UNDERSTANDING TUMOR HETEROGENEITY AND ALTERED METABOLISM IN GLIOMAS

EDITED BY: Yaohua Liu, Lingtao Jin and Shouwei Li

PUBLISHED IN: Frontiers in Oncology and Frontiers in Neurology

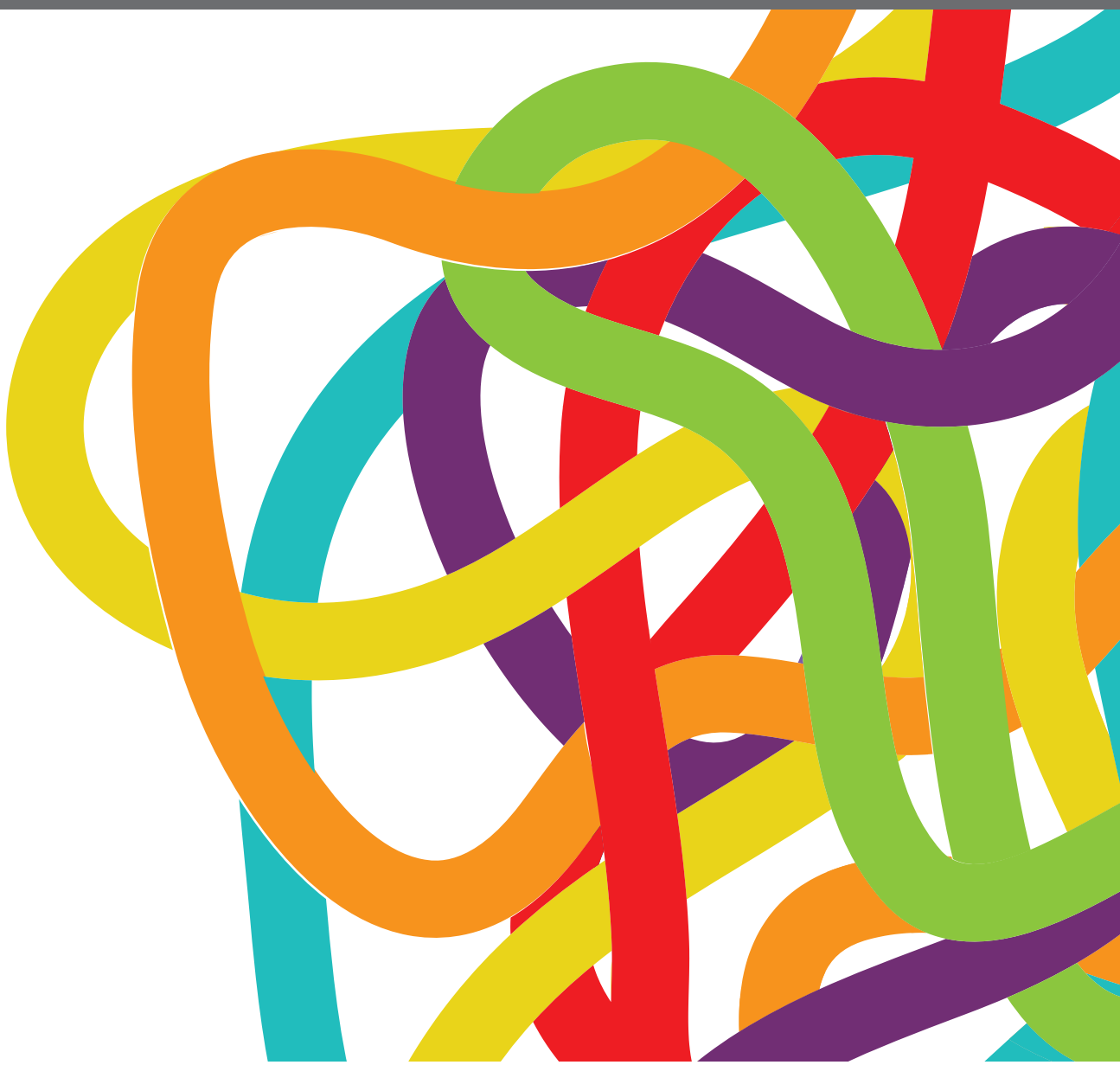

frontiers Research Topics

frontiers

ISSN 1664-8714
ISBN 978-2-83250-527-4
DOI 10.3389/978-2-83250-527-4

About Frontiers

Frontiers is more than just an open-access publisher of scholarly articles: it is a pioneering approach to the world of academia, radically improving the way scholarly research is managed. The grand vision of Frontiers is a world where all people have an equal opportunity to seek, share and generate knowledge. Frontiers provides immediate and permanent online open access to all its publications, but this alone is not enough to realize our grand goals.

Frontiers Journal Series

The Frontiers Journal Series is a multi-tier and interdisciplinary set of open-access, online journals, promising a paradigm shift from the current review, selection and dissemination processes in academic publishing. All Frontiers journals are driven by researchers for researchers; therefore, they constitute a service to the scholarly community. At the same time, the Frontiers Journal Series operates on a revolutionary invention, the tiered publishing system, initially addressing specific communities of scholars, and gradually climbing up to broader public understanding, thus serving the interests of the lay society, too.

Dedication to Quality

Each Frontiers article is a landmark of the highest quality, thanks to genuinely collaborative interactions between authors and review editors, who include some of the world's best academicians. Research must be certified by peers before entering a stream of knowledge that may eventually reach the public - and shape society; therefore, Frontiers only applies the most rigorous and unbiased reviews.
Frontiers revolutionizes research publishing by freely delivering the most outstanding research, evaluated with no bias from both the academic and social point of view. By applying the most advanced information technologies, Frontiers is catapulting scholarly publishing into a new generation.

What are Frontiers Research Topics?

Frontiers Research Topics are very popular trademarks of the Frontiers Journals Series: they are collections of at least ten articles, all centered on a particular subject. With their unique mix of varied contributions from Original Research to Review Articles, Frontiers Research Topics unify the most influential researchers, the latest key findings and historical advances in a hot research area! Find out more on how to host your own Frontiers Research Topic or contribute to one as an author by contacting the Frontiers Editorial Office: frontiersin.org/about/contact

UNDERSTANDING TUMOR HETEROGENEITY AND ALTERED METABOLISM IN GLIOMAS

Topic Editors:
Yaohua Liu, Shanghai First People's Hospital, China
Lingtao Jin, University of Florida, United States
Shouwei Li, Capital Medical University, China

Citation: Liu, Y., Jin, L., Li, S., eds. (2022). Understanding Tumor Heterogeneity and Altered Metabolism in Gliomas. Lausanne: Frontiers Media SA.
doi: 10.3389/978-2-83250-527-4

Table of Contents

frontiers in Oncology

REVIEW
published: 03 February 2021
doi: 10.3389/fonc.2020.625884

Emerging Role of Long Non-Coding RNAs in the Pathobiology of Glioblastoma

Omidvar Rezaei[1], *Kasra Honarmand Tamizkar*[2], *Guive Sharifi*[1], *Mohammad Taheri*[3]* *and Soudeh Ghafouri-Fard*[2]*

[1] Skull Base Research Center, Loghman Hakim Hospital, Shahid Beheshti University of Medical Sciences, Tehran, Iran, [2] Department of Medical Genetics, Shahid Beheshti University of Medical Sciences, Tehran, Iran, [3] Urogenital Stem Cell Research Center, Shahid Beheshti University of Medical Sciences, Tehran, Iran

Glioblastoma is the utmost aggressive diffuse kind of glioma which is originated from astrocytes, neural stem cells or progenitors. This malignant tumor has a poor survival rate. A number of genetic aberrations and somatic mutations have been associated with this kind of cancer. In recent times, the impact of long non-coding RNAs (lncRNAs) in glioblastoma has been underscored by several investigations. Up-regulation of a number of oncogenic lncRNAs such as H19, MALAT1, SNHGs, MIAT, UCA, HIF1A-AS2 and XIST in addition to down-regulation of other tumor suppressor lncRNAs namely GAS5, RNCR3 and NBAT1 indicate the role of these lncRNAs in the pathogenesis of glioblastoma. Several *in vitro* and a number of *in vivo* studies have demonstrated the contribution of these transcripts in the regulation of cell proliferation and apoptosis, cell survival, invasion and metastasis of glioblastoma cells. Moreover, some lncRNAs such as SBF2-AS1 are involved in conferring resistance to temozolomide. Finally, few circularRNAs have been identified that influence the evolution of glioblastoma. In this paper, we discuss the impacts of lncRNAs in the pathogenesis of glioblastoma, their applications as markers and their implications in the therapeutic responses in this kind of cancer.

Keywords: lncRNA, circRNA, glioblastoma, expression, polymorphism

OPEN ACCESS

Edited by:
Yaohua Liu,
Shanghai First People's Hospital, China

Reviewed by:
Maite Verreault,
INSERM U1127 Institut du Cerveau et de la Moelle épinière (ICM), France
Kristin Huntoon,
University of Texas MD Anderson Cancer Center, United States

***Correspondence:**
Mohammad Taheri
mohammad_823@yahoo.com
Soudeh Ghafouri-Fard
s.ghafourifard@sbmu.ac.ir

Specialty section:
This article was submitted to Neuro-Oncology and Neurosurgical Oncology, a section of the journal Frontiers in Oncology

Received: *04 November 2020*
Accepted: *22 December 2020*
Published: *03 February 2021*

Citation:
Rezaei O, Tamizkar KH, Sharifi G, Taheri M and Ghafouri-Fard S (2021) Emerging Role of Long Non-Coding RNAs in the Pathobiology of Glioblastoma. Front. Oncol. 10:625884. doi: 10.3389/fonc.2020.625884

INTRODUCTION

Being considered as grade IV glioma tumors, glioblastomas are the utmost aggressive diffuse kind of glioma originating from the astrocytes, neural stem cells or progenitors (1). This type of brain tumor includes about half of all glioma tumors and less than 20% of all primary brain tumors (2). Although being a rare tumor, the poor prognosis and low survival rate of glioblastoma have made it an important public health problem (3). It is more frequent in men compared with females, in Western countries compared with developing world and in some ethnicities such as Asians, Latinos and Whites (3). The etiology of this kind of tumor is largely unclarified, as no causal carcinogen has been linked with it. High dose ionizing radiation is the solitary environmental element that is highly associated with risk of glioblastoma (4). A number of genetic aberrations such as activation of growth factor cascade through amplification and mutations in receptor tyrosine kinase genes,

induction of the PI3K proteins and loss of the p53 and Rb tumor suppressor genes have been identified in glioblastoma (5). Genome-wide and direct sequencing techniques have also detected recurrent disease-causing mutations in glioblastoma samples in a number of genes such as *IDH1* (6) and *TERT* promoter (7). Moreover, contemporary studies have conveyed anomalous expression of long non-coding RNAs (lncRNAs) in glioblastoma samples indicating the impact of these transcripts in the pathobiology of this kind of cancer (8). These transcripts are larger than 200 nucleotides and regulate expression of numerous genes at transcriptional, post-transcriptional, and epigenetic phases (9). In the current paper, we discuss the impact of lncRNAs in the pathobiology of glioblastoma and their effects on the regulation of cell proliferation and apoptosis, cell survival, invasion and metastatic aptitude of glioblastoma cells.

ONCOGENIC LNCRNAS IN GLIOBLASTOMA

Several oncogenic lncRNAs have been up-regulated in glioblastoma samples. For instance, MIR22HG is an oncogenic lncRNA which has been shown to be highly dysregulated in glioblastoma *via* assessment of accessible datasets. This lncRNA hosts miR-22-3p and miR-22-5p. Further studies have unraveled over-expression of the MIR22HG/miR-22 route in glioblastoma and glioma stem-like cells. Over-expression of MIR22HG in glioblastoma samples has been related with poor patients' outcome. Knock down of this lncRNA has led to inactivation of the Wnt/β-catenin route *via* modulating miR-22-3p and miR-22-5p expressions. Functionally, MIR22HG silencing has diminished cell proliferation, invasion and tumor growth in xenograft models. The mentioned miRNAs have been shown to target SFRP2 and PCDH15. Taken together, MIR22HG has been acknowledged as an important activator of the Wnt/β-catenin signaling pathway, and its silencing has been proposed as a therapeutic modality in this kind of cancer (10). The small nucleolar RNA host gene 5 (SNHG5) is another up-regulated lncRNA in glioblastoma which enhances cell proliferation and suppresses cell apoptosis in these cells. Expression of this lncRNA is activated by the Yin Yang 1 (YY1) transcription factor. This lncRNA exerts its oncogenic role *via* stimulation of the p38/MAPK axis (11). SNHG9 has also been demonstrated to be over-expressed in glioblastoma samples in association with poor survival of patients. SNHG9 has a role in suppression of miR-199a-5p expression and enhancement of Wnt2 expression in glioblastoma cells. This lncRNA has been revealed to enhance aerobic glycolysis and cell proliferation (12). Expression of SAMMSON has been increased in the plasma of patients with glioblastoma but not in those with diffuse neurosarcoidosis, a disorder that shares MRI signs with glioblastoma. This lncRNA has been displayed to suppress expression of miR-622 in glioblastoma cells and subsequently enhance cell (13). MIAT is another up-regulated lncRNA in glioblastoma. Bountali et al. have knocked down this lncRNA in glioblastoma cell lines and analyzed RNA profile of these cells *via* RNA sequencing method. They reported differential expression of several genes including those participating in cancer-associated functions, namely cell growth and viability, apoptotic features, reactive oxygen species creation and migration. Functionally, MIAT silencing abolishes long-term viability and migration and enhances apoptosis in these cells (14). A genome-wide expression profiling in glioblastoma cells has identified MALAT1 as one of the most remarkably over-expressed genes following treatment with temozolomide (TMZ). Expression of this lncRNA has been co-regulated by p50 and p53 through κB- and p53-binding sites which are located in coding sequence of this lncRNA. MALAT1 silencing has increased sensitivity of patient-originated glioblastoma cells to TMZ and improved the effects of this drug in xenograft mice models (15). UCA1 is another oncogenic lncRNA which enhances cell proliferation and migration, while suppressing cell apoptosis. **Figure 1** depicts the molecular mechanisms through which UCA1 participates in the pathogenesis of glioblastoma.

Table 1 reviews the function of oncogenic lncRNAs in glioblastoma.

TUMOR SUPPRESSOR LNCRNAS IN GLIOBLASTOMA

Expression of GAS5 has been decreased in glioblastoma and its levels have been negatively correlated with miR-34a levels (61). In addition, expression of AC016405.3 has been decreased in glioblastoma tissues in association with numerous aggressive characteristics of this type of cancer. Up-regulation of this lncRNA inhibits proliferation and metastatic ability of glioblastoma cells. The oncogenic miRNA, miR-19a-5p has been identified as a downstream miRNA of AC016405.3. AC016405.3 has been shown to be targeted by miR-19a-5p. Functionally, AC016405.3 inhibits cell proliferation and metastasis *via* regulation of TET2 by serving as a sponge for miR-19a-5p (62). LINC00657 is another tumor suppressor lncRNA whose expression has been decreased in glioblastoma sections compared with neighboring normal section. Up-regulation of this lncRNA has suppressed cell proliferation, colony formation, invasiveness and migratory potential of glioma cells through activating cell apoptosis. LINC00657 has been acknowledged as a direct target of miR-190a-3p, a miRNA that negatively regulates PTEN expression. The tumor suppressive role of LINC00657 has also been verified in xenograft models (63). The lncRNA AC003092.1 has been shown to be down-regulated in TMZ resistance cells compared with their original cells. Moreover, down-regulation of this lncRNA has been correlated with resistance to TMZ, higher possibility of tumor relapse, and poor patients' outcome. Cell line studies has shown improvement of TMZ sensitivity following up-regulation of AC003092.1. The effect of this lncRNA in the modulation of TMZ sensitivity is exerted *via* regulation of TFPI-2–associated cell apoptosis through sponging miR-195 (64). RNCR3 is another down-regulated lncRNA in glioblastoma. Over-expression of this lncRNA significantly suppresses cell

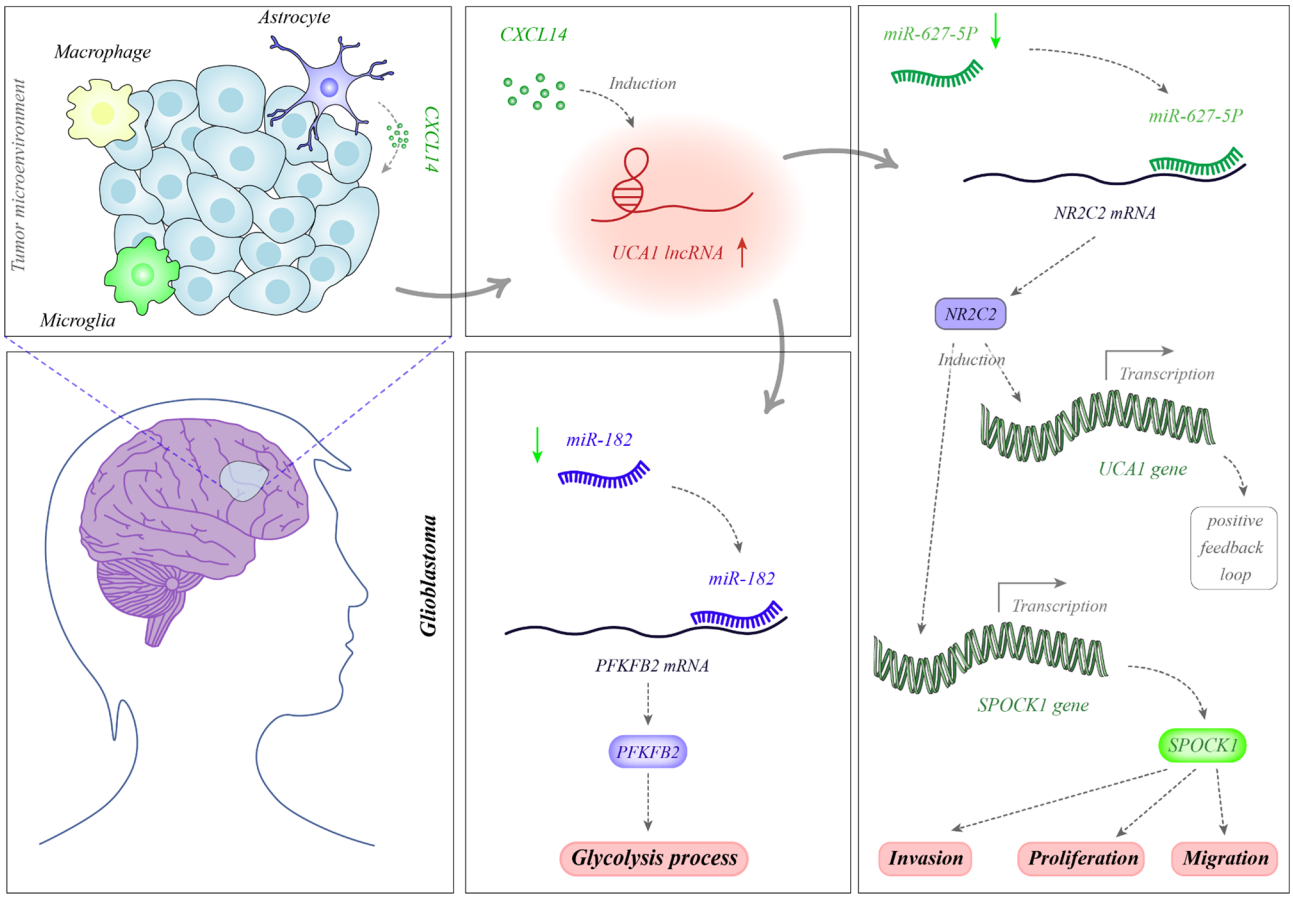

FIGURE 1 | Glioblastoma-associated stromal cells (GASCs) are special cells in the tumor microenvironment which are phenotypically and functionally similar to the cancer-associated fibroblasts. These cells produce CXCL14 which functions as a paracrine factor to enhance expression of UCA1. UCA1 serves as a sponge for miR-182. Since miR-182 suppresses expression of PFKFB2, UCA1 up-regulation results in up-regulation of PFKFB2 through sequestering miR-182. PFKFB2 protein increases glycolysis in the tumor cells (16). In addition, UCA1 decreases miR-627-5p levels. As miR-627-5p inhibits NR2C2 expression, down-regulation of miR-627-5p by UCA1 enhances expression of NR2C2. NR2C2 binds with the promoter region of UCA1 and increase its expression through a positive feedback loop. Moreover, NR2C2 enhances expression of SPOCK1 increasing cell proliferation, migration and invasiveness of tumor cells (17).

survival and proliferation of glioblastoma cells, while enhancing cell apoptosis and activity caspase-3/7. Besides, up-regulation of this lncRNA enhances expression of Krüppel-like factor 16 (KLF16) *via* suppressing miR-185-5p (65). **Table 2** gives an outline of studies which assessed function of tumor suppressor lncRNAs in glioblastoma.

DIAGNOSTIC AND PROGNOSTIC VALUE OF LNCRNAS IN GLIOBLASTOMA

Expression levels of lncRNAs can distinguish patients with glioblastoma from cancer-free individuals. Moreover, these transcripts can possibly differentiate different brain tumors. For instance, plasma levels of SAMMSON can differentiate glioblastoma from both diffuse neurosarcoidosis and healthy controls (13). Among lncRNAs whose diagnostic power has been assessed in glioblastoma, HOTAIR has exhibited the most promising results. Tan et al. have demonstrated significant higher levels of this lncRNA in sera of glioblastoma patients compared with controls. The area under the receiver operating characteristic (ROC) curve was 0.913 indicating the ideal feature of HOTAIR for this purpose. Moreover, they reported significant correlation between its levels and high tumor grade. Notably, there was significant correlation between tumor and serum levels of this lncRNA. Finally, exosomes extracted from the serum samples have been shown to contain this lncRNA, further emphasizing the application of this lncRNA in the prognostic and diagnostic processes in glioblastoma (49). In addition, Kaplan-Meier analysis has indicated the correlation between expression levels of several lncRNAs such as SNHG9, TRG-AS1, AGAP2-AS1, lnc-TALC, SBF2-AS1, SNHG20, AC016405.3, LINC-ROR, HOXB-AS1, H19, LINC00152, RAMP2-AS1 and GAS5 and patients' prognosis in the terms of overall survival, disease-free survival and progression free survival. **Table 3** gives a summary of studies which assessed such aspect of lncRNAs in glioblastoma.

TABLE 1 | List of over-expressed lncRNAs in glioblastoma.

lncRNA	Patients' specimens	Cell line	Targets/ Regulators	Signaling pathways	Functional impact	Impact of high expression on patient's prognosis	Reference
MIR22HG	18 gliomas and 5 NBT	U87MG, LN229, and LN18	b-catenin, miR-22-3p, SFRP2, PCDH15	Wnt	MIR22HG is over-expressed in glioma and glioma stem-like cells. Its silencing constrains the Wnt/b-catenin axis *via* loss of miR-22-3p and -5p. This diminishes proliferation, invasion and tumor growth.	poor survival	(10)
SNHG5	–	U251, U87, LN229 and HEB	ELK1, caspase-3, STAT1, p-p38/ YY1, TNF-a	p38/MAPK	SNHG5 enhances GBM proliferation and suppresses apoptosis in GBM. YY1 is the activator of SNHG5 transcription in GBM.	–	(11)
SNHG9	–	U87 and U251	miR-199a-5p and Wnt2	Wnt/b-catenin	SNHG9 enhances aerobic glycolysis and cell proliferation, which can be weakened by miR-199a-5p.	lower survival rate	(12)
SAMMSON	56 patients with GBM, 34 patients with diffuse neurosarcoidosis and 35 healthy controls	U87, U-373	miR-622	–	SAMMSON overexpression down-regulates miR-622 and increases proliferation rate.	–	(13)
DLEU1	10 GBM tissues and 10 adjacent NBT	SHG-44, U251	TRA F4	–	Over-expression of DLEU enhances viability and cell proliferation.	–	(18)
TRG-AS1	51 glioma tissues and 51 NBTs	U251, U87, A172, LN229, NHAs	miR-877-5p	–	TRG-AS1 inhibits miR-877-5p while miR-877-5p inhibits SUZ12 expression.	poor prognosis	(19)
LINC01579	51 patients with GBM	U251, U87, U87MG, LN229, NHA	miR-139-5p	–	LINC01579 regulates cell proliferation and apoptosis through binding with miR-139-5p.	–	(20)
AGAP2-AS1	58 GBM patients	A172, U87/MG, U251/ MG, LN229, SHG44, NHA	EZH2 and LSD1	–	Up-regulation of AGAP2-AS1 enhances cell proliferation and apoptosis.	Poor prognosis	(21)
lnc-TALC	79 GBM patients	LN229, U251, 551W, HG7, 229R, 251R, 551WR, HG7R	miR-20b-3p/ phosphorylated AKT/FOXO3 axis	c-MET	lnc-TALC is associated with TMZ resistance through interacting with miR-20b-3p to enhance c-Met expression.	Low lnc-TALC expression improved prognosis after receiving TMZ.	(22)
LncSBF2-AS1	20 primary and their corresponding recurrent GBM specimens (each pair from the same patient who was under TMZ treatment)	U87, LN229, A172, T98, U251, HEK293T, N3 primary culture cell	miR-151a-3p/ ZEB1	–	SBF2-AS1 is up-regulated in TMZ-resistant GBM cells and tissues.	Recurrent GBM patients cases with high serum exosomal SBF2-AS1 amounts had poor outcome and a resistance to TMZ.	(23)
SNHG20	78 pairs of human glioblastoma tissues and adjacent tissues	U87MG, U343, U251, LN215, NHA	Cyclin D1, CDK4, caspase 9, PI3K, Akt and mTOR	PI3K/Akt/ mTOR	SNHG20 overexpression enhanced cell proliferation, decreased apoptosis and increased stem properties.	Low survival rate	(24)
MALAT1	Patients expressing MALAt1 were separated into two low (n=19) and high (n=15) expressing groups	U87, A172, and U251, patient-derived GSCs, GBM34 and GBM44	-/p50 and p52	NF-κB	MALAT1 silencing sensitizes GBM cells to TMZ.	–	(15)
	–	U251, U87	ZEB1, MDR1, MRP5, LRP1	–	MALAT1silencing down-regulated MDR1, MRP5, and LRP1 levels, increased response to TMZ, and decreased ZEB1 level.	–	(25)
	–	U251	miR-101, GSK3β, MGMT	–	MALAT1 levels were higher in TMZ-resistant GBM cells. MALAT1 silencing reduces TMZ resistance by inhibiting cell proliferation and promoting apoptosis.	–	(26)
	140 GBM patients: 70 responsive to TMZ and 70 non-responsive	U87, U251	miR-203, TS	–	MALAT1 induces resistance to TMZ *via* inhibiting miR-203 and enhancing thymidylate synthase expression.	Poor OS and RFS	(27)

(Continued)

TABLE 1 | Continued

lncRNA	Patients' specimens	Cell line	Targets/ Regulators	Signaling pathways	Functional impact	Impact of high expression on patient's prognosis	Reference
miR155HG	24 GBM tissues and 15 adjacent NBTs	normal human astrocyte cell line NHA, U87, U251, Ln229, T98, and A172, GP1 and GP2	miR-185/ANXA2, STAT3	PI3K-Akt	miR155HG enhances epithelial-to-mesenchymal transition in glioma. miR155HG silencing inhibited GBM cell proliferation, stimulated G1/S-phase cell cycle arrest, and enhanced apoptosis.	–	(28)
TP73-AS1	TCGA and GTEx datasets: 207 normal, 518 low grade glioma and 163 GBM	G26 and G7	ALDH1A1	–	TP73-AS1 increases TMZ resistance in GBM cancer stem cells and enhances tumor aggressiveness.	Poor prognosis	(29)
LINC-ROR	57 GBM tissues and 10 NBTs	–	caspase 3 and p53	–	Patients with OS less than 15 months had up-regulation of LINC-ROR.	poor PDF and overall survival	(30)
MIAT	–	SH-SY5Y, GBM 1321N1, GBMT98G	Many genes	MAPK, Phospholipase D, TGF-β, NOD-like receptor, EGFR	MIAT enhances cell growth, survival, production of reactive oxygen species and migration, and decreases basal apoptosis.	–	(14)
HOXB-AS1	486 low grade glioma (LGG) and 154 glioblastoma (GBM) tissues	HA, LN229, U87 and U251 cell lines	miR-885-3p, HOXB2		HOXB-AS1silencing suppresses cell proliferation through inducing S phase cell cycle arrest, and suppresses the migration and invasion capacity.	Poor prognosis	(31)
GAPLINC	High GAPLINC expressing group (n=80) and low GAPLINC expressing group (n=81)	NHAs,T98G, U251, LN18, LN229, and A172	miR-331-3p	–	GAPLINC enhances GBM cells proliferation, migration, and invasion, and reduces apoptosis.	shorter overall survival and disease-free survival	(32)
AHIF	–	U87-MG and T98G GBM cell	Bax, Bcl-2, and caspase 7	–	AHIF was up-regulated in GBM cells after radiotherapy and affects GBM cell clonogenic formation, DNA repair and apoptosis.	–	(33)
	31 GBM patients and 7 adjacent NBT	U87-MG, U251-MG, A172, T98G	VEGF, angiogenin, Bcl-2, Bcl-xl, Mcl-1	–	AHIF enhances viability and invasiveness, and reduced the proportion of apoptotic cells. Exosomes originated from AHIF–overexpressing GBM cells enhanced viability, invasion and radio-resistance.	–	(34)
AGAP2-AS1	116 GBM tissues, 20 low-grade glioma samples and 20 adjacent NBTs	U87, U251, human astrocyte cell line (HA)	–	–	Up-regulation of AGAP2-AS1 enhances cell proliferation, migration, and invasion, but reduces cell apoptosis.	Shorter overall survival	(35)
lnc-UCA1	Glioma samples: Grade I–II (n=5), Grade III–IV (n=5) and normal human brain tissues (n=5)	Human U87 and U251 glioma cell	miR-627-5p, NR2C2	–	UCA1 overexpression enhances proliferation, migration, and invasion, but suppresses apoptosis.	–	(17)
	42 paired glioma tissues and NBTs	U251, U87MG	miR-182, PFKFB2/CXCL14	–	UCA1/miR-182/PFKFB2 axis induces glycolysis and invasion.	Poor survival	(16)
H19	50 FFPE brain tissue from GBM patients and 10 cancer-free brain tissue samples	–	miR-326	–	H19 over-expression confers poor OS and progression-free survival.	Poor OS	(36)
	–	U87, U251, Ln229, U373, U118, GP1, GP2	miR-181d, β-catenin/Hif-1α, PTEN, SP1	–	H19 expression is increased by Hif-1α under hypoxia. H19 contributes in hypoxia-associated migration and invasion.	Lower survival rate	(37)
	30 glioblastoma tissues and adjacent NBT	U87, U373, HUVECs	–	–	H19 enhances glioblastoma cell invasion, neurosphere formation, tumor growth and angiogenesis.	Lower PFS	(38)

(Continued)

TABLE 1 | Continued

lncRNA	Patients' specimens	Cell line	Targets/ Regulators	Signaling pathways	Functional impact	Impact of high expression on patient's prognosis	Reference
	–	U87MG, U251, U343, Hs683, LN215, A172, NHA	–	–	H19 silencing reduced cellular proliferation and increased apoptosis rate when induced by TMZ. Cancer stem cell markers (CD133, Nanog, Oct-4, and Sox2) are increased by H19 upregulation.	–	(39)
LINC00152	35 samples (5 normal, 10 with grade two, 9 with grade three and 11 with grade four GBM)	LN229, U87-MG and N9 (patient-derived cells)	miR-612	AKT2/NF-κB	LINC00152 regulates malignant progression and proneural–mesenchymal transition.	Poor prognosis	(40)
	–	U87	TPM2, PTX3, IGFBP4, TGM2, SPP1, LUM	–	LINC00152 increases cellular invasion and EMT.	Poor survival	(41)
	40 glioblastoma samples and matched NBTs	U87, U251, LN229, A172, U118, NHA	E-cadherin, N-cadherin, Vimentin, and Snail, HMGA2	–	LINC00152 enhances cell proliferation, EMT and invasion.	–	(42)
LINC00470	50 GBM samples and 10 NBTs	U251, U87 and U118	ELFN2, miR-101, AurkA. and eIF2a		LINC00470 increases expression of ELFN2 and regulates methylation of ELFN2. LINC00470 suppresses ELFN2-induced GBM cell autophagy.	Poor prognosis	(43)
	60 astrocytoma tissues and 12 NBT	U251, U87	FUS and AKT	–	Higher pAKT induced by LINC00470 decreased ubiquitination of HK1 and suppressed autophagy. Higher LINC00470 expression was associated poor patient outcome.	Poor prognosis	(44)
LINC01446	31 pairs of GBM samples and adjacent normal tissues	NHA, A172, U87, U251 and T98G	miR-489-3p, TPT1		LINC01446 silencing suppressed GBM cell proliferation, arrested cell-cycle progression, decreased tumor growth and attenuated invasion.	poor prognosis and OS	(45)
CASP5	40 pairs of GBM and NBTs	A172, U87MG, U251MG, T98G, U118MG and the human astrocyte cell line HA	Cyclin D1, MMP-9, MMP-2, E-cadherin, N-cadherin, and Vimentin	–	CASP5 silencing has suppressed GBM proliferation and arrested cells in G1.	–	(46)
LOXL1-AS1	169 GBM RNA-seq data (68 MES and 101 PN)	U87MG	RELB	NF-kB	GBM cell proliferation was inhibited by LOXL1-AS1 silencing.	Poor prognosis and low OS	(47)
MNX1-AS1	44 pairs of GBM samples and adjacent normal tissues	U138, LN229, T98, U251	miR-4443	–	MNX1-AS1 enhanced the proliferation, migration, and invasion of GBM cells.	–	(48)
HOTAIR	43 GBM patients and 40 controls	–	–	–	HOTAIR expression correlates with high grade brain tumors.	–	(49)
	123 GBM cases from TCGA, 34 cases from CGGA2, 227 cases from Rembrandt, 79 cases from TTseq, and 77 cases from GSE4290	U87, U87vIII	NLK	β-catenin	HOTAIR silencing suppressed GBM cell migration and invasion.	Poorer survival	(50)
	TCGA dataset: 220 glioma	U87, LN229	EZH2	–	HOTAIR enhances cell cycle progression.	Lower survival	(51)
SNHG7	53 pairs of GBM tissues and NBTs	HEB, A172, U87, T98G, SHG44	miR-5095	Wnt/b-catenin	SNHG7 silencing inhibited proliferation, migration and invasion and induced apoptosis.	Poorer prognosis	(52)

(Continued)

TABLE 1 | Continued

lncRNA	Patients' specimens	Cell line	Targets/ Regulators	Signaling pathways	Functional impact	Impact of high expression on patient's prognosis	Reference
NEAT1	–	N5, N9 and N33 patient-derived cells	b-catenin, ICAT, GSK3B, Axin2, EZH2/STAT3, p65	WNT/b-catenin, EGFR, NFkB	NEAT1 enhances proliferation, clone formation, and invasion but suppresses cell apoptosis.	–	(53)
	120 glioma tissues and 30 NBTs	U87, T98G, U251, A272, U373, HEK293T	miR-let7e, Argonaute 2, NRAS	–	NEAT1 silencing suppressed GSC cell proliferation, migration and invasion and promoted GSC apoptosis.	–	(54)
SOX2OT	Human glioma tissues (grade one=5, grade two=5, grade three=8, grade four=8) and 5 NBTs	U87 and U251	miR-194-5p and miR-122/SOX3	JAK/STAT	SOX2OT promoted the proliferation, migration and invasion of GSCs, and inhibited GSCs apoptosis.	–	(55)
TUG1	20 GBM specimens (grade one to four, each 5) and 5 normal brain tissues	U251 MG, U87MG, 293T	miR-299, VEGFA	–	TUG1 promotes tumor-induced endothelial cell proliferation, migration and tube formation and enhances spheroid-based angiogenesis.	–	(56)
HIF1A-AS2	–	Primary human GSCs	IGF2BP2, DHX9, HMGA1	–	This lncRNA regulates GSC growth, self-renewal, hypoxia-associated molecular reprogramming and adaptation to hypoxia within the tumor niche.	Poor OS	(57)
XIST	–	Human embryonic kidney (HEK) 293T cells	miR-152	–	XIST promotes cell proliferation, migration and invasion and suppresses apoptosis.	–	(58)
MCM3AP-AS	422 GBM patients (TCGA dataset)	–	MCM3AP	–	MCM3AP-AS corresponds to the coding-gene MCM3AP, which is involved in initiation of DNA replication.	Lower OS	(59)
LINC01057	12 paired frozen fresh GBM and adjacent NBTs and the paraffin-embedded human GBM samples	LN229, T98G, HEK293T	IKKα	NF-κB	LINC01057 up-regulation increases mesenchymal differentiation in proneural cells.	–	(60)

GBM, glioblastoma multiform; TMZ, temozolomide; OS, overall survival; GSC, glioblastoma stem cell; NBT, normal brain tissues.

TABLE 2 | List of under-expressed lncRNAs in glioblastoma.

lncRNA	Patients' specimens	Cell line	Targets/ Regulators	Signaling pathways	Functional role	Impact of low expression on patient's prognosis	Reference
AC016405.3	3 GBM samples and paired NBTs, 64 FFPE GBM specimens	U87MG, U251MG	miR-19a-5p, TET2	–	AC016405.3 inhibits proliferation and metastasis *via* affecting expression of TET2.	Poor prognosis	(62)
LINC00657	40 pairs of GBM tissues and adjacent normal tissues	HA1800, U-87, LN-18, and U-118 MG	miR-190a-3p	pTEN	LINC00657 suppresses viability and colony formation in through increasing cell apoptosis.	Poor progonosis	(63)
AC003092.1	108 human glioma tissue samples (75 grade IV, 5 grade III, 13 grade II, and 15 grade I astrocytoma cases)	U87, U251 and their TMZ-resistant lines, U87TR and U251TR	TFPI-2, miR-195	–	Down-regulation of AC003092.1 correlates with TMZ resistance, higher risk of relapse, and poor outcome.	Poor prognosis	(64)
GAS5	50 FFPE GB specimens and 10 NBTs	–	miR-34a	–	GAS5 level in reduced in GBM.	Poor overall survival	(61)
RNCR3	–	U87, U251, U373, A172	miR-185-5p, KLF16	–	RNCR3 overexpression suppresses cell survival and proliferation, enhances cell apoptosis and activity of caspase-3/7.	–	(65)
NBAT1	48 cases of GBM (two groups of low=24 and high=24 expression of NBAT1) and 30 cases of normal brain tissues	SVGP12, U251, U87, U373, T98, and LZ229	Akt	–	NBAT1 down-regulation correlates with proliferation ability, tumor size, degree of malignancy and cell viability.	Lower OS and poor prognosis	(66)
TUSC7	116 GBM specimens, 72 insensitive and 44 sensitive to TMZ treatment	U87	miR-10a	–	Under-expression of TUSC7 confers resistant to TMZ.	–	(67)
RAMP2-AS1	20 GBM patients and adjacent normal tissue	U87 and U251	NOTCH3, P21, DHC10	NOTCH	RAMP2-AS1 suppresses GBM cell growth and enhances cell cycle progression.	Poor prognosis	(68)
RP11-838N2.4	53 patients: 38 GBM cases, 3 grade III astrocytoma cases, 10 grade II astrocytoma cases, 2 grade I astrocytoma cases	U87TR, U251TR, U87, U251	miR-10a, EphA8	TGF-β	Down-regulation of RP11-838N2.4 was correlated with higher probability of tumor relapse.	Poorer survival	(69)

GBM, glioblastoma multiform; TMZ, temozolomide; OS, overall survival; GSC, glioblastoma stem cell; FFPE, formalin-fixed, paraffin paraffin-embedded.

TABLE 3 | Diagnostic/prognostic value of lncRNAs in glioblastoma.

Sample number	Area under curve	Sensitivity	Specificity	Kaplan–Meier analysis	Univariate/Multivariate Cox regression	Reference
Two groups of high and low SNHG9 expressing patients, each contained 20 patients	–	–	–	OS and PFS in patients with high SNHG9 expression were lower than those with down-regulation of SNHG9. High SNHG9 expression was correlated with high tumor grade, greater tumor dimension, and metastasis.	SNHG9 was an independent prognostic factor for worse OS.	(12)
56 patients with GBM, 34 patients with diffuse neurosarcoidosis and 35 healthy controls/SAMMSON levels	GBM versus diffuse neurosarcoidosis: 0.92 GBM versus healthy controls: 0.88	–	–	–	–	(13)
51 samples of glioma tissues	–	–	–	TRG-AS1 has been related with poor prognosis.	–	(19)
58 GBM patients	–	–	–	Higher levels of AGAP2-AS1 correlated with lower OS.	–	(21)
79 GBM patients	–	–	–	OS in patients with TMZ therapy and low expression of lnc-TALC was increased, whereas high expression of lnc-TALC and therapy with TMZ reduced OS.	TMZ chemotherapy was correlated with the OS of patients with low lnc-TALC expression.	(22)
77 with high levels of SBF2-AS1 and 77 with low levels of SBF2-AS1	–	–	–	OS decreases in patients with high levels of SBF2-AS1.	–	(23)
45 patients with low levels of SNHG20 and 33 patients with high levels of SNHG20	–	–	–	High levels of SNHG20 was correlated with lower rate of OS.	–	(24)
Two groups of 32 patients with high and low levels of AC016405.3	–	–	–	Low expression of AC016405.3 was correlated with a shorter survival rate, a larger size of tumor, a higher grade, and more common distant metastasis.	–	(62)
57 glioblastoma patients	0.653 ± 0.078	65.4	77.8	Patients with high LINC-ROR amounts had poor survival.	–	(30)
LGG (n=486) and GMB (n=154)	–	–	–	High expression of HOXB-AS1 was associated with poorer prognosis in GBM.	–	(31)
136 glioma patients	–	–	–	High levels of AGAP2-AS1was correlated with lower OS.	–	(35)
high (n = 37) and low (n = 38) AC003092.1 expression group	–	–	–	High AC003092.1 expression group indicated higher OS.	–	(64)
50 FFPE brain tissue from GBM patients	0.686 (0.537–0.836)	71.4	59.6	H19 overexpression correlates with poorer OS.	–	(36)
CGGA GBM (high expression= 45 and low expression= 45), TCGA GBM (high expression = 77 and low expression= 78)	–	–	–	Higher expression of LINC00152 correlates with lower OS.	LINC00152 levels, age, chemotherapy and radiotherapy have been associated with OS in CGGA database. LINC00152 levels, age, IDH status, and chemotherapy have been associated with OS database.	(40)
Low group (n=15) and high group (n=16)	–	–	–	Patients with a higher LINC01446 expression had a poor survival rate in five years.	–	(45)
15 patients with GBM/HOTAIR	0.913	86.1	87.5	–	–	(49)
53 patients with GBM	–	–	–	Higher expression of SNHG7 correlated with poorer survival rate.	–	(52)
20 patients with GBM	–	–	–	Lower survival rate with lower expression of RAMP2-AS1.	–	(68)
53 patients: 38 GBM cases, 3 grade III astrocytoma cases, 10 grade II astrocytoma cases, 2 grade I astrocytoma cases	–	–	–	High level of lncRNA RP11-838N2.4 has been correlated with longer survival.	–	(69)

(Continued)

TABLE 3 | Continued

Sample number	Area under curve	Sensitivity	Specificity	Kaplan–Meier analysis	Univariate/Multivariate Cox regression	Reference
LINC00470 expression levels in two groups: high=37, low=38	–	–	–	High LINC00470 amounts were correlated with shorter survival times and poor prognosis.	LINC00470 levels, astrocytoma grade, age, and tumor site were associated with OS.	(44)
7 low HOTAIR and 26 high HOTAIR (for survival), 22 low HOTAIR and 46 high HOTAIR (for DFS), 10 high GAS5 and 23 low GAS5 (for survival), 21 high GAS5 and 47 low GAS5 (for DFS)	–	–	–	Patients with high HOTAIR and low GAS5 levels had worse survival rates relative to patients with low HOTAIR and high GAS5 levels.	–	(70)
Low (54) and high (54) groups of HOTAIR expression (CGGA1 dataset)	–	–	–	Low HOTAIR expression has increased OS.	HOTAIR over-expression, age at diagnosis, IDH1 mutation, KPS score, and Ki-67 expression were associated with OS.	(50)
Expression of H19 in two groups: high=14, low=16	–	–	–	H19 over-expression was significantly associated with a poor PFS.	–	(38)
70 high and 70 low patients of MALAT1 expression	0.775	71.51	62.82	MALAT1 over-expression was correlated with poor OS and RFS.	Serum MALAT1 levels and tumor grade were independent prognostic factors for OS of patients receiving TMZ.	(27)

GB, glioblastoma multiform; TMZ, temozolomide; OS, overall survival; PFS, progression-free survival; RFS, recurrence-free survival; DFS, disease-free survival.

TABLE 4 | List of circRNAs which participate in the development of glioblastoma.

circRNA	Pattern of expression	Patients' specimens	Cell line	Targets/Regulators	Signaling pathways	Function	Patient's prognosis	Reference
circNT5E	↑	39 pairs of glioma and NBTs	U87, U251	miR-422a/ADARB2	–	circNT5E suppresses activity of miRNAs with tumor-suppressor like features, and increase several pathologic processes, such as cell proliferation, migration, and invasion.	–	(71)
circ_0001946	↓	–	U87, U251	miR-671-5p, CDR1	–	Circ_0001946 inhibits expression of miR-671-5p, and increases CDR1 levels. Circ_0001946 and CDR1 decrease proliferation, migration, and invasion and upsurge apoptosis.	–	(73)
circMTO1	↓	59 pairs of GBM and NBTs	NHA, A172, U251, U87, SNB19, SHG44	WWOX, miR-92	–	circMTO1 suppresses proliferation of tumorous cells. circMTO1 increases expression of WWOX, and WWOX mediates circMTO1-associated suppression of proliferation of U251 cells. circMTO1 directly interact with miR-92.	Lower OS	(74)
circ-PITX1	↑	58 pairs of GBM and NBTs	A172, LN229, U251, U87, NHA	miR-379–5p, MAP3K2	MAPK	Down-regulation of circ-PITX1 inhibits cell proliferation and enhances cell apoptosis.	–	(75)
hsa_circ_0076248	↑	–	U251, U87, HEB	miR-181a, SIRT1, p53	–	hsa_circ_0076248 sponges miR-181a and down-regulates it. Down-regulation of hsa_circ_0076248 depresses the proliferation and invasion of glioma, and enhances the TMZ sensitivity.	–	(76)
circMMP9	↑	18 pairs of GBM and NBTs	U87, U251	miR-124, CDK4, AURKA/eIF4A3	–	circMMP9 enhances the proliferation, migration and invasion capacities.	–	(77)
circ_0074027	↑	50 pairs of GBM and NBTs	U87, U251, A172, LN229, NHA	miR-518a-5p, IL17RD	–	Cell growth, clone formation, migration and invasion were increased by circ_0074027.	–	(78)

GBM, glioblastoma multiform; TMZ, temozolomide; OS, overall survival; NBT, normal brain tissue.

CIRCULAR RNAS AND GLIOBLASTOMA

In addition to lncRNAs, Circular RNAs (circRNAs) can act as miRNA sponges to modulate expression of their target genes. Numerous studies have assessed expression and function of circRNAs in glioblastoma. For instance, Wang et al. have reported over-expression of some circRNAs and lncRNAs in miR-422a–downregulated glioblastoma samples. They have also recognized a new circRNA originated from NT5E, termed circNT5E. Expression of this circRNA is modulated by ADARB2 through binding to sites neighboring circRNA-creating introns. circNT5E has been shown to regulate cell proliferation, migration, and invasion of glioblastoma cells through binding with miR-422a and suppressing its activity (71). Li et al. have demonstrated down-regulation of circ_0001946 and *CDR1*, while up-regulation of miR-671-5p in glioblastoma cells. Circ_0001946 has been shown to inhibit expression of miR-671-5p, therefore enhancing *CDR1* expression. Circ_0001946 and *CDR1* decrease cell proliferation, migration, and invasion and induce apoptosis in glioblastoma cells as verified by both *in vitro* and *in vivo* assays (72). **Table 4** summarizes the expression and function of circRNAs in glioblastoma.

DISCUSSION

Both candidate gene and high throughput expression studies have reported anomalous expression of several lncRNAs in glioblastoma samples indicating the oncogenic roles for some lncRNAs and tumor suppressor roles for a number of other lncRNAs. Yet, the function of the former group of lncRNAs has been more assessed in this kind of cancer. Like other cancers, the role of lncRNAs in the pathogenesis of glioblastoma can be exerted through their effects on the expression of miRNAs. Accordingly, several lncRNA/miRNA/mRNA axes have been identified in this context among them are SNHG9/miR-199a-5p/Wnt2, MIR155HG/miR-185/ANXA2, TRG-AS1/miR-877-5p/SUZ12, LINC01579/miR-139-5p/EIF4G2, AC016405.3/miR-19a-5p/TET2, AC003092.1/miR-195/TFPI-2, LINC00657/miR-190a-3p/PTEN, RNCR3/miR-185-5p/KLF16, and MALAT1/miR-203/thymidylate synthase axes. Thus, comprehensive assessment of these three types of transcripts would facilitate identification of the molecular pathways underlying the pathogenesis of this type of cancer. Moreover, a number of recent studies revealed the role of circRNAs in regulation of expression of miRNAs, thus adding an extra level of complexity in gene regulation networks. An example of the circRNA/miRNA/mRNA functional axis in glioblastoma is represented by circ_0001946/miR-671-5p/*CDR1*.

Association between lncRNA expression levels and resistance to TMZ has been assessed in several studies. Notably, expressions of oncogenic lncRNAs lnc-TALC, LncSBF2-AS1, MALAT1, TP73-AS1, and H19 as well as expression of tumor suppressor lncRNAs AC003092.1, TUSC7, and RP11-838N2.4 have been shown to alter this phenotype in glioblastoma cells. Therefore, a panel of these lncRNAs might be applied to predict response of pateints to this chemotherapeutic agent and establish a personalized strategy for these patients.

Finally, several oncogenic and tumor suppressor lncRNAs have been identified as modulators of glioblastoma patients' survival indicating the appropriateness of these transcripts as prognostic biomarkers. The diagnostic power of lncRNAs SAMMSON, HOTAIR, MALAT1, H19, and LINR-ROR has been assessed in serum or tissue samples of pateints with glioblastoma revealing the best results for the first two mentioned lncRNAs based on the high values of the area under the reciver operating characteristic curves. Considering the unavialbility of tissue samples for the purpose of early diagnosis and ambiguity of imaging techniques in early stages of the disease, assessment of expression of lncRNAs in serum samples provides a non-invasive method for early detection of this kind of malignant tumor.

In brief, dysregulation of several lncRNAs has been deteceted in glioblastoma cells leading to abnormal regualtion of cancer-associated pathways and cellular processes namely apoptosis, proliferation and survival. These transcripts provide promising tools for early detection of glioblastoma and prediction of patients' prognosis and response to therapeutic choices particularly TMZ. However, a limitation of *in vitro* studies in this regard is that most of them has been executed using traditional serum-grown cell lines such as U87 or U251. Furhther functional *in vitro* and *in vivo* investigations are required to verify the obtained data.

AUTHOR CONTRIBUTIONS

MT and SG-F wrote the draft and revised it. KHT, GS, and OR performed the data collection and designed the tables. All authors contributed to the article and approved the submitted version.

REFERENCES

1. Louis DN, Perry A, Reifenberger G, von Deimling A, Figarella-Branger D, Cavenee WK, et al. The 2016 World Health Organization Classification of Tumors of the Central Nervous System: a summary. *Acta Neuropathol* (2016) 131(6):803–20. doi: 10.1007/s00401-016-1545-1
2. Ostrom QT, Gittleman H, Farah P, Ondracek A, Chen Y, Wolinsky Y, et al. CBTRUS statistical report: Primary brain and central nervous system tumors diagnosed in the United States in 2006-2010. *Neuro-oncology* (2013) 15 Suppl 2(Suppl 2):ii1–56. doi: 10.1093/neuonc/not151
3. Hanif F, Muzaffar K, Perveen K, Malhi SM, Simjee SU. Glioblastoma Multiforme: A Review of its Epidemiology and Pathogenesis through Clinical Presentation and Treatment. *Asian Pac J Cancer Prev* (2017) 18 (1):3–9. doi: 10.22034/APJCP.2017.18.1.3
4. Braganza MZ, Kitahara CM, Berrington de González A, Inskip PD, Johnson KJ, Rajaraman P. Ionizing radiation and the risk of brain and central nervous system tumors: a systematic review. *Neuro-oncology* (2012) 14(11):1316–24. doi: 10.1093/neuonc/nos208
5. Network CGAR. Comprehensive genomic characterization defines human glioblastoma genes and core pathways. *Nature* (2008) 455(7216):1061. doi: 10.1038/nature07385
6. Parsons DW, Jones S, Zhang X, Lin JC-H, Leary RJ, Angenendt P, et al. An integrated genomic analysis of human glioblastoma multiforme. *Science* (2008) 321(5897):1807–12. doi: 10.1126/science.1164382

7. Nonoguchi N, Ohta T, Oh J-E, Kim Y-H, Kleihues P, Ohgaki H. TERT promoter mutations in primary and secondary glioblastomas. *Acta Neuropathol* (2013) 126(6):931–7. doi: 10.1007/s00401-013-1163-0
8. Li J, Zhu Y, Wang H, Ji X. Targeting Long Noncoding RNA in Glioma: A Pathway Perspective. *Mol Ther Nucleic Acids* (2018) 13:431–41. doi: 10.1016/j.omtn.2018.09.023
9. Mercer TR, Dinger ME, Mattick JS. Long non-coding RNAs: insights into functions. *Nat Rev Genet* (2009) 10(3):155–9. doi: 10.1038/nrg2521
10. Han M, Wang S, Fritah S, Wang X, Zhou W, Yang N, et al. Interfering with long non-coding RNA MIR22HG processing inhibits glioblastoma progression through suppression of Wnt/β-catenin signalling. *Brain* (2020) 143(2):512–30. doi: 10.1093/brain/awz406
11. Chen L, Gong X, Huang M. YY1-activated long noncoding RNA SNHG5 promotes Glioblastoma cell proliferation through p38/MAPK signaling pathway. *Cancer Biother Radiopharm* (2019) 34(9):589–96. doi: 10.1089/cbr.2019.2779
12. Zhang H, Qin D, Jiang Z, Zhang J. SNHG9/miR-199a-5p/Wnt2 axis regulates cell growth and aerobic glycolysis in glioblastoma. *J Neuropathol Exp Neurol* (2019) 78(10):939–48. doi: 10.1093/jnen/nlz078
13. Xie J, Wang X, Liu S, Chen C, Jiang F, Mao K, et al. LncRNA SAMMSON overexpression distinguished glioblastoma patients from patients with diffuse neurosarcoidosis. *NeuroReport* (2019) 30(12):817–21. doi: 10.1097/WNR.0000000000001278
14. Bountali A, Tonge DP, Mourtada-Maarabouni M. RNA sequencing reveals a key role for the long non-coding RNA MIAT in regulating neuroblastoma and glioblastoma cell fate. *Int J Biol Macromol* (2019) 130:878–91. doi: 10.1016/j.ijbiomac.2019.03.005
15. Voce DJ, Bernal GM, Wu L, Crawley CD, Zhang W, Mansour NM, et al. Temozolomide treatment induces lncRNA MALAT1 in an NF-κB and p53 codependent manner in glioblastoma. *Cancer Res* (2019) 79(10):2536–48. doi: 10.1158/0008-5472.CAN-18-2170
16. He Z, You C, Zhao D. Long non-coding RNA UCA1/miR-182/PFKFB2 axis modulates glioblastoma-associated stromal cells-mediated glycolysis and invasion of glioma cells. *Biochem Biophys Res Commun* (2018) 500(3):569–76. doi: 10.1016/j.bbrc.2018.04.091
17. Fan Z, Zheng J, Xue Y, Liu X, Wang D, Yang C, et al. NR2C2-uORF targeting UCA1-miR-627-5p-NR2C2 feedback loop to regulate the malignant behaviors of glioma cells. *Cell Death Dis* (2018) 9(12):1–18. doi: 10.1038/s41419-018-1149-x
18. Wang J, Quan X, Peng D, Hu G. Long non−coding RNA DLEU1 promotes cell proliferation of glioblastoma multiforme. *Mol Med Rep* (2019) 20(2):1873–82. doi: 10.3892/mmr.2019.10428
19. Xie H, Shi S, Chen Q, Chen Z. LncRNA TRG-AS1 promotes glioblastoma cell proliferation by competitively binding with miR-877-5p to regulate SUZ12 expression. *Pathol-Res Pract* (2019) 215(8):152476. doi: 10.1016/j.prp.2019.152476
20. Chai Y, Xie M. LINC01579 promotes cell proliferation by acting as a ceRNA of miR-139-5p to upregulate EIF4G2 expression in glioblastoma. *J Cell Physiol* (2019) 234(12):23658–66. doi: 10.1002/jcp.28933
21. Luo W, Li X, Song Z, Zhu X, Zhao S. Long non-coding RNA AGAP2-AS1 exerts oncogenic properties in glioblastoma by epigenetically silencing TFPI2 through EZH2 and LSD1. *Aging (Albany NY)* (2019) 11(11):3811. doi: 10.18632/aging.102018
22. Wu P, Cai J, Chen Q, Han B, Meng X, Li Y, et al. Lnc-TALC promotes O 6-methylguanine-DNA methyltransferase expression via regulating the c-Met pathway by competitively binding with miR-20b-3p. *Nat Commun* (2019) 10(1):1–15. doi: 10.1038/s41467-019-10025-2
23. Zhang SY, Huang SH, Gao SX, Wang YB, Jin P, Lu FJ. Upregulation of lncRNA RMRP promotes the activation of cardiac fibroblasts by regulating miR−613. *Mol Med Rep* (2019) 20(4):3849–57. doi: 10.3892/mmr.2019.10634
24. Gao X, He H, Zhu X, Xie S, Cao Y. LncRNA SNHG20 promotes tumorigenesis and cancer stemness in glioblastoma via activating PI3K/Akt/mTOR signaling pathway. *Neoplasma* (2019) 2019:532–42. doi: 10.4149/neo_2018_180829N656
25. Li H, Yuan X, Yan D, Li D, Guan F, Dong Y, et al. Long non-coding RNA MALAT1 decreases the sensitivity of resistant glioblastoma cell lines to temozolomide. *Cell Physiol Biochem* (2017) 42(3):1192–201. doi: 10.1159/000478917
26. Cai T, Liu Y, Xiao J. Long noncoding RNA MALAT 1 knockdown reverses chemoresistance to temozolomide via promoting micro RNA-101 in glioblastoma. *Cancer Med* (2018) 7(4):1404–15. doi: 10.1002/cam4.1384
27. Chen W, Xu X-K, Li J-L, Kong K-K, Li H, Chen C, et al. MALAT1 is a prognostic factor in glioblastoma multiforme and induces chemoresistance to temozolomide through suppressing miR-203 and promoting thymidylate synthase expression. *Oncotarget* (2017) 8(14):22783. doi: 10.18632/oncotarget.15199
28. Wu W, Yu T, Wu Y, Tian W, Zhang J, Wang Y. The miR155HG/miR-185/ANXA2 loop contributes to glioblastoma growth and progression. *J Exp Clin Cancer Res* (2019) 38(1):1–14. doi: 10.1186/s13046-019-1132-0
29. Mazor G, Levin L, Picard D, Ahmadov U, Carén H, Borkhardt A, et al. The lncRNA TP73-AS1 is linked to aggressiveness in glioblastoma and promotes temozolomide resistance in glioblastoma cancer stem cells. *Cell Death Dis* (2019) 10(3):1–14. doi: 10.1038/s41419-019-1477-5
30. Toraih EA, El-Wazir A, Hussein MH, Khashana MS, Matter A, Fawzy MS, et al. Expression of long intergenic non-coding RNA, regulator of reprogramming, and its prognostic value in patients with glioblastoma. *Int J Biol Markers* (2019) 34(1):69–79. doi: 10.1177/1724600818814459
31. Chen X, Li L, Qiu X, Wu H. Long non-coding RNA HOXB-AS1 promotes proliferation, migration and invasion of glioblastoma cells via HOXB-AS1/miR-885-3p/HOXB2 axis. *Neoplasma* (2019) 2019. doi: 10.4149/neo_2018_180606N377
32. Chen H, Zong J, Wang S. LncRNA GAPLINC promotes the growth and metastasis of glioblastoma by sponging miR-331-3p. *Eur Rev Med Pharmacol Sci* (2019) 23(1):262–70. doi: 10.26355/eurrev_201901_16772
33. Liao K, Ma X, Chen B, Lu X, Hu Y, Lin Y, et al. Upregulated AHIF-mediated radioresistance in glioblastoma. *Biochem Biophys Res Commun* (2019) 509(2):617–23. doi: 10.1016/j.bbrc.2018.12.136
34. Dai X, Liao K, Zhuang Z, Chen B, Zhou Z, Zhou S, et al. AHIF promotes glioblastoma progression and radioresistance via exosomes. *Int J Oncol* (2019) 54(1):261–70. doi: 10.3892/ijo.2018.4621
35. Tian Y, Zheng Y, Dong X. AGAP2-AS1 serves as an oncogenic lncRNA and prognostic biomarker in glioblastoma multiforme. *J Cell Biochem* (2019) 120(6):9056–62. doi: 10.1002/jcb.28180
36. Fawzy MS, Ellawindy A, Hussein MH, Khashana MS, Darwish MK, Abdel-Daim MM, et al. Long noncoding RNA H19, and not microRNA miR-326, is over-expressed and predicts survival in glioblastoma. *Biochem Cell Biol* (2018) 96(6):832–9. doi: 10.1139/bcb-2018-0122
37. Wu W, Hu Q, Nie E, Yu T, Wu Y, Zhi T, et al. Hypoxia induces H19 expression through direct and indirect Hif-1α activity, promoting oncogenic effects in glioblastoma. *Sci Rep* (2017) 7:45029. doi: 10.1038/srep45029
38. Jiang X, Yan Y, Hu M, Chen X, Wang Y, Dai Y, et al. Increased level of H19 long noncoding RNA promotes invasion, angiogenesis, and stemness of glioblastoma cells. *J Neurosurg* (2016) 124(1):129–36. doi: 10.3171/2014.12.JNS1426
39. Li W, Jiang P, Sun X, Xu S, Ma X, Zhan R. Suppressing H19 modulates tumorigenicity and stemness in U251 and U87MG glioma cells. *Cell Mol Neurobiol* (2016) 36(8):1219–27. doi: 10.1007/s10571-015-0320-5
40. Cai J, Zhang J, Wu P, Yang W, Ye Q, Chen Q, et al. Blocking LINC00152 suppresses glioblastoma malignancy by impairing mesenchymal phenotype through the miR-612/AKT2/NF-κB pathway. *J Neuro-Oncol* (2018) 140(2):225–36. doi: 10.1007/s11060-018-2951-0
41. Reon BJ, Karia BTR, Kiran M, Dutta A. LINC00152 promotes invasion through a 3′-hairpin structure and associates with prognosis in glioblastoma. *Mol Cancer Res* (2018) 16(10):1470–82. doi: 10.1158/1541-7786.MCR-18-0322
42. Liu X, Zhao H, Luo Y, Ma X, Xu M. LncRNA LINC00152 promoted glioblastoma progression through targeting the miR-107 expression. *Environ Sci Pollut Res* (2018) 25(18):17674–81. doi: 10.1007/s11356-018-1784-x
43. Liu C, Fu H, Liu X, Lei Q, Zhang Y, She X, et al. LINC00470 Coordinates the Epigenetic Regulation of ELFN2 to Distract GBM Cell Autophagy. *Mol Ther* (2018) 26(9):2267–81. doi: 10.1016/j.ymthe.2018.06.019
44. Liu C, Zhang Y, She X, Fan L, Li P, Feng J, et al. A cytoplasmic long noncoding RNA LINC00470 as a new AKT activator to mediate glioblastoma cell autophagy. *J Hematol Oncol* (2018) 11(1):77. doi: 10.1186/s13045-018-0619-z
45. Zhang L, Wang Q, Wang F, Zhang X, Tang Y, Wang S. LncRNA LINC01446 promotes glioblastoma progression by modulating miR-489-3p/TPT1 axis. *Biochem Biophys Res Commun* (2018) 503(3):1484–90. doi: 10.1016/j.bbrc.2018.07.067

46. Zhou Y, Dai W, Wang H, Pan H, Wang Q. Long non-coding RNA CASP5 promotes the malignant phenotypes of human glioblastoma multiforme. *Biochem Biophys Res Commun* (2018) 500(4):966–72. doi: 10.1016/j.bbrc.2018.04.217
47. Wang H, Li L, Yin L. Silencing LncRNA LOXL1-AS1 attenuates mesenchymal characteristics of glioblastoma via NF-κB pathway. *Biochem Biophys Res Commun* (2018) 500(2):518–24. doi: 10.1016/j.bbrc.2018.04.133
48. Gao Y, Xu Y, Wang J, Yang X, Wen L, Feng J. LncRNA MNX1-AS1 promotes glioblastoma progression through inhibition of miR-4443. *Oncol Res Featuring Preclinical Clin Cancer Ther* (2019) 27(3):341–7. doi: 10.3727/096504018X15228909735079
49. Tan SK, Pastori C, Penas C, Komotar RJ, Ivan ME, Wahlestedt C, et al. Serum long noncoding RNA HOTAIR as a novel diagnostic and prognostic biomarker in glioblastoma multiforme. *Mol Cancer* (2018) 17(1):74. doi: 10.1186/s12943-018-0822-0
50. Zhou X, Ren Y, Zhang J, Zhang C, Zhang K, Han L, et al. HOTAIR is a therapeutic target in glioblastoma. *Oncotarget* (2015) 6(10):8353. doi: 10.18632/oncotarget.3229
51. Zhang K, Sun X, Zhou X, Han L, Chen L, Shi Z, et al. Long non-coding RNA HOTAIR promotes glioblastoma cell cycle progression in an EZH2 dependent manner. *Oncotarget* (2015) 6(1):537. doi: 10.18632/oncotarget.2681
52. Ren J, Yang Y, Xue J, Xi Z, Hu L, Pan S-J, et al. Long noncoding RNA SNHG7 promotes the progression and growth of glioblastoma via inhibition of miR-5095. *Biochem Biophys Res Commun* (2018) 496(2):712–8. doi: 10.1016/j.bbrc.2018.01.109
53. Chen Q, Cai J, Wang Q, Wang Y, Liu M, Yang J, et al. Long noncoding RNA NEAT1, regulated by the EGFR pathway, contributes to glioblastoma progression through the WNT/β-catenin pathway by scaffolding EZH2. *Clin Cancer Res* (2018) 24(3):684–95. doi: 10.1158/1078-0432.CCR-17-0605
54. Gong W, Zheng J, Liu X, Ma J, Liu Y, Xue Y. Knockdown of NEAT1 restrained the malignant progression of glioma stem cells by activating microRNA let-7e. *Oncotarget* (2016) 7(38):62208. doi: 10.18632/oncotarget.11403
55. Su R, Cao S, Ma J, Liu Y, Liu X, Zheng J, et al. Knockdown of SOX2OT inhibits the malignant biological behaviors of glioblastoma stem cells via up-regulating the expression of miR-194-5p and miR-122. *Mol Cancer* (2017) 16(1):1–22. doi: 10.1186/s12943-017-0737-1
56. Cai H, Liu X, Zheng J, Xue Y, Ma J, Li Z, et al. Long non-coding RNA taurine upregulated 1 enhances tumor-induced angiogenesis through inhibiting microRNA-299 in human glioblastoma. *Oncogene* (2017) 36(3):318–31. doi: 10.1038/onc.2016.212
57. Mineo M, Ricklefs F, Rooj AK, Lyons SM, Ivanov P, Ansari KI, et al. The long non-coding RNA HIF1A-AS2 facilitates the maintenance of mesenchymal glioblastoma stem-like cells in hypoxic niches. *Cell Rep* (2016) 15(11):2500–9. doi: 10.1016/j.celrep.2016.05.018
58. Yao Y, Ma J, Xue Y, Wang P, Li Z, Liu J, et al. Knockdown of long non-coding RNA XIST exerts tumor-suppressive functions in human glioblastoma stem cells by up-regulating miR-152. *Cancer Lett* (2015) 359(1):75–86. doi: 10.1016/j.canlet.2014.12.051
59. Cao Y, Wang P, Ning S, Xiao W, Xiao B, Li X. Identification of prognostic biomarkers in glioblastoma using a long non-coding RNA-mediated, competitive endogenous RNA network. *Oncotarget* (2016) 7(27):41737. doi: 10.18632/oncotarget.9569
60. Tang G, Luo L, Zhang J, Zhai D, Huang D, Yin J, et al. lncRNA LINC01057 promotes mesenchymal differentiation by activating NF-κB signaling in glioblastoma. *Cancer Lett* (2020) 498:152–64. doi: 10.1016/j.canlet.2020.10.047
61. Toraih EA, Alghamdi SA, El-Wazir A, Hosny MM, Hussein MH, Khashana MS, et al. Dual biomarkers long non-coding RNA GAS5 and microRNA-34a co-expression signature in common solid tumors. *PLoS One* (2018) 13(10):e0198231. doi: 10.1371/journal.pone.0198231
62. Ren S, Xu Y. AC016405. 3, a novel long noncoding RNA, acts as a tumor suppressor through modulation of TET2 by microRNA-19a-5p sponging in glioblastoma. *Cancer Sci* (2019) 110(5):1621. doi: 10.1111/cas.14002
63. Chu L, Yu L, Liu J, Song S, Yang H, Han F, et al. Long intergenic non-coding LINC00657 regulates tumorigenesis of glioblastoma by acting as a molecular sponge of miR-190a-3p. *Aging (Albany NY)* (2019) 11(5):1456. doi: 10.18632/aging.101845
64. Xu N, Liu B, Lian C, Doycheva DM, Fu Z, Liu Y, et al. Long noncoding RNA AC003092. 1 promotes temozolomide chemosensitivity through miR-195/TFPI-2 signaling modulation in glioblastoma. *Cell Death Dis* (2018) 9(12):1–16. doi: 10.1038/s41419-018-1183-8
65. Zhang L, Cao Y, Wei M, Jiang X, Jia D. Long noncoding RNA-RNCR3 overexpression deleteriously affects the growth of glioblastoma cells through miR-185-5p/Krüppel-like factor 16 axis. *J Cell Biochem* (2018) 119(11):9081–9.
66. Liu J, Wang W, Zhang X, Du Q, Li H, Zhang Y. Effect of downregulated lncRNA NBAT1 on the biological behavior of glioblastoma cells. *Eur Rev Med Pharmacol Sci* (2018) 22(9):2715–22. doi: 10.26355/eurrev_201805_14968
67. Shang C, Tang W, Pan C, Hu X, Hong Y. Long non-coding RNA TUSC7 inhibits temozolomide resistance by targeting miR-10a in glioblastoma. *Cancer Chemother Pharmacol* (2018) 81(4):671–8. doi: 10.1007/s00280-018-3522-y
68. Liu S, Mitra R, Zhao M-M, Fan W, Eischen CM, Yin F, et al. The potential roles of long noncoding RNAs (lncRNA) in glioblastoma development. *Mol Cancer Ther* (2016) 15(12):2977–86. doi: 10.1158/1535-7163.MCT-16-0320
69. Liu Y, Xu N, Liu B, Huang Y, Zeng H, Yang Z, et al. Long noncoding RNA RP11-838N2. 4 enhances the cytotoxic effects of temozolomide by inhibiting the functions of miR-10a in glioblastoma cell lines. *Oncotarget* (2016) 7(28):43835. doi: 10.18632/oncotarget.9699
70. Shen J, Hodges TR, Song R, Gong Y, Calin GA, Heimberger AB, et al. Serum HOTAIR and GAS5 levels as predictors of survival in patients with glioblastoma. *Mol Carcinog* (2018) 57(1):137–41. doi: 10.1002/mc.22739
71. Wang R, Zhang S, Chen X, Li N, Li J, Jia R, et al. CircNT5E acts as a sponge of miR-422a to promote glioblastoma tumorigenesis. *Cancer Res* (2018) 78(17):4812–25. doi: 10.1158/0008-5472.CAN-18-0532
72. Li X, Diao H. Circular RNA circ_0001946 acts as a competing endogenous RNA to inhibit glioblastoma progression by modulating miR-671-5p and CDR1. *J Cell Physiol* (2019) 234(8):13807–19. doi: 10.1002/jcp.28061
73. Qi X, Yu XJ, Wang XM, Song TN, Zhang J, Guo XZ, et al. Knockdown of KCNQ1OT1 Suppresses Cell Invasion and Sensitizes Osteosarcoma Cells to CDDP by Upregulating DNMT1-Mediated Kcnq1 Expression. *Mol Ther Nucleic Acids* (2019) 17:804–18. doi: 10.1016/j.omtn.2019.06.010
74. Zhang X, Zhong B, Zhang W, Wu J, Wang Y. Circular RNA CircMTO1 inhibits proliferation of Glioblastoma cells via miR-92/WWOX signaling pathway. *Med Sci Monit: Int Med J Exp Clin Res* (2019) 25:6454. doi: 10.12659/MSM.918676
75. Lv X, Wang M, Qiang J, Guo S. Circular RNA circ-PITX1 promotes the progression of glioblastoma by acting as a competing endogenous RNA to regulate miR-379–5p/MAP3K2 axis. *Eur J Pharmacol* (2019) 863:172643. doi: 10.1016/j.ejphar.2019.172643
76. Lei B, Huang Y, Zhou Z, Zhao Y, Thapa AJ, Li W, et al. Circular RNA hsa_circ_0076248 promotes oncogenesis of glioma by sponging miR-181a to modulate SIRT1 expression. *J Cell Biochem* (2019) 120(4):6698–708. doi: 10.1002/jcb.27966
77. Wang R, Zhang S, Chen X, Li N, Li J, Jia R, et al. EIF4A3-induced circular RNA MMP9 (circMMP9) acts as a sponge of miR-124 and promotes glioblastoma multiforme cell tumorigenesis. *Mol Cancer* (2018) 17(1):1–12. doi: 10.1186/s12943-018-0911-0
78. Qian L, Guan J, Wu Y, Wang Q. Upregulated circular RNA circ_0074027 promotes glioblastoma cell growth and invasion by regulating miR-518a-5p/IL17RD signaling pathway. *Biochem Biophys Res Commun* (2019) 510(4):515–9. doi: 10.1016/j.bbrc.2019.01.140

Conflict of Interest: The authors declare that the research was conducted in the absence of any commercial or financial relationships that could be construed as a potential conflict of interest.

frontiers in Oncology

ORIGINAL RESEARCH
published: 18 March 2021
doi: 10.3389/fonc.2021.622430

Novel Molecular Hallmarks of Group 3 Medulloblastoma by Single-Cell Transcriptomics

Chaoying Qin†, *Yimin Pan*†, *Yuzhe Li*, *Yue Li*, *Wenyong Long** *and Qing Liu**

Department of Neurosurgery in Xiangya Hospital, Central South University, Changsha, China

Medulloblastoma (MB) is a highly heterogeneous and one of the most malignant pediatric brain tumors, comprising four subgroups: Sonic Hedgehog, Wingless, Group 3, and Group 4. Group 3 MB has the worst prognosis of all MBs. However, the molecular and cellular mechanisms driving the maintenance of malignancy are poorly understood. Here, we employed high-throughput single-cell and bulk RNA sequencing to identify novel molecular features of Group 3 MB, and found that a specific cell cluster displayed a highly malignant phenotype. Then, we identified the glutamate receptor metabotropic 8 (GRM8), and AP-1 complex subunit sigma-2 (AP1S2) genes as two critical markers of Group 3 MB, corresponding to its poor prognosis. Information on 33 clinical cases was further utilized for validation. Meanwhile, a global map of the molecular cascade downstream of the MYC oncogene in Group 3 MB was also delineated using single-cell RNA sequencing. Our data yields new insights into Group 3 MB molecular characteristics and provides novel therapeutic targets for this relentless disease.

Keywords: group 3 medulloblastoma, single-cell sequencing, hallmark, prognosis, molecular cascades

OPEN ACCESS

Edited by:
Shouwei Li,
Capital Medical University, China

Reviewed by:
Manjari Pandey,
West Cancer Center,
United States
Yang Yi,
Northwestern University,
United States

****Correspondence:***
Qing Liu
liuqingdr@csu.edu.cn
Wenyong Long
wylongdr@csu.edu.cn

†*These authors have contributed equally to this work*

Specialty section:
This article was submitted to Neuro-Oncology and Neurosurgical Oncology, a section of the journal Frontiers in Oncology

Received: *02 November 2020*
Accepted: *01 March 2021*
Published: *18 March 2021*

Citation:
Qin C, Pan Y, Li Y, Li Y, Long W and Liu Q (2021) Novel Molecular Hallmarks of Group 3 Medulloblastoma by Single-Cell Transcriptomics. Front. Oncol. 11:622430. doi: 10.3389/fonc.2021.622430

INTRODUCTION

Medulloblastoma (MB) is one of the most prevalent malignant (WHO IV) brain tumors in children, accounting for 15–20% of pediatric central nervous system tumors (1). Unfortunately, over 40% of patients with MB are diagnosed with metastases, with a grim median survival (2–4). Multimodal therapy, including combination of surgical resection, radiation, and adjuvant chemotherapy, has become a standard for MB, even though approximately one-third of patients with MB die from the disease (5). Thus, the identification of critical regulators that control MB malignance could facilitate the development of more effective therapeutics.

Current consensus identifies the existence of four major MB subgroups (Sonic Hedgehog [SHH], Wingless [WNT], Group 3, and Group 4) with different molecular characteristics. Group 3 MB is refractory to intensive multimodal therapy and displays the worst prognosis. However, the molecular

Abbreviations: MB, Medulloblastoma; WHO, World Health Organization; GRM8, Glutamate Receptor Metabotropic 8; MGLUR8, Metabotropic Glutamate Receptor 8; CNS, Central Nervous System; scRNA-seq, Single cell RNA sequencing; PDX, Patient-derived Xenograft; GSVA, Gene Set Variation Analysis; GO/KEGG, Gene ontology/Kyoto Encyclopedia of Genes and Genomes; PCR, Polymerase Chain Reaction; RT-Qpcr, Real Time Quantitative Polymerase Chain Reaction; IOD, Integrated option density; GSEA, Gene Set Enrichment Analysis; t-SNE, t-distributed Stochastic Neighbor Embedding.

characterization of Group 3 MB remains largely unknown, even less than the cells of origin. In contrast to WNT and SHH MBs, Group 3 tumors contain fewer nucleotide variants and germline mutations (6–9). Previous studies demonstrated that a subset of Group 3 tumors exhibits overexpression of transcription factors of the growth factor independent 1 family as a result of DNA structural changes that transform the genes encoding these factors almost into super enhancers (10). Pathway analysis indicated that transforming growth factor beta signaling pathways are also activated in Group 3 MB. However, the significance of MB tumorigenesis remains to be determined (7, 10, 11). Currently, the most validated prognostic marker is *MYC* oncogene amplification, found in approximately 20% of patients with Group 3 MB. However, how *MYC* drives tumorigenesis in a subset of Group 3 tumor cells remains to be defined.

Systematic search and analysis using multi-omics sequencing showed that MB is highly heterogeneous with intratumoral and intertumoral heterogeneity. Recently, single-cell transcriptomic methods have been utilized (12–16) to resolve tumor heterogeneity (17, 18), reconstruct tumor lineages (19–21), explore rare subpopulations (22, 23), and provide insights into the phenotypes of stromal and tumor cells in different cancers (24–26). It has been documented that single-cell sequencing could remove the barriers that previously challenged bulk genomic studies of patients with Group 3 MB, and hopefully, unearth Group 3 MB applicable molecular hallmarks and pathways for clinical utilization, similarly to the isocitrate dehydrogenase (IDH) and BRAF V600E mutations for glioblastoma.

In this study, we took advantage of one cohort (GSE119926) of scRNA-seq data composed of 25 tumor samples and 11 patient-derived xenograft (PDX) models (27). A total of 2762 cells were gathered from surgically removed Group 3 MB scRNA-seq data of eight patients according to their matching subtype information. Through detailed analysis of cellular heterogeneity, we identified a specific cell cluster with the tumorigenesis signature of Group 3 MB and interrelated molecular cascades initiated by MYC. The marker genes of this specific cluster were selected, followed by validation and selection, performed with tumor samples from 33 patients with Group 3 MB. Consequently, we unearthed the GRM8 gene, encoding metabotropic glutamate receptor 8 (MGLUR8), a G-protein coupled glutamate receptor reported to significantly influence the risk of central nervous system (CNS) disease (28–30), and the AP1S2 gene, encoding AP-1 complex subunit sigma-2, a component of adaptor protein complex 1 and correlating with CNS disorder (31), as novel hallmarks linked to poor prognosis of Group 3 MB. Thus, our findings identified GRM8 and AP1S2 as potential targets for treatment of patients with MYC+ Group 3 MB in the future.

MATERIALS AND METHODS

Patient Selection and Data Preprocessing

For MB single-cell transcriptome expression data, we searched in the Gene Expression Omnibus (GEO) and finally included one cohort (GSE119926) with scRNA-seq data of 25 tumor samples and 11 patient-derived xenograft (PDX) models for downstream analysis (27). According to its matching subtype information, normalized scRNA-seq data of eight patients with Group 3 MB (MUV11, SJ17, SJ917, SJ617, MUV29, BCH1205, MUV34, and BCH825) were extracted from the original downloaded scRNA-seq expression matrix. In total, after removing data with <2500 gene expression, we obtained an scRNA-seq expression matrix of 2762 cells from the surgically removed Group 3 MB sample in our study. For bulk transcriptome expression data, we applied Gliovis (gliovis.bioinfo.cnio.es), a web tool collecting brain tumor sequencing data from GEO, and the Cancer Genome Atlas database (32) to search for bulk data with MB clinical information and follow-up data. We included two MB cohorts (Cavalli et al., n = 763 and Griesinger et al., n = 130) in our study (33, 34). These two MB cohorts were sequenced by Affymetrix arrays (HG-U133_Plus_2, HG-U133A, HG_U95Av2, and HuGene-1_0-st), normalized by a multi-array average method using R package "affy." For genes with several probe sets, we chose the median value as the ultimate expression level. Using function "Combat" in R package sva, the batch effect produced by technical biases during the sequencing process was removed to reduce its side effects on downstream analysis.

Single-Cell Sequencing Data Analysis

For the obtained scRNA-seq data of Group 3 MB, R package "seurat" was applied for initial normalization and an unsupervised clustering process was subsequently performed (35). Then, the function "Find Variable Features" in Seurat was performed to find genes with high variability for downstream analysis, choosing the top 2000 genes with high standardized variance. Through integration of principle components analysis and t-distributed stochastic neighbor embedding (t-SNE), we reduced the dimension of expression data and divided 2762 cells of Group 3 MB into clusters with distinct expression patterns. Simultaneously, marker genes for each cluster were found according to its adjusted p-value and average log-transformed fold change value.

Microarray Data Analysis

Based on R package "limma," a differentially expression analysis was performed on the normalized microarray data by applying a Bayesian algorithm to find differentially expressed genes between tumor and normal sample, only data with adjusted p-value < 0.05 were included in our study for further analysis. According to the corresponding follow-up information, we conducted a Kaplan-Meier survival analysis on the genes of interest.

Cell Trajectory Analysis

In addition, the R package Monocle was adopted to conduct a time-series analysis of single-cell expression data, which orders every cell in pseudo-time and arranges them along a trajectory corresponding to a biological process such as cell differentiation, without knowing in advance which gene determines that progress (36). The Monocle reduces marker gene expression data of individual clusters from a high dimension form into a low-dimension form through a machine learning algorithm called reversed graph embedding. In that low-dimensional form, each cell is arranged into a branching line according to the sequence of the biological process.

Gene Set Variation Analysis (GSVA) and GO/KEGG Enrichment Analysis

To compare the enrichment degree of pathways and functions between each cluster, we used a GSVA algorithm, a gene set enrichment (GSE) method that estimates the variation of pathway activity for microarray and transcriptome data, to calculate the GSVA score of each cluster on different gene sets (37). For the calculation of tumor characteristics and pathway enrichment degree, input gene sets were obtained from the molecular signature database (MsigDB) (https://www.gsea-msigdb.org/gsea/msigdb). The gene sets of the KEGG pathway come from the C2 collection (curated gene sets) in MsigDB, and the tumor characteristic gene set comes from the H collection (hallmark gene sets) in MsigDB. By comparing the GSVA scores of each cluster, we could compare the relative enrichment levels of tumor-related pathways or features. In addition, the R package "ClusterProfiler" was used to conduct a hypergeometric distribution test on each cluster's marker genes to perform GO and KEGG annotation (38).

Protein-Protein Interaction (PPI) Network Development

Using the STRING database, a PPI network was developed according to the marker genes of each cell cluster. We then utilized Cytoscape to rearrange the PPI network downloaded for the STRING database according to its interaction characteristic (39). In Cytoscape, the CytoHubba plug-in was used to calculate and rank the interaction degree between downstream proteins of marker genes. Additionally, according to the interaction degree, we adjusted the color and position of the protein node, turning the highest degree node darker and placing it in the center.

Immunohistochemistry

Tumor tissues from 33 patients with Group 3 MB were perfused with 4% paraformaldehyde and fixed in 10% neutral buffered formalin mixed with 70% ethanol. Immunohistochemistry staining was performed according to protocols from Cell Signaling Technology. The antibodies used for immunostaining were Anti-MAGP1 (encoded by MFAP2, ab231344, Abcam) and Anti-MGLUR8 (encoded by GRM8, ab176301, Abcam). Quantification of mean fluorescence intensity was achieved using Image-Pro-Plus software.

Real-Time Quantitative PCR

RT-qPCR was performed using total RNA from the central tissues of eight (Numbered 1–8) patients with normal brain tissues (1–2), WNT/SHH (3–5), and Group 3 (6–8) MB. Total RNA was extracted using TRI Reagent (Molecular Research Center, Inc.) according to the manufacturer's protocol, and cDNA was synthesized using random hexamer and oligo (dT) primers using Thermo ScriptTM RT-PCR (Invitrogen). The gene-specific primers employed were purchased from the NDT Corporation. PCR was performed for 40 cycles of 95 °C for 15 s and 60 °C for 30 s. H-actin was amplified as a control (Forward: ACCCTGAAGTACCCCATCGAG; reverse: AGCACAGCC TGGATAGCAAC). Specific expression of MFAP2 and GRM8 in cell lines was established using total RNA obtained from tumor tissues and amplified with primers for each one (MAGP: Forward, CAGTCCCAGCAGCAAGTCCA and Reverse, AAGCAGACCTCGTTGAGACAC; GRM8: Forward, ACCTGCATCATTTGGTTAGCTT, and Reverse, AAACCTTGGGCATATAGAGCA) using SYBR Green PCR Master Mix (ThermoFisher Scientific).

Statistical Analysis

The correlation coefficient between the IOD area and numerical variables including age (year), tumor size (mm^3), and Ki67 (%) was separately calculated using the Spearman and Pearson correlation analysis. Random Grouping t-test was used to assess the relevance between the IOD area and binary clinical information including sex, cystic change, hydrocephalus, while one-way ANOVA was used to compare the differences among multi-grouped variables including tumor location. In addition, we applied Kaplan-Meier survival analysis and log-ranked test to conduct a survival comparison, where the median value was implemented to cut the relative genes expression level into high and low Groups. All the above-mentioned statistical analyses were conducted using R software (version 3.6.0). All p-values < 0.05 were considered statistically significant.

RESULTS

Landscape of Cellular Heterogeneity at Single-Cell Level Within Group 3 MB

Identification of critical cell clusters regulating cancer initiation and progression may help develop novel and effective strategies to overcome the treatment resistance associated with Group 3 MB. Thus, we initially selected the MB single-cell RNA sequencing (seq) datasets published in the GEO and finally included one cohort (GSE119926) of 25 tumor samples and 11 patient-derived xenograft (PDF) models for downstream analysis. According to its matching subtype information, normalized scRNA-seq data of eight patients with Group 3 MB (MUV11, SJ17, SJ917, SJ617, MUV29, BCH1205, MUV34, and BCH825) were extracted from the original scRNA-seq expression matrix, including a total of six male patients (three adults and three children) and two female patients (one adult and one child) (**Figure 1A**). A total of 2762 single-cell datasets of the above eight patients were organized into an expression matrix. Data preprocessing was initiated by normalizing the RNA expression of each cell and then removing mitochondrial RNAs. All single cells were divided into individual clusters according to their distance distribution after dimensionality reduction through t-SNE, gene set enrichment analysis, and functional annotations such as GSEA and GSVA scores on specific cell clusters was performed (**Figure 1A**). The normalization for the expression matrix was initiated by calculating the standard deviation of the gene expression in 2762 cells. We selected 2000 sufficient genes with a high standard deviation (**Figure 1B**). The normalized gene type (n-Feature-RNA), gene counts (n-Count-RNA), and mitochondrial gene numbers (MT-RNA) of each patient's tumor cells (mitochondrial genes were previously removed) were plotted, revealing that RNA levels in each of the patient's tumor cells were

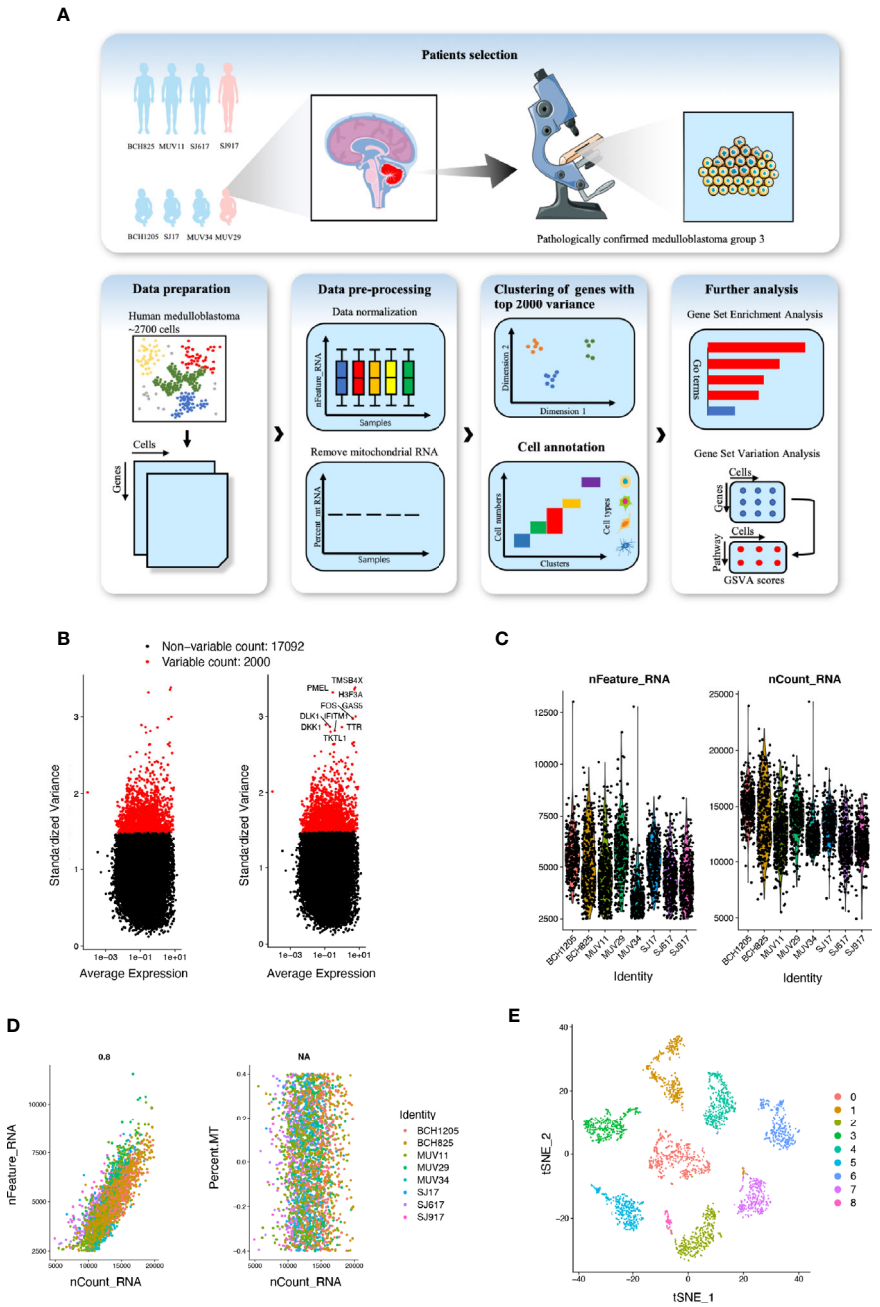

FIGURE 1 | **(A)** Overall data analysis process of single-cell transcriptome expression landscape of Group 3 medulloblastoma (MB) (n=8). **(B)** Genes with top 2000 standard variance selected for subsequent analysis. **(C)** Violin plot of RNA features, and RNA counts in patients with MB. **(D)** Scatter plot of expression level of mitochondrial RNA, RNA features and RNA counts. **(E)** T-distributed stochastic neighbor embedding (t-SNE) plot of Group 3 MB cells revealing 0–8 cell clusters.

expressed in a similar scope without apparent dispersion (**Figure 1C**). Notably, the gene sequencing depth was found to be consistent with the scatter diagram since the relationship between the number of gene types and the number of counts was positively correlated (**Figure 1D**). To further explore the expression feature of the scRNA data, we initially normalized the gene expression matrix and selected characteristic genes with a high standardized deviation for downstream analysis. After principle components analysis (PCA) and identification of distinct principle components, the representative principle components were chosen subsequently for unsupervised clustering process. Finally, we conducted a clustering using t-distributed stochastic neighbor embedding (t-SNE) and divided the cells into nine individual cell clusters (Numbered 0–8) with various differentiation features. Finally, we divided the cells into nine individual cell clusters (Numbered 0–8) with various

differentiation features (**Figure 1E**). These data suggest that Group 3 MB is highly heterogeneous with different cell subgroups and genetic characteristics.

Cell Clusters Reflect Transcriptional Heterogeneity and Trajectory

We next sought to investigate the transcriptional heterogeneity of cells in each cluster by depicting the gene expression profile using a heatmap that showed distinguishable differences in gene expression preferences in each cluster. Except for cluster 0, we identified significantly upregulated genes in clusters different from each other, indicating the transcriptional heterogeneity of the nine clusters (**Figure 2A**). Then, we performed scatter plots by t-SNE colored by the expression of a single gene in all nine cell clusters. The genes showing the highest expression level in each individual cluster were selected for mapping. Consistently, these genes were

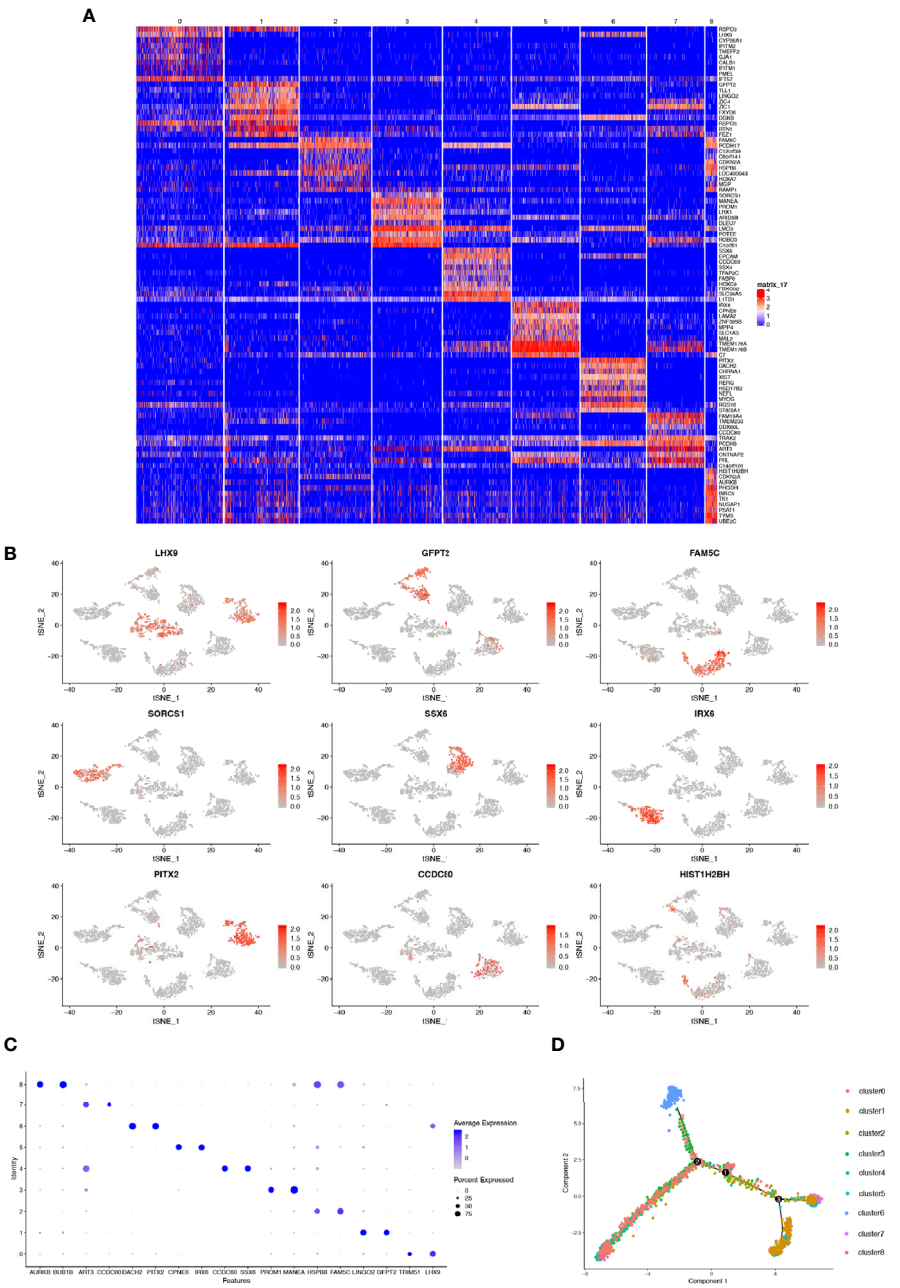

FIGURE 2 | **(A)** Heatmap showing the genes differentially expressed in each cluster. **(B)** t-SNE plots of marker gene expression levels in each cluster. **(C)** Bubble plot depicting the expression level of selected genes in each cluster. Color depth represents average expression level and bubble size the percentage of expression. **(D)** Cell trajectory analysis showing five main cell branches.

only specifically expressed in their own cluster (**Figure 2B**). Moreover, the bubble graph was also plotted to further identify the genes that were most upregulated. Notably, the bubble color refers to the average gene expression in all cells of each cluster, whereas bubble size represented the gene expression percentage in the cluster. The top genes containing the highest level of the above two criteria in each cluster were emphasized with a large size and darker color (**Figure 2C**). Due to transcriptional heterogeneity among the nine cell clusters, we speculated that single-cell RNA-seq may uncover the heterogeneity of biological features correlated with MB formation. To test our hypothesis, the R package Monocle was adopted to conduct a time-series analysis of the single-cell expression data to address this point. We ordered every cell in pseudo-time and arranged them along a trajectory corresponding to a biological process such as cell differentiation, without knowing in advance which gene determines that progress (36). Each cell of the nine clusters was arranged into a branching line according to the sequence of the biological process (**Figure 2D**). We observed that cluster 6 (colored blue) was relatively isolated at the beginning of a differentiation tree at point "A," indicating that cell cluster 6 may play a key role in cancer initiation and progression.

Annotation of the Tumorigenesis Featured Cluster and Its Downstream Cascades

With regards to the aforementioned feature of cluster 6, we next sought to verify its exclusive tumorigenesis feature among the nine cell clusters. To compare the enrichment degree of pathways and functions among each cluster, we used the GSVA and GSE methods to estimate the variation in pathway activity from microarray and transcriptome data, to calculate the GSVA score of each cluster on different gene sets (37). For the calculation of tumor characteristics and pathway enrichment degree, the input gene sets were obtained from the molecular signature database (MsigDB). Among them, the KEGG pathway gene sets derived from the C2 collection (curated gene sets) (**Figure 3A**). Further, we performed a violin plot by selecting the pathways demonstrating specific up- or down-regulation in cluster 6 compared to the others, quantified by the GSVA score. The degree of enrichment of cluster 6 in some tumor-related pathways was significantly higher than that of the other clusters, such as cell adhesion molecules cams, and arginine and proline metabolism for metastasis of tumors (40). Nevertheless, in immune-related pathways such as antigen procession and presentation, and natural killer cell mediated cytotoxicity which have been correlated to antitumor cytotoxicity, the enrichment was significantly lower (**Figure 3B**). Consistently, tumor characteristic genes set from H collection (hallmark gene sets) in MsigDB (**Figure 3C**) revealed that the degree of enrichment of cluster 6 in MYC targets V1/V2 was remarkably higher than that of other clusters identified as critical for Group 3 MB. The enrichment of antitumor cytotoxicity in cluster 6, such as interferon alpha response and interferon gamma response, were much lower than those of other clusters (**Figure 3D**). Collectively, these results demonstrated the pivotal role of cluster 6 in the malignant behavior of Group 3 MB and were marked for further validation.

To depict the detailed annotation of the signaling pathways involved in cluster 6, we then performed GO enrichment analysis for the marker genes of the six clusters, and suggested that the most active pathways were neuron- and axon-related, such as axon development, axonogenesis, cell morphogenesis involved in neuron differentiation, axon guidance, neuron projection guidance, and regulation of neuron projection development. Meanwhile, genes associated directly or indirectly to these signaling pathways were shown (**Figures 4A, B**). The main pathways for KEGG enrichment in cluster 6 were also analyzed. Interestingly, the top pathways obtaining the highest scores were tumor- or cancer-related, corresponding to previous observations. For example, transcriptional misregulation in cancer, hepatocellular carcinoma, gastric cancer, and the WNT signaling pathway. We also plotted a heatmap of the genes related to these pathways (**Figures 4C, D**). These findings supported our hypothesis that cluster 6 cells were responsible for the tumorigenic character of Group 3 MB. To gain insight into downstream protein interaction and cascades, we constructed a PPI network according to cluster 6 marker genes by using the STRING database. We then utilized Cytoscape to rearrange the PPI network downloaded for the STRING database according to its interaction characteristic (39). In addition, according to the interaction degree, we adjusted the color and position of the protein by turning the highest degree node darker and placing it in the center of the map. Importantly, our data showed that MYC had the highest degree of interaction among all marker genes in cluster 6, consistent with the previous findings that amplification of the *MYC* oncogene is the most common genetic alteration in patients with Group 3 MB (**Figure 4E**). Together, our findings indicated that cluster 6 drives malignancy in Group 3 MB with MYC positivity.

Identification of Novel Hallmarks in Group 3 MB

Given the stepwise dissection of cluster 6 in Group 3 MB, the malignance signature of this cluster became relatively clear. We selected a set of microarray data from a cohort consisting of common pediatric malignant brain tumors containing 15 pilocytic astrocytomas, 46 ependymomas, 20 glioblastomas, 22 MBs, and 13 non-tumor brain control samples obtained from epilepsy surgery to generate the bulk transcriptional dataset for differential expression analysis (34) (**Figure 5A**). We performed a variation analysis with normalized microarray data of this mixed pediatric tumor cohort to compare the expression level of cluster 6 marker genes in variant tumor types and normal brain, and found that 54 genes in total showed specific upregulation either in one tumor type or in the normal brain (**Figure 5A**, **Supplementary Materials**). Notably, some genes were specifically upregulated in MB, consistent with their high expression in Group 3 MB in our previous analysis. Meanwhile, another cohort of 763 patients with MB was included to conduct a Kaplan-Meier survival analysis on the marker genes of cluster 6. In total, 20 genes correlated with the survival of patients with MB. By combining these results, 10 genes showed significant differences of either expression levels or survival analysis, including TUBB4A, TSHZ1, SLITRK1, POU4F1, MPHOSPH6, MFAP2,

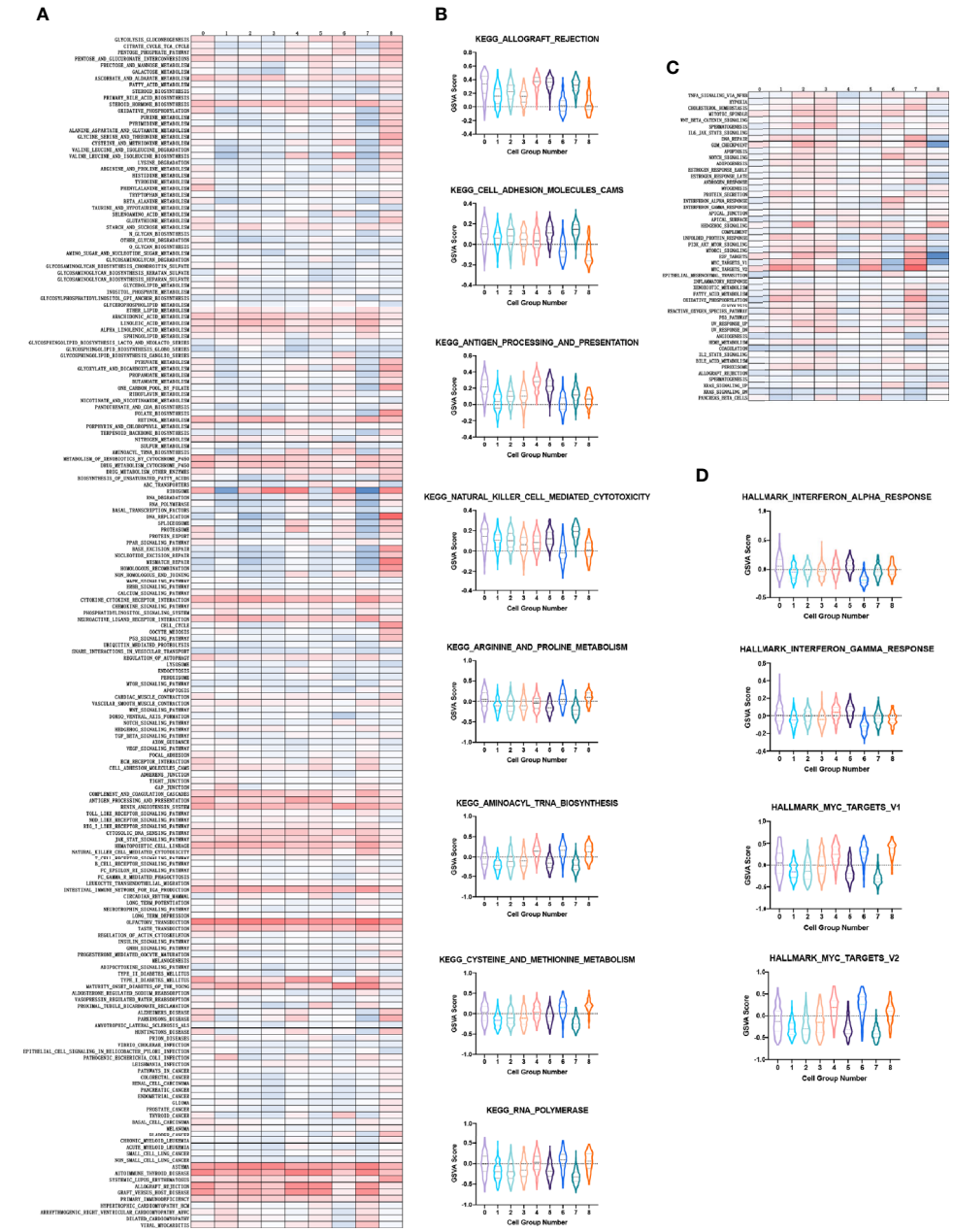

FIGURE 3 | **(A)** Heatmap showing the gene set variation analysis (GSVA) scores of each cell cluster in the KEGG pathway. **(B)** Violin plot depicting the GSVA score of specific KEGG pathways in each cell cluster. **(C)** Same as A in H collection in molecular signature database (MsigDB). **(D)** Same as B in H collection in MsigDB.

KIF5C, GRM8, CCND2, and AP1S2 (**Figure 5A**). Among them, TSHZ1, MFAP2, GRM8, CCND2, and AP1S2 showed dramatically higher expression levels in MB than other tumors and the normal brain (**Figure 5B**). Of note, the prognosis of the patients highly expressing TSHZ1, GRM8, CCND2, AP1S2 was poorer than low expressing patients, while only MFAP2 showed an adverse correlation between its gene expression and prognosis (**Figure 5C**). Taken together, these data indicate that some marker genes in cluster 6 were truly upregulated in Group 3 MB and affected its prognosis; hence, these five genes were initially identified as potential hallmarks of Group 3 MB.

GRM8 and AP1S2 Are Hallmarks Indicating Poor Prognosis of Patients With Group 3 MB

Based upon the stepwise bioinformatic analysis with single-cell and bulk datasets, we narrowed down the pool of Group 3 MB's potential hallmarks. However, for further validation a biochemical

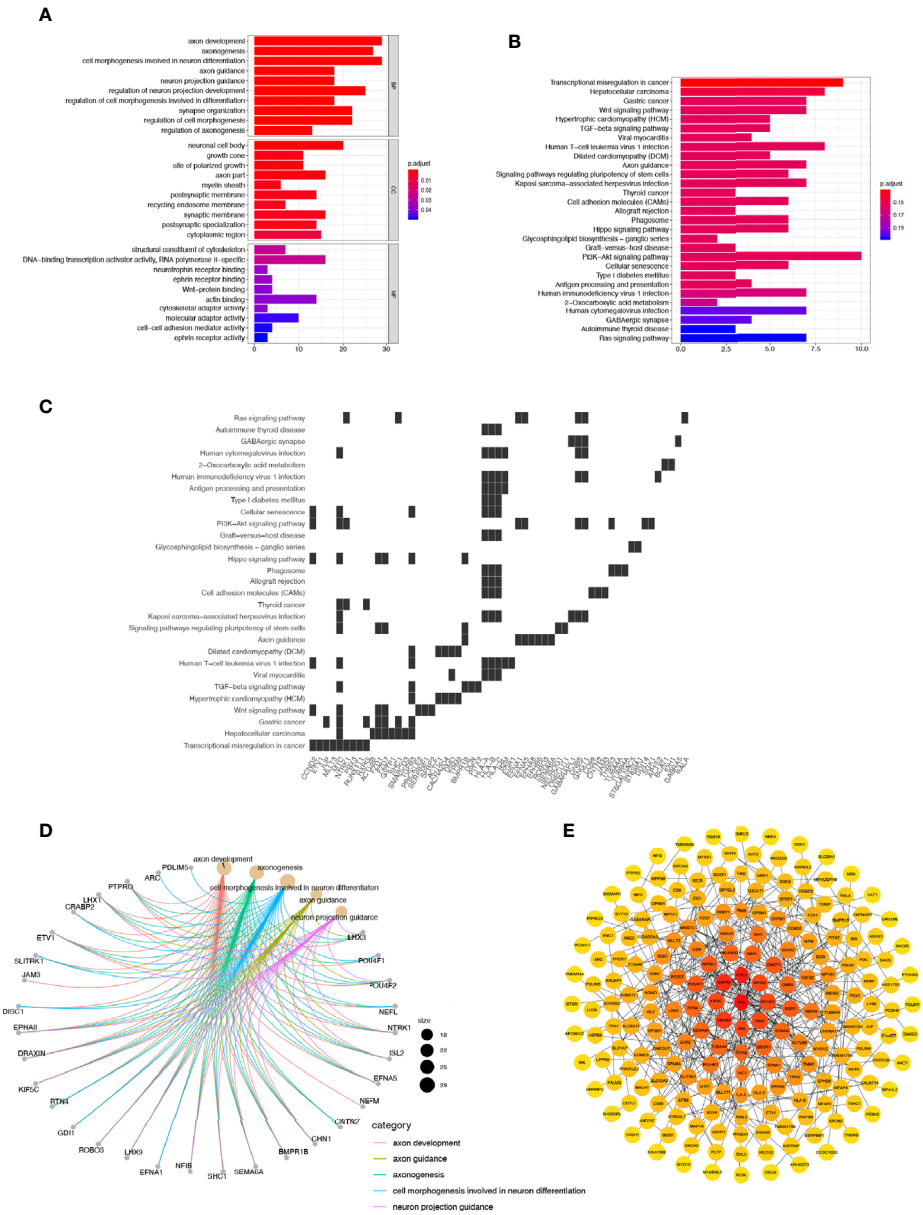

FIGURE 4 | **(A)** GO annotation of cluster 6. **(B)** Gene net plot showing the common genes in multiple GO entries. **(C)** Heatmap showing the genes involved in each pathway. 6. **(D)** KEGG annotation of cluster 6. **(E)** Protein-Protein Interaction network of marker genes in cluster 6, where the node with the highest degree of interaction is darker and located in the center.

verification was needed; therefore, we performed quantitative PCR with samples from two normal brain tissues obtained from epilepsy surgery (Numbered 1 and 2), three WNT/SHH MBv (Numbered 3–5), and three Group 3 MB (Numbered 6–8) to test the gene expression levels of TSHZ1, MFAP2, GRM8, CCND2, and AP1S2. Among them, MFAP2, GRM8, and AP1S2 were highly expressed in patients 6, 7, and 8, diagnosed with Group 3 MB through pathological tests (**Figure 6A**), while TSHZ1 and CCND2 did not exhibit the same expression trends (**Supplementary Materials**). This result supported the provisional exclusion of these two genes and to focus on MFAP2, GRM8, and AP1S2. Then, with samples of 33 patients pathologically diagnosed with Group 3 MB, we performed immunohistochemistry (IHC) staining to test the expression level of MAGP1 encoded by MFAP2, MGLUR8 encoded by GRM8, and AP1S2 encoded by AP1S2 in each patient, aiming to combine clinical data with gene regulation for analysis. The heatmap of the "IOD/Area" of each gene was plotted (**Figure 6B**). By implementing the median value of "IOD/Area," 33 patients were divided into high and low groups, respectively. Consistently, Kaplan-Meier survival analysis indicated that GRM8 and AP1S2 expression was negatively correlated with prognosis (**Figure 6C**),

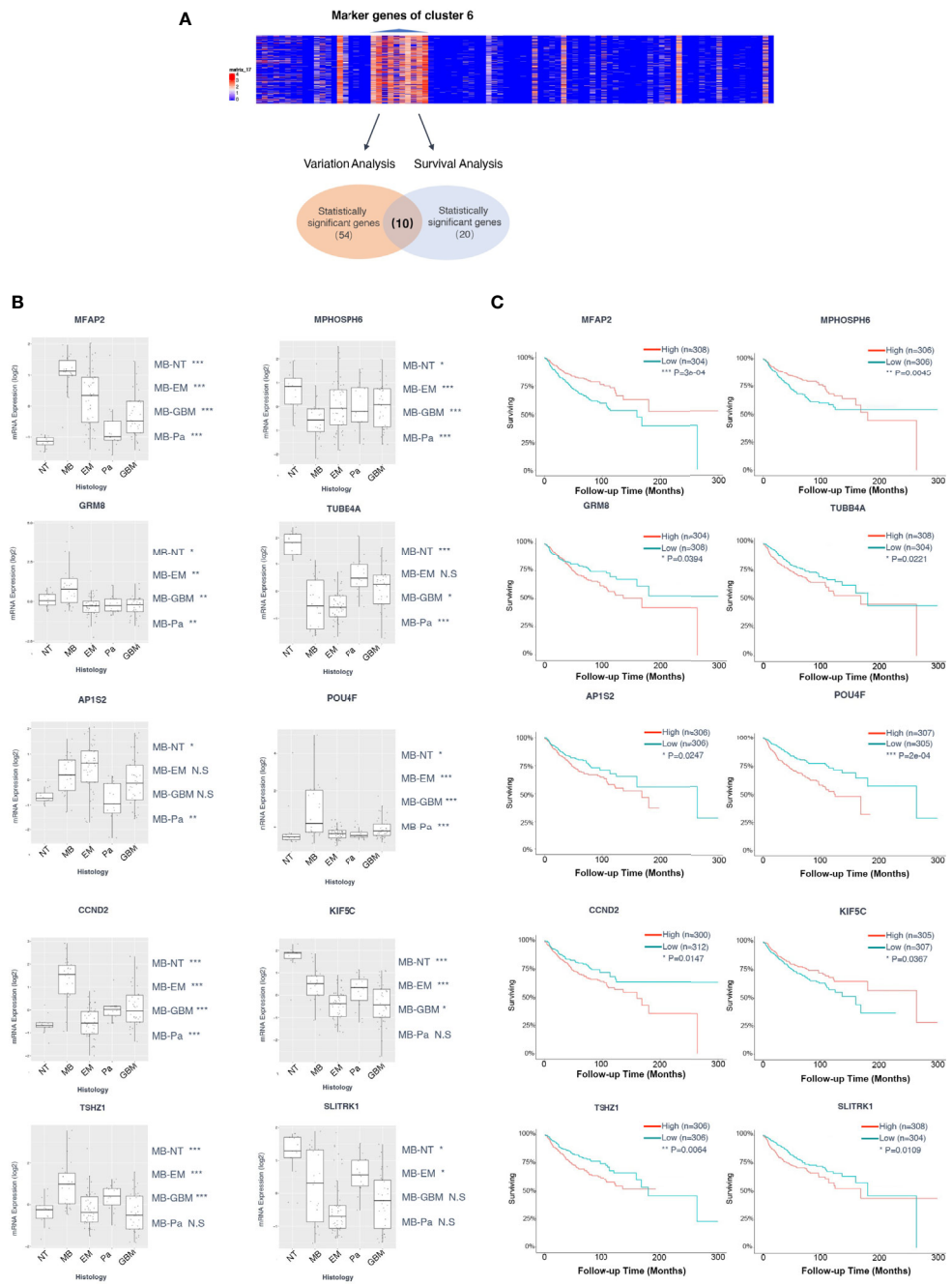

FIGURE 5 | **(A)** Diagram of the screen process of Kaplan-Meier survival and variation analyses for the marker genes of cluster 6 with two cohorts of microarray data. Fifty-four genes showed specific upregulation in one tumor type or normal brain. Twenty genes exhibited correlation with the survival of patients with medulloblastoma (MB). Ten genes contained significant differences of either expression or survival analysis, including TUBB4A, TSHZ1, SLITRK1, POU4F1, MPHOSPH6, MFAP2, KIF5C, GRM8, CCND2, and AP1S2. **(B)** Box plot of variant analysis of microarray data of the MB patient cohort grouped showing expression levels of TUBB4A, TSHZ1, SLITRK1, POU4F1, MPHOSPH6, MFAP2, KIF5C, GRM8, CCND2, and AP1S2 in various brain tumors and normal brain. NT, normal tissue; MB, medulloblastoma; EM, ependymoma; Pa, pilocytic astrocytoma; GBM, glioblastoma. **(C)** Kaplan-Meier survival curve of microarray data of the MB patient cohort grouped by TUBB4A, TSHZ1, SLITRK1, POU4F1, MPHOSPH6, MFAP2, KIF5C, GRM8, CCND2, and AP1S2 expression level. Data are mean ± s.e.m. *P ≤ 0.05; **P ≤ 0.01; ***P ≤ 0.001; ****P < 0.0001; NS, not significant (P > 0.05).

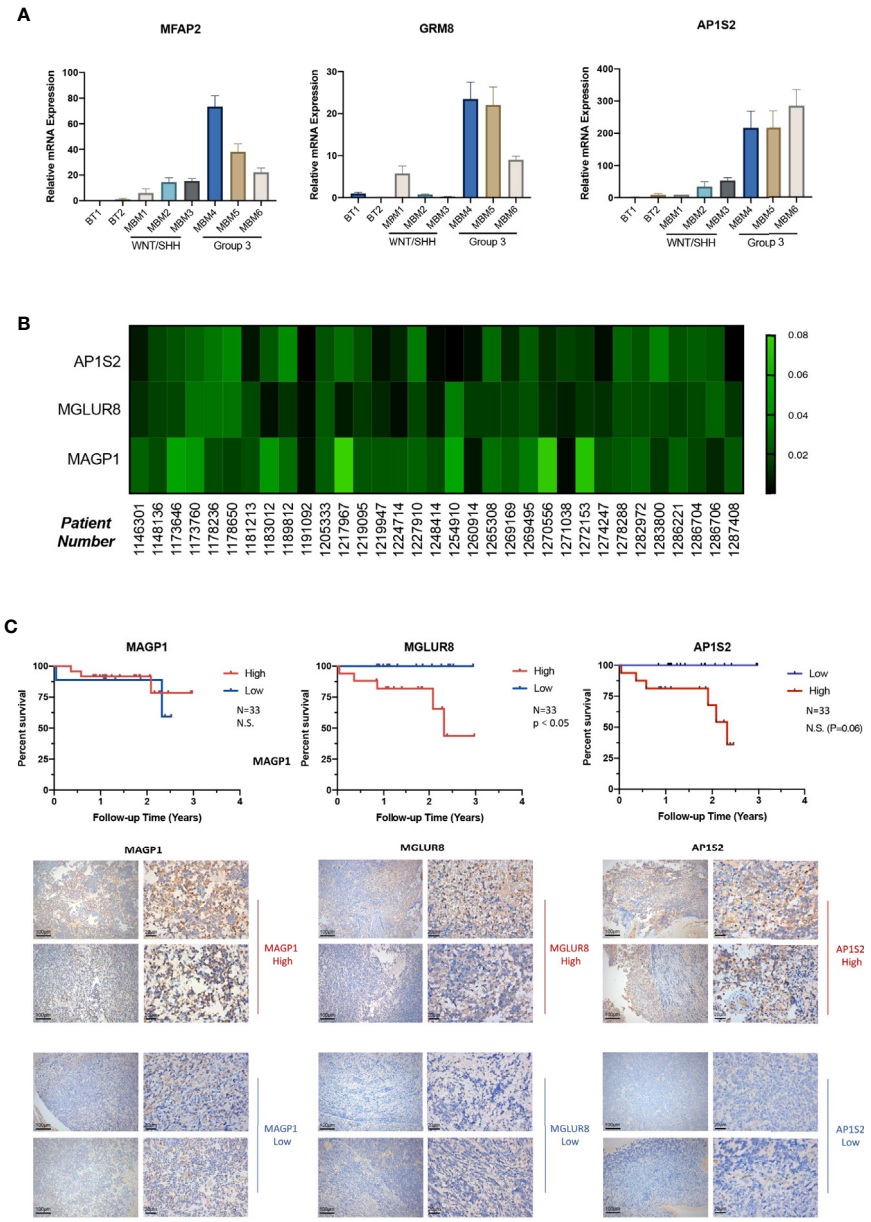

FIGURE 6 | **(A)** GRM8, AP1S2, and MFAP2 mRNA levels of two normal brain tissue obtained from epilepsy surgery (Numbered 1 and 2), three Wingless/Sonic Hedgehog medulloblastoma (MB) (Numbered 3–5), and three Group 3 MB (Numbered 6–8). H-actin was used as the endogenous reference gene. The expression level is presented with graphs. **(B)** Heatmap of Immunohistochemistry staining with (GRM8 encoding), (AP1S2 encoding), and (MFAP2 encoding) antibodies for the 33 Group 3 MB. Protein IOD/Are is represented by the indicated color. **(C)** Images of immunohistochemistry staining showing high and low expression of MGLUR8 (GRM8 encoding), AP1S2 (AP1S2 encoding), and MAGP1 (MFAP2 encoding) in the series of Group 3 MB patients (10X and 40X magnification). Kaplan-Meier survival curve of the 33 patients with Group 3 MB grouped by expression level of GRM8, AP1S2, and MFAP2 encoding. Data are mean ± s.e.m. ****P < 0.0001; NS, not significant (P > 0.05).

which demonstrated that these two genes were specific indicators of poor diagnosis of Group 3 MB. However, with respect to MFAP2, the protein level was not significantly correlated with prognosis in our 33-patient series. Next, we collected detailed clinical data of the 33 patients in addition to postoperative survival time, such as sex, age, tumor cystic change, hydrocephalus, location of tumor body, tumor size, and Ki67 (%), to explore the deeper association of tumor phenotypes with the genetic hallmarks. However, most correlation coefficients were not statistically significant for GRM8, MFAP2, and AP1S2 (**Supplementary Tables 1–3**). Therefore, our study identified GRM8 and AP1S2 as two key regulators of Group 3 MB malignancy, which could serve as important biomarkers for Group 3 MB diagnosis and therapeutics.

DISCUSSION

Despite intensive conventional post-surgery treatments, half of the patients with Group 3 MB die from recurrent disease. *MYC* amplification and overexpression is known to play a vital role in maintaining the malignancy of Group 3 MB; however, an incomplete understanding of how MYC drives tumorigenesis in a subset of Group 3 tumor cells has hampered the development of novel therapeutic approaches for this lethal disease. The elucidation of novel critical factors regulating the malignant phenotype of MB cells is of great significance to increase our knowledge of this type of cancer, and subsequently bring more selective and efficient therapeutic options for patients with Group 3 MB.

Single-cell RNA sequencing allows us to understand how cellular heterogeneity contributes to the origination, progression, and invasion of Group 3 MB. MB single-cell RNA-seq datasets from the Gene Expression Database were analyzed in eight patients with Group 3 MB. Nine individual cell clusters were identified according to their distance distribution after dimensionality reduction through t-SNE. The genetic expression features of the cell clusters showed specific transcription preferences. Based on the cells' pseudo-time, a trajectory analysis was performed showing the potent tumorigenesis characteristic of cluster 6 since cells congregated at the beginning of a differentiation tree. A differentiation trajectory might represent the degree of differentiation from a pluripotent cell to a terminal state (41). Therefore, cluster 6 is a potential tumorigenesis signature of Group 3 MB, and could be a foundation for further studies.

It has been shown that *MYC* amplifications are the most frequently observed driver events in Group 3 (42). In this study, PPI analysis showed that *MYC* is at the center of the network and crosstalks with critical downstream factors/targets pathways. Several immune system-related anti-tumor pathways such as antigen procession and presentation, and natural killer cell mediated cytotoxicity were specifically downregulated in cluster 6. Therefore, one potential therapeutic option for Group 3 would be to develop immunotherapy targeting the immune-related pathways and their correlated genes in cluster 6 cells, besides, to upregulate the immune response to tumor. This observation further clarifies the vital and specific role of cluster 6 cells in Group 3 MB.

Increasing evidence suggests that metabolic dysfunction is a key cause of cancer development, including MB. Interestingly, some amino acid synthesis pathways were enriched in cluster 6. Notably, previous studies have proven the important role of amino acids in cancer metabolism in both a tumorigenic and tumor-suppressive manner (43). These amino acid-related pathways specifically enriched in cluster 6 may be attributed to cancer formation and metastasis. Aminoacyl-tRNAs are substrates for translation, capable also of interacting with various proteins to regulate tumorigenesis (44). Consistently, proline and (or) arginine metabolism supports metastasis formation (40). In addition, cysteine is necessary to promote cancer cell proliferation and survival. The metabolic demands of a cell from the stresses associated with proliferation by oncogenic transformation must be met through extracellular sources of cysteine and *de novo* cysteine generation (45). Moreover, RNA polymerase (pol) III transcription contributes to the regulation of the cell's biosynthetic capacity, and a direct link exists between cancer cell proliferation and deregulation of RNA pol III transcription (46). Further studies on the metabolism in Group 3 MB are warranted.

A pivotal role of cluster 6 has been identified and verified from several perspectives. Naturally, marker genes of this cell cluster are candidates for future therapeutic targets. From over thousands of genes, microarray data screening for survival and expression differences excluded most of them, only those prolonging or shortening survival while specifically expressed in MBs were selected. Therapy de-escalation of these genes requires prospective testing using clinical samples. Only GRM8, MFAP2, and AP1S2 were specifically upregulated in Group 3 MB; however, GRM8 and MFAP2 both interact with MYC as its downstream factors. The 33 cases of Group 3 MB provide us with valuable data showing that higher expression levels of GRM8 and AP1S2 are associated with poorer patient outcomes. All 33 patients pathologically diagnosed with Group 3 MB underwent craniotomy and achieved gross resection; adjuvant radiation therapy and chemotherapy were also performed. Thus, the correlation of the expression with survival is convincing to propose GRM8 and AP1S2 as novel hallmarks of Group 3 MB. Nevertheless, MFAP2 remains a potential tumor suppression feature based on previous results. However, the scale of the 33 clinical samples may be too small to uncover all associations.

GRM8 encodes MGLUR8, a G-protein coupled glutamate receptor reported to significantly influence the risk of diseases affecting the CNS including behavior, mental disorder, cognition as well as tumorigenesis of the CNS and other systems (28–30). Of note, GRM8 expression has been shown to characterize Group 4 MB (47) which overlaps in molecular features with Group 3 tumors. AP1S2 is a component of adaptor protein complex 1, and AP1S2 mutation could cause various brain diseases, including hydrocephalus and Dandy-Walker malformation, among others (31). To the best of our knowledge, this is the first study to reveal the functional significance of AP1S2 in Group 3 MB.

Clinical features such as cystic change, location, and tumor size have not been clearly related to molecular MB markers, or prognosis. Its large volume and cystic tumors can easily occlude the fourth ventricle causing hydrocephalus, while the location of the main tumor body is also important. Substantial Group 3 MBs originate and extend to the fourth ventricle, and obstructive hydrocephalus and cerebral fluid metastasis more often occur. In contrast, most SHH MBs are laterally located in the cerebral hemisphere; and therefore, hydrocephalus is not as common as Group 3 MB (48, 49). The Ki-67 index has been considered a valuable independent prognostic biomarker for adult MB (50), so we also included this index in the study. However, on comparing the above tumor features including age, sex, and hydrocephalus with the expression of GRM8 and AP1S2 within these 33 patients with Group 3 MB, no remarkable correlation between GRM8 and AP1S2 gene levels was found; therefore, a larger scale clinical sample is needed for further investigation.

CONCLUSION

To summarize, using single-cell transcriptomics, this study identified GRM8 and AP1S2 as two novel hallmarks of Group 3 MB indicating poor prognosis, while simultaneously delineating a global picture of the molecular cascade of Group 3 MB downstream of the *MYC* oncogene. With the development of novel single-cell techniques combined with clinical cases, new insights into Group 3 MB molecular characteristics may promote clinical treatment and offer more selective and efficient therapeutic targets for this disease.

DATA AVAILABILITY STATEMENT

The datasets presented in this study can be found in online repositories. The names of the repository/repositories and accession number(s) can be found in the article/**Supplementary Material**.

ETHICS STATEMENT

The studies involving human participants were reviewed and approved by Xiangya Hospital ethics committee. The patients/participants provided their written informed consent to participate in this study.

AUTHOR CONTRIBUTIONS

YP performed the experiments and interpreted the data. CQ wrote the manuscript. YuzL and YueL performed the experiments. WL and QL designed the experiments, interpreted the data, wrote the manuscript, and provided supervision. All authors contributed to the article and approved the submitted version.

FUNDING

This work was supported by the National Natural Science Foundation of China (grant number 81802974).

SUPPLEMENTARY MATERIAL

The Supplementary Material for this article can be found online at: https://www.frontiersin.org/articles/10.3389/fonc.2021.622430/full#supplementary-material

Supplementary Figure 1 | CCND2, MPHOSPH6, TUBB4A, POU4F1, SLITRK1, KIF5C, and TSHZ1 mRNA levels of two normal brain tissues obtained from epilepsy surgery (Numbered 1 and 2), three Wingless/Sonic Hedgehog medulloblastoma (MB) (Numbered 3–5), and three Group 3 MB (Numbered 6–8). H-actin was used as endogenous reference gene. The expression level is presented with graphs.

REFERENCES

1. Kumar V, Kumar V, McGuire T, Coulter DW, Sharp JG, Mahato RI. Challenges and Recent Advances in Medulloblastoma Therapy. *Trends Pharmacol Sci* (2017) 38(12):1061–84. doi: 10.1016/j.tips.2017.09.002
2. Ward E, DeSantis C, Robbins A, Kohler B, Jemal A. Childhood and adolescent cancer statistics, 2014. *CA Cancer J Clin* (2014) 64(2):83–103. doi: 10.3322/caac.21219
3. Ellison DW, Kocak M, Dalton J, Megahed H, Lusher ME, Ryan SL, et al. Definition of disease-risk stratification groups in childhood medulloblastoma using combined clinical, pathologic, and molecular variables. *J Clin Oncol* (2011) 29(11):1400–7. doi: 10.1200/JCO.2010.30.2810
4. Wen PY, Chang SM, Van den Bent MJ, Vogelbaum MA, Macdonald DR, Lee EQ. Response Assessment in Neuro-Oncology Clinical Trials. *J Clin Oncol* (2017) 35(21):2439–49. doi: 10.1200/JCO.2017.72.7511
5. Ramaswamy V, Taylor MD. Medulloblastoma: From Myth to Molecular. *J Clin Oncol* (2017) 35(21):2355–63. doi: 10.1200/JCO.2017.72.7842
6. Waszak SM, Northcott PA, Buchhalter I, Robinson GW, Sutter C, Groebner S, et al. Spectrum and prevalence of genetic predisposition in medulloblastoma: a retrospective genetic study and prospective validation in a clinical trial cohort. *Lancet Oncol* (2018) 19(6):785–98. doi: 10.1016/s1470-2045(18)30242-0.
7. Northcott PA, Korshunov A, Witt H, Hielscher T, Eberhart CG, Mack S, et al. Medulloblastoma comprises four distinct molecular variants. *J Clin Oncol* (2011) 29(11):1408–14. doi: 10.1200/JCO.2009.27.4324
8. Sharma T, Schwalbe EC, Williamson D, Sill M, Hovestadt V, Mynarek M, et al. Second-generation molecular subgrouping of medulloblastoma: an international meta-analysis of Group 3 and Group 4 subtypes. *Acta Neuropathol* (2019) 138(2):309–26. doi: 10.1007/s00401-019-02020-0
9. Robinson G, Parker M, Kranenburg TA, Lu C, Chen X, Ding L, et al. Novel mutations target distinct subgroups of medulloblastoma. *Nature* (2012) 488 (7409):43–8. doi: 10.1038/nature11213.
10. Northcott PA, Lee C, Zichner T, Stutz AM, Erkek S, Kawauchi D, et al. Enhancer hijacking activates GFI1 family oncogenes in medulloblastoma. *Nature* (2014) 511(7510):428–34. doi: 10.1038/nature13379.
11. Kool M, Jones DT, Jager N, Northcott PA, Pugh TJ, Hovestadt V, et al. Genome sequencing of SHH medulloblastoma predicts genotype-related response to smoothened inhibition. *Cancer Cell* (2014) 25(3):393–405. doi: 10.1016/j.ccr.2014.02.004.
12. Laks E, McPherson A, Zahn H, Lai D, Steif A, Brimhall J, et al. Clonal Decomposition and DNA Replication States Defined by Scaled Single-Cell Genome Sequencing. *Cell* (2019) 179(5):1207–21.e22. doi: 10.1016/j.cell.2019.10.026.
13. Casasent AK, Schalck A, Gao R, Sei E, Long A, Pangburn W, et al. Multiclonal Invasion in Breast Tumors Identified by Topographic Single Cell Sequencing. *Cell* (2018) 172(1-2):205–17.e12. doi: 10.1016/j.cell.2017.12.007.
14. Gao R, Kim C, Sei E, Foukakis T, Crosetto N, Chan LK, et al. Nanogrid single-nucleus RNA sequencing reveals phenotypic diversity in breast cancer. *Nat Commun* (2017) 8(1):228. doi: 10.1038/s41467-017-00244-w
15. Islam S, Zeisel A, Joost S, La Manno G, Zajac P, Kasper M, et al, et al. Quantitative single-cell RNA-seq with unique molecular identifiers. *Nat Methods* (2014) 11(2):163–6. doi: 10.1038/nmeth.2772
16. Tirosh I, Izar B, Prakadan SM, Wadsworth MH 2nd, Treacy D, Trombetta JJ, et al. Dissecting the multicellular ecosystem of metastatic melanoma by single-cell RNA-seq. *Science* (2016) 352(6282):189–96. doi: 10.1126/science.aad0501.
17. Grun D, Lyubimova A, Kester L, Wiebrands K, Basak O, Sasaki N, et al. Single-cell messenger RNA sequencing reveals rare intestinal cell types. *Nature* (2015) 525(7568):251–5. doi: 10.1038/nature14966
18. Habib N, Li Y, Heidenreich M, Swiech L, Avraham-Davidi I, Trombetta JJ, et al. Div-Seq: Single-nucleus RNA-Seq reveals dynamics of rare adult newborn neurons. *Science* (2016) 353(6302):925–8. doi: 10.1126/science.aad7038
19. Navin N, Kendall J, Troge J, Andrews P, Rodgers L, McIndoo J, et al. Tumour evolution inferred by single-cell sequencing. *Nature* (2011) 472(7341):90–4. doi: 10.1038/nature09807
20. Wang Y, Waters J, Leung ML, Unruh A, Roh W, Shi X, et al. Clonal evolution in breast cancer revealed by single nucleus genome sequencing. *Nature* (2014) 512(7513):155–60. doi: 10.1038/nature13600

21. Kim C, Gao R, Sei E, Brandt R, Hartman J, Hatschek T, et al. Chemoresistance Evolution in Triple-Negative Breast Cancer Delineated by Single-Cell Sequencing. *Cell* (2018) 173(4):879–93.e13. doi: 10.1016/j.cell.2018.03.041.
22. Lohr JG, Adalsteinsson VA, Cibulskis K, Choudhury AD, Rosenberg M, Cruz-Gordillo P, et al. Whole-exome sequencing of circulating tumor cells provides a window into metastatic prostate cancer. *Nat Biotechnol* (2014) 32(5):479–84. doi: 10.1038/nbt.2892.
23. Martelotto LG, Baslan T, Kendall J, Geyer FC, Burke KA, Spraggon L, et al. Whole-genome single-cell copy number profiling from formalin-fixed paraffin-embedded samples. *Nat Med* (2017) 23(3):376–85. doi: 10.1038/nm.4279
24. Goodwin S, McPherson JD, McCombie WR. Coming of age: ten years of next-generation sequencing technologies. *Nat Rev Genet* (2016) 17(6):333–51. doi: 10.1038/nrg.2016.49
25. Meyer M, Reimand J, Lan X, Head R, Zhu X, Kushida M, et al. Single cell-derived clonal analysis of human glioblastoma links functional and genomic heterogeneity. *Proc Natl Acad Sci U.S.A.* (2015) 112(3):851–6. doi: 10.1073/pnas.1320611111
26. Patel AP, Tirosh I, Trombetta JJ, Shalek AK, Gillespie SM, Wakimoto H, et al. Single-cell RNA-seq highlights intratumoral heterogeneity in primary glioblastoma. *Science* (2014) 344(6190):1396–401. doi: 10.1126/science.1254257
27. Hovestadt V, Smith KS, Bihannic L, Filbin MG, Shaw ML, Baumgartner A, et al. Resolving medulloblastoma cellular architecture by single-cell genomics. *Nature* (2019) 572(7767):74–9. doi: 10.1038/s41586-019-1434-6.
28. Jantas D, Grygier B, Gołda S, Chwastek J, Zatorska J, Tertil M. An endogenous and ectopic expression of metabotropic glutamate receptor 8 (mGluR8) inhibits proliferation and increases chemosensitivity of human neuroblastoma and glioma cells. *Cancer Lett* (2018) 432:1–16. doi: 10.1016/j.canlet.2018.06.004
29. Zhang P, Kang B, Xie G, Li S, Gu Y, Shen Y, et al. Genomic sequencing and editing revealed the GRM8 signaling pathway as potential therapeutic targets of squamous cell lung cancer. *Cancer Lett* (2019) 442:53–67. doi: 10.1016/j.canlet.2018.10.035
30. Boccella S, Marabese I, Guida F, Luongo L, Maione S, Palazzo E. The Modulation of Pain by Metabotropic Glutamate Receptors 7 and 8 in the Dorsal Striatum. *Curr Neuropharmacol* (2020) 18(1):34–50. doi: 10.2174/1570159X17666190618121859
31. Huo L, Teng Z, Wang H, Liu X. A novel splice site mutation in AP1S2 gene for X-linked mental retardation in a Chinese pedigree and literature review. *Brain Behav* (2019) 9(3):e01221. doi: 10.1002/brb3.1221
32. Bowman RL, Wang Q, Carro A, Verhaak RG, Squatrito M. GlioVis data portal for visualization and analysis of brain tumor expression datasets. *Neuro Oncol* (2017) 19(1):139–41. doi: 10.1093/neuonc/now247
33. Cavalli FMG, Remke M, Rampasek L, Peacock J, Shih DJH, Luu B, et al. Intertumoral Heterogeneity within Medulloblastoma Subgroups. *Cancer Cell* (2017) 31(6):737–54.e6. doi: 10.1016/j.ccell.2017.05.005
34. Griesinger AM, Birks DK, Donson AM, Amani V, Hoffman LM, Waziri A, et al. Characterization of distinct immunophenotypes across pediatric brain tumor types. *J Immunol* (2013) 191(9):4880–8. doi: 10.4049/jimmunol.1301966
35. Stuart T, Butler A, Hoffman P, Hafemeister C, Papalexi E, Mauck WM 3rd, et al. Comprehensive Integration of Single-Cell Data. *Cell* (2019) 177(7):1888–902.e21 doi: 10.1016/j.cell.2019.05.031.
36. Qiu X, Hill A, Packer J, Lin D, Ma YA, Trapnell C. Single-cell mRNA quantification and differential analysis with Census. *Nat Methods* (2017) 14 (3):309–15. doi: 10.1038/nmeth.4150
37. Hanzelmann S, Castelo R, Guinney J. GSVA: gene set variation analysis for microarray and RNA-seq data. *BMC Bioinf* (2013) 14:7. doi: 10.1186/1471-2105-14-7
38. Senabouth A, Lukowski SW, Hernandez JA, Andersen SB, Mei X, Nguyen QH, et al. ascend: R package for analysis of single-cell RNA-seq data. *Gigascience* (2019) 8(8):giz087. doi: 10.1093/gigascience/giz087
39. Shannon P, Markiel A, Ozier O, Baliga NS, Wang JT, Ramage D, et al. Cytoscape: a software environment for integrated models of biomolecular interaction networks. *Genome Res* (2003) 13(11):2498–504. doi: 10.1101/gr.1239303
40. Elia I, Broekaert D, Christen S, Boon R, Radaelli E, Orth MF, et al. Proline metabolism supports metastasis formation and could be inhibited to selectively target metastasizing cancer cells. *Nat Commun* (2017) 8:15267. doi: 10.1038/ncomms15267
41. Nestorowa S, Hamey FK, Pijuan Sala B, Diamanti E, Shepherd M, Laurenti E, et al. A single-cell resolution map of mouse hematopoietic stem and progenitor cell differentiation. *Blood* (2016) 128(8):e20–31. doi: 10.1182/blood-2016-05-716480
42. Northcott PA, Shih DJ, Remke M, Cho YJ, Kool M, Hawkins C, et al. Rapid, reliable, and reproducible molecular sub-grouping of clinical medulloblastoma samples. *Acta Neuropathol* (2012) 123(4):615–26. doi: 10.1007/s00401-011-0899-7
43. Lieu EL, Nguyen T, Rhyne S, Kim J. Amino acids in cancer. *Exp Mol Med* (2020) 52(1):15–30. doi: 10.1038/s12276-020-0375-3
44. Ibba M, Soll D. Aminoacyl-tRNA synthesis. *Annu Rev Biochem* (2000) 69:617–50. doi: 10.1146/annurev.biochem.69.1.617
45. Combs JA, DeNicola GM. The Non-Essential Amino Acid Cysteine Becomes Essential for Tumor Proliferation and Survival. *Cancers (Basel)* (2019) 11 (5):678. doi: 10.3390/cancers11050678
46. Cabarcas S, Schramm L. RNA polymerase III transcription in cancer: the BRF2 connection. *Mol Cancer* (2011) 10:47. doi: 10.1186/1476-4598-10-47
47. Northcott PA, Dubuc AM, Pfister S, Taylor MD. Molecular subgroups of medulloblastoma. *Expert Rev Neurother* (2012) 12(7):871–84. doi: 10.1586/ern.12.66
48. Gibson P, Tong Y, Robinson G, Thompson MC, Currle DS, Eden C, et al. Subtypes of medulloblastoma have distinct developmental origins. *Nature* (2010) 468(7327):1095–9 doi: 10.1038/nature09587.
49. Wang J, Garancher A, Ramaswamy V, Wechsler-Reya RJ. Medulloblastoma: From Molecular Subgroups to Molecular Targeted Therapies. *Annu Rev Neurosci* (2018) 41:207–32. doi: 10.1146/annurev-neuro-070815-013838
50. Zhao F, Zhang J, Li P, Zhou Q, Zhang S, Zhao C, et al. Prognostic value of Ki-67 index in adult medulloblastoma after accounting for molecular subgroup: a retrospective clinical and molecular analysis. *J Neurooncol* (2018) 139(2):333–40. doi: 10.1007/s11060-018-2865-x

Conflict of Interest: The authors declare that the research was conducted in the absence of any commercial or financial relationships that could be construed as a potential conflict of interest.

frontiers in Oncology

REVIEW
published: 25 March 2021
doi: 10.3389/fonc.2021.619300

The Role of 2-Oxoglutarate Dependent Dioxygenases in Gliomas and Glioblastomas: A Review of Epigenetic Reprogramming and Hypoxic Response

Rebekah L. I. Crake[1†], *Eleanor R. Burgess*[1†], *Janice A. Royds*[2], *Elisabeth Phillips*[1], *Margreet C. M. Vissers*[3] *and Gabi U. Dachs*[1*]

[1] Mackenzie Cancer Research Group, Department of Pathology and Biomedical Science, University of Otago Christchurch, Christchurch, New Zealand, [2] Department of Pathology, University of Otago, Dunedin, New Zealand, [3] Centre for Free Radical Research, Department of Pathology and Biomedical Science, University of Otago Christchurch, Christchurch, New Zealand

OPEN ACCESS

Edited by:
Yaohua Liu,
Shanghai First People's Hospital, China

Reviewed by:
Chuanlu Jiang,
Second Affiliated Hospital of Harbin Medical University, China
Maite Verreault,
INSERM U1127 Institut du Cerveau et de la Moelle Épinière (ICM), France

***Correspondence:**
Gabi U. Dachs
gabi.dachs@otago.ac.nz

[†]These authors have contributed equally to this work

Specialty section:
This article was submitted to Neuro-Oncology and Neurosurgical Oncology, a section of the journal Frontiers in Oncology

Received: 20 October 2020
Accepted: 25 January 2021
Published: 25 March 2021

Citation:
Crake RLI, Burgess ER, Royds JA, Phillips E, Vissers MCM and Dachs GU (2021) The Role of 2-Oxoglutarate Dependent Dioxygenases in Gliomas and Glioblastomas: A Review of Epigenetic Reprogramming and Hypoxic Response. Front. Oncol. 11:619300. doi: 10.3389/fonc.2021.619300

Gliomas are a heterogeneous group of cancers that predominantly arise from glial cells in the brain, but may also arise from neural stem cells, encompassing low-grade glioma and high-grade glioblastoma. Whereas better diagnosis and new treatments have improved patient survival for many cancers, glioblastomas remain challenging with a highly unfavorable prognosis. This review discusses a super-family of enzymes, the 2-oxoglutarate dependent dioxygenase enzymes (2-OGDD) that control numerous processes including epigenetic modifications and oxygen sensing, and considers their many roles in the pathology of gliomas. We specifically describe in more detail the DNA and histone demethylases, and the hypoxia-inducible factor hydroxylases in the context of glioma, and discuss the substrate and cofactor requirements of the 2-OGDD enzymes. Better understanding of how these enzymes contribute to gliomas could lead to the development of new treatment strategies.

Keywords: hypoxia, brain cancer, PHD, HIF-1, TET, IDH, ascorbate

INTRODUCTION

Gliomas and glioblastomas are brain cancers with significant morbidity and mortality, and limited treatment options. Our review will briefly describe these neoplasms, then concentrate on a super-family of enzymes, the 2-oxoglutarate dependent dioxygenase enzymes (2-OGDD), with dozens of members currently known (**Figure 1**). 2-OGDDs participate in numerous processes including collagen and hormone synthesis, fatty acid metabolism, stress signaling, epigenetic modifications and oxygen sensing (2–7). We will discuss specific members of the 2-OGDD family that have attracted recent interest, including the DNA demethylases [ten-eleven translocases (TET)], the histone demethylases [Jumonji-C domain-containing demethylases (JmjC)], and the hypoxia-inducible factor (HIF) hydroxylases. These enzymes require molecular oxygen and 2-oxoglutarate [2-OG, produced by isocitrate dehydrogenase (IDH)] as substrates, and non-ferrous iron (Fe^{2+}) and

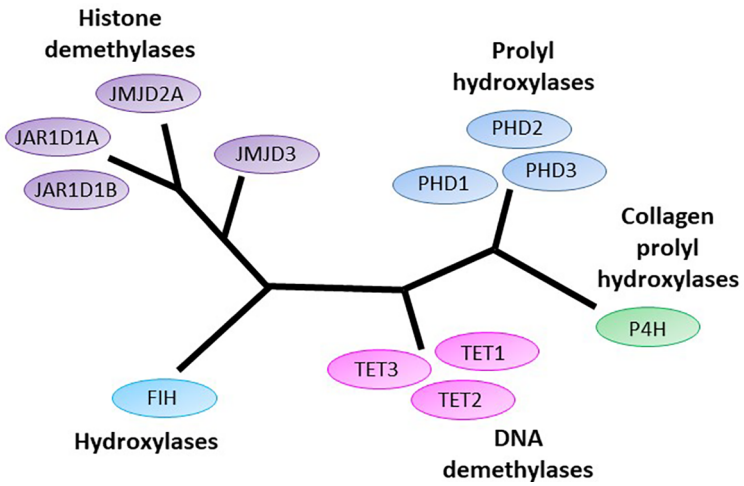

FIGURE 1 | The human 2-oxoglutarate dependent dioxygenases implicated in initiation and progression of gliomas. 2-oxoglutarate dependent dioxygenases (2-OGDDs) include the DNA demethylases Ten-eleven translocases (TETs), the Jumonji-C domain containing histone demethylases (JMJD and JAR1Ds), the prolyl hydroxylases (PHDs) and hydroxylases that control hypoxic response (factor inhibiting HIF, FIH), and the collagen prolyl hydroxylases (P4H). Colors are used to indicate close phylogenetic relationships [adapted from Johansson (1)].

vitamin C (ascorbate) as cofactors. Decreased availability of either substrate or co-factors reduces 2-OGDD enzyme activity, resulting in these enzymes acting as cellular sensors of energy metabolism, oxygen availability, and iron homeostasis (2–4, 8–14). Finally, we consider the potential means of modifying the activity of the 2-OGDDs, specifically by modulating ascorbate availability.

GLIOMA AND GLIOBLASTOMA AND TREATMENT OPTIONS

Gliomas are a heterogeneous group of neoplasms that arise from glial cells in the brain (15, 16), or neural stem cells (17). Low-grade gliomas, grades II and III, include astrocytomas and oligodendrogliomas which predominantly develop from astrocytes or oligodendrocytes, respectively. Glioblastomas (GBM) are grade IV and can develop either as a high-grade lesion (primary GBM), or from astrocytoma progression (secondary GBM) (15, 16).

Gliomas accounted for 1.6% of cancer diagnoses and 2.5% of cancer related deaths worldwide in 2018 (18). Astrocytomas, oligodendrogliomas and secondary GBM tend to develop in younger individuals (median age 35, 45, and 38 years, respectively), compared to primary GBM (median age of 55 years) (17, 19). Gliomas are identified by magnetic resonance imaging (MRI) or computed tomography (CT/CAT). Although treatment options are available as detailed below, high grade gliomas are incurable (20–23). Some low grade gliomas can be cured, although these are rare (17). Following diagnosis, the median survival for patients with oligodendroglioma can be up to 16 years, for astrocytoma 5–8 years, and for GBM only 15–31 months (17, 24).

The current standard treatment for gliomas focuses on extending patient survival and includes maximal safe debulking surgery followed by radiotherapy and concomitant or adjuvant chemotherapy (20), usually with the alkylating agent temozolomide (20, 21, 25, 26). Debulking surgery is performed to reduce intracranial pressure and neurological symptoms, while resected tissue is utilized for tumor classification (17, 22, 23). Post-treatment recurrence is common with approximately 80% of gliomas recurring in close proximity to the primary site (27). Gliomas treated with temozolomide often hypermutate at recurrence leading to treatment resistance, as evidenced by the mere 20% of recurring gliomas showing response to the same agent (17, 28). Dissemination beyond the brain is uncommon, but some high grade gliomas may spread into the meninges or opposing brain hemisphere (17).

Besides traditional oncogenic drivers, gliomas are characterized by deregulated epigenetics and high levels of hypoxia (low oxygen), processes which are largely regulated by 2-OGDDs.

2-OGDD'S AND EPIGENETIC REPROGRAMMING

A significant proportion of 2-OGDDs in mammals are demethylases involved in epigenetic reprogramming (6, 29). Methylation and demethylation of DNA and histones are the fundamental processes guiding epigenetic inheritance and regulating transcriptional activation and repression (30, 31). Consequently, aberrant modifications to these epigenetic processes, causing hyper- and hypo-methylating events, have emerged as hallmarks of cancer progression (32, 33).

Demethylases regulate the epigenome through either the conversion of methylated cytosine (5-mC) to hydroxymethylcytosine (5-hmC) on DNA (**Figure 2**), or the removal of methyl groups from lysine residues on histones (**Figure 3**).

Global Methylcytosine Status in Glioma

Epigenetic modifications are considered key mechanisms regulating occurrence and prognosis of glioma (34), and are used as classifiers of glioma subtypes (15, 16). Early genome-wide 5-mC analyses revealed that many low-grade gliomas and secondary GBMs contained large numbers of hypermethylated loci referred to as the glioma CpG island methylator phenotype (G-CIMP), and this was closely associated with the presence of somatic *IDH1* mutations, and improved prognosis (35–37). *IDH1* mutations are considered to occur early during the genesis of glioma, persisting during progression to secondary GBM, but they rarely appear in primary GBM (24, 38). Although initial reports suggested that G-CIMP remains stable during disease progression (35, 37), more recent analyses have shown their loss upon recurrence of *IDH1*-mutant gliomas (39–42). Loss of G-CIMP at recurrence resembled genome-wide 5-mC patterns seen in *IDH1* wild-type primary GBM, and was associated with poorer outcomes (41). A novel 7-CpG signature has been identified in non-G-CIMP primary GBMs, where high-risk signatures correlated with poorer overall survival in patients treated with temozolomide and radiation (43), suggesting that even in the absence of G-CIMP and *IDH1* mutations, 5-mC marks may be prognostic.

Interestingly however, earlier approaches for quantifying methylation, such as those used in the identification of G-CIMP (35, 36), relied on bisulfite conversion techniques, which cannot differentiate between 5-mC and 5-hmC. It was the introduction of oxidative bisulfide chemistry that made the distinction between 5-mC and 5-hmC possible (44), and consequently, led to the discovery of 5-hmC-specific binding proteins that are not only involved in DNA repair, but also transcriptional regulation (45, 46). These findings suggest that 5-hmC, in addition to being an intermediate in DNA demethylation, may have its own unique epigenetic role.

Many studies report a loss of global 5-hmC content in glioma compared to healthy brain tissues (47–52). Clinically, lower levels of 5-hmC have been associated with high tumor grade and poorer prognosis in glioma (48, 50, 53). More recent investigations moved beyond measuring global 5-hmC levels, to delineate, with base resolution, specific genomic locations to show 5-hmC patterns; all reporting higher than expected levels of 5-hmC at intronic CpG dinucleotides of high-grade gliomas and GBMs (50, 51, 54). Higher intronic 5-hmC levels correlated with elevated expression of the corresponding gene (54), with 5-hmC levels enriched within enhancer elements (50, 54), and 5-hmC levels associated with histone marks for open chromatin (50, 51). Thus, despite global loss of 5-hmC, genomic locations associated with transcriptional regulation and expression were commonly enriched for 5-hmC in glioma.

Ten-Eleven Translocases (TETs)

The TET family consists of three members (TET1/2/3). TET enzymes are involved in both passive and active DNA demethylation (55). During active DNA demethylation, oxidized cytosine intermediates (5-hmC) are excised by thymine DNA glycosylase and repaired with base-excision repair (BER) to generate an unmethylated cytosine (56, 57) (**Figure 2**). Passive DNA demethylation on the other hand occurs

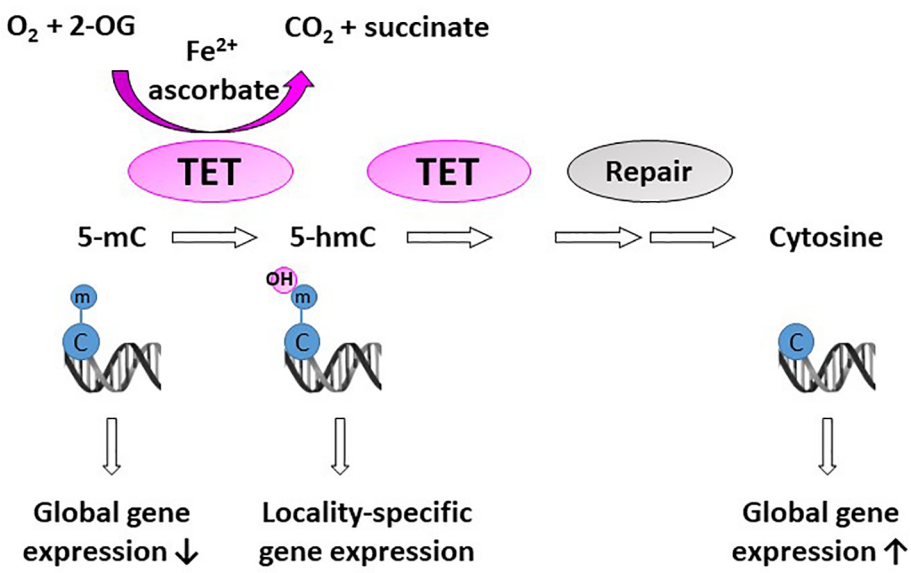

FIGURE 2 | Activity of DNA demethylases. The ten-eleven translocases (TET1-3) hydroxylate methyl cytosine (5-mC). Hydroxy-methyl cytosine (5-hmC) are further converted to several intermediates, which are excised and repaired by thymine DNA glycosylase and base-excision repair (Repair) to generate an unmethylated cytosine. Methylation at CpG islands tends to repress gene expression, but some evidence suggests that gene expression is increased when 5-mC is converted to 5-hmC in gene promoters and enhancers (locality-specific); however, the exact biological role of 5-hmC is not yet known.

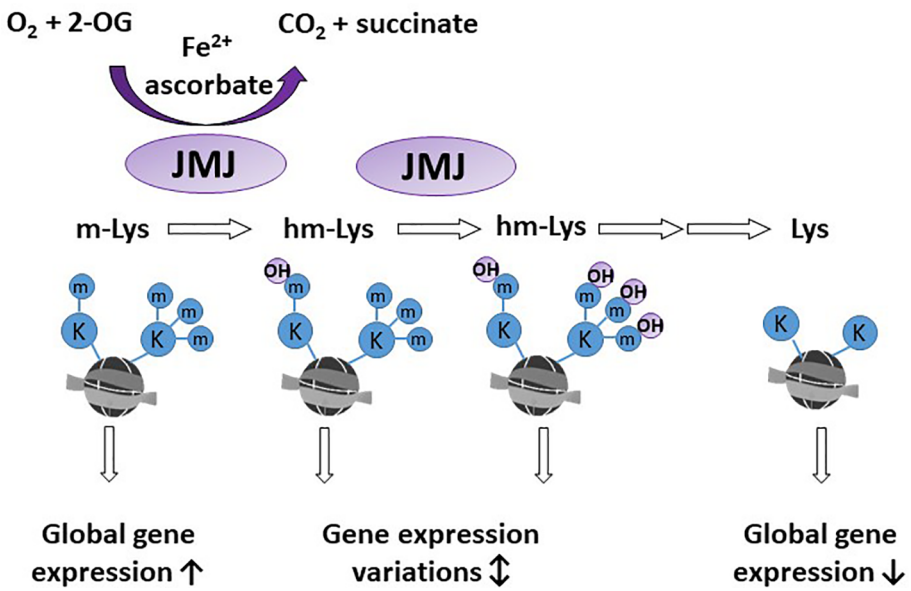

FIGURE 3 | Activity of histone demethylases. Jumonji-C domain-containing demethylases (JMJ) act on lysine residues of the histone tails. Methylated lysine (m-Lys, mK) are hydroxylated (hm-Lys, hmK), which *via* several intermediates, leads to demethylated lysine residues. The effect of m-Lys and hm-Lys on histone structure and subsequent gene expression is very complex. Global gene expression tends to be increased in the more open methylated histone structure, compared to compact, demethylated histones.

during cell replication, when 5-mC at CpG sites are not recognized and replaced with unmethylated cytosine (58). In humans, TET1 is located on chromosome 10q21.3, TET2 on chromosome 4q24, and TET3 on chromosome 2p13.1. It is noteworthy that 10q21.3 is commonly deleted in gliomas (59–61).

TET2 is the most studied isoform in glioma. In comparison to normal human brain tissue, TET2 gene and protein expression is reduced in GBM and other gliomas (62, 63). TET2 expression is significantly decreased with increased grade, and lower TET2 was associated with poorer overall survival (62). Similar observations have been reported for the other two isoforms (53). In glioma, reduction in TET3 expression was associated with a genome-wide reduction in 5-hmC levels compared to normal brain, and decreased TET3 expression correlated with poorer prognosis (64). Together, these findings imply a tumor suppressive role for TET enzymes in glioma.

Numerous studies highlight the potential mechanisms by which TET expression and activity are dysregulated in gliomas. A likely mechanism for reduced TET activity is the indirect inhibition *via* mutated IDH1/2 (65). Mutant IDH1 enzymes often exhibit neomorphic activity, converting isocitrate into 2-hydroxyglutarate (2-HG), instead of 2-OG, which is required for TET activity (66, 67). In *IDH1*-mutant gliomas it has been suggested that 2-HG generation is responsible for the presence of G-CIMP, likely due to reduced TET demethylase activity (35, 36). Independent of IDH status, a complete absence of 5-hmC immunoreactivity was associated with nuclear exclusion of TET1 in 61% of gliomas (52). Transcription of TET2 may be repressed by zinc finger E-box-binding homeobox 1 (ZEB1) in gliomas. ZEB1 levels were inversely correlated with TET2 levels in tumors, and physical binding of ZEB1 to the TET2 promoter in glioma cells was observed *in vitro* (62). However, reductions in TET2 expression and activity are unlikely to be due to TET2 mutations, as direct sequencing of TET2 revealed very few mutations and minimal association of mutations with levels of 5-hmC in gliomas (68, 69). In humans, intragenic CpG sites within *TET2* showed higher levels of 5-mC and lower levels of 5-hmC in GBM compared to normal brain, although within the *TET2* promoter low levels of both 5-mC and 5-hmC were detected at CpG sites of normal brain and GBM (63). Therefore, it is unlikely that lower TET2 expression in glioma is transpiring as a result of promoter methylation-mediated transcriptional suppression, but may be an effect of transcription prevention due to intragenic DNA methylation. Interestingly though, in a cohort of low-grade gliomas that had promoter hypermethylation, all were wild-type *IDH1/2* (68). From this we hypothesize that in the absence of *IDH1/2* mutations, a small portion of IDH wildtype tumors may instead remodel TET2 promoter methylation in an attempt to disrupt TET2 activity. Taken together, these studies demonstrate the tumor suppressive role of TET enzymes in glioma, and highlight the potential mechanisms by which TET expression and activity may be dysregulated. Restoration of TET function to resemble healthy brain tissue may aid in regulating epigenetic processors that can counteract glioma progression and improve treatment outcomes.

Jumonji-C Domain Containing Histone Demethylases

Many 2-OGDDs are from the large family of evolutionary conserved jumonji-C (JmjC) domain-containing proteins that

are responsible for catalysing the removal of methyl groups from lysine residues on histones (29, 70) (**Figure 3**). There are several subfamilies of JmjC domain-containing histone lysine demethylases with substrate specificity to different methylated lysine residues, and this specificity is mediated by the functional domains unique to each subfamily (2, 29). The dynamic interplay between histone methylation and demethylation can result in either gene activation [via histone 3 lysine 4 (H3K4), H3K36 and H3K79] or inactivation (H3K9 and H3K27) (71, 72).

JmjC-domain containing demethylase isoforms are heterogeneously expressed in different brain locations and adult brain cell types (73, 74). Under hypoxic conditions, JMJD3 expression increased in neurons (75), but the modulation of specific histone methylation marks in response to varying oxygen tensions, and ranges of iron and 2-OG levels in brain cells, has yet to be determined.

In gliomas, changes in JmjC-dependent demethylase expression have been associated with differences in genome-wide histone methylation patterns (76, 77), and lower global histone methylation was associated with poorer patient survival (78). Conflicting reports on expression patterns of JmjC-dependent demethylases in glioma and GBM tissues have been published (77, 79–83). Overall, whether JmjC-dependent demethylases promote or suppress gliomagenesis is likely enzyme-dependent, although the majority of studies show these enzymes to promote tumor progression.

Introduction of the $IDH1^{R132H}$ mutation in astrocytoma cells has been associated with both global histone hypermethylation (84), and enrichment of specific histone methylation marks (85). Mutant IDH1 enzymes generate the oncometabolite 2-HG instead of 2-OG, and 2-HG has been shown to competitively inhibit histone demethylase activity (65, 86). Despite the fact that reduced histone demethylase activity has been linked with higher histone methylation in astrocytoma cells, most clinical gliomas show increased levels of JmjC-dependent demethylases and lower histone methylation (76–81). Thus, further investigations of the biological mechanisms causing increased expression of JmjC-dependent demethylases in glioma is needed.

2-OGDDs AND THE HYPOXIC PATHWAY

Gliomas are highly hypoxic tumors and this is associated with poor patient prognosis (23, 87–89). Hypoxia induces adverse tumor characteristics including genomic instability, decreased apoptotic potential, increased expression of oncogenes and increased angiogenesis, which have all been described in gliomas (90). These characteristics are driven by the hypoxia inducible factors (HIFs) which are regulated by microenvironmental oxygen levels and the 2-OGDD enzymes, prolyl hydroxylases (PHD) and factor inhibiting HIF (FIH) (**Figure 4**) (91). As these HIF hydroxylases are dependent on oxygen for optimal function their activity is likely impaired in gliomas (92–95).

Hypoxia-Inducible Factors

Hypoxic conditions typical of most solid tumors result in accumulation of the HIF transcription factors (11, 96). The HIFs (HIF-1,2,3) are heterodimeric transcription factors, consisting of one of three oxygen-sensitive α-subunits and a constitutive β-subunit (also known as aryl hydrocarbon receptor nuclear translocator (ARNT)) (97–99). HIF-1α is located on chromosome 14q23 (100); HIF-2α, also known as endothelial PAS domain protein 1 (EPAS1), is on 2p21, and HIF-3α is on 19q13 (101). Active HIF complexes accumulate in the nucleus and bind to specific hypoxic response elements (HREs) in promoter regions of HIF target genes, inducing their expression (102, 103). HREs contain the consensus sequence $^{5'}CGTG^{3'}$, targets of CpG methylation, and CpG methylation blocks HIF-1 binding and transactivation (104). Even though HIF-1 and HIF-2 have identical HREs, their response to hypoxia, tissue distribution, target genes and their pro- or anti-tumor effects are distinct (105). Binding of HIF-1 and HIF-2 to their canonical HREs vary according to histone modifications, with HIF-1 preferentially associating with H3K4me3 modifications and HIF-2 with H3K4me1 (106). These binding patterns were interpreted as HIF-1 binding predominantly at regulatory regions within promoters, and HIF-2 binding to enhancer regions (106).

HIF's modulate expression of hundreds of genes, and as a result, promote tumor growth and spread, adaptation to the tumor microenvironment, and resistance to chemo- and radio-therapy (107, 108). HIF activity also affects DNA methylation, histone acetylation and regulates noncoding RNAs (109), demonstrating the complexities of the hypoxic pathway.

HIF-1α has been proposed to drive glioma progression from low-grade astrocytoma to high-grade GBM (23, 110). Higher HIF-1α expression in human astrocytoma and GBM has been correlated with worse prognosis (111–114). Moreover, expression of HIF-1α, and its downstream target genes vascular endothelial growth factor (VEGF), glucose transporter (GLUT1), and carbonic anhydrase (CA9), show increased expression in higher grade gliomas compared to lower grade (115). In addition, increases in VEGF expression were shown to localize to hypercellular and necrotic regions that form as result of decreased oxygen and nutrient delivery (113, 116).

In comparison to HIF-1α, HIF-2α may be a specifically attractive target in GBMs, as it is expressed in glioma stem cells but not normal neuronal progenitors and it is activated by long-term hypoxia, in addition to its association with poor patient survival (117).

HIF Hydroxylases

HIF activity is regulated at the post-translational level by two families of HIF hydroxylases, the prolyl hydroxylase domain (PHD) and factor inhibiting HIF (FIH) 2-OGDDs (**Figure 4**). PHDs hydroxylate specific proline residues on the HIF-α subunit targeting the subunit for proteasomal degradation (9, 92, 118). FIH hydroxylates an asparagine residue and prevents binding of the co-activators CBP/p300 and nuclear translocation (93, 119). The instability of HIF-α and the inhibition of transcriptional activators binding results in a reduction in both HIF-α protein and expression of target genes. Protein hydroxylation was considered irreversible, but a recent study showed evidence that FIH-mediated asparagine hydroxylation may be reversible by as yet unknown cellular enzymes (120).

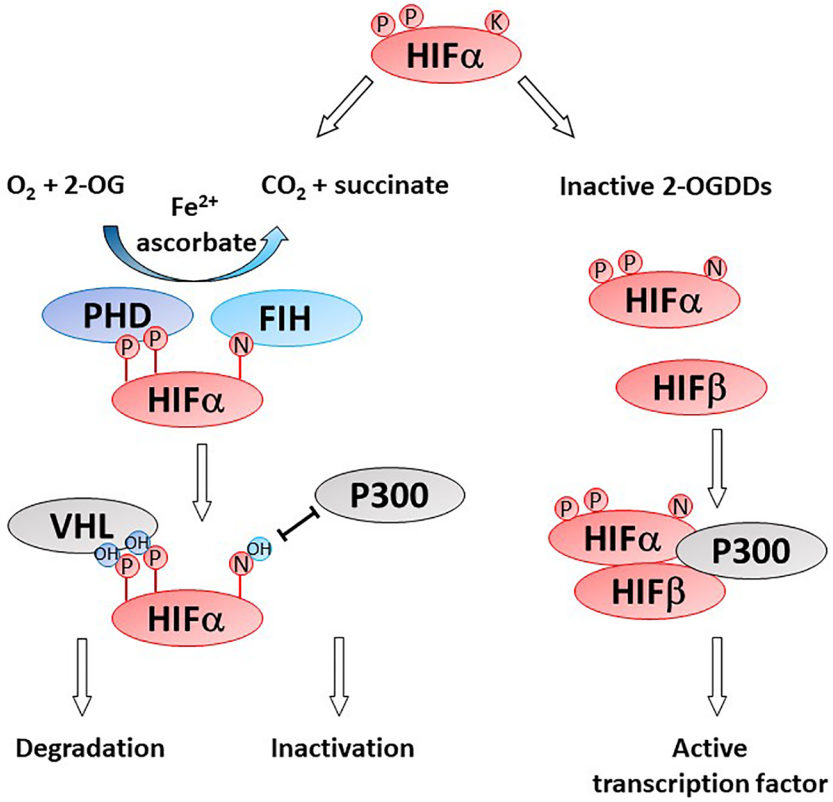

FIGURE 4 | Activity of HIF-hydroxylases. Response to low oxygen (hypoxia) is regulated *via* the prolyl (PHD) and asparaginyl hydroxylases (factor inhibiting HIF, FIH). Specific proline (P) and asparagine (N) residues on the alpha subunit of the hypoxia inducible factor (HIFα) are hydroxylated by PHD and FIH, respectively. Proline hydroxylation enables recognition by von Hippel Lindau (VHL) as part of the proteasome and HIFα degradation. Asparagine hydroxylation prevent binding of the cofactor P300, thereby inactivating the HIF transcription factor. In the absence of one or more of the OGDD substrates or cofactors, PHD and FIH enzymes become inactive, enabling the accumulation of HIFα and formation of an active HIF transcription factor *via* binding to HIFβ. Genes under HIF control regulate cancer pathways such as angiogenesis, metastasis, glycolysis, etc.

The PHDs and the FIH enzymes have specific roles in oxygen and metabolic sensing due to their exquisite requirements for molecular oxygen and 2-OG, respectively (11). PHDs have higher affinity for oxygen (9, 13), bind unusually tightly to Fe^{2+} (121), and have a lower affinity for ascorbate compared to FIH (3), possibly due to the narrower opening to the enzyme active site of PHDs (122). PHD2 and FIH bind 2-OG with distinct residues, with FIH sharing more homology with JmjC-domain containing protein family of enzymes (94), suggesting evolutionary divergence (122). The HIF hydroxylases therefore have different sensitivities to loss of enzyme substrates and/or co-factors.

PHD2 (encoded by *EGLN1*) is generally acknowledged as the primary mediator of HIF-1α protein degradation, with PHD1 and 3 more likely to be involved in fine-tuning of the hypoxic response (123). This may be reflected in the subcellular localisation of each isoform, with PHD1 detected exclusively in the nucleus, PHD2 (and FIH) in the cytoplasm, and PHD3 in both compartments (124). Interestingly, PHD2 is activated, rather than inhibited, by the R-enantiomer of 2-HG as it mimics 2-OG, suggesting that IDH mutations may lead to HIF-α degradation (125–127). It has been shown, using immunohistochemistry, that HIF-1α and IDH^{R132H} expression are not related, supporting the ability of 2-HG to activate PHD2 (128).

FIH (also known as *HIF1AN*) is mapped to chromosome 10q24 (93). Full or partial deletions of chromosome 10q often occur in gliomas, and the frequency of these deletions increases with tumor grade (59–61). Thus, *FIH* mRNA expression often decreases with increasing tumor grade (129, 130). Investigation of FIH in GBMs has shown that FIH reduces the interaction between p300 and HIF-1α which is essential for transcriptional activity (131), and correspondingly higher FIH expression was associated with reduced *GLUT1* and *VEGF* expression in GBM cells (131). Loss of *FIH* through deletion of chromosome 10q24 may increase the hypoxic response, and thus contribute to an aggressive and treatment resistant glioma phenotype associated with hypoxia (23, 87, 88). While PHD2 is activated by the mutant IDH metabolite, 2-HG, FIH is inhibited, resulting in p300 interacting with HIF-α and inducing target gene expression (125). However, FIH has been shown to interact with a glioma tumor suppressor gene (*ANKDD1A*), which increased FIH activity, thereby reducing HIF-α activation and preventing HIF target gene expression (132).

SUBSTRATE AND COFACTOR REQUIREMENTS OF 2-OGDDs

2-OGDDs contain a non-heme iron (Fe^{2+}) in the active site, and utilize 2-OG (also known as α-ketoglutarate) and molecular oxygen as substrates (**Figure 5**). Ascorbate is an essential cofactor, and is thought to be required to maintain the active site Fe^{2+} in the reduced state (11–14, 133, 134).

Molecular Oxygen as 2-OGDD Substrate and its Availability in Gliomas

Oxygen is an absolute requirement for all 2-OGDDs, but not all 2-OGDDs function as oxygen sensors. The PHDs have a K_m for oxygen of 230-250 μM, slightly above dissolved oxygen concentrations in air (20.9% O_2 in gas phase ~ 200 μM dissolved O_2) (135), and this property makes these proteins the predominant cellular oxygen sensors. These K_m values are significantly greater than for FIH at 90 μM, and the collagen prolyl 4-hydroxylases (C-P4H) at 40 μM (13, 135, 136).

Tissue partial pressure of oxygen (PO_2) in the human body range from 104–108 mmHg in the alveola of the lung, to arterial PO_2 of 90 mmHg and venous PO_2 of 40 mmHg, to most tissues that have between tissue PO_2 of 20–70 mmHg (137). Oxygen levels in the brain are heterogeneous and difficult to measure, with levels of 30–48 mmHg in normal brain recorded. Hypoxia is defined as <5 mmHg, and levels below 2.5 mmHg are known to

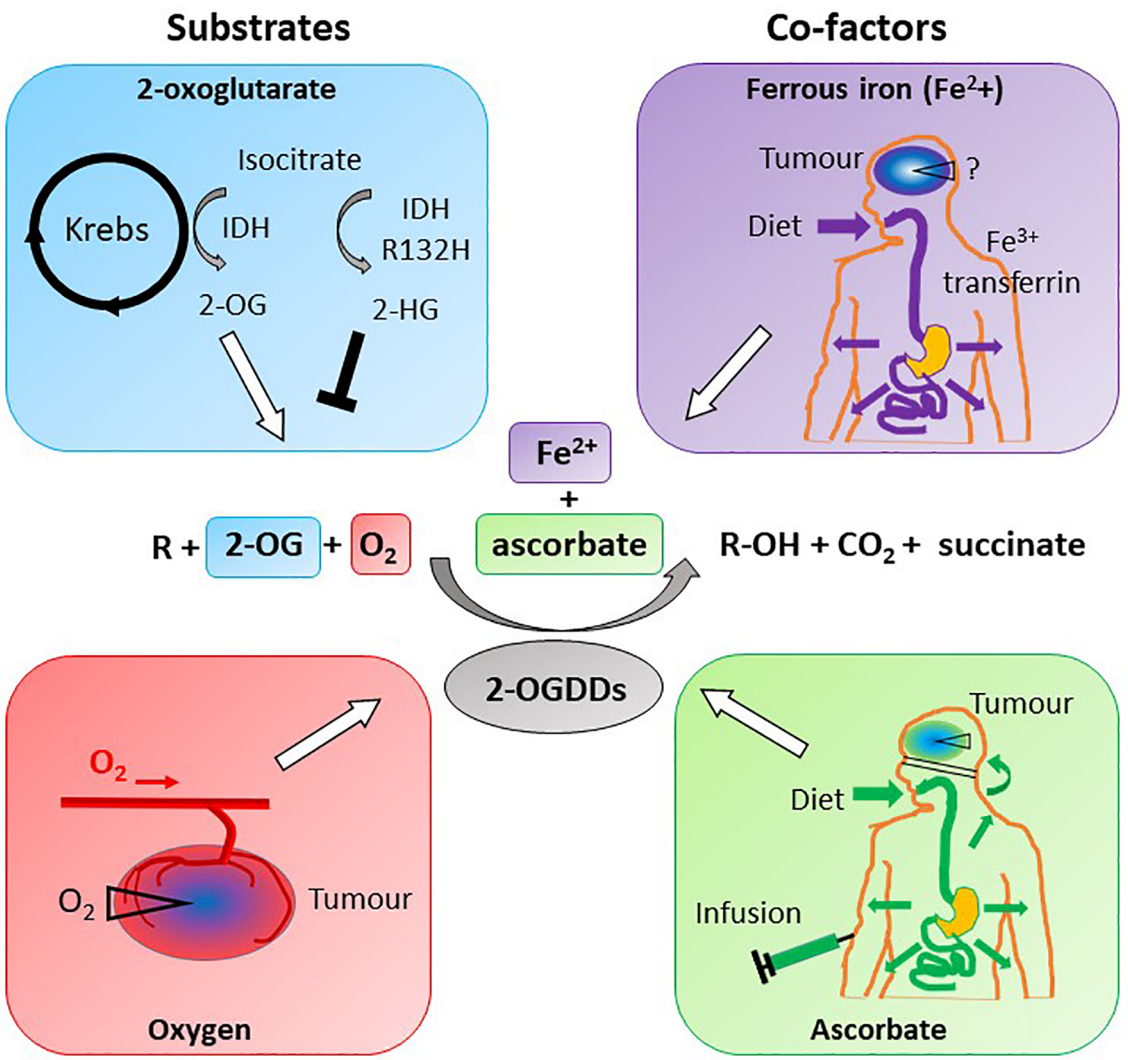

FIGURE 5 | Substrate and cofactor requirements of the 2-oxoglutarate dependent dioxygenases. These enzymes hydroxylate nucleotides or amino acids (R), forming a hydroxylated product (R-OH). 2-OGDDs require 2-oxoglutarate (2-OG) and molecular oxygen (O_2) as substrates, and ferrous iron (Fe^{2+}) and ascorbate as cofactors. Isocitrate from the Krebs cycle is converted to 2-OG by isocitrate dehydrogenase (IDH), but mutant IDH (IDH^{R132H}) produces the competitive inhibitor 2-hydroxyglutarate (2-HG). Low oxygen (hypoxia) is a characteristic of most solid tumors, thus reducing activity of 2-OGDDs. Iron obtained from the diet is transported *via* transferrin and taken up across the BBB *via* transferrin receptors; the content in tumors is unknown. Ascorbate is obtained *via* a healthy diet or infusions, and cannot cross the BBB but will travel *via* the choroid plexus. Cellular ascorbate uptake is *via* sodium vitamin C transporters; tumors may be low in the vitamin.

induce clinical radioresistance (138–145). Theoretical modelling suggests the minimum oxygen level requirement for brain tissue is 17 mmHg and that a critical range for hypoxic injury is 4–11 mmHg (140).

Hypoxia is a prominent feature of gliomas. Oxygen levels in tumors have been measured using a range of techniques, including injection of hypoxia markers (146–149), direct measurements using polarographic O_2 microelectrodes (145, 150) and MRI/CT scans (151). Using these techniques, oxygen levels were observed to be lower in gliomas and peritumoral regions compared to normal brain tissues, and readings below 2.5 mmHg were more common in tumors of increasing grade (145, 150, 152), with the most severe hypoxia detected in GBMs (23, 88, 89). A review of six studies reported a median PO_2 of 13 mmHg in gliomas (144). This suggests that in high grade gliomas, the activity of 2-OGDD enzymes is likely to be reduced, but hypoxia is not routinely measured.

As ionizing radiation remains the mainstay of glioma treatment, and since hypoxia governs radioresistance, considerable clinical effort has been focused on reducing tumor hypoxia. With regards to 2-OGDD activity, these strategies may also improve enzyme activity, and are thus briefly discussed here. In an attempt to improve tumor oxygenation, patients have been given pure oxygen in a pressurized environment (hyperbaric oxygen) to breath (153). Alternatively, patients breathed 95% O_2 with 5% CO_2 (carbogen), which, together with hypercapnic-induced vasodilation, increases the amount of dissolved plasma O_2 at the capillary level (154). Carbogen was tested in combination with nicotinamide, which is believed to prevent transient cessations in blood flow, thus inhibiting the development of acute hypoxia (154). Drugs have been developed to improve oxygen delivery (eg trans sodium crocetinate, TSC) (155), to normalize the tumor vasculature (e.g., anti-VEGF bevacizumab) (156), or to reduce oxygen consumption rate *via* mitochondrial poisons (e.g., anti-parasitic drugs atovaquone, ivermectin, proguanil, mefloquine, and quinacrine) and tested in patients with GBM (157). Overall, the results of these clinical trials have been disappointing and none of the approaches have been adopted into clinical practice, and actual oxygen measurements were largely lacking.

2-Oxoglutarate and Oncometabolites as 2-OGDD Substrates in Gliomas

The substrate 2-oxoglutarate (2-OG) is a product of the reaction in which isocitrate dehydrogenase enzymes (IDH) convert isocitrate to 2-OG (**Figure 5**). This reaction occurs in the TCA cycle *via* IDH3 and in the cytosol *via* IDH1 and IDH2. A number of *IDH1* and *IDH2* mutations have been reported in glioma, with the most common a base substitution in codon 132 of *IDH1* resulting in an arginine to histidine replacement ($IDH1^{R132H}$) (24, 67). $IDH1^{R132H}$ has been identified in more than 70% of grade II/III astrocytic and oligodendroglial diffuse gliomas, and in more than 80% of secondary GBM, but rarely in primary GBM (24, 158, 159). $IDH1^{R132H}$ enzymes generate 2-HG, instead of 2-OG (66, 67), which binds competitively to 2-OGDD enzymes and inhibits their function (**Figure 5**). Studies have, however, also reported that accumulation of 2-HG does not universally occur in all $IDH1^{R132H}$ and, conversely, that some wild type IDH cells accumulate 2-HG (160, 161). Further research is required to understand the impact of IDH mutations on patients with glioma, and how 2-HG accumulation interacts with other 2-OGDD substrates and co-factors to influence their activity in these tumors.

In gliomas with $IDH1^{R132H}$ mutations, drugs that inhibit the mutant IDH1 enzymes may improve 2-OGDD activity by reducing 2-HG production. A number of mutant IDH1 inhibitors are currently being evaluated in clinical trials with glioma patients, including AG-120 (Ivosidenib), AG-881 (Vorasidenib), BAY1436032 (Bayer), and DS-1001b (NCT02746081) (162–166). Pre-clinical investigations have reported anti-proliferative effects, reductions in tumor growth rates, and lower levels of 2-HG in both glioma cells and tumors from animal models (167–170). To date, 2-HG levels have only been measured in the plasma of human glioma patients following intervention with Ivosidenib, reporting no difference compared to those without treatment (163). Despite this, interest remains high and data from a Phase I study of Ivosidenib and Vorasidenib in patients with recurrent, non-enhancing, IDH1-mutant, low-grade glioma is currently pending (162). In addition to inhibitors, vaccines against mutant IDH1 have been tested in mice (171, 172). Mice with mutant $IDH1^{R132H}$ gliomas treated with the vaccine showed longer survival than non-immunized mice, and had higher levels of peripheral anti- $IDH1^{R132H}$ antibodies, IFN-γ, and CD8+ T cells (172). However, 2-HG levels in tumors were not measured, and thus the vaccine effect on 2-OGDDs remains to be tested.

Iron as Cofactor for 2-OGDDs and Availability in the Brain

Iron is the most abundant transition metal in the brain (173) and is more concentrated in some regions than in others (range; 13.5–1.75 μmol/g dry weight) (174), including the iron-rich substantia nigra, caudate nucleus and globus pallidus (175). Most gliomas arise in the frontal/temporal lobe, areas rich in glial cells and, potentially, relatively lower in iron. Astrocytes secrete hepcidin, which modulates the expression of ferroportin and other iron regulatory proteins, and thereby function as iron sensors to regulate and communicate the iron requirement of the brain through paracrine signaling (176–178).

Iron uptake into the brain is tightly regulated through the endothelial cells and neighboring astrocytes in the blood brain barrier (BBB) (176, 179, 180), primarily through the transferrin bound iron (TBI) pathway (174, 181, 182) however, when this pathway becomes saturated, non-TBI pathways are used (183). Through the canonical TBI uptake pathway, ferric iron (Fe^{3+}) forms halotransferrin (174), which is able to pass through the BBB by binding to transferrin receptors on the apical surface of brain microvascular endothelial cells (BMVECs). Within the BMVEC, excess iron is stored in the cytosolic labile iron pool, which is the principle source of metals for metabolism (184). Efflux of iron through the abluminal membrane into the brain interstitium occurs through ferroportin (185, 186), expressed on

the basolateral side of the BMVEC cells (186, 187). Once iron has crossed the BBB barrier, it is taken up by neurons, astrocytes, oligodendrocytes and microglia through TBI and nonTBI uptake pathways (183).

Iron plays a role in carcinogenesis, with proteins that modulate and regulate iron metabolism often dysregulated in gliomas (188–191). GBM cancer-stem-like cells were shown to upregulate transferrin expression, and to extract iron more effectively from the tumor microenviroment than non-stem-like tumor cells in an *ex vivo* explant model (192). The Fe^{2+} content in gliomas has not been reported but reduced levels may impede 2-OGDD function in tumors and cancer stem cells.

Ascorbate as Cofactor for 2-OGDDs and its Availability in the Brain

As a cofactor for 2-OGDDs, ascorbate acts to reduce Fe^{3+} back to active Fe^{2+} (**Figure 5**). This activity appears to be specific to ascorbate as alternative reducing agents such as glutathione or N-Acetylcysteine are unable to substitute for ascorbate in 2-OGDD activity (12, 193, 194). Ascorbate is also involved in stabilizing cysteine residues in PHD enzymes, preventing intramolecular oxidation and supporting catalytic activity (126).

Normal brain tissue has one of the highest ascorbate levels of all tissues in the body, reaching intracellular concentrations of 2–10 mM depending on the cell type (195–197). In times of ascorbate insufficiency, the brain is one of the last tissues to lose ascorbate, supporting its importance to brain function (195, 198). The specific vitamin C transporters (sodium-dependent vitamin C transporters) are not expressed on the endothelial cells lining the BBB (198), and ascorbate enters the central nervous system through the choroid plexus where it can diffuse through the cerebrospinal fluid to the brain (195, 198). Cells within the brain express ascorbate transporters allowing intracellular ascorbate accumulation (198).

Data on ascorbate content in gliomas is limited to a single study that reported ascorbate levels in astrocytomas from eleven patients (199). While ascorbate levels were not different between astrocytoma tissue and non-neoplastic tissue, DNA content was significantly higher in astrocytoma (tumor) tissues indicating increased cell density (or cellularity) of the tissues. This suggests that intracellular ascorbate per cell may be reduced in astrocytoma tissue compared to normal, non-necrotic tissue (199). These intriguing findings need to be confirmed.

Ascorbate and Epigenetic Reprogramming

Evidence for the effects of ascorbate on epigenetic reprogramming is largely from embryonic cells (200, 201), but data in gliomas is missing. In patients with myeloid malignancies, oral ascorbate supplementation resulted in an increase in the ratio of 5-hmC compared to 5-mC in mononuclear myeloid cells (202). Here, DNA demethylation was not associated with changes in TET expression (202, 203), but instead appear to result from ascorbate-mediated restoration of endogenous TET activity, which was supported by studies with *Tet2*-deficient mice (204). Gliomas show lower TET expression independent of *TET* mutations (63, 68, 69), and we hypothesize that ascorbate may compensate for lower TET expression by upregulating residual TET2 function as was observed in a case study of acute myeloid leukemia (205).

Low-grade primary gliomas commonly harbor *IDH* mutations that persist during progression to secondary GBM (24). *In vitro*, ascorbate was able to circumventing competitive inhibition by 2-HG in colon cancer and HOXA9-immortalized mouse bone marrow cells with $IDH1^{R132H}$ mutations (206, 207). One *in vitro* study reported the effects of ascorbate on epigenetic marks in LN229 glioma cells, showing increased *TET3* mRNA expression, as well as increased 5-hmC, but these cells did not harbor an IDH mutation (64). Yet, these findings, together with reported associations between higher 5-hmC levels and better prognosis in patients with GBM (50), support the notion that sufficient ascorbate levels in glioma tumors may induce demethylation activity and promote more favorable outcomes, although whether sufficient ascorbate can overcome high levels of 2-HG remains to be determined.

In addition to TET-mediated effects, ascorbate induced H3K9me2/3 and H3K36me2/3 demethylation *via* JmjC-dependent demethylases in embryonic stem, embryonic fibroblast and Th17 cells from mice (208–210). Ascorbate caused reductions in H3K9 methylation and increased expression of the JmjC-dependent demethylases, JHDM2A-C and JHDM3B, as well as widespread DNA demethylation at CpG island boundaries in human embryonic stem cells (211). However, investigations in gliomas are lacking, despite the well-established link between glioma formation and global 5-hmC deficiency.

Ascorbate and the Hypoxic Pathway

The relationship between intracellular ascorbate levels and HIF pathway activity has been investigated in numerous cancers, but not yet in gliomas. *In vitro* investigations of intracellular ascorbate levels and HIF pathway activity have been performed in varying cancer types, findings from which have guided further *in vivo* studies (212–215). In relevant mouse models (using ascorbate-dependent $Gulo^{-/-}$ mice), increased ascorbate intake or administration was associated with increased tumor ascorbate levels, reduced HIF pathway activity and reduced tumor growth (216). In clinical samples of endometrial (217), colorectal (218), thyroid (214), papillary cell renal cell carcinomas (215, 219), and breast cancer (220), high tumor ascorbate levels were associated with low HIF-1α protein levels and low HIF target gene expression. This relationship was not evident in clear cell renal cell carcinoma (215, 219), that have a mutated von Hippel-Lindau factor which prevents proteasomal degradation of hydroxylated HIF-α (219). Higher levels of tumor ascorbate were associated with improved disease-free survival in patients with colorectal cancer (218) and improved disease-specific survival in patients with breast cancer (220).

HIGH DOSE ASCORBATE AS CANCER TREATMENT

Infusion with high dose ascorbate as an alternative or complementary therapy for cancer is widespread (221), but

lacks evidence of efficacy (222, 223), despite early promising data (224, 225). Since then, pharmacokinetic data have demonstrated that infusion results in supra-physiological plasma ascorbate levels that are not achievable by oral administration (226–229). Case studies and small clinical trials continue to surface that suggest there may be circumstances under which high dose ascorbate infusion can provide a clinical benefit (230–239).

Preclinical Models of High Dose Ascorbate Treatment in Gliomas

In a mouse xenograft glioma model, analysis of ascorbate levels in plasma, tumor, and cerebrospinal fluid samples showed that ascorbate increased 1 h post intraperitoneal injection with 4 g/kg of ascorbate (240). One study, using an intracranial GL261 glioma mouse model, reported that radiation treatment slowed tumor growth, whereas ascorbate treatment made no difference, and the combination of ascorbate and radiotherapy induced faster progression (241), in conflict to *in vitro* findings of radiosensitisation by ascorbate in numerous glioma cell lines, including GL261 cells (242–244). However, ascorbate levels in the intracranial model were not measured, and thus the impact of ascorbate on glioma response to radiation remain uncertain.

Clinical Trials in Patients With Gliomas and GBMs

Preclinical data led to phase I clinical trials administering intravenous ascorbate to glioma patients, with and without standard radiotherapy and temozolomide (245). High dose vitamin C (HDVC) was found to be safe and well tolerated, reaching target 20 mM plasma levels (240, 245), but tumor ascorbate levels were not measured. A trend of improved overall survival was reported, but participant numbers were too small to determine statistical significance (240). Two case reports for the use of HDVC infusions in patients with glioma have also been reporting (237, 246).

Previous research has shown an association between a lower proportion of methylation at the O-6-methylguanine-DNA methyltransferase (MGMT) promoter in glioma tumors and poorer patient prognosis (247). MGMT is a DNA repair enzyme responsible for resistance to temozolomide, and hypermethylation of the *MGMT* promoter is evident in 40–45% of gliomas (248, 249), with higher methylation levels in low-grade gliomas compared to GBMs (53). Interestingly, in glioma patients with low methylation levels at the *MGMT* promoters, HDVC infusions resulted in improved overall survival (240), but unfortunately, ascorbate levels in the glioma tissue were not measured. Plasma ascorbate levels do not necessarily reflect tumor ascorbate levels due reduced functioning vasculature and BBB in gliomas. Overall, the clinical worth of HDVC in cancer remains unproven.

CONCLUSION

The superfamily of 2-OGDD enzymes play a vital role in glioma progression and patient prognosis, being involved in epigenetic modifications and oxygen sensing. Limiting supplies of one or more of their substrates or cofactors in gliomas is likely although reported measurements are rare. Restoration of epigenetic modifications offers a promising target in the treatment of cancer, as these alterations are reversible, as opposed to genetic mutations. Attempts at increasing tumor oxygenation to improve effectiveness of radiation and chemotherapy in glioma are not (yet) in clinical practice (250), and new strategies are sought. Ascorbate infusion is a safe and cheap option that may be able to normalize 2-OGDD function in a subset of glioma tumor subtypes. However, this will likely depend on mutation status and on the ability to increase intracellular ascorbate levels in these tumors. Future research will need to confirm ascorbate status of clinical glioma tumors, on measuring 5-hmC levels and HIF activity in clinical samples, and on determining an optimal ascorbate dose for patients, before embarking on phase III trials to determine clinical efficiency.

AUTHOR CONTRIBUTIONS

Conceptualization, RC, EB, JR, and GD. Funding acquisition, EP and GD. Supervision, EP, MV, and GD. Writing—original draft, RC and EB. Writing—review and editing, JR, MV, and GD. All authors contributed to the article and approved the submitted version.

FUNDING

We received funding from the Mackenzie Charitable Foundation (EP and GD), the Canterbury Medical Research Foundation (RC, EP, and GD) and the University of Otago (RC and GD).

ACKNOWLEDGMENTS

We would like to acknowledge receipt of the doctoral scholarship from the University of Otago (EB).

REFERENCES

1. Johansson C, Tumber A, Che K, Cain P, Nowak R, Gileadi C, et al. The roles of Jumonji-type oxygenases in human disease. *Epigenomics* (2014) 6(1):89–120. doi: 10.2217/epi.13.79
2. McDonough MA, Loenarz C, Chowdhury R, Clifton IJ, Schofield CJ. Structural studies on human 2-oxoglutarate dependent oxygenases. *Curr Opin Struct Biol* (2010) 20:659–72. doi: 10.1016/j.sbi.2010.08.006
3. Ozer A, Bruick RK. Non-heme dioxygenases: Cellular sensors and regulators jelly rolled into one? *Nat Chem Biol* (2007) 3:144–53. doi: 10.1038/nchembio863
4. Schofield CJ, Ratcliffe PJ. Oxygen sensing by HIF hydroxylases. *Nat Rev Mol Cell Biol* (2004) 5:343–54. doi: 10.1038/nrm1366
5. Wu Y-C, Ling Z-Q. The role of TET family proteins and 5-hydroxymethylcytosine in human tumors. *Histol Histopathol* (2014) 29:991–7. doi: 10.14670/HH-29.991

6. Islam MS, Leissing TM, Chowdhury R, Hopkinson RJ, Schofield CJ. 2-Oxoglutarate-Dependent Oxygenases. *Annu Rev Biochem* (2018) 87:585–620. doi: 10.1146/annurev-biochem-061516-044724
7. Vissers MC, Das AB. Ascorbate as an Enzyme Cofactor. In: Vitamin C. CRC Press Taylor and Francis Group, Florida, USA. (2020) pp 71–98. CRC Press Taylor and Francis Group (2020).
8. Grosso G, Bei R, Mistretta A, Marventano S, Calabrese G, Masuelli L, et al. Effects of vitamin C on health: A review of evidence. *Front Biosci* (2013) 18:1017–29. doi: 10.2741/4160
9. Epstein ACR, Gleadle JM, McNeill LA, Hewitson KS, O'Rourke J, Mole DR, et al. C. elegans EGL-9 and mammalian homologs define a family of dioxygenases that regulate HIF by prolyl hydroxylation. *Cell* (2001) 107:43–54. doi: 10.1016/S0092-8674(01)00507-4
10. Mandl J, Szarka A, Bánhegyi G. Vitamin C: update on physiology and pharmacology. *Br J Pharmacol* (2009) 157:1097–110. doi: 10.1111/j.1476-5381.2009.00282.x
11. Vissers MCM, Kuiper C, Dachs GU. Regulation of the 2-oxoglutarate-dependent dioxygenases and implications for cancer. *Biochem Soc Trans* (2014) 42:945–51. doi: 10.1042/BST20140118
12. Dickson KM, Gustafson CB, Young JII, Züchner S, Wang G. Ascorbate-induced generation of 5-hydroxymethylcytosine is unaffected by varying levels of iron and 2-oxoglutarate. *Biochem Biophys Res Commun* (2013) 439:522–7. doi: 10.1016/j.bbrc.2013.09.010
13. Koivunen P, Hirsilä M, Günzler V, Kivirikko KII, Myllyharju J. Catalytic Properties of the Asparaginyl Hydroxylase (FIH) in the Oxygen Sensing Pathway Are Distinct from Those of Its Prolyl 4-Hydroxylases. *J Biol Chem* (2004) 279:9899–904. doi: 10.1074/jbc.M312254200
14. Nytko KJ, Spielmann P, Camenisch G, Wenger RH, Stiehl DP. Regulated function of the prolyl-4-hydroxylase domain (PHD) oxygen sensor proteins. *Antioxid Redox Signal* (2007) 9:1329–38. doi: 10.1089/ars.2007.1683
15. Louis DN, Perry A, Reifenberger G, von Deimling A, Figarella-Branger D, Cavenee WK, et al. The 2016 World Health Organization Classification of Tumors of the Central Nervous System: a summary. *Acta Neuropathol* (2016) 131:803–20. doi: 10.1007/s00401-016-1545-1
16. Wesseling P, Capper D. WHO 2016 Classification of gliomas. *Neuropathol Appl Neurobiol* (2018) 44:139–50. doi: 10.1111/nan.12432
17. Behin A, Hoang-Xuan K, Carpentier AF, Delattre JY. Primary brain tumours in adults. *Lancet* (2003) 361:323–31. doi: 10.1016/S0140-6736(03)12328-8
18. Bray F, Ferlay J, Soerjomataram I, Siegel RL, Torre LA, Jemal A, et al. Global cancer statistics 2018: GLOBOCAN estimates of incidence and mortality worldwide for 36 cancers in 185 countries. *CA Cancer J Clin* (2018) 68:394–424. doi: 10.3322/caac.21492
19. Watanabe K, Tachibana O, Sato K, Yonekawa Y, Kleihues P, Ohgaki H. Overexpression of the EGF Receptor and p53 Mutations are Mutually Exclusive in the Evolution of Primary and Secondary Glioblastomas. *Brain Pathol* (1996) 6:217–23. doi: 10.1111/j.1750-3639.1996.tb00848.x
20. Stupp R, Mason WP, Van Den Bent MJ, Weller M, Fisher B, Taphoorn MJB, et al. Radiotherapy plus Concomitant and Adjuvant Temozolomide for Glioblastoma. *N Engl J Med* (2005) 352:987–96. doi: 10.1056/NEJMoa043330
21. Stupp R, Hegi ME, Mason WP, van den Bent MJ, Taphoorn MJ, Janzer RC, et al. Effects of radiotherapy with concomitant and adjuvant temozolomide versus radiotherapy alone on survival in glioblastoma in a randomised phase III study: 5-year analysis of the EORTC-NCIC trial. *Lancet Oncol* (2009) 10:459–66. doi: 10.1016/S1470-2045(09)70025-7
22. Annovazzi L, Mellai M, Schiffer D. Chemotherapeutic drugs: DNA damage and repair in glioblastoma. *Cancers* (2017) 9:57–73 doi: 10.3390/cancers9060057
23. Huang WJ, Chen WW, Zhang X. Glioblastoma multiforme: Effect of hypoxia and hypoxia inducible factors on therapeutic approaches (review). *Oncol Lett* (2016) 12:2283–8. doi: 10.3892/ol.2016.4952
24. Yan H, Parsons DW, Jin G, McLendon R, Rasheed BA, Yuan W, et al. IDH1 and IDH2 Mutations in Gliomas. *N Engl J Med* (2009) 360:765–73. doi: 10.1016/S0513-5117(09)79085-4
25. Van Den Bent MJ, Hegi ME, Stupp R. Recent developments in the use of chemotherapy in brain tumours. *Eur J Cancer* (2006) 42:582–8. doi: 10.1016/j.ejca.2005.06.031
26. Hirst TC, Vesterinen HM, Sena ES, Egan KJ, Macleod MR, Whittle IR. Systematic review and meta-analysis of temozolomide in animal models of glioma: Was clinical efficacy predicted. *Br J Cancer* (2013) 108:64–71. doi: 10.1038/bjc.2012.504
27. Hou LC, Veeravagu A, Hsu AR, Tse VCK. Recurrent glioblastoma multiforme: a review of natural history and management options. *Neurosurg Focus* (2006) 20:E5. doi: 10.3171/foc.2006.20.4.2
28. Touat M, Li YY, Boynton AN, Spurr LF, Iorgulescu JB, Bohrson CL, et al. Mechanisms and therapeutic implications of hypermutation in gliomas. *Nature* (2020) 580:517–23. doi: 10.1038/s41586-020-2209-9
29. Dong C, Zhang H, Xu C, Arrowsmith CH, Min J. Structure and function of dioxygenases in histone demethylation and DNA/RNA demethylation. *IUCrJ* (2014) 1:540–9. doi: 10.1107/S2052252514020922
30. Shi Y. Histone lysine demethylases: Emerging roles in development, physiology and disease. *Nat Rev Genet* (2007) 8:829–33. doi: 10.1038/nrg2218
31. Fu Y, He C. Nucleic acid modifications with epigenetic significance. *Curr Opin Chem Biol* (2012) 16:516–24. doi: 10.1016/j.cbpa.2012.10.002
32. Berdasco M, Esteller M. Developmental Cell Review Aberrant Epigenetic Landscape in Cancer: How Cellular Identity Goes Awry. (2010) 19:698–711. doi: 10.1016/j.devcel.2010.10.005
33. Hanahan D, Weinberg RA. Hallmarks of cancer: the next generation. *Cell* (2011) 144:646–74. doi: 10.1016/j.cell.2011.02.013
34. Gusyatiner O, Hegi ME. Glioma epigenetics: From subclassification to novel treatment options. *Semin Cancer Biol* (2018) 51:50–8. doi: 10.1016/j.semcancer.2017.11.010
35. Noushmehr H, Weisenberger DJ, Diefes K, Phillips HS, Pujara K, Berman BP, et al. Identification of a CpG Island Methylator Phenotype that Defines a Distinct Subgroup of Glioma. *Cancer Cell* (2010) 17:510–22. doi: 10.1016/j.ccr.2010.03.017
36. Turcan S, Rohle D, Goenka A, Walsh LA, Fang F, Yilmaz E, et al. IDH1 mutation is sufficient to establish the glioma hypermethylator phenotype. *Nature* (2012) 483:479–83. doi: 10.1038/nature10866
37. Laffaire J, Everhard S, Idbaih A, Crinière E, Marie Y, de Reyniès A, et al. Methylation profiling identifies 2 groups of gliomas according to their tumorigenesis. *Neuro Oncol* (2011) 13:84–98. doi: 10.1093/neuonc/noq110
38. Parsons DW, Jones S, Zhang X, Lin JC, Leary RJ, Angenendt P, et al. An integrated genomic analysis of human glioblastoma multiforme. *Science* (2008) 321:1807–12. doi: 10.1126/science.1164382
39. Bai H, Harmanci AS, Erson-Omay EZ, Li J, Coşkun S, Simon M, et al. Integrated genomic characterization of IDH1-mutant glioma malignant progression. *Nat Genet* (2015) 48:59–66. doi: 10.1038/ng.3457
40. Mazor T, Pankov A, Johnson BE, Hong C, Hamilton EG, Bell RJA, et al. DNA Methylation and Somatic Mutations Converge on the Cell Cycle and Define Similar Evolutionary Histories in Brain Tumors. *Cancer Cell* (2015) 28:307–17. doi: 10.1016/j.ccell.2015.07.012
41. de Souza CF, Sabedot TS, Malta TM, Stetson L, Morozova O, Sokolov A, et al. A Distinct DNA Methylation Shift in a Subset of Glioma CpG Island Methylator Phenotypes during Tumor Recurrence. *Cell Rep* (2018) 23:637–51. doi: 10.1016/j.celrep.2018.03.107
42. Nomura M, Saito K, Aihara K, Nagae G, Yamamoto S, Tatsuno K, et al. DNA demethylation is associated with malignant progression of lower-grade gliomas. *Sci Rep* (2019) 9:1–12. doi: 10.1038/s41598-019-43790-7
43. Yin AA, He Y-L, Etcheverry A, Liu Y-H, Aubry M, Barnholtz-Sloan J, et al. Novel predictive epigenetic signature for temozolomide in non-G-CIMP glioblastomas. *Clin Epigenet* (2019) 11:76. doi: 10.1186/s13148-019-0670-9
44. Booth MJ, Ost TWB, Beraldi D, Bell NM, Branco MR, Reik W, et al. Oxidative bisulfite sequencing of 5-methylcytosine and 5- hydroxymethylcytosine. *Nat Protoc* (2013) 8:1841–51. doi: 10.1038/nprot.2013.115
45. Spruijt CG, Gnerlich F, Smits AH, Pfaffeneder T, Jansen PWTC, Bauer C, et al. Dynamic readers for 5-(Hydroxy)methylcytosine and its oxidized derivatives. *Cell* (2013) 152:1146–59. doi: 10.1016/j.cell.2013.02.004
46. Iurlaro M, Ficz G, Oxley D, Raiber EA, Bachman M, Booth MJ, et al. A screen for hydroxymethylcytosine and formylcytosine binding proteins suggests functions in transcription and chromatin regulation. *Genome Biol* (2013) 14. doi: 10.1186/gb-2013-14-10-r119
47. Jin S-G, Jiang Y, Qiu R, Rauch TA, Wang Y, Schackert G, et al. 5-Hydroxymethylcytosine Is Strongly Depleted in Human Cancers but Its Levels Do Not Correlate with IDH1 Mutations. (2011) 71:7360–5. doi: 10.1158/0008-5472.CAN-11-2023
48. Kraus T, Globisch D, Wagner M, Eigenbrod S, Widmann D, Münzel M, et al. Low values of 5-hydroxymethylcytosine (5hmC), the 'sixth base,' are

associated with anaplasia in human brain tumors. *Int J Cancer* (2012) 131:1577–90. doi: 10.1002/ijc.27429
49. Kraus T, Kolck G, Greiner A, Schierl K, Guibourt V, Kretzschmar HA, et al. Loss of 5-hydroxymethylcytosine and intratumoral heterogeneity as an epigenomic hallmark of glioblastoma. *Tumor Biol* (2015) 36:8439–46. doi: 10.1007/s13277-015-3606-9
50. Johnson KC, Houseman EA, King JE, Von Herrmann KM, Fadul CE, Christensen BC. 5-Hydroxymethylcytosine localizes to enhancer elements and is associated with survival in glioblastoma patients. *Nat Commun* (2016) 7:1–11. doi: 10.1038/ncomms13177
51. Fernandez AF, Bayó GF, Sierra MI, Urdinguio RG, Tora EG, García MG, et al. Loss of 5hmC identifies a new type of aberrant DNA hypermethylation in glioma. *Orig Artic Hum Mol Genet* (2018) 27:3046–59. doi: 10.1093/hmg/ddy214
52. Waha A, Müller T, Gessi M, Waha A, Isselstein LJ, Luxen D, et al. Nuclear exclusion of TET1 is associated with loss of 5- hydroxymethylcytosine in IDH1 wild-type gliomas. *Am J Pathol* (2012) 181:675–83. doi: 10.1016/j.ajpath.2012.04.017
53. Orr BA, Haffner MC, Nelson WG, Yegnasubramanian S, Eberhart CG. Decreased 5-Hydroxymethylcytosine is associated with neural progenitor phenotype in normal brain and shorter survival in malignant glioma. *PloS One* (2012) 7:e41036. doi: 10.1371/journal.pone.0041036
54. Glowacka WK, Jain H, Okura M, Maimaitiming A, Mamatjan Y, Nejad R, et al. 5-Hydroxymethylcytosine preferentially targets genes upregulated in isocitrate dehydrogenase 1 mutant high-grade glioma. *Acta Neuropathol* (2018) 135:617–34. doi: 10.1007/s00401-018-1821-3
55. Kohli RM, Zhang Y. TET enzymes, TDG and the dynamics of DNA demethylation. *Nature* (2013) 502:472–9. doi: 10.1038/nature12750
56. He YF, Li BZ, Li Z, Liu P, Wang Y, Tang Q, et al. Tet-mediated formation of 5-carboxylcytosine and its excision by TDG in mammalian DNA. *Science* (2011) 333:1303–7. doi: 10.1126/science.1169786
57. Dalton SR, Bellacosa A. DNA demethylation by TDG. *Epigenomics* (2012) 4:459–67. doi: 10.2217/epi.12.36
58. Otani J, Kimura H, Sharif J, Endo TA, Mishima Y. Cell Cycle-Dependent Turnover of 5-Hydroxymethyl Cytosine in Mouse Embryonic Stem Cells. *PloS One* (2013) 8:82961. doi: 10.1371/journal.pone.0082961
59. Fults D, Pedone CA, Thompson GE, Uchiyama CM, Gumpper KL, Iliev D, et al. Microsatellite deletion mapping on chromosome 10q and mutation analysis of MMAC1, FAS, and MXI1 in human glioblastoma multiforme. *Int J Oncol* (1998) 12:905–10. doi: 10.3892/ijo.12.4.905
60. Ichimura K, Ohgaki H, Kleihues P, Collins VP. Molecular pathogenesis of astrocytic tumours. *J Neurooncol* (2004) 70:137–60. doi: 10.1007/s11060-004-2747-2
61. Sonoda Y, Murakami Y, Tominaga T, Kayama T, Yoshimoto T, Sekiya T. Deletion Mapping of Chromosome 10 in Human Glioma. *Japan J Cancer Res* (1996) 87:363–7. doi: 10.1111/j.1349-7006.1996.tb00231.x
62. Chen B, Lei Y, Wang H, Dang Y, Fang P, Wang J, et al. Repression of the expression of TET2 by ZEB1 contributes to invasion and growth in glioma cells. *Mol Med Rep* (2017) 15:2625–32. doi: 10.3892/mmr.2017.6288
63. García MG, Carella A, Urdinguio RG, Bayón GF, Lopez V, Tejedor JR, et al. Epigenetic dysregulation of TET2 in human glioblastoma. *Oncotarget* (2018) 9:25922–34. doi: 10.18632/oncotarget.25406
64. Carella A, Tejedor JR, García MG, Urdinguio RG, Bayón GF, Sierra M, et al. Epigenetic downregulation of TET3 reduces genome-wide 5hmC levels and promotes glioblastoma tumorigenesis. *Int J Cancer* (2020) 146:373–87. doi: 10.1002/ijc.32520
65. Xu W, Yang H, Liu Y, Yang Y, Wang P, Kim SH, et al. Oncometabolite 2-hydroxyglutarate is a competitive inhibitor of α-ketoglutarate-dependent dioxygenases. *Cancer Cell* (2011) 19:17–30. doi: 10.1016/j.ccr.2010.12.014
66. Dang L, White DW, Gross S, Bennett BD, Bittinger MA, Driggers EM, et al. Cancer-associated IDH1 mutations produce 2-hydroxyglutarate. *Nature* (2009) 462:739–44. doi: 10.1038/nature08617
67. Cohen AL, Holmen SL, Colman H. IDH1 and IDH2 mutations in gliomas. *Curr Neurol Neurosci Rep* (2013) 13:345. doi: 10.1007/s11910-013-0345-4
68. Kim YH, Pierscianek D, Mittelbronn M, Vital A, Mariani L, Hasselblatt M, et al. TET2 promoter methylation in low-grade diffuse gliomas lacking IDH1/2 mutations. *J Clin Pathol* (2011) 64:850–2. doi: 10.1136/jclinpath-2011-200133
69. Kraus T, et al. Genetic characterization of ten-eleven-translocation methylcytosine dioxygenase alterations in human glioma. *J Cancer* (2015) 6:832–42. doi: 10.7150/jca.12010
70. Klose RJ, Kallin EM, Zhang Y. JmjC-domain-containing proteins and histone demethylation. *Nat Rev Genet* (2006) 7:715–27. doi: 10.1038/nrg1945
71. Martin C, Zhang Y. The diverse functions of histone lysine methylation. *Nat Rev Mol Cell Biol* (2005) 6:838–49. doi: 10.1038/nrm1761
72. Mosammaparast N, Shi Y. Reversal of Histone Methylation: Biochemical and Molecular Mechanisms of Histone Demethylases. *Annu Rev Biochem* (2010) 79:155–79. doi: 10.1146/annurev.biochem.78.070907.103946
73. Smith SMC, Kimyon RS, Watters JJ. Cell-type-specific Jumonji histone demethylase gene expression in the healthy rat CNS: Detection by a novel flow cytometry method. *ASN Neuro* (2014) 6:193–207. doi: 10.1042/AN20130050
74. Karuppagounder SS, Kumar A, Shao DS, Zille M, Bourassa MW, Caulfield JT, et al. Metabolism and epigenetics in the nervous system: Creating cellular fitness and resistance to neuronal death in neurological conditions via modulation of oxygen-, iron-, and 2-oxoglutarate-dependent dioxygenases. *Brain Res* (2015) 1628:273–87. doi: 10.1016/j.brainres.2015.07.030
75. Lee HY, Choi K, Oh H, Park YK, Park H. HIF-1-dependent induction of jumonji domain-containing protein (JMJD) 3 under hypoxic conditions. *Mol Cells* (2014) 37:43–50. doi: 10.14348/molcells.2014.2250
76. Liau BB, Sievers C, Donohue LK, Gillespie SM, Flavahan WA, Miller TE, et al. Adaptive Chromatin Remodeling Drives Glioblastoma Stem Cell Plasticity and Drug Tolerance. *Cell Stem Cell* (2017) 20:233–246.e7. doi: 10.1016/j.stem.2016.11.003
77. Li M, Cheng J, Ma Y, Guo H, Shu H, Huang H, et al. The histone demethylase JMJD2A promotes glioma cell growth via targeting Akt-mTOR signaling. *Cancer Cell Int* (2020) 20:101. doi: 10.1186/s12935-020-01177-z
78. Liu BL, Cheng JX, Zhang X, Wang R, Zhang W, Lin H, et al. Global histone modification patterns as prognostic markers to classify glioma patients. *Cancer Epidemiol Biomarkers Prev* (2010) 19:2888–96. doi: 10.1158/1055-9965.EPI-10-0454
79. Dai B, Hu Z, Huang H, Zhu G, Xiao Z, Wan W, et al. Overexpressed KDM5B is associated with the progression of glioma and promotes glioma cell growth via downregulating p21. *Biochem Biophys Res Commun* (2014) 454:221–7. doi: 10.1016/j.bbrc.2014.10.078
80. Banelli B, Carra E, Barbieri F, Würth R, Parodi F, Pattarozzi A, et al. The histone demethylase KDM5A is a key factor for the resistance to temozolomide in glioblastoma. *Cell Cycle* (2015) 14:3418–29. doi: 10.1080/15384101.2015.1090063
81. Staberg M, Rasmussen RD, Michaelsen SR, Pedersen H, Jensen KE, Villingshøj M, et al. Targeting glioma stem-like cell survival and chemoresistance through inhibition of lysine-specific histone demethylase KDM2B. *Mol Oncol* (2018) 12:406–20. doi: 10.1002/1878-0261.12174
82. Frescas D, Guardavaccaro D, Bassermann F, Koyama-Nasu R, Pagano M. JHDM1B/FBXL10 is a nucleolar protein that represses transcription of ribosomal RNA genes. *Nature* (2007) 450:309–13. doi: 10.1038/nature06255
83. Ene C, Edwards L, Riddick G, Baysan M, Woolard K, Kotliarova S, et al. Histone Demethylase Jumonji D3 (JMJD3) as a Tumor Suppressor by Regulating p53 Protein Nuclear Stabilization. *PloS One 7* (2012)7:e51407. doi: 10.1371/journal.pone.0051407
84. Lu C, Ward PS, Kapoor GS, Rohle D, Turcan S, Abdel-Wahab O, et al. IDH mutation impairs histone demethylation and results in a block to cell differentiation. *Nature* (2012) 483:474–8. doi: 10.1038/nature10860
85. Turcan S, Makarov V, Taranda J, Wang Y, Fabius AWM, Wu W, et al. Mutant-IDH1-dependent chromatin state reprogramming, reversibility, and persistence. *Nat Genet* (2018) 50:62–72. doi: 10.1038/s41588-017-0001-z
86. Chowdhury R, Yeoh KK, Tian YM, Hillringhaus L, Bagg EA, Rose NR, et al. The oncometabolite 2-hydroxyglutarate inhibits histone lysine demethylases. *Nat Publ Gr* (2011) 12:463–9. doi: 10.1038/embor.2011.43
87. Monteiro AR, Hill R, Pilkington GJ, Madureira PA. The role of hypoxia in glioblastoma invasion. *Cells* (2017) 6:45–64. doi: 10.3390/cells6040045
88. Spence AM, Muzi M, Swanson KR, O'Sullivan F, Rockhill JK, Rajendran JG, et al. Regional hypoxia in glioblastoma multiforme quantified with [18F] fluoromisonidazole positron emission tomography before radiotherapy:

Correlation with time to progression and survival. *Clin Cancer Res* (2008) 14:2623–30. doi: 10.1158/1078-0432.CCR-07-4995
89. Kaynar MY, Sanus GZ, Hnimoglu H, Kacira T, Kemerdere R, Atukeren P, et al. Expression of hypoxia inducible factor-1α in tumors of patients with glioblastoma multiforme and transitional meningioma. *J Clin Neurosci* (2008) 15:1036–42. doi: 10.1016/j.jocn.2007.07.080
90. Jensen RL. Brain tumor hypoxia: tumorigenesis, angiogenesis, imaging, pseudoprogression, and as a therapeutic target. *J Neuro-oncol Neurooncol* (2009) 92:317–35. doi: 10.1007/s11060-009-9827-2
91. Semenza GL. Defining the role of hypoxia-inducible factor 1 in cancer biology and therapeutics. *Oncogene* (2010) 29:625–34. doi: 10.1038/onc.2009.441
92. Ivan M, Kondo K, Yang H, Kim W, Valiando J, Ohh M, et al. HIFα targeted for VHL-mediated destruction by proline hydroxylation: Implications for O2 sensing. *Science* (2001) 292:464–8. doi: 10.1126/science.1059817
93. Mahon PC, Hirota K, Semenza GL. FIH-1: A novel protein that interacts with HIF-1α and VHL to mediate repression of HIF-1 transcriptional activity. *Genes Dev* (2001) 15:2675–86. doi: 10.1101/gad.924501
94. Hewitson KS, McNeill LA, Riordan MV, Tian Y-M, Bullock AN, Welford RW, et al. Hypoxia-inducible Factor (HIF) Asparagine Hydroxylase Is Identical to Factor Inhibiting HIF (FIH) and Is Related to the Cupin Structural Family*. (2002)277:26351–5. doi: 10.1074/jbc.C200273200
95. Jaakola P, Mole DR, Tian Y, Wilson MI, Gielbery J, Gaskell, et al. Targeting of HIF-alpha to to the von Hippel–Lindau Ubiquitylation Complex by O2-Regulated Prolyl Hydroxylation. *Science* (2001) 292:468–72. doi: 10.1126/science.1059817
96. Kaelin WG, Ratcliffe PJ. Oxygen Sensing by Metazoans: The Central Role of the HIF Hydroxylase Pathway. *Mol Cell* (2008) 30:393–402. doi: 10.1016/j.molcel.2008.04.009
97. Schödel J, Oikonomopoulos S, Ragoussis J, Pugh CW, Ratcliffe PJ, Mole DR. High-resolution genome-wide mapping of HIF-binding sites by ChIP-seq. *Blood* (2011) 117. doi: 10.1182/blood-2010-10-314427
98. Semenza GL. Hypoxia-inducible factors: Mediators of cancer progression and targets for cancer therapy. *Trends Pharmacol Sci* (2012) 33:207–14. doi: 10.1016/j.tips.2012.01.005
99. Mole DR, Blancher C, Copley RR, Pollard PJ, Gleadle JM, Ragousis J, et al. Genome-wide association of hypoxia-inducible factor (HIF)-1α and HIF-2α DNA binding with expression profiling of hypoxia-inducible transcripts. *J Biol Chem* (2009) 284:16767–75. doi: 10.1074/jbc.M901790200
100. Semenza GL, Rue EA, Iyer NV, Pang MG, Kearns WG. Assignment of the hypoxia-inducible factor 1α gene to a region of conserved synteny on mouse chromosome 12 and human chromosome 14q. *Genomics* (1996) 34:437–9. doi: 10.1006/geno.1996.0311
101. https://www.ensembl.org/index.html?redirect=no. (Accessed on 26/02/2021).
102. Maxwell PH, Dachs GU, Gleadle JM, Nicholls LG, Harris AL, Stratford IJ, et al. Hypoxia-inducible factor-1 modulates gene expression in solid tumors and influences both angiogenesis and tumor growth. *Proc Natl Acad Sci U S A* (1997) 94:8104–9. doi: 10.1073/pnas.94.15.8104
103. Dachs GU, Patterson AV, Firth JD, Ratcliffe PJ, Stuart Townsend KM, Stratford IJ, et al. Targeting gene expression to hypoxic tumor cells. *Nat Med* (1997) 3:515–20. doi: 10.1038/nm0597-515
104. Wenger RH, Grassmann M. Molecular Biology of Hypoxia-Inducible Factor-1. *Mol Biol Hematopoiesis* (1999) pp:269–77. doi: 10.1007/978-1-4615-4797-6_34
105. Keith B, Johnson RS, Simon MC. HIF1 α and HIF2 α: sibling rivalry in hypoxic tumour growth and progression. *Nat Rev Cancer* (2012) 12:9–22. doi: 10.1038/nrc3183
106. Smythies JA, Sun M, Masson N, Salama R, Simpson PD, Murray E, et al. Inherent DNA binding specificities of the HIF-1α and HIF-2α transcription factors in chromatin. *EMBO Rep* (2019) 20. doi: 10.15252/embr.201846401
107. Majmundar AJ, Wong WJ, Simon MC. Hypoxia-inducible factors and the response to hypoxic stress. *Mol Cell* (2010) 2:294–309. doi: 10.1016/j.molcel.2010.09.022
108. Chowdhury R, Hardy A, Schofield CJ. The human oxygen sensing machinery and its manipulation. *Chem Soc Rev* (2008) 37:1308–19. doi: 10.1039/b701676j
109. Choudhry H, Harris AL. Advances in Hypoxia-Inducible Factor Biology. *Cell Metab* (2018) 27:281–98. doi: 10.1016/j.cmet.2017.10.005
110. Jensen RL. Hypoxia in the tumorigenesis of gliomas and as a potential target for therapeutic measures. *Neurosurg Focus* (2006) 20:E24. doi: 10.3171/foc.2006.20.4.16
111. Korkolopoulou P, Patsouris E, Konstantinidou AE, Pavlopoulos PM, Kavantzas N, Boviatsis E, et al. Hypoxia-inducible factor 1a/vascular endothelial growth factor axis in astrocytomas. Associations with microvessel morphometry, proliferation and prognosis. *Neuropathol Appl Neurobiol* (2004) 30:267–78. doi: 10.1111/j.1365-2990.2003.00535.x
112. Chen W, Cheng X, Wang X, Wang J, Wen X, Xie C, et al. Clinical implications of hypoxia-inducible factor-1alpha and caveolin-1 overexpression in isocitrate dehydrogenase-wild type glioblastoma multiforme. *Oncol Lett* (2019) 17:2867–73. doi: 10.3892/ol.2019.9929
113. Zagzag D, Zhong H, Scalzitti JM, Laughner E, Simons JW, Semenza GL. Expression of hypoxia-inducible factor 1α in brain tumors: Association with angiogenesis, invasion, and progression. *Cancer* (2000) 88:2606–18. doi: 10.1002/1097-0142(20000601)88:11<2606::AID-CNCR25>3.0.CO;2-W
114. Lo Dico A, Martelli C, Diceglie C, Lucignani G, Ottobrini L. Hypoxia-Inducible Factor-1alpha Activity as a Switch for Glioblastoma Responsiveness to Temozolomide. *Front Oncol* (2018) 8:249. doi: 10.3389/fonc.2018.00249
115. Jensen RL, Ragel BT, Whang K, Gillespie D. Inhibition of hypoxia inducible factor-1a (HIF-1a) decreases vascular endothelial growth factor (VEGF) secretion and tumor growth in malignant gliomas. *J Neurooncol* (2006) 78:233–47. doi: 10.1007/s11060-005-9103-z
116. Brat DJ, Castellano-Sanchez AA, Hunter SB, Pecot M, Cohen C, Hammond EH, et al. Pseudopalisades in Glioblastoma Are Hypoxic, Express Extracellular Matrix Proteases, and Are Formed by an Actively Migrating Cell Population. *Cancer Res* (2004) 64:920–7. doi: 10.1158/0008-5472.CAN-03-2073
117. Renfrow JJ, Soike MH, Debinski W, Ramkissoon SH, Mott RT, Frenkel MB, et al. Hypoxia-inducible factor 2α: A novel target in gliomas. *Future Med Chem* (2018) 10:2227–36. doi: 10.4155/fmc-2018-0163
118. Yu F, White SB, Zhao Q, Lee FS. HIF-1α binding to VHL is regulated by stimulus-sensitive proline hydroxylation. *Proc Natl Acad Sci U S A* (2001) 98:9630–5. doi: 10.1073/pnas.181341498
119. Lando D, Peet DJ, Gorman JJ, Whelan DA, Whitelaw ML, Bruick RK. FIH-1 is an asparaginyl hydroxylase enzyme that regulates the transcriptional activity of hypoxia-inducible factor. *Genes Dev* (2002) 16:1466–71. doi: 10.1101/gad.991402
120. Rodriguez J, Haydinger CHD, Peet DJ, Nguyen L, von Kriegsheim A. Asparagine hydroxylation is a reversible post-translational modification. *Mol Cell Proteomics* (2020) 13:1777–89. doi: 10.1101/2020.03.22.002436
121. McNeill LA, Flashman E, Buck MRG, Hewitson KS, Clifton IJ, Jeschke G, et al. Hypoxia-inducible factor prolyl hydroxylase 2 has a high affinity for ferrous iron and 2-oxoglutarate. *Mol Biosyst* (2005) 1:321–4. doi: 10.1039/b511249b
122. McDonough MA, Li V, Flashman E, Chowdhury R, Mohr C, R Lié nard BM, et al. Cellular oxygen sensing: Crystal structure of hypoxia-inducible factor prolyl hydroxylase (PHD2). *Proc Natl Acad Sci USA* (2006) 103:9814–9. doi: 10.1073/pnas.0601283103
123. Berra E, Benizri E, Ginouvès A, Volmat V, Roux D, Pouysségur J. HIF prolyl-hydroxylase 2 is the key oxygen sensor setting low steady-state levels of HIF-1α in normoxia. *EMBO J* (2003) 22:4082–90. doi: 10.1093/emboj/cdg392
124. Metzen E, Berchner-Pfannschmidt U, Stengel P, Marxsen JH, Stolze I, Klinger M, et al. Intracellular localisation of human HIF-1α hydroxylases: Implications for oxygen sensing. *J Cell Sci* (2003) 116:1319–26. doi: 10.1242/jcs.00318
125. Ježek P. 2-hydroxyglutarate in cancer cells. *Antioxid Redox Signaling* (2020) 33:903–26. doi: 10.1089/ars.2019.7902
126. Losman J-A, Koivunen P, Kaelin WG. 2-Oxoglutarate-dependent dioxygenases in cancer. *Nat Rev Cancer* (2020) 20:710–26. doi: 10.1038/s41568-020-00303-3
127. Koivunen P, Lee S, Duncan CG, Lopez G, Lu G, Ramkissoon S, et al. Transformation by the (R)-enantiomer of 2-hydroxyglutarate linked to EGLN activation. *Nature* (2012) 483:484–8. doi: 10.1038/nature10898
128. Williams SC, Karajannis MA, Chiriboga L, Golfinos JG, Von Deimling A, Zagzag D, et al. R132H-mutation of isocitrate dehydrogenase-1 is not sufficient for HIF-1α upregulation in adult glioma. *Acta Neuropathol* (2011). doi: 10.1007/s00401-010-0790-y

129. Womeldorff M, Gillespie D, Jensen RL. Hypoxia-inducible factor-1 and associated upstream and downstream proteins in the pathophysiology and management of glioblastoma. *Neurosurg Focus* (2014) 37:1–17. doi: 10.3171/2014.9.FOCUS14496
130. Rhodes DR, Yu J, Shanker K, Deshpande N, Varambally R, Ghosh D, et al. ONCOMINE: A Cancer Microarray Database and Integrated Data-Mining Platform. *Neoplasia* (2004) 6:1–6. doi: 10.1016/S1476-5586(04)80047-2
131. Wang E, Zhang C, Polavaram N, Liu F, Wu G, Schroeder MA, et al. The Role of Factor Inhibiting HIF (FIH-1) in Inhibiting HIF-1 Transcriptional Activity in Glioblastoma Multiforme. *PloS One* (2014) 9:e86102. doi: 10.1371/journal.pone.0086102
132. Feng J, Zhang Y, She X, Sun Y, Fan L, Ren X, et al. Hypermethylated gene ANKDD1A is a candidate tumor suppressor that interacts with FIH1 and decreases HIF1α stability to inhibit cell autophagy in the glioblastoma multiforme hypoxia microenvironment. *Oncogene* (2019) 38:103–19. doi: 10.1038/s41388-018-0423-9
133. Kuiper C, Vissers MCM. Ascorbate as a cofactor for Fe-and 2-oxoglutarate dependent dioxygenases: Physiological activity in tumour growth and progression. *Front Oncol* (2014) 4:359. doi: 10.3389/fonc.2014.00359
134. Rebouche, Charles J. Ascorbic acid and carnitine biosynthesis. *Am J Clin Nutr* (1991) 54:1147S–52S. doi: 10.1093/ajcn/54.6.1147s
135. Hirsilä M, Koivunen P, Günzler V, Kivirikko KII, Myllyharju J. Characterization of the human prolyl 4-hydroxylases that modify the hypoxia-inducible factor. *J Biol Chem* (2003) 278:30772–80. doi: 10.1074/jbc.M304982200
136. Myllyharju J, Kivirikko KII. Characterization of the iron- and 2-oxoglutavate binding sites of human prolyl 4-hydroxylase. *EMBO J* (1997) 16:1173–80. doi: 10.1093/emboj/16.6.1173
137. Ortiz-Prado E, Dunn JF, Vasconez J, Castillo D, Viscor G. Partial pressure of oxygen in the human body: a general review. *Am J Blood Res* (2019) 9:1–14.
138. Charbel FT, Hoffman WE, Misra M, Hannigan K, Ausman JII. Cerebral interstitial tissue oxygen tension, pH, HCO3, CO2. *Surg Neurol* (1997) 48:414–7. doi: 10.1016/S0090-3019(96)00473-9
139. Baker NA. A galvanic cell suitable for monitoring cortical oxygen in man. *Med Biol Eng* (1975) 13:443–9. doi: 10.1007/BF02477117
140. Hoffman WE, Charbel FT, Edelman G. Brain tissue oxygen, carbon dioxide, and pH in neurosurgical patients at risk for ischemia. *Anesth Analg* (1996) 82:582–6. doi: 10.1213/00000539-199603000-00027
141. Assad F, Schultheiss R, Leniger-Follert E, Wüllenweber R. Measurement of Local Oxygen Partial Pressure (PO2) of the Brain Cortex in Cases of Brain Tumors. Berlin, Heidelberg: Springer (1984), 263–70. doi: 10.1007/978-3-642-69360-1_45
142. Meixensberger J, Dings J, Kuhnigk H, Roosen K. Studies of tissue PO2 in normal and pathological human brain cortex. *Acta Neurochir Suppl (Wien)* (1993) 59:58–63. doi: 10.1007/978-3-7091-9302-0_10
143. Dings J, Meixensberger J, Jäger A, Roosen K. Clinical Experience with 118 Brain Tissue Oxygen Partial Pressure Catheter Probes. *Neurosurgery* (1998) 43:1082–94. doi: 10.1097/00006123-199811000-00045
144. Vaupel P, Höckel M, Mayer A. Detection and characterization of tumor hypoxia using pO2 histography. *Antioxid Redox Signaling* (2007) 9:1221–35. doi: 10.1089/ars.2007.1628
145. Rampling R, Cruickshank G, Lewis AD, Fitzsimmons SA, Workman P. Direct measurement of pO2 distribution and bioreductive enzymes in human malignant brain tumors. *Radiat Oncol Biol Phys* (1994) 29:427–31. doi: 10.1016/0360-3016(94)90432-4
146. Qian Y, Von Eyben R, Liu Y, Chin FT, Miao Z, Apte S, et al. 18F-EF5 PET-based Imageable Hypoxia Predicts Local Recurrence in Tumors Treated With Highly Conformal Radiation Therapy. *Int J Radiat Oncol Biol Phys* (2018) 102:1183–92. doi: 10.1016/j.ijrobp.2018.06.287
147. Valk PE, Mathis CA, Prados M, Gilbert JC, Budinger TF. Hypoxia in human gliomas: Demonstration by PET with fluorine-18-fluoromisonidazole. *Artic J Nucl Med* (1993) 33:2133–7.
148. Evans SM, Jenkins KW, Chen HI, Jenkins WT, Judy KD, Hwang WT, et al. The relationship among hypoxia, proliferation, and outcome in patients with de nouo glioblastoma: A pilot study. *Transl Oncol* (2010) 3:160–9. doi: 10.1593/tlo.09265
149. Koch CJ. Measurement of absolute oxygen levels in cells and tissues using oxygen sensors and 2-nitroimidazole EF5. *Methods Enzymol* (2002) 352:3–31. doi: 10.1016/S0076-6879(02)52003-6
150. Collingridge DR, Piepmeier JM, Rockwell S, Knisely JPS. Polarographic measurements of oxygen tension in human glioma and surrounding peritumoural brain tissue. *Radiother Oncol* (1999) 53:127–31. doi: 10.1016/S0167-8140(99)00121-8
151. Kaur B, Khwaja FW, Severson EA, Matheny SL, Brat DJ, Van Meir EG, et al. Hypoxia and the hypoxia-inducible-factor pathway in glioma growth and angiogenesis. *Neuro Oncol* (2005) 7:134–53. doi: 10.1215/S1152851704001115
152. Cruickshank GS, Rampling R. Peri-tumoural hypoxia in human brain: peroperative measurement of the tissue oxygen tension around malignant brain tumours. *Acta Neurochir Suppl (Wien)* (1994) 60:375–7. doi: 10.1007/978-3-7091-9334-1_101
153. Stępień K, Ostrowski RP, Matyja E. Hyperbaric oxygen as an adjunctive therapy in treatment of malignancies, including brain tumours. *Med Oncol* (2016) 33:1–9. doi: 10.1007/s12032-016-0814-0
154. Miralbell R, Mornex F, Greiner R, Bolla M, Storme G, Hulshof M, et al. Accelerated radiotherapy, carbogen, and nicotinamide in glioblastoma multiforme: Report of European Organization for Research and Treatment of Cancer Trial 22933. *J Clin Oncol* (1999) 17:3143–9. doi: 10.1200/JCO.1999.17.10.3143
155. Gainer JL, Sheehan JP, Larner JM, Jones DR. Trans sodium crocetinate with temozolomide and radiation therapy for glioblastoma multiforme. *J Neurosurg* (2017) 126:460–6. doi: 10.3171/2016.3.JNS152693
156. Bindra RS, Chalmers AJ, Evans S, Dewhirst M. GBM radiosensitizers: dead in the water…or just the beginning? *J Neuro-Oncol* (2017) 134:513–21. doi: 10.1007/s11060-017-2427-7
157. Mudassar F, Shen H, O'Neill G, Hau E. Targeting tumor hypoxia and mitochondrial metabolism with anti-parasitic drugs to improve radiation response in high-grade gliomas. *J Exp Clin Cancer Res* (2020) 39:1–17. doi: 10.1186/s13046-020-01724-6
158. Balss J, Meyer J, Mueller W, Korshunov A, Hartmann C, Von Deimling A. Analysis of the IDH1 codon 132 mutation in brain tumors. *Acta Neuropathol* (2008) 116:597–602. doi: 10.1007/s00401-008-0455-2
159. Bleeker FE, Lamba S, Leenstra S, Troost D, Hulsebos T, Vandertop WP, et al. IDH1 mutations at residue p.R132 (IDH1R132) occur frequently in high-grade gliomas but not in other solid tumors. *Hum Mutat* (2009) 30:7–11. doi: 10.1002/humu.20937
160. Fan J, Teng X, Liu L, Mattaini KR, Looper RE, Vander Heiden MG, et al. Human phosphoglycerate dehydrogenase produces the oncometabolite D-2-hydroxyglutarate. *ACS Chem Biol* (2015) 10:510–6. doi: 10.1021/cb500683c
161. Terunuma A, Putluri N, Mishra P, Mathé EA, Dorsey TH, Yi M, et al. MYC-driven accumulation of 2-hydroxyglutarate is associated with breast cancer prognosis. *J Clin Invest* (2014) 124:398–412. doi: 10.1172/JCI71180
162. MellinghoffI, Maher E, Wen P, Cloughesy T, Peters K, Choi C, et al. A phase 1, multicenter, randomized, openlabel, perioperative study of ag-120 (ivosidenib) and AG-881 in patients with recurrent, nonenhancing, IDH1-mutant, low-grade glioma. *Neuro Oncol* (2018). doi: 10.1093/neuonc/noy148.973
163. Fan B, Mellinghoff IK, Wen PY, Lowery MA, Goyal L, Tap WD, et al. Clinical pharmacokinetics and pharmacodynamics of ivosidenib, an oral, targeted inhibitor of mutant IDH1, in patients with advanced solid tumors. *Invest New Drugs* (2020) 38:433–44. doi: 10.1007/s10637-019-00771-x
164. Natsume A, Wakabayashi T, Miyakita Y, Narita Y, Mineharu Y, Arakawa Y, et al. Phase I study of a brain penetrant mutant IDH1 inhibitor DS-1001b in patients with recurrent or progressive IDH1 mutant gliomas. *J Clin Oncol* (2019) 15:2004. doi: 10.1200/jco.2019.37.15_suppl.2004
165. Karpel-Massler G, Nguyen TTT, Shang E, Siegelin MD. Novel IDH1-Targeted Glioma Therapies. *CNS Drugs* (2019) 33:1155–66. doi: 10.1007/s40263-019-00684-6
166. Han S, Liu Y, Cai SJ, Qian M, Ding J, Larion M, et al. IDH mutation in glioma: molecular mechanisms and potential therapeutic targets. *Br J Cancer* (2020) 122:1580–9. doi: 10.1038/s41416-020-0814-x
167. Urban DJ, Martinez NJ, Davis MI, Brimacombe KR, Cheff DM, Lee TD, et al. Assessing inhibitors of mutant isocitrate dehydrogenase using a suite of

pre-clinical discovery assays. *Sci Rep* (2017) 7:12758. doi: 10.1038/s41598-017-12630-x
168. Nakagawa M, Nakatani F, Matsunaga H, Seki T, Endo M, Ogawara Y, et al. Selective inhibition of mutant IDH1 by DS-1001b ameliorates aberrant histone modifications and impairs tumor activity in chondrosarcoma. *Oncogene* (2019) 38:6835–49. doi: 10.1038/s41388-019-0929-9
169. Nicolay B, Narayanaswamy R, Amatangelo MD, Aguado E, Nagaraja R, Murtie J, et al. EXTH-34. Combined use of the pan IDH mutant inhibitor AG-881 with radiation therapy shoes added benefit in an orthotopic IDH1 mutant glioma model in vivo. *Neuro Oncol* (2017) 19: vi79. doi: 10.1093/neuonc/nox168.326
170. Pusch S, Krausert S, Fischer V, Balss J, Ott M, Schrimpf D, et al. Pan-mutant IDH1 inhibitor BAY 1436032 for effective treatment of IDH1 mutant astrocytoma in vivo. *Acta Neuropathol* (2017) 133:629–44. doi: 10.1007/s00401-017-1677-y
171. Schumacher T, Bunse L, Pusch S, Sahm F, Wiestler B, Quandt J, et al. A vaccine targeting mutant IDH1 induces antitumour immunity. *Nature* (2014) 512:324–7. doi: 10.1038/nature13387
172. Pellegatta S, Valletta L, Corbetta C, Patanè M, Zucca I, Riccardi Sirtori F, et al. Effective immuno-targeting of the IDH1 mutation R132H in a murine model of intracranial glioma. *Acta Neuropathol Commun* (2015) 3:4. doi: 10.1186/s40478-014-0180-0
173. Ward RJ, Zucca FA, Duyn JH, Crichton RR, Zecca L. The role of iron in brain ageing and neurodegenerative disorders. *Lancet Neurol* (2014) 13:1045–60. doi: 10.1016/S1474-4422(14)70117-6
174. Bradbury MW. Transport of iron in the blood-brain-cerebrospinal fluid system. *J Neurochem* (1997) 69:443–54. doi: 10.1046/j.1471-4159.1997.69020443.x
175. Berg D, Hochstrasser H. Iron metabolism in parkinsonian syndromes. *Mov Disord* (2006) 21:1299–310. doi: 10.1002/mds.21020
176. Beydoun R, Hamood MA, Gomez Zubieta DM, Kondapalli KC. Na+/H+ Exchanger 9 Regulates Iron Mobilization at the Blood-Brain Barrier in Response to Iron Starvation *. (2017) 292:4293–301. doi: 10.1074/jbc.M116.769240
177. McCarthy RC, Kosman DJ. Glial Cell Ceruloplasmin and Hepcidin Differentially Regulate Iron Efflux from Brain Microvascular Endothelial Cells. *PloS One* (2014) 9:89003. doi: 10.1371/journal.pone.0089003
178. Du F, Qian C, Ming Qian Z, Wu X-M, Xie H, Yung W-H, et al. Hepcidin directly inhibits transferrin receptor 1 expression in astrocytes via a cyclic AMP-protein kinase a pathway. *Glia* (2011)59:936–45. doi: 10.1002/glia.21166
179. Duck KA, Simpson IA, Connor JR. Regulatory mechanisms for iron transport across the blood-brain barrier. *Biochem Biophys Res Commun* (2017) 494:70–5. doi: 10.1016/j.bbrc.2017.10.083
180. Torti SV, Torti FM. Cellular iron metabolism in prognosis and therapy of breast cancer. *Crit Rev Oncog* (2013) 18:435–48. doi: 10.1615/CritRevOncog.2013007784
181. Khan AII, Liu J, Dutta P. Iron transport kinetics through blood-brain barrier endothelial cells. *Biochim Biophys Acta Gen Subj* (2018) 1862:1168–79. doi: 10.1016/j.bbagen.2018.02.010
182. Malecki EA, Devenyi AG, Beard JL, Connor JR. Existing and emerging mechanisms for transport of iron and manganese to the brain. *J Neurosci Res* (1999) 56:113–22. doi: 10.1002/(SICI)1097-4547(19990415)56:2<113::AID-JNR1>3.0.CO;2-K
183. Qian ZM, Ke Y. Brain iron transport. *Biol Rev* (2019) 94:1672–84. doi: 10.1111/brv.12521
184. Cabantchik ZII. Labile iron in cells and body fluids: physiology, pathology, and pharmacology. *Front Pharmacol* (2014) 5:45. doi: 10.3389/fphar.2014.00045
185. McCarthy RC, Kosman DJ. Iron transport across the blood-brain barrier: Development, neurovascular regulation and cerebral amyloid angiopathy. *Cell Mol Life Sci* (2015) 72:709–27. doi: 10.1007/s00018-014-1771-4
186. McCarthy RC, Kosman DJ. Ferroportin and exocytoplasmic ferroxidase activity are required for brain microvascular endothelial cell iron efflux. *J Biol Chem* (2013) 288:17932–40. doi: 10.1074/jbc.M113.455428
187. Wu LJC, Leenders AGM, Cooperman S, Meyron-Holtz E, Smith S, Land W, et al. Expression of the iron transporter ferroportin in synaptic vesicles and the blood-brain barrier. *Brain Res* (2004) 1001:108–17. doi: 10.1016/j.brainres.2003.10.066
188. Weston C, Klobusicky J, Weston J, Connor J, Toms SA, Marko NF. Aberrations in the Iron Regulatory Gene Signature Are Associated with Decreased Survival in Diffuse Infiltrating Gliomas. *PloS One* (2016) 11: e0166593. doi: 10.1371/journal.pone.0166593
189. Legendre C, Garcion E. Iron metabolism: a double-edged sword in the resistance of glioblastoma to therapies. *Trends Endocrinol Metab* (2015) 26:322–31. doi: 10.1016/j.tem.2015.03.008
190. Magri S, Pinton L, Masetto E, Cassandro S, Pozzuoli A, Belluzzi E, et al. Role of iron metabolism in the immunosuppression mediated by myeloid cells in glioblastoma patients. *Ann Oncol* (2019) 30:xi56. doi: 10.1093/annonc/mdz452.029
191. Vela D. Hepcidin, an emerging and important player in brain iron homeostasis. *J Trans Med* (2018) 16:25. doi: 10.1186/s12967-018-1399-5
192. Schonberg DL, Miller TE, Wu Q, Flavahan WA, Das NK, Hale JS, et al. Preferential Iron Trafficking Characterizes Glioblastoma Stem-like Cells. *Cancer Cell* (2015) 28:441–55. doi: 10.1016/j.ccell.2015.09.002
193. Flashman E, Davies SL, Yeoh KK, Schofield CJ. Investigating the dependence of the hypoxia-inducible factor hydroxylases (factor inhibiting HIF and prolyl hydroxylase domain 2) on ascorbate and other reducing agents. *Biochem J* (2010) 427:135–42. doi: 10.1042/BJ20091609
194. Minor EA, Court BL, Young JII, Wang G. Ascorbate induces ten-eleven translocation (Tet) methylcytosine dioxygenase-mediated generation of 5-hydroxymethylcytosine. *J Biol Chem* (2013) 288:13669–74. doi: 10.1074/jbc.C113.464800
195. Harrison FE, May JM. Vitamin C function in the brain: vital role of the ascorbate transporter SVCT2. *Free Radic Biol Med* (2009) 46:719–30. doi: 10.1016/j.freeradbiomed.2008.12.018
196. Figueroa-Méndez R, Rivas-Arancibia S. Vitamin C in health and disease: Its role in the metabolism of cells and redox state in the brain. *Front Physiol* (2015) 6. doi: 10.3389/fphys.2015.00397
197. Hornig D. Distribution of ascorbic acid, metabolites and analogues in man and animals. (1975) 258:103–18. doi: 10.1111/j.1749-6632.1975.tb29271.x
198. Nualart F. Vitamin C Transporters, Recycling and the Bystander Effect in the Nervous System: SVCT2 versus Gluts. *J Stem Cell Res Ther* (2014) 04:209. doi: 10.4172/2157-7633.1000209
199. Landolt H, Langemann H, Probst A, Gratzl O. Levels of water-soluble antioxidants in astrocytoma and in adjacent tumor-free tissue. *J Neurooncol* (1994) 21:127–33. doi: 10.1007/BF01052896
200. Blaschke K, Ebata KT, Karimi MM, Zepeda-Martínez JA, Goyal P, Mahapatra S, et al. Vitamin C induces Tet-dependent DNA demethylation and a blastocyst-like state in ES cells. *Nature* (2013) 500:222–6. doi: 10.1038/nature12362
201. Hore TA, Von Meyenn F, Ravichandran M, Bachman M, Ficz G, Oxley D, et al. Retinol and ascorbate drive erasure of Epigenetic memory and enhance reprogramming to naïve pluripotency by complementary mechanisms. *Proc Natl Acad Sci USA* (2016) 113:12202–7. doi: 10.1073/pnas.1608679113
202. Gillberg L, Ørskov AD, Nasif A, Ohtani H, Madaj Z, Hansen JW, et al. Oral vitamin C supplementation to patients with myeloid cancer on azacitidine treatment: Normalization of plasma vitamin C induces epigenetic changes. *Clin Epigenet* (2019) 11:143. doi: 10.1186/s13148-019-0739-5
203. Peng D, Ge G, Gong Y, Zhan Y, He S, Guan B, et al. Vitamin C increases 5-hydroxymethylcytosine level and inhibits the growth of bladder cancer. *Clin Epigenet* (2018) 10. doi: 10.1186/s13148-018-0527-7
204. Cimmino L, Dolgalev I, Wang Y, Yoshimi A, Martin GH, Wang J, et al. Restoration of TET2 Function Blocks Aberrant Self-Renewal and Leukemia Progression. *Cell* (2017) 170:1079–1095.e20 doi: 10.1016/j.cell.2017.07.032.
205. Das AB, Kakadia PM, Wojcik D, Pemberton L, Browett PJ, Bohlander SK, et al. Clinical remission following ascorbate treatment in a case of acute myeloid leukemia with mutations in TET2 and WT1. *Blood Cancer J* (2019) 9:82. doi: 10.1038/s41408-019-0242-4
206. Gerecke C, Schumacher F, Berndzen A, Homann T, Kleuser B. Vitamin C in combination with inhibition of mutant IDH1 synergistically activates TET enzymes and epigenetically modulates gene silencing in colon cancer cells. *Epigenetics* (2020) 15:307–22. doi: 10.1080/15592294.2019.1666652
207. Mingay M, Chaturvedi A, Bilenky M, Cao Q, Jackson L, Hui T, et al. Vitamin C-induced epigenomic remodelling in IDH1 mutant acute myeloid leukaemia. *Leukemia* (2018) 32:11–20. doi: 10.1038/leu.2017.171

208. Wang T, Chen K, Zeng X, Yang J, Wu Y, Shi X, et al. The histone demethylases Jhdm1a/1b enhance somatic cell reprogramming in a vitamin-C-dependent manner. *Cell Stem Cell* (2011) 9:575–87. doi: 10.1016/j.stem.2011.10.005
209. Ebata KT, Mesh K, Liu S, Bilenky M, Fekete A, Acker MG, et al. Vitamin C induces specific demethylation of H3K9me2 in mouse embryonic stem cells via Kdm3a/b. *Epigenet Chromatin* (2017) 10:36. doi: 10.1186/s13072-017-0143-3
210. Song MH, Nair VS, Oh KII. Vitamin C enhances the expression of IL17 in a Jmjd2-dependent manner. *BMB Rep* (2017) 50:49–54. doi: 10.5483/BMBRep.2017.50.1.193
211. Chung TL, Brena RM, Kolle G, Grimmond SM, Berman BP, Laird PW, et al. Vitamin C promotes widespread yet specific DNA demethylation of the epigenome in human embryonic stem cells. *Stem Cells* (2010) 28:1848–55. doi: 10.1002/stem.493
212. Kuiper C, Dachs GU, Currie MJ, Vissers MCM. Intracellular ascorbate enhances hypoxia-inducible factor (HIF)-hydroxylase activity and preferentially suppresses the HIF-1 transcriptional response. *Free Radic Biol Med* (2014) 69:308–17. doi: 10.1016/j.freeradbiomed.2014.01.033
213. Dachs G, Campbell EJ, Vissers MC. Ascorbate availability affects tumor implantation-take rate and increases tumor rejection in gulo-/- mice. *Hypoxia* (2016) 4:41. doi: 10.2147/HP.S103088
214. Jóźwiak P, Ciesielski P, Zaczek A, Lipińska A, Pomorski L, Wieczorek M, et al. Expression of hypoxia inducible factor 1α and 2α and its association with Vitamin C level in thyroid lesions. *J Biomed Sci* (2017) 24:83. doi: 10.1186/s12929-017-0388-y
215. Wohlrab C, Kuiper C, Vissers MCM, Phillips E, Robinson BA, Dachs GU. Ascorbate modulates the hypoxic pathway by increasing intracellular activity of the HIF hydroxylases in renal cell carcinoma cells. *Hypoxia* (2019) 7:17–31. doi: 10.2147/HP.S201643
216. Campbell EJ, Vissers MCM, Bozonet S, Dyer A, Robinson BA, Dachs GU. Restoring physiological levels of ascorbate slows tumor growth and moderates HIF-1 pathway activity in Gulo $^{-/-}$ mice. *Cancer Med* (2015) 4:303–14. doi: 10.1002/cam4.349
217. Kuiper C, Molenaar IG, Dachs GU, Currie MJ, Sykes PH, Vissers MCM. Low ascorbate levels are associated with increased hypoxia-inducible factor-1 activity and an aggressive tumor phenotype in endometrial cancer. *Cancer Res* (2010) 70:5749–58. doi: 10.1158/0008-5472.CAN-10-0263
218. Kuiper C, Dachs GU, Munn D, Currie MJ, Robinson BA, Pearson JF, et al. Increased tumor ascorbate is associated with extended disease-free survival and decreased hypoxia-inducible factor-1 activation in human colorectal cancer. *Front Oncol* (2014) 4:10. doi: 10.3389/fonc.2014.00010
219. Wohlrab C, Vissers MCM, Phillips E, Morrin HR, Robinson BA, Dachs GU. The Association Between Ascorbate and the Hypoxia-Inducible Factors in Human Renal Cell Carcinoma Requires a Functional Von Hippel-Lindau Protein. *Front Oncol* (2018) 8:574. doi: 10.3389/fonc.2018.00574
220. Campbell EJ, Dachs GU, Morrin HR, Davey VC, Robinson BA, Vissers MCM. Activation of the hypoxia pathway in breast cancer tissue and patient survival are inversely associated with tumor ascorbate levels. *BMC Cancer* (2019) 19:307. doi: 10.1186/s12885-019-5503-x
221. Padayatty SJ, Sun AY, Chen Q, Espey MG, Drisko J, Levine M. Vitamin C: Intravenous Use by Complementary and Alternative Medicine Practitioners and Adverse Effects. *PloS One* (2010) 5:e11414. doi: 10.1371/journal.pone.0011414
222. Creagan ET, Moertel CG, O'Fallon JR, Schutt AJ, O'Connell MJ, Rubin J, et al. Failure of high-dose vitamin C therapy to benefit patients with advanced cancer. *N Engl J Med* (1979) 301. doi: 10.1056/NEJM197909273011303
223. Moertel CG, Fleming TR, Creagan ET, Rubin J, O'Connell MJ, Ames MM. High-dose vitamin C versus placebo in the treatment of patients with advanced cancer who have had no prior chemotherapy. *N Engl J Med* (1985) 312. doi: 10.1056/NEJM198501173120301
224. Cameron E, Pauling L. Supplemental ascorbate in the supportive treatment of cancer: Reevaluation of prolongation of survival times in terminal human cancer. *Proc Natl Acad Sci* (1978) 75:4538–42. doi: 10.1073/pnas.75.9.4538
225. Cameron E, Campbell A. The orthomolecular treatment of cancer II. Clinical trial of high-dose ascorbic acid supplements in advanced human cancer. *Chem Interact* (1974) 9:285–315. doi: 10.1016/0009-2797(74)90019-2
226. Padayatty S, Sun H, Wang Y, Riordan, Hugh D, Hewitt SM, et al. Vitamin C Pharmacokinetics : Implications for Oral and IV use. *Ann Intern Med* (2004) 140:533–8. doi: 10.7326/0003-4819-140-7-200404060-00010
227. Stephenson CM, Levin RD, Spector T, Lis CG. Phase I clinical trial to evaluate the safety, tolerability, and pharmacokinetics of high-dose intravenous ascorbic acid in patients with advanced cancer. *Cancer Chemother Pharmacol* (2013) 72:139–46. doi: 10.1007/s00280-013-2179-9
228. Nielsen TK, Højgaard M, Andersen JT, Poulsen HE, Lykkesfeldt J, Mikines KJ, et al. Elimination of Ascorbic Acid following High-Dose Infusion in Prostate Cancer Patients: A Pharmacokinetic Evaluation. *Basic Clin Pharmacol Toxicol* (2014) 116:(15AD). doi: 10.1111/bcpt.12323
229. Hoffer LJ, Levine M, Assouline S, Melnychuk D, Padayatty SJ, Rosadiuk K, et al. Phase I clinical trial of i.v. ascorbic acid in advanced malignancy. *Ann Oncol* (1969) 19. doi: 10.1093/annonc/mdn377
230. Drisko JA, Chapman J, Hunter VJ. The Use of Antioxidants with First-Line Chemotherapy in Two Cases of Ovarian Cancer. *J Am Coll Nutr* (2003) 22:118–23. doi: 10.1080/07315724.2003.10719284
231. Padayatty SJ, Riordan HD, Hewitt SM, Katz A, Hoffer LJ, Levine M, et al. Intravenously administered vitamin C as cancer therapy: Three cases. *CMAJ* (2006) 174:937–42. doi: 10.1503/cmaj.050346
232. Mikirova N, Casciari J, Rogers A, Taylor P. Effect of high-dose intravenous vitamin C on inflammation in cancer patients. *J Transl Med* (2012) 10. doi: 10.1186/1479-5876-10-189
233. Welsh J, Wagner BA, van't Erve TJ, Zehr PS, Berg DJ, Halfdanarson TR, et al. Pharmacological ascorbate with gemcitabine for the control of metastatic and node-positive pancreatic cancer (PACMAN): results from a phase I clinical trial. *Cancer Chemother Pharmacol* (2013) 71:765–75. doi: 10.1007/s00280-013-2070-8
234. Ma Y, Chapman J, Levine M, Polireddy K, Drisko J, Chen Q. High-dose parenteral ascorbate enhanced chemosensitivity of ovarian cancer and reduced toxicity of chemotherapy. *Sci Transl Med* (2014) 6:222ra18–222ra18. doi: 10.1126/scitranslmed.3007154
235. Seo M-S, Kim J-K, Shim J-Y. High-Dose Vitamin C Promotes Regression of Multiple Pulmonary Metastases Originating from Hepatocellular Carcinoma. *Yonsei Med J* (2015) 56:1449–52. doi: 10.3349/ymj.2015.56.5.1449
236. Raymond YCF, Glenda CSL, Meng LK. Effects of High Doses of Vitamin C on Cancer Patients in Singapore: Nine Cases. *Integr Cancer Ther* (2016) 15:197–204. doi: 10.1177/1534735415622010
237. Mikirova N, Hunnunghake R, Scimeca RC, Chinshaw C, Ali F, Brannon C, et al. High-dose intravenous vitamin C treatment of a child with neurofibromatosis type 1 and optic pathway glioma: A case report. *Am J Case Rep* (2016) 17:774–81. doi: 10.12659/AJCR.899754
238. Polireddy K, Dong R, Reed G, Yu J, Chen P, Williamson S, et al. High dose parenteral ascorbate inhibited pancreatic cancer growth and metastasis: Mechanisms and a phase I/IIa study. *Sci Rep* (2017) 7:1–15. doi: 10.1038/s41598-017-17568-8
239. Wang F, He M-M, Wang Z-X, Li S, Jin Y, Ren C, et al. Phase I study of high-dose ascorbic acid with mFOLFOX6 or FOLFIRI in patients with metastatic colorectal cancer or gastric cancer. *BMC Cancer* (2019) 19. doi: 10.1186/s12885-019-5696-z
240. Schoenfeld JD, Sibenaller ZA, Mapuskar KA, Wagner BA, Cramer-Morales KL, Furqan M, et al. O 2 ·– and H 2 O 2 -Mediated Disruption of Fe Metabolism Causes the Differential Susceptibility of NSCLC and GBM Cancer Cells to Pharmacological Ascorbate. *Cancer Cell* (2017) 31:487–500.e8. doi: 10.1016/j.ccell.2017.02.018
241. Grasso C, Fabre M-S, Collis SV, Castro ML, Field CS, Schleich N, et al. Pharmacological doses of daily ascorbate protect tumors from radiation damage after a single dose of radiation in an intracranial mouse glioma model. *Front Oncol* (2014) 4:356. doi: 10.3389/fonc.2014.00356
242. Herst PM, Broadley KW, Harper JL, McConnell MJ. Pharmacological concentrations of ascorbate radiosensitize glioblastoma multiforme primary cells by increasing oxidative DNA damage and inhibiting G2/M arrest. *Free Radic Biol Med Biol Med* (2012) 52:1486–93. doi: 10.1016/j.freeradbiomed.2012.01.021
243. Ma E, Chen P, Wilkins HM, Wang T, Swerdlow RH, Chen Q. Pharmacologic ascorbate induces neuroblastoma cell death by hydrogen peroxide mediated DNA damage and reduction in cancer cell glycolysis. *Free Radic Biol Med* (2017) 113:36–47. doi: 10.1016/j.freeradbiomed.2017.09.008
244. Castro ML, McConnell MJ, Herst PM. Radiosensitisation by pharmacological ascorbate in glioblastoma multiforme cells, human glial cells, and HUVECs depends on their antioxidant and DNA repair capabilities and is not cancer

specific. *Free Radic Biol Med* (2014) 74:200–9. doi: 10.1016/j.freeradbiomed.2014.06.022

245. Bodeker KL, Allen BG, Smith MC, Monga V, Sandhu S, Hohl RJ, et al. First-in-human phase 1 clinical trial of pharmacological ascorbate combined with radiation and temozolomide for newly diagnosed glioblastoma. *Clin Cancer Res* (2019) 25:6590–7. doi: 10.1158/1078-0432.CCR-19-0594
246. Baillie N, Carr AC, Peng S. The use of intravenous vitamin C as a supportive therapy for a patient with glioblastoma multiforme. *Antioxidants* (2018) 7. doi: 10.3390/antiox7090115
247. Hegi ME, Diserens A-C, Gorlia T, Hamou M-F, de Tribolet N, Weller M, et al. MGMT Gene Silencing and Benefit from Temozolomide in Glioblastoma. *N Engl J Med* (2005) 352:997–1003. doi: 10.1056/NEJMoa043331
248. Pegg AE, Dolan ME, Moschel RC. Structure, Function, and Inhibition of O6-Alkylguanine-DNA Alkyltransferase. *Prog Nucleic Acid Res Mol Biol* (1995) 51:167–223. doi: 10.1016/S0079-6603(08)60879-X
249. Esteller M, Garcia-Foncillas J, Andion E, Goodman SN, Hidalgo OF, Vanaclocha V, et al. Inactivation of the DNA-repair gene MGMT and the clinical response of gliomas to alkylating agents. *N Engl J Med* (2000) 343:1350–4. doi: 10.1056/NEJM200011093431901
250. Huang L, Boling W, Zhang J. Hyperbaric oxygen therapy as adjunctive strategy in treatment of glioblastoma multiforme. *Med Gas Res* (2018) 8:24–8. doi: 10.4103/2045-9912.229600

Conflict of Interest: The authors declare that the research was conducted in the absence of any commercial or financial relationships that could be construed as a potential conflict of interest.

frontiers in Oncology

ORIGINAL RESEARCH
published: 26 March 2021
doi: 10.3389/fonc.2021.625838

Correlation Between APOBEC3B Expression and Clinical Characterization in Lower-Grade Gliomas

Hao Zhang[1†], Zhiyang Chen[2†], Zeyu Wang[1], Ziyu Dai[1], Zhengang Hu[1], Xun Zhang[1], Min Hu[2], Zhixiong Liu[1] and Quan Cheng[1,3*]*

[1] Department of Neurosurgery, Xiangya Hospital, Central South University, Changsha, China, [2] Department of Laboratory Medicine, The Second Xiangya Hospital, Central South University, Changsha, China, [3] Department of Clinical Pharmacology, Xiangya Hospital, Central South University, Changsha, China

Background: As the most aggressive tumors in the central nervous system, gliomas have poor prognosis and limited therapy methods. Immunotherapy has become promising in the treatment of gliomas. Here, we explored the expression pattern of APOBEC3B, a genomic mutation inducer, in gliomas to assess its value as an immune biomarker and immunotherapeutic target.

Methods: We mined transcriptional data from two publicly available genomic datasets, TCGA and CGGA, to investigate the relevance between APOBEC3B and clinical characterizations including tumor classifications, patient prognosis, and immune infiltrating features in gliomas. We especially explored the correlation between APOBEC3B and tumor mutations. Samples from Xiangya cohort were used for immunohistochemistry staining.

Results: Our findings demonstrated that APOBEC3B expression level was relatively high in advanced gliomas and other cancer types, which indicated poorer prognosis. APOBEC3B also stratified patients' survival in Xiangya cohort. APOBEC3B was significantly associated with infiltrating immune and stromal cell types in the tumor microenvironment. Notably, APOBEC3B was involved in tumor mutation and strongly correlated with the regulation of oncogenic genes.

Conclusion: Our findings identified that APOBEC3B could be a latent molecular target in gliomas.

Keywords: glioma, APOBEC3B, tumor microenvironment, immune response, prognosis

OPEN ACCESS

Edited by:
Lingtao Jin,
University of Florida, United States

Reviewed by:
Loic P. Deleyrolle,
University of Florida, United States
Guo Chen,
Jinan University, China

****Correspondence:***
Quan Cheng
chengquan@csu.edu.cn
Zhixiong Liu
zhixiongliu@csu.edu.cn

†These authors have contributed equally to this work

Specialty section:
This article was submitted to Neuro-Oncology and Neurosurgical Oncology, a section of the journal Frontiers in Oncology

Received: *18 November 2020*
Accepted: *28 January 2021*
Published: *26 March 2021*

Citation:
Zhang H, Chen Z, Wang Z, Dai Z, Hu Z, Zhang X, Hu M, Liu Z and Cheng Q (2021) Correlation Between APOBEC3B Expression and Clinical Characterization in Lower-Grade Gliomas. Front. Oncol. 11:625838. doi: 10.3389/fonc.2021.625838

INTRODUCTION

Diffuse gliomas, including lower-grade gliomas (LGGs) and glioblastomas (GBMs), are the most malignant brain tumor in adults (1). Glioma patients always had high mortality rate, high recurrence risk and dismal prognosis (2). LGGs comprised of diffuse low-grade and intermediated-grade gliomas. Nowadays, the primary therapeutic methods for LGG is surgery with concurrent radiotherapy and chemotherapy (3). Despite the advances in treatment methods, the median overall survival of LGG patients is less than 2 years due to limitations in therapeutic options. Therefore, novel therapeutic strategies are urgently needed. In recent years, immunotherapy, including immune checkpoint inhibitors, has demonstrated remarkable results in cancer treatment and casted new lights on clinical management of glioma (4, 5).

The tumor microenvironment (TME) is a highly dynamic composition of various cell types and is considered being responsible for the effectiveness of immunotherapies. An immunosuppressive TME was formed during the progression and recurrence of glioma (6). Immune infiltrating cells account for the major part of TME and sometimes can protect tumor cells from being detected and exterminated by the immune system. For example, regulatory T cells (Tregs) and tumor-associated macrophages (TAMs) have been proved to exert immunosuppressive effect in glioma (7). As another important member in the TME, immune checkpoint molecules are also involved in immunosuppressive mechanism. Immunotherapy of immune checkpoint blockade has become a promising treatment modality for cancers (8).

APOBEC3B, a member of APOBEC (apolipoprotein B mRNA editing enzyme, catalytic-polypeptide-like) enzymes with cytidine deaminase activity (9), can induce prevalent mutagen of genomic DNA in multiple cancers. APOBEC3B has been found to be upregulated in various cancer types with poor prognosis (10–12), and is also considered as a mediator regulating the growth, the metastatic outgrowths, and the emerging therapeutic resistance of cancer cells (13). High expression of APOBEC3B is associated with immune evasion of cancer (14). Notably, high expression of APOBEC3B also enhances the sensitivity to immune checkpoint blockade in melanoma (15). However, the relationship between TME and the APOBEC3B expression in gliomas remains largely unknown.

Therefore, we integrated and analyzed the RNA-sequencing data of glioma patients from The Cancer Genome Atlas (TCGA) and Chinese Glioma Genome Atlas (CGGA) databases to reveal the immune features and clinical characteristics of APOBEC3B in gliomas.

METHODS

Data Collection

This study was ethically approved by Xiangya Hospital, Central South University. Archived paraffin embedded glioma tissues (WHO grades II–IV) were collected from patients (n = 58) who underwent surgery in the Department of Neurosurgery, Xiangya Hospital, Central South University. We collected transcriptomic data of LGG and GBM samples from the TCGA and CGGA datasets, and RNA seq was used for the analysis. RNA-seq data about specific tumor anatomic structure in GBM was downloaded from Ivy Glioblastoma Atlas Project (http://glioblastoma.alleninstitute.org/). APOBEC3B expression data in distinct radiographical areas of normal brain and GBM was downloaded from the Gill dataset.

Immunohistochemistry

Tissues of different grades of human gliomas (WHO grades II–IV) were formalin-fixed and paraffin-embedded to obtain sections (4 mm). Sections were then boiled in sodium citrate buffer (pH 6.0) for antigen retrieval, 3% H_2O_2 was used for blockage of endogenous HRP activity. Slides were blocked with 10% normal goat serum and incubated with primary antibody (rabbit polyclonal anti-APOBEC3B antibody, 1:50; Proteintech; Wuhan, China) at 4°C overnight. Signal was visualized with horse radish peroxidase conjugated secondary antibody and 3, 3′-diaminobenzidine (DAB) as the substrate. Slides were counterstained with hematoxylin, and representative images were obtained using an Olympus inverted microscope. H-score of glioma samples was subsequently calculated.

Bioinformatic Analysis

We acquired the chromosome localization of APOBEC3B on the GeneCards database (https://www.genecards.org/). APOBEC3B gene structure was analyzed on the Ensembl database (http://asia.ensembl.org/), with its protein structure analyzed in the Uniprot database (http://www.uniprot.org/). APOBEC3B gene structure was then visualized by using Illustrator for biological sequences software (IBS, http://ibs.biocuckoo.org/). The protein sequence comparison among different species was analyzed by DNAMAN software (lynnonBiosoft, USA). Correlation analysis of APOBEC3B was performed using gene expression profiles from the TCGA and CGGA datasets with R language (https://www.r-project.org/). Somatic mutations and somatic copy number alternations (CNAs) of the cases with the corresponding RNA-seq data were downloaded from TCGA database. GSITIC analysis was adopted to determine the genomic event enrichment. CNAs associated with APOBEC3B expression and the threshold copy number (CN) at alteration peaks were from GISTIC 2.0 analysis (https://gatkforums.broadinstitute.org). GSITIC analysis was performed based on the first 25% and last 25% of samples. The gene sets variation analysis (GSVA) package was used to analyze the differential expression in GO terms of immune related process and immune cell lineages from TCGA and CGGA. As for somatic mutations, software VarScan2 was used to detect WES data of $APOBEC3B^{high}$ and $APOBEC3B^{low}$ groups. $P < 0.05$ was set as the criteria for selecting differentially mutated genes, and Fisher's exact test was used to identify the differentially mutation pattern. CoMEt algorithm was used to detect the co-occurrence and mutually exclusive mutations. R package maftools was used for the visualization of the somatic mutations. Correlation analysis was performed by the expression values of APOBEC3B and GO term, and the items with $p < 0.05$ and high correlation coefficient were selected. After Spearman correlation analysis, Heatmap was used to construct gene ontology (GO) analysis of the most correlated genes. The relevant immune signaling pathways of high level of APOBEC3B expression from GO were analyzed by ClueGO (16). ClueGO: a Cytoscape

plug-in to decipher functionally grouped gene ontology and pathway annotation networks. ESTIMATE (Estimation of Stromal and Immune cells in Malignant Tumor tissues using Expression) algorithm was used to evaluate the infiltration of immune cells and the presence of stromal cells in tumor samples, which generated three results including immune score (reflecting the level of immune cells infiltrations in tumor tissue), stromal score (reflecting the presence of stroma in tumor tissue), and estimate score (reflecting tumor purity).

We analyzed the relationship between APOBEC3B expression and overall survival (OS) in adrenocortical carcinoma (ACC), cholangiocarcinoma (CHOL), esophageal carcinoma (ESCA), liver hepatocellular carcinoma (LIHC), lung adenocarcinoma (LUAD), pancreatic adenocarcinoma (PAAD), Uterine Corpus Endometrial Carcinoma (UCEC), Uterine Carcinosarcoma (UCS), and Kidney Chromophobe (KICH) cancer types based on the pan-cancer data in TCGA dataset. We also analyzed the correlation between APOBEC3B expression and the abundance of six immune infiltrating cell types, including activated $CD4^+$T cell, central memory $CD8^+$T cell, macrophage, Myeloid-derived suppressor cells (MDSCs), memory B cell and type 2 helper cell in pan-cancer from TCGA.

The weighted gene co-expression network analysis (WGCNA) package in R was used to perform WGCNA. The expression profile of 2,559 APOBEC3B related genes (correlation efficient >0.4) was applied as the input of WGCNA. The association between individual genes and APOBEC3B density was quantified by gene significance, and the correlation between module eigengenes and gene expression profiles was represented by module membership. A power of $\beta = 3$ and a scale-free R2 = 0.87 were set as soft-threshold parameters to ensure a scale-free topology network. A total of eight modules were generated, and yellow module showed the highest correlation (r = 0.96, p = 1.6e-112). Genes within the yellow module were chosen for further GO and KEGG enrichment analysis.

Statistical Analysis

Spearman correlation analysis was used to evaluate the correlations between continuous variables. The survival probability was described by Kaplan–Meier survival curves. Patients were stratified according to the median value of APOBEC3B or the cutpoint value automatically calculated. The Student t-test was used to determine the expression levels of APOBEC3B with regard to pathological characteristics. The linear relationship between gene expression levels was evaluated by the Pearson correlation. All statistical analyses were performed using R project (version 3.6.1, https://www.r-project.org/). P-values <0.05 were considered to be statistically significant. And all tests were two-sided.

RESULTS

The Expression Level of APOBEC3B Is Increased in Aggressive Glioma and Other Cancers

The mRNA expression levels of APOBEC3B were measured using data from publicly accessed databases including over 1,600 gliomas samples: TCGA. n = 672: CGGA, n = 1013. We found that APOBEC3B was upregulated in GBM compared to LGG (P <.05, respectively; **Figure 1A**). The expression level of APOBEC3B was also increased in order of grade II, grade III, and grade IV (WHO classification) (P <.05,respectively; **Figure 1B**). Based on gene expression profiling, glioblastoma can be classified into four distinct molecular subtypes: classical (CL), mesenchymal (ME), proneural (PN) and neural (NE). Practically, the CL and ME types predict worse clinical prognosis. To figure out the relationship between APOBEC3B and molecular subtypes, we further investigated the expression level of APOBEC3B among subtypes: increased expression level of APBOEC3B was found in CL and ME compared to PN and NE (P <.05, respectively; **Figure 1C**). ROC further indicated that APOBEC3B expression level can distinguish CL and ME from GBM (area under curve (AUC) value = 0.85; P < 0.05; **Figure 1C**).

We also examined the relationship between APOBEC3B and certain genomic alterations. Glioma patients with codeletion of 1p and 19q derived more benefits in several clinical trials (17). We observed that the expression of APOBEC3B was decreased in the 1p19q codeletion cluster in pan-glioma analysis (P <.05, respectively; **Figure 1D**). Better clinical outcome was accompanied by MGMT promoter methylated subtype (18) and IDH*mut* (19), similarly, down-regulated of APOBEC3B mRNA expression level was found in these two types compared to wild type patients (**Figures 1E, F**), and receiver operating characteristic (ROC) curve analysis indicated that the expression of APOBEC3B discriminated IDH mutation from non-IDH mutation in pan-glioma analysis (the area under the curve (AUC) value = 0.807; P < 0.05; **Figure 1F**). Among nine methylation probes designed for APOBEC3B from TCGA, all of them exhibited remarkable negative association with expression of APOBEC3B, which most of the association was statistically significant (**Figure S1**).

Furthermore, we analyzed various clinically related characteristics of APOBEC3B in gliomas. Pathologically, APOBEC3B has been found to be most adequately expressed in microvascular proliferation (MVP) (**Figure S2A**). In copy number (CN) analysis, glioma with APOBEC3B CN loss expressed higher level of APOBEC3B mRNA (**Figure S2B**). Radiographically, APOBEC3B was upregulated in contrast enhancing area compared with non-contrast enhancing and normal brain area (**Figure S2C**). Moreover, the expression pattern of APOBEC3B with regard to the histology of gliomas was shown in **Figure S2D**. We also examined APOBEC3B level in primary, recurrent, and secondary patients respectively; statistics revealed that APOBEC3B expression was higher in recurrent patients than in primary patients (**Figure S2E**). And in patients with different treatment outcomes, the expression of APOBEC3B was significantly higher in progressive patients than in patients who were in complete remission (**Figure S2F**).

APOBEC3B mRNA expression levels were analyzed in pan-cancer (**Figure 1G**) and interactive body map of APOBEC3B (**Figure 1H**). The results elucidated that besides LGG and GBM, expression of APOBEC3B was higher in multiple cancers

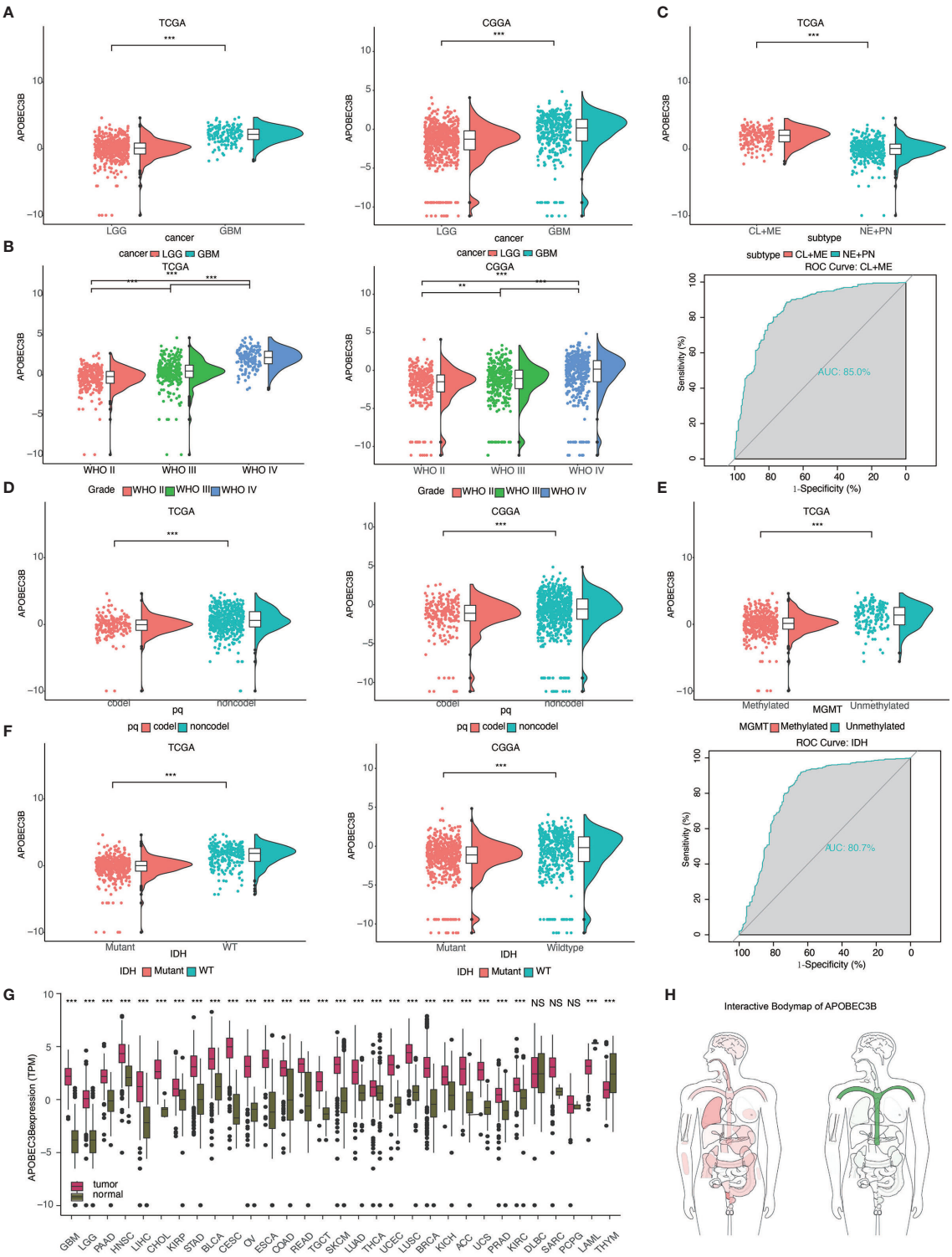

FIGURE 1 | The expression level of APOBEC3B is increased in aggressive glioma and other cancers. Analysis of APOBEC3B mRNA levels in **(A)** LGG and GBM **(B)** WHO grade II–IV gliomas **(D)** 1p19q codeletion and non-codeletion from TCGA and CGGA datasets. **(C)** APOBEC3B expression in distinct subclasses(upper), ROC curve indicating sensitivity and specificity of APOBEC3B expression as a discriminative biomarker for CL+ME subtypes and GBM (lower). **(E)** APOBEC3B expression in MGMT methylated and unmethylated. **(F)** Analysis of APOBEC3B level in IDH mutant and wildtype from TCGA and CGGA. ROC curve indicates the sensitivity and specificity of APOBEC3B expression as a diagnostic biomarker for discriminate IDH mutation from non-IDH mutation. **(G)** APOBEC3B mRNA expression levels in pan-cancer. **(H)** The median expression of tumor (red) and normal (green) samples in bodymap. NS, Not Statistically Significant; *P < 0.05; **P < 0.01; ***P < 0.001; ****P < 0.0001.

including PAAD, Head and Neck Squamous Cell Carcinoma (HNSC), LIHC, CHOL, kidney renal papillary cell carcinoma (KIRP), stomach adenocarcinoma (STAD), Bladder Urothelial Carcinoma (BLCA), cervical squamous cell carcinoma and endocervical adenocarcinoma (CESC), ovarian cancer (OV), ESCA, colon adenocarcinoma (COAD), rectal adenocarcinoma (READ), Testicular Germ Cell Tumors (TGCT), Skin Cutaneous Melanoma (SKCM), LUAD, Thyroid Carcinoma (THCA), UCEC, lung squamous cell carcinoma (LUSC), Breast Invasive Carcinoma (BRCA), KICH, ACC, UCS, Prostate Adenocarcinoma (PRAD), kidney renal clear cell carcinoma (KIRC) than adjacent normal tissues, respectively, while lower in Thymoma (THYM).

APOBEC3B Expression Is Elevated in Aggressive Glioma and Related to Poor Prognosis

APOBEC3B was located at 22q13.1 (**Figure 2A**), and the protein structure of APOBEC3B consisted of CMP/dCMP-type deaminase 1 and CMP/dCMP-type deaminase 2 (**Figure 2B**). In order to study the conservation of APOBEC3B among distinct species, we compared protein sequences encoded by APOBEC3B among seven different species (**Figure 2C**). Statistics showed that Homo sapiens APOBEC3B shared 75.71, 54.19, 78.73, 73.81, 44.76 and 74.52% identity to PANTR, pig, rat, whale, bovine, and dolphin, respectively. It presented that APOBEC3B was highly conserved in most kinds of mammals, but varied significantly between human and bovine. To confirm that APOBEC3B expression was also upregulated at the protein level, we performed IHC staining of APOBEC3B based on an independent cohort consisting of different pathological grades of glioma samples (n = 58) from our institution. APOBEC3B was located in the nucleus and cytoplasm, and increase in order of WHO classification (**Figure 2D**). The quantification of IHC staining was shown in **Figures 2E, F**, in which there was an increase of APOBEC3B expression as tumor grade increased. We further investigated the prognostic value of APOBEC3B in glioma based on 27 clinical samples with survival information, and patients with higher expression of APOBEC3B are more likely to have shorter overall survival (**Figure 2G**).

Higher APOBEC3B Expression Is Related to Poor Survival in Glioma and Multiple Cancers

We used Kaplan–Meier analysis to subsequently explore the prognostic value of APOBEC3B in both TCGA and CGGA datasets. We revealed that APOBEC3B^{high} patients showed shorter overall survival (OS) than APOBEC3B^{low} patients in pan-glioma, LGG, and GBM (P <.05, respectively; **Figures 3A, B**). Thus, APOBEC3B might be a latent marker for prognosis in glioma patients. We further investigated the prognostic value of ABPOEC3B for pan-cancer, in which patients were divided into high and low APOBEC3B groups. High APOBEC3B expression was significantly correlated to worse prognosis in nine cancer types, including ACC, CHOL, ESCA, LIHC, LUAD, PAAD, UCEC, UCS, and KICH (P <.0001, respectively; **Figure 3C**).

APOBEC3B Expression Is Related to Genomic Alterations in Glioma

Genomic alterations can be easily found in glioma. Thus, we performed copy number variation (CNV) and somatic mutation analysis to examine whether there is a link between APOBEC3B expression levels and specific genomic alterations in glioma. An overall CNV profile comparison of APOBEC3B^{high}(n = 158) and APOBEC3B^{low}(n = 158) cluster was carried out. Besides the variation of chr1 and chr19, amplification of chr7 and deletion of chr10 most frequently occurred in glioma patients (**Figure 4A**). As a genomic symbol of oligodendroglioma, deletion of 1p and 19q tended to appear in APOBEC3B^{low} cluster (**Figure 4B**). Using GSITIC analysis, we found distinct genomic alterations in different clusters (**Figures 4B, C**). In APOBEC3B^{low} patients, PD-1 (2q37.3), CLPTM1L (5p15.33), CDKN2A (9p21.3), SAA1 (11p15.5) were frequently deleted, while HAS2 (8q24.13), NDRG1 (8q24.22), FGF23 (12p13.32) and CDK4 (12q14.1) were most frequently amplified. In APOBEC3B^{high} group, CDKN2A (9p21.3), PARK7 (1p36.23) and PTEN (10q23.31) were most frequently deleted, at the same time, EGFR (7p11.2) and CDK4(12q14.1) were most commonly amplified genes. Based on the level of APOBEC3B, somatic mutation profiles were analyzed. In low APOBEC3B group, IDH-1 (77%), TP53 (44%), ATRX (29%), and CIC (11%) are altered in high frequency, while TP53 (33%), EGFR (28%), TTN (26%), and PTEN (23%) were more frequently mutated in high APOBEC3B group (**Figures 4D, E**). Taken together, our results demonstrated that APOBEC3B expression level was pertinent to chromosomal alterations in glioma.

Comparisons of Somatic Mutations Among Different Immune Infiltration Levels

We further used the R package maftools to analyze somatic mutations including the single-nucleotide variant (SNV), single-nucleotide polymorphism (SNP), insertion (INS), and deletion (DEL) under different expression levels of APOBEC3B, based on the WES data from TCGA portal in which the mutations had been called by VarScan2. As shown in **Figure 5A**, most genomic variants were nonsense mutation, missense mutation, and silent in the APOBEC3B^{high} and APOBEC3B^{low} groups. As for SNVs, the mutation numbers of T>A, C>T, C>G, and C>A in APOBEC3B^{high} cohort were significantly higher than those in APOBEC3B^{low} cohort (**Figure 5B**). Furthermore, SNPs in the APOBEC3B^{low} cohort were outnumbered by those in the APOBEC3B^{high} cohort; however, INS and DEL in two cohorts showed no significant difference (**Figure 5C**). Moreover, the mutation frequencies of some genes differed from these two groups, and the top 10 mutated genes were exhibited in **Figure 5D**. Common carcinogenic pathways were found to be more active in APOBEC3B^{high} group (**Figures 5E, G**). The strongest co-occurrent pairs of gene alteration in the APOBEC3B^{high} group were ATRX-TP53, and in the APOBEC3B^{low} groups were ATRX-TP53 as well as ATRX-IDH1, which was in line with previous studies> (19–21) Meanwhile, the most mutually exclusive pairs in APOBEC3B^{high} and APOBEC3B^{low} groups were CIC-TP53 and EGFR-IDH1, respectively (**Figures 5F, H**).

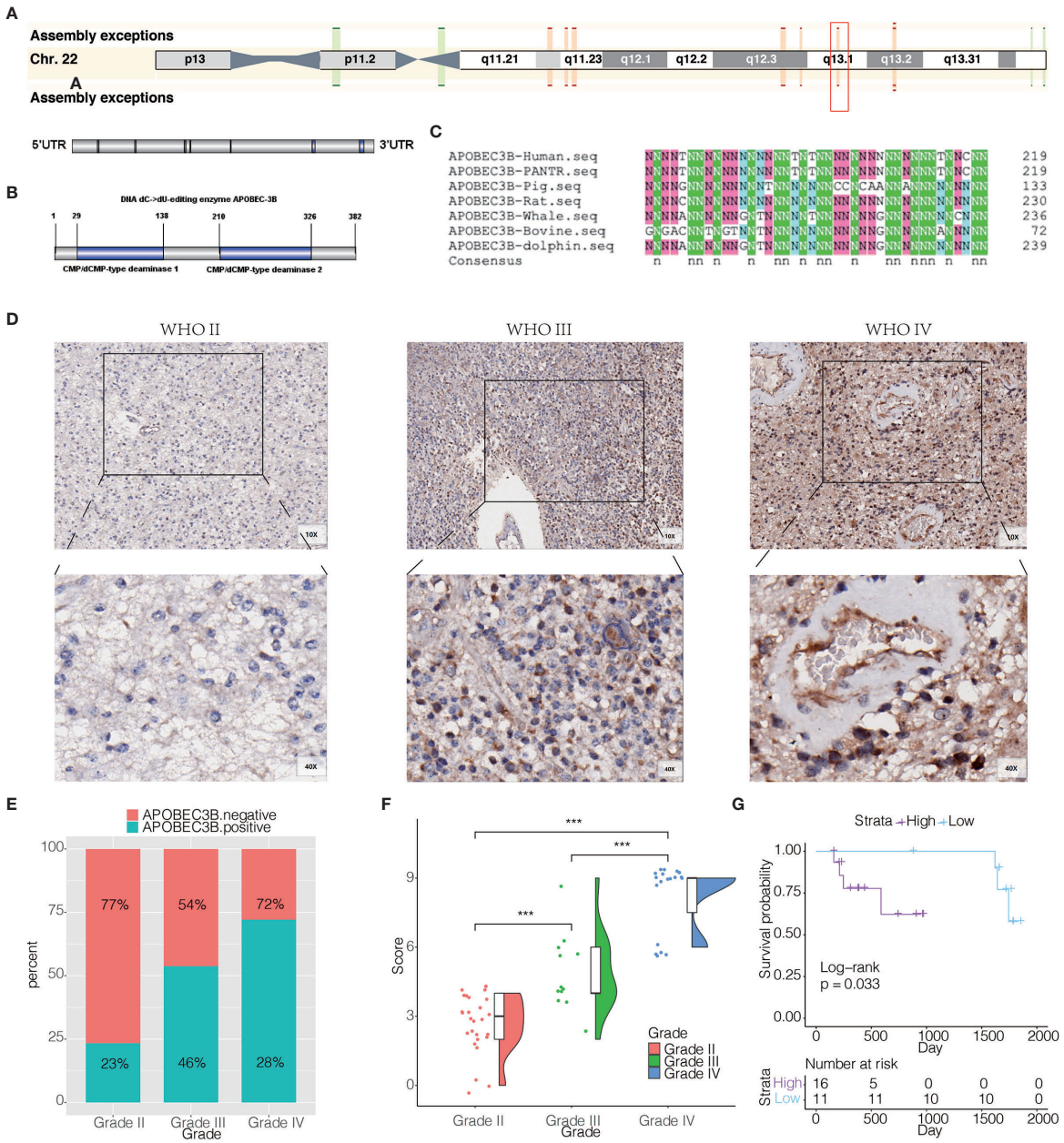

FIGURE 2 | APOBEC3B expression is elevated in aggressive glioma and related to poor prognosis. **(A)** Chromosome localization and gene structure of APOBEC3B in human. **(B)** Structure of APOBEC3B. **(C)** Comparison of protein sequences encoded by APOBEC3B among seven different species. **(D)** Representative images of IHC staining for APOBEC3B in different pathological grades of gliomas [WHO II (27), WHO III (12), WHO IV (19)]. **(E)** Quantification of APOBEC3B IHC staining regarding the positive rate. **(F)** Quantification of APOBEC3B IHC staining regarding the H-score. **(G)** Overall survival based on high *vs* low expression of APOBEC3B in glioma patients (n = 27). The patients were stratified according to the H score of APOBEC3B in IHC staining. The H score has the range of 0–12. High group was defined as expression intensity >=6. Low group was defined as expression intensity <6. NS, Not Statistically Significant; *P < 0.05; **P < 0.01; ***P < 0.001; ****P < 0.0001.

Genes Positively Related to APOBEC3B Are Enriched in Immune and Inflammatory Related Pathways

We using GO analysis and KEGG pathway analysis to further investigate the potential function of APOBEC3B in the development of human glioma. Our results revealed that several immune and inflammatory related pathways were involved in APOBEC3B-mediated immune microenvironment. GO results revealed APOBEC3B was significantly correlated with type 1 interferon, MHC-I and cytokine-mediated signaling

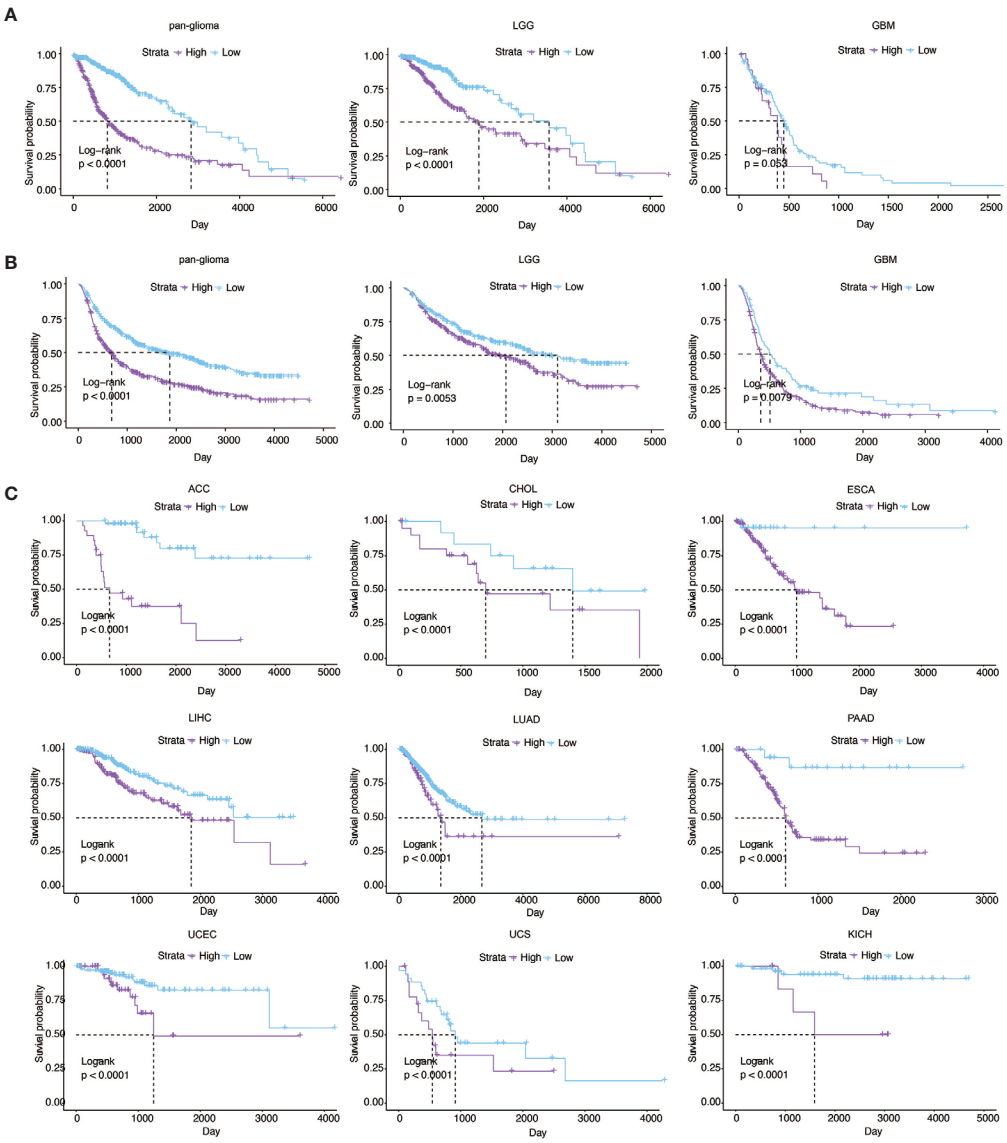

FIGURE 3 | Higher APOBEC3B expression is related to poor survival in glioma and multiple cancers. Kaplan–Meier analysis of overall survival (OS) based on high *vs* low expression of APOBEC3B in pan-glioma analysis, LGG, and GBM patients in **(A)** TCGA and **(B)** CGGA datasets. GBM patients were stratified according to the cutpoint value automatically calculated in TCGA, and the cutpoint value was 3.1278. Kaplan–Meier analysis of overall survival (OS) based on high *vs* low expression of APOBEC3B in **(C)** ACC, CHOL, ESCA, LIHC, LUAD, PAAD, UCEC, UCS and KICH.

pathway, negatively regulates differentiation of T cell, positively regulates regulatory T cell and macrophage as well as fibroblast proliferation in LGG (**Figures 6A, C**) and pan-glioma analysis (**Figures S3A, C**) from TCGA and CGGA. The signaling network from KEGG pathway analysis further elucidates the relevance between APOBEC3B and immune and inflammation related pathways including antigen processing and presentation, p53, JAK-STAT and T, B cell receptor signaling pathway in LGG patients (**Figures 6B, D**) and pan-glioma analysis (**Figures S3B, D**). As shown in **Figure 6E**, the result of GO pathway analysis revealed that APOBEC3B was significantly related to immune infiltrating, such as monocyte chemotaxis, neutrophil chemotaxis, lymphocyte chemotaxis, and lymphocyte mediated pathways. These data suggest APOBEC3B might play an immunosuppression role in the TME of glioma.

APOBEC3B Is Correlated With Inflammatory Activities in Gliomas

A positive feedback loop of APOBEC3B and inflammatory response mediator IL-6 has been found in hepatocellular carcinoma through the JAK1/STAT3 pathway (22). Meanwhile, based on our analysis, APOBEC3B was also involved in inflammatory responses in glioma. We further observed that APOBEC3B was positively correlated with MHC-1, MHC-2, STAT1, IFN, LCK, and HCK metagenes, but

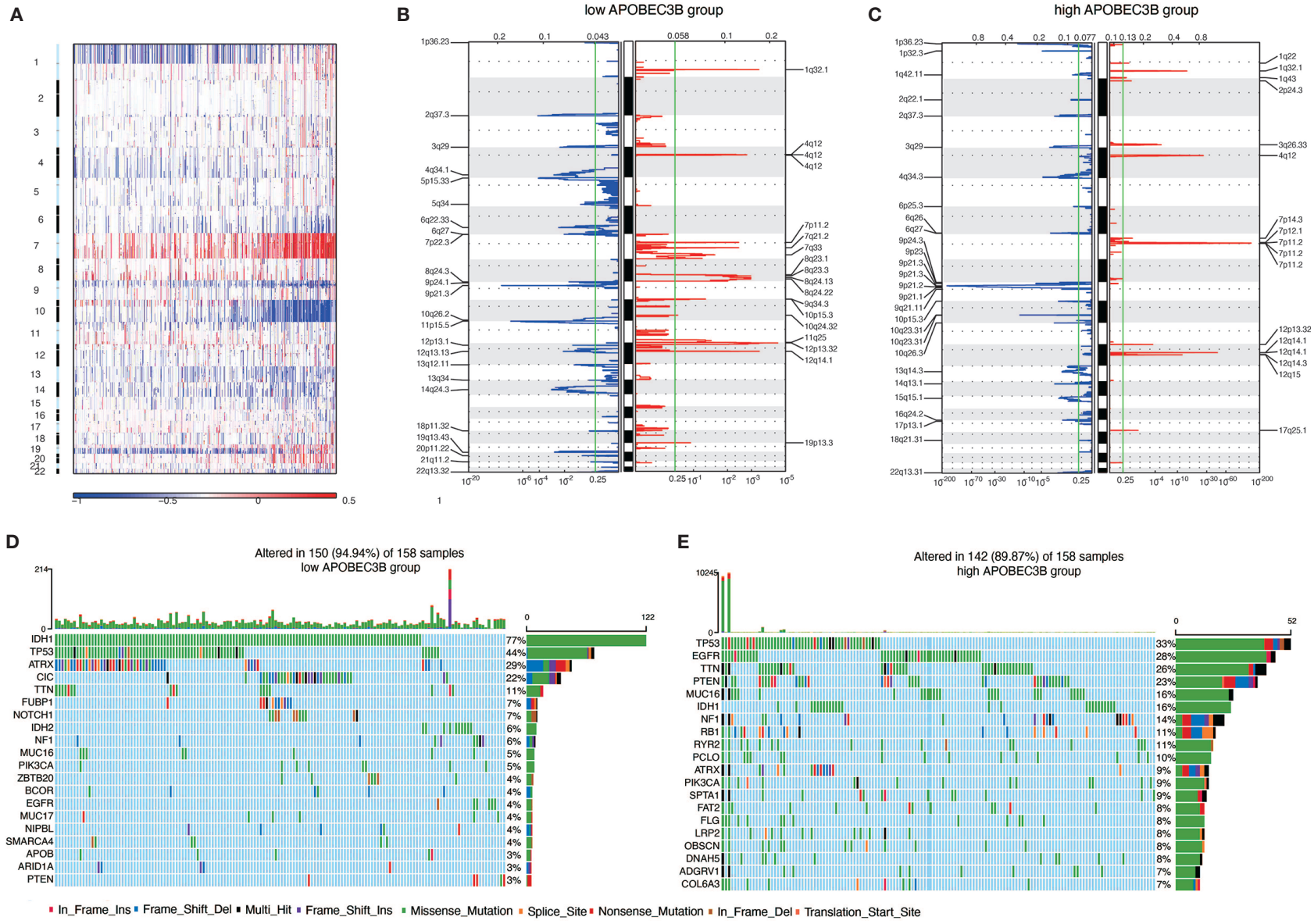

FIGURE 4 | APOBEC3B expression is related to genomic alterations in glioma. **(A)** Overall CNV profile according to high *vs* low APOBEC3B expression. Blue (deletion); Red (amplification). Frequency of specific changes based on **(B)** APOBEC3B^{low} and **(C)** APOBEC3B^{high} groups. The X-axis represents the frequency of chromosomal deletion (blue) or amplification (red). Spectrum of somatic mutations in gliomas from **(D)** APOBEC3B^{low} and **(E)** APOBEC3B^{high} groups.

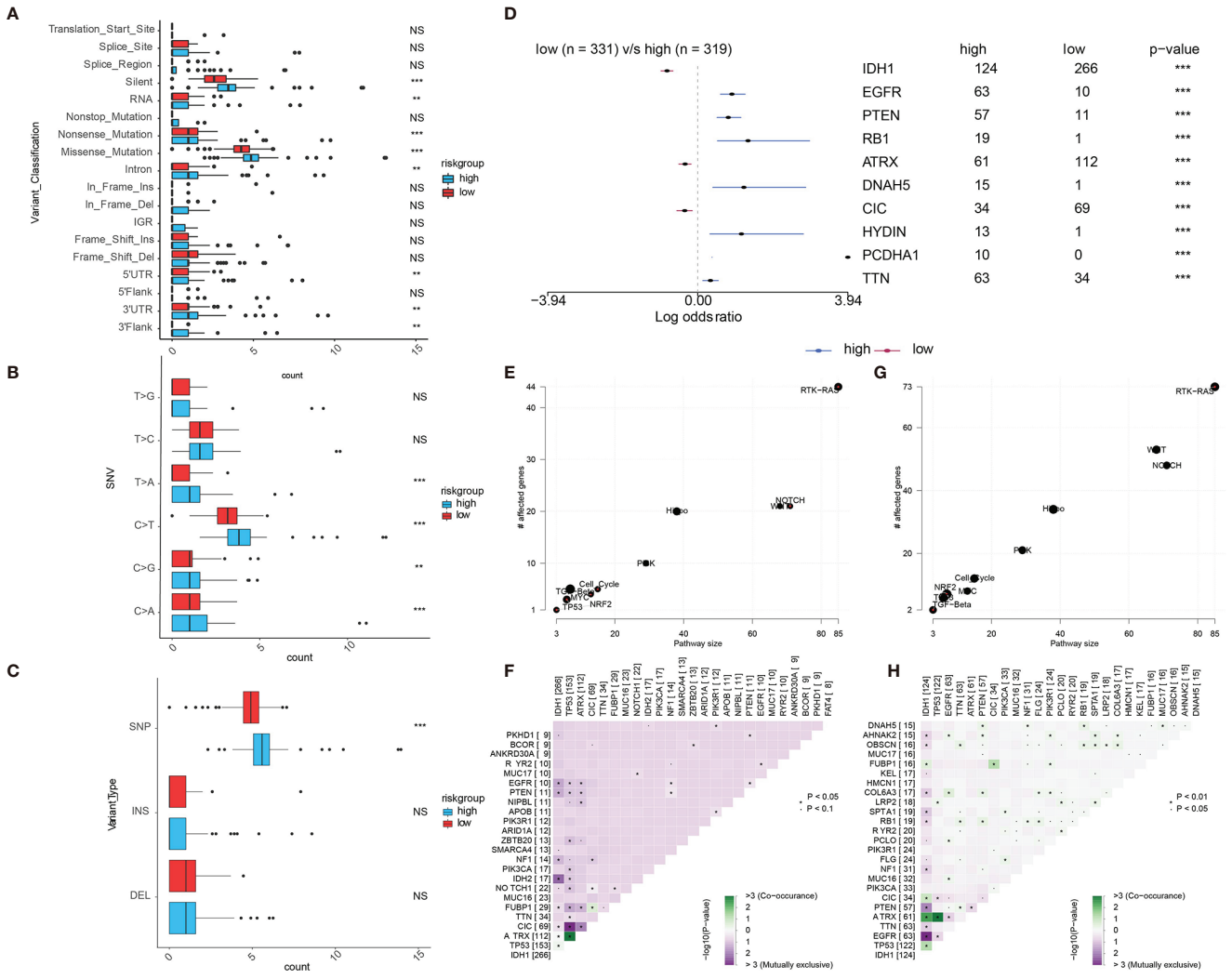

FIGURE 5 | Landscape of somatic mutation in APOBEC3B^{high} and APOBEC3B^{low} groups. **(A–C)** the comparisons of mutation frequencies of **(A)** every mutation type classified by effects, **(B)** SNVs, **(C)** INDEL and SNP. **(D)** Forest plot shows the top 10 most significantly differentially mutated genes between two groups. Common carcinogenic pathways in **(E)** APOBEC3B^{low} and **(G)** APOBEC3N^{high} group. The heatmap indicates the mutually exclusive mutations and co-occurring of the frequently mutated genes in **(F)** APOBEC3B^{low} and **(H)** APOBEC3N^{high} groups. NS, Not Statistically Significant; *P < 0.05; **P < 0.01; ***P < 0.001; ****P < 0.0001.

negatively related to IgG metagene, a marker for B cells in LGG patients (**Figures S4A, B**) and pan-glioma analysis (**Figures S4C, D**) in TCGA and CGGA datasets.

APOBEC3B Is Related to Immune and Stromal Cell Infiltration in Gliomas

We further explore the relevance of APOBEC3B expression and ESTIMATE scores. Our results illuminated that APOBEC3B expression was positively related to the immune score, stromal score, and estimate score in the pan-glioma analysis (**Figure S5A**) and LGG (**Figure S5B**) respectively. Immune suppression is a significant feature of human gliomas which partly ascribes to TME components. To further understand in-depth the relevance between elevated APOBEC3B and immune tumor microenvironment, we examined which immune-related cell types are influenced by APOBEC3B in glioma. Using cell type enrichment analysis, we observed that APOBEC3B was strongly positively correlated with activated CD4$^+$ T cell, $\gamma\delta$ T cell, NK cells, dendritic cells and myeloid-derived suppressor cells in LGG patients (**Figures 7A, B**) and pan-glioma analysis (**Figures S6A, B**). Moreover, specific stromal cell types like fibroblasts, epithelial cells, and monocyte are related to glioma in LGG patients (**Figures S5C, D**) and pan-glioma analysis as well (**Figures S6C, D**). Taken together, our results suggested that increased APOBEC3B tend to recruit immune and stromal cells into the tumor microenvironment in glioma.

Correlation Between APOBEC3B and Immune Cells in Pan-Cancer

To further understand the relationships between APOBEC3B and infiltrating immune cells in TME, we analyzed the

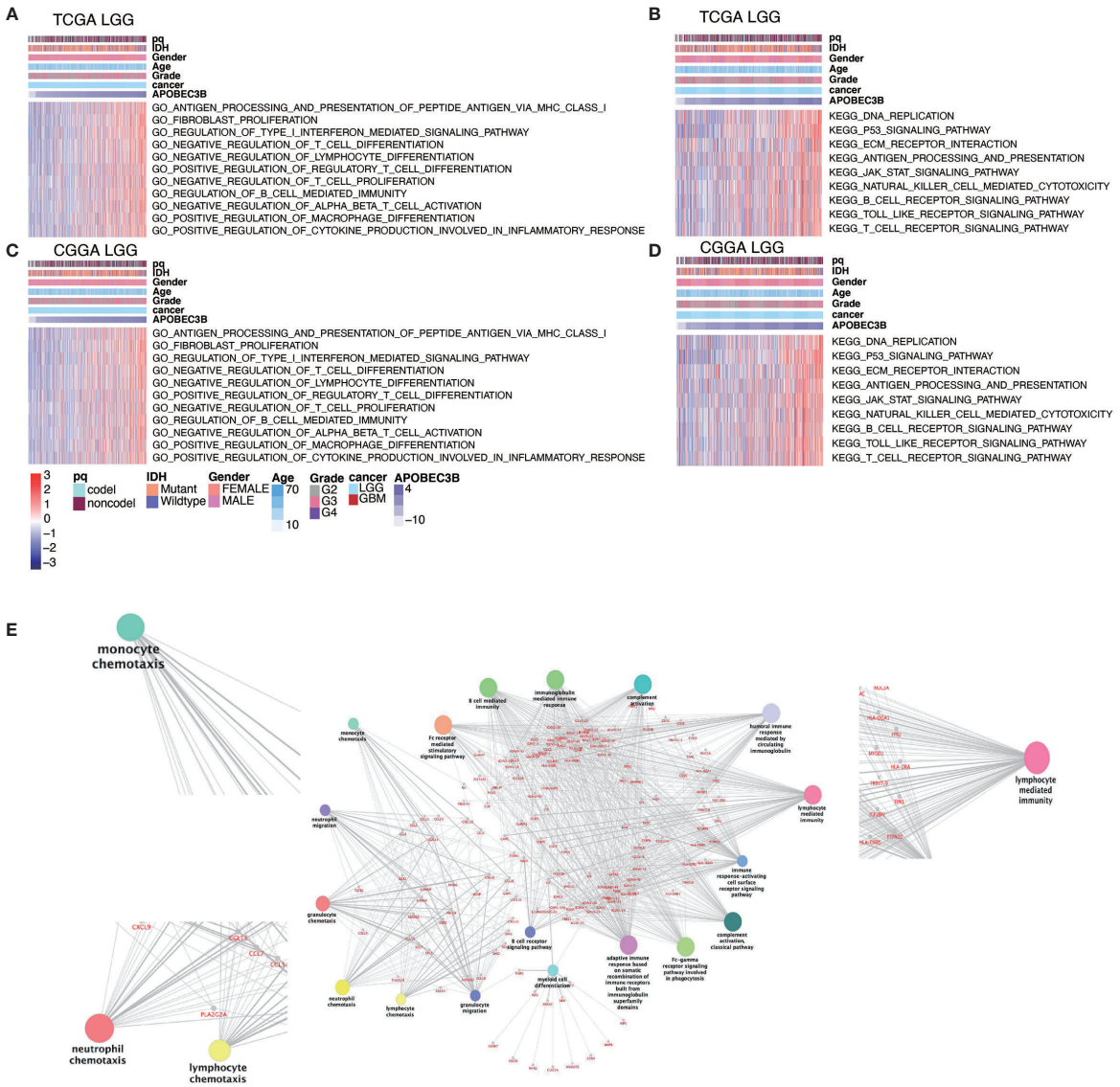

FIGURE 6 | APOBEC3B-related biological functions in LGG. GO analysis based on APOBEC3B levels in **(A)** TCGA and **(C)** CGGA datasets in LGG patients. KEGG pathway analysis based on APOBEC3B expression levels in **(B)** TCGA and **(D)** CGGA datasets in LGG patients. **(E)** The APOBEC3B related pathway revealed by APOBEC3B positively associated genes in TCGA datasets with ClueGO.

correlation between APOBEC3B and several immune cells such as activated $CD4^+$ T cells, central memory $CD8^+$ T cells, macrophages, MDSCs, memory B cells, regulatory T cells, and type 2 T helper cells in pan-cancer. And we found in KICH (**Figure 7C**), PAAD (**Figure 7D**) and UCS (**Figure 7E**), APOBEC3B expression was positively correlated with these immune cells. In accordance with the results in gliomas, APOBEC3B expression in UCS was mostly correlated with macrophage, MDSC, regulatory T cell and type 2 helper cell, which contributed to immunosuppression in TME, but these immunosuppressive cells are less significantly correlated with APOBEC3B in KICH and PAAD.

APOBEC3B Is Correlated With Other Immune Checkpoint Molecules in Gliomas

Regarded as a prospective immunotherapy, immune checkpoint inhibitors take an important role in the regulation of immune response in cancers. We investigated the relationship between APOBEC3B and several immune checkpoint genes in gliomas. We found APOBEC3B was associated with CD276(B7-H3), PDCD1LG2(PD-L2), IDO1, CD274(PD-L1), HAVCR2(TIM-3), and CD80(B7-1) in pan-glioma analysis (**Figure 8A**) and LGG (**Figure 8B**) in TCGA and CGGA datasets. We further analyzed the prognostic value of APOBEC3B in combination with CD276, PDCD1LG2, IDO1, and CD274. Significant worse

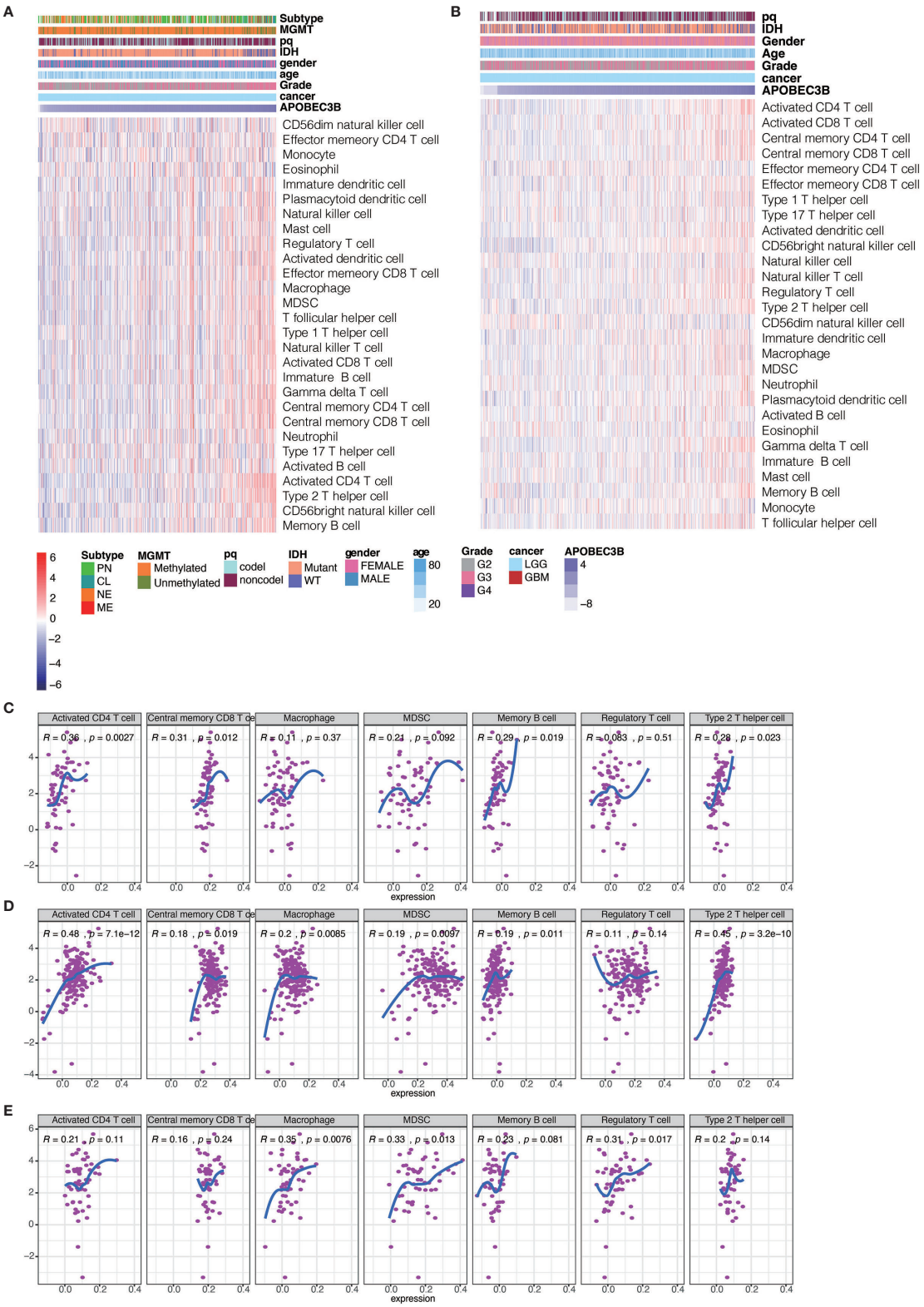

FIGURE 7 | Heatmaps illustrating the relationship between APOBEC3B and immune cell populations based on **(A)** TCGA and **(B)** CGGA in LGG patients. Correlation of APOBEC3B expression with immune infiltration cells including activated CD4+T cells, central memory CD8+T cells, macrophages, MDSC, memory B cell, regulatory T cells and Th2 cells in **(C)** KICH, **(D)** PAAD< **(E)** UCS.

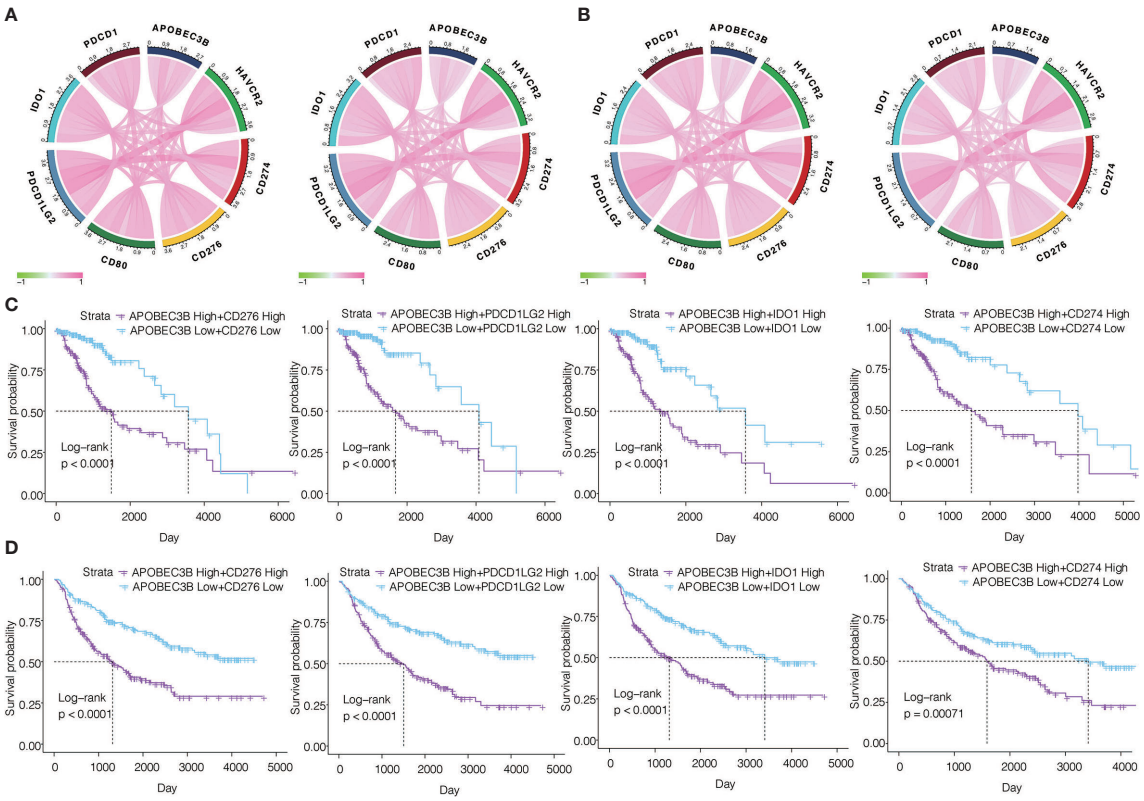

FIGURE 8 | Correlation of APOBEC3B expression with other immune checkpoint molecules in gliomas. Correlation analyses of APOBEC3B and other immune checkpoints in **(A)** pan-glioma analysis and **(B)** LGG patients from TCGA (left) and CGGA (right) datasets. Analyzing combined prognostic value of APOBEC3B and CD276, PDCD1LG2, IDO1 and CD274 expression in LGG patients from **(C)** TCGA and **(D)** CGGA datasets.

prognosis was observed in the patient group with the co-upregulation of APOBEC3B and these genes in LGG patients from TCGA and CGGA databases (**Figures 8C, D**).

Identification of a Gene Signature Associated With Immune Cells

WGCNAs were applied to determine the genes most correlated with high expression of APOBEC3B. Genes were clustered into eight modules (**Figures 9A**), and the correlation between the eight modules and the expression level of APOBEC3B was shown in **Figure 9B**. The yellow module showed the highest correlation coefficient with high APOBEC3B expression level. A significant correlation between module membership in the yellow module and gene significance for APOBEC3B^{high} was observed (**Figure 9C**). Then, GO enrichment analysis revealed that the neutrophil activation, neutrophil chemotaxis, and chemokine-mediated signaling pathway were the most related gene functions associated with the high expression of APOBEC3B (**Figure 9D**). And KEGG enrichment analysis revealed that Th17 cell differentiation, IL-17 signaling pathway, antigen processing and presentation, Th1 and Th2 cell differentiation as well as NF-kappa B signaling pathway were the most related pathways involved in high expression of APOBEC3B (**Figure 9E**).

DISCUSSION

Somatic mutations are responsible for the transformation from normal cells to cancer cells. Generally, somatic mutation has been considered as a therapy evasion promoter of cancer. Correspondingly, mutation can also promote antitumor T-cell response. As the only member of the deaminase family with constitutive nuclear localization, APOBEC3B, the endogenous mutagenic factor, can induce genomic C-to-U lesions that are correlated with a variety of mutagenic outcomes (23). Therefore, we are interested in the characteristics of APOBEC3B in the development of glioma.

To the best of our knowledge, studies about expression and prognostic value of APOBEC3B have been conducted in several cancer types. For example, highly expressed APOBEC3B is regarded as an unfavorable prognostic factors in myeloma (11), ovarian cancer (24), and clear cell renal cell carcinoma (25). Immune-oncology has become a hot area for tumor therapy nowadays. However, the immune-related and mutation-related role of APOBEC3B in cancer metastasis has not been thoroughly investigated. Most recently, the duality of APOBEC3B in immunotherapy has been demonstrated, in which APOBEC3B not only acts as the general driving force of therapy escape but

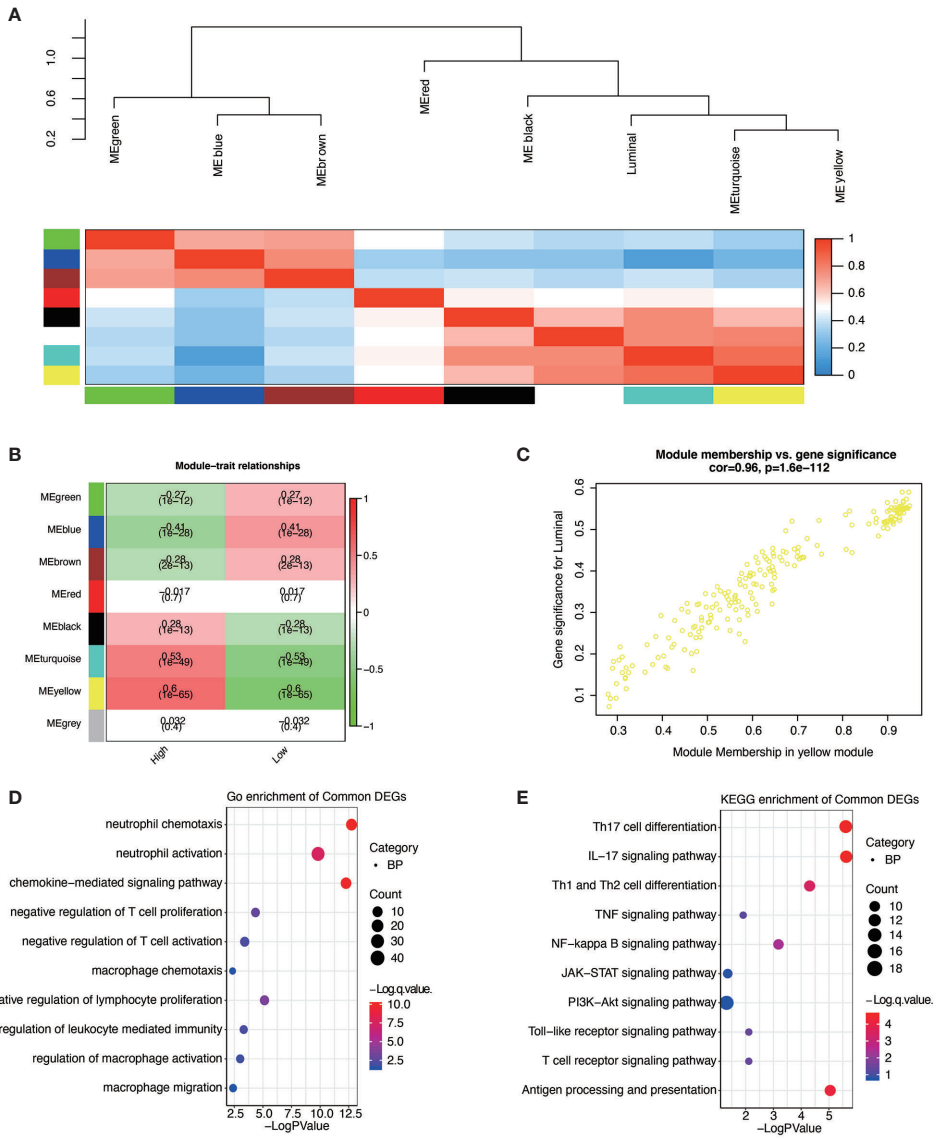

FIGURE 9 | Higher expression of APOBEC3B related gene signature identification. **(A)** WGCNA was applied to identify the clustered eigengene modules. **(B)** Seven modules are identified by WGCNA. **(C)** The yellow module has the highest correlation (r = 0.96, P = 1.6e-112). **(D)** Go analysis was performed based on APOBEC3B^{high} related genes. **(E)** KEGG analysis was performed based on APOBEC3B ^{high} related genes.

also significantly activates the immune system in melanoma (15). As important parts of TME, inflammatory cells and infiltrating immune cells are closely related to curative effect. Thus, understanding the TME can help to unveil the mechanisms of tumor development and shed light on tumor therapy. Previous study has proved that APOBEC3B is related to an active immune infiltration in high-grade serous ovarian carcinoma (26). But the activation of tumor-infiltrating immune cells also mediates APOBEC3B deletion in breast cancer in Asian patients (27).

In the current study, we characterized the landscape of APOBEC3B among glioma and other cancers *via* a large-scale bioinformatic analysis. We observed that APOBEC3B expression was upregulated in numerous cancer categories. In gliomas, the increasing expression level of APOBEC3B is consistent with the increasing grade of gliomas based on WHO classification. Presumable worse prognosis was observed in glioma patients with higher expression of APOBEC3B, and the result was further verified in ACC, CHOL, ESCA, LIHC, LUAD, PAAD, UCEC, UCS, and KICH in our study. Meanwhile, APOBEC3B was closely related to oncogenic mutation in our study, indicating its role in carcinogenesis. Thus, APOBEC3B has prognostic value in pan-cancer.

In GO and KEGG analysis, another major finding of our study was that elevated APOBEC3B was significantly accompanied by inflammatory, stromal and immune related signaling pathways in LGG, among which fibroblast

proliferation, negative regulation of T cell, positive regulation of Tregs and cytokines productions were most significant. Furthermore, upregulated APOBEC3B was significantly associated with immune cells and stromal cells' infiltration in glioma based on ESTIMATE algorithm. Several immune infiltrating cell types possess the features of immunosuppression: It is well documented that MDSC is able to inhibit innate and adaptive immunity (28), and macrophages have been indicated to promote cancer cell proliferation, immunosuppression, and angiogenesis in cancers (29). Treg not only can suppress the activation and expansion of different effector cells from mediating autoimmunity, but also can negatively affect immune therapies concerning immune checkpoints inhibitors (30, 31). Moreover, Th2 responses are generally considered undesirable since they mitigate against cytotoxic antitumor immune mechanisms in glioma (31). Cell type enrichment analysis further revealed that APOBEC3B was significantly correlated with MDSC, macrophage, regulatory T cells, and Th2 cells in glioma, KICH, PAAD, and UCS, providing evidence to the statement that APOBEC3B was an immunotherapy escape driver in LGG. Taken together, we proposed that APOBEC3B may be involved in the regulation of immunosuppressive microenvironment by recruiting immunosuppression cells and might become a selective target to inhibit immunosuppression.

The efficient treatment option for glioma is limited. Diverse cancer immunotherapeutic approaches have exhibited significant and exciting treatment outcomes for several cancer types, and have also triggered unparalleled research interest in glioma. Nowadays, glioma immunotherapy research predominantly focuses on immunosuppressive ICBs, CAR-T cells, vaccine, and oncolytic viruses (7). Although blood brain barrier and immunosuppressive TME in glioma patients suppress the efficiency of ICB treatment, ICBs do have revolutionized the treatment of solid malignant tumor. Our analysis illuminated that APOBEC3B was correlated with immune checkpoints including CD276, PDCD1LG2, IDO1, CD274, and TIM-3 in LGG and pan-glioma analysis. These immune checkpoints are promising immunotherapeutic targets for glioma, which CD276, PDCD1LG2, IDO1 and TIM-3 are both unfavorable prognosticator for glioma patients (32–35). In our current study, the co-upregulation of APOBEC3B and CD276, PDCD1LG2, IDO1, and CD274 suggested worse survival probability. CD276 has become a novel Cart-T target for GBM (36) while inhibition of PD-1/PD-L1 pathway can be a latent treatment strategy for glioma (37). Other promising immune checkpoint molecules like 4-1BB, GITR, and TIGIT are further being considered to enter early phase clinical trials (38). Immune checkpoints also take part in immunosuppression: upregulating PD-L1 can bind receptors on immune cells and suppress lymphocyte activation (39, 40). The correlation between APOBEC3B and these classic immune checkpoint molecules indicates that targeting APOBEC3B may become a potential approach for mediating immunotherapeutic response in LGG patients.

WGCNA is well applied to classify the high-throughput sequencing data into subsets of genes with cell-specific expression; therefore, we applied WGCNA to identify the APOBEC3B^{high} related genes. In our study, the yellow module was the most correlated one; further GO analysis revealed that neutrophil activities and chemokine-mediated signaling pathway were the most represented activities related to higher expression of APOBEC3B. Moreover, negative regulation of T cell activities further demonstrated that higher expression of APOBEC3B was correlated with activated inflammation and immunosuppression. In the KEGG analysis, IL-17 signaling pathway was the most relevant activity that occurred in patients with higher level of APOBEC3B. IL-17 is a cytokine produced by Th17 cell, suggesting the crucial role of Th17 cell in glioma pathogenesis.

In summary, our results revealed that APOBEC3B overexpression was related to aggressive clinicopathologic features, poor prognosis, inflammatory and immune pathways in glioma. These findings may be helpful in further optimizing diagnosis and immune treatments for LGG.

DATA AVAILABILITY STATEMENT

All data used in this work can be acquired from the Cancer Genome Atlas (TCGA) datasets (https://xenabrowser.net/), the Chinese Glioma Genome Atlas (CGGA) datasets (http://www.cgga.org.cn/).

AUTHOR CONTRIBUTIONS

HZ and QC conceptualized and designed the study. QC and ZL provided foundation support. HZ and ZC acquired and analyzed the data. HZ and ZC interpreted the data. HZ, ZC, ZW, ZD, ZH, XZ and QC drafted the manuscript and revised it for submission quality. All authors contributed to the article and approved the submitted version. QC supervised the study.

FUNDING

This work was supported by the National Natural Science Foundation of China (Nos. 82073893, 81703622, 81472693, and 81873635), China Postdoctoral Science Foundation (No. 2018M633002), Hunan Provincial Natural Science Foundation of China (No. 2018JJ3838), Hunan Provincial Health and Health Committee Foundation of China (C2019186).

SUPPLEMENTARY MATERIAL

The Supplementary Material for this article can be found online at: https://www.frontiersin.org/articles/10.3389/fonc.2021.625838/full#supplementary-material

Supplementary Figure 1 | Relationship between APOBEC3B and methylation statues. **(A).** Relationship between APOBEC3B and the mean value of methylation status at promoter region in TCGA. Relationship between APOBEC3B and methylation status at promoter region in TCGA: **(B)** cg01089751, **(C)** cg06837067, **(D)** cg11816043, **(E)** cg14194956, **(F)** cg14387414, **(G)** cg16045423, **(H)** cg21707131, **(I)** cg25787886, **(J)** cg26000393. The orange dots represent IDH-mutant samples, and cyan dots represent IDH wild-type samples, respectively. The orange line and cyan line represent linear regression between APOBEC3B expression and promoter region methylation in IDH-mutant samples and IDH wild-type samples, respectively.

Supplementary Figure 2 | Relationship between APOBEC3B and **(A)** anatomic structure analysis. CT (Cellular Tumour), HBV (Hyperplastic Blood Vessels), IT (Infiltrating Tumour), LE (Leading Edge), MVP (Microvascular Proliferation), PAN (Pseudopalisading Cells Around Necrosis) and PNZ (Perinecrotic Zone). **(B)** APOBEC3B copy number in TCGA pan-glioma. **(C)** distinct radiographical regions of glioma. **(D)** different histology analysis from CGGA database. **(E)** different disease conditions including primary, recurrent and secondary from CGGA database. **(F)** different treatment outcomes.

Supplementary Figure 3 | APOBEC3B-related biological functions in gliomas. GO analysis based on APOBEC3B levels in **(A)** TCGA and **(C)** CGGA datasets in pan-glioma analysis. KEGG pathway analysis based on APOBEC3B expression levels in **(B)** TCGA and **(D)** CGGA datasets in pan-glioma analysis.

Supplementary Figure 4 | Heatmaps illuminating APOBEC3B related inflammatory activities in LGG and pan-glioma. Analysis between APOBEC3B and inflammatory metagenes in LGG from **(A)** TCGA and **(B)** CGGA datasets and pan-glioma analysis from **(C)** TCGA and **(D)** CGGA.

Supplementary Figure 5 | Correlation between APOBEC3B expression and ESTIMATE algorithm scores in gliomas. APOBEC3B expression was positively correlated with immune score, stromal score and ESTIMATE score in **(A)** pan-glioma analysis and **(B)** LGG patients. The relationship between APOBEC3B and stromal cell populations based on **(C)** TCGA and **(D)** CGGA in LGG patients.

Supplementary Figure 6 | Heatmaps illustrating the relationship between APOBEC3B and immune cell populations based on **(A)** TCGA and **(B)** CGGA in pan-glioma analysis. The relationship between APOBEC3B and stromal cell populations based on **(C)** TCGA and **(D)** CGGA in pan-glioma analysis.

REFERENCES

1. Miller AM, Shah RH, Pentsova EI, Pourmaleki M, Briggs S, Distefano N, et al. Tracking tumour evolution in glioma through liquid biopsies of cerebrospinal fluid. *Nature* (2019) 565:654–8. doi: 10.1038/s41586-019-0882-3
2. Wen PY, Reardon DA. Neuro-oncology in 2015: Progress in glioma diagnosis, classification and treatment. *Nat Rev Neurol* (2016) 12:69–70. doi: 10.1038/nrneurol.2015.242
3. Zhang H, Wang R, Yu Y, Liu J, Luo T, Fan F. Glioblastoma Treatment Modalities besides Surgery. *J Cancer* (2019) 10:4793–806. doi: 10.7150/jca.32475
4. Goel G, Sun W. Cancer immunotherapy in clinical practice – the past, present, and future. *Chin J Cancer* (2014) 33:445–57. doi: 10.5732/cjc.014.10123
5. Ribas A, Wolchok JD. Cancer immunotherapy using checkpoint blockade. *Science* (2018) 359:1350–5. doi: 10.1126/science.aar4060
6. Roesch S, Rapp C, Dettling S, Herold-Mende C. When Immune Cells Turn Bad-Tumor-Associated Microglia/Macrophages in Glioma. *Int J Mol Sci* (2018) 19(2):436. doi: 10.3390/ijms19020436
7. Wang H, Xu T, Huang Q, Jin W, Chen J. Immunotherapy for Malignant Glioma: Current Status and Future Directions. *Trends Pharmacol Sci* (2020) 41:123–38. doi: 10.1016/j.tips.2019.12.003
8. Peng Z, Chen Y, Cao H, Zou H, Wan X, Zeng W, et al. Protein disulfide isomerases are promising targets for predicting the survival and tumor progression in glioma patients. *Aging (Albany NY)* (2020) 12:2347–72. doi: 10.18632/aging.102748
9. Alexandrov LB, Nik-Zainal S, Wedge DC, Aparicio SA, Behjati S, Biankin AV, et al. Signatures of mutational processes in human cancer. *Nature* (2013) 500:415–21. doi: 10.1038/nature12477
10. Sieuwerts AM, Doebar SC, de Weerd V, Verhoef EI, Beauford CM, Agahozo MC, et al. APOBEC3B Gene Expression in Ductal Carcinoma In Situ and Synchronous Invasive Breast Cancer. *Cancers (Basel)* (2019) 11(8):1062. doi: 10.3390/cancers11081062
11. Yamazaki H, Shirakawa K, Matsumoto T, Hirabayashi S, Murakawa Y, Kobayashi M, et al. Endogenous APOBEC3B Overexpression Constitutively Generates DNA Substitutions and Deletions in Myeloma Cells. *Sci Rep* (2019) 9:7122. doi: 10.1038/s41598-019-43575-y
12. Wang S, Jia M, He Z, Liu XS. APOBEC3B and APOBEC mutational signature as potential predictive markers for immunotherapy response in non-small cell lung cancer. *Oncogene* (2018) 37:3924–36. doi: 10.1038/s41388-018-0245-9
13. Roberts SA, Lawrence MS, Klimczak LJ, Grimm SA, Fargo D, Stojanov P, et al. An APOBEC cytidine deaminase mutagenesis pattern is widespread in human cancers. *Nat Genet* (2013) 45:970–6. doi: 10.1038/ng.2702
14. Evgin L, Huff AL, Kottke T, Thompson J, Molan AM, Driscoll CB, et al. Suboptimal T-cell Therapy Drives a Tumor Cell Mutator Phenotype That Promotes Escape from First-Line Treatment. *Cancer Immunol Res* (2019) 7:828–40. doi: 10.1158/2326-6066.CIR-18-0013
15. Driscoll CB, Schuelke MR, Kottke T, Thompson JM, Wongthida P, Tonne JM, et al. APOBEC3B-mediated corruption of the tumor cell immunopeptidome induces heteroclitic neoepitopes for cancer immunotherapy. *Nat Commun* (2020) 11:790. doi: 10.1038/s41467-020-14568-7
16. Bindea G, Mlecnik B, Hackl H, Charoentong P, Tosolini M, Kirilovsky A, et al. ClueGO: a Cytoscape plug-in to decipher functionally grouped gene ontology and pathway annotation networks. *Bioinformatics* (2009) 25:1091–3. doi: 10.1093/bioinformatics/btp101
17. van den Bent MJ, Brandes AA, Taphoorn MJ, Kros JM, Kouwenhoven MC, Delattre JY, et al. Adjuvant procarbazine, lomustine, and vincristine chemotherapy in newly diagnosed anaplastic oligodendroglioma: long-term follow-up of EORTC brain tumor group study 26951. *J Clin Oncol* (2013) 31:344–50. doi: 10.1200/JCO.2012.43.2229
18. Rivera AL, Pelloski CE, Gilbert MR, Colman H, De La Cruz C, Sulman EP, et al. MGMT promoter methylation is predictive of response to radiotherapy and prognostic in the absence of adjuvant alkylating chemotherapy for glioblastoma. *Neuro Oncol* (2010) 12:116–21. doi: 10.1093/neuonc/nop020
19. Cancer Genome Atlas Research, N, rat DJ, Verhaak RG, Aldape KD, Yung WK, Salama SR, et al. Comprehensive, Integrative Genomic Analysis of Diffuse Lower-Grade Gliomas. *N Engl J Med* (2015) 372:2481–98. doi: 10.1056/NEJMoa1402121
20. Liu XY, Gerges N, Korshunov A, Sabha N, Khuong-Quang DA, Fontebasso AM, et al. Frequent ATRX mutations and loss of expression in adult diffuse astrocytic tumors carrying IDH1/IDH2 and TP53 mutations. *Acta Neuropathol* (2012) 124:615–25. doi: 10.1007/s00401-012-1031-3
21. Ichimura K. Molecular pathogenesis of IDH mutations in gliomas. *Brain Tumor Pathol* (2012) 29:131–9. doi: 10.1007/s10014-012-0090-4
22. Li S, Bao X, Wang D, You L, Li X, Yang H, et al. APOBEC3B and IL-6 form a positive feedback loop in hepatocellular carcinoma cells. *Sci China Life Sci* (2017) 60:617–26. doi: 10.1007/s11427-016-9058-6
23. Burns MB, Temiz NA, Harris RS. Evidence for APOBEC3B mutagenesis in multiple human cancers. *Nat Genet* (2013) 45:977–83. doi: 10.1038/ng.2701
24. Du Y, Tao X, Wu J, Yu H, Yu Y, Zhao H. APOBEC3B up-regulation independently predicts ovarian cancer prognosis: a cohort study. *Cancer Cell Int* (2018) 18:78. doi: 10.1186/s12935-018-0572-5
25. Xu L, Chang Y, An H, Zhu Y, Yang Y, Xu J, et al. High APOBEC3B expression is a predictor of recurrence in patients with low-risk clear cell renal cell carcinoma. *Urol Oncol* (2015) 33:340 e341–348. doi: 10.1016/j.urolonc.2015.05.009
26. Ruder U, Denkert C, Kunze CA, Jank P, Lindner J, Johrens K, et al. APOBEC3B protein expression and mRNA analyses in patients with high-grade serous ovarian carcinoma. *Histol Histopathol* (2019) 34:405–17. doi: 10.14670/HH-18-050

27. Wen WX, Soo JS, Kwan PY, Hong E, Khang TF, Mariapun S, et al. Germline APOBEC3B deletion is associated with breast cancer risk in an Asian multi-ethnic cohort and with immune cell presentation. *Breast Cancer Res* (2016) 18:56. doi: 10.1186/s13058-016-0717-1
28. Bronte V, Brandau S, Chen SH, Colombo MP, Frey AB, Greten TF, et al. Recommendations for myeloid-derived suppressor cell nomenclature and characterization standards. *Nat Commun* (2016) 7:12150. doi: 10.1038/ncomms12150
29. Ngambenjawong C, Gustafson HH, Pun SH. Progress in tumor-associated macrophage (TAM)-targeted therapeutics. *Adv Drug Deliv Rev* (2017) 114:206–21. doi: 10.1016/j.addr.2017.04.010
30. Grauer OM, Nierkens S, Bennink E, Toonen LW, Boon L, Wesseling P, et al. CD4+FoxP3+ regulatory T cells gradually accumulate in gliomas during tumor growth and efficiently suppress antiglioma immune responses in vivo. *Int J Cancer* (2007) 121:95–105. doi: 10.1002/ijc.22607
31. Wainwright DA, Chang AL, Dey M, Balyasnikova IV, Kim CK, Tobias A, et al. Durable therapeutic efficacy utilizing combinatorial blockade against IDO, CTLA-4, and PD-L1 in mice with brain tumors. *Clin Cancer Res* (2014) 20:5290–301. doi: 10.1158/1078-0432.CCR-14-0514
32. Zhang C, Zhang Z, Li F, Shen Z, Qiao Y, Li L, et al. Large-scale analysis reveals the specific clinical and immune features of B7-H3 in glioma. *Oncoimmunology* (2018) 7:e1461304. doi: 10.1080/2162402X.2018.1461304
33. Wang ZL, Li GZ, Wang QW, Bao ZS, Wang Z, Zhang CB, et al. PD-L2 expression is correlated with the molecular and clinical features of glioma, and acts as an unfavorable prognostic factor. *Oncoimmunology* (2019) 8:e1541535. doi: 10.1080/2162402X.2018.1541535
34. Zhai L, Ladomersky E, Lauing KL, Wu M, Genet M, Gritsina G, et al. Infiltrating T Cells Increase IDO1 Expression in Glioblastoma and Contribute to Decreased Patient Survival. *Clin Cancer Res* (2017) 23:6650–60. doi: 10.1158/1078-0432.CCR-17-0120
35. Li G, Wang Z, Zhang C, Liu X, Cai J, Wang Z, et al. Molecular and clinical characterization of TIM-3 in glioma through 1,024 samples. *Oncoimmunology* (2017) 6:e1328339. doi: 10.1080/2162402X.2017.1328339
36. Tang X, Zhao S, Zhang Y, Wang Y, Zhang Z, Yang M, et al. B7-H3 as a Novel CAR-T Therapeutic Target for Glioblastoma. *Mol Ther Oncolytics* (2019) 14:279–87. doi: 10.1016/j.omto.2019.07.002
37. Xue S, Hu M, Iyer V, Yu J. Blocking the PD-1/PD-L1 pathway in glioma: a potential new treatment strategy. *J Hematol Oncol* (2017) 10:81. doi: 10.1186/s13045-017-0455-6
38. Kelly WJ, Giles AJ, Gilbert M. T lymphocyte-targeted immune checkpoint modulation in glioma. *J Immunother Cancer* (2020) 8(1):e000379. doi: 10.1136/jitc-2019-000379
39. Lim M, Xia Y, Bettegowda C, Weller M. Current state of immunotherapy for glioblastoma. *Nat Rev Clin Oncol* (2018) 15:422–42. doi: 10.1038/s41571-018-0003-5
40. Liu F, Huang J, Xiong Y, Li S, Liu Z. Large-scale analysis reveals the specific clinical and immune features of CD155 in glioma. *Aging (Albany NY)* (2019) 11:5463–82. doi: 10.18632/aging.102131

Conflict of Interest: The authors declare that the research was conducted in the absence of any commercial or financial relationships that could be construed as a potential conflict of interest.

frontiers in Oncology

ORIGINAL RESEARCH
published: 13 May 2021
doi: 10.3389/fonc.2021.632663

Differential Predictors and Clinical Implications Associated With Long-Term Survivors in IDH Wildtype and Mutant Glioblastoma

Haihui Jiang[1,2†], Kefu Yu[3], Yong Cui[1,2], Xiaohui Ren[1,2], Mingxiao Li[1,2], Guobin Zhang[1,2], Chuanwei Yang[1,2], Xuzhe Zhao[1,2], Qinghui Zhu[1,2] and Song Lin[1,2,4†]*

[1] Department of Neurosurgery, Beijing Tiantan Hospital, Capital Medical University, Beijing, China, [2] National Clinical Research Center for Neurological Diseases, Center of Brain Tumor, Beijing Institute for Brain Disorders and Beijing Key Laboratory of Brain Tumor, Beijing, China, [3] Department of Pharmacy, Beijing Tiantan Hospital, Capital Medical University, Beijing, China, [4] Beijing Neurosurgical Institute, Capital Medical University, Beijing, China

OPEN ACCESS

Edited by:
Yaohua Liu,
Shanghai First People's Hospital, China

Reviewed by:
Elizabeth Jane Hovey, New South Wales Department of Health, Australia
Simon Hanft, Westchester Medical Center, United States

***Correspondence:**
Song Lin
linsong2005@126.com

†ORCID:
Haihui Jiang
orcid.org/0000-0002-8114-9741
Song Lin
orcid.org/0000-0001-5721-274X

Specialty section:
This article was submitted to Neuro-Oncology and Neurosurgical Oncology, a section of the journal Frontiers in Oncology

Received: 23 November 2020
Accepted: 26 April 2021
Published: 13 May 2021

Citation:
Jiang H, Yu K, Cui Y, Ren X, Li M, Zhang G, Yang C, Zhao X, Zhu Q and Lin S (2021) Differential Predictors and Clinical Implications Associated With Long-Term Survivors in IDH Wildtype and Mutant Glioblastoma. Front. Oncol. 11:632663. doi: 10.3389/fonc.2021.632663

Background: Glioblastoma (GBM) is the most aggressive intracranial tumor which can be divided into two subtypes based on status of isocitrate dehydrogenase (IDH). A small fraction of patients after receiving standard treatment can be long-term survivors (LTS). This study was designed to disclose the predictors and clinical implications associated with LTS in IDH wildtype and mutant GBM.

Methods: Patients who survived beyond five years after diagnosis of GBM were defined as LTS, while those with a survival less than one year were defined as short-term survivors (STS). A total of 211 patients with diagnosis of GBM in Beijing Tiantan Hospital from January 2007 to January 2015 were enrolled, including 44 (20.9%) LTS and 167 (79.1%) STS. The clinical, radiological and molecular features between groups were systematically compared.

Results: Compared with STS, LTS were a subgroup of patients with a younger age at diagnosis (P=0.006), a higher KPS score (P=0.011), higher rates of cystic change (P=0.037), O^6-methylguanine-DNA methyltransferase (MGMT) promoter methylation (P=0.007), and IDH mutation (P=0.049), and more likely to have undergone gross total resection (P<0.001). Survival analysis demonstrated that LTS with wildtype IDH conferred a longer progression-free survival (66.0 *vs.* 27.0 months, P=0.04), but a shorter post-progression survival (46.5 months *vs.* not reached, P=0.0001) than those of LTS with mutant IDH. LTS with mutant IDH showed a trend towards increased survival after receiving re-operation (P=0.155) and reirradiation (P=0.127), while this clinical benefit disappeared in the subset of LTS with wildtype IDH (P>0.05).

Conclusion: The prognostic value and therapeutic implications associated with LTS in GBM population significantly differed on the basis of IDH status. Our findings provide a new approach for physicians to better understand the two subtypes of GBM, which may assist in making more tailored treatment decisions for patients.

Keywords: glioblastoma, long-term survivor, IDH, precision medicine, treatment

INTRODUCTION

Glioblastoma (GBM) is one of the worldwide intractable malignancies in adults (1). Despite advances in the therapeutic regimens during past few decades, the clinical outcomes of patients with GBM have not been substantially improved (2–4). It is reported that most of patients will progress within one year after resection, and the median survival is less than two years (4). Although the survival rate of GBM remains unfavorable, there are still a few patients who demonstrate an extraordinary response to treatment with a prolonged progression-free survival (PFS); some patients even survive more than five years (5–7). But unfortunately, the intrinsic characteristics of these long-term survivors (LTS) are still unclear (5).

Previous studies have established that isocitrate dehydrogenase (IDH) mutation was a strong predictor associated with long-term survival of patients with GBM (8, 9), which has led the neuropathologists to reclassify GBM into two molecular subtypes: IDH-wildtype (IDH-wt) GBM and IDH-mutant (IDH-mut) GBM (10). Traditionally, IDH-mut GBM is regarded as a secondary malignancy that had transformed from a low-grade diffuse glioma (11). Meanwhile, IDH-wt GBM, which represents the major component (>90%) of the whole GBM cohort, is clinically defined as primary GBM (10). There are some studies that have explored the predictors for becoming a long-term survivor within the GBM population (5, 6, 8, 9). But up to now, no studies have compared the characteristics and clinical implications associated with LTS between IDH-wt and IDH-mut GBM.

Therefore, in the present study, we systematically compared the clinical, radiological and molecular characteristics between LTS and short-term survivors (STS) in the cohort of GBM. Furthermore, the intrinsic characteristics and clinical implications correlated with LTS between IDH-wt and IDH-mut GBM have also been explored. We found that the clinical, radiological, and molecular features of IDH-wt and IDH-mut LTS were significantly different and the two subtypes of LTS showed distinct PFS and post-progression survival (PPS), which can help the physicians to better understand GBM and may contribute to making more tailored treatment decisions for patients.

MATERIALS AND METHODS

Patient Cohort

Forty-four patients who survived beyond five years after diagnosis of GBM (LTS) and 167 patients who survived less than one years after diagnosis of GBM (STS) between January 2007 and January 2015 in Beijing Tiantan Hospital affiliated to Capital Medical University were selected for inclusion in this study. Pathology review was performed by two experienced neuropathologists according to the 2016 World Health Organization (WHO) classification schema (10). All the patients, in our institution, once diagnosed with GBM are recommended to proceed with post-operative combination radiation and chemotherapy. However, there are still a small number of patients who missed out on chemotherapy or radiation for personal reasons. Radiation was performed within one month after operation, with a total dose of 60 Gy which was further divided into 30 fractions. The adjuvant chemotherapy regimen was mainly nimostine (ACNU) and temozolomide (TMZ), according to the previously described protocol (12). When tumor progressed, re-operation and reirradiation were performed if possible. Rechallenge with chemotherapy which commonly consisted of a combination of bevacizumab and temozolomide (TMZ) could be also attempted if patients showed relatively normal laboratory tests and maintained a reasonable performance status (ECOG: 0-2) (13).

Radiological Evaluation

The radiological evaluation was performed by 3 experienced neuroradiologists who were blind to the clinical outcome of patients. Radiological features included tumor location, tumor size, enhancement, cystic change, and extent of resection. The calculation of tumor size was mainly based on the T1-weighted imaging (T1WI) contrast enhanced area. Enhancement was classified into three subtypes: solid, ring, irregular (**Figure 1**) (14). Solid subtype was relatively uniformly enhanced and concurrent with a well-circumscribed edge. Ring subtype was characterized by a ring-like enhancement with central necrosis or cyst. Irregular subtype had scattered enhancement which was irregularly shaped. A cystic tumor was defined as those with a large cyst cavity comprising at least half of the whole tumor and the cyst was filled with fluid that showed a radiographic appearance similar to cerebrospinal fluid on T2-weighted imaging (T2WI) (**Figure 1**) (15). Hence, tumors with fluid-filled cysts and those with large central necrosis were both regarded as cystic tumors in this study. Within 72 hours after operation, an enhanced magnetic resonance imaging (MRI) was carried out to assess the extent of resection (EOR). EOR was calculated on the basis of contrast-enhanced T1WI, according to the following equation: (preoperative tumor volume - postoperative tumor volume)/preoperative tumor volume.

Molecular Biomarkers Detection

Abnormality of chromosome 1p/19q, IDH mutation and O^6-methylguanine-DNA methyltransferase (MGMT) promoter methylation were respectively analyzed by fluorescence *in situ* hybridization (FISH) (16), Sanger sequencing (17) and pyrosequencing (18), according to previously described methods (**Figure 2**). Ki-67 index was detected by immunohistochemistry (IHC) staining which was done with a monoclonal mouse antibody (1:80 dilution, Dako) (**Figure 2**). The expression level of the Ki-67 index was defined as either high (≥30%) or low (<30%) for interpretation, according to the percentage of IHC-positive cells (19).

Follow-Up

After operation, patients were regularly followed up with brain MRI scans until death. MRIs were performed at an interval of three months, or more frequent in the event of clinical changes,

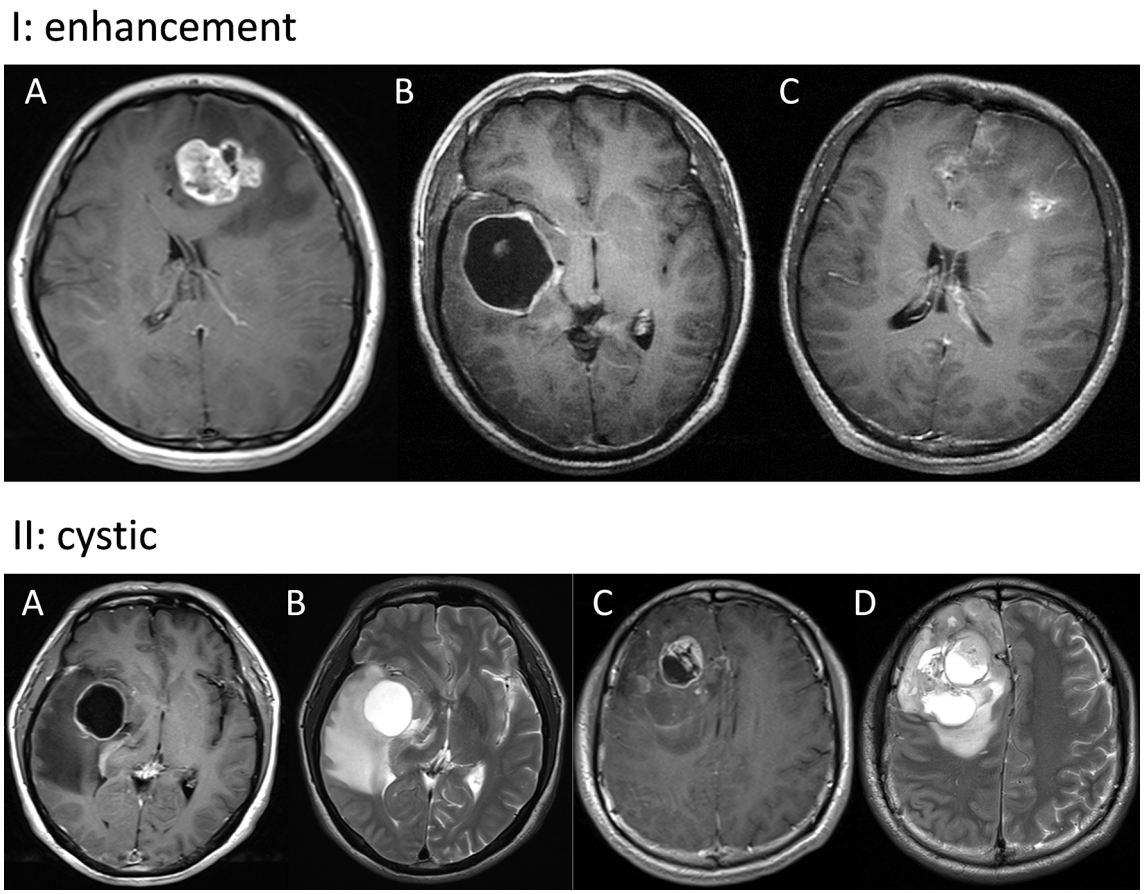

FIGURE 1 | Panel I: Representative images of solid **(A)**, ring **(B)**, and irregular **(C)** enhancement. Panel II: Typical images of cystic GBM. A tumor in the right insular lobe with fluid-filled cysts **(A, B)** and a tumor in the right frontal lobe with large central necrosis **(C, D)**.

such as seizures or neurologic deterioration. Progression pattern was divided into local and non-local subtypes based on the preoperative and serial postoperative radiographic images (**Figure S1**). Local recurrence was those with lesion located in the resection cavity or in continuity with it, or less than 2 cm from the primary tumor margins, while the recurrence lesion border beyond 2 cm from the original cavity was defined as non-local failure (20). PFS was defined as the time period from the date of operation to the date of progression or recurrence demonstrated by MRI, death or last follow up. Overall survival (OS) was defined as the time period from the date of initial operation to the date of death or last follow-up. Timespan between the first progression and death/last follow-up was defined as post-progression survival (PPS). The median follow-up of this cohort was 71.5 (range: 1.0-130.0) months. There were 195 (92.4%) patients with progression and 176 (83.4%) patients had died by the time of data analysis.

Statistical Analysis

All the analyses were performed with SPSS (version 22.0, Chicago, IL, USA) and R software (http://www.r-project.org, The R Foundation). Comparisons of categorical variables between the groups were performed using chi-square test or Fisher's exact test, while differences in age at diagnosis, tumor size and Karnofsky performance scale (KPS) score were evaluated by student t-test. The variables with P values less than 0.05 were entered into the multivariate logistic regression analysis to identify the independent predictors of LTS. Survival rates were calculated using the Kaplan-Meier methods, and differences were compared by log-rank tests. All tests were two-sided, and difference with a *P* value less than 0.05 was considered to be statistically significant.

RESULTS

Patient Population

We identified 211 patients, including 44 (20.9%) LTS and 167 (79.1%) STS. Of these 44 LTS, there were 17 (38.6%) patients with wildtype IDH and 27 (61.4%) patients with mutant IDH. Our cohort consisted of 126 males and 85 females with a mean age of 49.0 ± 11.8 years. All the clinical, radiological, and molecular characteristics of patients were summarized in **Table 1**.

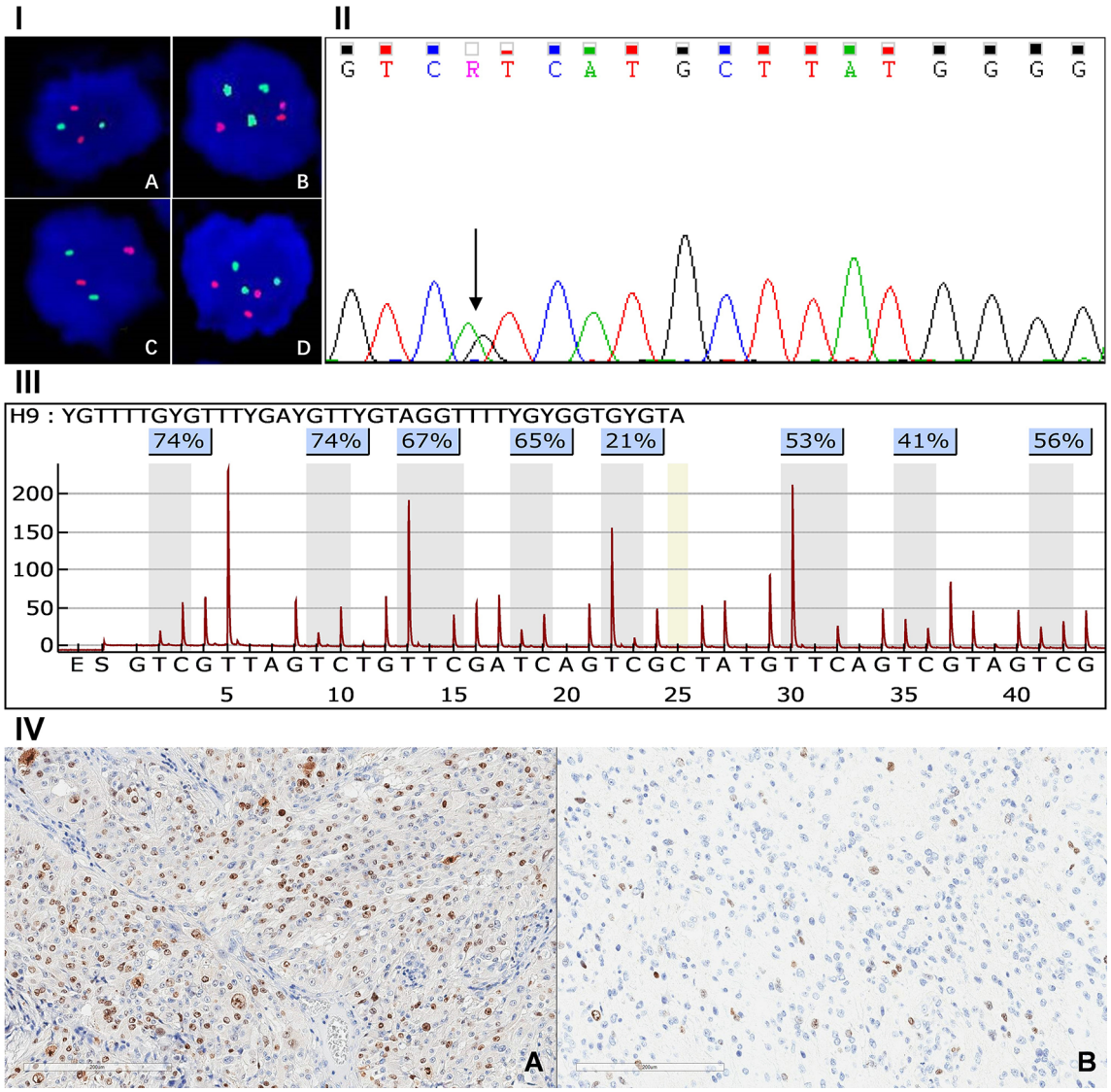

FIGURE 2 | Panel I, FISH detection result of 1q/19p polysomy: 1p intact **(A)**, 1q polysomy **(B)**, 19q intact **(C)**, 19p polysomy **(D)**. Panel II: Sanger sequence of IDH1 mutation. Panel III: Assay of MGMT promoter methylation in GBM. Panel IV: Immunohistochemical staining of high **(A)** and low **(B)** Ki-67 index.

Comparison of Baseline Characteristics Between STS and LTS

LTS patients were younger (41.2 ± 11.1 *vs.* 49.9 ± 11.3, $P < 0.001$), and had higher KPS score (82.2 ± 8.3 *vs.* 76.2 ± 14.9, $P = 0.002$) than the STS. But they shared a similar gender ratio and tumor size ($P > 0.05$). There were more frontal tumors in LTS (59.1% *vs.* 35.9%, $P = 0.039$), but no significant difference has been observed in the laterality ($P = 0.138$). The enhancement features were also similar between STS and LTS ($P = 0.139$), while LTS showed a higher frequency of cystic change (56.8% *vs.* 19.2%, $P < 0.001$). With respect to the treatment information, LTS patients were more likely to have undergone gross-total resection (GTR) (86.4% *vs.* 31.7%, $P < 0.001$), and to have received chemotherapy (100.0% *vs.* 91.6%, $P = 0.084$) and radiotherapy (100.0% *vs.* 86.2%, $P = 0.005$), compared with the STS. The molecular profile of LTS patients was characterized by a higher rate of MGMT promoter methylation (70.6% *vs.* 34.9%, $P<0.001$), IDH mutation (61.4% *vs.* 13.2%, $P < 0.001$), and 1q/19p co-polysomy (25.7% *vs.* 12.6%, $P = 0.047$). The Ki-67 index was similar among groups ($P = 0.510$) (**Table 1**).

On the basis of these predictors identified by univariate analyses, a multivariate logistic regression model was built. The final results showed that age < 50 years (odds ratio [OR] = 1.081, 95% confidence interval [CI]: 1.022-1.141, $P = 0.006$), KPS score ≥ 70 (OR = 22.354, 95% CI: 2.028-246.449, $P = 0.011$), cystic change (OR = 3.791, 95% CI: 1.082-13.275, $P = 0.037$), GTR (OR = 18.731, 95% CI: 4.636-75.690, $P < 0.001$), MGMT promoter methylation

TABLE 1 | Comparisons of baseline characteristics between short- and long-term survivors.

Variables	All (n=211)	STS (n=167)	LTS (n=44)	*P* value
Age at diagnosis (years)	49.0 ± 11.8	49.9 ± 11.3	41.2 ± 11.1	<0.001
Gender				0.432
Male	126/211	102/167	24/44	
KPS score	80.0 ± 14.2	76.2 ± 14.9	82.2 ± 8.3	0.002
Tumor size (mm)	49.2 ± 18.9	49.5 ± 19.1	48.1 ± 18.3	0.652
Tumor location				0.039*
Frontal	86/211	60/167	26/44	
Temporal	56/211	45/167	11/44	
Parietal	35/211	32/167	3/44	
Occipital	18/211	16/167	2/44	
Others	16/211	14/167	2/44	
Laterality				0.138
Right	92/211	67/167	25/44	
Left	95/211	80/167	15/44	
Bilateral	24/211	20/167	4/44	
Enhancement				0.139
Solid	144/211	118/167	26/44	
Ring	38/211	30/167	8/44	
Irregular	29/211	19/167	10/44	
Cystic change				<0.001
Yes	57/211	32/167	25/44	
Extent of resection				<0.001
GTR	91/211	53/167	38/44	
Chemotherapy				0.084
Temozolomide	170/211	134/167	36/44	
Nimostine	27/211	19/167	8/44	
None	14/211	14/167	0/44	
Radiotherapy				0.005*
Yes	188/211	144/167	44/44	
Recurrence pattern				0.838
Local	156/195	134/167	22/28	
MGMT promotor				<0.001
Methylation	68/160	44/126	24/34	
IDH				<0.001
Mutation	55/211	28/167	27/44	
1q/19p co-polysomy				0.047
Yes	30/202	21/167	9/35	
Ki-67 index				0.510
High	70/193	59/158	11/35	

KPS, Karnofsky performance scale; GTR, gross-total resection; MGMT, O^6-methylguanine-DNA-methyltransferase; IDH, isocitrate dehydrogenase.
**by Fisher exact test.*

(OR = 5.553, 95% CI: 1.591-19.379, $P = 0.007$), and IDH mutation (OR = 4.321, 95% CI: 1.007-18.535, $P = 0.049$) were confirmed as predictive factors for LTS (**Table 2**).

Comparison of Baseline Characteristics Between IDH-Wt and IDH-Mut LTS

Compared with the IDH-wt LTS, IDH-mut LTS had a lower rate of solid enhancement (44.4% *vs.* 82.3%, $P = 0.036$), but higher rates of cystic change (70.4% *vs.* 35.3%, $P = 0.022$), local recurrence (95.0% *vs.* 37.5%, $P = 0.003$), and 1q/19p co-polysomy (44.4% *vs.* 5.9%, $P = 0.018$). The Ki-67 index of IDH-mut LTS was lower than that in the IDH-wt LTS, but the difference was not statistically significant (16.7% *vs.* 47.1%, $P = 0.053$) (**Table 3**).

TABLE 2 | Results of multivariate logistic regression analysis.

Variables	Odds ratio (OR)	95% Confidence interval (CI)	*P* value
Age at diagnosis			
<50 years	1.081	1.022-1.141	0.006
KPS score			
≥70	22.354	2.028-246.449	0.011
Cystic change			
Yes	3.791	1.082-13.275	0.037
Extent of resection			
GTR	18.731	4.636-75.690	<0.001
MGMT promotor			
Methylation	5.553	1.591-19.379	0.007
IDH			
Mutation	4.321	1.007-18.535	0.049

KPS, Karnofsky performance scale; GTR, gross-total resection; MGMT, O^6-methylguanine-DNA-methyltransferase; IDH, isocitrate dehydrogenase.

TABLE 3 | Comparisons of baseline characteristics between IDH-wt and IDH-mut long-term survivors.

Variables	IDH-wt (n=17)	IDH-mut (n=27)	*P* value
Age at diagnosis (years)	41.1 ± 12.3	41.3 ± 10.5	0.938
Gender			0.651
Male	10/17	14/27	
KPS score	80.0 ± 8.7	84.7 ± 7.4	0.115
Tumor size (mm)	52.4 ± 16.3	45.3 ± 19.2	0.213
Tumor location			0.351
Frontal	10/17	16/27	
Temporal	6/17	5/27	
Parietal	0/17	3/17	
Occipital	1/17	1/27	
Others	0/17	2/27	
Laterality			0.342
Right	8/17	17/27	
Left	8/17	7/27	
Bilateral	1/17	3/27	
Enhancement			0.036
Solid	14/17	12/27	
Ring	2/17	6/27	
Irregular	1/17	9/27	
Cystic change			0.022
Yes	6/17	19/27	
Extent of resection			0.380*
GTR	16/17	22/27	
Chemotherapy			0.125*
Temozolomide	16/17	20/27	
Nimostine	1/17	7/27	
Radiotherapy			NA
Yes	17/17	27/27	
Recurrence pattern			0.003*
Local	3/8	19/20	
MGMT promotor			1.0
Methylation	12/17	12/17	
1q/19p co-polysomy			0.018*
Yes	1/17	8/18	
Ki-67 index			0.053
High	8/17	3/18	

IDH, isocitrate dehydrogenase; KPS, Karnofsky performance scale; GTR, gross-total resection; MGMT, O^6-methylguanine-DNA-methyltransferase; NA, not applicable.
**by Fisher exact test.*

Differential Clinical Implications Between IDH-wt and IDH-Mut LTS

With respect to the prognostic implication of IDH in LTS patients, the survival rates between IDH-wt and IDH-mut subgroups in terms of PFS, OS, and PPS were compared. Results demonstrated that IDH-wt LTS shared a similar survival rate with IDH-mut LTS in regard to OS (P = 0.262) (**Figure 3A**). But interestingly, the median PFS of IDH-wt LTS was unexpectedly longer than that of IDH-mut LTS (66.0 *vs.* 27.0 months, P = 0.040). Conversely, the median PPS of IDH-wt LTS was significantly shorter than that of IDH-mut LTS (46.5 months *vs.* not reached, P = 0.0001) (**Figures 3B, C**).

Considering the distinct survival distribution in PFS and PPS between IDH-wt and IDH-mut LTS, we explored the clinical implication of recurrence pattern in LTS patients. Of these 44 LTS, 22 patients (including 3 IDH-wt LTS and 19 IDH-mut LTS) experienced local recurrence at a median period of 18.5 (10.0-29.0) months and 6 patients (including 5 IDH-wt LTS and 1 IDH-mut LTS) experienced non-local recurrence at a median period of 45.0 (16.2-76.8) months, which imparted a significant difference (P = 0.043) (**Figure 4A**). Moreover, the percent of death was also markedly different between patients with local and non-local recurrence (P = 0.006) (**Figure 4B**).

Of the 28 patients who underwent tumor progression, 12 (42.9%) patients (including 4 IDH-wt LTS and 8 IDH-mut LTS) received re-operation, 15 (53.6%) patients (including 5 IDH-wt LTS and 10 IDH-mut LTS) received reirradiation, and all (100.0%) patients (including 8 IDH-wt LTS and 20 IDH-mut LTS) received rechallenge with chemotherapy (**Figure S2**). Kaplan-Meier plots demonstrated that IDH-mut LTS showed a trend towards increased survival after receiving re-operation (P = 0.155) and reirradiation (P = 0.127), while this clinical benefit disappeared in the subset of IDH-wt (P>0.05) (**Figure 5**).

DISCUSSION

GBM is the most aggressive intracranial malignancy, with rapid growth, inevitable recurrence and high mortality (4). Only a small fraction of patients can achieve a long-term survival after surgical resection and chemoradiotherapy. But the diagnostic threshold of LTS varies significantly in the pre-existing literatures, ranging from 2 years to 5 years (5, 9, 18, 21). As the median survival of patients with GBM is about 1 year and 5-years survival rate is regarded as a predictor of better tumor control, patients who survived beyond 5 years after diagnosis, in this study, were identified as LTS, while those with a survival less than 1 year were defined as STS (5). We systematically compared the clinical, radiological, and molecular features between STS and LTS. Although the characteristics of LTS in GBM have been

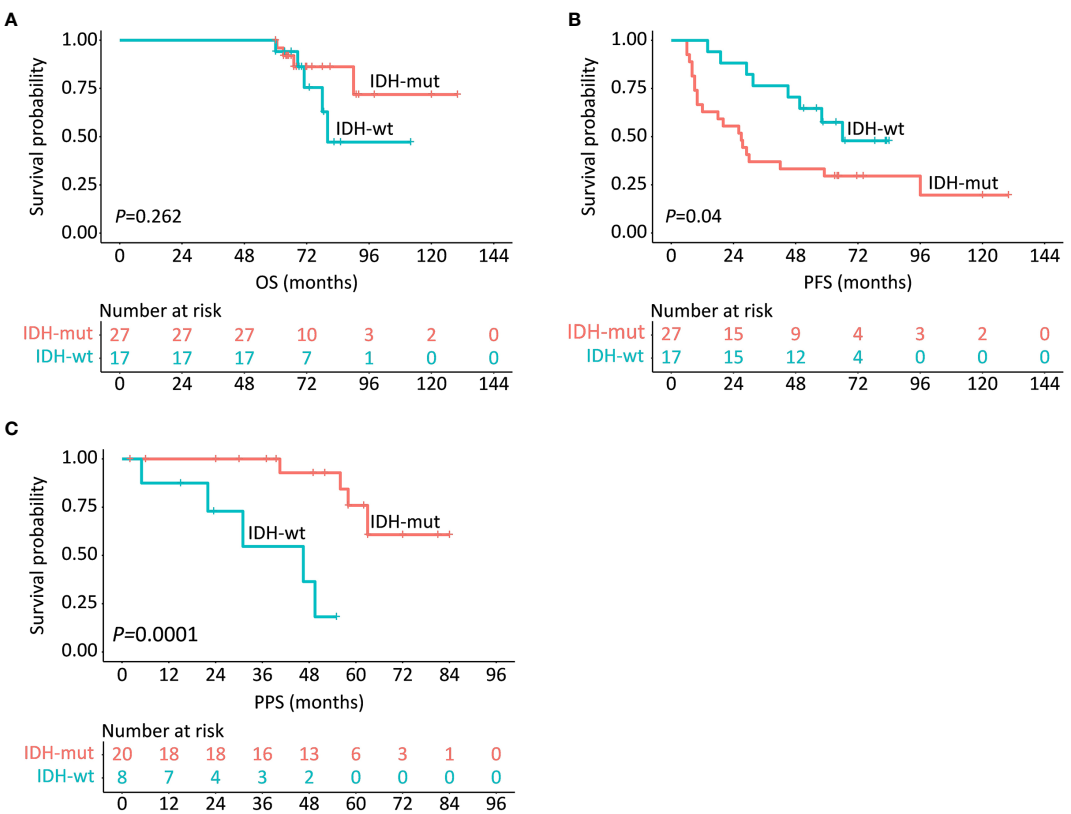

FIGURE 3 | Survival comparisons in regards to OS **(A)**, PFS **(B)** and PPS **(C)** between IDH-wt and IDH-mut LTS.

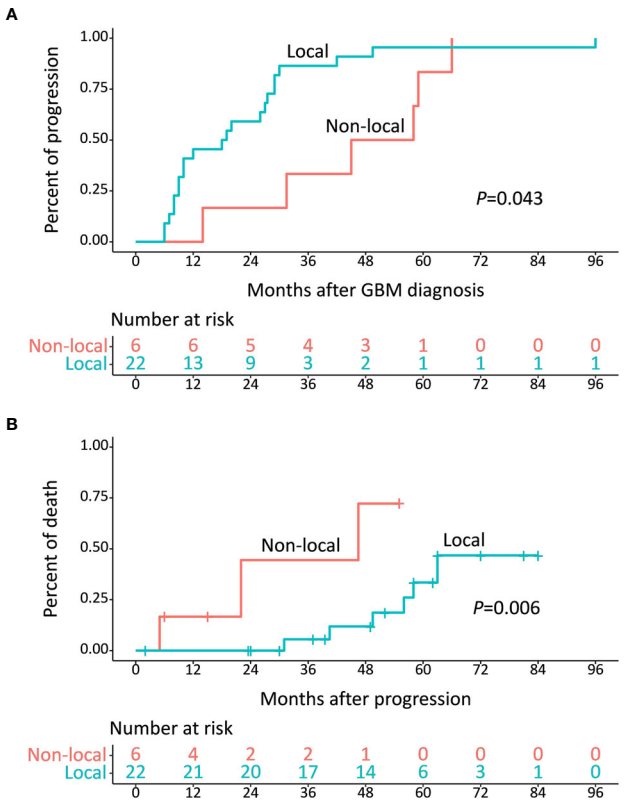

FIGURE 4 | **(A)** Median time from diagnosis to development of progression was 18.5 months for local recurrence and 45.0 months for non-local recurrence (P = 0.043). **(B)** Median survival after diagnosis of non-local recurrence was 46.5 months, which was shorter than that of local recurrence (P = 0.006).

widely investigated (5, 6, 8, 9, 18, 21, 22), there is no study devoted to exploring the intrinsic properties of IDH-wt and IDH-mut LTS. To our knowledge, it's the first study that was aimed to disclose the differential predictors and clinical implications between IDH-wt and IDH-mut LTS. Our results demonstrated that IDH-mut LTS had a lower rate of solid enhancement, but higher rates of cystic change, 1q/19p co-polysomy, and local recurrence. IDH-mut LTS showed a shorter PFS, but a significantly prolonged PPS than those of IDH-wt LTS.

Younger age, better performance status, and higher resection degree are universally regarded as predictors of superior survival in GBM (5, 23–27). In this study, we found that LTS were a subgroup of patients who had a younger age, a higher KPS score, and a more radical resection. In 2014, Field et al. compared the characteristics between patients who survived more than 2 years and those with a survival less than 6 months (23). Final results showed that younger age, better performance status, gross macroscopic resection, and clinical trial participation were independent predictors of LTS (23). Similarly, some authors have explored the features of LTS who were defined as surviving over 3 years by comparing with controls and found that LTS were younger, had better performance status, and were more likely to have received GTR and adjuvant chemotherapy (24, 25). These studies, however, enrolled a small number of LTS, which to a certain extent decreased the reliability of conclusions. Recently, a report of 2249 LTS from National Cancer Database maintained that factors associated with improved 5-year survival were younger age, female gender, less medical comorbidities, non-white race, higher salary, left-sided tumors and tumors outside the brainstem, and radiotherapy (5). However, the molecular parameters have not been explored in the study.

In addition to the clinical factors, the molecular biomarkers, such as IDH and MGMT, are also closely correlated with patient's survival (18, 24, 28–30). Most of the prior studies repeatedly demonstrated that IDH mutation was a prognostic factor associated with prolonged survival (18, 31). GBM was divided into two major categories based on the status of IDH since 2016 when the latest World Health Organization classification schema of brain tumor was issued (10). In our study, the frequencies of IDH mutation and MGMT promoter methylation in LTS were significantly higher than those in STS, which was consistent with previous findings (18). Barbus et al. found that IDH mutation was more prevalent in LTS (28). However, in a larger cohort study of comparative patients, the presence of IDH mutation was not significantly associated with LTS (9). Of note, their further analysis showed that significantly more LTS were MGMT methylated and IDH mutant (9). MGMT is a DNA repair protein involved in reversing methylation damage from alkylating agent (32). It's universally acknowledged that methylated MGMT is linked to increased chemosensitivity and generally confers an improved survival (32). The frequency of MGMT promoter methylation of LTS was 70.6% in our study, which was in accordance with prior results (6, 9, 24, 29, 30). It is well-established that methylated MGMT is more prevalent in LTS of GBM, compared with the STS patients (18, 24, 29, 30). Together these suggest that MGMT methylation is one of the most important features of LTS.

Within the group of LTS, solid enhancement seemed to be more likely occurred in IDH-wt LTS, while cystic change was predominant in IDH-mut group. Rathore and colleagues divided GBM into three distinct subtypes based on the signature of enhancement and found that classical tumors were more prevalent in the solid subtype which showed the worst clinical outcome (14). Cystic change is confirmed as a prognostic factor associated with favorable outcomes (33, 34). Some authors held that cystic GBM may develop from malignant transformation of a previously undiagnosed cystic low-grade glioma (34). This explained why cystic change occurred more frequently in IDH-mut GBM cases which had a history of low-grade glioma within our cohort. Utsuki et al. (34) believed cystic GBM was less aggressive and had little infiltration of the peritumoral brain tissue, which is consistent with the lower Ki-67 index demonstrated in the tumors of the IDH-mut GBM group in our study. Furthermore, we found IDH-mut LTS presented with a higher rate of 1q/19p co-polysomy than IDH-wt GBM. In 2017, Zeng et al. analyzed the prognostic implication of 1q/19p

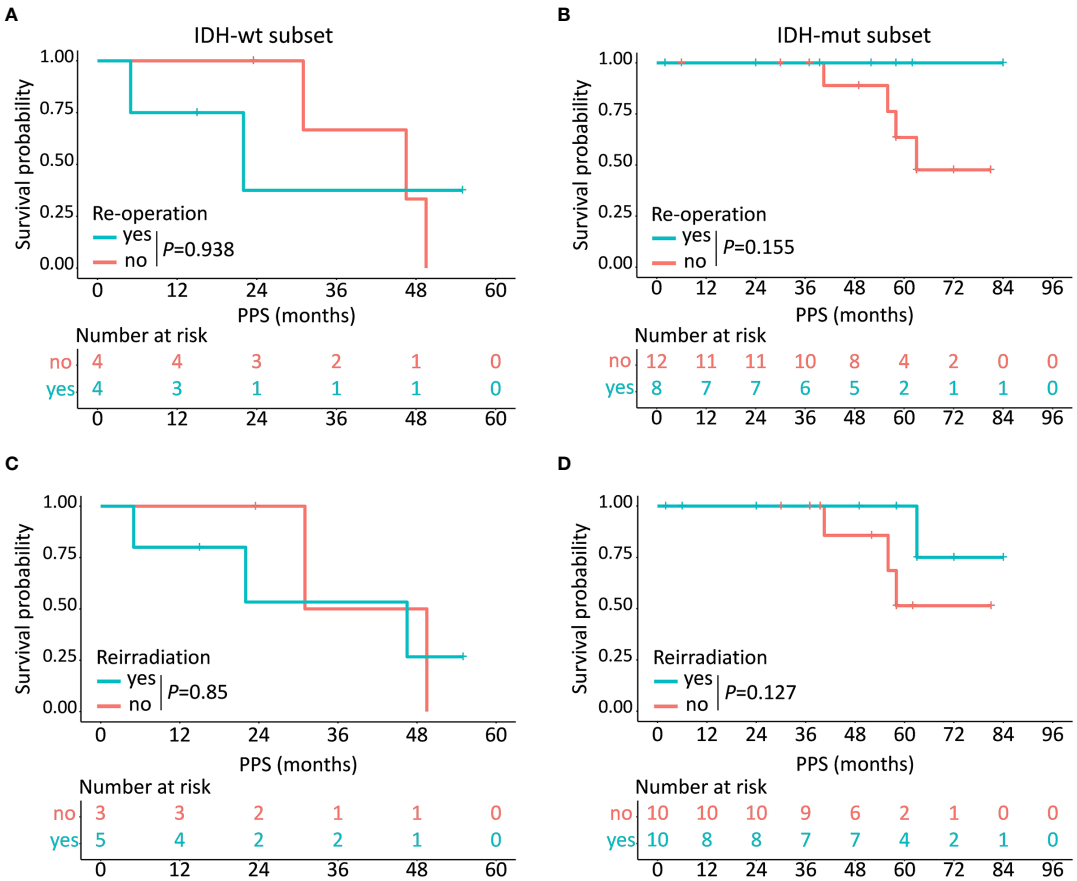

FIGURE 5 | Prognostic implications of different kinds of treatment regimens in IDH-wt and IDH-mut subtypes. In the subset of IDH-wt LTS, no obvious clinical benefit has been observed after receiving re-operation **(A)** or reirradiation **(C)** while IDH-mut LTS show a trend towards increased survival after receiving re-operation **(B)** and reirradiation **(D)**.

polysomy in two large cohorts of astrocytic gliomas and found co-polysomy was an independent prognostic factor associated with prolonged survival (35). All the findings imply that IDH-mut GBM seems to be a less aggressive brain tumor, compared with IDH-wt GBM.

The most interesting finding of our study was that IDH-wt LTS showed a significantly higher rate of non-local failure compared with that in IDH-mut group, which determined the different survival distribution spectrum between IDH-wt and IDH-mut LTS. As we all know, non-local failure is a fatal event which commonly occurs later than local failure (20). In our study, the median time period from diagnosis to local failure was 18.5 months, which was shorter than the interval between diagnosis and non-local failure. Meanwhile, IDH-wt LTS had a higher rate of non-local failure than that of IDH-mut LTS. Therefore, the favorable PFS among IDH-wt LTS could be ascribed to a higher rate of non-local failure. Notably, although IDH-wt LTS conferred a longer PFS, the PPS of these patients was significantly shorter than IDH-mut LTS. With an attempt to interpret the opposite result observed in PPS, we explored the relationship between post-progression treatments and PPS. Finally, the survival analyses demonstrated that IDH-mut LTS showed a trend towards increased survival after receiving re-operation and reirradiation, while the clinical benefits disappeared in the subset of IDH-wt. Hence, non-local failure can be regarded as an endpoint event that predicts a poor treatment response.

There are several limitations of this study. Firstly, the fact that it is a retrospective study, means that there has been bias relating to our patient selection. Secondly, given the wide confidence intervals in some subgroups, our results should be interpreted with caution. Additionally, we should continue this study until the last patient reached the endpoint in order to recheck and confirm the results and conclusions in the future. Finally, functional and employment status of LTS in addition to cognition was not recorded which was of great importance in terms of assessing the quality of life (36).

CONCLUSIONS

Despite improvements of median survival achieved in recent years, the percentage of patients surviving more than five years after diagnosis of GBM remains low. IDH-wt and IDH-mut LTS

are two distinct subgroups which differ radically in terms of clinical, radiological, and molecular characteristics. Our findings provide a new approach for physicians to better understand the IDH-wt and IDH-mut GBM, which may contribute to developing more tailored therapeutic strategies for patients.

DATA AVAILABILITY STATEMENT

The original contributions presented in the study are included in the article/**Supplementary Material**. Further inquiries can be directed to the corresponding author.

ETHICS STATEMENT

The studies involving human participants were reviewed and approved by Institutional Review Board of Capital Medical University. The patients/participants provided their written informed consent to participate in this study.

AUTHOR CONTRIBUTIONS

Acquisition of data: HJ, ML, CY, XZ, and QZ. Analysis and interpretation of data: HJ, KY, YC, and XR. Statistical analysis: HJ and KY. Drafting the article: HJ and SL. Funding acquisition: SL and YC. Conception and design: HJ, GZ, and SL. Study supervision: SL. All authors contributed to the article and approved the submitted version.

FUNDING

This work was supported by the National Natural Science Foundation of China (81771309) and the Capital's Funds for Health Improvement and Research (2020-2-1075).

ACKNOWLEDGMENTS

The authors appreciate Dr. Hongyan Chen, Dr. Xiaobin Zhao, and Prof. Xuzhu Chen for their help in evaluating radiological features and resection degree, Department of Neuroradiology, Beijing Tiantan Hospital, Capital Medical University.

SUPPLEMENTARY MATERIAL

The Supplementary Material for this article can be found online at: https://www.frontiersin.org/articles/10.3389/fonc.2021.632663/full#supplementary-material

Supplementary Figure 1 | Panel I: Representative images of local recurrence **(A–C)**. Preoperative image showed a lesion in the left frontal lobe, which was totally removed during operation. While 38 months after operation, the tumor recurred at the resection cavity. Panel II: Representative images of non-local recurrence **(A–F)**. Preoperative images showed a lesion in the left temporal lobe, which was totally removed during operation. After 45 months follow-up, a new non-enhanced lesion far from the original resection cavity was found in the corpus callosum.

Supplementary Figure 2 | No significant difference was observed between IDH-wt and IDH-mut LTS in the number of patients who received re-operation **(A)**, reirradiation **(B)**, and rechallenge with chemotherapy **(C)**. NA, not applicable.

REFERENCES

1. Ostrom QT, Cioffi G, Gittleman H, Patil N, Waite K, Kruchko C, et al. Cbtrus Statistical Report: Primary Brain and Other Central Nervous System Tumors Diagnosed in the United States in 2012-2016. *Neuro Oncol* (2019) 21:v1–v100. doi: 10.1093/neuonc/noz150
2. Stupp R, Mason WP, van den Bent MJ, Weller M, Fisher B, Taphoorn MJ, et al. Radiotherapy Plus Concomitant and Adjuvant Temozolomide for Glioblastoma. *N Engl J Med* (2005) 352:987–96. doi: 10.1056/NEJMoa043330
3. Stupp R, Taillibert S, Kanner A, Read W, Steinberg D, Lhermitte B, et al. Effect of Tumor-Treating Fields Plus Maintenance Temozolomide vs Maintenance Temozolomide Alone on Survival in Patients With Glioblastoma: A Randomized Clinical Trial. *JAMA* (2017) 318:2306–16. doi: 10.1001/jama.2017.18718
4. Marenco-Hillembrand L, Wijesekera O, Suarez-Meade P, Mampre D, Jackson C, Peterson J, et al. Trends in Glioblastoma: Outcomes Over Time and Type of Intervention: A Systematic Evidence Based Analysis. *J Neurooncol* (2020) 147:297–307. doi: 10.1007/s11060-020-03451-6
5. Cantrell JN, Waddle MR, Rotman M, Peterson JL, Ruiz-Garcia H, Heckman MG, et al. Progress Toward Long-Term Survivors of Glioblastoma. *Mayo Clin Proc* (2019) 94:1278–86. doi: 10.1016/j.mayocp.2018.11.031
6. Burgenske DM, Yang J, Decker PA, Kollmeyer TM, Kosel ML, Mladek AC, et al. Molecular Profiling of Long-Term IDH-Wildtype Glioblastoma Survivors. *Neuro Oncol* (2019) 21:1458–69. doi: 10.1093/neuonc/noz129
7. Wong D, Yip S. Finding a Four-Leaf Clover-Identifying Long-Term Survivors in IDH-Wildtype Glioblastoma. *Neuro Oncol* (2019) 21:1352–3. doi: 10.1093/neuonc/noz174
8. Cantero D, Rodriguez de Lope A, Moreno de la Presa R, Sepulveda JM, Borras JM, Castresana JS, et al. Molecular Study of Long-Term Survivors of Glioblastoma by Gene-Targeted Next-Generation Sequencing. *J Neuropathol Exp Neurol* (2018) 77:710–6. doi: 10.1093/jnen/nly048
9. Hartmann C, Hentschel B, Simon M, Westphal M, Schackert G, Tonn JC, et al. Long-Term Survival in Primary Glioblastoma With Versus Without Isocitrate Dehydrogenase Mutations. *Clin Cancer Res* (2013) 19:5146–57. doi: 10.1158/1078-0432.CCR-13-0017
10. Louis DN, Perry A, Reifenberger G, von Deimling A, Figarella-Branger D, Cavenee WK, et al. The 2016 World Health Organization Classification of Tumors of the Central Nervous System: A Summary. *Acta Neuropathol* (2016) 131:803–20. doi: 10.1007/s00401-016-1545-1
11. Ohgaki H, Kleihues P. The Definition of Primary and Secondary Glioblastoma. *Clin Cancer Res* (2013) 19:764–72. doi: 10.1158/1078-0432.CCR-12-3002
12. Jiang H, Cui Y, Liu X, Ren X, Lin S. Patient-Specific Resection Strategy of Glioblastoma Multiforme: Choice Based on a Preoperative Scoring Scale. *Ann Surg Oncol* (2017) 24:2006–14. doi: 10.1245/s10434-017-5843-1
13. Jiang H, Yu K, Li M, Cui Y, Ren X, Yang C, et al. Classification of Progression Patterns in Glioblastoma: Analysis of Predictive Factors and Clinical Implications. *Front Oncol* (2020) 10:590648. doi: 10.3389/fonc.2020.590648
14. Rathore S, Akbari H, Rozycki M, Abdullah KG, Nasrallah MP, Binder ZA, et al. Radiomic MRI Signature Reveals Three Distinct Subtypes of Glioblastoma With Different Clinical and Molecular Characteristics, Offering Prognostic Value Beyond IDH1. *Sci Rep* (2018) 8:5087. doi: 10.1038/s41598-018-22739-2
15. Kaur G, Bloch O, Jian BJ, Kaur R, Sughrue ME, Aghi MK, et al. A Critical Evaluation of Cystic Features in Primary Glioblastoma as a Prognostic Factor for Survival. *J Neurosurg* (2011) 115:754–9. doi: 10.3171/2011.5.JNS11128
16. Jiang H, Ren X, Zhang Z, Zeng W, Wang J, Lin S. Polysomy of Chromosomes 1 and 19: An Underestimated Prognostic Factor in Oligodendroglial Tumors. *J Neurooncol* (2014) 120:131–8. doi: 10.1007/s11060-014-1526-y

17. Jiang H, Ren X, Cui X, Wang J, Jia W, Zhou Z, et al. 1p/19q Codeletion and IDH1/2 Mutation Identified a Subtype of Anaplastic Oligoastrocytomas With Prognosis as Favorable as Anaplastic Oligodendrogliomas. *Neuro Oncol* (2013) 15:775–82. doi: 10.1093/neuonc/not027
18. Zhang GB, Cui XL, Sui DL, Ren XH, Zhang Z, Wang ZC, et al. Differential Molecular Genetic Analysis in Glioblastoma Multiforme of Long- and Short-Term Survivors: A Clinical Study in Chinese Patients. *J Neurooncol* (2013) 113:251–8. doi: 10.1007/s11060-013-1102-x
19. Jiang H, Ren X, Zhang W, Ma J, Sui D, Jiang Z, et al. A New Prognostic Scoring Scale for Patients With Primary WHO Grade III Gliomas Based on Molecular Predictors. *J Neurooncol* (2013) 111:367–75. doi: 10.1007/s11060-012-1026-x
20. Tejada S, Aldave G, Marigil M, Gallego Perez-Larraya J, Dominguez PD, Diez-Valle R. Factors Associated With a Higher Rate of Distant Failure After Primary Treatment for Glioblastoma. *J Neurooncol* (2014) 116:169–75. doi: 10.1007/s11060-013-1279-z
21. Gately L, McLachlan SA, Philip J, Ruben J, Dowling A. Long-Term Survivors of Glioblastoma: A Closer Look. *J Neurooncol* (2018) 136:155–62. doi: 10.1007/s11060-017-2635-1
22. Gately L, McLachlan SA, Philip J, Rathi V, Dowling A. Molecular Profile of Long-Term Survivors of Glioblastoma: A Scoping Review of the Literature. *J Clin Neurosci* (2019) 68:1–8. doi: 10.1016/j.jocn.2019.08.017
23. Field KM, Rosenthal MA, Yilmaz M, Tacey M, Drummond K. Comparison Between Poor and Long-Term Survivors With Glioblastoma: Review of an Australian Dataset. *Asia Pac J Clin Oncol* (2014) 10:153–61. doi: 10.1111/ajco.12076
24. Sonoda Y, Kumabe T, Watanabe M, Nakazato Y, Inoue T, Kanamori M, et al. Long-Term Survivors of Glioblastoma: Clinical Features and Molecular Analysis. *Acta Neurochir (Wien)* (2009) 151:1349–58. doi: 10.1007/s00701-009-0387-1
25. Scott JN, Rewcastle NB, Brasher PM, Fulton D, MacKinnon JA, Hamilton M, et al. Which Glioblastoma Multiforme Patient Will Become a Long-Term Survivor? A Population-Based Study. *Ann Neurol* (1999) 46:183–8. doi: 10.1002/1531-8249(199908)46:2<183::AID-ANA7>3.0.CO;2-7
26. Armocida D, Pesce A, Di Giammarco F, Frati A, Santoro A, Salvati M. Long Term Survival in Patients Suffering From Glio-blastoma Multiforme: A Single-Center Observational Cohort Study. *Diagnostics (Basel)* (2019) 9:209. doi: 10.3390/diagnostics9040209
27. Krex D, Klink B, Hartmann C, von Deimling A, Pietsch T, Simon M, et al. Long-Term Survival With Glioblastoma Multiforme. *Brain* (2007) 130:2596–606. doi: 10.1093/brain/awm204
28. Barbus S, Tews B, Karra D, Hahn M, Radlwimmer B, Delhomme N, et al. Differential Retinoic Acid Signaling in Tumors of Long- and Short-Term Glioblastoma Survivors. *J Natl Cancer Inst* (2011) 103:598–606. doi: 10.1093/jnci/djr036
29. Smrdel U, Popovic M, Zwitter M, Bostjancic E, Zupan A, Kovac V, et al. Long-Term Survival in Glioblastoma: Methyl Guanine Methyl Transferase (MGMT) Promoter Methylation as Independent Favourable Prognostic Factor. *Radiol Oncol* (2016) 50:394–401. doi: 10.1515/raon-2015-0041
30. Nakagawa Y, Sasaki H, Ohara K, Ezaki T, Toda M, Ohira T, et al. Clinical and Molecular Prognostic Factors for Long-Term Survival of Patients With Glioblastomas in Single-Institutional Consecutive Cohort. *World Neurosurg* (2017) 106:165–73. doi: 10.1016/j.wneu.2017.06.126
31. Zou P, Xu H, Chen P, Yan Q, Zhao L, Zhao P, et al. IDH1/IDH2 Mutations Define the Prognosis and Molecular Profiles of Patients With Gliomas: A Meta-Analysis. *PloS One* (2013) 8:e68782. doi: 10.1371/journal.pone.0068782
32. Hegi ME, Diserens AC, Gorlia T, Hamou MF, de Tribolet N, Weller M, et al. MGMT Gene Silencing and Benefit From Temozolomide in Glioblastoma. *N Engl J Med* (2005) 352:997–1003. doi: 10.1056/NEJMoa043331
33. Maldaun MV, Suki D, Lang FF, Prabhu S, Shi W, Fuller GN, et al. Cystic Glioblastoma Multiforme: Survival Outcomes in 22 Cases. *J Neurosurg* (2004) 100:61–7. doi: 10.3171/jns.2004.100.1.0061
34. Utsuki S, Oka H, Suzuki S, Shimizu S, Tanizaki Y, Kondo K, et al. Pathological and Clinical Features of Cystic and Noncystic Glioblastomas. *Brain Tumor Pathol* (2006) 23:29–34. doi: 10.1007/s10014-006-0195-8
35. Zeng W, Ren X, Cui Y, Jiang H, Zhang X, Lin S. 1q/19p Co-Polysomy Predicts Longer Survival in Patients With Astrocytic Gliomas. *Oncotarget* (2017) 8:67104–16. doi: 10.18632/oncotarget.17947
36. Weller J, Tzaridis T, Mack F, Steinbach JP, Schlegel U, Hau P, et al. Health-Related Quality of Life and Neurocognitive Functioning With Lomustine-Temozolomide Versus Temozolomide in Patients With Newly Diagnosed, MGMT-methylated Glioblastoma (CeTeG/NOA-09): A Randomised, Multicentre, Open-Label, Phase 3 Trial. *Lancet Oncol* (2019) 20:1444–53. doi: 10.1016/S1470-2045(19)30502-9

Conflict of Interest: The authors declare that the research was conducted in the absence of any commercial or financial relationships that could be construed as a potential conflict of interest.

frontiers in Oncology

CASE REPORT
published: 20 May 2021
doi: 10.3389/fonc.2021.642683

Primary Intracranial Leiomyosarcoma Secondary to Glioblastoma: Case Report and Literature Review

*Liyan Zhao[1], Yining Jiang[2], Yubo Wang[2], Yang Bai[2], Ying Sun[1] and Yunqian Li[2]**

[1] Department of Clinical Laboratory, Second Hospital of Jilin University, Changchun, China, [2] Department of Neurosurgery, First Hospital of Jilin University, Changchun, China

Background: Leiomyosarcoma is a highly malignant soft-tissue sarcoma with a poor prognosis. In recent years, treatment for leiomyosarcoma has not shown much progress. Primary intracranial leiomyosarcoma (PILMS) is a much rarer type of neoplasm, which occurs more frequently in immunocompromised patients. PILMS cases reported in the literature are scarce and treatment strategy and prognosis are still under debate. In this study, a case of PILMS secondary to the total resection of giant cell glioblastoma is reported.

Case Description: A 38-year-old male was hospitalized with a three-month history of a temporal opisthotic bump. His medical history included a total resection of a tumor located in the right temporal lobe performed 4 years earlier. Pathological examination led to a diagnosis of giant cell glioblastoma, and the patient underwent postoperative chemotherapy with temozolomide for 6 weeks plus simultaneous radiotherapy with 63.66 Gary. Four years later, during regular follow-up, a preoperative MRI brain scan resulted in a well-defined signal pointing out two nodule-like features located at the right temporal lobe and subcutaneous soft tissue, respectively, and near the area where the previous giant cell glioblastoma was located. The mass was completely removed by a transtemporal approach and postoperative pathology revealed that the mass was a leiomyosarcoma. The patient underwent postoperative radiotherapy and no recurrence occurred until now.

Conclusions: To date, research on soft-tissue sarcoma, especially PILMS, has not made much progress, and a limited number of studies have provided few details on the management of PILMS. The treatment of choice for PILMS is aggressive multimodal treatment based on total tumor resection and radiotherapy. Moreover, systemic treatment with chemotherapy and targeted therapy, such as olaratumab, as well as further research still needs to be performed as many questions are left unanswered. To our knowledge, this is the first report on a case of PILMS secondary to glioblastoma, which might serve as a potential reference for clinicians and clinical studies.

Keywords: primary intracranial leiomyosarcoma, glioblastoma, leiomyosarcoma, treatment, prognosis, genetic diagnosis

OPEN ACCESS

Edited by:
Yaohua Liu,
Shanghai First People's Hospital, China

Reviewed by:
Antonio Silvani,
Fondazione Istituto Neurologio Carlo Besta (IRCCS), Italy
Maria Caffo,
University of Messina, Italy

***Correspondence:**
Yunqian Li
yunqian@jlu.edu.cn

Specialty section:
This article was submitted to Neuro-Oncology and Neurosurgical Oncology, a section of the journal Frontiers in Oncology

Received: *16 December 2020*
Accepted: *26 April 2021*
Published: *20 May 2021*

Citation:
Zhao L, Jiang Y, Wang Y, Bai Y, Sun Y and Li Y (2021) Primary Intracranial Leiomyosarcoma Secondary to Glioblastoma: Case Report and Literature Review. Front. Oncol. 11:642683. doi: 10.3389/fonc.2021.642683

INTRODUCTION

Intracranial leiomyosarcoma (LMS) is rare, and most often occurs as a result of metastasis of primary smooth muscle tissue tumors that can therefore develop in different organs due to the ubiquitous presence of the smooth muscle tissue in the body (1–4). Primary intracranial leiomyosarcoma (PILMS) is extremely rare in the central nervous system (CNS) and previous studies suggested that less than 1% of brain biopsies (or 3 out of 25,000 brain tumors) are positive for LMS (5). They are speculated to derive from smooth muscle cells of the blood vessels or dura mater pluripotent mesenchymal cells (1, 2, 6–9), and display strong smooth muscle differentiation (10). In addition, PILMS usually occurs in immunocompromised patients or after exposure to radiation (8, 11, 12). Here we report a case of PILMS arising on the right temporal robe near to the location of a previous giant cell glioblastoma (GCG) totally excised 4-year earlier. The patient was not immunocompromised. To the best of our knowledge, this is the first report describing a case of PILMS secondary to a glioblastoma. Relevant literature has been reviewed, and diagnosis, and prognosis, especially regarding treatment strategy have been discussed.

CASE REPORT

History and Examination

A 38-year-old male with a 3-month history of a temporal opisthotic bump was admitted to the hospital. The patient had no history of immunosuppressive medical treatment, intravenous drug use, previous organ transplantation or sexual promiscuity. Moreover, he did not experience any signs of headaches, dizziness, nausea, vomiting nor did he have any other sensory or motor deficits. Routine laboratory analysis showed standard parameters within normal limits, and the serologic test was negative for Human Immunodeficiency Virus (HIV), Hepatitis-B Virus (HBV), Hepatitis-C Virus (HCV), and Epstein Barr virus (EBV). According to his medical history, the patient underwent craniotomy 4 years earlier, because of the presence of an abnormal and heterogeneous magnetic resonance imaging (MRI) enhancement signal located in the right temporal and parietal lobe, together with evident edema (**Figures 1A–C**). The MRI performed 3 months after follow-up (**Figures 1D–F**) revealed that the tumor was successfully removed. Postoperative pathological examination of the tumor led to a diagnosis of GCG, with a Ki-67 index of 50%. Histological examination showed that many giant tumor cells were densely arranged, with blood vessel hyperplasia and focal necrosis. The tumor cells had obvious atypia and eosinophilic cytoplasm, and the nuclei were eccentric with mitosis that was easy to observe (**Figure 2A**). Moreover, pathological findings were evaluated. Pyrosequencing presented that no O6-methylguanine-DNA methyltransferase promoter methylation was shown (**Figure 3**). Fluorescence *in situ* hybridization suggested no loss of heterozygosity in 1p/19q chromosome (**Figures 2B, C**). Levels of *IDH1*, *TERT*, and *BRAF* were determined by multiple polymerase chain reaction amplification combined with high-throughput sequencing, which did not indicate a mutation of *IDH1-R132/R172*, *TERT-C228T/C250T* or *BRAF-V600E*. The patient accepted to be subjected to postoperative chemotherapy with temozolomide for 6 weeks, and concomitant local 63.66 Gray radiotherapy. Follow-up was not stopped after the first surgery. During a visit after 4 years when the patient presented the bump, the MRI brain scan resulted in a well-defined signal pointing out two nodule-like features of 3.1x2.5 cm and 4.0x1.8x3.7 cm located kin the right temporal lobe and subcutaneous soft tissue, respectively (**Figures 4A–F**), with a slightly hypointense signal on T1-weighted imaging (T1WI, **Figure 4A**), isointense and slightly hyperintense signal on T2-weighted imaging (T2WI, **Figure 4B**), and isointense signal on fluid attenuated inversion recovery (**Figure 4C**). The lesion showed significant edge enhancement and heterogeneous reinforcement inside the tumor (**Figures 4D–F**). A preoperative diagnosis of a recurrent glioblastoma was made.

Surgery

The patient underwent transtemporal craniotomy under preoperative and intraoperative neuronavigation, together with electrophysiological monitoring. The tumor was pinkish in color, solid, bloody, and was closely adherent to the brain parenchyma and subcutaneous tissue. The entire tumor was removed.

Histopathological Findings

The postoperative histopathological examination led to a diagnosis of leiomyosarcoma. The microscopic examination revealed the tumor was composed of spindle-shaped cells (**Figure 2D**) with an abundant mitotic activity (**Figure 2E**), and the Ki-67 labeling index was 10-20%. Immunohistochemical staining was positive for h-caldesmon (**Figure 2F**), vimentin, SMA, and desmin, but negative for S-100, epithelial membrane antigen (EMA), glial fibrillary acidic protein (GFAP), CK-pan, CD34, CD31, CD117, Oligo-2, Dog-1, PR, and STAT6.

Postoperative Course

The postoperative course was uneventful and no postoperative complications occurred. In addition, positron emission tomography (PET) was performed to identify potential extracranial primary sites, and serum tumor markers were measured; both were negative. One month after surgery, the patient underwent postoperative 54 Gray radiotherapy. Immediate post-operative cranial CT (**Figure 4G**) and follow-up MRI were performed 3 months after surgery (**Figures 4H, I**), and demonstrated complete removal of the tumor and no signs of recurrence. During the last telephone follow-up in December 2020, the patient stated that he did not report any abnormal condition and that he was leading a normal daily life. Based on these results,

Abbreviations: CT, computed tomography; LMS, leiomyosarcoma; PILMS, primary intracranial leiomyosarcoma; STS, soft-tissue sarcomas; GCG, giant cell glioblastoma; IDH, isocitrate dehydrogenase; MGMT, O6-methylguanine-DNA methyltransferase; EMA, epithelial membrane antigen; GFAP, glial fibrillary acidic protein; HIV, human immunodeficiency virus; HBV, hepatitis-B virus; HCV, hepatitis-C virus; EBV, Epstein-Barr virus; MRI, magnetic resonance imaging; PET, positron emission tomography; CNS, central nervous system; T1WI, T1-weighted imaging; T2WI, T2-weighted imaging; BBBP, blood brain barrier permeability; PFS, progression-free survival; OS, overall survival; GTR, gross tumor resection; PDGFR, platelet-derived growth factor receptor.

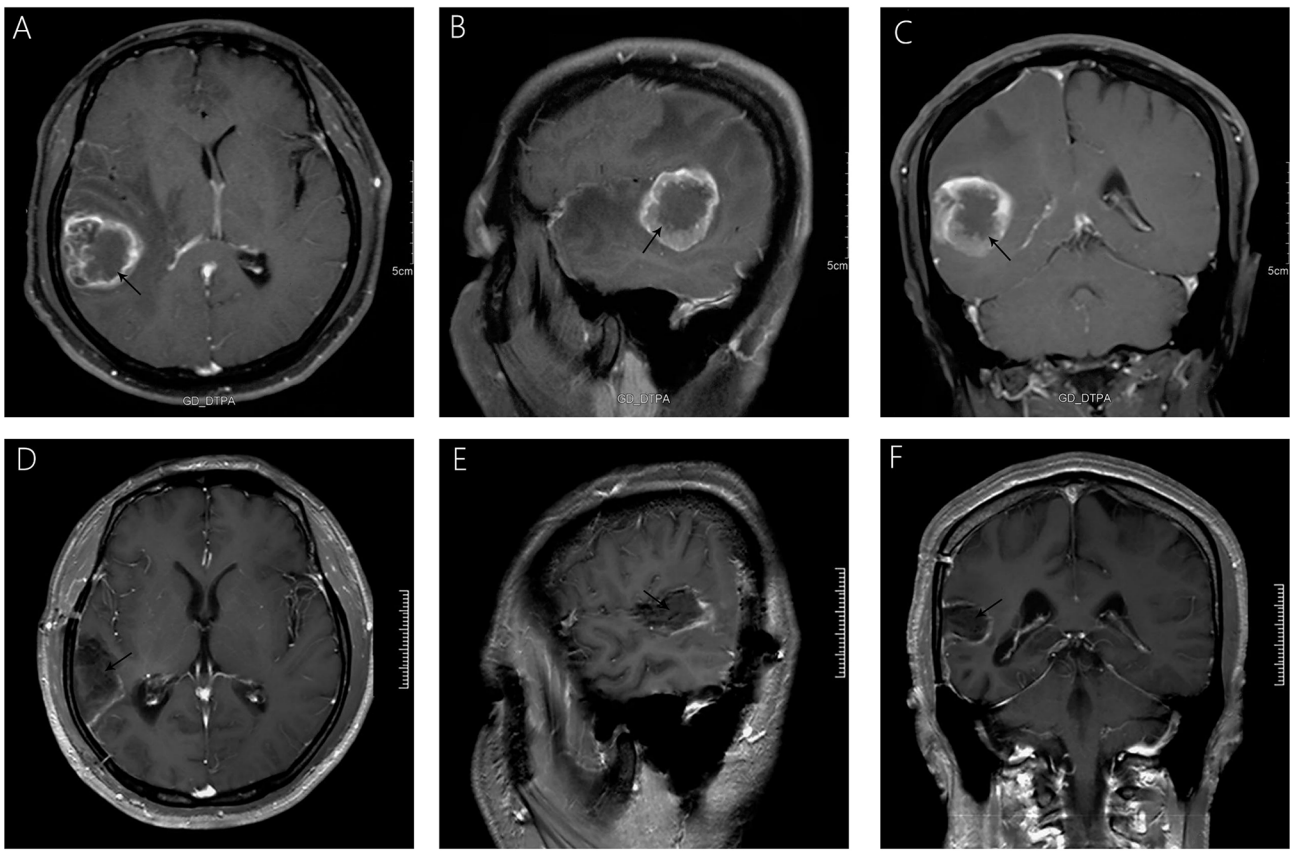

FIGURE 1 | Significant heterogeneous enhancement is observed with evident edema after gadolinium administration **(A–C)**. A follow-up MRI, 3 months after surgery **(D–F),** showed that the lesion was completely removed, without any signs of recurrence.

his conditions seem stable and therefore, the patients will undergo routine follow-up with MRI.

DISCUSSION

Epidemiology

LMS is an uncommon malignant tumor, accounting for 1% of the head and neck soft-tissue sarcomas (STS) (13), being usually the result of metastasis of primary smooth muscle tissue tumors (1–4, 14). PILMS is rare and sporadically reported (4, 14), indeed accounting for approximately 0.1% of all the intracranial tumors (3). The onset range is quite wide, from 4 to 75 years of age (2, 15, 16), commonly appearing in the second and third decades of life (1, 6, 17–19), and in previous studies, a slight male predominance was observed (2, 20).

Etiology

The cellular origin and tumorigenesis of PILMS is considered as deriving from the smooth muscle cells of the blood vessels or the pluripotent mesenchymal stem cells in the dura mater (1, 2, 6–9). LMS also mostly occur in immunocompromised patients compared to the immunocompetent ones (11), especially patients with HIV (7, 12, 17, 21, 22) or EBV (1, 5, 12, 21, 23, 24) infection, subjected to organ transplantation (18), with malignancies (20), genetic disorders (18), after radiation exposure (25), and especially in children (8). Therefore, immunodeficiency plays a role in the occurrence and development of PILMS.

Co-infection with EBV in immunosuppressed patients with HIV is considered a leading factor in the development of LMS (9, 22, 26, 27), and EBV-transformed and infected smooth muscle cells may contribute to the pathogenesis of LMS in patients with AIDS (2, 3, 17). However, immunocompetent patients in whom LMS occurred, were invariably negative for EBV (2, 17, 24, 28). Radiotherapy (2) and chemotherapy (27, 29) are also considered as potential factors inducing PILMS. Radiation oncogenesis was first defined by Cahan et al. (30), in 1948. Since then, it was clear that radiation doses above 50 Gray cause cell death, while lower doses (e.g.< 30 Gray) are associated with genomic instability and cell repair mechanisms of the caused damages (2). Suzuki et al. (31), also described a radiation-induced sarcoma usually within or at the edge of the tumor. Since the radiation is not uniformly distributed within the tissue, a sufficient dose does not reach the edge to ensure the killing of all tumor cells (31). Furthermore, Fujimoto et al. (9), described a case of LMS arising after the

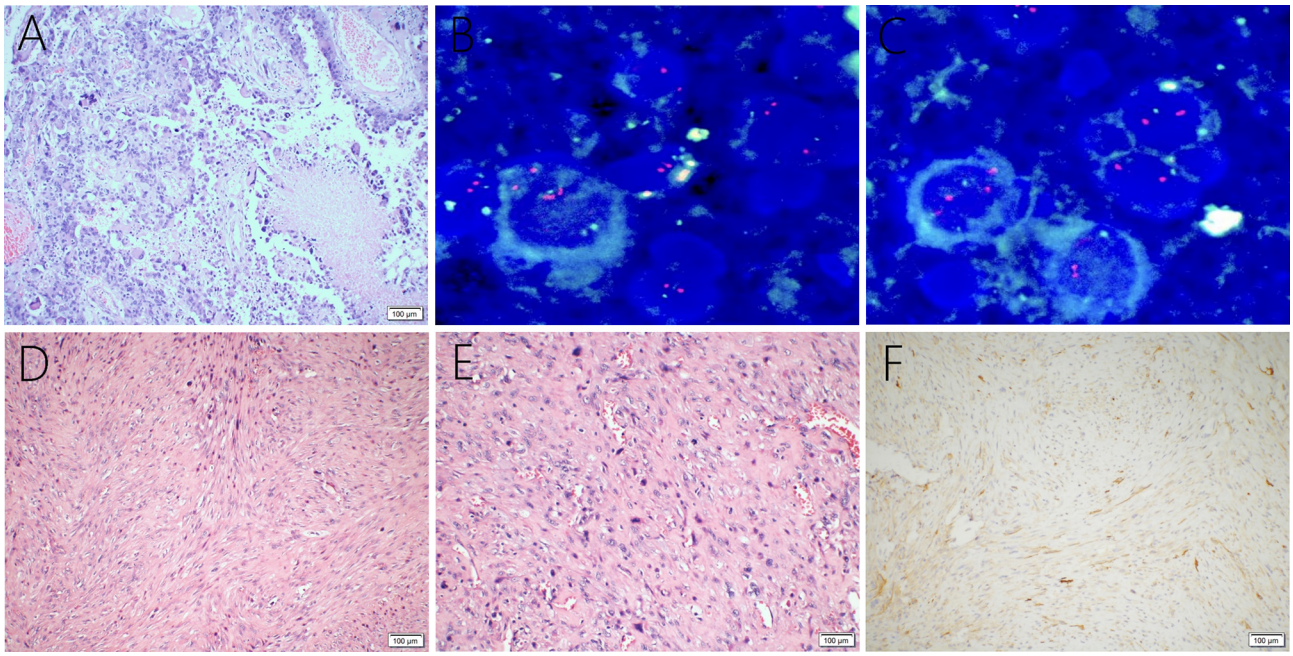

FIGURE 2 | Giant cell glioblastoma is composed of large, closely-arranged cells, with an eosinophilic cytoplasm and obvious nuclear atypia. There are also scattered multinucleated giant cells. Local necrosis and vascular proliferation are observed **(A)**. FISH detection suggests no loss of heterozygosity in *1p* **(B)** or *19q* **(C)** chromosomes. Primary intracranial leiomyosarcoma showing spindle–shaped cells **(D)** and abundant mitotic activity **(E)** through the tumor, hematoxylin, and eosin staining. Immunohistochemical examination was positive for H-caldesmon **(F)**.

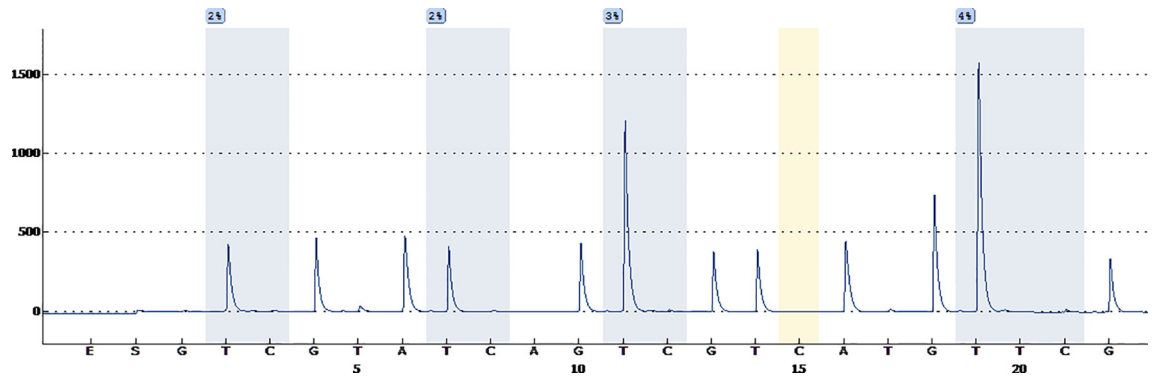

FIGURE 3 | Pyrosequencing demonstrates that no O6-methylguanine-DNA methyltransferase promoter methylation was found.

resection of a neurofibroma at the left cerebellopontine angle and concluded that the mechanical and/or heat stimulation during a previous surgery was associated with the development of LMS. The patient in this case report is the first ever described with PILMS secondary to a glioblastoma, and the pathogenesis was hypothesized as associated with the history of malignant tumor and radiation exposure together with the mechanical and heat stimulation during the first surgery. Nevertheless, these hypotheses did not explain all cases of PILMS in immunocompetent patients and further studies are needed to clarify the clinical features involved.

Clinical Presentation

No specific symptoms are shown in patients with PILMS, and they largely depend on the location of the tumor and the mass effect (3, 4, 16, 32); the average length of the symptoms approximately 4 months (3, 33). General symptoms include headache (1, 32), memory impairment (17), gait instability (1), altered mental status (34), and seizures (1). In addition, some patients may present subdural hematoma (3, 20) or intratumoral apoplexy (15, 20). The subdural hematoma is hypothesized to be developed from new capillary formation, vascular hyperpermeability,

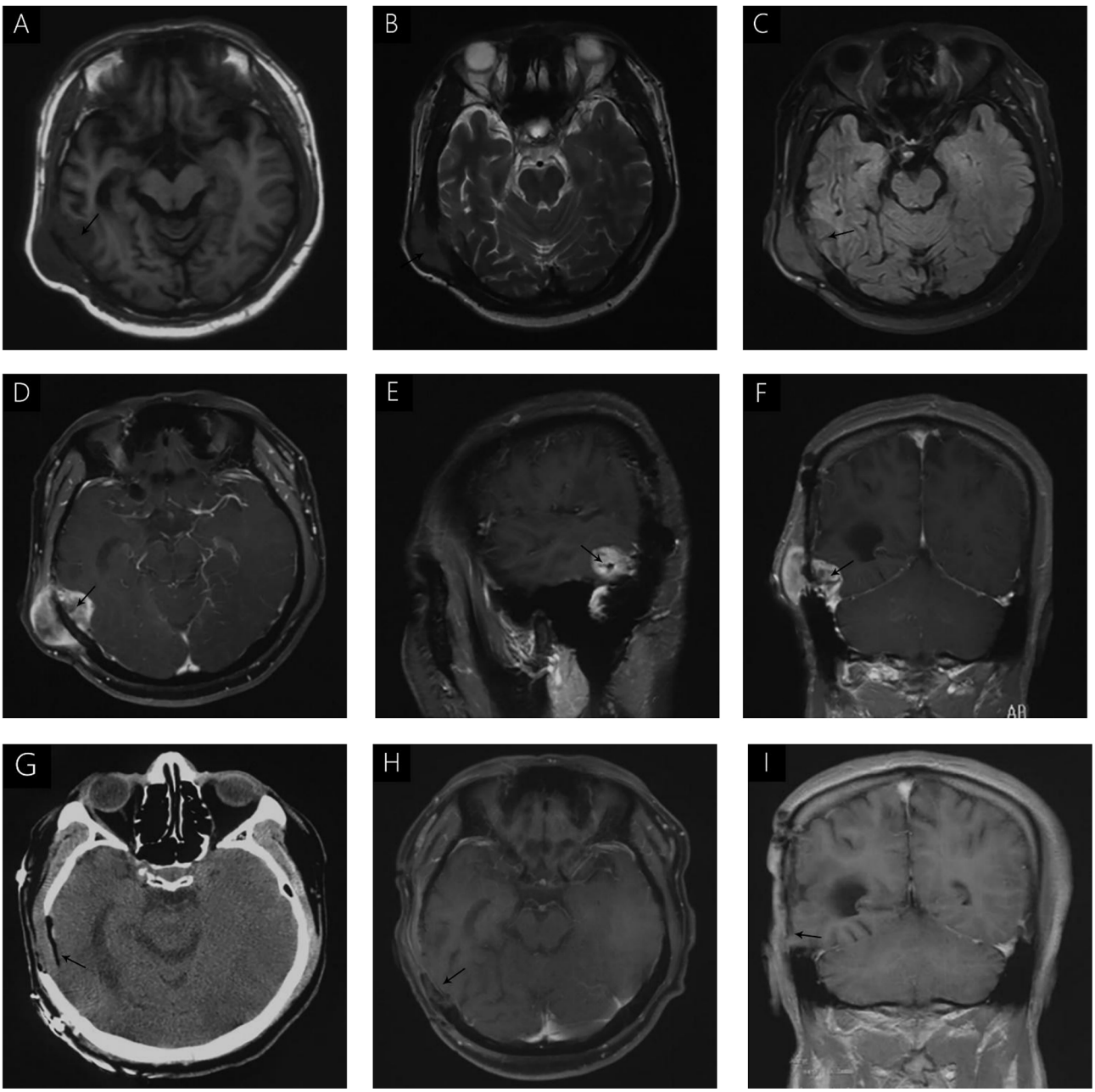

FIGURE 4 | **(A)** hypointense signal is seen on T1WI **(A)**. Isointense and slightly hyperintense signals were seen on T2WI **(B)**; Isointense signal on FLAIR **(C)**. Significant enhancement was seen after gadolinium administration, without uniform enhancement in the center of the lesion **(D–F)**. Immediate postoperative CT **(G)** and follow-up MRI, 3 months after surgery **(H, I)** demonstrated complete removal of the tumor and no signs of recurrence.

and serum protein exudation, as a result of a typical inflammatory reactions (3).

Radiological Characteristic

Due to the rarity of PILMS, radiological details describing it are lacking in the literature. In general, PILMS presents a hyperdense signal on CT and homogenous enhancement on enhanced scanning images (3, 16). In addition, calcifications can be observed (16, 35). MRI is considered the primary neurological approach to assess PILMS, which is also important for surgical planning (14). PILMS can develop as either extra-axial or intra-axial tumor, and the imaging features are different in these two locations (4). The extra-axial PILMS is usually characterized by uniform hypointense or isointense T1WI and T2WI (4, 36). After gadolinium enhancement, well-defined homogeneous (22, 23, 28) or inhomogeneous (17, 37) enhancement with (6) or

without (4) dural tail signal is detected, resembling meningioma (18, 22, 23, 28, 38). Moreover, the tumors were always significantly enhanced (18, 36). No significant differences in survival were observed in patients with dura involvement (39). Intra-axial PILMS often appears as an irregular mass presenting a heterogeneous intense and heterogeneous enhanced pattern (2, 24, 26, 40). Ultra-sound examination could also be performed for patients with skull involvement (36).

Diagnosis

The diagnosis and differential diagnosis of PILMS depend on the comprehensive analysis of all the laboratory tests, MRI and pathological examination (2, 5, 6, 9). Histological examination revealed the presence of elongated spindle-shaped cells with pleomorphism and coagulative necrosis (17, 41), and most of these cells grow following a fascicular pattern (6, 16, 36). Moreover, PILMS is often positive for desmin, actin, h-caldesmon, α-SMA, and occasionally vimentin (6, 9, 16, 28), and is negative in S-100, EMA and GFAP (6, 9, 16, 28). In addition, PILMS showed a high Ki-67 index and mitotic index (16). H-caldesmon is considered a specific and valuable biomarker characterizing smooth muscle cells and LMS (9, 24). Extra-axial PILMS is sometimes difficult to differentiate from meningioma on radiological examination (6, 9, 24, 34). However, EMA is immunohistochemically positive in meningioma, meningosarcoma and hemangiopericytomas (9, 24), thereby helping in the differential diagnosis. Notably, thorough investigation, including whole-body CT, bone scans, lumbar punctures, and PET scans were imperative to exclude extracranial lesions.

Treatment

Due to the rarity of PILMS, standard management guidelines have not yet been established (39). However, currently, a multimodal approach, including surgery, radiotherapy, and chemotherapy is the main treatment (12, 21, 42). In addition, surgical resection is the leading treatment to perform gross tumor resection (GTR) and the achievement of negative surgical margins due to extension of the resection is one of the most frequently reported predictors of recurrence and survival (2, 15, 16, 28, 33). Zhang et al. (39) demonstrated that the extent of excision might result in differences because of the difference in score systems that are presented in the literature, which needs further unification.

Radiotherapy

In PILMS, postoperative radiotherapy is used to control local recurrence (2, 43). In many previous studies, GTR combined with postoperative radiotherapy is indeed the main treatment strategy for PILMS (1, 3, 26, 27, 44, 45). However, the specific benefit of radiotherapy in terms of the survival of PILMS patients is not clear (39). To date, there is no consensus that patients with PILMS should undergo radiotherapy regardless of the extent of resection. In several studies, radiotherapy was not recommended for patients with GTR (15). However, considering the aggressive character, immediate adjuvant radiotherapy after GTR was approved in some cases (3, 28, 37). In this case, the patient underwent radiotherapy immediately after GTR, and had a relatively good survival without recurrence. In addition, radiation therapy represents an adjuvant option in patients with relapse or progression (39). In case of recurrent LMS, Gallagher et al. (28), suggested to perform a re-irradiation according to their experience in the treatment of recurrent glioblastoma. Recently, gamma knife radiosurgery (43, 46) and stereotactic robotic cyber knife radiosurgery (47) have been performed to treat PILMS, revealing their feasibility and effectiveness in treating this type of tumor, although the number of patients was small, thus, they can be considered potential treatment strategies. The specific treatment advantage needs to be verified in future multicenter prospective studies.

Chemotherapy

In previous studies, it was demonstrated that PILMS is inclined to progress to extra-cranial metastasis, such as the spinal cord, lung, pleural, spleen, and hip (6, 26, 48). Although the role of chemotherapy in preventing extracranial metastasis is currently unknown, we speculate that it is difficult for radiation alone to confine the aggressive behavior of LMS. Chemotherapy is not a routine treatment of PILMS (9, 17), and the choice of effective chemotherapeutic agents remains unclear (28). Because of its good blood brain barrier permeability (BBBP) and acceptable level of toxicity, temozolomide was the first chemotherapy drug used in the treatment of PILMS (49). Temozolomide has moderate activity in residual or metastatic STS, with a response rate of 8% (41, 49, 50), which makes it a promising drug in the treatment of PILMS. In some studies, it was revealed that temozolomide was effective at a dose that was equivalent to that of dacarbazine (9, 51, 52). However, the validity of monotherapy of chemotherapeutic drugs has been questioned (3), and the combination with other therapeutic approaches seems somewhat effective (1–3, 6). In a recent study, Francisco et al. (53), reported a case of PILMS where maintenance treatment involved temozolomide and nimotuzumab. Nimotuzumab is an epidermal growth factor receptor monoclonal antibody. STS, like LMS, can express epidermal growth factor receptor-34, and its blocking promoted tumor inactivation and decreased chemoresistance (54). However, in this study, no improvement in survival was observed. For the current treatment of sarcomas, anthracyclines (doxorubicin and epirubicin) remain the first-line standard treatment regimens of advanced STSs (55), with a median overall survival (OS) of 12-18 months (56, 57). When combined with other drugs, such as ifosfamide, a significant improvement in the response rate and progression free survival (PFS), but not in OS, was observed (58, 59). The treatment experience with anthracyclines in PILMS is limited and controversial, and no improvement in survival was observed (60, 61), due to its poor BBBP and limited treatment experience of this disease (12, 42).

Targeted Therapy

Here, we describe the application and research progress of targeted drugs in PILMS. To date, monoclonal antibodies to LMS, especially to PILMS, are scarce (28). However, along with increasing the understanding of the pathophysiology and

underlying molecular mechanisms of action of LMS, there is an increase in research studies. For example, somatostatin receptor subtypes have been detected in moderate and malignant sarcomas. In 2016, Crespo-Jara A et al. (62), reported a case of metastatic and multiple drug-resistant sarcoma, which was successfully treated with radiolabeled somatostatin analogs. However, this agent has not been approved in China. Moreover, platelet-derived growth factor receptor (PDGFR), especially the alpha (α) isoform, has been confirmed to be associated with the metastasis and proliferation of LMS cells. Therefore, drugs that block the action of PDGFR could be a promising antitumor regimen (63, 64). Lartruvo® (olaratumab) is a PDGFR-α antagonist, a first-in-class recombinant human immunoglobulin-G subclass-1 monoclonal antibody that blocks binding and activation of the PDGF receptor (55). In 2016, a Phase 1b study and randomized Phase II clinical trials, showed that advanced STS treated with olaratumab plus doxorubicin had a significant prolonged OS when compared to doxorubicin monotherapy (26.5 *vs* 14.7 months; HR 0.46, 95% CI 0.30-0.71, p=0.0003), and slight PFS extension (6.6 *vs* 4.1 months; HR 0.672, 95% CI 0.442-1.021, p=0.0615) (65), with manageable toxicity. This was the first randomized trial showing a significant improvement in OS, compared to doxorubicin monotherapy, which brings light for advanced STS and PILMS patients. From 2016 to 2019, olaratumab was considered the most effective PDGFRα neutralizing antibody for LMS (56). However, the latest Phase 3 multicenter randomized clinical trials in 2020 failed to demonstrate OS benefits of doxorubicin plus olaratumab when compared to doxorubicin plus placebo in advanced STS (20.4 *vs* 19.7 months; HR 1.05, 95% CI 0.84-1.30, p=0.69) and LMS (21.6 months *vs* 21.9 months; HR 0.95, 95% CI 0.69-1.31, p=0.76) (66). The reason for the differences between the results of the second and third clinical trial has not yet been identified. Gennatas et al. (67), reviewed eight patients with advanced STS who underwent at least two treatment cycles of doxorubicin plus olaratumab between May 2017 and March 2019, and none of the patients experienced survival benefits. At present, the treatment of STS with olaratumab has been suspended by the drug manufacturer of olaratumab (66), and further studies are needed. Moreover, no studies have been performed with olaratumab for PILMS or its BBBP. Other recent first-line studies of advanced STS included the comparison of doxorubicin monotherapy with docetaxel plus gemcitabine (58) or doxorubicin plus ifosfamide (51, 59), palifosfamide (68), or evofosfamide (65). However, historical OS (12-18 months) and the 2-year survival rate (20-30%) did not show improvement. Thus, identifying new and effective treatment for advanced STS, especially PILMS, is of utmost importance. Mathieson et al. (3), described a treatment including the combination of vincristine, ifosfamide, doxorubicin, and etoposide with radiotherapy on a pediatric PILMS patient, which did not result in recurrence in 18 months. The use of the vascular endothelial growth factor inhibitor bevacizumab is also a promising approach, and has been increasingly used to treat LMS (32, 52). Three Phase II clinical trials demonstrated that bevacizumab is an effective treatment for some STS (69, 70). Gallagher et al. (28), also reported recurrence of PILMS treated with re-operation and bevacizumab (7.5mg/kg, 4 doses at 3-week intervals), and the follow-up was lost two-months after the re-operation. Notably, active antiretroviral therapy is imperative for PILMS patients with retroviral infections, such as HIV (28).

Prognosis

The prognosis of PILMS is overall poor (3, 4, 15, 32, 33), and the long-term prognosis is not clear (53). A limited number of studies reported a survival range from 6 to 44 months (4, 37, 45), and the average follow-up was 12 months, although Niwa et al. (19), reported a patient who died 8 years after the initial surgery, which represented the longest survival ever published. The poor prognosis and high local recurrence rate were considered as associated with the difficulty in obtaining negative surgical resection margins and an inadequate radiotherapeutic dose (6, 14, 28). Vos et al. (71), contrasted the survival period of patients with STS between 2010-2014 and 1989-1994, and found that the OS had improved, but was not statistically significant. In some studies, it was shown that gender, age, immunosuppressive status, dural origin, or EBV infection did not have a significant impact on treatment outcome, but tumor size, location, mitotic rate, residual tumor, and inadequate dose of radiation were all unfavorable factors with a negative effect on survival (2, 15, 16, 72). However, Zhang, et al. (39), demonstrated that age, tumor size, and location were not statistically linked with clinical outcome. Shotton et al. (73), also suggested that the perineural invasion is an important predictor of survival and recurrence (10). The local recurrence rate is approximately 25.9% after radiotherapy on the initial lesion (15). Taken together, GTR has a significant and unexpected favorable outcome on survival (17, 24, 39).

CONCLUSION

Since PILMS is an extremely rare type of neoplasm, studies reporting on PILMS cases are rare. More future clinical trials, treatment experience, and long-term follow-up are required to fully understand this disease. Olaratumab might be a potential targeted drug for the treatment of PILMS, but has never been applied to PILMS patients. Thus, further studies are needed for its validity and BBBP. Here, we reported on PILMS secondary to GCG for the first time, and represented an additional reference among the few available, which might serve as a potential guide for clinicians and clinical studies.

ETHICS STATEMENT

The studies involving human participant was reviewed and approved by Ethics Committee of the First Hospital of Jilin University. The patient/participant provided his written informed consent to participate in this study. Written informed consent was obtained from the individual(s) for the publication of any potentially identifiable images or data included in this article.

AUTHOR CONTRIBUTIONS

LZ and YJ made study design, data collection, data analysis and interpretation, and composed the manuscript and literature review. YL and YW were the surgeons that performed the surgery, and did data collection, data analysis, and interpretation. YS and YB made English and grammar corrections, critical revisions, and approved final version. YL had the acquisition, analysis or interpretation of data for the work, revising it critically for important intellectual content, final approval of the version to be published, and agreed to be accountable for all aspects of the work in ensuring that questions related to the accuracy or integrity of any part of the work are appropriately investigated and resolved. All authors contributed to the article and approved the submitted version.

REFERENCES

1. Lee TT, Page LK. Primary Cerebral Leiomyosarcoma. *Clin Neurol Neurosurg* (1997) 99(3):210–2. doi: 10.1016/s0303-8467(97)00018-8
2. Zhang H, Dong L, Huang Y, Zhang B, Ma H, Zhou Y, et al. Primary Intracranial Leiomyosarcoma: Review of the Literature and Presentation of a Case. *Onkologie* (2012) 35(10):609–16. doi: 10.1159/000342676
3. Mathieson CS, St George EJ, Stewart W, Sastry J, Jamal S. Primary Intracranial Leiomyosarcoma: A Case Report and Review of the Literature. *Childs Nerv Syst* (2009) 25(8):1013–7. doi: 10.1007/s00381-009-0845-3
4. Li XL, Ren J, Niu RN, Jiang X, Xu GH, Zhou P, et al. Primary Intracranial Leiomyosarcoma in an Immunocompetent Patient: Case Report With Emphasis on Imaging Features. *Med (Baltimore)* (2019) 98(17):e15269. doi: 10.1097/md.0000000000015269
5. Paulus W, Slowik F, Jellinger K. Primary Intracranial Sarcomas: Histopathological Features of 19 Cases. *Histopathology* (1991) 18(5):395–402. doi: 10.1111/j.1365-2559.1991.tb00869.x
6. Hussain S, Nanda A, Fowler M, Ampil FL, Burton GV. Primary Intracranial Leiomyosarcoma: Report of a Case and Review of the Literature. *Sarcoma* (2006) 2006:52140. doi: 10.1155/srcm/2006/52140
7. Ritter AM, Amaker BH, Graham RS, Broaddus WC, Ward JD. Central Nervous System Leiomyosarcoma in Patients With Acquired Immunodeficiency Syndrome: Report of Two Cases. *JJon* (2000) 92(4):688–92. doi: 10.3171/jns.2000.92.4.0688
8. Aeddula NR, Pathireddy S, Samaha T, Ukena T, Hosseinnezhad A. Primary Intracranial Leiomyosarcoma in an Immunocompetent Adult. *J Clin Oncol* (2011) 29(14):e407–10. doi: 10.1200/jco.2010.33.4805
9. Fujimoto Y, Hirato J, Wakayama A, Yoshimine T. Primary Intracranial Leiomyosarcoma in an Immunocompetent Patient: Case Report. *J Neurooncol* (2011) 103(3):785–90. doi: 10.1007/s11060-010-0450-z
10. Barbiero FJ, Huttner AJ, Judson BL, Baehring JM. Leiomyosarcoma of the Infratemporal Fossa With Perineurial Spread Along the Right Mandibular Nerve: A Case Report. *CNS Oncol* (2017) 6(4):281–5. doi: 10.2217/cns-2017-0004
11. Patel U, Patel N. Primary Intracranial Leiomyoma in Renal Transplant Recipient. *Saudi J Kidney Dis Transplant an Off Publ Saudi Center Organ Transplant Saudi Arabia* (2017) 28(4):921–4.
12. Gupta S, Havens PL, Southern JF, Firat SY, Jogal SS. Epstein-Barr Virus-Associated Intracranial Leiomyosarcoma in an HIV-positive Adolescent. *JJopho* (2010) 32(4):e144–e7. doi: 10.1097/MPH.0b013e3181c80bf3
13. Akcam T, Oysul K, Birkent H, Gerek M, Yetiser S. Leiomyosarcoma of the Head and Neck: Report of Two Cases and Review of the Literature. *Auris Nasus Larynx* (2005) 32(2):209–12. doi: 10.1016/j.anl.2005.01.012
14. Alijani B, Yousefzade S, Aramnia A, Mesbah A. Primary Intracranial Leiomyosarcoma. *Arch Iran Med* (2013) 16(10):606–7. doi: 0131610/aim.0012
15. Torihashi K, Chin M, Yoshida K, Narumi O, Yamagata S. Primary Intracranial Leiomyosarcoma With Intratumoral Hemorrhage: Case Report and Review of Literature. *World Neurosurg* (2018) 116:169–73. doi: 10.1016/j.wneu.2018.05.004
16. Gautam S, Meena RK. Primary Intracranial Leiomyosarcoma Presenting With Massive Peritumoral Edema and Mass Effect: Case Report and Literature Review. *Surg Neurol Int* (2017) 8:278. doi: 10.4103/sni.sni_219_17
17. Sivendran S, Vidal CI, Barginear MF. Primary Intracranial Leiomyosarcoma in an HIV-infected Patient. *Int J Clin Oncol* (2011) 16(1):63–6. doi: 10.1007/s10147-010-0110-5
18. Selbi W, Sims-Williams H, Ince P, Carroll TA. Skull Base Angiomatous Leiomyoma: A Case Report and Review of Literature. *Br J Neurosurg* (2019) 1–3. doi: 10.1080/02688697.2018.1555636
19. Niwa J, Hashi K, Minase T. Radiation Induced Intracranial Leiomyosarcoma: its Histopathological Features. *Acta Neurochir (Wien)* (1996) 138(12):1470–1. doi: 10.1007/bf01411129
20. Saito A, Ninomiya A, Ishida T, Inoue T, Inoue T, Suzuki S, et al. Intractable Repeated Intracerebral Hemorrhage Due to Primary Dural Leiomyosarcoma: Case Report and Literature Review. *World Neurosurg* (2019) 122:116–22. doi: 10.1016/j.wneu.2018.10.132
21. Suankratay C, Shuangshoti S, Mutirangura A, Prasanthai V, Lerdlum S, Shuangshoti S, et al. Epstein-Barr Virus Infection-Associated Smooth-Muscle Tumors in Patients With AIDS. *Clin Infect Dis* (2005) 40:(10):1521–8. doi: 10.1086/429830
22. Brown HG, Burger PC, Olivi A, Sills AK, Barditch-Crovo PA, Lee RR. Intracranial Leiomyosarcoma in a Patient With AIDS. *Neuroradiology* (1999) 41(1):35–9. doi: 10.1007/s002340050701
23. Zevallos-Giampietri E-A, Yañes HH, Puelles JO, Barrionuevo CJAI, Morphology M. Primary Meningeal Epstein-Barr Virus-Related Leiomyosarcoma in a Man Infected With Human Immunodeficiency Virus: Review of Literature, Emphasizing the Differential Diagnosis and Pathogenesis. *Appl Immunohistochem Mol Morphol* (2004) 12: (4):387–91. doi: 10.1097/00129039-200412000-00018
24. Takei H, Powell S, Rivera A. Concurrent Occurrence of Primary Intracranial Epstein-Barr Virus-Associated Leiomyosarcoma and Hodgkin Lymphoma in a Young Adult. *J Neurosurg* (2013) 119(2):499–503. doi: 10.3171/2013.3.Jns121707
25. Paulino AC, Fowler BZ. Secondary Neoplasms After Radiotherapy for a Childhood Solid Tumor. *Pediatr Hematol Oncol* (2005) 22(2):89–101. doi: 10.1080/08880010590896459
26. Eckhardt BP, Brandner S, Zollikofer CL, Wentz KU. Primary Cerebral Leiomyosarcoma in a Child. *Pediatr Radiol* (2004) 34(6):495–8. doi: 10.1007/s00247-003-1123-2
27. Jhas S, Henriques L, Hawkins C, Bouffet E, Rutka JT. An Intracranial Leiomyosarcoma in a Child With Neurofibromatosis Type 1. *Can J Neurol Sci* (2009) 36(4):491–5. doi: 10.1017/s031716710000785x
28. Gallagher SJ, Rosenberg SA, Francis D, Salamat S, Howard SP, Kimple RJ. Primary Intracranial Leiomyosarcoma in an Immunocompetent Patient: Case Report and Review of the Literature. *Clin Neurol Neurosurg* (2018) 165:76–80. doi: 10.1016/j.clineuro.2017.12.014
29. Winn H. *Youmans Neurological Surgery. 6th Edn* Vol 3. Philadelphia. PA: Elsevier (2011).
30. Cahan WG, Woodard HQ, Higinbotham NL, Stewart FW, Coley BL. Sarcoma Arising in Irradiated Bone: Report of Eleven Cases. 1948. *Cancer* (1998) 82 (1):8–34. doi: 10.1002/(sici)1097-0142(19980101)82:1<8::aid-cncr3>3.0.co;2-w
31. Suzuki K, Yokoyama S, Waseda S, Kodama S, Watanabe M. Delayed Reactivation of p53 in the Progeny of Cells Surviving Ionizing Radiation. *Cancer Res* (2003) 63(5):936–41.
32. Polewski PJ, Smith AL, Conway PD, Marinier DE. Primary CNS Leiomyosarcoma in an Immunocompetent Patient. *J Oncol Pract* (2016) 12 (9):827–9. doi: 10.1200/jop.2016.012310
33. Morales RL, Alvarez A, Norena MP, Torres F, Esguerra J. Low-Grade Leiomyosarcoma of the Cavernous Sinus in an HIV Positive Patient: Case Report. *Cureus* (2020) 12(1):e6758. doi: 10.7759/cureus.6758
34. Louis DN, Richardson EP Jr., Dickersin GR, Petrucci DA, Rosenberg AE, Ojemann RG. Primary Intracranial Leiomyosarcoma. Case Report. *J Neurosurg* (1989) 71(2):279–82. doi: 10.3171/jns.1989.71.2.0279
35. Asai A, Yamada H, Murata S, Matsuno A, Tsutsumi K, Takemura T, et al. Primary Leiomyosarcoma of the Dura Mater. Case Report. *J Neurosurg* (1988) 68(2):308–11. doi: 10.3171/jns.1988.68.2.0308

36. Pop M, Botar Jid C, Hotoleanu C, Vasilescu D, Sfrangeu S. Superficial Leiomyosarcoma of the Scalp: A Case Report. *Med Ultrasonogr* (2011) 13 (3):237–40.
37. Almubaslat M, Stone JC, Liu L, Xiong Z. Primary Intracranial Leiomyosarcoma in an Immunocompetent Patient. *Clin Neuropathol* (2011) 30(3):154–7. doi: 10.5414/npp30154
38. Smith AB, Horkanyne-Szakaly I, Schroeder JW, Rushing EJ. From the Radiologic Pathology Archives: Mass Lesions of the Dura: Beyond Meningioma-Radiologic-Pathologic Correlation. *Radiographics Rev Publ Radiol Soc North America Inc* (2014) 34(2):295–312. doi: 10.1148/rg.342130075
39. Zhang GJ, Weng JC, Huo XL, Ma JP, Wang B, Wang L, et al. Surgical Management and Long-Term Outcomes of Primary Intracranial Leiomyosarcoma: A Case Series and Review of Literature. *Neurosurg Rev* (2020). doi: 10.1007/s10143-020-01422-z
40. Kumar S, Santi M, Vezina G, Rosser T, Chandra RS, Keating R. Epstein-Barr Virus-Associated Smooth Muscle Tumor of the Basal Ganglia in an HIV+ Child: Case Report and Review of the Literature. *Pediatr Dev Pathol* (2004) 7 (2):198–203. doi: 10.1007/s10024-003-7079-2
41. Purgina B, Rao UN, Miettinen M, Pantanowitz L. Aids-Related EBV-Associated Smooth Muscle Tumors: A Review of 64 Published Cases. *Pathol Res Int* (2011) 2011:561548. doi: 10.4061/2011/561548
42. Litofsky NS, Pihan G, Corvi F, Smith TW. Intracranial Leiomyosarcoma: A Neuro-Oncological Consequence of Acquired Immunodeficiency Syndrome. *J Neurooncol* (1998) 40(2):179–83. doi: 10.1023/a:1006167629968
43. Flannery T, Kano H, Niranjan A, Monaco EA3rd, Flickinger JC, Kofler J, et al. Gamma Knife Radiosurgery as a Therapeutic Strategy for Intracranial Sarcomatous Metastases. *Int J Radiat Oncol Biol Phys* (2010) 76(2):513–9. doi: 10.1016/j.ijrobp.2009.02.007
44. Anderson WR, Cameron JD, Tsai SH. Primary Intracranial Leiomyosarcoma. Case Report With Ultrastructural Study. *J Neurosurg* (1980) 53(3):401–5. doi: 10.3171/jns.1980.53.3.0401
45. Skullerud K, Stenwig AE, Brandtzaeg P, Nesland JM, Kerty E, Langmoen I, et al. Intracranial Primary Leiomyosarcoma Arising in a Teratoma of the Pineal Area. *Clin Neuropathol* (1995) 14(4):245–8.
46. Shepard MJ, Fezeu F, Lee CC, Sheehan JP. Gamma Knife Radiosurgery for the Treatment of Gynecologic Malignancies Metastasizing to the Brain: Clinical Article. *J Neurooncol* (2014) 120(3):515–22. doi: 10.1007/s11060-014-1577-0
47. Saito N, Akoi K, Hirari N, Ishii M, Fujita S, Hiramoto YJ. Primary Intracranial Leiomyosarcoma of the Cavernous Sinus: Case Report. *AJMO* (2014) 1(2):2.
48. Aumüller M, Sykora KW, Hartmann C, Hermann EJ, Krauss JK. Primary Intracranial Leiomyosarcoma of the Torcular Herophili Associated With Fanconi Anemia and Allogenic Stem Cell Transplantation. *Childs Nerv Syst* (2014) 30(9):1613–6. doi: 10.1007/s00381-014-2422-7
49. Ridolfi C, Pasini G, Drudi F, Barzotti E, Santelmo C, Polselli A, et al. Long Lasting Clinical Response to Chemotherapy for Advanced Uterine Leiomyosarcoma: A Case Report. *J Med Case Rep* (2013) 7:29. doi: 10.1186/1752-1947-7-29
50. Talbot SM, Keohan ML, Hesdorffer M, Orrico R, Bagiella E, Troxel AB, et al. A Phase II Trial of Temozolomide in Patients With Unresectable or Metastatic Soft Tissue Sarcoma. *Cancer* (2003) 98(9):1942–6. doi: 10.1002/cncr.11730
51. Amant F, Coosemans A, Debiec-Rychter M, Timmerman D, Vergote I. Clinical Management of Uterine Sarcomas. *Lancet Oncol* (2009) 10 (12):1188–98. doi: 10.1016/s1470-2045(09)70226-8
52. Jain A, Sajeevan KV, Babu KG, Lakshmaiah KC. Chemotherapy in Adult Soft Tissue Sarcoma. *Indian J Cancer* (2009) 46(4):274–87. doi: 10.4103/0019-509x.55547
53. Francisco CN, Alejandria M, Salvana EM, Andal VMV. Primary Intracranial Leiomyosarcoma Among Patients With AIDS in the Era of New Chemotherapeutic and Biological Agents. *BMJ Case Rep* (2018) 2018. doi: 10.1136/bcr-2018-225714
54. Kersting C, Packeisen J, Leidinger B, Brandt B, von Wasielewski R, Winkelmann W, et al. Pitfalls in Immunohistochemical Assessment of EGFR Expression in Soft Tissue Sarcomas. *J Clin Pathol* (2006) 59(6):585–90. doi: 10.1136/jcp.2005.028373
55. Moroncini G, Maccaroni E, Fiordoliva I, Pellei C, Gabrielli A, Berardi R. Developments in the Management of Advanced Soft-Tissue Sarcoma - Olaratumab in Context. *OncoTargets Ther* (2018) 11:833–42. doi: 10.2147/ott.S127609
56. Shirley M. Olaratumab: First Global Approval. *Drugs* (2017) 77(1):107–12. doi: 10.1007/s40265-016-0680-2
57. Knepper TC, Saller J, Walko CM. Novel and Expanded Oncology Drug Approvals of 2016-PART 1: New Options in Solid Tumor Management. *Oncol (Williston Park NY)* (2017) 31(2):110–21.
58. Seddon B, Strauss SJ, Whelan J, Leahy M, Woll PJ, Cowie F, et al. Gemcitabine and Docetaxel Versus Doxorubicin as First-Line Treatment in Previously Untreated Advanced Unresectable or Metastatic Soft-Tissue Sarcomas (GeDDiS): A Randomised Controlled Phase 3 Trial. *Lancet Oncol* (2017) 18 (10):1397–410. doi: 10.1016/s1470-2045(17)30622-8
59. Judson I, Verweij J, Gelderblom H, Hartmann JT, Schöffski P, Blay JY, et al. Doxorubicin Alone Versus Intensified Doxorubicin Plus Ifosfamide for First-Line Treatment of Advanced or Metastatic Soft-Tissue Sarcoma: A Randomised Controlled Phase 3 Trial. *Lancet Oncol* (2014) 15(4):415–23. doi: 10.1016/s1470-2045(14)70063-4
60. Kamian S, Ebrahimi A, Zadeh KE, Behzadi B. Primary Intracranial Leiomyosarcoma Presenting With Frontal Bone Mass: A Case Report. *Radiat Oncol J* (2020) 38(4):282–6. doi: 10.3857/roj.2020.00577
61. Kaphan E, Eusebio A, Witjas T, Donnet A, Vacher-Coponat H, Figarella-Branger D, et al. [Primary Leiomyosarcoma of the Cavernous Sinus Associated With Epstein-Barr Virus in a Kidney Graft]. *Rev Neurol (Paris)* (2003) 159(11):1055–9.
62. Crespo-Jara A, González Manzano R, Lopera Sierra M, Redal Peña MC, Brugarolas Masllorens A. A Patient With Metastatic Sarcoma was Successfully Treated With Radiolabeled Somatostatin Analogs. *Clin Nucl Med* (2016) 41 (9):705–7. doi: 10.1097/rlu.0000000000001288
63. Ehnman M, Missiaglia E, Folestad E, Selfe J, Strell C, Thway K, et al. Distinct Effects of Ligand-Induced Pdgfrα and Pdgfrβ Signaling in the Human Rhabdomyosarcoma Tumor Cell and Stroma Cell Compartments. *Cancer Res* (2013) 73(7):2139–49. doi: 10.1158/0008-5472.Can-12-1646
64. Board R, Jayson GC. Platelet-Derived Growth Factor Receptor (PDGFR): A Target for Anticancer Therapeutics. *Drug Resist Updates Rev Comment Antimicrob Anticancer Chemother* (2005) 8(1-2):75–83. doi: 10.1016/j.drup.2005.03.004
65. Tap WD, Jones RL, Van Tine BA, Chmielowski B, Elias AD, Adkins D, et al. Olaratumab and Doxorubicin Versus Doxorubicin Alone for Treatment of Soft-Tissue Sarcoma: An Open-Label Phase 1b and Randomised Phase 2 Trial. *Lancet (London England)* (2016) 388(10043):488–97. doi: 10.1016/s0140-6736(16)30587-6
66. Tap WD, Wagner AJ, Schöffski P, Martin-Broto J, Krarup-Hansen A, Ganjoo KN, et al. Effect of Doxorubicin Plus Olaratumab vs Doxorubicin Plus Placebo on Survival in Patients With Advanced Soft Tissue Sarcomas: The Announce Randomized Clinical Trial. *JAMA* (2020) 323(13):1266–76. doi: 10.1001/jama.2020.1707
67. Gennatas S, Chamberlain F, Carter T, Slater S, Cojocaru E, Lambourn B, et al. Real-World Experience With Doxorubicin and Olaratumab in Soft Tissue Sarcomas in England and Northern Ireland. *Clin Sarcoma Res* (2020) 10:9. doi: 10.1186/s13569-020-00131-x
68. Ryan CW, Merimsky O, Agulnik M, Blay JY, Schuetze SM, Van Tine BA, et al. Picasso Iii: A Phase III, Placebo-Controlled Study of Doxorubicin With or Without Palifosfamide in Patients With Metastatic Soft Tissue Sarcoma. *J Clin Oncol* (2016) 34(32):3898–905. doi: 10.1200/jco.2016.67.6684
69. D'Adamo DR, Anderson SE, Albritton K, Yamada J, Riedel E, Scheu K, et al. Phase II Study of Doxorubicin and Bevacizumab for Patients With Metastatic Soft-Tissue Sarcomas. *J Clin Oncol* (2005) 23(28):7135–42. doi: 10.1200/jco.2005.16.139
70. Agulnik M, Yarber JL, Okuno SH, von Mehren M, Jovanovic BD, Brockstein BE, et al. An Open-Label, Multicenter, Phase II Study of Bevacizumab for the Treatment of Angiosarcoma and Epithelioid Hemangioendotheliomas. *Ann Oncol* (2013) 24(1):257–63. doi: 10.1093/annonc/mds237
71. Vos M, Ho VKY, Oosten AW, Verhoef C, Sleijfer S. Minimal Increase in Survival Throughout the Years in Patients With Soft Tissue Sarcoma With Synchronous Metastases: Results of a Population-Based Study. *Oncol* (2019) 24(7):e526–e35. doi: 10.1634/theoncologist.2017-0383
72. Bartosch C, Afonso M, Pires-Luis AS, Galaghar A, Guimaraes M, Antunes L, et al. Distant Metastases in Uterine Leiomyosarcomas: The Wide Variety of Body Sites and Time Intervals to Metastatic Relapse. *Int J Gynecol Pathol* (2017) 36(1):31–41. doi: 10.1097/pgp.0000000000000284

73. Shotton JC, Kuhwoede R, Fisch U. Mesenchymal Tumors of the Skull Base With Particular Reference to Surgical Management and Outcome. *Skull Base Surg* (1992) 2(2):112–7. doi: 10.1055/s-2008-1057120

Conflict of Interest: The authors declare that the research was conducted in the absence of any commercial or financial relationships that could be construed as a potential conflict of interest.

frontiers in Oncology

REVIEW
published: 11 June 2021
doi: 10.3389/fonc.2021.688027

Roles of Long Noncoding RNAs in Conferring Glioma Progression and Treatment

Jie Qin, Chuanlu Jiang, Jinquan Cai and Xiangqi Meng**

Department of Neurosurgery, The Second Affiliated Hospital of Harbin Medical University, Harbin, China

Accompanying the development of biomedicine, our knowledge of glioma, one of the most common primary intracranial carcinomas, is becoming more comprehensive. Unfortunately, patients with glioblastoma (GBM) still have a dismal prognosis and a high relapse rate, even with standard combination therapy, namely, surgical resection, postoperative radiotherapy and chemotherapy. The absence of validated biomarkers is responsible for the majority of these poor outcomes, and reliable therapeutic targets are indispensable for improving the prognosis of patients suffering from gliomas. Identification of both precise diagnostic and accurate prognostic markers and promising therapeutic targets has therefore attracted considerable attention from researchers. Encouragingly, accumulating evidence has demonstrated that long noncoding RNAs (lncRNAs) play important roles in the pathogenesis and oncogenesis of various categories of human tumors, including gliomas. Nevertheless, the underlying mechanisms by which lncRNAs regulate diverse biological behaviors of glioma cells, such as proliferation, invasion and migration, remain poorly understood. Consequently, this review builds on previous studies to further summarize the progress in the field of lncRNA regulation of gliomas over recent years and addresses the potential of lncRNAs as diagnostic and prognostic markers and therapeutic targets.

Keywords: lncRNAs, glioma, biomarker, therapeutic target, prognosis, chemoresistance

OPEN ACCESS

Edited by:
Yaohua Liu,
Shanghai First People's Hospital, China

Reviewed by:
Karanbir Brar,
University of Toronto, Canada
Ye Zhang,
China Medical University, China
Wenhua Liang,
First Affiliated Hospital of Guangzhou Medical University, China

****Correspondence:***
Jinquan Cai
caijinquan666777@126.com
Xiangqi Meng
neptune_mxq@126.com

Specialty section:
This article was submitted to Neuro-Oncology and Neurosurgical Oncology, a section of the journal Frontiers in Oncology

Received: *30 March 2021*
Accepted: *26 May 2021*
Published: *11 June 2021*

Citation:
Qin J, Jiang C, Cai J and Meng X (2021) Roles of Long Noncoding RNAs in Conferring Glioma Progression and Treatment. Front. Oncol. 11:688027. doi: 10.3389/fonc.2021.688027

INTRODUCTION

Gliomas, originating from glial or precursor cells, which are categorized into astrocytomas, ependymomas and oligodendrogliomas, are the most common malignant primary tumors of the central nervous system (CNS) (1, 2). In addition, gliomas are graded by the World Health Organization (WHO) into four classifications based on their malignancy. Gliomas with WHO grades I-II are known as low-grade gliomas (LGGs), including angiocentric glioma and diffuse astrocytoma, while those with WHO grades III-IV are considered high-grade gliomas (HGGs), including mesenchymal astrocytoma and glioblastoma multiform gliomas (GBMs) (3, 4). In the 2016 WHO classification of CNS tumors, molecular parameters, including IDH, ATRX, TP53 and 1p/19, were considered in the classification of glioma subtypes, which is more detailed than its 2007 predecessor (5, 6). GBM has high mortality and recurrence rates and represents the most malignant CNS tumor (3). The present criteria for treating GBM continue to be neurosurgical resection of the

neoplasm accompanied by chemotherapy with temozolomide (TMZ) and radiotherapy (7). Unfortunately, the median survival for GBM patients is only 15 months, even with this combination treatment (8). Therefore, exploring the specific mechanisms of the occurrence and progression of glioma has drawn widespread interest in recent years. Studies on precise biomarkers and reliable therapeutic targets are urgently needed.

Approximately 98% of transcripts do not encode proteins in the human genome, and this category of RNA is known as noncoding RNA (ncRNA). Long noncoding RNAs (lncRNAs), accounting for approximately 80-90% of ncRNAs, are transcripts consisting of more than 200 nucleotides that typically lack protein-coding capability and were once regarded as transcriptional noise (9). Open reading frames are generally absent in lncRNAs (10). Intriguingly, this "transcriptional noise" has been extensively researched and demonstrated to not only serve an important function in normal cellular physiological procedures but also play an invaluable role in regulating the malignant behavior of tumors (11). LncRNAs can be divided into sense lncRNAs, antisense lncRNAs, bidirectional lncRNAs, intronic lncRNAs and intergenic lncRNAs (LINCRNAs) based on genomic location (12). The order of nucleotide arrangement constitutes the primary structure of lncRNAs, and intricate secondary and tertiary structures guarantee the multiple functions of lncRNAs. However, the relationship between lncRNA secondary structure and functions remains unclear. Recent evidence has indicated that lncRNAs regulate gene expression at three levels: transcriptional, post-transcriptional and epigenetic modification (13).

As mentioned above, lncRNAs are associated with both cellular physiology and disease origination and progression by regulating gene expression (11). Additionally, an increasing number of investigations have suggested that lncRNAs play pivotal roles in regulating the tumorigenesis, proliferation, aggression, metastasis, and drug resistance of gliomas. Consequently, as the molecular mechanism of lncRNA regulation of glioma is further investigated, the etiology of glioma will gradually be revealed. Furthermore, along with the advancement of sequencing technology, we will gradually recognize the entire spectrum of lncRNAs, implying that lncRNAs could be not only effective indicators for early diagnosis and determination of prognosis but also therapeutic targets for glioma.

THE FUNCTIONS AND MECHANISMS OF LNCRNAS IN GLIOMAS

MiRNAs are a category of noncoding RNAs of approximately 20 nucleotides in length that can bind to target mRNAs *via* microRNA response elements (MREs) and thus perform negative regulatory functions, exerting critical post-transcriptional regulatory effects (14). MREs are short sequences of both lncRNAs and mRNAs that combine with miRNAs. Therefore, lncRNAs absorb miRNAs as sponges, enabling the expression of mRNAs that were previously repressed by miRNAs, and such lncRNAs are referred to as competitive endogenous RNAs (**Figure 1**) (15). Many studies have been conducted to demonstrate that lncRNAs, as ceRNAs, impact the progression of tumors at the post-transcriptional regulatory level (**Table 1**).

By analyzing GSE4290, Liu and colleagues showed that LINC00689 was highly expressed in glioma tissue compared to normal brain tissue. The expression of pyruvate kinase M2 (PKM2) was enhanced by LINC00689-mediated elimination of miR-338-3p, which facilitated malignant progression of glioma cells. As a consequence, the LINC00689/miR-338-3p/PKM2 axis functions as a carcinogenic driver in gliomas (16). Moreover, LINC01857 could promote tumorigenesis of glioma by sponging miR-1281 to upregulate TRIM65 expression (17). MALAT1 has been proved to have a crucial role in the progression of multiple neoplasms such as lung, colorectal and gastric cancers, and shows a comparable regulatory role in glioma. MALAT1 promoted the level of ZHX1 by serving as a ceRNA of miR-199a, leading to augmented glioma development (18). LINC01579 accelerated cell proliferation and apoptosis of GBM by the competitive binding of miR-139-5p to affect EIF4G2 (19). Furthermore, the lncRNA SNHG1 is considered a sponge that absorbs miR-194 to promote glioma progression by regulating PHLDA1 expression (20). MiR-605-3p was eliminated by lncRNA BLACAT1 to accelerate VASP expression, contributing to glioma proliferation (21). The expression level of NAMPT was regulated by lncRNA-GACAT3 to promote glioma progression as a sponge for miR135a (22). LncRNA MATN1-AS1 competitively binding with miR-200b/c/429 also promoted the progression of glioma by modulating CHD1 expression (23). Chai et al. demonstrated that exosomal lncRNAe-ROR1-AS1 enhanced glioma progression by suppressing miR-4686 (24). LEF1-AS1 promoted glioma formation by competitively binding miR-489-3p to increase the expression of HIGD1A (25). Oncogenic lncRNA FOXD1-AS1 promoted the proliferation and metastasis of GBM cells by targeting miR339/342 (26). However, lncRNA could also act as a repressor to inhibit tumor progression. Zhen et al. indicated that NEAT1 sponged miR-107 to inhibit the expression of cyclin-dependent kinase 14 (CDK14) to repress the malignant progression of glioma (27). The anti-oncogene AC016405.3 restrained GBM cell proliferation and migration by sponging miR-19a through regulation of ten-eleven translocation-2 (TET2) (28). LncRNA TPT1-AS1 inhibited glioma cell autophagy by decreasing the expression of miR-110-5p, and upregulating STMN1 expression promoted the proliferation of glioma cells (29). In addition, mRNAs can indirectly regulate gene phenotypes by signaling pathways *via* the post-transcriptional regulation of ceRNAs. For instance, miR-183-2-3p was sponged by lncRNA NCK1-AS1. Low levels of miR-183-2-3p promoted TRIM24 expression and thereby activated the Wnt/β-catenin pathway to contribute to glioma progression (30). Correspondingly, the lncRNA AGAP2-AS1 exhibited analogous mechanisms in contributing to the development of glioma advancement *via* the miR-15a/b-5p/HDGF/WNT axis (31). The oncogene lncRNA SNHG16, in contrast, functioned in the proliferation, aggression and migration of glioma cells through the miR373/EGFR/PI3K/

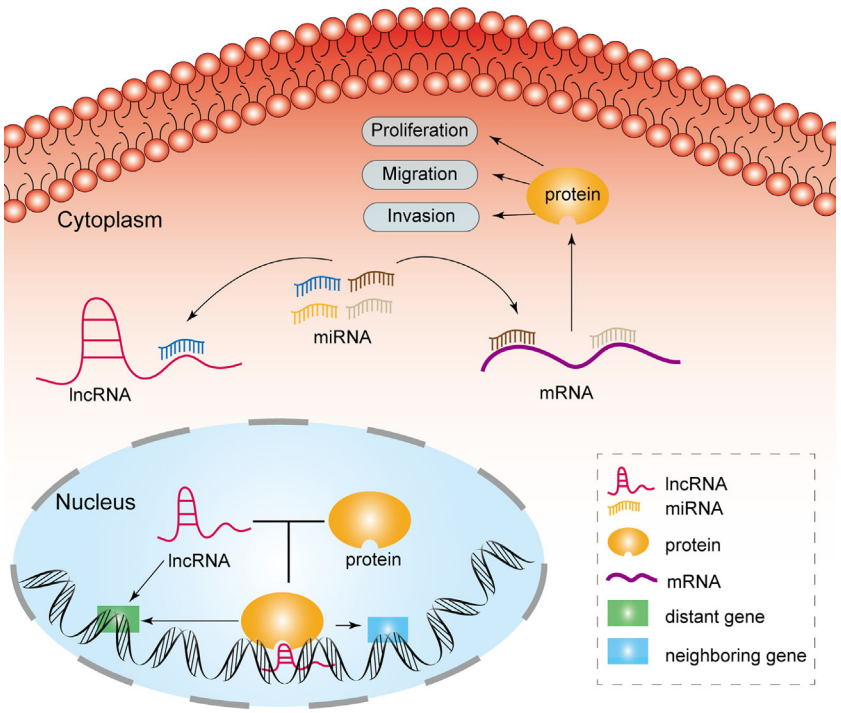

FIGURE 1 | Mechanisms of lncRNAs in glioma cell.

AKT axis (32). These researches illustrated that lncRNAs could not only promote but also inhibit tumor progression.

By interacting with signaling pathways, lncRNAs can facilitate tumorigenesis. For example, silencing lncRNA MIR22HG inhibited GBM aggressiveness by suppressing the Wnt/β-catenin signaling pathway (33), while cancer susceptibility candidate 7 (CASC7) restrained the progression of glioma through the Wnt/β-catenin pathway (34). BCAR4 promoted glioma cell progression by stimulating the EGFR/PI3K/AKT pathway (35). LncRNA LPP-AS2 plays an important role in regulating the miR-7-5p/EGFR/PI3K/AKT/c-MYC feedback loop, which is correlated with glioma tumorigenesis (36). LncRNA BCYRN1 could suppress tumorigenesis of glioma as a molecular sponge of miR-619-5p to modulate the PTEN/AKT/p21 pathway and CUEDC2 expression (37). Furthermore, lncRNA MT1JP suppressed proliferation, invasion, and migration and promoted apoptosis of glioma cells through stimulation of the PTEN/Akt signaling pathway (38). LncRNA-THOR silencing accelerated human glioma cell apoptosis by activating the MAGEA6-AMPK signaling pathway (39). Accumulating studies have suggested that lncRNA is involved in the regulation of diverse biological behaviors in glioma through the regulation of signaling pathways including but not limited to Wnt/β, PI3K/AKT and NF-κB. Therefore, lncRNAs are promising biomarkers for glioma diagnosis, prognosis and treatment in theory.

The interaction between RNA-binding proteins (RBPs) and lncRNAs plays a non-negligible role in the advancement of glioma. The expression level of EZH2 positively correlated with the malignancy of glioma and promoted the malignant behavior of glioma (40). Chen et al. first addressed the mechanism of the participation of lncRNA NEAT1 in tumorigenesis as a scaffold for EZH2. LncNEAT1 recruited EZH2 to interact with the promoter regions of downstream genes (Axin2, ICAT, GSK3B) to promote trimethylation modification of H3K27, thereby silencing these three genes. Further, the WNT/β-catenin pathway was activated, resulting in tumorigenesis (41). Moreover, RBP DGCR8 could bind with ZFAT-AS1, the interaction between DGCR8/ZFAT-AS1 and CDX2 contributed to the malignant progression of glioma (42). RBP, lncRNA and downstream gene could form negative or positive feedback loop to modulate biological behavior of glioma. SNHG1 regulated the miRNA154-5p/miR-376b-3p-FOXP2-KDM5B positive feedback loop to promote the malignant phenotype of glioma cells (43). LINC00475 silencing acted as a tumor suppressor in glioma under hypoxic conditions by impairing miRNA-449b-5p-dependent upregulation of AGAP2 expression (44). TRPM2-AS inhibited the growth, migration, and invasion of gliomas through JNK, c-Jun, and RGS4 (45). HCG11 inhibited glioma progression by modulating miR-496 to upregulate cytoplasmic polyadenylation element binding protein 3 (CPEB3) expression (46). The lncRNA MNX1-AS1 reduced the level of miR-4443, leading to the promotion of proliferation, invasion and migration in glioma (47). NEAT1 and CDK6 could promote tumorigenesis of glioma cells; additionally, miR-139-5p restrained the biological functions of glioma cells (48). LncRNAs has diverse roles in glioma processes, such as

TABLE 1 | The role of lncRNAs as ceRNA in the glioma.

LncRNA	MiRNA	Expression of mRNA	Function	Study
LINC00689	miR-338-3p	Upregulated PKM2	Promoting growth, metastasis and glycolysis	16
LINC01857	miR-1281	Upregulated TRIM65	Promoting growth, migration, and invasion	17
MALAT1	miR-199a	Upregulated ZHX1	Promoting proliferation and progression.	18
SNHG1	miR-194	Upregulated PHLDA1	Promoting progression	19
BLACAT1	miR-605-3p	Upregulated VASP	Promoting progression	20
AC016405.3	miR-19a-5p	Upregulated TET2	Acting as tumor suppressor	21
GACAT3	miR-135a.	Upregulated NAMPT	Promoting progression	22
MATN1-AS1	miR-200b/c/429	Upregulated CHD1	Promoting progression	23
TPT1-AS1	miRNA-770-5p	Upregulated STMN1	Inhibiting autophagy and promoting proliferation	24
LEF1-AS1	miR-489-3p	Upregulated HIGD1A	Promoting tumorigenesis	26
NCK1-AS1	miR-138-2-3p	Upregulated TRIM24	Promoting tumorigenesis	28
AGAP2-AS1	miR-15a/b-5p	Upregulated HDGF	Promoting proliferation	29
SNHG16	miR-373	Upregulated EGFR	Promoting tumorigenicity	30
LINC00475	miR-449b-5p	Upregulated AGAP2	Acting as a tumor suppressor	41
HCG11	miR-496	Upregulated CPEB3	Promoting progression	43
NEAT1	miR-139-5p	Upregulated CDK6	Promoting proliferation, invasion and migration	45
NEAT1	miR-107	Upregulated CDK14	Promoting progression	52
BCYRN1	miR-619-5p	Upregulated CUEDC2	Inhibiting tumorigenesis	50
LINC00174	miR-152-3p	Upregulated SLC2A1	Promoting glycolysis and tumor progression	51
LPP-AS2	miR-7-5p	Upregulated EGFR	Promoting tumorigenesis	54
LINC00645	miR-205-3p	Upregulated ZEB1	Promoting epithelial-mesenchymal transition (EMT)	55
HOTAIR	miR-148b-3p	Upregulated USF1	Regulating blood-tumor barrier (BTB) permeability	58
MIAT	miR-140-3p	Upregulated ZAK	Regulating BTB permeability	59
Lnc00462717	miR-186-5p	Upregulated PTBP1	Regulating BTB permeability	61
LINC00174	miR-138-5p/miR-150-5p	Upregulated FOSL2	Regulating BTB permeability	62
TALC	miR-20b-3p	Upregulated c-Met	Promoting MGMT expression	66
SNHG15	miR-726	Upregulated CDK6	Overcoming temozolomide (TMZ) resistance	68
AC003092.1	miR-195	Upregulated TFPI-2	Promoting TMZ chemosensitivity	71
CASC2	miR-181a	Upregulated PTEN	Promoting glioma growth and resistance to TMZ	72
SNHG16	miR-212-3p	Upregulated USF1	Promoting vasculogenic mimicry	78
LINC00667	miR-429	Upregulated USF1	Promoting vasculogenic mimicry	78
SNHG1	miR-154-5p/miR-376b-3p	Upregulated FOXP2	Promoting growth, migration, and invasion	39
PDIA3P1	miR-124-3p	Upregulated RELA	Promoting EMT	83
LINC01579	miR-139-5p	Upregulated EIF4G2	Promoting proliferation	84

proliferation, migration, apoptosis and angiogenesis, by distinct mechanisms, including ceRNA, interaction with RBPs and regulation of mRNA. **Figure 2** portrays the lncRNAs associated with glioma proliferation, metastasis, apoptosis and angiogenesis.

LNCRNAS AS DIAGNOSTIC AND PROGNOSTIC BIOMARKERS OF GLIOMAS

Medical diagnosis in the twenty-first century is gradually moving from clinical pathology to molecular pathology. With the development of bioinformatics, an increasing number of studies have identified lncRNAs as biomarkers for glioma diagnosis and prognosis by exploring RNA microarrays, and advances in microarray and high-throughput RNA-seq technologies have provided numerous valuable lncRNAs for the diagnosis and prognosis of gliomas.

The detection of serum HOTAIR levels can be employed for the clinical diagnosis of glioma, as reported by Tan et al. (49) These researchers also observed that the serum levels of HOTAIR were significantly higher in GBM patients than in controls, with a sensitivity of 86.1% and specificity of 87.5% (49). This report first showed that HOTAIR can function as a novel diagnostic and prognostic peripheral biomarker of GBM. Lin et al. screened six lncRNAs associated with low-grade glioma prognosis by TCGA and GTEx RNA-seq databases. These researchers constructed a prognostic risk signature with 6 lncRNAs in LGG, and this research illustrated that AL031722.1 and LINC00844 decreased when the risk score was increased, while the expression of AL354740.1, FGD5-AS1, and NEAT1 increased (50). The team of Li et al. indicated that the expression of LINC01060 was upregulated in glioma and significantly related to tumor grade and poor clinical prognosis (51). Furthermore, Liu et al. revealed that the level of RMST was related to histological grade, and 95.6% of HGGs had higher RMST expression (52). The lncRNA HOTAIRM1 was identified as a prognostic factor for glioma because it can maintain the tumorigenicity of GSCs by regulating HOX gene expression (53). And, LINC00115 was shown to act as a key role in GSC self-renewal and tumorigenicity by Tang et al. (54) LINC00174 accelerated glycolysis and tumor progression by competitively binding with miR-152-3p in glioma, indicating this molecule might act as a molecular target for glioma diagnosis (55). LncRNA H19, which mediates the effect of curcumin in treating glioma accompanied by miR-675 and VDR, could act as a novel diagnostic biomarker (56). Li et al. showed that

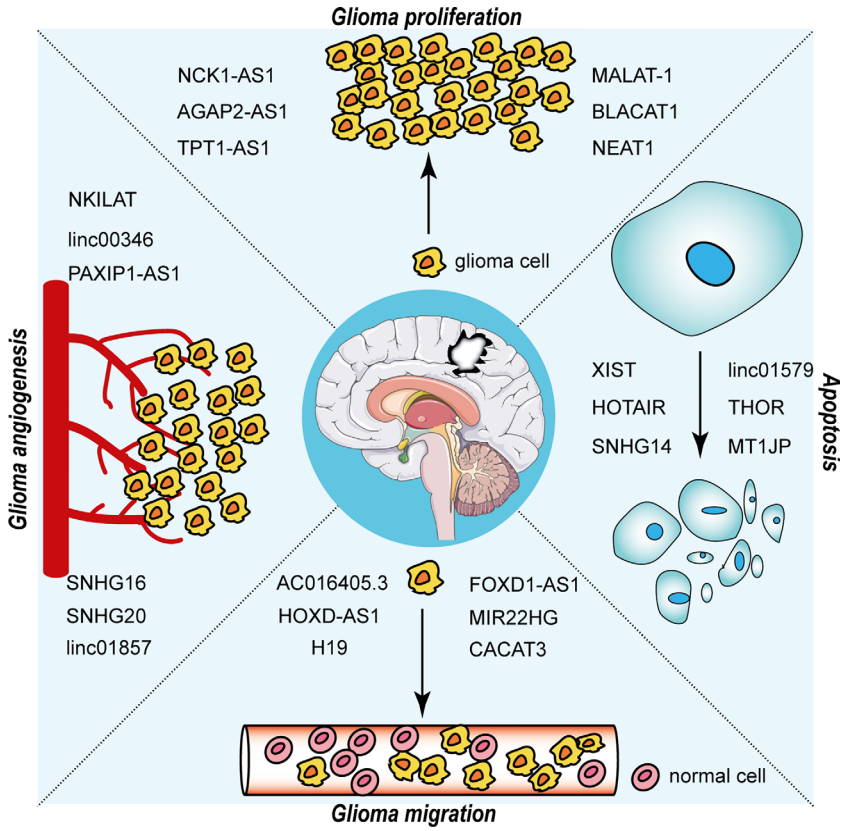

FIGURE 2 | LncRNAs in the proliferation, migration, apoptosis and angiogenesis of glioma.

LINC00645 could promote EMT, which was indispensable in the invasion and migration of glioma cells involving TGF-β by regulating the miR-205-3p-ZEB1 axis; thus, LINC00645 could be a prognostic indicator for glioma (57). A novel lncRNA-TOCN that targets the Smad2/PKCα signaling pathway to inhibit malignant progression of glioma was highlighted by Tang et al. and could serve as a prognostic indicator of GBM (58). The expression of multiple lncRNAs has been documented to correlate with the malignancy of gliomas and to be involved in their malignant progression, providing powerful theoretical evidence for their application as diagnostic and prognostic markers.

LNCRNAS AS RELIABLE THERAPEUTIC TARGETS

Treatment Strategies Involving LncRNAs as Regulators Modulating the BTB

The BTB parallels the blood-brain barrier (BBB) and is comprised of vascular endothelial cells, basement membrane, and glioma cells. This structure can seriously impede the entry of drugs into the tumor microenvironment, resulting in poor drug efficacy and extremely unfavorable patient prognosis (59–61). Consequently, exploring lncRNAs that can regulate BTB permeability to promote chemotherapy and thus improve drug efficacy is one of the research directions for targeted glioma therapy. Li et al. showed that silencing HOTAIR could increase BTB permeability by eliminating miR-148b-3p, thereby further reducing the expression of glioma-microvascular endothelial cell tight junction (TJ)-related proteins by targeting USF1 (62). He et al. also indicated that MIAT regulated the expression of ZAK to promote the delivery efficiency of doxorubicin across the BTB (63). In addition, the IGF2BP2/FBXL19-AS1/ZNF765 axis could regulate the permeability of the BTB to improve the antitumor effect of doxorubicin (64). Lnc00462717 regulated BTB permeability by interacting with PTBP1 to restrain the miR-1865p/Occludin signaling pathway (65). Moreover, BTB permeability was shown to be augmented by silencing LINC00174 in glioma tissue (66). Overcoming the obstacle of the BTB to increase the local concentration of chemotherapeutic agents in glioma and then enhance therapeutic efficacy is a prospective strategy. As such, identifying appropriate targets has been a major concern. The formulation of individual drug delivery routes based on the corresponding targets is another strategy that can potentially enhance chemotherapeutic efficacy.

Treatment Strategies Involving LncRNAs Overcoming TMZ Resistance

Temozolomide (TMZ) is an oral alkylating agent that passes through the BBB, adding methyl groups to the purines of DNA to cause DNA damage and apoptosis for therapeutic effects (67, 68). Conversely, this process is reversed by the DNA damage repair enzyme O^6-methyl-guanine-DNA methyltransferase (MGMT), which restores the damage caused by TMZ, resulting in the resistance of glioma cells to TMZ (69). A novel lncRNA, lnc-TALC, was found to be highly expressed in TMZ-resistant GBM cells by Wu et al. Lnc-TALC modulated the c-Met pathway by functioning as a ceRNA for miR-20b-3p, facilitating MGMT performance and in turn leading to TMZ resistance in GBM cells (70). Sun and colleagues revealed that the overexpression of miR-29c-3p could promote chemosensitivity to cisplatin, and CRNDE, which competitively binds with miR-29c-3p, plays a critical role in regulating the chemoresistance of medulloblastoma (71). In addition, tumorigenesis of glioma was attenuated with the downregulation of lncRNA-SNHG15 expression, and TMZ sensitivity was increased (72). Recently, a study reported that combining p50 and p53 with the proximal κB and p53 sites of the MALAT1 coding region, respectively, cooperatively downregulated MALAT1 expression, which in turn increased the chemosensitivity of GBM cells (73). The tumor microenvironment was remodeled with the secretion of oncogenic lncSBF2-AS1-enriched exosomes by GBM cells, resulting in tumor drug resistance (74). The lncRNA AC003092.1 inhibited miR-195, increasing the expression of tfpi-2, which promoted TMZ-induced apoptosis and thus made GBM cells more sensitive to TMZ (75). CASC2 has an essential function in the sensitivity of glioma to TMZ by upregulating PTEN expression through direct inhibition of miR-181a (76). High expression of SNHG12 in TMZ-resistant cells served as a molecular sponge for miR-129-5p to raise the levels of MAPK1 and E2F7 to enhance the sensitivity of GBM cells to TMZ. In contrast, knockdown of SNHG12 restored TMZ sensitivity (77). LncRNA SOX2OT activates the Wnt5a/β-catenin signaling pathway through upregulation of SOX2 expression, thereby inhibiting apoptosis, promoting cell proliferation, and resulting in resistance to TMZ (78). LncRNAs are not only linked to chemotherapy but also closely correlated with radioresistance. For instance, LINC-RA1 inhibited autophagy and enhanced radioresistance by inhibiting the H2Bub1/USP44 combination in glioma cells (79). In summary, lncRNA on the one hand can increase sensitivity of glioma to TMZ and on the other hand induce TMZ resistance of glioma. TMZ is currently the main chemotherapeutic agent for the treatment of glioma, however, glioma is prone to become resistance to it. Thus, it is feasible to target lncRNA to find drugs to overcome TMZ resistance in glioma.

Treatment Strategy Involving LncRNAs Mediating Angiogenesis

Angiogenesis is a requirement for the growth and metastasis of gliomas, which are solid tumors. Additionally, extensive evidence has demonstrated that the formation of novel blood vessels participates in the development and metabolic processes of tumors. Therefore, vasculogenic mimicry is considered a hallmark of malignant tumor development. Hence, antiangiogenic treatment is anticipated to be an additional efficacious strategy for glioma. Chen and colleagues demonstrated that overexpression of NKILAT was negatively correlated with survival time in glioma patients, and NKILAT augmented the Warburg effect and angiogenesis in glioma, suggesting that it may be a promising therapeutic strategy (80). In addition, Yang et al. elucidated the key role of the ANKHD1/LINC00346/ZNF655 feedback loop in regulating angiogenesis in glioma (81). Likewise, Wang et al. demonstrated that knockdown of USF1 suppressed angiogenesis in gliomas by stressing SNHG16/miR-212-3p and the LINC00667/miR-429 axis (82). Furthermore, overexpression of lncRNA PAXIP1-AS1 promoted glioma vasculogenic mimicry by recruiting the transcription factor EST to upregulate KIF4 expression (83). SNHG20 played a crucial role in the ZRANB2/SNHG20/FOXK1 axis to regulate vasculogenic mimicry of glioma (84). These studies provide compelling evidence that lncRNAs potentially act as therapeutic targets by regulating angiogenesis in gliomas.

In addition, lncRNAs that exert regulatory effects by binding to RBP also have the potential to become therapeutic targets. Lin28a elevated the expression and stability of SNHG14, while deletion of SNHG14 increased the expression of IRF6, which inhibited the transcription of PKM2 and GLUT1 and thus impaired glycolysis and proliferation of glioma cells and induced apoptosis. Therefore, considering the lin28a/SNHG14/IRF6 axis as a target provides novel insight for the treatment of glioma (85). Additionally, the TAF15/LINC00665/MTF1(YY2)/GTSE1 axis is crucial for regulating the malignant biological behaviors of glioma cells, which might help in the development of a novel therapeutic strategy for human glioma (86). The PABPC1-BDNF-AS-RAX2-DLG5 axis was shown to play the same role as the TAF15/LINC00665/MTF1(YY2)/GTSE1 axis in regulating the biological behavior of gliomas (87). LncRNA PDIA3P1 promoted glioma mesenchymal transition by competitively binding to miR-124-3p in a hypoxic environment to regulate RELA expression and activate the downstream NF-κB pathway. Consequently, the PDIA3P1-miR-124-3p-RELA axis is a possible target for glioma therapy (88, 89). SChLAP1 forms a complex with HNRNPL to maintain the stability of ACTN4 and thus activates the NF-κB pathway to promote the growth of GBM cells (90). The identification of this complex provided a new perspective for the treatment of glioma. The UPF1-LINC00313-miR-342-3p/miR-485-5p-Zic4-SHCBP1 positive feedback loop was capable of modulating the biological behaviors of glioma cells, demonstrating that this loop is probably a potential therapeutic target (91). The combination of lncRNA and RBP forms a complex that regulates downstream target gene to contribute to TMZ resistance of glioma. This regulatory model provides a novel insight into the therapeutic strategy for glioma. Thus, targeting lncRNA-regulated angiogenesis, BTB permeability and TMZ resistance of glioma as novel strategies for the treatment of glioma shows potential.

CONCLUSION

Over the previous decades, lncRNA studies have made major progress in the field of glioma research due to the rapid development of bioinformatics, and a series of lncRNAs have been found to act as indispensable factors in the occurrence and progression of glioma. LncRNAs act as ceRNAs in the cytoplasm to regulate glioma progression at the post-transcriptional level or to regulate gene expression through interactions with proteins in the nucleus. However, the mechanisms of most lncRNAs remain unclear. Therefore, the specific mechanisms of lncRNAs need to be further clarified. Glioma continues to be a major challenge to human health, and its advanced aggressiveness, chemoresistance and recurrence are the main factors contributing to the poor prognosis. Theoretically, there are numerous lncRNAs, such as HOTAIR, H19 and NEAT1, that can be applied as diagnostic and prognostic indicators of glioma. It is also possible that many lncRNAs can overcome TMZ resistance, modulate BTB permeability and control glioma angiogenesis, all of which are theoretically effective therapeutic strategies. Regrettably, no successful clinical use of lncRNAs has been achieved yet. In prospective research, lncRNA-centered gene regulatory networks should be constructed to elucidate the regulatory mechanisms of lncRNAs in tumor cells and then used as diagnostic, prognostic, and therapeutic indicators in clinical practice to improve the survival of glioma patients. One of the focuses of basic research is translation to the clinic to improve the survival of patients. Translating basic research into clinical strategies is a long road that will require generations of researchers to eventually understand the full picture of the function of lncRNAs in glioma at both the scientific and clinical levels.

AUTHOR CONTRIBUTIONS

JQ and XM wrote the draft and revised it. JC and CJ designed the tables. All authors contributed to the article and approved the submitted version.

FUNDING

This study was supported by The National Natural Science Foundation of China (No. 81874204, No. 81772666, No. 81972817, No. 82073298, No. 82003022), Excellent Young Talents Project of Central Government Supporting Local University Reform and Development Fund (0202-300011190006), Karolinska Institutet Research Foundation Grants 2020-2021 (No. FS-2020:0007), The Heilongjiang Postdoctoral Science Foundation (LBH-Z18103, LBH-Z19029), and The Research Project of the Health and Family Planning Commission of Heilongjiang Province (2019-102).

REFERENCES

1. Chen Q, Han B, Meng X, Duan C, Yang C, Wu Z, et al. Immunogenomic Analysis Reveals LGALS1 Contributes to the Immune Heterogeneity and Immunosuppression in Glioma. *Int J Cancer* (2019) 145(2):517–30. doi: 10.1002/ijc.32102
2. Lapointe S, Perry A, Butowski NA. Primary Brain Tumours in Adults. *Lancet* (2018) 392(10145):432–46. doi: 10.1016/s0140-6736(18)30990-5
3. Louis DN, Perry A, Reifenberger G, von Deimling A, Figarella-Branger D, Cavenee WK, et al. The 2016 World Health Organization Classification of Tumors of the Central Nervous System: A Summary. *Acta Neuropathol* (2016) 131(6):803–20. doi: 10.1007/s00401-016-1545-1
4. Louis DN, Ohgaki H, Wiestler OD, Cavenee WK, Burger PC, Jouvet A, et al. The 2007 WHO Classification of Tumours of the Central Nervous System. *Acta Neuropathol* (2007) 114(2):97–109. doi: 10.1007/s00401-007-0243-4
5. Yang P, Cai J, Yan W, Zhang W, Wang Y, Chen B, et al. Classification Based on Mutations of TERT Promoter and IDH Characterizes Subtypes in Grade II/III Gliomas. *Neuro Oncol* (2016) 18(8):1099–108. doi: 10.1093/neuonc/now021
6. Han B, Cai J, Gao W, Meng X, Gao F, Wu P, et al. Loss of ATRX Suppresses ATM Dependent DNA Damage Repair by Modulating H3K9me3 to Enhance Temozolomide Sensitivity in Glioma. *Cancer Lett* (2018) 419:280–90. doi: 10.1016/j.canlet.2018.01.056
7. Stupp R, Mason WP, van den Bent MJ, Weller M, Fisher B, Taphoorn MJ, et al. Radiotherapy Plus Concomitant and Adjuvant Temozolomide for Glioblastoma. *N Engl J Med* (2005) 352(10):987–96. doi: 10.1056/NEJMoa043330
8. Van Meir EG, Hadjipanayis CG, Norden AD, Shu HK, Wen PY, Olson JJ. Exciting New Advances in Neuro-Oncology: The Avenue to a Cure for Malignant Glioma. *CA Cancer J Clin* (2010) 60(3):166–93. doi: 10.3322/caac.20069
9. Ulitsky I, Bartel DP. Lincrnas: Genomics, Evolution, and Mechanisms. *Cell* (2013) 154(1):26–46. doi: 10.1016/j.cell.2013.06.020
10. Derrien T, Johnson R, Bussotti G, Tanzer A, Djebali S, Tilgner H, et al. The GENCODE V7 Catalog of Human Long Noncoding RNAs: Analysis of Their Gene Structure, Evolution, and Expression. *Genome Res* (2012) 22(9):1775–89. doi: 10.1101/gr.132159.111
11. Zhang XQ, Leung GK. Long Non-Coding RNAs in Glioma: Functional Roles and Clinical Perspectives. *Neurochem Int* (2014) 77:78–85. doi: 10.1016/j.neuint.2014.05.008
12. Li J, Zhu Y, Wang H, Ji X. Targeting Long Noncoding RNA in Glioma: A Pathway Perspective. *Mol Ther Nucleic Acids* (2018) 13:431–41. doi: 10.1016/j.omtn.2018.09.023
13. Bonasio R, Shiekhattar R. Regulation of Transcription by Long Noncoding Rnas. *Annu Rev Genet* (2014) 48:433–55. doi: 10.1146/annurev-genet-120213-092323
14. Salmena L, Poliseno L, Tay Y, Kats L, Pandolfi PP. A ceRNA Hypothesis: The Rosetta Stone of a Hidden RNA Language? *Cell* (2011) 146(3):353–8. doi: 10.1016/j.cell.2011.07.014
15. Tay Y, Rinn J, Pandolfi PP. The Multilayered Complexity of ceRNA Crosstalk and Competition. *Nature* (2014) 505(7483):344–52. doi: 10.1038/nature12986
16. Liu X, Zhu Q, Guo Y, Xiao Z, Hu L, Xu Q. Lncrna LINC00689 Promotes the Growth, Metastasis and Glycolysis of Glioma Cells by Targeting miR-338-3p/PKM2 Axis. *BioMed Pharmacother* (2019) 117:109069. doi: 10.1016/j.biopha.2019.109069
17. Hu G, Liu N, Wang H, Wang Y, Guo Z. Lncrna LINC01857 Promotes Growth, Migration, and Invasion of Glioma by Modulating miR-1281/TRIM65 Axis. *J Cell Physiol* (2019) 234(12):22009–16. doi: 10.1002/jcp.28763
18. Liao K, Lin Y, Gao W, Xiao Z, Medina R, Dmitriev P, et al. Blocking Lncrna MALAT1/miR-199a/ZHX1 Axis Inhibits Glioblastoma Proliferation and Progression. *Mol Ther Nucleic Acids* (2019) 18:388–99. doi: 10.1016/j.omtn.2019.09.005
19. Chai Y, Xie M. LINC01579 Promotes Cell Proliferation by Acting as a ceRNA of miR-139-5p to Upregulate EIF4G2 Expression in Glioblastoma. *J Cell Physiol* (2019) 234(12):23658–66. doi: 10.1002/jcp.28933

20. Liu L, Shi Y, Shi J, Wang H, Sheng Y, Jiang Q, et al. The Long non-Coding RNA SNHG1 Promotes Glioma Progression by Competitively Binding to miR-194 to Regulate PHLDA1 Expression. *Cell Death Dis* (2019) 10(6):463. doi: 10.1038/s41419-019-1698-7
21. Liu N, Hu G, Wang H, Wang Y, Guo Z. Lncrna BLACAT1 Regulates VASP Expression Via Binding to miR-605-3p and Promotes Giloma Development. *J Cell Physiol* (2019) 234(12):22144–52. doi: 10.1002/jcp.28778
22. Wang J, Zhang M, Lu W. Long Noncoding RNA GACAT3 Promotes Glioma Progression by Sponging Mir-135a. *J Cell Physiol* (2019) 234(7):10877–87. doi: 10.1002/jcp.27946
23. Zhu J, Gu W, Yu C. Matn1-AS1 Promotes Glioma Progression by Functioning as ceRNA of miR-200b/c/429 to Regulate CHD1 Expression. *Cell Prolif* (2020) 53(1):e12700. doi: 10.1111/cpr.12700
24. Chai Y, Wu HT, Liang CD, You CY, Xie MX, Xiao SW. Exosomal Lncrna ROR1-AS1 Derived From Tumor Cells Promotes Glioma Progression Via Regulating Mir-4686. *Int J Nanomed* (2020) 15:8863–72. doi: 10.2147/IJN.S271795
25. Cheng Z, Wang G, Zhu W, Luo C, Guo Z. Lef1-AS1 Accelerates Tumorigenesis in Glioma by Sponging miR-489-3p to Enhance HIGD1A. *Cell Death Dis* (2020) 11(8):690. doi: 10.1038/s41419-020-02823-0
26. Gao YF, Liu JY, Mao XY, He ZW, Zhu T, Wang ZB, et al. Lncrna FOXD1-AS1 Acts as a Potential Oncogenic Biomarker in Glioma. *CNS Neurosci Ther* (2020) 26(1):66–75. doi: 10.1111/cns.13152
27. Zhen Y, Nan Y, Guo S, Zhang L, Li G, Yue S, et al. Knockdown of NEAT1 Repressed the Malignant Progression of Glioma Through Sponging miR-107 and Inhibiting CDK14. *J Cell Physiol* (2019) 234(7):10671–9. doi: 10.1002/jcp.27727
28. Ren S, Xu Y. Ac016405.3, a Novel Long Noncoding RNA, Acts as a Tumor Suppressor Through Modulation of TET2 by microRNA-19a-5p Sponging in Glioblastoma. *Cancer Sci* (2019) 110(5):1621–32. doi: 10.1111/cas.14002
29. Jia L, Song Y, Mu L, Li Q, Tang J, Yang Z, et al. Long Noncoding RNA Tpt1-AS1 Downregulates the microRNA-770-5p Expression to Inhibit Glioma Cell Autophagy and Promote Proliferation Through STMN1 Upregulation. *J Cell Physiol* (2020) 235(4):3679–89. doi: 10.1002/jcp.29262
30. Huang L, Li X, Ye H, Liu Y, Liang X, Yang C, et al. Long non-Coding RNA Nck1-AS1 Promotes the Tumorigenesis of Glioma Through Sponging microRNA-138-2-3p and Activating the TRIM24/Wnt/beta-Catenin Axis. *J Exp Clin Cancer Res* (2020) 39(1):63. doi: 10.1186/s13046-020-01567-1
31. Zheng Y, Lu S, Xu Y, Zheng J. Long non-Coding RNA Agap2-AS1 Promotes the Proliferation of Glioma Cells by Sponging miR-15a/b-5p to Upregulate the Expression of HDGF and Activating Wnt/beta-catenin Signaling Pathway. *Int J Biol Macromol* (2019) 128:521–30. doi: 10.1016/j.ijbiomac.2019.01.121
32. Zhou XY, Liu H, Ding ZB, Xi HP, Wang GW. LncRNA SNHG16 Promotes Glioma Tumorigenicity Through miR-373/EGFR Axis by Activating PI3K/AKT Pathway. *Genomics* (2020) 112(1):1021–9. doi: 10.1016/j.ygeno.2019.06.017
33. Han M, Wang S, Fritah S, Wang X, Zhou W, Yang N, et al. Interfering With Long Non-Coding RNA MIR22HG Processing Inhibits Glioblastoma Progression Through Suppression of Wnt/beta-catenin Signalling. *Brain* (2020) 143(2):512–30. doi: 10.1093/brain/awz406
34. Gong X, Liao X, Huang M. Lncrna CASC7 Inhibits the Progression of Glioma Via Regulating Wnt/beta-Catenin Signaling Pathway. *Pathol Res Pract* (2019) 215(3):564–70. doi: 10.1016/j.prp.2019.01.018
35. Wei L, Yi Z, Guo K, Long X. Long Noncoding RNA BCAR4 Promotes Glioma Cell Proliferation Via EGFR/PI3K/AKT Signaling Pathway. *J Cell Physiol* (2019) 234(12):23608–17. doi: 10.1002/jcp.28929
36. Zhang X, Niu W, Mu M, Hu S, Niu C. Long non-Coding RNA Lpp-AS2 Promotes Glioma Tumorigenesis Via miR-7-5p/EGFR/PI3K/AKT/c-MYC Feedback Loop. *J Exp Clin Cancer Res* (2020) 39(1):196. doi: 10.1186/s13046-020-01695-8
37. Mu M, Niu W, Zhang X, Hu S, Niu C. Lncrna BCYRN1 Inhibits Glioma Tumorigenesis by Competitively Binding With miR-619-5p to Regulate CUEDC2 Expression and the PTEN/AKT/p21 Pathway. *Oncogene* (2020) 39(45):6879–92. doi: 10.1038/s41388-020-01466-x
38. Zhang Y, Sui R, Chen Y, Liang H, Shi J, Piao H. Long Noncoding RNA MT1JP Inhibits Proliferation, Invasion, and Migration While Promoting Apoptosis of Glioma Cells Through the Activation of PTEN/Akt Signaling Pathway. *J Cell Physiol* (2019) 234(11):19553–64. doi: 10.1002/jcp.28553
39. Xue J, Zhong S, Sun BM, Sun QF, Hu LY, Pan SJ. Lnc-THOR Silencing Inhibits Human Glioma Cell Survival by Activating MAGEA6-AMPK Signaling. *Cell Death Dis* (2019) 10(11):866. doi: 10.1038/s41419-019-2093-0
40. Han B, Meng X, Wu P, Li Z, Li S, Zhang Y, et al. ATRX/EZH2 Complex Epigenetically Regulates FADD/PARP1 Axis, Contributing to TMZ Resistance in Glioma. *Theranostics* (2020) 10(7):3351–65. doi: 10.7150/thno.41219
41. Chen Q, Cai J, Wang Q, Wang Y, Liu M, Yang J, et al. Long Noncoding Rna NEAT1, Regulated by the EGFR Pathway, Contributes to Glioblastoma Progression Through the WNT/beta-Catenin Pathway by Scaffolding Ezh2. *Clin Cancer Res* (2018) 24(3):684–95. doi: 10.1158/1078-0432.CCR-17-0605
42. Zhang F, Ruan X, Ma J, Liu X, Zheng J, Liu Y, et al. Dgcr8/Zfat-As1 Promotes Cdx2 Transcription in a PRC2 Complex-Dependent Manner to Facilitate the Malignant Biological Behavior of Glioma Cells. *Mol Ther* (2020) 28(2):613–30. doi: 10.1016/j.ymthe.2019.11.015
43. Li H, Xue Y, Ma J, Shao L, Wang D, Zheng J, et al. SNHG1 Promotes Malignant Biological Behaviors of Glioma Cells Via Microrna-154-5p/Mir-376b-3p- FOXP2- KDM5B Participating Positive Feedback Loop. *J Exp Clin Cancer Res* (2019) 38(1):59. doi: 10.1186/s13046-019-1063-9
44. Yu L, Gui S, Liu Y, Qiu X, Qiu B, Zhang X, et al. Long Intergenic non-Protein Coding RNA 00475 Silencing Acts as a Tumor Suppressor in Glioma Under Hypoxic Condition by Impairing Microrna-449b-5p-Dependent AGAP2 Up-Regulation. *Ther Adv Med Oncol* (2020) 12:1758835920940936. doi: 10.1177/1758835920940936
45. Bao MH, Lv QL, Szeto V, Wong R, Zhu SZ, Zhang YY, et al. Trpm2-AS Inhibits the Growth, Migration, and Invasion of Gliomas Through JNK, c-Jun, and RGS4. *J Cell Physiol* (2020) 235(5):4594–604. doi: 10.1002/jcp.29336
46. Chen Y, Bao C, Zhang X, Lin X, Huang H, Wang Z. Long non-Coding RNA HCG11 Modulates Glioma Progression Through Cooperating With miR-496/CPEB3 Axis. *Cell Prolif* (2019) 52(5):e12615. doi: 10.1111/cpr.12615
47. Gao Y, Xu Y, Wang J, Yang X, Wen L, Feng J. Lncrna MNX1-AS1 Promotes Glioblastoma Progression Through Inhibition of Mir-4443. *Oncol Res* (2019) 27(3):341–7. doi: 10.3727/096504018X15228909735079
48. Wu DM, Wang S, Wen X, Han XR, Wang YJ, Fan SH, et al. Long Noncoding RNA Nuclear Enriched Abundant Transcript 1 Impacts Cell Proliferation, Invasion, and Migration of Glioma Through Regulating miR-139-5p/ Cdk6. *J Cell Physiol* (2019) 234(5):5972–87. doi: 10.1002/jcp.27093
49. Tan SK, Pastori C, Penas C, Komotar RJ, Ivan ME, Wahlestedt C, et al. Serum Long Noncoding RNA HOTAIR as a Novel Diagnostic and Prognostic Biomarker in Glioblastoma Multiforme. *Mol Cancer* (2018) 17(1):74. doi: 10.1186/s12943-018-0822-0
50. Lin JZ, Lin N, Zhao WJ. Identification and Validation of a six-lncRNA Prognostic Signature With its ceRNA Networks and Candidate Drugs in Lower-Grade Gliomas. *Genomics* (2020) 112(5):2990–3002. doi: 10.1016/j.ygeno.2020.05.016
51. Li J, Liao T, Liu H, Yuan H, Ouyang T, Wang J, et al. Hypoxic Glioma Stem Cell-Derived Exosomes Containing LINC01060 Promote Progression of Glioma by Regulating the MZF1/C-Myc/HIF-1alpha. *Cancer Res* (2021) 81(1):114–28. doi: 10.1158/0008-5472
52. Liu C, Peng Z, Li P, Fu H, Feng J, Zhang Y, et al. Lncrna RMST Suppressed GBM Cell Mitophagy Through Enhancing FUS Sumoylation. *Mol Ther Nucleic Acids* (2020) 19:1198–208. doi: 10.1016/j.omtn.2020.01.008
53. Xia H, Liu Y, Wang Z, Zhang W, Qi M, Qi B, et al. Long Noncoding Rna HOTAIRM1 Maintains Tumorigenicity of Glioblastoma Stem-Like Cells Through Regulation of HOX Gene Expression. *Neurotherapeutics* (2020) 17(2):754–64. doi: 10.1007/s13311-019-00799-0
54. Tang J, Yu B, Li Y, Zhang W, Alvarez AA, Hu B, et al. TGF-Beta-Activated Lncrna LINC00115 Is a Critical Regulator of Glioma Stem-Like Cell Tumorigenicity. *EMBO Rep* (2019) 20(12):e48170. doi: 10.15252/embr.201948170
55. Shi J, Zhang Y, Qin B, Wang Y, Zhu X. Long Non-Coding RNA LINC00174 Promotes Glycolysis and Tumor Progression by Regulating miR-152-3p/SLC2A1 Axis in Glioma. *J Exp Clin Cancer Res* (2019) 38(1):395. doi: 10.1186/s13046-019-1390-x
56. Pan JX, Chen TN, Ma K, Wang S, Yang CY, Cui GY. A Negative Feedback Loop of H19/miR-675/VDR Mediates Therapeutic Effect of Cucurmin in the Treatment of Glioma. *J Cell Physiol* (2020) 235(3):2171–82. doi: 10.1002/jcp.29127
57. Li C, Zheng H, Hou W, Bao H, Xiong J, Che W, et al. Long Non-Coding RNA LINC00645 Promotes TGF-Beta-Induced Epithelial-Mesenchymal Transition by Regulating miR-205-3p-ZEB1 Axis in Glioma. *Cell Death Dis* (2019) 10(10):717. doi: 10.1038/s41419-019-1948-8

58. Tang C, Wang Y, Zhang L, Wang J, Wang W, Han X, et al. Identification of Novel LncRNA Targeting Smad2/PKCalpha Signal Pathway to Negatively Regulate Malignant Progression of Glioblastoma. *J Cell Physiol* (2020) 235 (4):3835–48. doi: 10.1002/jcp.29278
59. Vogelbaum MA. Targeted Therapies for Brain Tumors: Will They Ever Deliver? *Clin Cancer Res* (2018) 24(16):3790–1. doi: 10.1158/1078-0432.CCR-18-0855
60. Wang X, Sun N, Meng X, Chen M, Jiang C, Cai J. Review of Clinical Nerve Repair Strategies for Neurorestoration of Central Nervous System Tumor Damage. *J Neurorestoratol* (2020) 8(3):172–81. doi: 10.26599/jnr.2020.9040018
61. Huang H, Chen L, Mao G, Sharma HS. Clinical Neurorestorative Cell Therapies: Developmental Process, Current State and Future Prospective. *J Neurorestoratol* (2020) 8(2):61–82. doi: 10.26599/jnr.2020.9040009
62. Sa L, Li Y, Zhao L, Liu Y, Wang P, Liu L, et al. The Role of HOTAIR/miR-148b-3p/USF1 on Regulating the Permeability of BTB. *Front Mol Neurosci* (2017) 10:194. doi: 10.3389/fnmol.2017.00194
63. He J, Xue Y, Wang Q, Zhou X, Liu L, Zhang T, et al. Long non-Coding RNA MIAT Regulates Blood Tumor Barrier Permeability by Functioning as a Competing Endogenous RNA. *Cell Death Dis* (2020) 11(10):936. doi: 10.1038/s41419-020-03134-0
64. Liu X, Wu P, Su R, Xue Y, Yang C, Wang D, et al. IGF2BP2 Stabilized FBXL19-AS1 Regulates the Blood-Tumour Barrier Permeability by Negatively Regulating ZNF765 by STAU1-mediated mRNA Decay. *RNA Biol* (2020) 17 (12):1777–88. doi: 10.1080/15476286.2020.1795583
65. Zhang C, Zhang X, Wang J, Di F, Xue Y, Lin X, et al. Lnc00462717 Regulates the Permeability of the Blood-Brain Tumor Barrier Through Interaction With PTBP1 to Inhibit the miR-186-5p/Occludin Signaling Pathway. *FASEB J* (2020) 34(8):9941–58. doi: 10.1096/fj.202000045R
66. Guo J, Shen S, Liu X, Ruan X, Zheng J, Liu Y, et al. Role of LINC00174/miR-138-5p (Mir-150-5p)/FOSL2 Feedback Loop on Regulating the Blood-Tumor Barrier Permeability. *Mol Ther Nucleic Acids* (2019) 18:1072–90. doi: 10.1016/j.omtn.2019.10.031
67. Karachi A, Dastmalchi F, Mitchell DA, Rahman M. Temozolomide for Immunomodulation in the Treatment of Glioblastoma. *Neuro Oncol* (2018) 20(12):1566–72. doi: 10.1093/neuonc/noy072
68. Zhang J, Stevens MF, Bradshaw TD. Temozolomide: Mechanisms of Action, Repair and Resistance. *Curr Mol Pharmacol* (2012) 5(1):102–14. doi: 10.2174/1874467211205010102
69. Banerjee A, Vest KE, Pavlath GK, Corbett AH. Nuclear Poly(a) Binding Protein 1 (PABPN1) and Matrin3 Interact in Muscle Cells and Regulate RNA Processing. *Nucleic Acids Res* (2017) 45(18):10706–25. doi: 10.1093/nar/gkx786
70. Wu P, Cai J, Chen Q, Han B, Meng X, Li Y, et al. Lnc-TALC Promotes O(6)-Methylguanine-DNA Methyltransferase Expression Via Regulating the c-Met Pathway by Competitively Binding With Mir-20b-3p. *Nat Commun* (2019) 10 (1):2045. doi: 10.1038/s41467-019-10025-2
71. Sun XH, Fan WJ, An ZJ, Sun Y. Inhibition of Long Noncoding RNA Crnde Increases Chemosensitivity of Medulloblastoma Cells by Targeting Mir-29c-3p. *Oncol Res* (2020) 28(1):95–102. doi: 10.3727/096504019X15742472027401
72. Li Z, Zhang J, Zheng H, Li C, Xiong J, Wang W, et al. Modulating Lncrna SNHG15/CDK6/miR-627 Circuit by Palbociclib, Overcomes Temozolomide Resistance and Reduces M2-Polarization of Glioma Associated Microglia in Glioblastoma Multiforme. *J Exp Clin Cancer Res* (2019) 38(1):380. doi: 10.1186/s13046-019-1371-0
73. Voce DJ, Bernal GM, Wu L, Crawley CD, Zhang W, Mansour NM, et al. Temozolomide Treatment Induces Lncrna MALAT1 in an NF-kappaB and P53 Codependent Manner in Glioblastoma. *Cancer Res* (2019) 79(10):2536–48. doi: 10.1158/0008-5472.CAN-18-2170
74. Zhang Z, Yin J, Lu C, Wei Y, Zeng A, You Y. Exosomal Transfer of Long Non-Coding RNA Sbf2-AS1 Enhances Chemoresistance to Temozolomide in Glioblastoma. *J Exp Clin Cancer Res* (2019) 38(1):166. doi: 10.1186/s13046-019-1139-6
75. Xu N, Liu B, Lian C, Doycheva DM, Fu Z, Liu Y, et al. Long Noncoding RNA AC003092.1 Promotes Temozolomide Chemosensitivity Through miR-195/TFPI-2 Signaling Modulation in Glioblastoma. *Cell Death Dis* (2018) 9 (12):1139. doi: 10.1038/s41419-018-1183-8
76. Liao Y, Shen L, Zhao H, Liu Q, Fu J, Guo Y, et al. Lncrna CASC2 Interacts With miR-181a to Modulate Glioma Growth and Resistance to TMZ Through PTEN Pathway. *J Cell Biochem* (2017) 118(7):1889–99. doi: 10.1002/jcb.25910
77. Lu C, Wei Y, Wang X, Zhang Z, Yin J, Li W, et al. DNA-Methylation-Mediated Activating of Lncrna SNHG12 Promotes Temozolomide Resistance in Glioblastoma. *Mol Cancer* (2020) 19(1):28. doi: 10.1186/s12943-020-1137-5
78. Liu B, Zhou J, Wang C, Chi Y, Wei Q, Fu Z, et al. Lncrna SOX2OT Promotes Temozolomide Resistance by Elevating SOX2 Expression Via ALKBH5-mediated Epigenetic Regulation in Glioblastoma. *Cell Death Dis* (2020) 11 (5):384. doi: 10.1038/s41419-020-2540-y
79. Zheng J, Wang B, Zheng R, Zhang J, Huang C, Zheng R, et al. Linc-RA1 Inhibits Autophagy and Promotes Radioresistance by Preventing H2Bub1/USP44 Combination in Glioma Cells. *Cell Death Dis* (2020) 11(9):758. doi: 10.1038/s41419-020-02977-x
80. Chen Z, Li S, Shen L, Wei X, Zhu H, Wang X, et al. NF-Kappa B Interacting Long Noncoding RNA Enhances the Warburg Effect and Angiogenesis and Is Associated With Decreased Survival of Patients With Gliomas. *Cell Death Dis* (2020) 11(5):323. doi: 10.1038/s41419-020-2520-2
81. Yang C, Zheng J, Liu X, Xue Y, He Q, Dong Y, et al. Role of ANKHD1/LINC00346/ZNF655 Feedback Loop in Regulating the Glioma Angiogenesis Via Staufen1-Mediated mRNA Decay. *Mol Ther Nucleic Acids* (2020) 20:866–78. doi: 10.1016/j.omtn.2020.05.004
82. Wang D, Zheng J, Liu X, Xue Y, Liu L, Ma J, et al. Knockdown of USF1 Inhibits the Vasculogenic Mimicry of Glioma Cells Via Stimulating Snhg16/miR-212-3p and LINC00667/miR-429 Axis. *Mol Ther Nucleic Acids* (2019) 14:465–82. doi: 10.1016/j.omtn.2018.12.017
83. Xu H, Zhao G, Zhang Y, Jiang H, Wang W, Zhao D, et al. Long Non-Coding RNA Paxip1-AS1 Facilitates Cell Invasion and Angiogenesis of Glioma by Recruiting Transcription Factor ETS1 to Upregulate KIF14 Expression. *J Exp Clin Cancer Res* (2019) 38(1):486. doi: 10.1186/s13046-019-1474-7
84. Li X, Xue Y, Liu X, Zheng J, Shen S, Yang C, et al. Zranb2/Snhg20/Foxk1 Axis Regulates Vasculogenic Mimicry Formation in Glioma. *J Exp Clin Cancer Res* (2019) 38(1):68. doi: 10.1186/s13046-019-1073-7
85. Lu J, Liu X, Zheng J, Song J, Liu Y, Ruan X, et al. Lin28A Promotes IRF6-Regulated Aerobic Glycolysis in Glioma Cells by Stabilizing SNHG14. *Cell Death Dis* (2020) 11(6):447. doi: 10.1038/s41419-020-2650-6
86. Ruan X, Zheng J, Liu X, Liu Y, Liu L, Ma J, et al. Lncrna LINC00665 Stabilized by TAF15 Impeded the Malignant Biological Behaviors of Glioma Cells Via STAU1-Mediated mRNA Degradation. *Mol Ther Nucleic Acids* (2020) 20:823–40. doi: 10.1016/j.omtn.2020.05.003
87. Su R, Ma J, Zheng J, Liu X, Liu Y, Ruan X, et al. PABPC1-Induced Stabilization of BDNF-AS Inhibits Malignant Progression of Glioblastoma Cells Through STAU1-Mediated Decay. *Cell Death Dis* (2020) 11(2):81. doi: 10.1038/s41419-020-2267-9
88. Wang S, Qi Y, Gao X, Qiu W, Liu Q, Guo X, et al. Hypoxia-Induced Lncrna PDIA3P1 Promotes Mesenchymal Transition Via Sponging of miR-124-3p in Glioma. *Cell Death Dis* (2020) 11(3):168. doi: 10.1038/s41419-020-2345-z
89. Zhang M-B, Song C-C, Li G-Z, Chen L-F, Ma R, Yu X-H, et al. Transplantation of Umbilical Cord Blood Mononuclear Cells Attenuates the Expression of IL-1β Via the TLR4/NF-κb Pathway in Hypoxic-Ischemic Neonatal Rats. *J Neurorestoratol* (2020) 8(2):122–30. doi: 10.26599/jnr.2020.9040015
90. Ji J, Xu R, Ding K, Bao G, Zhang X, Huang B, et al. Long Noncoding Rna SChLAP1 Forms a Growth-Promoting Complex With HNRNPL in Human Glioblastoma Through Stabilization of ACTN4 and Activation of NF-kappaB Signaling. *Clin Cancer Res* (2019) 25(22):6868–81. doi: 10.1158/1078-0432.CCR-19-0747
91. Shao L, He Q, Liu Y, Liu X, Zheng J, Ma J, et al. UPF1 Regulates the Malignant Biological Behaviors of Glioblastoma Cells Via Enhancing the Stability of LINC-00313. *Cell Death Dis* (2019) 10(9):629. doi: 10.1038/s41419-019-1845-1

Conflict of Interest: The authors declare that the research was conducted in the absence of any commercial or financial relationships that could be construed as a potential conflict of interest.

frontiers in Oncology

ORIGINAL RESEARCH
published: 11 June 2021
doi: 10.3389/fonc.2021.692097

Epidemiology and Survival of Patients With Brainstem Gliomas: A Population-Based Study Using the SEER Database

Huanbing Liu[1†], *Xiaowei Qin*[1†], *Liyan Zhao*[2], *Gang Zhao*[1*] *and Yubo Wang*[1*]

[1] Department of Neurosurgery, First Hospital of Jilin University, Changchun, China, [2] Department of Clinical Laboratory, Second Hospital of Jilin University, Changchun, China

OPEN ACCESS

Edited by:
Yaohua Liu,
Shanghai First People's Hospital, China

Reviewed by:
Kristin Schroeder,
Duke Cancer Institute, United States
Gerardo Caruso,
University Hospital of Policlinico G. Martino, Italy

***Correspondence:**
Gang Zhao
gzhao@jlu.edu.cn
Yubo Wang
wangyubo@jlu.edu.cn

[†]These authors have contributed equally to this work and share first authorship

Specialty section:
This article was submitted to Neuro-Oncology and Neurosurgical Oncology, a section of the journal Frontiers in Oncology

Received: 07 April 2021
Accepted: 26 May 2021
Published: 11 June 2021

Citation:
Liu H, Qin X, Zhao L, Zhao G and Wang Y (2021) Epidemiology and Survival of Patients With Brainstem Gliomas: A Population-Based Study Using the SEER Database. Front. Oncol. 11:692097. doi: 10.3389/fonc.2021.692097

Background: Brainstem glioma is a primary glial tumor that arises from the midbrain, pons, and medulla. The objective of this study was to determine the population-based epidemiology, incidence, and outcomes of brainstem gliomas.

Methods: The data pertaining to patients with brainstem gliomas diagnosed between 2004 and 2016 were extracted from the SEER database. Descriptive analyses were conducted to evaluate the distribution and tumor-related characteristics of patients with brainstem gliomas. The possible prognostic indicators were analyzed by Kaplan-Meier curves and a Cox proportional hazards model.

Results: The age-adjusted incidence rate was 0.311 cases per 100,000 person-years between 2004 and 2016. A total of 3387 cases of brainstem gliomas were included in our study. Most of the patients were white and diagnosed at 5-9 years of age. The most common diagnosis confirmed by histological review was ependymoma/anaplastic ependymoma. The median survival time was 24 months. Patients with tumors less than 3 cm in size had a better prognosis. Surgery was effective at improving overall survival. There was no evidence that radiotherapy and chemotherapy improved overall survival.

Conclusion: Brainstem gliomas can be diagnosed at any age. Ependymoma/anaplastic ependymoma is the most common pathological diagnosis. The prognosis is poor, and timely diagnosis and surgery are effective at improving the prognosis. We suggest that more attention should be given to the treatment of patients with brainstem gliomas.

Keywords: brainstem glioma, epidemiology, survival, SEER Program, CNS disease

INTRODUCTION

Gliomas are primary brain tumors that are thought to arise from neuroglial stem or progenitor cells (1). Gliomas are the most common malignant primary brain tumor, and 4.3% of gliomas are localized at the brainstem (2). Brainstem glioma is a primary glial tumor that arises from the midbrain, pons, and medulla. In most instances, the term refers to a highly aggressive tumor of the pons (3). Diffuse intrinsic pontine glioma has been reported to account for ~75% of brain stem

tumors in children (2). Because of poor survival, brainstem glioma has been a main research focus for decades (4).

The Surveillance, Epidemiology, and End Results (SEER) program of the National Cancer Institute represents approximately 35% of the US population (based on the 2000 census) (5). Our goal is to use SEER data to analyze the epidemiology and survival of patients with brainstem gliomas in the United States.

METHODS

Data Extraction and Incidence Rates

The data from SEER are available to the public for research purposes. Therefore, ethics committee approval and informed consent were not necessary to perform the analyses. Patients with a diagnosis of primary brainstem gliomas were included. The term glioma was defined by setting the variable "Histology recode - broad groupings" as "9380-9489: gliomas". Brainstem gliomas were defined by setting the variable "Primary Site - labeled" as "C71.7-Brainstem". The research period was set from 2004 to 2016. Age-adjusted incidence rates (directly standardized to the 2000 US standard population) between 2004 and 2016 were retrieved from the SEER 18 database (November 2019 submission) (6). The detailed patient data were obtained from SEER 18 Regs Custom Data (November 2018 submission) (7). All the data were obtained by using the SEER*Stat 8.3.8 program.

Variables and Population Analysis

The demographic and clinical features included age at diagnosis (0-19 years, ≥20 years), sex (Male, Female), race (White, Black, Asian or Pacific Islander, American Indian/Alaska Native, Unknown), Purchased/Referred Care Delivery Area (PRCDA) Region (Alaska, eastern region, north plains, Pacific coast, southwestern region), tumor size (≤3 cm, >3 cm and Unknown), diagnostic confirmation (positive microscopic confirm, others), behavior code (benign, borderline malignancy, malignant) according to the International Classification of Diseases for Oncology 3 (ICD-O-3), surgery (Yes, None/Unknown), radiation therapy (Yes, None/Unknown), chemotherapy (Yes, None/Unknown), survival months and vital status. The pathology types (according to the code of "Histology recode - Brain groupings") of the patients diagnosed with positive microscopic confirmation were analyzed. Descriptive analyses were conducted to evaluate the distribution and tumor-related characteristics of patients with brainstem gliomas. Bar graphs and pie charts were also used to further describe the distribution of patients.

Survival Analysis

The Kaplan-Meier method was used to estimate overall survival (OS) at 1, 3, 5, and 10 years. Survival time was defined as the time from diagnosis to death from any cause. We also used this method to estimate the OS in different groups. The differences between the curves were analyzed by the log-rank test. Univariate and multivariate Cox proportional hazard models were performed to estimate the hazard ratios (HRs) and 95% confidence intervals (CIs) to analyze the independent prognostic factors associated with OS in patients with brainstem gliomas, and statistical significance was defined as $p < 0.05$. All the data were analyzed by IBM SPSS Statistics 25 software (IBM Corporation, Armonk, New York, USA).

RESULTS

Population Analysis

The age-adjusted incidence rate was 0.311 cases per 100,000 person-years between 2004 and 2016. A total of 3387 cases of brainstem gliomas were indexed between 2004 and 2016. The demographic and clinical characteristics of the patients are shown in **Table 1**. There were 1535 female patients (45.3%) and 1852 male patients (54.7%). The median age was 18 years (range 0 to 103 years). The majority of patients were diagnosed when they were between 5 and 9 years old, and the distribution of patient age at diagnosis is shown in a histogram (**Figure 1**). Children and adolescents (0-19 years old) accounted for 34.3% of all patients. White patients accounted for 80.2% of all patients (**Figure 2**). Most of the patients were from the Pacific coast (n=1740, 51.4%) and eastern region (n=1187, 35.0%). According to ICD-0-3, most of the tumors were malignant (n=3040, 89.8%). Among this cohort, 2023 cases were diagnosed with positive microscopic confirmation. We analyzed pathology type among these patients, and the results are shown in a pie chart (**Figure 3**). We found that ependymoma/anaplastic ependymoma (n=438, 21.7%) and pilocytic astrocytoma (n=377, 18.6%) were the most common pathology types. A total of 37.2% of the tumors were less than 3 cm in size, and 33.5% of the tumors were larger than 3 cm. Radiation was the first choice of therapy for patients with brainstem gliomas. Surgery was performed in 1479 (43.7%) cases, radiation therapy was performed in 1746 (51.6%) cases, and chemotherapy was performed in 1166 (34.4%) cases. The median survival time was 24 months (range 0 to 155 months). At the time of data collection, 1931 (57.0%) patients were alive, and 1456 (43.0%) were deceased.

Survival Analysis

The OS rates at 1, 3, 5 and 10 years after diagnosis were 70.8%, 56.3%, 53.3% and 48.8%, respectively. A Kaplan-Meier curve was created to show the OS for the full cohort (**Figure 4A**). The Kaplan-Meier log-rank test indicated that the variables age at diagnosis (**Figure 4B**), race (**Figure 4C**), tumor size (**Figure 4D**), behavior (**Figure 4E**), surgery (**Figure 4F**), radiation (**Figure 4G**) and chemotherapy (**Figure 4H**) were possibly related to OS. The results of multivariate Cox proportional hazard regression analysis showed that race, age and sex were not independent prognostic factors. Patients with tumors less than 3 cm in size or benign or borderline tumors had a better prognosis. The results also showed that surgery was effective for improving prognosis, but radiation and chemotherapy did not help patients obtain a better prognosis. The results generated by the log-rank test and univariate and multivariate Cox proportional hazard models are listed in **Table 2**.

TABLE 1 | Demographic and clinical characteristics of patients with brainstem gliomas.

Variables	Number	%
Sex		
Female	1535	45.3
Male	1852	54.7
Age at diagnosis (years)		
Mean±SD	26.86±23.244	
Median	18.00	
Range	0-103	
0-19	1161	34.3
≥20	2226	65.7
Race		
White	2715	80.2
Others	672	19.8
PRCDA Region		
Alaska	6	0.2
East	1187	35.0
North plains	258	7.6
Pacific coast	1740	51.4
Southwest	196	5.8
Tumor Size		
≤3cm	1259	37.2
>3cm	1134	33.5
Unknown	994	29.3
Diagnostic confirmation		
Positive microscopic confirm	2023	59.7
Others	1364	40.3
Behavior code		
Benign	113	3.3
Borderline malignancy	234	6.9
Malignant	3040	89.8
Surgery		
Yes	1479	43.7
None/Unknown	1908	56.3
Radiation		
Yes	1746	51.6
None/Unknown	1641	48.4
Chemotherapy		
Yes	1166	34.4
None/Unknown	2221	65.6
Survival months		
Mean±SD	44.22±44.404	
Median	24.00	
Range	0-155	
Vital status		
Alive	1931	57.0
Dead	1456	43.0

DISCUSSION

Brainstem glioma is a primary glial tumor that arises within the brainstem and is believed to be a heterogeneous group of gliomas. Some authors divided brainstem gliomas into 2 categories. Twenty percent are considered to be focal low-grade lesions with good prognosis, and the remaining 80% of tumors arise in and occupy the majority of the pons and are diffuse in nature and associated with poor prognosis (8–10). We could not define whether the tumor originated from the midbrain, medulla, or pons, and we also could not define whether the tumor was focal or diffuse based on the data available in the SEER database. Some authors have conducted cohort studies with data on high-grade glioma (11, 12) or low-grade glioma (13) based on the SEER database. Brainstem glioma is a relative rare lesion, and previous reports have included limited numbers of cases. We believe that this limitation might prevent us from obtaining a better understanding of the general characteristics of the patients diagnosed with brainstem glioma. The SEER program represents approximately 35% of the US population, and the data were collected from most parts of the United States (5). To better understand brainstem glioma, we conducted this large-scale cohort study including 3387 cases. To the best of our knowledge, this is the largest brainstem glioma cohort to date. We believe our report can explain the epidemiology and survival of patients with brainstem gliomas in the United States to some extent.

First, we wanted to conduct an analysis of cancer-specific survival. However, because the brainstem glioma was not the first malignant tumor in some patients, cancer-specific survival was not applicable for approximately 10% of the cohort. Progression-free survival cannot be adopted because we cannot obtain data about progression from the SEER database. To include all of the data and make the analysis accurate, we chose to analyze OS. The World Health Organization (WHO) grade classification is widely used by neuro-oncology doctors, but half of the tumors were not clearly classified according to WHO grade. Therefore, we chose the behavior code according to ICD-O-3; in our cohort, more than 80% of the tumors were malignant, which is in agreement with a previous study (3).

According to the report from The Central Brain Tumor Registry of the United States (14), in children and adolescents, brainstem tumors account for 10.8% of all primary central nervous system tumors. Brainstem gliomas were also reported to account for up to 20% or more of primary brain tumors (15). In our cohort, the highest incidence was found in individuals between 5 and 9 years old, and the median age at diagnosis was 18 years old. However, we found that brainstem gliomas could be diagnosed at every age. Children and adolescents (0-19 years old) accounted for 34.3% of all patients, and more than half of the patients were adults. The predominance of white patients was also very significant in our study, which is consistent with the findings of other cohort studies of gliomas based on the SEER program (13, 16). Males and females are almost equally affected. We have also analyzed the pathological classification of the tumors in these patients, with the intention of providing information that could be useful when biopsy or surgery cannot be performed but a treatment needs to be selected. According to a previous report, diffuse intrinsic tumors account for approximately 80% of all brainstem gliomas. These tumors are generally high-grade anaplastic astrocytoma (WHO grade 3), glioblastoma multiforme (WHO grade 4), or occasionally well-differentiated diffuse astrocytoma (WHO grade 2) (17). However, in our cohort, we found that the most common pathology type was ependymoma/anaplastic ependymoma and pilocytic astrocytoma. Glioblastoma accounted for only 9% of all cases with positive histology. Because the anatomical location of the tumor precludes surgery, radiation is the standard therapy for patients with diffuse intrinsic tumors (17), and tumor resection or biopsy is

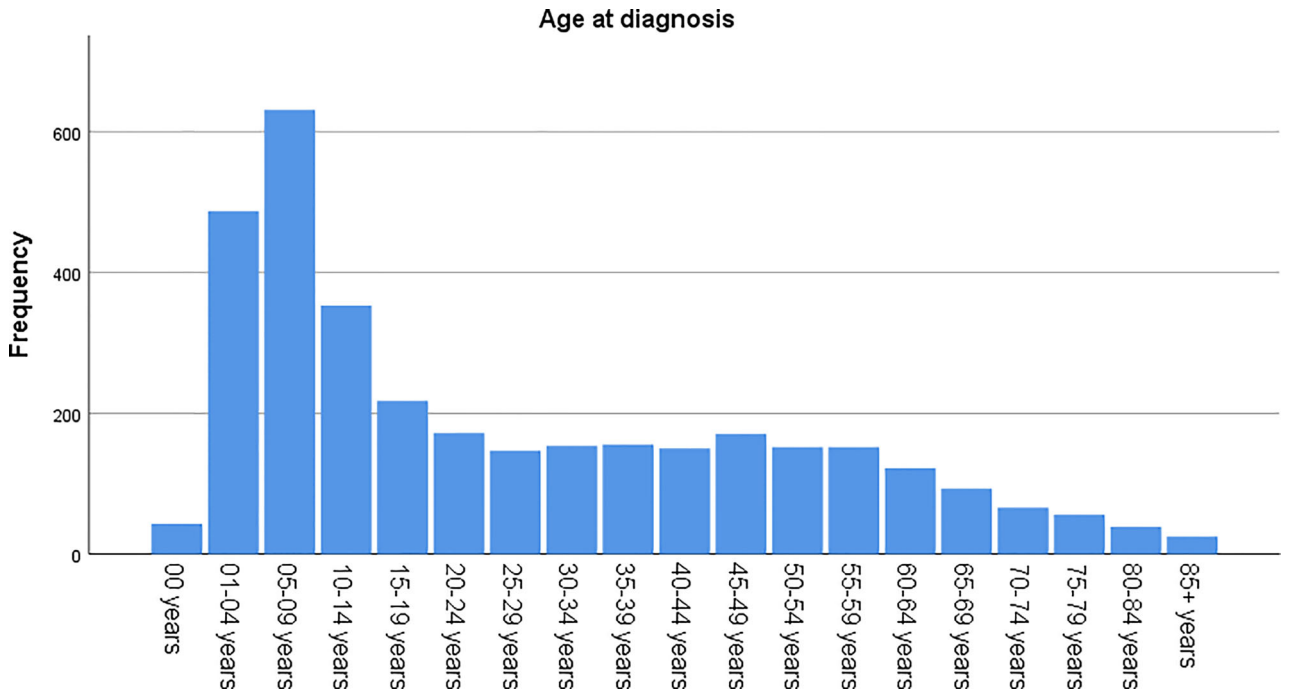

FIGURE 1 | Age distribution of the patients at diagnosis.

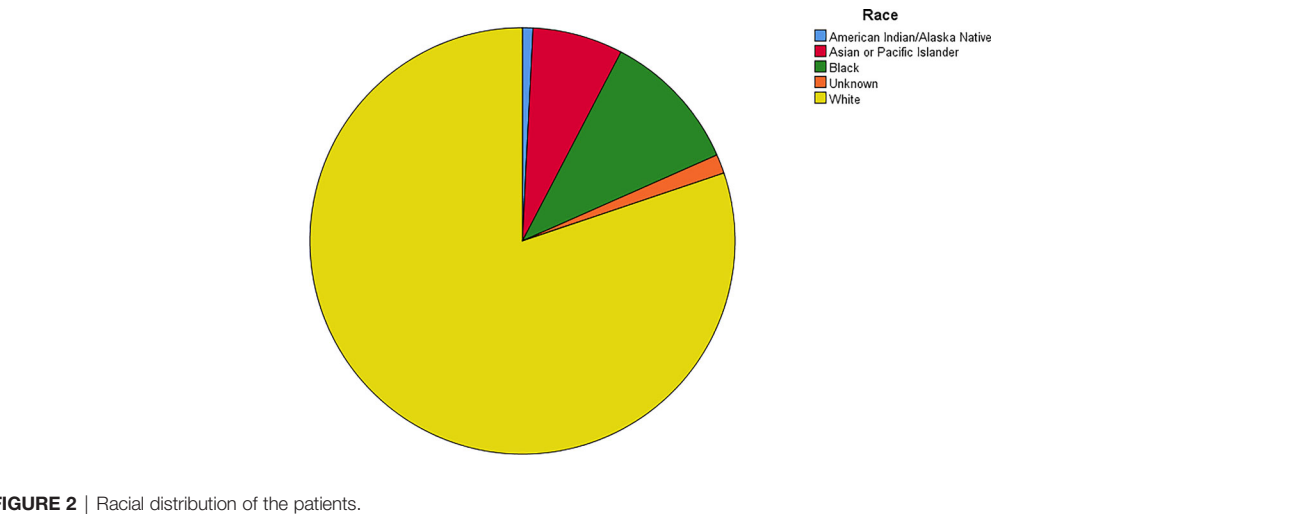

FIGURE 2 | Racial distribution of the patients.

not recommended for some patients. In our cohort, 59.7% of the cases were diagnosed with a positive microscopic method. There could be some bias in our research of the pathological characteristics because the data were not fully included. We believe further investigation should be conducted to clarify the findings, and further research about molecular pathology is also needed.

In our study, we found that race, age and sex were not independent prognostic factors. However, patients with tumors less than 3 cm in size had a better prognosis than patients with tumors larger than 3 cm. We believe that timely diagnosis and treatment are essential for patients. Focal radiation therapy is the current standard of care for children with diffuse intrinsic pontine glioma (18). We also found that radiation therapy was chosen more frequently than surgery and chemotherapy. However, the results of the survival analysis showed that radiation and chemotherapy did not improve overall survival. The systematic review conducted by Xu et al. (19) also could not make definitive conclusions regarding whether radiotherapy can help patients obtain better survival. We believe that further high-

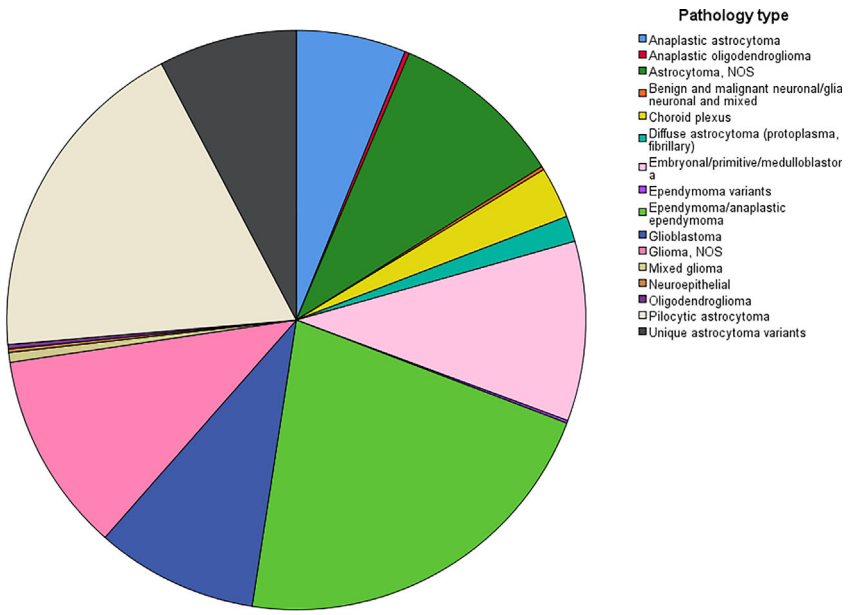

FIGURE 3 | The distribution of the patients with different pathological types.

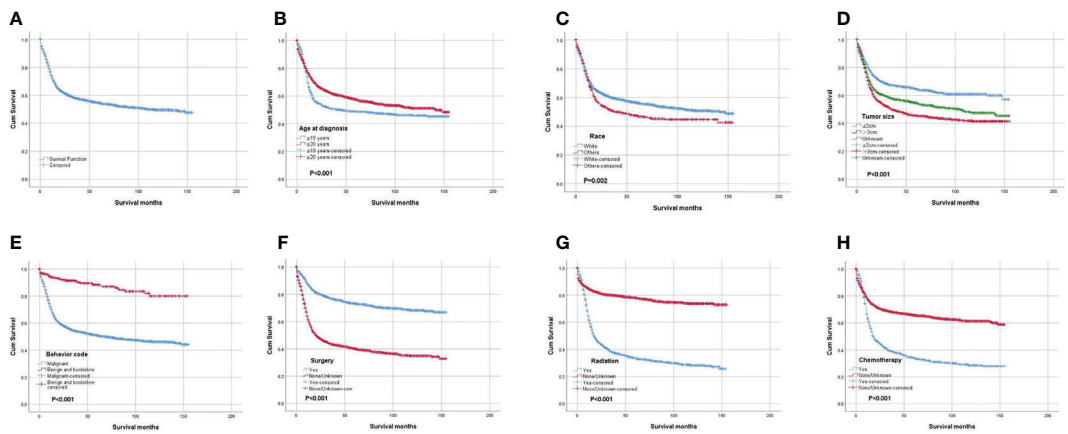

FIGURE 4 | Kaplan-Meier survival analysis: **(A)** The overall survival for the whole cohort. The survival analysis of patients classified based on **(B)** age at diagnosis, **(C)** race, **(D)** tumor size, **(E)** behavior, **(F)** surgery, **(G)** radiation and **(H)** chemotherapy.

quality studies are needed to establish the role of radiotherapy in the management of brainstem gliomas. Brainstem glioma is believed to be composed of a heterogeneous group of gliomas, and individualized treatment is needed based on pathology. Our results also showed that surgery can improve prognosis. The extent of surgery in some cases was difficult to clarify based on the code provided. In particular, biopsy and ventricular peritoneal shunts are widely used for patients with brainstem gliomas. We did not analyze the impact of surgery extent on survival. Based on the results, the prognosis of brainstem glioma is poor, and the median survival time is 24 months. Different attempts have been made to treat patients with brainstem gliomas (4, 18, 20), and we hope that more effective treatments can be discovered in the future.

There are several limitations of our analysis that must be considered. The availability of some important information was limited, such as information on the tumor location (midbrain, pons, and medulla), focality of diffuse glioma, molecular pathology, more specific treatment, tumor progression and so on. The specific location and molecular features are very important factors affecting progression, and molecular pathological investigations have been widely implemented in clinical practice. We hope that we can obtain more detailed information from the SEER database in the future. Although it would necessitate the inclusion of a

TABLE 2 | Results of the log-rank test and univariate and multivariate Cox regression analysis.

Variable	Log-Rank Test	Univariate Analysis		Multivariate Analysis	
	P value	HR (95%CI)	P value	HR (95%CI)	P value
Sex	0.270				
Female		Reference		Reference	
Male		0.944 (0.851-1.047)	0.275	0.998 (0.899-1.108)	0.973
Age at diagnosis (years)	<0.001				
≤19		Reference		Reference	
≥20		0.802 (0.721-.892)	<0.001	0.908 (0.812-1.016)	0.092
Race	0.002				
White		Reference		Reference	
Others/Unknown		1.210 (1.069-1.370)	0.003	1.003 (0.885-1.137)	0.959
Tumor Size	<0.001				
≤3cm		Reference		Reference	
>3cm		1.662 (1.462-1.889)	<0.001	1.240 (1.079-1.424)	0.002
Unknown		1.408 (1.227-1.616)	<0.001	1.159 (1.008-1.332)	0.038
Behavior	<0.001				
Malignant		Reference		Reference	
Benigan and Borderline		0.212 (0.155-0.290)	<0.001	0.507 (0.366-0.703)	<0.001
Surgery	<0.001				
None/Unknown		Reference		Reference	
Yes		0.337 (0.299-0.380)	<0.001	0.337 (0.298-0.381)	<0.001
Radiation	<0.001				
None/Unknown		Reference		Reference	
Yes		3.651 (3.235-4.121)	<0.001	2.832 (2.465-3.254)	<0.001
Chemotherapy	<0.001				
None/Unknown		Reference		Reference	
Yes		2.188 (1.972-2.428)	0.001	1.234 (1.100-1.384)	<0.001

substantial amount of information, it would assist in the realization of a better understanding of primary CNS tumors.

CONCLUSION

Brainstem gliomas can be diagnosed at every age. Ependymoma/anaplastic ependymoma is the most common pathological diagnosis. The predominance of white patients was significant. The prognosis was poor, and the median survival time was 24 months. Timely diagnosis and surgery are effective in improving the prognosis, and individualized treatment is essential for patients. We suggest that more attention should be paid to the treatment of patients with brainstem gliomas.

DATA AVAILABILITY STATEMENT

The original contributions presented in the study are included in the article/supplementary material. Further inquiries can be directed to the corresponding authors.

AUTHOR CONTRIBUTIONS

YW and GZ: Conceptualization, methodology, and reviewing and editing. YW: Data curation, software, and validation. HL, XQ, LZ, and YW: Original draft preparation, and reviewing and editing. All authors contributed to the article and approved the submitted version.

REFERENCES

1. Weller M, Wick W, Aldape K, Brada M, Berger M, Pfister SM, et al. Glioma. *Nat Rev Dis Primers* (2015) 1:15017. doi: 10.1038/nrdp.2015.17
2. Ostrom QT, Patil N, Cioffi G, Waite K, Kruchko C, Barnholtz-Sloan JS. Cbtrus Statistical Report: Primary Brain and Other Central Nervous System Tumors Diagnosed in the United States in 2013-2017. *Neuro-Oncology* (2020) 22:iv1–96. doi: 10.1093/neuonc/noaa200
3. Grimm SA, Chamberlain MC. Brainstem Glioma: A Review. *Curr Neurol Neurosci Rep* (2013) 13:346. doi: 10.1007/s11910-013-0346-3
4. Chen LH, Pan C, Diplas BH, Xu C, Hansen LJ, Wu Y, et al. The Integrated Genomic and Epigenomic Landscape of Brainstem Glioma. *Nat Commun* (2020) 11:3077. doi: 10.1038/s41467-020-16682-y
5. Overview of the SEER Program. (2020). Available at: https://seer.cancer.gov/about/overview.html (Accessed Jan, 2020).
6. Surveillance, Epidemiology, and End Results (SEER) Program. *Seer*Stat Database: Incidence - SEER Research Data, 18 Registries, Nov 2019 Sub (2000-2017) - Linked to County Attributes - Time Dependent (1990-2017) Income/Rurality, 1969-2018 Counties*. National Cancer Institute, DCCPS, Surveillance Research Program. Available at: www.seer.cancer.gov. released April 2020, based on the November 2019 submission.
7. Surveillance, Epidemiology, and End Results (SEER) Program. *Seer*Stat Database: Incidence - SEER 18 Regs Custom Data (With Additional Treatment Fields), Nov 2018 Sub (1975-2016 Varying) - Linked to County Attributes - Total U.S., 1969-2017 Counties, National Cancer Institute, Dccps*. Surveillance Research Program. Available at: www.seer.cancer.gov. released April 2019, based on the November 2018 submission.
8. Dellaretti M, Reyns N, Touzet G, Dubois F, Gusmão S, Pereira JL, et al. Diffuse Brainstem Glioma: Prognostic Factors. *J Neurosurg* (2012) 117:810–4. doi: 10.3171/2012.7.JNS111992
9. Hargrave D, Bartels U, Bouffet E. Diffuse Brainstem Glioma in Children: Critical Review of Clinical Trials. *Lancet Oncol* (2006) 7:241–8. doi: 10.1016/S1470-2045(06)70615-5

10. Laigle-Donadey F, Doz F, Delattre JY. Brainstem Gliomas in Children and Adults. *Curr Opin Oncol* (2008) 20:662–7. doi: 10.1097/CCO.0b013e32831186e0
11. Maxwell R, Luksik AS, Garzon-Muvdi T, Yang W, Huang J, Bettegowda C, et al. Population-Based Study Determining Predictors of Cancer-Specific Mortality and Survival in Pediatric High-Grade Brainstem Glioma. *World Neurosurg* (2018) 119:e1006–15. doi: 10.1016/j.wneu.2018.08.044
12. Doyle J, Khalafallah AM, Yang W, Sun Y, Bettegowda C, Mukherjee D. Association Between Extent of Resection on Survival in Adult Brainstem High-Grade Glioma Patients. *J Neuro Oncol* (2019) 145:479–86. doi: 10.1007/s11060-019-03313-w
13. Liu Z, Feng S, Li J, Cao H, Huang J, Fan F, et al. The Epidemiological Characteristics and Prognostic Factors of Low-Grade Brainstem Glioma: A Real-World Study of Pediatric and Adult Patients. *Front Oncol* (2020) 10:391. doi: 10.3389/fonc.2020.00391
14. Ostrom QT, Cioffi G, Gittleman H, Patil N, Waite K, Kruchko C, et al. Cbtrus Statistical Report: Primary Brain and Other Central Nervous System Tumors Diagnosed in the United States in 2012-2016. *Neuro-Oncology* (2019) 21:v1–v100. doi: 10.1093/neuonc/noz150
15. Smith MA, Freidlin B, Ries LA, Simon R. Trends in Reported Incidence of Primary Malignant Brain Tumors in Children in the United States. *J Natl Cancer Inst* (1998) 90:1269–77. doi: 10.1093/jnci/90.17.1269
16. Ostrom QT, Cote DJ, Ascha M, Kruchko C, Barnholtz-Sloan JS. Adult Glioma Incidence and Survival by Race or Ethnicity in the United States From 2000 to 2014. *JAMA Oncol* (2018) 4:1254–62. doi: 10.1001/jamaoncol.2018.1789
17. Donaldson SS, Laningham F, Fisher PG. Advances Toward an Understanding of Brainstem Gliomas. *J Clin Oncol Off J Am Soc Clin Oncol* (2006) 24:1266–72. doi: 10.1200/JCO.2005.04.6599
18. Deland K, Starr BF, Mercer JS, Byemerwa J, Crabtree DM, Williams NT, et al. Tumor Genotype Dictates Radiosensitization After Atm Deletion in Primary Brainstem Glioma Models. *J Clin Invest* (2021) 131(1):e142158. doi: 10.1172/JCI142158
19. Hu X, Fang Y, Hui X, Jv Y, You C. Radiotherapy for Diffuse Brainstem Glioma in Children and Young Adults. *Cochrane Database Syst Rev* (2016) 6: Cd010439. doi: 10.1002/14651858.CD010439.pub2
20. Osorio DS, Patel N, Ji L, Sposto R, Stanek J, Gardner SL, et al. Pre-Irradiation Intensive Induction and Marrow-Ablative Consolidation Chemotherapy in Young Children With Newly Diagnosed High-Grade Brainstem Gliomas: Report of the "Head-Start" I and II Clinical Trials. *J Neuro Oncol* (2018) 140:717–25. doi: 10.1007/s11060-018-03003-z

Conflict of Interest: The authors declare that the research was conducted in the absence of any commercial or financial relationships that could be construed as a potential conflict of interest.

frontiers in Neurology

ORIGINAL RESEARCH
published: 06 July 2021
doi: 10.3389/fneur.2021.633390

Development of a Prognostic Five-Gene Signature for Diffuse Lower-Grade Glioma Patients

Qiang Zhang[1†], *Wenhao Liu*[2†], *Shun-Bin Luo*[3], *Fu-Chen Xie*[4], *Xiao-Jun Liu*[5], *Ren-Ai Xu*[6*], *Lixi Chen*[7*] and *Zhilin Su*[8*]

[1] Department of Clinical Laboratory, The People's Hospital of Lishui, Lishui, China, [2] Guangdong-Hong Kong-Macao Greater Bay Area (GBA) Research Innovation Institute for Nanotechnology, Guangzhou, China, [3] Department of Clinical Pharmacy, The People's Hospital of Lishui, Lishui, China, [4] Department of Urinary Surgery, The People's Hospital of Lishui, Lishui, China, [5] Pathology Department, The People's Hospital of Lishui, Lishui, China, [6] The First Affiliated Hospital of Wenzhou Medical University, Wenzhou, China, [7] Department of Gynecology in Xiahe Branch, Xiamen University Affiliated Zhongshan Hospital, Xiamen, China, [8] Department of Laboratory Medicine, The First Affiliated Hospital of Xiamen University, Xiamen, China

OPEN ACCESS

Edited by:
Yaohua Liu,
Shanghai First People's Hospital, China

Reviewed by:
Christine Marosi,
Medical University of Vienna, Austria
Ann-Christin Hau,
Laboratoire National de Santé (LNS), Luxembourg

***Correspondence:**
Ren-Ai Xu
wmu_xra@163.com
Lixi Chen
lixichen2008@126.com
Zhilin Su
SUZL2003@163.com

[†] These authors have contributed equally to this work

Specialty section:
This article was submitted to Neuro-Oncology and Neurosurgical Oncology, a section of the journal Frontiers in Neurology

Received: 25 November 2020
Accepted: 02 June 2021
Published: 06 July 2021

Citation:
Zhang Q, Liu W, Luo S-B, Xie F-C, Liu X-J, Xu R-A, Chen L and Su Z (2021) Development of a Prognostic Five-Gene Signature for Diffuse Lower-Grade Glioma Patients. Front. Neurol. 12:633390. doi: 10.3389/fneur.2021.633390

Background: Diffuse lower-grade gliomas (LGGs) are infiltrative and heterogeneous neoplasms. Gene signature including multiple protein-coding genes (PCGs) is widely used as a tumor marker. This study aimed to construct a multi-PCG signature to predict survival for LGG patients.

Methods: LGG data including PCG expression profiles and clinical information were downloaded from The Cancer Genome Atlas (TCGA) and the Chinese Glioma Genome Atlas (CGGA). Survival analysis, receiver operating characteristic (ROC) analysis, and random survival forest algorithm (RSFVH) were used to identify the prognostic PCG signature.

Results: From the training ($n = 524$) and test ($n = 431$) datasets, a five-PCG signature which can classify LGG patients into low- or high-risk group with a significantly different overall survival (log rank $P < 0.001$) was screened out and validated. In terms of prognosis predictive performance, the five-PCG signature is stronger than other clinical variables and IDH mutation status. Moreover, the five-PCG signature could further divide radiotherapy patients into two different risk groups. GO and KEGG analysis found that PCGs in the prognostic five-PCG signature were mainly enriched in cell cycle, apoptosis, DNA replication pathways.

Conclusions: The new five-PCG signature is a reliable prognostic marker for LGG patients and has a good prospect in clinical application.

Keywords: lower-grade glioma, signature, prognostic biomarker, survival, gene expression

INTRODUCTION

Glioma is the most common primary CNS tumor and was classified into grades I–IV according to histopathological characteristics. Glioblastoma (WHO grade IV glioma) accounts for 70–75% of all diagnosed diffuse gliomas, with a median overall survival of 14–17 months (1). Diffuse low-grade (WHO grade II) and intermediate-grade (WHO grade III) gliomas are considered lower-grade gliomas (LGGs), and their clinical behavior is highly variable, with a prognosis of 1–15 years (2). Overall, the prognosis of glioma patients is not satisfactory. For LGGs, the great prognostic variance among patients subjected

to the same therapeutic regimen is the highlighted clinical problem. Thus, identification of patients with bad survival is very important for instructing subsequent treatment.

Glioma is a fatal tumor that derives from glial cell and grows in the central nervous system, including diffuse gliomas and nondiffuse gliomas (3). Diffuse gliomas are the most frequently occurring intracranial malignant tumors, encompassing various histologic types (astrocytic or oligodendroglial) and malignancy grades [World Health Organization (WHO) grades II, III, and IV] tumors. Astrocytomas and oligodendrogliomas in the low grade (WHO II) and intermediate grade (WHO III) are incorporated into diffuse lower-grade glioma (LGG) and perform better than IV grade glioblastoma in both malignancy and prognosis. However, it is difficult to predict the clinical outcome of LGG patients because LGG are a highly heterogeneous group of tumors. Firstly, there is a difference in the speed of tumor progression within LGG. Some are relatively inert, while others quickly progress to high-grade glioma or glioblastoma. Secondly, therapeutic sensitivity varies in LGG patients. Some people have effective treatments, while others have poor treatment results. Finally, LGG patients differ greatly in the prognosis, ranging from 1 to 15 years (2). Due to the limitations of histologic classification of LGG, finding molecular markers that can accurately predict prognosis and treatment response has become an urgent task (4).

In recent years, significant progress has been made in the study of molecular pathology of gliomas, and a series of molecular markers have been discovered that are helpful for clinical diagnosis, prognostic judgment, and treatment guidance, such as IDH1/2 gene mutation, chromosome 1p/19q co-deletion, and MGMT promoter methylation (5). Especially, the revised 2016 WHO classification of CNS tumors made fundamental changes and classified diffuse gliomas based on IDH mutation and 1p/19q co-deletion status. This innovative measure highlights the important role of novel and reliable gene biomarkers in the diagnosis and prognosis of gliomas.

With the development of next-generation sequencing technology, a large amount of high-throughput sequencing data and a variety of bioinformatics methods have prompted researchers to further understand tumorigenesis and find prognostic markers. Hu et al. (6) selected a prognostic 35-gene signature from 374 glioma patients carrying the 1p/19q co-deletion. Wu constructed a six-gene signature that could classify IDH-mutant GBM patients into high or low risk of poor outcome using 33 samples from the Chinese Glioma Genome Atlas RNA-sequencing data and 21 cases from Chinese Glioma Genome Atlas microarray data (7). Deng found a four-gene immune prognostic signature for predicting prognosis in LGGs through analyzing 511 LGG samples from the TCGA database and 172 LGG samples from the CGGA dataset (8). Therefore, gene signature has become the research focus of glioma prognostic markers.

Abbreviations: TCGA, The Cancer Genome Atlas; CGGA, the Chinese Glioma Genome Atlas; ROC, receiver operating characteristic; Kaplan–Meier, KM; AUC, area under the ROC curve; GO, Gene ontology; KEGG, Kyoto Encyclopedia of Genes and Genomes; CI, confidence interval; OS, overall survival.

In the present study, the protein-coding gene (PCG) expression data from a total of 955 LGG patients were collected from the Cancer Genome Atlas (TCGA) database and the Chinese Glioma Genome Atlas (CGGA). We aimed to mine the large queue of gene expression data and clinical information to identify a prognostic PCG signature and explore its significance of treatment guidance.

MATERIALS AND METHODS

Data Collection of Diffuse LGG Patients

The clinical information and mRNA expression data of LGG patients were obtained from the TCGA database (http://cancergenome.nih.gov/; https://xenabrowser.net/datapages/). Another independent dataset used as validation or test dataset was downloaded from the CGGA database (http://www.cgga.org.cn/). LGG cases with clinical survival information including survival status and survival time were selected for building the prognostic model. Clinical details of LGG patients in the training and test datasets are shown in **Supplementary Table 1**. Genes with missing expression values in >20% samples were removed in subsequent analysis (9).

TABLE 1 | Relationship of the five-gene signature with features in the two groups with LGG.

Feature	Training set		*P*	Test set		*P*
	Low#	High#		Low#	High#	
Age (years)			0.02			0.99
≤40	144	117		111	110	
>40	118	145		105	105	
Gender			0.99			0.88
Female	119	118		98	95	
Male	143	144		118	120	
Grade			<0.001			<0.001
G2	169	88		111	69	
G3	92	174		105	146	
Unknown	1	0		0	0	
IDH mutation status			<0.001			<0.001
Mutant	69	22		183	114	
Wild type	9	25		13	83	
Unknown	184	215		20	18	
Radiotherapy			<0.001			0.31
No	119	54		47	39	
Yes	113	171		157	157	
Unknown	30	37		12	19	
Chemotherapy						0.04
No				74	50	
Yes				124	141	
Unknown				18	24	
1p19q co-deletion status						<0.001
Co-deletion				99	29	
Non-co-deletion				98	167	
Unknown				19	19	

The median risk score was used to classify patients into low- and high risk groups.

The Process of Developing the Prognostic Signatures in the Training Dataset

Using Kaplan–Meier (KM) and receiver operating characteristic (ROC) analysis, we identified the PCGs significantly associated with patients' OS with AUC > 0.6 from the TCGA group. Then we reduced the number of the PCGs by the random survival forest algorithm (RSFVH). Further, prognostic models were constructed as follows:

$$Riskscore = \sum_{i}^{N}{}_{=1}(Expression_i \times coefficient_i)$$

where N is the number of PCG, Expression is the PCG expression value, and coefficient is the PCG expression in Cox regression analysis. The final prognostic PCG signature was screened out with the largest AUC value in all the constructed models (10).

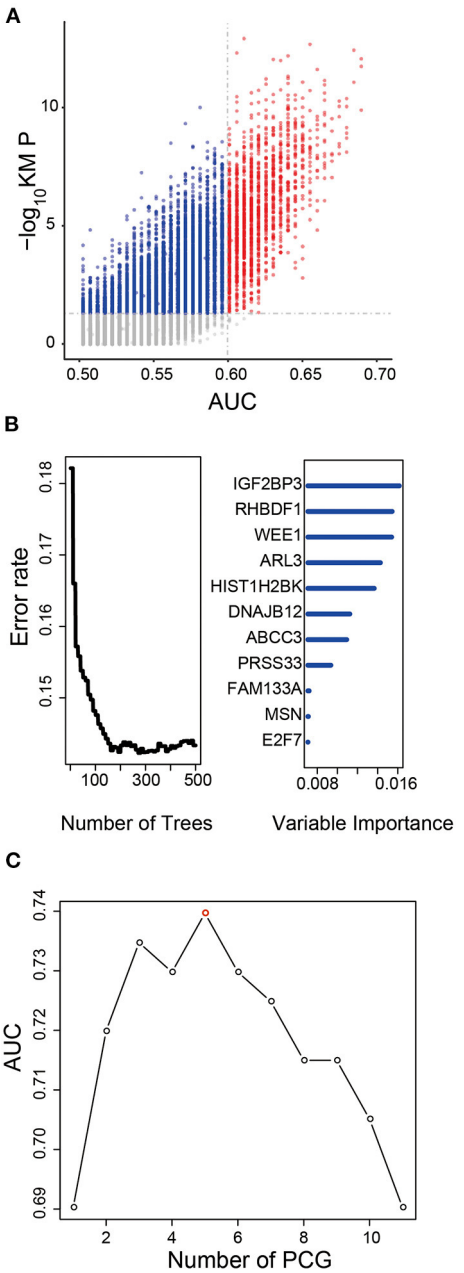

FIGURE 1 | Development of the prognostic signature in the training dataset. **(A)** The survival-associated PCGs in Kaplan–Meier analysis were displayed as red dots in the scatter diagram. **(B)** Random forest supervised classification algorithm reduced the prognosis-associated PCGs to 11 PCGs. **(C)** The prognostic five-PCG signature was selected because its AUC was the largest (AUC = 0.739) among the $2^{11}-1 = 2{,}047$ signatures.

Statistical and Bioinformatics Analysis

Kaplan–Meier analysis was used to assess the two survival risk groups separated by the median risk score. Cox regression

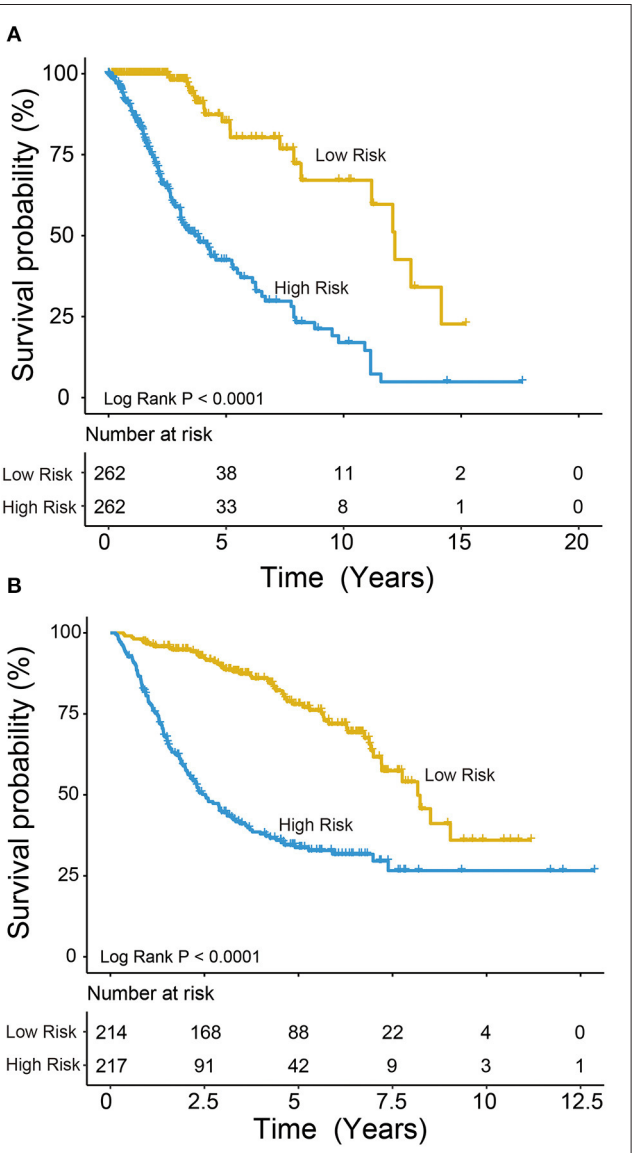

FIGURE 2 | Kaplan–Meier plots indicated that LGG patients could be classified into high- and low-risk groups according to the five-gene signature in the training **(A)** and test **(B)** datasets.

analysis was performed to explore the independence of the signature. ROC and TimeROC were used to analyze survival prediction performance. Function prediction of prognostic PCGs was analyzed by clusterProfiler (11). R program (www.r-project.org) with R packages including pROC, TimeROC, randomForestSRC, and survival was used to perform the above analyses.

RESULTS

The Process of Developing the Prognostic Signatures in the Training Dataset

All 955 patients diagnosed with LGG were collected from the TCGA (n = 524) and CGGA (n = 431) datasets, and a total of 16,246 expressed PCGs were identified. From **Table 1**, we found that the median age of the enrolled patients was 40 years (11–87 years) and that there were more male patients than female patients, indicating that LGG is more likely to occur in adult males. When focusing on the survival status and survival time of these patients, we found that more than one-third of patients (326 of 955) had died and the median survival time was only 2.11 years (0.2–14.15 years). In addition, we also obtained IDH mutation status, 1p19q co-deletion, radiotherapy, and chemotherapy information for further analysis.

After Kaplan–Meier and ROC analysis in the TCGA dataset, a total of 1,702 PCGs were discovered (red dots in **Figure 1A**), which were significantly associated with OS and had a good ability to predict survival (KM $P < 0.05$ and AUC > 0.6, **Supplementary Table 2**). Further, we screened out 11 prognostic PCGs by RSFVH analysis based on importance scores (**Figure 1B**). Then, we brought the prognostic PCGs into the risk prediction model and got 2^{11}-1 = 2,047 possible signatures in the training dataset. ROC analyses were performed in all the 2,047 signatures to find out the signature with the strongest predictive ability (**Supplementary Table 3**). The final signature including five PCGs (ABCC3, SMC4,

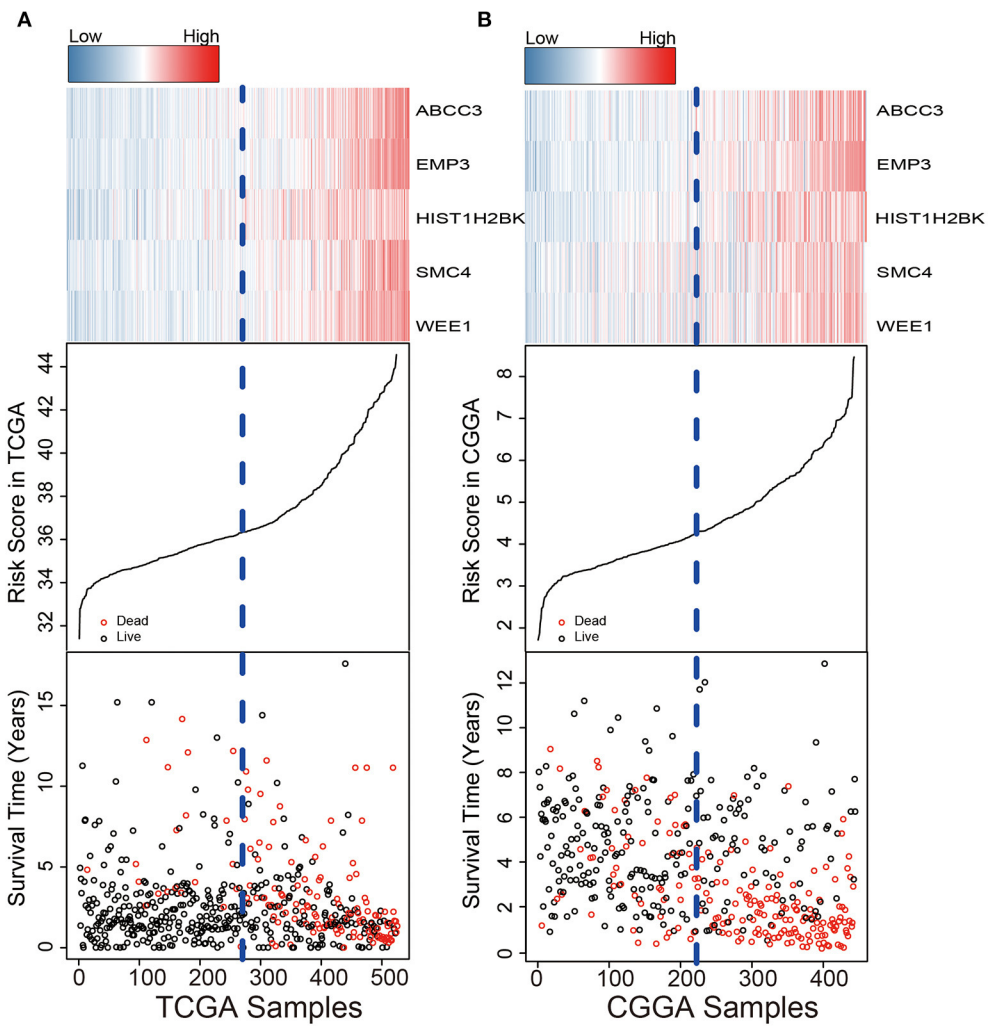

FIGURE 3 | Risk score distribution, survival status, and PCG expression patterns for LGG patients in the training **(A)** and test **(B)** datasets.

EMP3, WEE1, and HIST1H2BK) related to LGG prognosis significantly (**Supplementary Figure 1A**) was screened out with the maximum AUC (AUCsignature = 0.739; **Figure 1C**). The selected risk model is as follows: risk score = (0.28 × expression value of ABCC3) + (0.66 × expression value of SMC4) + (0.44 × expression value of EMP3) + (0.61 × expression value of WEE1) + (0.45 × expression value of HIST1H2BK). In addition, the survival curves with univariable Cox hazard ratio for each gene in the signature in the CGGA group are also shown in **Supplementary Figure 1B**. The five genes, significantly associated with LGG prognosis, were also observed in the CGGA dataset. The result suggested that the five genes were reliable prognostic biomarkers for patients with LGG.

The Performance of PCG Signature in Predicting LGG Patient Survival

We used the risk model to calculate the risk scores for each patient. The median risk score was used to divide patients in the training dataset into either the high-risk ($n = 262$) or low-risk group ($n = 262$). The Kaplan–Meier analysis results showed that patients in the low-risk group lived longer than patients in the high-risk group (median survival time: 12.18 years vs. 3.84 years, $P < 0.001$; **Figure 2A**). Then, we tested the prognostic value of the PCG signature in another large independent LGG dataset (CGGA, $n = 431$). After the median risk score in CGGA-separated patients into high- or low-risk group, Kaplan–Meier analysis found that the 5-year survival of patients with high risk scores was lower than that of patients with low risk scores (5-year survival: 34.16 vs. 77.05%, log-rank test $P < 0.001$; **Figure 2B**). We showed the relationship of PCG expression, risk score, and survival information in **Figure 3**. With the increase of gene expression value, risk scores and death toll increased in the training (**Figure 3A**) and test datasets (**Figure 3B**).

The Five-PCG Signature Is an Independent Predictive Factor

In the two LGG groups ($n = 524/431$), we found that the signature was related with clinical variables such as IDH mutation status and Grade by chi-square test ($P < 0.001$; **Table 1**). In addition, we found that the 1p19q co-deletion status could predict the patients with LGG significantly (**Supplementary Figure 2**) and the signature was also associated with 1p19q co-deletion status based on the CGGA dataset ($P < 0.001$; **Table 1**). Then, we further performed univariate and multivariable Cox regression analyses to test the predictive independence of the signature. Multivariable Cox regression results verified that the signature was an independent predictive factor and could independently predict patients' clinical outcome in training or test datasets (high- vs. low-risk, HR training = 1.70, 95% CI 1.31–2.21, $P < 0.001$, $n = 524$; HR test = 3.01, 95% CI: 2.12–4.27, $P < 0.001$, $n = 431$; **Table 2**).

Predictive Performance Comparison Between the Five-PCG Signature With Other Clinical Variables

We performed ROC analysis to compare the predictive performance of the five-PCG signature with other clinical variables including IDH mutation status, age, and grade. **Figures 4A,B** shows that the PCG signature outperformed the above clinical variables in both the training and test sets (AUCsignature 0.739/0.678 vs. AUCIDH 0.712/0.585; AUCgrade 0.625/0.632; AUCage 0.57/0.527). Further, TimeROC analysis found that the AUC values of the signature from 1 to 5 years were greater than that of IDH mutation status, grade, or age, indicating that the PCG signature had better survival prediction when integrating the TCGA and CGGA datasets (**Figure 4C**).

TABLE 2 | Univariable and multivariable Cox regression of the signature with patient survival in two LGG datasets.

Variables		Univariable				Multivariable			
		HR	95% CI of HR		*P*	HR	95% CI of HR		*P*
			Lower	Upper			Lower	Upper	
TCGA set									
Age	>40 vs. ≤40	2.82	1.96	4.04	<0.001	1.99	0.52	7.60	0.32
Gender	Male vs. female	1.14	0.81	1.60	0.45	2.00	0.66	6.09	0.22
IDH status	Wild type vs. mutant	5.53	2.07	14.82	<0.001	0.94	0.22	4.07	0.94
LGG Grade	G3 vs. G2	3.31	2.28	4.79	<0.001	0.79	0.22	2.81	0.72
Signature	High risk vs. low risk	6.86	4.26	11.04	<0.001	1.70	1.31	2.21	<0.001
CGGA set									
Age	>40 vs. ≤40	1.19	0.89	1.58	0.24	1.10	0.82	1.48	0.54
Gender	Male vs. female	1.00	0.75	1.34	0.98	1.14	0.85	1.54	0.38
IDH status	Wild type vs. mutant	2.24	1.64	3.07	<0.001	1.48	1.06	2.07	0.02
Grade	G3 vs. G2	2.62	1.89	3.64	<0.001	2.58	1.81	3.66	<0.001
Signature	High risk vs. low risk	3.68	2.69	5.03	<0.001	3.01	2.12	4.27	<0.001

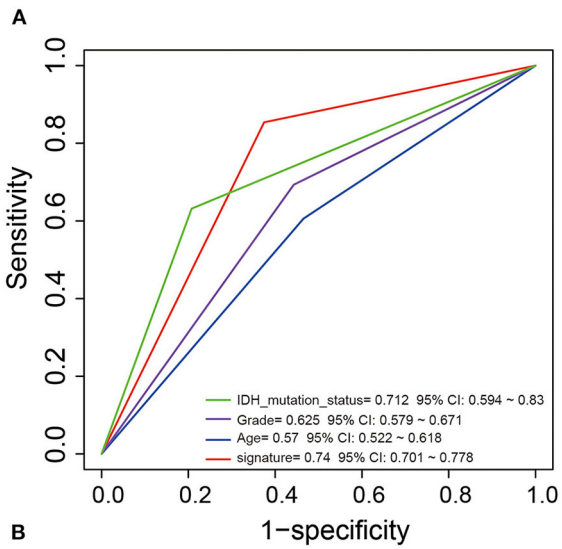

FIGURE 4 | Comparison of the survival predictive power of the signature with grade, age, and IDH mutation by ROC in the training **(A)** and test **(B)** sets. TimeROC analysis of survival predictive power for the signature, grade, age, and IDH mutation **(C)**.

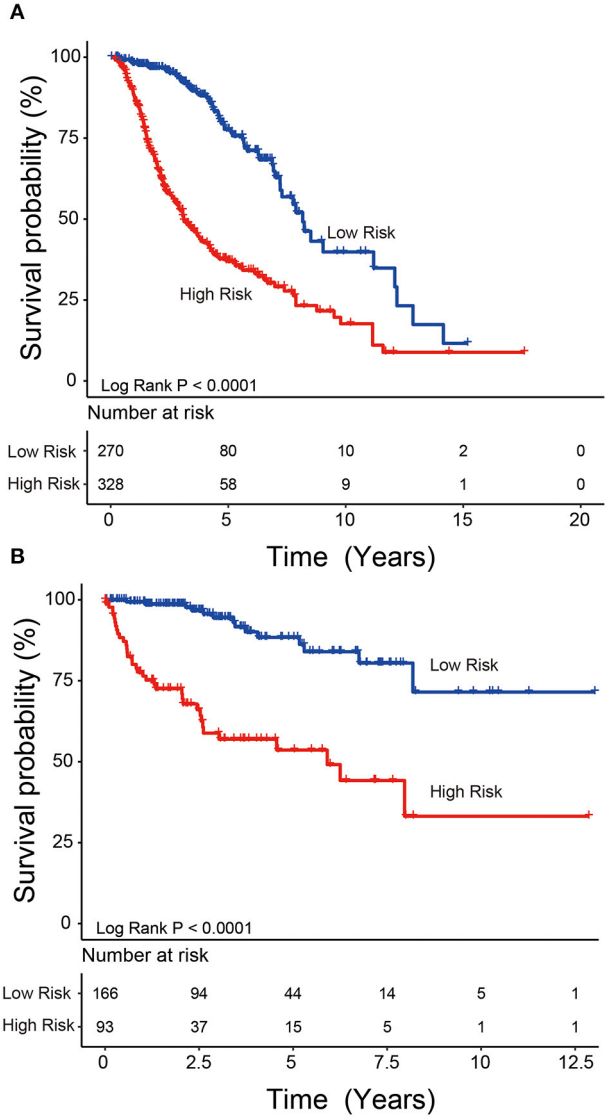

FIGURE 5 | Radiotherapy stratification analysis. The five-PCG signature could further divide patients with radiotherapy **(A)** or patients without radiotherapy **(B)** into two groups with significantly different survival.

Radiotherapy Stratification Analysis

Because radiotherapy is the most commonly used treatment in LGGs, we further explore the clinical value of the signature in LGG patients treated with radiotherapy in TCGA and CGGA. According to the radio-status information of all the 955 LGG patients, we found that 598 received radiotherapy, 259 patients did not, and 98 patients had unknown radiotherapy information. For patients after radiotherapy, the five-PCG signature could further divide patients into low- and high-risk groups with significantly different survival (5- or 10-year survival: 77.70/39.84% vs. 37.10/17.69%, log-rank test $P < 0.001$; **Figure 5A**). Patients without radiotherapy can also be grouped into different risk groups by the five-PCG signature (5- or 10-year

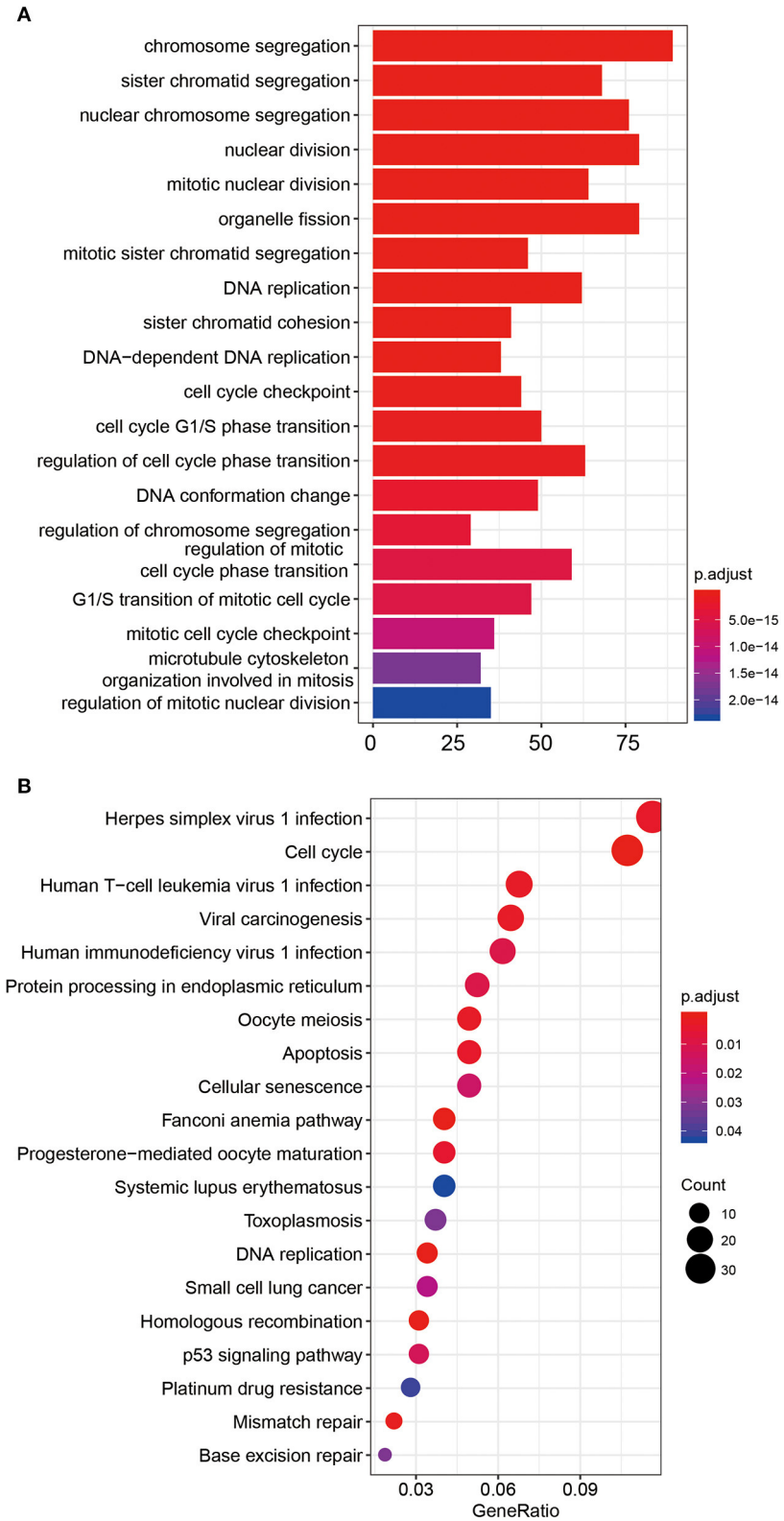

FIGURE 6 | GO **(A)** and KEGG **(B)** functional enrichment analysis of the five PCGs in the signature.

survival: 88.39/71.53% vs. 53.59/33.15%, log-rank test $P < 0.001$; **Figure 5B**).

Function Prediction for the Five Selected PCGs

To explore the role and function of the five selected PCGs screened in this study, we obtained a total of 741 co-expressing PCGs (Pearson coefficient $>0.5/<-0.5$, $P < 0.05$) using the Pearson test in the TCGA and CGGA datasets, respectively, and then performed KEGG and GO analysis. The co-expressing genes of the five PCGs were significantly enriched in 425 Go terms and 21 KEGG pathways ($P < 0.05$), such as cell cycle, DNA replication, and p53 signaling pathway, indicating the specific pathway or mechanism in which the prognostic PCGs might play a key role (top 20 shown; **Figure 6**).

DISCUSSION

The heterogeneity among patients is a major contributing factor in the adverse clinical outcome of gliomas (12). Consequently, the latest edition (2016 edition) of the WHO glioma classification incorporates molecular features into the classification criteria, thereby improving the homogeneity of clinical outcomes in patients with the same subtype (1). However, as one of histological subtypes of glioma, LGG has substantial variation in patient survival and lacks effective prognostic markers. In the current study, we analyzed the survival and gene expression information of 955 patients with LGG and found that the five-PCG signature could be a good prognostic molecular marker. In addition to predicting prognosis of LGG patients, the five-PCG signature has also been found to have a role in guiding radiotherapy.

Tumor heterogeneity and therapeutic advancements have prompted clinicians to make individualized prognosis and treatment choices for cancer patients, thereby achieving precision medicine. Gene biomarkers have always been at the forefront of the development of personalized medicine, especially in the field of cancer. Gene signature-based RNA expression obtained by analyzing gene profiling has been shown to predict the tumor behavior and to distinguish patients with specific tumor grades and/or prognosis (13, 14) in various types of cancer, such as esophageal squamous cell carcinoma, hepatocellular carcinoma, bladder carcinoma, breast cancer, and glioblastoma. In the current study, we aimed to analyze the gene expression profile and develop an effective gene signature for accurate prognosis prediction of LGG patients. After a detailed analysis of gene expression profiles of 955 patients with LGG from the TCGA training set and CGGA validation set, a five-PCG-based prognostic risk model and the five-PCG signature that could distinguish LGG patients with high risk of poor prognosis from patients with low risk were developed. The five-PCG signature has the following two advantages in prognosis prediction: First, it is an independent factor and does not depend on known prognostic factors such as IDH mutation and tumor grade II/III; second, it has excellent prediction performance for its AUC value was higher than IDH mutation and tumor grade.

Notably, the five-PCG signature was found to be a predictive marker for radiotherapy in LGG patients. More specifically, the marker can identify who can benefit from radiotherapy or who is suitable for radiotherapy. As a result, LGG patients have more scientific guidance on whether to accept radiotherapy, and clinicians can also have more standardized guidelines for radiotherapy to facilitate their implementation. This finding shows that the five-PCG signature not only makes the prognosis assessment of patients more precise but also can play the role of individualized treatment. In addition, we noted that the five PCGs in the signature had positive risk factors, meaning they were all prognostic risk factors. By searching the existing literature, we found that the important role of these genes in prognosis prediction had been reported in a variety of tumors. ATP-binding cassette subfamily C member 3 (ABCC3), also named multidrug resistance-associated protein 3 (MRP3), is an organic anion transporter and contributes to drug resistance of cancer cells (15). Consistent with the results in this article, the poor prognosis predictive role of ABCC3 has been reported not only in acute myeloid leukemia (16), gastric cancer (17), pancreatic cancer (18), and lung cancer (19) but also in gliomas (20). In addition to being found as a prognostic marker for gliomas in this article, structural maintenance of chromosomes 4 (SMC4) has also been found to be a survival marker for colorectal cancer (21), breast cancer (22), and prostate cancer (23). Epithelial membrane protein 3 (EMP3) is considered to be a tumor suppressor, but this article found that this gene is a prognostic risk gene for LGG. Similar to our results, Wang et al. (24) also found that EMP3 was associated with the worse prognosis of LGG patients and Guo et al. (25) discovered that EMP3 was also a risk gene in the process of developing a prognostic four-gene panel for glioblastoma patients. WEE1 G2 checkpoint kinase (WEE1) is reported to be an oncogenic nuclear kinase and a regulator of the G2 checkpoint. Expression of WEE1 has been found to be associated with poor prognosis in a variety of tumor types including gliomas (26). Two other gene signatures constructed to predict the prognosis of LGG are also consistent with the results of this article and found that WEE1 is a prognostic risk factor (27, 28). H2B-clustered histone 12 (H2BC12 or HIST1H2BK) is a replication-dependent histone and belongs to the histone H2B family. The prognostic role of HIST1H2BK was identified in ovarian cancer (29), breast cancer (30), and pancreatic ductal adenocarcinoma (31). Although we had some findings on the function of the five prognostic genes by KEGG and GO analysis, further functional exploration of these genes is needed.

CONCLUSION

Our study developed a prognostic five-PCG signature for LGG patients that can predict individual clinical outcome with high accuracy. Surprisingly, the five-gene signature can also predict radiotherapy response, which makes the biomarker have a broad clinical value.

DATA AVAILABILITY STATEMENT

Publicly available datasets were analyzed in this study. This data can be found here: TCGA: https://xenabrowser.net/datapages/; CGGA: http://www.cgga.org.cn/download.jsp.

AUTHOR CONTRIBUTIONS

QZ and WL: data collection, data analysis, interpretation, and drafting. X-JL, R-AX, LC, and ZS: study design, study supervision, and final approval of the manuscript. S-BL and F-CX: technical support and critical revision of the manuscript. All the authors read and approved the final manuscript.

SUPPLEMENTARY MATERIAL

The Supplementary Material for this article can be found online at: https://www.frontiersin.org/articles/10.3389/fneur.2021.633390/full#supplementary-material

REFERENCES

1. Molinaro AM, Taylor JW, Wiencke JK, Wrensch MR. Genetic and molecular epidemiology of adult diffuse glioma. *Nat Rev Neurology.* (2019) 15:405–17. doi: 10.1038/s41582-019-0220-2
2. Cancer Genome Atlas Research Network, Brat DJ, Verhaak RG, Aldape KD, Yung WK, Salama SR, et al. Comprehensive, integrative genomic analysis of diffuse lower-grade gliomas. *N Engl J Med.* (2015) 372:2481–98. doi: 10.1056/NEJMoa1402121
3. Wesseling P, Capper D. WHO 2016 Classification of gliomas. *Neuropathol Appl Neurobiol.* (2018) 44:139–50. doi: 10.1111/nan.12432
4. Ramaswamy V, Taylor MD. Fall of the optical wall: freedom from the tyranny of the microscope improves glioma risk stratification. *Cancer Cell.* (2016) 29:137–8. doi: 10.1016/j.ccell.2016.01.009
5. Chen R, Smith-Cohn M, Cohen AL, Colman H. Glioma subclassifications and their clinical significance. *Neurotherapeutics.* (2017) 14:284–97. doi: 10.1007/s13311-017-0519-x
6. Hu X, Martinez-Ledesma E, Zheng S, Kim H, Barthel F, Jiang T, et al. Multigene signature for predicting prognosis of patients with 1p19q co-deletion diffuse glioma. *Neurooncology.* (2017) 19:786–95. doi: 10.1093/neuonc/now285
7. Wu F, Chai RC, Wang Z, Liu YQ, Zhao Z, Li GZ, et al. Molecular classification of IDH-mutant glioblastomas based on gene expression profiles. *Carcinogenesis.* (2019) 40:853–60. doi: 10.1093/carcin/bgz032
8. Deng X, Lin D, Chen B, Zhang X, Xu X, Yang Z, et al. Development and validation of an IDH1-associated immune prognostic signature for diffuse lower-grade glioma. *Front Oncol.* (2019) 9:1310. doi: 10.3389/fonc.2019.01310
9. Xu J, Li Y, Lu J, Pan T, Ding N, Wang Z, et al. The mRNA related ceRNA-ceRNA landscape and significance across 20 major cancer types. *Nucleic Acids Res.* (2015) 43:8169–82. doi: 10.1093/nar/gkv853
10. Guo JC, Li CQ, Wang QY, Zhao JM, Ding JY, Li EM, et al. Protein-coding genes combined with long non-coding RNAs predict prognosis in esophageal squamous cell carcinoma patients as a novel clinical multi-dimensional signature. *Mol Biosyst.* (2016) 12:3467–77. doi: 10.1039/C6MB00585C
11. Yu G, Wang LG, Han Y, He QY. clusterProfiler: an R package for comparing biological themes among gene clusters. *Omics.* (2012) 16:284–7. doi: 10.1089/omi.2011.0118
12. Cheng J, Meng J, Zhu L, Peng Y. Exosomal noncoding RNAs in Glioma: biological functions and potential clinical applications. *Mol Cancer.* (2020) 19:66. doi: 10.1186/s12943-020-01189-3
13. Sato K, Tahata K, Akimoto K. Five genes associated with survival in patients with lower-grade gliomas were identified by information-theoretical analysis. *Anticancer Res.* (2020) 40:2777–85. doi: 10.21873/anticanres.14250
14. Burska AN, Roget K, Blits M, Soto Gomez L, van de Loo F, Hazelwood LD, et al. Gene expression analysis in RA: towards personalized medicine. *Pharmacogenomics J.* (2014) 14:93–106. doi: 10.1038/tpj.2013.48
15. Kool M, van der Linden M, de Haas M, Scheffer GL, de Vree JM, Smith AJ, et al. MRP3, an organic anion transporter able to transport anti-cancer drugs. *Proc Natl Acad Sci U S A.* (1999) 96:6914–9. doi: 10.1073/pnas.96.12.6914
16. Benderra Z, Faussat AM, Sayada L, Perrot JY, Tang R, Chaoui D, et al. MRP3, BCRP, and P-glycoprotein activities are prognostic factors in adult acute myeloid leukemia. *Clin Cancer Res.* (2005) 11:7764–72. doi: 10.1158/1078-0432.CCR-04-1895
17. Mao X, He Z, Zhou F, Huang Y, Zhu G. Prognostic significance and molecular mechanisms of adenosine triphosphate-binding cassette subfamily C members in gastric cancer. *Medicine.* (2019) 98:e18347. doi: 10.1097/MD.0000000000018347
18. Adamska A, Ferro R, Lattanzio R, Capone E, Domenichini A, Damiani V, et al. ABCC3 is a novel target for the treatment of pancreatic cancer. *Adv Biol Regul.* (2019) 73:100634. doi: 10.1016/j.jbior.2019.04.004
19. Zhao Y, Lu H, Yan A, Yang Y, Meng Q, Sun L, et al. ABCC3 as a marker for multidrug resistance in non-small cell lung cancer. *Sci Rep.* (2013) 3:3120. doi: 10.1038/srep03120
20. Wang F, Zheng Z, Guan J, Qi D, Zhou S, Shen X, et al. Identification of a panel of genes as a prognostic biomarker for glioblastoma. *EBioMedicine.* (2018) 37:68–77. doi: 10.1016/j.ebiom.2018.10.024
21. Feng XD, Song Q, Li CW, Chen J, Tang HM, Peng ZH, et al. Structural maintenance of chromosomes 4 is a predictor of survival and a novel therapeutic target in colorectal cancer. *Asian Pac J Cancer Prev.* (2014) 15:9459–65. doi: 10.7314/APJCP.2014.15.21.9459
22. Ma RM, Yang F, Huang DP, Zheng M, Wang YL. The prognostic value of the expression of SMC4 mRNA in breast cancer. *Dis Markers.* (2019) 2019:2183057. doi: 10.1155/2019/2183057
23. Zhao SG, Evans JR, Kothari V, Sun G, Larm A, Mondine V, et al. The landscape of prognostic outlier genes in high-risk prostate cancer. *Clin Cancer Res.* (2016) 22:1777–86. doi: 10.1158/1078-0432.CCR-15-1250
24. Wang H, Wang X, Xu L, Zhang J, Cao H. Prognostic significance of age related genes in patients with lower grade glioma. *J Cancer.* (2020) 11:3986–99. doi: 10.7150/jca.41123
25. Guo XX, Su J, He XF. A 4-gene panel predicting the survival of patients with glioblastoma. *J Cell Biochem.* (2019) 120:16037–43. doi: 10.1002/jcb.28883
26. Mir SE, De Witt Hamer PC, Krawczyk PM, Balaj L, Claes A, Niers JM, et al. *In silico* analysis of kinase expression identifies WEE1 as a gatekeeper against mitotic catastrophe in glioblastoma. *Cancer Cell.* (2010) 18:244–57. doi: 10.1016/j.ccr.2010.08.011
27. Xiao K, Liu Q, Peng G, Su J, Qin CY, Wang XY. Identification and validation of a three-gene signature as a candidate prognostic biomarker for lower grade glioma. *PeerJ.* (2020) 8:e8312. doi: 10.7717/peerj.8312
28. Pang FM, Yan H, Mo JL, Li D, Chen Y, Zhang L, et al. Integrative analyses identify a DNA damage repair gene signature for prognosis prediction in lower grade gliomas. *Future Oncol.* (2020) 16:367–82. doi: 10.2217/fon-2019-0764

29. Li N, Zhan X. Signaling pathway network alterations in human ovarian cancers identified with quantitative mitochondrial proteomics. *EPMA J.* (2019) 10:153–72. doi: 10.1007/s13167-019-00170-5
30. Han J, Lim W, You D, Jeong Y, Kim S, Lee JE, et al. Chemoresistance in the human triple-negative breast cancer cell line MDA-MB-231 induced by doxorubicin gradient is associated with epigenetic alterations in histone deacetylase. *J Oncol.* (2019) 2019:1345026. doi: 10.1155/2019/1345026
31. Yu S, Li Y, Liao Z, Wang Z, Wang Z, Li Y, et al. Plasma extracellular vesicle long RNA profiling identifies a diagnostic signature for the detection of pancreatic ductal adenocarcinoma. *Gut.* (2020) 69:540–50. doi: 10.1136/gutjnl-2019-318860

Conflict of Interest: The authors declare that the research was conducted in the absence of any commercial or financial relationships that could be construed as a potential conflict of interest.

frontiers in Neurology

ORIGINAL RESEARCH
published: 08 July 2021
doi: 10.3389/fneur.2021.627431

Expression of TCF7L2 in Glioma and Its Relationship With Clinicopathological Characteristics and Patient Overall Survival

*Shiyuan Jing, Lei Chen, Song Han, Ning Liu, MingYang Han, Yakun Yang and Changxiang Yan**

Sanbo Brain Hospital, Capital Medical University, Beijing, China

Background: The TCF7L2 gene is known as transcription factor 7-like 2 which has been identified as a novel transcription factor epithelial-mesenchymal transition (EMT) in tumor cells at 10q25.3. TCF7L2 may affect cancer progression and plays a central role in cancer proliferation, migration, and invasion. However, its clinical and prognostic value have not been researched in glioma. The purpose of our study was to research TCF7L2 expression and evaluate the clinical value of prognosis.

Method: We collected glioma specimens including low-grade glioma ($n = 46$) and glioblastoma ($n = 51$) from September 2015 to September 2017. Expression of TCF7L2 in 97 specimens was detected by quantitative real-time PCR (qRT-PCR). The chi-square test was applied to analyze the relationship between TCF7L2 expression and clinicopathological characteristics. The overall survival (OS) was estimated by log-rank tests among strata, and the survival curves were drawn by Kaplan-Meier. Univariate and multivariate analysis were utilized to analyze the relationship between prognosis and clinicopathological characteristics including TCF7L2 expression.

Results: Compared with the low-grade glioma group, the expression of TCF7L2 was significantly increased in the glioblastoma group ($p = 0.001$). TCF7L2 overexpression was associated with higher WHO grade ($p = 0.001$), isocitrate dehydrogenase (IDH) wild-type ($p = 0.001$), and lack of O(6)-methylguanine-DNA methyltransferase (MGMT) methylation ($p = 0.001$). Moreover, Kaplan-Meier analysis proved that overexpressed TCF7L2 was associated with poor OS ($p = 0.010$). The multivariate analysis suggested that TCF7L2 expression was an independent prognostic factor ($p = 0.020$).

Conclusions: Our research proved that TCF7L2 was overexpressed in glioblastoma, and related with tumor long-term prognosis, which, therefore, could be an independent prognostic factor for glioma patients.

Keywords: glioma, TCF7L2, overall survival, prognosis, clinicopathological characteristics

OPEN ACCESS

Edited by:
Yaohua Liu,
Shanghai First People's Hospital, China

Reviewed by:
Alissa A. Thomas,
University of Vermont, United States
Yinyan Wang,
Capital Medical University, China

****Correspondence:***
Changxiang Yan
yancx65828@sina.com

Specialty section:
This article was submitted to Neuro-Oncology and Neurosurgical Oncology, a section of the journal Frontiers in Neurology

Received: *09 November 2020*
Accepted: *13 May 2021*
Published: *08 July 2021*

Citation:
Jing S, Chen L, Han S, Liu N, Han M, Yang Y and Yan C (2021) Expression of TCF7L2 in Glioma and Its Relationship With Clinicopathological Characteristics and Patient Overall Survival. Front. Neurol. 12:627431. doi: 10.3389/fneur.2021.627431

BACKGROUND

Glioblastoma is a common malignant brain tumor owing to its stronger invasive ability and resistance to treatment. The morbidity rate of glioblastoma is approximately 0.59–0.69/100000 people worldwide, affecting those aged 20 years or older, especially those aged 40–70 years (1). The morbidity is higher in men (3.97/100,000) than in women (2, 3) (2.53/100,000).

According to NCCN Guidelines, the standard therapies include surgery, radiotherapy with concomitant temozolomide (TMZ), adjuvant TMZ chemotherapy, and TTF therapies, but the 5-year overall survival (OS) is only 9.8% (3). Despite comprehensive therapy, the median survival time is ∼12–15 months for GBM patients after diagnosis (4, 5).

An increasing number of molecular markers have been discovered, which improves our understanding of the mechanism of glioma and development. To date, the final histological diagnosis, final integrated diagnosis, pathological classification, and prognosis assessment are more accurate, which can help develop personalized therapy for glioma. Therefore, it is important to find novel biomarkers which can predict the prognosis, and explore its potential as a therapeutic target for glioma patients.

The Wnt/β-catenin signaling pathway is important in the majority of tumor progression. There is over 90% of aberrant activation of Wnt signaling in colorectal cancer (6). TCF7L2 is a member of the Wnt/β-catenin signaling pathway, which plays an important role in metabolism, cell differentiation/ proliferation, and cell death (7). Several meta-analyses have evaluated cancer risk induced by TCF7L2 gene variants (8–10).

A study (11) provided summary evidence that TCF7L2 genes are associated with the risk of breast, colorectal, and lung cancer and glioma. The loss of TCF7L2 enhances tumor cell growth, whereas a gain inhibits tumor cell growth (12). TCF7L2 plays a significant role in the pathogenesis of human cancers. A recent study (13) demonstrated that LEF/TCF-specific transcriptional regulation of Wnt target genes is associated with cancer progression and survival in human colorectal tumor samples.

However, the study of TCF7L2 mutation mainly focused on breast, colorectal, and lung cancer. Therefore, the aim of our study was to analyze the clinical value of TCF7L2 in glioma. We collected samples including 51 GBM tissues and 46 low-grade glioma tissues WHO (I-II). We focused on the TCF7L2 effect and the expression level in glioma tissue. Subsequently, we analyzed the relation between TCF7L2 expression level and clinicopathological characteristics. In our study, we performed a preliminary analysis between the expression level of TCF7L2 and overall survival risk of glioma among Chinese people.

Abbreviations: TCF7L2, Transcription factor 7-like 2; qRT-PCR, Real-time quantitative PCR; OS, Overall survival; TMZ, Temozolomide; EMT, Epithelial-mesenchymal transition; TTF, Tumor treating fields; GBM, Glioblastoma; cDNA, Complementary DNA; HR, Hazard ratios; CI, Confidence interval; MGMT, O(6)-methylguanine-DNA methyltransferase; IDH, Isocitrate dehydrogenase.

METHODS

Patients and Tissue Samples

Patients who underwent initial surgery in the Sanbo Brain Hospital of Capital Medical University from September 2015 to September 2017 were retrospectively selected for this research. All samples were diagnosed by pathologists and stored in liquid nitrogen.

As for patients with low-grade glioma, we identified high-risk patients according to the literature (14), including at least three factors (age >40 years old, astrocytomas, tumor maximum diameter ≧6 cm, tumors across the midline, and preoperative neurological impairment). Those patients were treated with radiochemotherapy, while the patients at low risk were followed up. Patients with glioblastoma received radiotherapy with concomitant temozolomide (TMZ) and adjuvant TMZ chemotherapy.

The patients' characteristics are described in **Table 1**. Tissue sample usage was approved by Ethics Committee of the Sanbo Brain Hospital of Capital Medical University and written informed consent was obtained from all study participants.

RNA Extraction and qRT-PCR Analyses

The total RNA was extracted from the frozen sample by TRIzol reagent (Invitrogen, Carlsbad, CA, USA). RNA was

TABLE 1 | Relationship between the expression level of TCF7L2 and clinicopathological parameters.

Characteristic	Case number	TCF7L2 expression R_s		*p*
		Low ($n = 47$)	High ($n = 50$)	
Age (years)				0.980
≤45	35	17	18	
>45	62	30	32	
Gender				0.970
Male	60	29	31	
Female	37	18	19	
Tumor size (cm)				0.085
≤3	33	20	13	
>3	64	27	37	
Necrosis				0.618
Yes	47	24	23	
No	50	23	27	
WHO grade			0.41	0.001
I-II	46	33	13	
IV	51	14	37	
IDH status			0.32	0.001
Wild-type	54	18	36	
Mutation	43	29	14	
1p/19q status				0.180
No deletion	72	32	40	
Co-deletion	25	15	10	
MGMT status			0.37	0.001
No methylation	55	17	38	
Methylation	42	30	12	

reverse-transcribed to complementary DNA (cDNA) using a PrimeScript RT reagent kit (Thermo, Beijing, China) according to the manufacturer's protocol. Its synthesis was conducted at 37°C for 15 min, then 85°C for 5 s according to the experimental protocols. Real-time PCR reactions were carried by Applied Biosystems 7500. Real-time PCR was carried in triplicate. We selected glyceraldehyde3-phosphate dehydrogenase (GAPDH) as a suitable endogenous reference gene. The relative TCF7L2 expression was computed and normalized using the $2^{-\Delta CT}$ method relative to GAPDH. The primers for TCF7L2: 5′-TGCT CTGCGGTTGCTATGTTGAC-3′, 3′-GCT GCGAGTCCTCAC CAATGTC-5′ and for GAPDH: 5′-CAGACCACAG TCCATGC CATCAC-3′, 3′-GACGCCTGCTTCACCACCTTC-5′.

Data Analysis

The comparison of the TCF7L2 expression level between GBM and low-grade glioma was performed by the two-sample Student's *t*-test. The chi-square test was used to examine the associations between TCF7L2 expression and the clinicopathological characteristics.

In addition, survival curves were drawn by the Kaplan-Meier method and analyzed with log-rank test. Cox proportional-hazards regression analysis was applied to estimate univariate and multivariate hazard ratios for OS. A value of $P < 0.05$ was considered as statistically significant. SPSS software 20.0 was applied in the present study.

RESULTS

TCF7L2 Was Upregulated in Glioblastoma Tissues

We measured TCF7L2 expression levels in 97 patients with glioma by qRT-PCR. The data revealed that TCF7L2 had a higher expression in GBM tissues than the low-grade group ($p = 0.001$) (**Figure 1**).

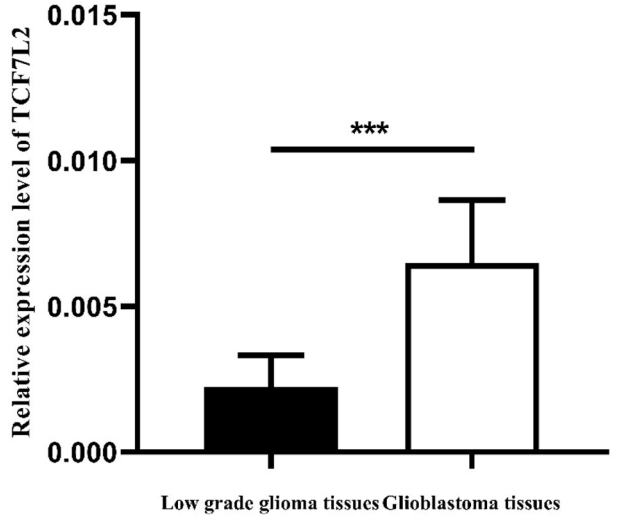

FIGURE 1 | Expression levels of TCF7L2 in GBM tissues were significantly higher (***$p = 0.001$).

Relation Between TCF7L2 Expression and Clinicopathological Factors of GBM Patients

We found high TCF7L2 expression in GBM. The median expression level of TCF7L2 was used as a dividing point, and we divided 97 patients into two groups (high and low expression). **Table 1** summarizes the relationship between TCF7L2 expression and clinicopathological parameters in glioma. The results showed that TCF7L2 high expression was significantly related to higher WHO grade ($p = 0.001$), isocitrate dehydrogenase (IDH) wild-type ($p = 0.001$), and lack of O(6)-methylguanine-DNA methyltransferase (MGMT) methylation ($p = 0.001$).

Upregulation of TCF7L2 Confers Poor Prognosis in Patients

Univariate and multivariate analyses were utilized to evaluate the association between OS and various clinicopathological features including TCF7L2 expression level (**Table 1**).

The Kaplan-Meier method indicated that the 5-year OS of patients was significantly shorter in patients with high TCF7L2 expression than in those with low TCF7L2 expression ($p = 0.010$), but there were no significant differences in 2-year OS ($p = 0.070$). The OS was significantly longer with small tumor size (≦3 cm) compared to those with large tumor size (>3 cm) ($p = 0.020$). The OS was significantly shorter in patients with IDH wild-type than in those with IDH mutation ($p = 0.010$). The OS was significantly shorter in patients receiving subtotal resection than those receiving total resection ($p = 0.010$), but was significantly longer in patients in the low-grade group compared to those with glioblastoma ($p = 0.001$). The OS was significantly shorter in patients with no 1p/19q deletion than in those with 1p/19q codeletion ($p = 0.001$). The OS was significantly shorter in patients with no MGMT methylation than in those with MGMT methylation ($p = 0.010$). There were no significant differences between necrosis and non-necrosis patients ($p = 0.420$) (**Figures 2**, **3**).

As for multivariate Cox regression analysis including TCF7L2 expression, WHO grade, extent of resection, 1p/19q status, IDH status, and MGMT status, we found a 5-year OS advantage of the low expression vs high expression of TCF7L2 (HR 2.56, 95% CI:1.16–5.68, $p = 0.020$), low-grade glioma vs. glioblastoma (HR 79.94, 95% CI:18.88–338.39, $p = 0.001$), total resection vs subtotal resection (HR 2.09, 95% CI:1.09–4.01, $p = 0.030$), IDH mutation vs IDH wild-type (HR 0.36, 95% CI:0.15–0.87, $p = 0.020$), 1p/19q codeletion vs no 1p/19q deletion (HR 0.33, 95% CI: 0.12–0.93, $p = 0.040$), and MGMT methylation vs no MGMT methylation (HR 0.34, 95% CI:0.16–0.71, $p = 0.010$) (**Table 2**).

DISCUSSION

TCF7L2 has been reported to have an effect on the suppression of cell proliferation, migration, and invasion in the literature (15). The transcription factor 7-like 2 (TCF7L2) gene may affect

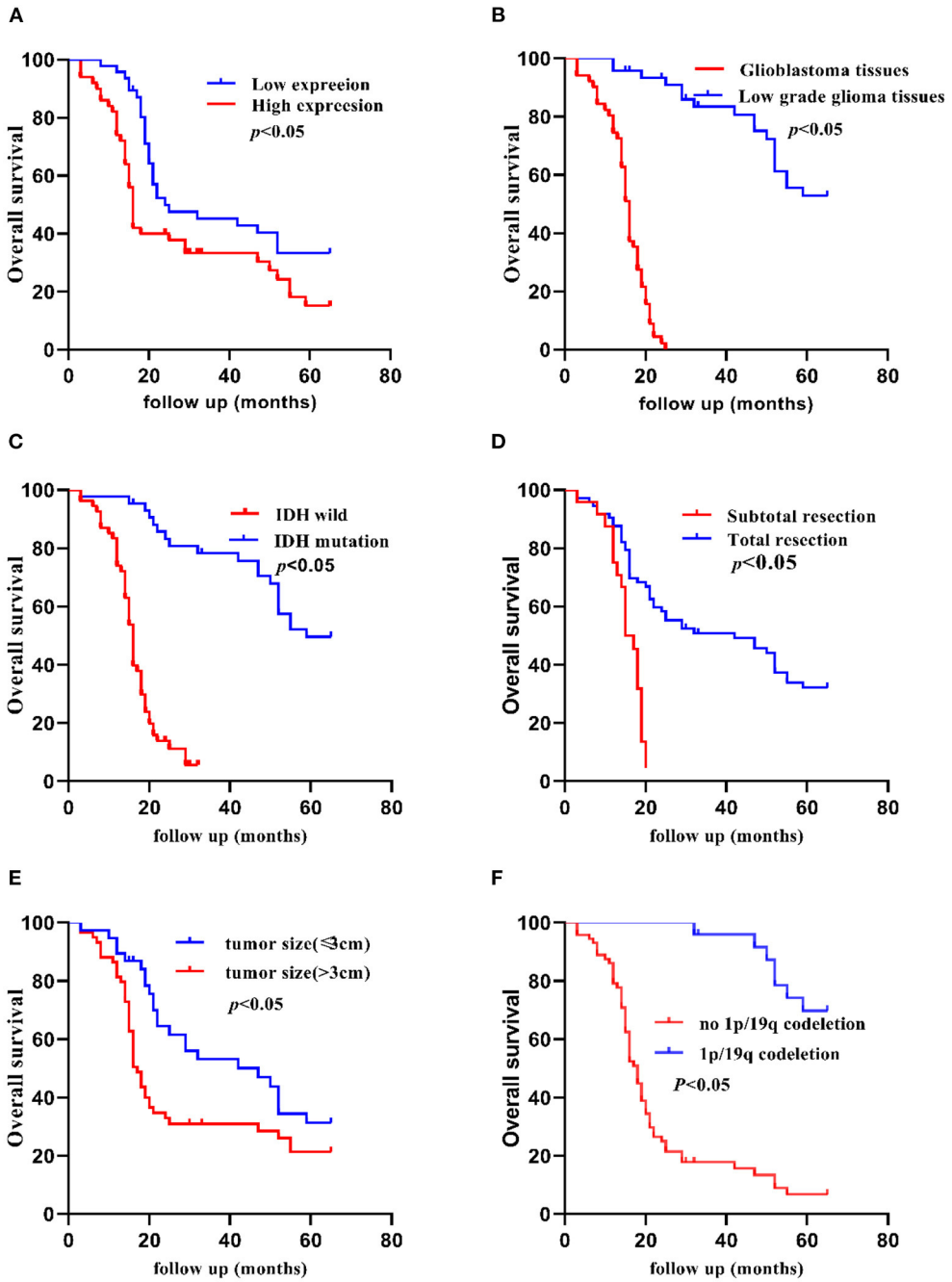

FIGURE 2 | Kaplan-Meier 5-year OS curves of patients with glioma according to clinicopathological features. **(A)** Patients with higher TCF7L2 expression showed shorter OS compared with those with a lower expression ($p = 0.010$), **(B)** Glioblastoma patients showed worse OS compared with low-grade patients ($p = 0.001$). **(C)** Patients with IDH wild-type showed worse OS compared with those with an IDH mutation ($p = 0.010$). **(D)** Patients who had a subtotal resection showed worse OS compared with those who had a total resection ($p = 0.010$). **(E)** Patients with a larger tumor size (>3 cm) showed worse OS compared with those with a small tumor size (≤3 cm) ($p = 0.020$). **(F)** Patients with no 1p/19q codeletion showed worse OS compared with those with 1p/19q codeletion ($p = 0.001$).

cancer development and prognosis because the TCF7L2 gene plays an important role in the Wnt/β-catenin signaling pathway (16, 17).

To date, various biological markers have been reported in glioma (18, 19). TCF7L2 represents a central factor in metabolism, cell proliferation, and cell apoptosis (20, 21). Bo Yu et al. (15) found that TCF7L2 overexpression increased cell viability, migration, and invasion in cells with CRNDE inhibition. The TCF7L2 expression and prognostic value in glioma have rarely been reported.

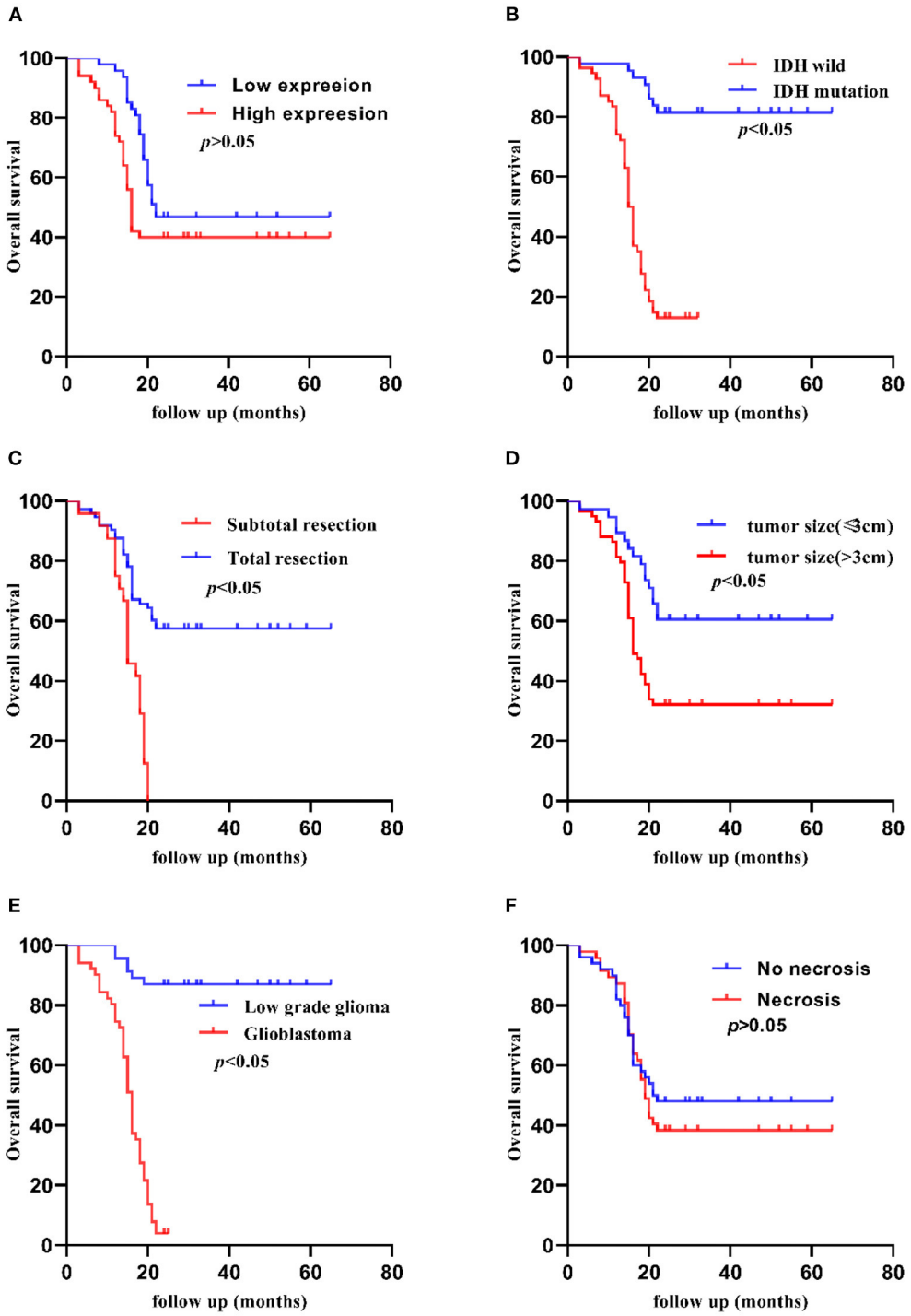

FIGURE 3 | Kaplan-Meier 2-year OS curves of patients with glioma according to clinicopathological features. **(A)** Patients with higher TCF7L2 expression showed no significant differences compared with those with a lower expression ($p = 0.008$). **(B)** Patients with IDH wild-type showed worse OS compared with those with an IDH mutation ($p = 0.001$). **(C)** Patients who had a subtotal resection showed worse OS compared with those who had a total resection ($p = 0.001$). **(D)** Patients with a larger tumor size (>3 cm) showed worse OS compared with those with a small tumor size (≤3 cm) ($p = 0.003$). **(E)** Glioblastoma patients showed worse OS compared with low-grade patients ($p = 0.001$). **(F)** Patients with necrosis showed no significant differences compared with those with no necrosis ($p = 0.486$).

TABLE 2 | Univariate and multivariate analyses of 5-year OS.

Parameter	Univariate			Multivariate		
	HR	95% CI	*P*	HR	95% CI	*P*
Age (≤45/>45)	1.01	1 0.61–1.67	0.960			
Sex (Male/female)	0.85	0.52–1.38	0.510			
Tumor size (≤3 cm/>3 cm)	1.77	1.07–2.92	0.020			
Necrosis (Yes/no)	1.21	0.75–1.95	0.430			
WHO grade (I-II/IV)	38.64	12.84–116.24	0.001	79.94	18.88–338.39	0.001
TCF7L2 expression (High/low)	1.86	1.14–3.01	0.010	2.56	1.16–5.68	0.020
IDH status (Wild-type/mutation)	0.09	0.04–0.19	0.010	0.36	0.15–0.87	0.020
Extent of resection (Subtotal/total)	6.12	3.36–11.17	0.010	2.09	1.09–4.01	0.030
1p/19q status (No deletion/co-deletion	0.10	0.05–0.23	0.001	0.33	0.12–0.93	0.040
MGMT status (No methylation/methylation	0.53	0.32–0.85	0.010	0.34	0.16–0.71	0.010

In our study, we detected significantly higher TCF7L2 expression in GBM tissues than in the low-grade group. Moreover, TCF7L2 overexpression was significantly related with higher WHO grade, IDH wild-type, and no MGMT methylation, and the coefficients were 0.41, 0.32, and 0.37, respectively.

Our study reported shorter OS in patients with higher TCF7L2 expression, however, there was no significant difference in 2-year OS in the two groups. We found that the 2-year OS was relatively high in the patients who underwent standard therapies including radiotherapy with concomitant temozolomide (TMZ) and adjuvant TMZ after surgery in the high expression group. There was statistical significance in 5-year survival rate. On the other hand, TCF7L2 might be more advantageous in judging long-term prognosis.

Multivariate analysis revealed that TCF7L2, WHO grade, IDH status, extent of resection, 1p/19q status, and MGMT methylation status were independent prognostic factors for OS. The hazard ratio in the high TCF7L2 expression group was 2.56 times more than the low expression group (95% CI: 1.16–5.68, $p = 0.020$). TCF7L2 expression was independently related with OS, indicating that higher TCF7L2 level was a marker of poor prognosis for patients.

IDH mutation was found in both low-grade glioma and glioblastoma in our study, suggesting the IDH gene played an important role in the pathogenesis of tumors in glioma. The mutation rate was 15.6%, which was practically consistent with that reported in the literature (22). The multivariate analysis revealed that the patients of IDH mutation were closely associated with better prognosis, as compared with those of IDH wild-type.

Previous studies have reported that IDH mutations have been identified as one of the most important diagnostic and prognostic factors of gliomas (23). Due to intra-group heterogeneity, we need additional prognostic factors to subdivide the prognosis results in gliomas. There was a correlation between IDH status and TCF7L2 expression level, therefore, we would combine IDH status and TCF7L2 expression to further refine the stratified study and better judge the prognosis in a future study.

Previous studies have reported that patients with 1p/19q co-deletion have better prognosis and response to treatment (24, 25). 1p/19q co-deletion is a typical molecular genetic feature of oligodendroglioma, which provides an important reference for pathological diagnosis. We found that patients with 1p/19q co-deletion had a better prognosis than those no 1p/19q co-deletion. The results were consistent with literature reports.

Surgical resection plays a critical role in glioma therapy, which can reduce tumor load and provide an opportunity for postoperative adjuvant therapy. We found that patients receiving gross total resection had a better prognosis than those receiving subtotal resection. The results were consistent with other literature reports (26).

Glioblastoma patients showed worse OS compared with low-grade patients. In our study, we did not include WHO III patients, therefore, the hazard ratio was larger in the multivariate analysis. In addition, the sample size of data was relatively small, which might have introduced a bias. Currently, MGMT methylation is a widely accepted biomarker in glioblastoma, which can predict the effect of chemotherapeutic drugs (27). Patients with MGMT methylation showed a better prognosis than those with no methylation.

The sample size of data was relatively small. Some patients were reluctant to attend follow-up appointments, or the follow-up was interrupted in our study. We will increase the sample size for detailed study in the future.

TCF7L2 could be a potential prognostic factor and therapeutic target for patients with glioma. The underlying molecular mechanisms of TCF7L2 involvement in the Wnt/β-catenin signaling pathway needs to be investigated in future studies.

DATA AVAILABILITY STATEMENT

The raw data supporting the conclusions of this article will be made available by the authors, without undue reservation.

ETHICS STATEMENT

The studies involving human participants were reviewed and approved by the Capital Medical University Hospital Ethics

Committees. The patients/participants provided their written informed consent to participate in this study.

AUTHOR CONTRIBUTIONS

LC, SH, and NL analyzed and interpreted the glioma patient data. SJ performed the qRT-PCR of the glioma tissues. CY and SJ were major contributors in writing the manuscript. All authors read and approved the final manuscript.

ACKNOWLEDGMENTS

We appreciated W-Y. Deng for providing constructive suggestions to the manuscript.

REFERENCES

1. Darlix A, Zouaoui S, Rigau V, Bessaoud F, Figarella-Branger D, Mathieu-Daudé H, et al. Erratum to: Epidemiology for primary brain tumors: a nationwide population-based study. *J Neurooncol.* (2017) 131:547. doi: 10.1007/s11060-016-2340-5
2. Ostrom QT, Gittleman H, Fulop J, Liu M, Blanda R, Kromer C, et al. CBTRUS statistical report: primary brain and central nervous system tumors diagnosed in the United States in 2008-2012. *Neuro Oncol.* (2015) 17(Suppl 4):iv1–62. doi: 10.1093/neuonc/nov189
3. Koshy M, Villano JL, Dolecek TA, Howard A, Mahmood U, Chmura SJ, et al. Improved survival time trends for glioblastoma using the SEER 17 population-based registries. *J Neurooncol.* (2012) 107:207–12. doi: 10.1007/s11060-011-0738-7
4. Stupp R, Hegi ME, Mason WP, van den Bent MJ, Taphoorn MJ, Janzer RC, et al. Effects of radiotherapy with concomitant and adjuvant temozolomide versus radiotherapy alone on survival in glioblastoma in a randomised phase III study: 5-year analysis of the EORTC-NCIC trial. *Lancet Oncol.* (2009) 10:459–66. doi: 10.1016/S1470-2045(09)70025-7
5. Stupp R, Mason WP, van den Bent MJ, Weller M, Fisher B, Taphoorn MJ, et al. Radiotherapy plus concomitant and adjuvant temozolomide for glioblastoma. *N Engl J Med.* (2005) 352:987–96. doi: 10.1056/NEJMoa043330
6. Cancer Genome Atlas Network. Comprehensive molecular characterization of human colon and rectal cancer. *Nature.* (2012) 487:330–7. doi: 10.1038/nature11252
7. Hrckulak D, Kolar M, Strnad H, Korinek V. TCF/LEF transcription factors: an update from the internet resources. *Cancers.* (2016) 8:70. doi: 10.3390/cancers8070070
8. Chen J, Yuan T, Liu M, Chen P. Association between TCF7L2 gene polymorphism and cancer risk: a meta-analysis. *PLoS ONE.* (2013) 8:e71730. doi: 10.1371/journal.pone.0071730
9. Lu XP, Hu GN, Du JQ, Li HQ. TCF7L2 gene polymorphisms and susceptibility to breast cancer: a meta-analysis. *Genet Mol Res.* (2015). 14:2860–7. doi: 10.4238/2015.March.31.16
10. Wang F, Jiang L, Li J, Yu X, Li M, Wu G, et al. Association between TCF7L2 polymorphisms and breast cancer susceptibility: a meta-analysis. *Int J Clin Exp Med.* (2015) 8:9355–61.
11. Zhang M, Tang M, Fang Y, Cui H, Chen S, Li J, et al. Cumulative evidence for relationships between multiple variants in the VTI1A and TCF7L2 genes and cancer incidence. *Int J Cancer.* (2018) 142:498–513. doi: 10.1002/ijc.31074
12. Angus-Hill ML, Elbert KM, Hidalgo J, Capecchi MR. T-cell factor 4 functions as a tumor suppressor whose disruption modulates colon cell proliferation and tumorigenesis. *Proc Natl Acad Sci USA.* (2011) 108:4914–9. doi: 10.1073/pnas.1102300108
13. Mayer CD, Giclais SM, Alsehly F, Hoppler S. Diverse LEF/TCF expression in human colorectal cancer correlates with altered Wnt-regulated transcriptome in a meta-analysis of patient biopsies. *Genes.* (2020) 11:538. doi: 10.3390/genes11050538
14. Pignatti F, van den Bent M, Curran D, Debruyne C, Sylvester R, Therasse P, et al. Prognostic factors for survival in adult patients with cerebral low-grade glioma. *J Clin Oncol.* (2002) 20:2076–84. doi: 10.1200/JCO.2002.08.121
15. Yu B, Ye X, Du Q, Zhu B, Zhai Q, Li XX. The long non-coding RNA CRNDE promotes colorectal carcinoma progression by competitively binding miR-217 with TCF7L2 and Enhancing the Wnt/β-catenin signaling pathway. *Cell Physiol Biochem.* (2017) 41:2489–502. doi: 10.1159/000475941
16. Spranger S, Bao R, Gajewski TF. Melanoma-intrinsic β-catenin signalling prevents anti-tumour immunity. *Nature.* (2015) 523:231–5. doi: 10.1038/nature14404
17. Zhao C, Deng Y, Liu L, Yu K, Zhang L, Wang H, et al. Dual regulatory switch through interactions of Tcf7l2/Tcf4 with stage-specific partners propels oligodendroglial maturation. *Nat Commun.* (2016) 7:10883. doi: 10.1038/ncomms10883
18. Qu DW, Xu HS, Han XJ, Wang YL, Ouyang CJ. Expression of cyclinD1 and Ki-67 proteins in gliomas and its clinical significance. *Eur Rev Med Pharmacol Sci.* (2014) 18:516–9. doi: 10.1016/j.jep.2013.12.015
19. Li W, Xie P, Ruan WH. Overexpression of lncRNA UCA1 promotes osteosarcoma progression and correlates with poor prognosis. *J Bone Oncol.* (2016) 5:80–5. doi: 10.1016/j.jbo.2016.05.003
20. Chen C, Cao F, Bai L, Liu Y, Xie J, Wang W, et al. IKKβ Enforces a LIN28B/TCF7L2 positive feedback loop that promotes cancer cell stemness and metastasis. *Cancer Res.* (2015) 75:1725–35. doi: 10.1158/0008-5472.CAN-14-2111
21. Weng Q, Tan B, Wang J, Wang J, Zhou H, Shi J, et al. Corrigendum to "5-Fluorouracil causes severe CNS demyelination by disruption of TCF7L2/HDAC1/HDAC2 complex in adolescent mice" [Toxicology 325 (2014) 144-150]. *Toxicology.* (2020) 430:152342. doi: 10.1016/j.tox.2019.152342
22. Ichimura K, Pearson DM, Kocialkowski S, Bäcklund LM, Chan R, Jones DT, et al. IDH1 mutations are present in the majority of common adult gliomas but rare in primary glioblastomas. *Neuro Oncol.* (2009) 11:341–7. doi: 10.1215/15228517-2009-025
23. Mirchia K, Richardson TE. Beyond IDH-mutation: emerging molecular diagnostic and prognostic features in adult diffuse gliomas. *Cancers.* (2020) 12:1817. doi: 10.3390/cancers12071817
24. Buckley PG, Alcock L, Heffernan J, Woods J, Brett F, Stallings RL, et al. Loss of chromosome 1p/19q in oligodendroglial tumors: refinement of chromosomal critical regions and evaluation of internexin immunostaining as a surrogate marker. *J Neuropathol Exp Neurol.* (2011) 70:177–82. doi: 10.1097/NEN.0b013e31820c765b
25. Durand KS, Guillaudeau A, Weinbreck N, DeArmas R, Robert S, Chaunavel A, et al. 1p19q LOH patterns and expression of p53 and Olig2 in gliomas: relation with histological types and prognosis. *Mod Pathol.* (2010) 23:619–28. doi: 10.1038/modpathol.2009.185
26. Lee JH, Jung TY, Jung S, Kim IY, Jang WY, Moon KS, et al. Performance status during and after radiotherapy plus concomitant and adjuvant temozolomide in elderly patients with glioblastoma multiforme. *J Clin Neurosci.* (2013) 20:503–8. doi: 10.1016/j.jocn.2012.03.044
27. Butler M, Pongor L, Su YT, Xi L, Raffeld M, Quezado M, et al. MGMT status as a clinical biomarker in glioblastoma. *Trends Cancer.* (2020) 6:380–91. doi: 10.1016/j.trecan.2020.02.010

Conflict of Interest: The authors declare that the research was conducted in the absence of any commercial or financial relationships that could be construed as a potential conflict of interest.

The Reviewer YW declared a shared affiliation, with no collaboration, with the authors SJ, LC, SH, NL, MH, YY, and CY.

frontiers in Oncology

ORIGINAL RESEARCH
published: 02 November 2021
doi: 10.3389/fonc.2021.673780

SPAG5 Is Involved in Human Gliomagenesis Through the Regulation of Cell Proliferation and Apoptosis

*Chunhong Wang, Haiyang Su, Rui Cheng and Hongming Ji**

Department of Neurosurgery, Shanxi Medical University Shanxi Provincial People's Hospital, Taiyuan, China

Background: Glioma is the most frequent malignant primary brain tumor in adults.

Objective: To explore the role of sperm-associated antigen 5 (SPAG5) in glioma.

Methods: The association between SPAG5 expression and clinical features was investigated based on The Cancer Genome Atlas (TCGA) datasets. The function of SPAG5 in glioma was analyzed using U87 and U251 cells. Knockdown glioma cells were constructed by shRNA interference. qRT-PCR and Western blotting were used to measure the expression of SPAG5 and Cadherin 2 (CDH2). Cell proliferation and apoptosis were measured by 3-(4,5-dimethylthiazol-2-yl)-2,5-diphenyltetrazolium bromide (MTT) assay, caspase 3/7 assay, and high-content screening (HCS) proliferation analysis and colony formation assay. Transwell assays and wound-healing assays were used to investigate cell migration and invasion.

Results: The increased expression of SPAG5 was correlated with poor outcomes in glioma patients. Knocking down SPAG5 could inhibit the proliferation and colony formation and promoted the apoptosis of glioma cells. Knocking down SPAG5 could also inhibit cell migration and invasion and the expression of CDH2. Overexpression of CDH2 with SPAG5 depletion could restore the proliferation and inhibit the apoptosis of glioma cells, which also promoted cell migration and invasion.

Conclusions: SPAG5 is a promising prognostic factor and potential therapeutic target for clinical intervention in glioma.

Keywords: SPAG5, glioma, proliferation, apoptosis, migration and invasion

OPEN ACCESS

Edited by:
Yaohua Liu,
Shanghai First People's Hospital, China

Reviewed by:
Jun Dong,
Second Affiliated Hospital of Soochow University, China
Zhao Wenyang,
The First Affiliated Hospital of Harbin Medical University, China

***Correspondence:**
Hongming Ji
jihongming1001@163.com

Specialty section:
This article was submitted to Neuro-Oncology and Neurosurgical Oncology, a section of the journal Frontiers in Oncology

Received: *28 February 2021*
Accepted: *04 October 2021*
Published: *02 November 2021*

Citation:
Wang C, Su H, Cheng R and Ji H (2021) SPAG5 Is Involved in Human Gliomagenesis Through the Regulation of Cell Proliferation and Apoptosis. Front. Oncol. 11:673780. doi: 10.3389/fonc.2021.673780

INTRODUCTION

Glioma is a neuroectodermal tumor arising from glial or precursor cells (1), which represents one of the most frequent malignant neoplasm in the central nervous system (2). Studies demonstrated that glioma accounts for about 75% of primary malignant brain tumors in adults (3, 4). Despite current advances in the therapy of glioma, the overall 5-year survival rate of glioma patients undergoing comprehensive treatments, including surgical resection, adjuvant radiotherapy, and chemotherapy, is disappointingly low (5). Particularly, most of the glioma patients with high grade succumb to this

disease within 2 years of diagnosis (6). Therefore, it poses great challenges to understand the potential molecular pathogenesis of glioma, to identify novel prognostic molecular markers, and to develop new therapeutic strategies (7).

Sperm-associated antigen 5 (SPAG5, also called astrin and hMAP126), which maps to Ch17q11.2 and codes for a mitotic spindle-associated protein (8), plays a key role in the regulatory network of mitosis by forming a molecular switch with a mass of protein partners (9). During mitosis, SPAG5 could interact with many proteins, such as CLASP1, astrin, and Kif2b, to regulate the centromere–microtubule dynamics and thus promotes mitotic processes and their fidelity (10). It was reported that SPAG5 has participated in growth and progression of various tumors, which was overexpressed in breast cancer (11, 12), osteosarcoma (13), lung cancer (14), bladder urothelial carcinoma (15), prostate cancer (16), and cervical cancer (17). Thus, it is deduced that SPAG5 may also take part in the tumorigenesis and progression of glioma. However, the clinical significance of SPAG5 and its biological role in glioma remain obscure.

The epithelial-to-mesenchymal transition (EMT) is a very complex process underlying cell movement during embryonic development and morphogenesis, in which several family transcription factors form a network through many signaling pathways, allowing cancer cells to acquire invasive properties and penetrate adjacent stroma (18, 19). *In vitro*, SPAG5 silencing inhibits the EMT process of osteosarcoma cells, and SPAG5 may serve as a prognostic indicator and potential therapeutic target for patients with osteosarcoma (13). Although the significance of EMT in gliomagenesis is still unclear, it has been confirmed to be closely related to glioblastomas (GBMs) (20). Cadherin 2 (CDH2) encodes N-cadherin, which is also a hallmark of EMT. Tumor endothelial cell-derived CDH2 promotes angiogenesis and has prognostic significance for lung adenocarcinoma (21). A growing body of evidence suggests that CDH2 is closely associated with glioma.

In the present study, we intended to characterize the role of SPAG5 in gliomagenesis and explore the underlying mechanisms. Our results provided the evidence that downregulation of SPAG5 represses glioma cell proliferation and attenuates glioma cell migration and invasion *in vitro*. To further explore the regulatory mechanism of SPAG5 in glioma cells, the relationship between SPAG5 and CDH2 was also analyzed. Taken together, these data demonstrate the biological and clinical significance of SPAG5 as a potential biomarker.

METHODS

The Cancer Genome Atlas Database Analysis

We downloaded clinical characteristics and the data of SPAG5 mRNA expression profile chip expression data from The Cancer Genome Atlas (TCGA) database (http://www.cbioportal.org), including 667 glioma specimens and 10 normal specimens. The RNA-seq level 3 data of the expression profile of these samples were downloaded and sorted and directly used for the analysis of the mRNA expression of SPAG5. For pathological analysis, the RNA-seq level 3 data from the 667 glioma specimens, which was divided into low-grade gliomas (LGGs, n = 515, WHO II and WHO III grade gliomas) and GBMs (n = 152). We use the Affy and Limma packages in the R language to standardize and T test our data and then filter according to P value <0.05 and $|FC| \geq 2$. According to the median of the SPAG5 mRNA expression, the 667 glioma specimens were further divided into low SPAG5 expression group (n = 334) and high SPAG5 expression group (n = 333). The association between the mRNA expression level of SPAG5 and the overall survival time of glioma patients was then analyzed by Kaplan–Meier curves.

Cell Culture and Transfection

Glioma cell lines (U87 and U251) were purchased from Shanghai Genechem Co., Ltd. (Shanghai, China). Cells were cultured in Dulbecco's modified Eagle's medium (DMEM; Corning) supplemented with 10% fetal bovine serum (FBS; Ausbian) and cultured in a 5% CO_2 incubator at 37°C. To knock down SPAG5 and overexpress CDH2, the plasmids specifically expressing SPAG5 shRNA and CDH2 mRNA were constructed using pAdTrack-CMV plasmid (Addgene, Cambridge, MA, USA) as the vector. The plasmids expressing the mRNA or shRNA that are not targeting any known human gene were used as the negative control. The cells were transfected with shSPAG5, CDH2 mRNA, or control mRNA or shRNA by Lipofectamine 2000 (Invitrogen, CA, USA) according to the instruction.

Quantitative Real-Time Polymerase Chain Reaction

The total RNAs were extracted with TRIzol reagent (Invitrogen, Carlsbad, CA, USA) according to the manufacturer's protocol and reversed to cDNA (Invitrogen, CA, USA). qRT-PCR was performed, and the sequences of the PCR primers are as follows: SPAG5 F: 5′-TTGAGGCCCGTTTAGATACCA-3′ and R: 5′-GCTTTCCTTGGAGC-AATGTAGTT-3′; glyceraldehyde 3-phosphate dehydrogenase (GAPDH), F: 5'-TGACTTC AACAGCGACACCCA-3′ and R: 5'-CACCCTGTTGC TGTAGCCAAA-3′. The relative expression of SPAG5 was presented as $2^{-\Delta\Delta Ct}$ value.

Western Blotting

Western blotting was carried out according to the literature description (17). The primary antibodies are as follows: rabbit polyclonal SPAG5 (1:200, Sigma-Aldrich, Germany), mouse monoclonal GAPDH (1:2,000, Santa-Cruz, CA, USA), rabbit polyclonal CDH2 (1:100, Cell Signaling Technology, MA, USA), rabbit IgG (1:2,000, Santa-Cruz, CA, USA). A horseradish peroxidase (HRP)-conjugated anti-rabbit or anti-mouse IgG antibody was used as the secondary antibody (1:2,000, Santa-Cruz, CA, USA).

Cell Proliferation and Apoptosis Assays

The 3-(4,5-dimethylthiazol-2-yl)-2,5-diphenyltetrazolium bromide (MTT) assay was used to measure cell proliferation rate. Glioma cells (2×10^3 cells/well) were seeded onto 96-well plates. Subsequently, 20 µl MTT (5 mg/ml) solution was added to each well and incubated for 4 h at 37°C. After aspirating the

medium, 100 µl dimethyl sulfoxide (DMSO) was added to solubilize the formazan crystals formed by viable cells. Optical density (OD) was measured at 490 nm. The observation duration lasted for 5 days.

Colony Formation Assay

Adherent glioma cells in the logarithmic phase were trypsinized and counted to measure viability. Then, viable cells (600 cells/well) were seeded onto each well of a six-well plate. Glioma cells were allowed to adhere and grow for 15 days. Media were replaced every 3 days. When colonies were formed, we removed media and added 1 ml 4% paraformaldehyde to each well to fix cells for 30 min and stained them with crystal violet solution (22). Finally, colonies were counted. Data gathered from three independent experiments were expressed as mean colony number ± SD.

Apoptosis Assay

Caspase 3/7 assay was used to assess apoptosis according to the manufacturer's instructions (Caspase-Glo® 3/7 Assay, Promega Corporation, Cat. No. G8092).

Wound-Healing Assay

The 5×10^4 glioma cells were inoculated in 96-well plate. When the cells grew to 90% confluence, we scratched the bottom of the dishes across each well using a scratch tester. Cells were rinsed 2–3 times with serum-free medium and cultivated in 0.5% FBS. The wound-healing process was observed for 24 h, and photos were taken at 8 and 24 h.

Cell Migration and Invasion Assays

The cell migration and invasion assays were carried out by Transwell kit (Corning, US) following the manufacturer's instructions. In brief, some chambers were inserted in a new 24-well plate, and 5×10^3 cells in 100 µl medium without FBS were seeded on the upper chamber in Transwell apparatus. Then, 600 µl medium with 10% FBS was added in the lower chamber. After the cells were incubated for 16 h at 37°C, the medium in chambers were removed with absorbent paper, and cells on the chambers were wiped off with a cotton swab. The cells adhering to chambers were treated with 4% paraformaldehyde for 30 min to fix and stained with Giemsa solution and counted and visualized under a microscope in nine random fields (×200). The process of the invasion assay was similar to the cell migration experiment, except that the Transwell membrane was precoated with Matrigel basement membrane and the cells were cultured for 18 h at 37°C. The cell count method was the same as the cell migration assay.

High-Content Screening Proliferation Analysis

Cells in the logarithmic growth phase were trypsinized and completely resuspended into cell suspension and counted. The cells (1,500 cells/well) were seeded onto each well of a 96-well plate and cultured at 37°C with 5% CO_2. The day after planking, the number of green fluorescent cells was counted under Celigo cytometry system (Nexcelom, Beijing, China) for 5 consecutive days. Lentivirus 2000 was used to infect cells to make the glioma cells express SPAG5 and green fluorescent proteins, so as to facilitate the automatic cell count. To further explore the effect of SPAG5 knockdown, CDH2 was overexpressed. The experiment was divided into the following: NC+NC group (parental glioma cells + vector), KD+NC group (parental glioma cells + knockdown-SPAG5 + vector), and KD+OE group (parental glioma cells + knockdown-SPAG5 + overexpression-CDH2).

Statistical Analysis

All quantified data were obtained from at least three independent experiments and analyzed using SPSS 17.0 software. Data are shown as mean ± SD. The Kaplan–Meier method was used for survival analysis. The log-rank test was used to assess differences in survival. Spearman's method was applied in analyzing the relationship between gene expression level and clinical variables. Comparison of gene expression between groups was conducted using Mann–Whitney *U*. The differences between groups were analyzed using two-tailed Student's *t*-test and ANOVA. Differences were considered statistically significant when $P < 0.05$.

RESULTS

SPAG5 Expression Is Correlated With Prognosis

Analysis of the mRNA expression profiles of SPAG5 in TCGA revealed that the mRNA expression of SPAG5 was higher in glioma tissues (n = 667) than that in normal tissues (n = 10) ($P < 0.05$; **Figure 1A**). Meanwhile, the mRNA expression of SPAG5 was higher in GBMs (n = 152) than that in LGGs (n = 515) ($P < 0.05$; **Figure 1B**).

We next analyzed the relationship between the mRNA expression of SPAG5 and clinic characteristics, including age, sex, and grade (**Table 1**) in 667 glioma patients. According to the median of the SPAG5 mRNA expression, the 667 glioma specimens were further divided into low SPAG5 expression group (n = 334) and high SPAG5 expression group (n = 333). The mRNA expression levels of SPAG5 were significantly associated with overall survival time. And the high mRNA level of SPAG5 indicated poor prognosis. The expression levels of SPAG5 were not significantly associated with sex but were significantly associated with age ($P < 0.001$) and grade ($P < 0.001$). Furthermore, the overall survival between glioma patients with low (n = 334) and high (n = 333) expression of SPAG5 was compared, who were grouped according to the median of the expression of SPAG5. A Kaplan–Meier curve was obtained (**Figure 1C**). Glioma patients with low expression of SPAG5 showed a higher overall survival rate than glioma patients with high expression of SPAG5 [log-rank $P = 0.03$; hazard ratio (HR) = 3.324, CI 2.521–4.328].

SPAG5 Knockdown Inhibited Cell Proliferation and Promoted Apoptosis *In Vitro*

The biological function of SPAG5 in glioma was next studied. Cell proliferation analysis was performed in the two cell lines (U87 and U251) transfected with SPAG5-shRNA. The mRNA and protein

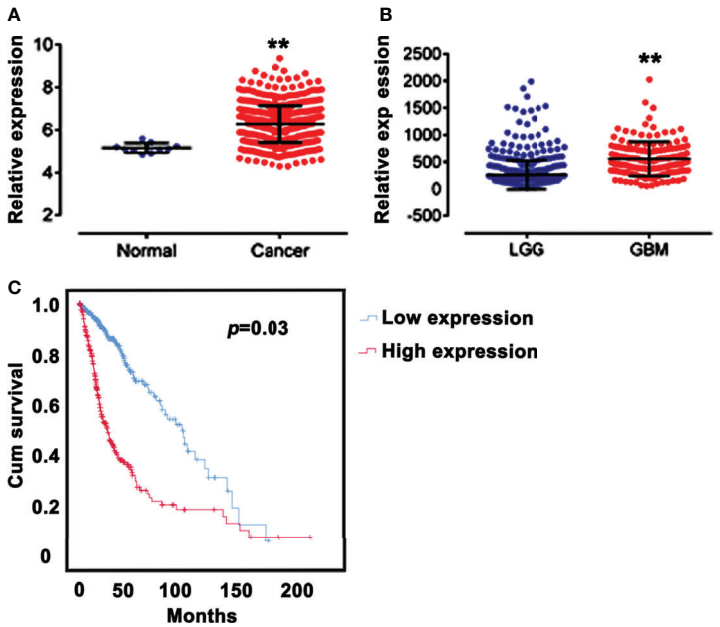

FIGURE 1 | SPAG5 expression is correlated with prognosis. **(A)** Relative expression of SPAG5 in normal (n = 10) and glioma tissues (n = 667). The SPAG5 mRNA expression profile chip data including 667 glioma specimens and 10 normal specimens were all from TCGA database. vs Normal group, $^{**}P < 0.01$. **(B)** Relative expression of SPAG5 in low-grade gliomas (LGGs, n = 515) and glioblastomas (GBM, n = 152). The SPAG5 mRNA expression data of 667 glioma specimens were from TCGA database. vs LGG group, $^{**}P < 0.01$. **(C)** Kaplan-Meier curves for glioma patients with low (n = 334) and high (n = 333) expression of SPAG5. According to the median, 667 glioma specimens from TCGA database were further divided into low SPAG5 expression group (n = 334) and high SPAG5 expression group (n = 333).

TABLE 1 | The relationship between SPAG5 expression level and clinic characteristics in glioma patients.

		SPAG5 expression level		Total	*P* value
		Low	High		
Age	≤46	212	128	340	<0.001
	>46	122	205	327	
Total		334	333	667	
Sex	Male	188	196	384	0.502
	Female	146	137	283	
Total		334	333	667	
Grade	LGG	317	198	515	<0.001
	GBM	17	135	152	
Total		334	333	667	

According to the median of the SPAG5 mRNA expression, the 667 glioma specimens were further divided into low SPAG5 expression group (n = 334) and high SPAG5 expression group (n = 333). LGG, low-grade glioma; GBM, glioblastoma; SPAG5, sperm-associated antigen 5.

of SPAG5 in stable cell lines were examined by qRT-PCR and Western blotting. After transfection with SPAG5-shRNA, the mRNA and protein expression levels of SPAG5 in U87 and U251 cell lines were all downregulated (**Figure 2**). Knockdown of SPAG5 markedly suppressed the cell proliferation in the U87 cell lines and U251 cell lines (all $P < 0.05$; **Figure 3**). In accordance, colony formation was also significantly decreased in shSPAG5 group compared with control group on the 15th day after shRNA transfection (**Figure 4**). Caspase 3/7 assay was further carried out to assess the effect of SPAG5 on apoptosis (**Figure 5**). In the glioma cell lines (U87 and U251) transfected with SPAG5-shRNA, cell apoptosis was significantly enhanced compared with that of the normal control group. Our results revealed that SPAG5 knockdown inhibited cell proliferation and promoted apoptosis *in vitro*.

SPAG5 Facilitates Cell Migration and Invasion

To further analyze the effect of SPAG5 on cell migration and invasion, wound-healing assays and invasion assays were performed. The results of wound-healing assays showed that SPAG5 depletion at 24 h inhibited the migrated cells in U87 cells ($P < 0.01$; **Figure 6A**) but had no obvious effect on U251 cells (**Figure 6B**). Invasion assays demonstrated that SPAG5 enhanced the ability of cell invasion in U87 and U251 cells (**Figure 7**). The results suggested that SPAG5 might be involved in tumor progression.

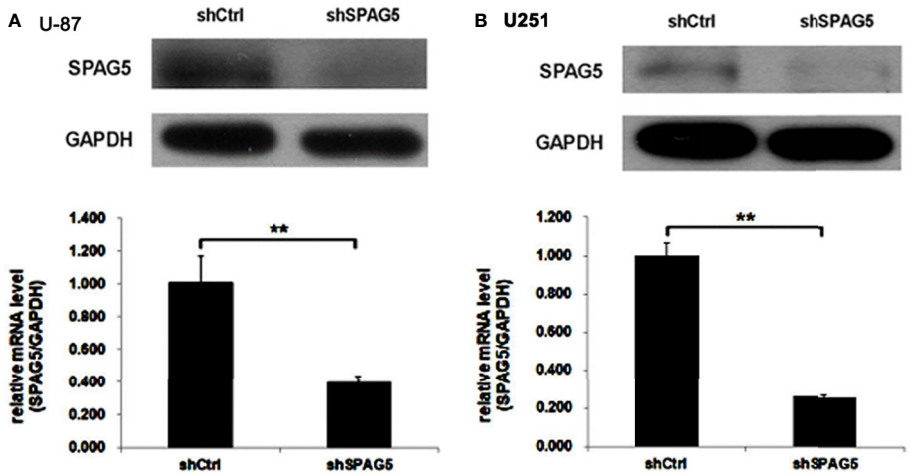

FIGURE 2 | The expression of sperm-associated antigen 5 (SPAG5) in **(A)** U-87 and **(B)** U251 cells transfected with SPAG5-shRNA was measured by Western blotting and qRT-PCR, respectively. Results were expressed as mean ± SD from three independent experiments. $^{**}P < 0.01$.

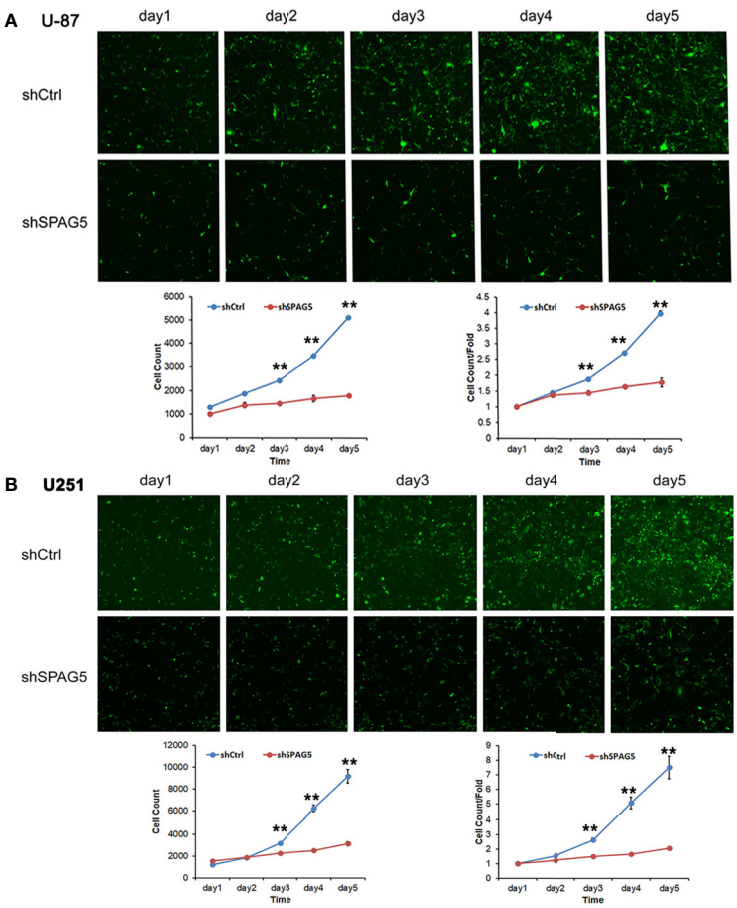

FIGURE 3 | The proliferation capacities were detected by Celigo cytometry system in **(A)** U-87 cells and **(B)** U251 cells transfected with SPAG5-shRNA. Results were expressed as mean ± SD from three independent experiments. vs shCtrl group, $^{**}P < 0.01$.

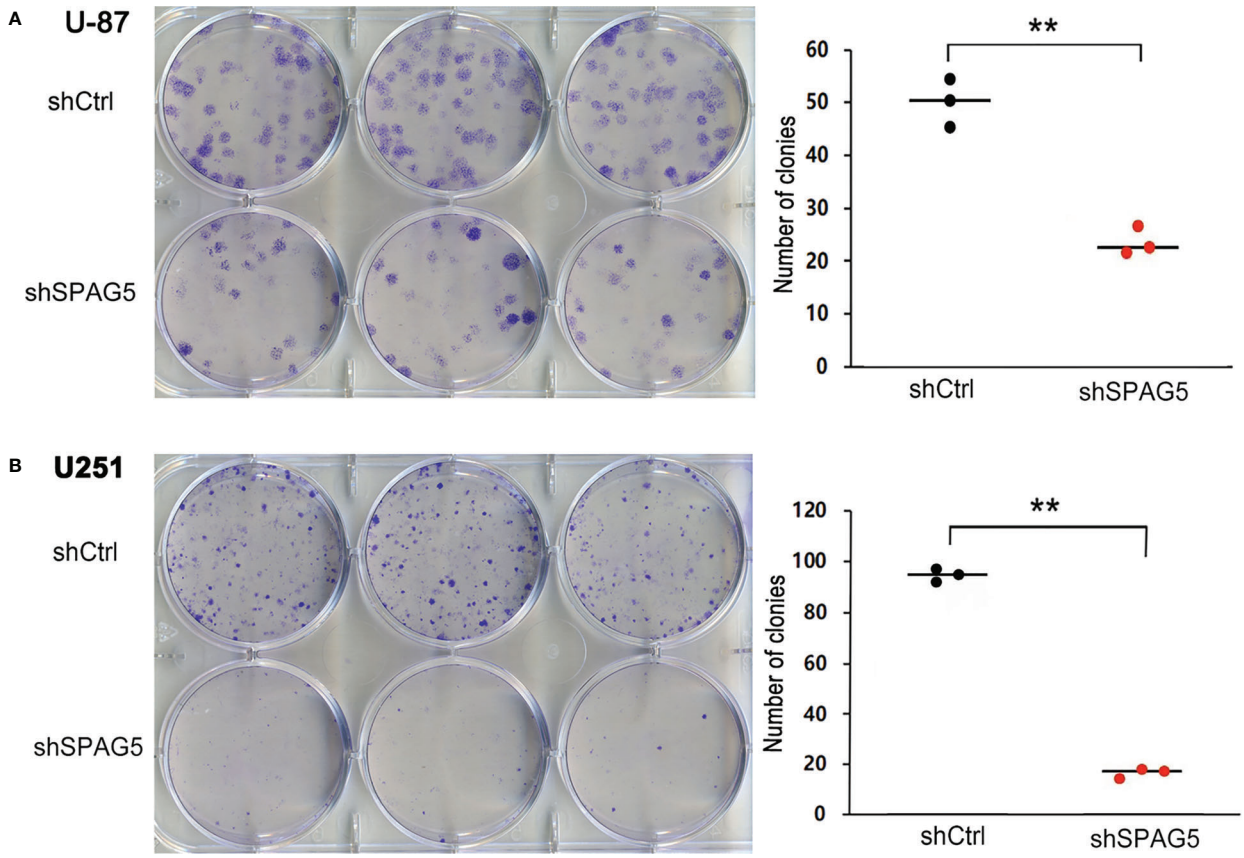

FIGURE 4 | Sperm-associated antigen 5 (SPAG5) silencing reduces colony formation of **(A)** U-87 cells and **(B)** U251 cells. Bar chart showed the number of colony formation on the 15th day. Results were expressed as mean ± SD from three independent experiments. $^{**}P < 0.01$.

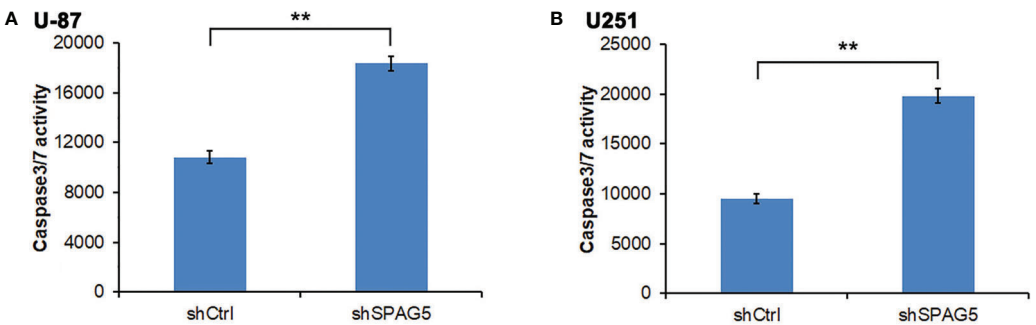

FIGURE 5 | Measurement of apoptotic cells under sperm-associated antigen 5 (SPAG5) downregulation in **(A)** U-87 cells and **(B)** U251 cells. Results are to calculate the percentage of Caspase 3/7-positive cell population. Results were expressed as mean ± SD from three independent experiments. $^{**}P < 0.01$.

SPAG5 Knockdown Could Reduce +CDH2 Expression in Glioma Cells and Overexpression of CDH2 Could Antagonize the Effects of SPAG5 Knockdown

To further explore the mechanisms of SPAG5 in glioma cells, several important signaling pathway molecules were examined using Western blotting. We found that the expression of CDH2 was correlated with SPAG5 knockdown (**Figures 8A, B**). The results of HCS proliferation screening analysis showed that compared with the NC group, the proliferation of the KD group was significantly reduced, which was consistent with the expectation. Compared with KD group, the expression of

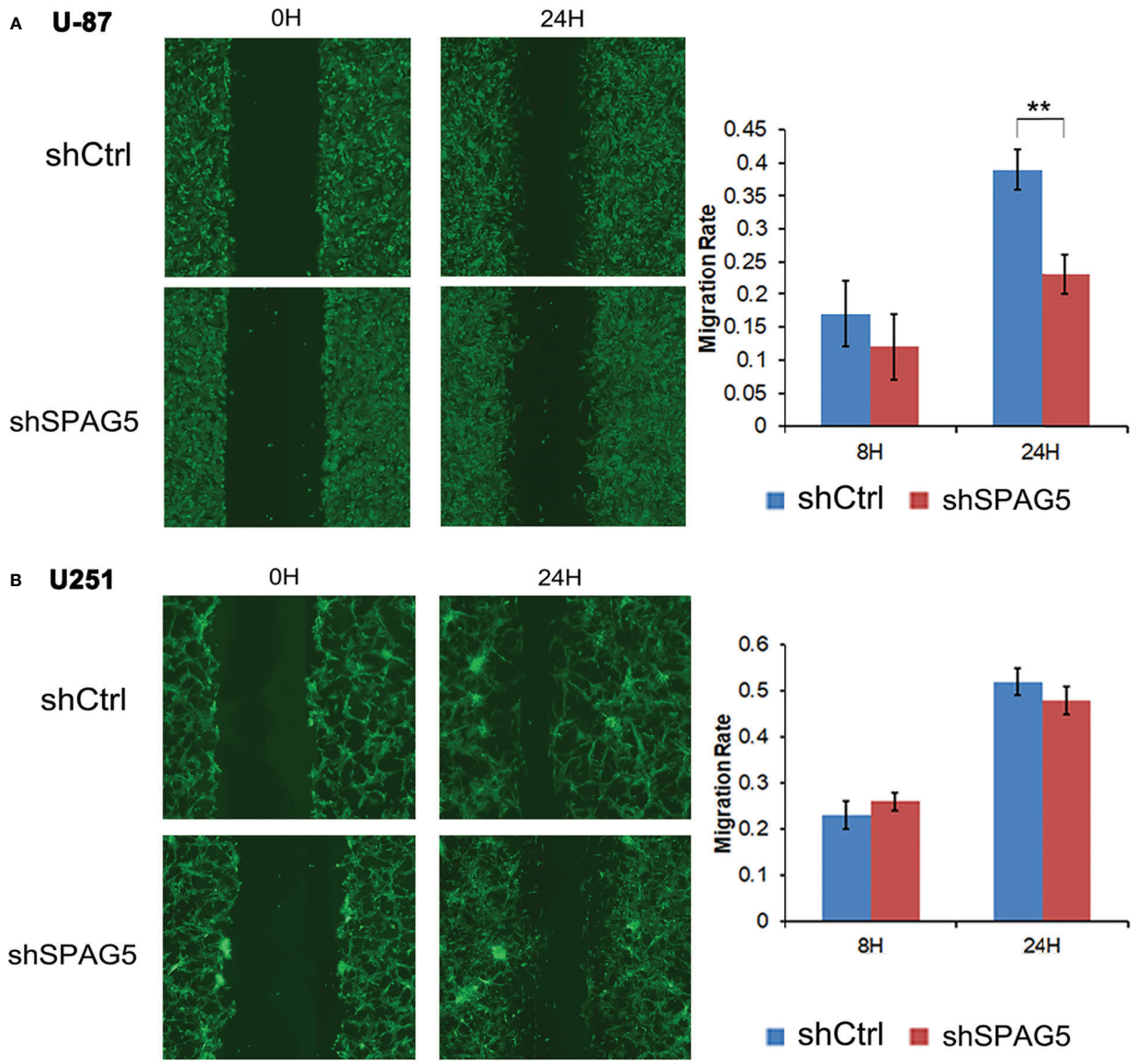

FIGURE 6 | Wound healing assay showed that shRNA-sperm-associated antigen 5 (SPAG5) transfection into **(A)** U-87 cells and **(B)** U251 cells for 24 h hampered cell migrating capacity compared with that of the negative control group. Bar chart showed the relative migration ability at 8 and 24 h Results were expressed as mean ± SD from three independent experiments. $^{**}P < 0.01$.

CDH2 gene in OE group was significantly increased (**Figures 8C, D**). MTT showed that the proliferation of KD +NC group was decreased compared with that in NC+NC group ($P < 0.05$). Compared with KD+NC group, glioma cell proliferation was increased in KD+OE group ($P < 0.05$) (**Figures 8E, F**). Compared with the NC+NC group, the Transwell transfer rate in the KD+NC group decreased ($P < 0.05$), and the Transwell transfer rate in the KD+NC group increased ($P < 0.05$) (**Figures 8G, H**). Our results revealed that SPAG5 knockdown could reduce CDH2 expression, and overexpression of CDH2 could antagonize the effects of SPAG5 knockdown in glioma cells.

DISCUSSION

Glioma represents the most common primary malignant cerebral tumor in adults, and especially GBM is a severe disease (7). Although glioma has a large number of studies, the precise molecular mechanisms about the disease's development are still unclear. Additional potential markers are needed to predict glioma progression and prognosis to provide clinical significance. In this study, we reported that SPAG5 overexpression was associated with the clinical poor prognosis of glioma patients in TCGA database. Notably, SPAG5 depletion by shRNA silencing led to reduced proliferation and viability of

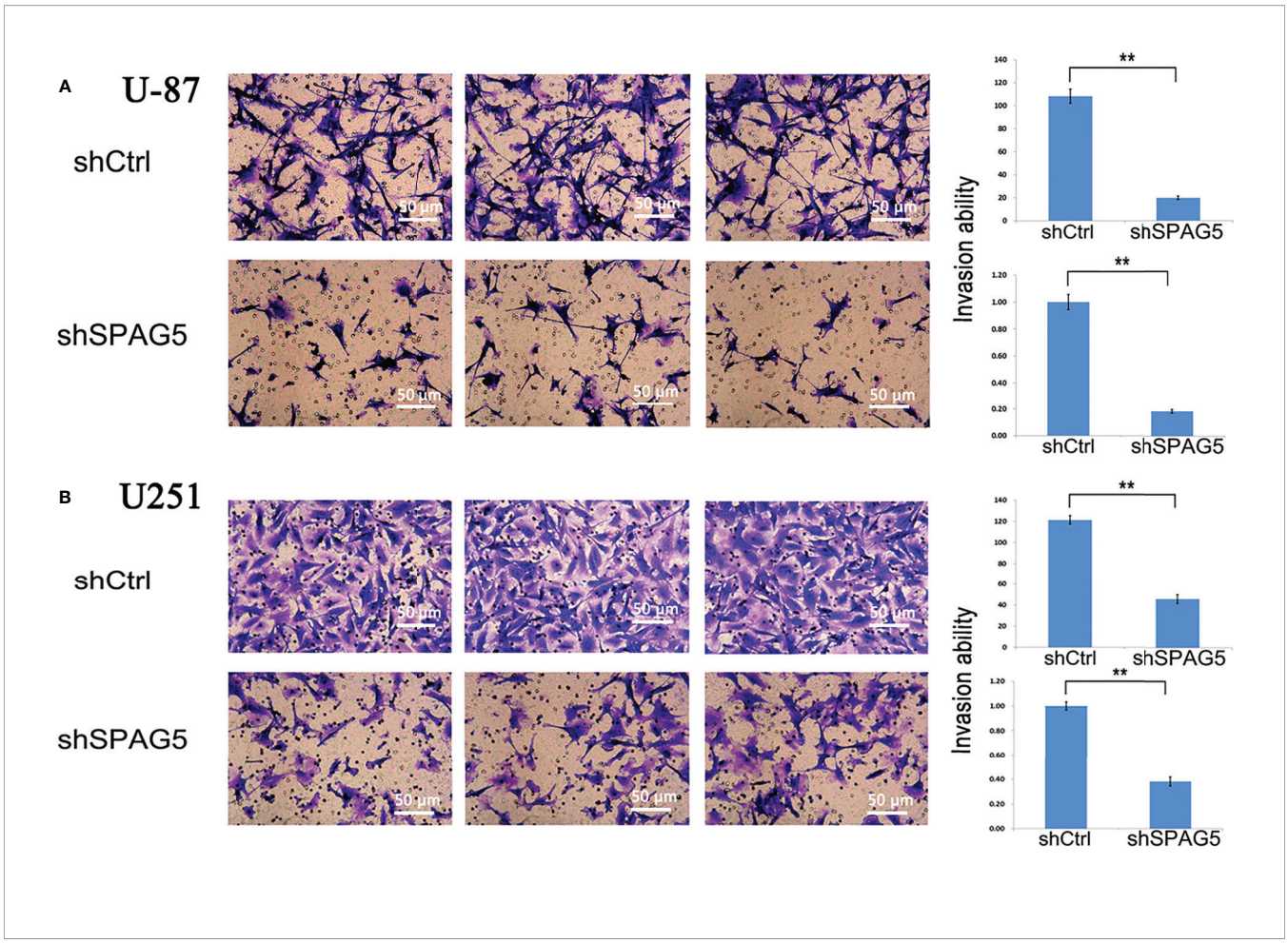

the glioma cells. In addition, SPAG5-depleted glioma cells displayed increased apoptosis *in vitro*. In agreement, clone formation was observably decreased after SPAG5 silencing. Our data suggest that SPAG5 is an oncogene that promotes glioma by downregulating CDH2.

Ideally, identification of genes contributing to tumor genesis and progression will improve the objectivity and accuracy of tumor diagnosis and grading and will probably lead to more accurate judgments of prognosis and treatment response (1). Therefore, identification of novel diagnostic markers and therapeutic targets in glioma is urgently needed. Previous studies have fully uncovered the clinical impact of SPAG5 in breast cancer (11, 12, 23–25). Copy number aberration resulting in SPAG5 gain or amplification, as well as the high-level expression of SPAG5 transcript and protein, were accompanied by shorter overall and tumor-specific survival of patients suffering from breast cancer (25). Upregulation of SPAG5 was associated with poor prognosis in cervical cancer (17). In two independent cohorts, it was reported that HCC patients who had enhanced expression of SPAG5 frequently had a shorter survival (26, 27). SPAG5, which interacts with centrosomal protein CEP55 resulting in the phosphorylation of AKT at Ser473, promotes hepatocellular carcinoma growth *via* CEP55-mediated Phosphatidyl inositol -3-hydroxykinase (PI3K)/(protein kinase B) AKT pathway (28). SPAG5 overexpression was an independent predictor of poor prognosis in gastric cancer patients. Mechanistically, SPAG5 facilitates the progression of gastric cancer cell *via* intensifying the Wnt/β-catenin/survivin signaling *in vitro* and *in vivo* (29). This probably may be due to the fact that overexpression of SPAG5 was associated with infaust clinical factors, including poor tumor histological differentiation, large tumor volume, advanced TNM stage, lymph node metastasis status, and tumor vascular invasion. Furthermore, our findings suggested that glioma cells overexpressing SPAG5 were more aggressive. EMT-related molecules have been reported to play a key role in glioma progression.

CDH2 encodes the N-cadherin protein, and the previous study has confirmed that the expression of CDH2 in patients with high-grade glioma is higher than that in patients with LGG, and patients with high expression of CDH2 show poor prognosis (30). Our results demonstrated that deletion of the SPAG5 gene reduced the expression of CDH2 and inhibited the proliferation of glioma cells, whereas restoration of CDH2 restored the proliferation of glioma cells. This suggests that in glioma cells, the SPAG5 gene regulates tumor cell proliferation through the CDH2 signaling pathway.

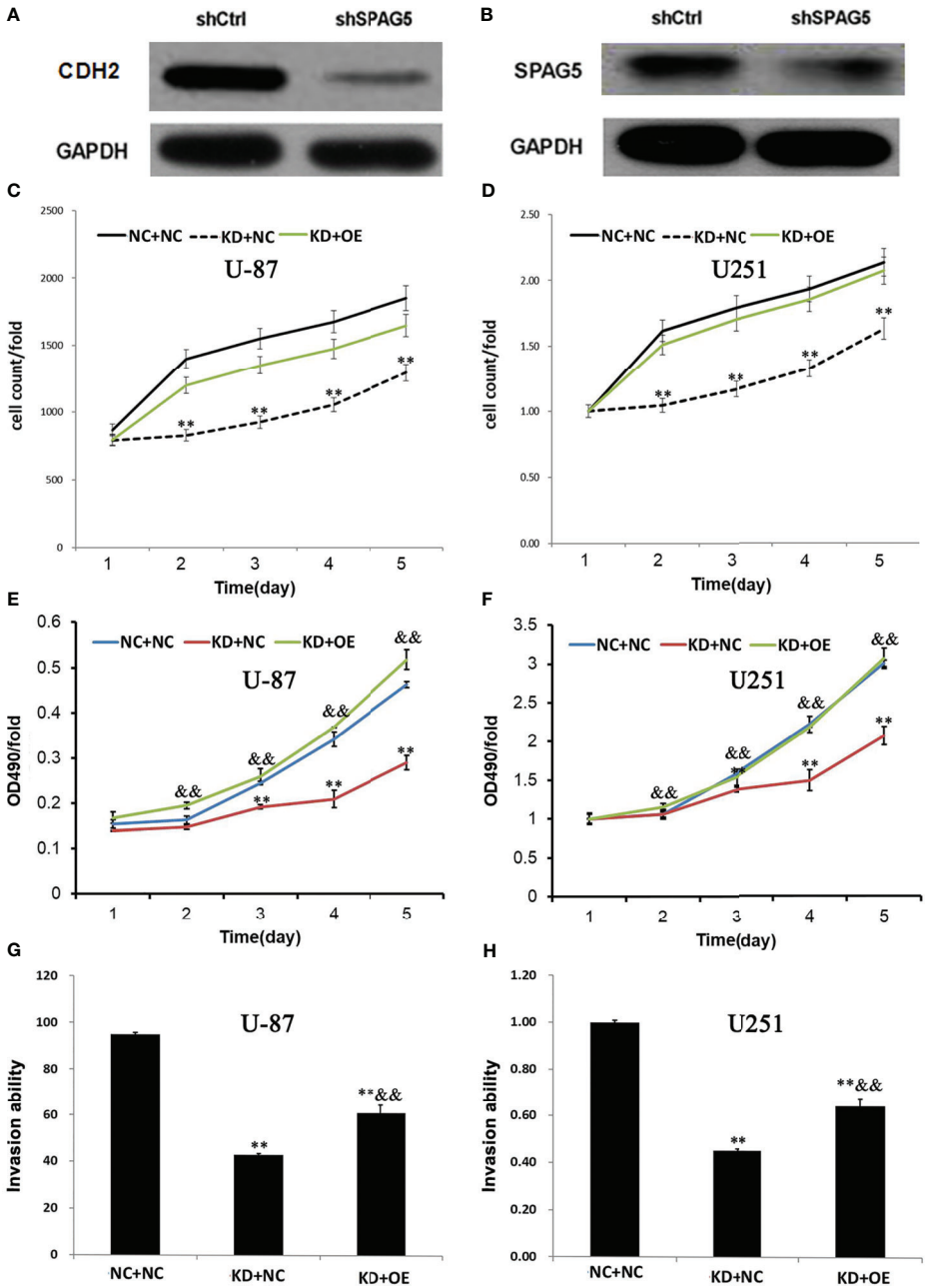

FIGURE 8 | SPAG5 knockdown decreased CDH2 expression in glioma cells. The expression of **(A)** CDH2 and **(B)** SPAG5 in cells transfected with SPAG5-shRNA were measured by western blotting. The HCS proliferation screening analysis of **(C)** U-87 cells and **(D)** U251 cells. ShRNA lentivirus-infected **(E)** U-87 and **(F)** U251 cells were cultured for 5 d and used in MTT assay. The absorption rate of light at wavelength of 490 nm was compared with time in each group. OD490 reflects the number of active cells. The invasion ability of transwell transferred **(G)** U-87 and **(H)** U251 cells in each experimental group was compared with that in the control group. NC+NC: Parental glioma cells+Vector; KD+NC: Parental glioma cells+Knockdown-SPAG5+Vector; KD+OE: Parental glioma cells +Knockdown-SPAG5+overexpression-CDH2. Results were expressed as mean ± SD from three independent experiments. vs NC+NC group, $^{**}P < 0.01$; vs KD +NC group, $^{\&\&}P < 0.01$.

Our findings imply that SPAG5 plays a role in the development of gliomas. Certain limitations of our research should be noted. Though we described that SPAG5 is related to proliferation, migration, and invasion of glioma cells at the molecular and cellular levels, the exact mechanism is not clear. Whether SPAG5 has an effect on glioma after overexpression and *in vivo* experiments are our next step need further investigation to unveil the mechanism.

CONCLUSIONS

In short, we show that increased expression of SPAG5 in glioma was closely correlated with poor prognosis, indicating that SPAG5 serves as a promising prognostic factor in glioma. SPAG5 may represent a potential therapeutic target for the clinical intervention of glioma.

DATA AVAILABILITY STATEMENT

The raw data supporting the conclusions of this article will be made available by the authors without undue reservation.

AUTHOR CONTRIBUTIONS

Conception: HJ. Interpretation or analysis of data: HS and RC. Preparation of the manuscript: CW, HS, and RC. Revision for important intellectual content: CW. Supervision: CW and HJ. All authors contributed to the article and approved the submitted version.

FUNDING

We thank Shanxi Province Natural Science Foundation (No. 201701D121091) for funding our study.

REFERENCES

1. Wesseling P, Capper D. WHO 2016 Classification of Gliomas. *Neuropathol Appl Neurobiol* (2018) 44:139–50. doi: 10.1111/nan.12432
2. Reni M, Mazza E, Zanon S, Gatta G, Vecht CJ. Central Nervous System Gliomas. *Crit Rev Oncol Hematol* (2017) 113:213–34. doi: 10.1016/j.critrevonc.2017.03.021
3. Izquierdo C, Joubert B, Ducray F. Anaplastic Gliomas in Adults: An Update. *Curr Opin Oncol* (2017) 29:434–42. doi: 10.1097/CCO.0000000000000409
4. Ostrom QT, Cioffi G, Gittleman H, Patil N, Waite K, Kruchko C, et al. CBTRUS Statistical Report: Primary Brain and Other Central Nervous System Tumors Diagnosed in the United States in 2012-2016. *Neuro-Oncology* (2019) 21:1–100. doi: 10.1093/neuonc/noz150
5. Im JH, Hong JB, Kim SH, Choi J, Chang JH, Cho J, et al. Recurrence Patterns After Maximal Surgical Resection and Postoperative Radiotherapy in Anaplastic Gliomas According to the New 2016 WHO Classification. *Sci Rep* (2018) 8:777. doi: 10.1038/s41598-017-19014-1
6. Back M, Jayamanne DT, Brazier D, Newey A, Bailey D, Schembri GP, et al. Influence of Molecular Classification in Anaplastic Glioma for Determining Outcome and Future Approach to Management. *J Med Imaging Radiat Oncol* (2019) 63:272–80. doi: 10.1111/1754-9485.12850
7. Oberheim Bush NA, Hervey-Jumper SL, Berger MS. Management of Glioblastoma, Present and Future. *World Neurosurg* (2019) 131:328–38. doi: 10.1016/j.wneu.2019.07.044
8. Chang MS, Huang CJ, Chen ML, Chen ST, Fan CC, Chu JM, et al. Cloning and Characterization of Hmap126, a New Member of Mitotic Spindle-Associated Proteins. *Biochem Biophys Res Commun* (2001) 287(1):116–21. doi: 10.1006/bbrc.2001.5554
9. Gruber J, Harborth J, Schnabel J, Weber K, Hatzfeld M, et al. The Mitotic-Spindle-Associated Protein Astrin Is Essential for Progression Through Mitosis. *J Cell Sci* (2002) 115:4053–9. doi: 10.1242/jcs.00088
10. Manning AL, Bakhoum SF, Maffini S, Correia-Melo C, Maiato H, Compton DA, et al. CLASP1, Astrin and Kif2b Form a Molecular Switch That Regulates Kinetochore-Microtubule Dynamics to Promote Mitotic Progression and Fidelity. *EMBO J* (2010) 29:3531–43. doi: 10.1038/emboj.2010.230
11. Zhu C, Menyhart O, Győrffy B, He X, et al. The Prognostic Association of SPAG5 Gene Expression in Breast Cancer Patients With Systematic Therapy. *BMC Cancer* (2019) 19:1046. doi: 10.1186/s12885-019-6260-6
12. Bertucci F, Viens P, Birnbaum D. SPAG5: The Ultimate Marker of Proliferation in Early Breast Cancer? *Lancet Oncol* (2016) 17(7):863–5. doi: 10.1016/S1470-2045(16)30092-4
13. Li Z, Li H, Chen J, Luo H, Duan M. SPAG5 Promotes Osteosarcoma Metastasis via Activation of FOXM1/MMP2 Axis. *Int J Biochem Cell Biol* (2020) 126:105797. doi: 10.1016/j.biocel.2020.105797
14. Wang T, Li K, Song H, Xu D, Liao Y, Jing B, et al. P53 Suppression is Essential for Oncogenic SPAG5 Upregulation in Lung Adenocarcinoma. *Biochem Biophys Res Commun* (2019) 513:319–25. doi: 10.1016/j.bbrc.2019.03.198
15. Liu JY, Zeng QH, Cao PG, Xie D, Yang F, He LY, et al. SPAG5 Promotes Proliferation and Suppresses Apoptosis in Bladder Urothelial Carcinoma by Upregulating Wnt3 via Activating the AKT/mTOR Pathway and Predicts Poorer Survival. *Oncogene* (2018) 37(29):3937–52. doi: 10.1038/s41388-018-0223-2
16. Zhang H, Li S, Yang X, Qiao B, Zhang Z, Xu Y. miR-539 Inhibits Prostate Cancer Progression by Directly Targeting SPAG5. *J Exp Clin Cancer Res: CR* (2016) 35:60. doi: 10.1186/s13046-016-0337-8
17. Yuan LJ, Li JD, Zhang L, Wang JH, Wan T, Zhou Y, et al. SPAG5 Upregulation Predicts Poor Prognosis in Cervical Cancer Patients and Alters Sensitivity to Taxol Treatment via the mTOR Signaling Pathway. *Cell Death Dis* (2015) 6:e1784–4. doi: 10.1038/cddis.2015.163
18. Sanchez-Tillo E, Barrios OD, Siles L, Cuatrecasas M, Castells A, Postigo A. β-Catenin/TCF4 Complex Induces the Epithelial-to-Mesenchymal Transition (EMT)-Activator ZEB1 to Regulate Tumor Invasiveness. *Proc Natl Acad Sci USA* (2011) 108(48):19204–9. doi: 10.1073/pnas.1108977108
19. Latorre E, Carelli S, Raimondi I, D'Agostino V, Castiglioni I, Zucal C, et al. The Ribonucleic Complex HuR-MALAT1 Represses CD133 Expression and Suppresses Epithelial-Mesenchymal Transition in Breast Cancer. *Cancer Res* (2016) 76(9):2626–36. doi: 10.1158/0008-5472.CAN-15-2018
20. Lu Y, Xiao L, Liu Y, Wang H, Li H, Zhou Q, et al. MIR517Cinhibits Autophagy and the Epithelial-to-Mesenchymal (-Like) Transition Phenotype in Human Glioblastoma Through KPNA2-Dependent Disruption of TP53 Nuclear Translocation. *Autophagy* (2015) 11(12):2213–32. doi: 10.1080/15548627.2015.1108507
21. Zhuo H, Zhao Y, Cheng X, Xu M, Wang L, Lin L, et al. Tumor Endothelial Cell-Derived Cadherin-2 Promotes Angiogenesis and has Prognostic Significance for Lung Adenocarcinoma. *Mol Cancer* (2019) 18(1):34. doi: 10.1186/s12943-019-0987-1
22. Matsui T, Oike T, Nuryadi E, Nakano T. Inter-Study Precision of Cancer Cell Radiosensitivity As Assessed By Colony Formation Assay. *Int J Radiat Oncol Biol Phys* (2019) 105(1):E671. doi: 10.1016/j.ijrobp.2019.06.978
23. Li M, Li A, Zhou S, Lv H, Yang W. SPAG5 Upregulation Contributes to Enhanced C-MYC Transcriptional Activity via Interaction With C-MYC Binding Protein in Triple-Negative Breast Cancer. *J Hematol Oncol* (2019) 12:14. doi: 10.1186/s13045-019-0700-2
24. Jiang J, Wang J, He X, Ma W, Sun L, Zhou Q, et al. High Expression of SPAG5 Sustains the Malignant Growth and Invasion of Breast Cancer Cells Through the Activation of Wnt/β-Catenin Signalling. *Clin Exp Pharmacol Physiol* (2019) 46:597–606. doi: 10.1111/1440-1681.13082
25. Abdel-Fatah TMA, Agarwal D, Liu D-X, Russell R, Rueda OM, Liu K, et al. SPAG5 as a Prognostic Biomarker and Chemotherapy Sensitivity Predictor in Breast Cancer: A Retrospective, Integrated Genomic, Transcriptomic, and Protein Analysis. *Lancet Oncol* (2016) 17:1004–18. doi: 10.1016/S1470-2045(16)00174-1
26. Liu H, Hu J, Wei R, Zhou L, Pan H, Zhu H, et al. SPAG5 Promotes Hepatocellular Carcinoma Progression by Downregulating SCARA5 Through Modifying β-Catenin Degradation. *J Exp Clin Cancer Res* (2018) 37(1):229–42. doi: 10.1186/s13046-018-0891-3
27. Chen W, Chen X, Li S, Ren B. Expression, Immune Infiltration and Clinical Significance of SPAG5 in Hepatocellular Carcinoma: A Gene Expression-Based Study. *J Gene Med* (2019) 22:e3155–5. doi: 10.1002/jgm.3155
28. Yang YF, Zhang MF, Tian QH, Jia F, Xia Y, Zhang CZ, et al. SPAG5 Interacts With CEP55 and Exerts Oncogenic Activities via PI3K/AKT Pathway in

Hepatocellular Carcinoma. *Mol Cancer* (2018) 17(1):117–29. doi: 10.1186/s12943-018-0872-3
29. Liu G, Liu S, Cao G, Luo W, Li P, Wang S, et al. SPAG5 Contributes to the Progression of Gastric Cancer by Upregulation of Survivin Depend on Activating the Wnt/β-Catenin Pathway. *Exp Cell Res* (2019) 379(1):83–91. doi: 10.1016/j.yexcr.2019.03.024
30. Chen Q, Cai J, Jiang C. CDH2 Expression is of Prognostic Significance in Glioma and Predicts the Efficacy of Temozolomide Therapy in Patients With Glioblastoma. *Oncol Lett* (2018) 15(5):7415–22. doi: 10.3892/ol.2018.8227

Conflict of Interest: The authors declare that the research was conducted in the absence of any commercial or financial relationships that could be construed as a potential conflict of interest.

Publisher's Note: All claims expressed in this article are solely those of the authors and do not necessarily represent those of their affiliated organizations, or those of the publisher, the editors and the reviewers. Any product that may be evaluated in this article, or claim that may be made by its manufacturer, is not guaranteed or endorsed by the publisher.

frontiers in Neurology

ORIGINAL RESEARCH
published: 24 November 2021
doi: 10.3389/fneur.2021.659921

Epidemiologic Features, Survival, and Prognostic Factors Among Patients With Different Histologic Variants of Glioblastoma: Analysis of a Nationwide Database

Li-Tsun Shieh[1†], *Chung-Han Ho*[2,3], *How-Ran Guo*[4,5†], *Chien-Cheng Huang*[2,6], *Yi-Chia Ho*[7] *and Sheng-Yow Ho*[1,8,9*]

[1] Department of Radiation Oncology, Chi Mei Medical Center, Liouying, Liouying, Tainan, Taiwan, [2] Department of Medical Research, Chi Mei Medical Center, Tainan, Taiwan, [3] Department of Hospital and Health Care Administration, Chia Nan University of Pharmacy and Science, Tainan, Taiwan, [4] Department of Environmental and Occupational Health, College of Medicine, National Cheng Kung University, Tainan, Taiwan, [5] Department of Occupational and Environmental Medicine, National Cheng Kung University Hospital, Tainan, Taiwan, [6] Department of Emergency Medicine, Chi Mei Medical Center, Tainan, Taiwan, [7] Departement of Medical Education, Chi Mei Medical Center, Tainan, Taiwan, [8] Department of Radiation Oncology, Chi Mei Medical Center, Tainan, Taiwan, [9] Graduate Institute of Medical Science, Chang Jung Christian University, Tainan, Taiwan

OPEN ACCESS

Edited by:
Yaohua Liu,
Shanghai First People's Hospital, China

Reviewed by:
Ashley Ghiaseddin,
University of Florida, United States
Bing-Fang Hwang,
China Medical University, Taiwan

***Correspondence:**
Sheng-Yow Ho
shengho@seed.net.tw
orcid.org/0000-0002-3997-6575

[†] *These authors have contributed equally to this work*

Specialty section:
This article was submitted to Neuro-Oncology and Neurosurgical Oncology, a section of the journal Frontiers in Neurology

Received: *28 January 2021*
Accepted: *01 October 2021*
Published: *24 November 2021*

Citation:
Shieh L-T, Ho C-H, Guo H-R, Huang C-C, Ho Y-C and Ho S-Y (2021) Epidemiologic Features, Survival, and Prognostic Factors Among Patients With Different Histologic Variants of Glioblastoma: Analysis of a Nationwide Database. Front. Neurol. 12:659921. doi: 10.3389/fneur.2021.659921

Background: Glioblastoma (GBM) is the most common primary intracranial malignancy. Previous studies found incidence of GBM varies substantially by age, sex, race and ethnicity, and survival also varies by country, ethnicity, and treatment. Gliosarcoma (GSM) and giant cell glioblastoma (GC-GBM) are different histologic variants of GBM with distinct clinico-pathologic entities. We conducted a study to compare epidemiology, survival, and prognostic factors among the three.

Methods: We identified GBM patients diagnosed between 2000 and 2016 using the Taiwan Cancer Registry and followed them using the death registry. Survival was compared among conventional GBM and two histologic variants. The potential confounding factors evaluated in this study included registered year, age, sex, and treatment modality (resection, radiotherapy, and chemotherapy).

Results: We enrolled 3,895 patients, including 3,732 (95.8%) with conventional GBM, 102 (2.6%) with GSM, and 61 (1.6%) with GC-GBM. GC-GBM patients had younger mean age at diagnosis (49.5 years) than conventional GBM patients (58.7 years) and GSM patients (61.3 years) ($p < 0.01$). The three groups had similar sex distributions ($p = 0.29$). GC-GBM had a longer median survival [18.5, 95% confidence interval (CI): 15.8–25.3 months] than conventional GBM (12.5, 95%CI: 12.0–13.0 months) and GSM (12.8, 95%CI: 9.2–16.2 months), and the differences in overall survival did not attain statistical significance ($p = 0.08$, log-rank test). In univariate analysis, GC-GBM had better survival than conventional GBM, but the hazard ratio (0.91) did not reach statistical significance (95%CI: 0.69–1.20) in the multivariate analysis. Young ages (≤40 years), female sex, resection, radiotherapy, and chemotherapy were factors

associated with better survival in overall GBMs. In subtype analyses, these factors remained statistically significant for conventional GBM, as well as radiotherapy for GSM.

Conclusion: Our analysis found conventional GBM and its variants shared similar poor survival. Factors with age ≤40 years, female sex, resection, radiotherapy, and chemotherapy were associated with better prognosis in conventional GBM patients.

Keywords: glioblastoma, gliosarcoma, giant cell glioblastoma, histologic variant, epidemiology

INTRODUCTION

Primary brain tumors account for about 1% of all malignant neoplasms. Glioma is the most common brain tumor, and glioblastoma (GBM) is the most common primary intracranial malignancy in adults, which has a dismal prognosis despite multimodality therapy (1). Previous studies found the incidence of central nervous system tumors in the Western world is higher than that in the Eastern world, and the occurrence is also higher in developed countries compared to less developed countries (2). The incidence of GBM varies substantially by age, sex, race, and ethnicity, and prognosis also vary by country, ethnicity, and treatment (2–5). Ostrom et al. reported that non-Hispanic whites had a higher incidence and lower survival rates compared to individuals of other racial or ethnic groups in the US (3). Chien et al. also found disparities by histologic type and grade of primary malignant brain and central nervous system tumors between the US and Taiwan (2).

Glioblastomas comprise a group of morphologically highly heterogeneous neoplasms, as the original designation "multiforme" implies (6). "Glioblastoma" is synonymous with WHO grade IV astrocytoma, GBM multiforme, or conventional GBM in the previous WHO classification. Variants are subtypes of entities that are sufficiently well-characterized pathologically to take a place in the classification and have potential clinical utility (6, 7). Two histologic variants of GBM are recognized as distinct clinicopathologic entities since the 2000 WHO classification: gliosarcoma (GSM) and giant cell glioblastoma (GC-GBM) (6–8). The variants of GSM and GC-GBM possess distinct histologic identities, which may be relevant for tumor behavior and clinical outcomes. The prognosis of GSM appears to be equal or even worse than that of conventional GBM (9–13). GC-GBN also bears a distinct clinico-pathologic picture, traditionally thought to occur more in younger patients and has better survival (13–16).

According to the literature, GSM accounts for 2–8% of overall GBM patients, while GC-GBM comprises only about 1–5% (11–17). The reported outcome of GC-GBM and GSM are limited in a retrospective hospital database or case series with small patient size. Nonetheless, the differences between GSM and GC-GBM may not be fully evaluated, especially in different countries, in the literature. Therefore, they may not fully reflect the distinct clinical features of GBM variants.

To overcome the limitations associated with low incidence, we used the Taiwan Cancer Registry (TCR) database to study histologic variants of GBM. The aims are to identify epidemiologic features, survival, and prognostic factors of the GBM patients with different histologic variants. Modest, yet clinically meaningfully, differences in the effects of treatment modality may surface with the study of a large series. We also conduct a literature review on the incidence and prognosis of histologic variants of GBM reported on the basis of population-based databases in the world.

MATERIALS AND METHODS

Database Sources

The databases of TCR and Taiwan's death registry from 1996 to 2016 were used in this study. The TCR has been organized and funded by the Ministry of Health and Welfare of Taiwan since 1979. Following the enactment of the Cancer Control Act in 2003, all hospitals are mandated to submit cancer data to TCR. The TCR had to monitor the completeness and audit data quality to assure the accuracy of cancer registration data from hospitals reporting, so lag time for reporting cancer incidence is about 4 years. Additionally, TCR data are subjected to periodic quality control audits. It is also overseen by an advisory board and run by the National Public Health Association, which works to standardize terminology, coding, and procedures for the registry. The TCR covers nearly 99% of the cancer patients in Taiwan and records their related information, including the individual demographics, cancer primary sites, tumor histology, and treatment modality. However, the database did not record the exact date of death before 2000. For research purposes, the Health and Welfare Data Science Center (HWDC) set an integrated database center to help academic usage of these databases with de-identified forms in an anonymous format.

Definition of Study Subjects

The subjects of this study were selected from patients registered in the TCR between 2000 and 2016, and we identified brain tumor patients with the coding of the International Classification of Diseases for Oncology, third edition (ICD-O-3). The percentage of microscopically confirmed cases of malignant brain and central nervous system tumors was around 90% in TCR. Three histologic types of brain tumor were chosen for comparison: GBM not otherwise specified (ICD-O-3 histology code: 9440/3; noted as conventional GBM in this study), GC-GBM (ICD-O-3 histology code: 9441/3), and GSM (ICD-O-3 histology code: 9442/3). Cases without pathologically confirmed, prior diagnosis of glioma or other brain tumor, and also those that were without required data on the TCR such as the date of registration, diagnosis, or treatment were excluded in our analysis.

Literature Search Strategy

We conducted a search of literature published between January 1995 and December 2019 in PubMed (National Library of Medicine) using "glioblastoma," "gliosarcoma," "giant cell glioblastoma," or "brain tumor" combined with "population-based" or "epidemiology" as keywords. We included epidemiological studies published in full-text English. Case reports, animal studies, reports of GBMs secondary to other conditions, and reports of surgical or radiological management of GBMs were not included.

Measurements

The primary outcome in this study was mortality. All study subjects were followed up until death or the end date of the study (December 31, 2016). Mortality was identified using the death registry database. The potential confounding factors evaluated in this study included registered year, age, sex, and treatment modality (resection, radiotherapy, and chemotherapy). The TCR database focuses on new cases and thus does not have information about the definite tumor recurrence. Therefore, we are unable to perform disease-free survival analysis.

Statistical Analysis

We used Pearson's chi-square tests to evaluate the differences in distributions of categorical variables among patients with conventional GBM, GC-GBM, and GSM and used analyses of variance to evaluate the differences in continuous variables. The survival curves were plotted using the Kaplan-Meier method, and the differences were evaluated using log-rank tests. We used Cox proportional regressions to compared survival among the three groups of patients. Multivariate analysis was performed to identify independent factors associated with survival and adjust for effects of potential confounders. We also conducted stratified analyses by histologic type and paired comparisons using conventional GBM as the reference group. We conducted all statistical analyses using SAS 9.4 (SAS Institute Inc., Cary, NC, USA) and performed statistical tests at a two-tailed significance level of 0.05.

RESULTS

From the TCR database, we enrolled 3,895 histologically confirmed GBM patients in the final analyses, including 3,732 (95.8%) with conventional GBM, 102 (2.6%) with GSM variant, and 61 (1.6%) with GC-GBM. We found the distribution of these three groups of GBMs was quite similar before and after 2007 ($p = 0.20$) (**Table 1**). Patients with GC-GBM had a younger mean age at diagnosis than patients with conventional GBM or GSM (49.5 vs. 58.7 or 61.3 years, $p < 0.01$). While 26.2% of GC-GBM patients were in the youngest age group (≤40 years), only 12.6% of conventional GBM patients and 6.9% of GSM patients were in this age group ($p < 0.01$). The differences in the distribution of sex among the three groups did not reach statistical significance ($p = 0.29$). Patients with conventional GBM were more likely to receive conservative operation (i.e., incisional biopsy only) compared to GC-GBM or GSM patients (18.8 vs. 6.6 or 5.9%, $p < 0.01$). Differences in the percentage of patients who received adjuvant radiotherapy among the three groups did not reach statistical significance ($p = 0.23$). However, a higher proportion of GSM patients (72.1%) had undergone adjuvant chemotherapy in comparison with patients with conventional GBM or GC-GBM (48.2 or 57.8%, $p < 0.01$).

The prognosis of overall GBM cohort is poor, with an overall median survival of 12.6 [95% confidence interval (CI): 12.1–13.2] months. GC-GBM patients had a median survival of 18.5 (95%CI: 15.8–25.3) months, longer than that of conventional GBM [12.5 (95%CI: 12.0–13.0) months] or GSM [12.8 (95%CI: 9.2–16.2) months]. The 5-year mortality of conventional GBM, GSM, and GC-GBM were 87.9%, 86.3%, and 82%, respectively ($p = 0.34$). The differences in overall survival did not reach statistical significance ($p = 0.08$, log-rank test) (**Figure 1**).

In univariate analyses, GC-GBM had better survival than conventional GBM with a hazard ratio (HR) of 0.73 (95%CI: 0.55–0.97) (**Table 2**). Older ages (HR = 1.34, 95%CI: 1.20–1.49 for 40–70 years old and HR = 2.64, 95%CI: 2.35–2.98 for ≥70 years old as compared to ≤40 years old) and male sex (HR = 1.16, 95%CI: 1.09–1.24) were also associated with poor survival. Tumor resection (HR = 0.64, 95%CI: 0.59–0.70), adjuvant radiotherapy (HR = 0.51, 95%CI: 0.48–0.55), and chemotherapy (HR = 0.57, 95%CI: 0.53–0.61) were all associated with favorable survival. In multivariate analyses, the 5-year mortality rates of patients with conventional GBM, GC-GBM, and GSM were similar after adjustment for other factors. Nonetheless, younger ages (≤40 years) ($p < 0.01$), female sex ($p < 0.01$), resection ($p < 0.01$), adjuvant radiotherapy ($p < 0.01$), and chemotherapy ($p < 0.01$) were shown to be associated with better prognosis of the overall GBM cohort following multivariate analyses (**Table 2**).

In stratified analyses by histologic type, older ages (HR = 1.46, 95%CI: 1.30–1.63 for 40–70 years old and HR = 2.58, 95%CI: 2.29–2.92 for ≥70 years old as compared to ≤40 years old) and male sex (HR = 1.13, 95%CI: 1.06–1.21) were still independent unfavorable factors for survival in conventional GBMs (**Table 3**). However, the HRs did not reach statistical significance in GC-GBM or GSM. In fact, a lower HR associated with 40–70 years old was observed for both GC-GBM (HR = 0.69, 95%CI: 0.35–1.38) and GSM (HR = 0.91, 95%CI: 0.38–2.20). Tumor resection was associated with a better survival for conventional GBM (HR = 0.81, 95%CI: 0.74–0.89), but not GC-GBM (HR = 2.49, 95%CI: 0.63–9.93); the HR associated with operation did not reach statistical significance for GSM (HR = 0.74, 95%CI: 0.31–1.81), neither. Radiotherapy was associated with better survival for all three histologic types (HR = 0.65, 95%CI: 0.60–0.71 for conventional GBM and HR = 0.46, 95%CI: 0.28–0.78 GSM), but the HR associated with GC-GBM did not reach statistical significance (HR = 0.51, 95%CI: 0.21–1.21). Chemotherapy was associated with better survival for all three histologic types (HR = 0.73, 95%CI: 0.67–0.79 for conventional GMB), but the associated HR did not reach statistical significance for GC-GBM (HR = 0.51, 95%CI: 0.24–1.07) or GSM (HR = 0.65, 95%CI: 0.40–1.08) (**Table 3**).

In paired comparisons, after adjusting for potential confounders, we found GC-GBM and GSM variants have similar survival compared to conventional GBM in all strata by age group, sex, and treatment modality (**Supplementary Table**).

TABLE 1 | Demographic and clinical characteristics of patients diagnosed with glioblastoma and its histologic variants in 2000–2016, Taiwan.

Characteristics	All patients	Histologic variants			*p*-value
		Conventional GBM	Giant cell GBM	Gliosarcoma	
Patients	3,895 (100.0)	3,732 (95.8)	61 (1.6)	102 (2.6)	
Period of diagnosis					0.20
2000–2007	1,647 (42.3)	1,603 (97.0)	17 (0.4)	27 (1.6)	
2008–2016	2,248 (57.7)	2,129 (94.7)	44 (2.0)	75 (3.3)	
Age at diagnosis (mean ± SD year)	58.6 ± 16.8	58.7± 16.8	49.5 ± 17.8	61.3 ± 15.5	<0.01
Age group (year)					<0.01
≤40	493 (12.7)	470 (12.6)	16 (26.2)	7 (6.9)	
40–70	2,266 (58.2)	2,174 (58.3)	35 (57.4)	57 (55.9)	
≥70	1,136 (29.2)	1,088 (29.2)	10 (16.4)	38 (37.3)	
Sex					0.29
Male	2,229 (57.2)	2,136 (54.8)	30 (49.2)	63 (61.8)	
Female	1,666 (42.8)	1,596 (45.2)	31 (50.8)	39 (38.2)	
M/F ratio	1.34	1.34	0.97	1.62	
Resection[a]					<0.01
Yes	3,185 (81.8)	3,032 (81.2)	57 (93.4)	96 (94.1)	
No	710 (18.2)	700 (18.8)	4 (6.6)	6 (5.9)	
Radiotherapy					0.23
Yes	2,669 (68.5)	2,548 (68.3)	47 (77.1)	74 (72.6)	
No	1,226 (31.5)	1,184 (31.7)	14 (22.9)	28 (27.4)	
Chemotherapy					<0.01
Yes	1,902 (48.8)	1,799 (48.2)	44 (72.1)	59 (57.8)	
No	1,993 (51.2)	1,933 (51.8)	17 (17.9)	43 (42.2)	

CI, confidence interval; GBM, glioblastoma; SD, standard deviation.
[a]*Subtotal or gross-total resection, other than biopsy only.*

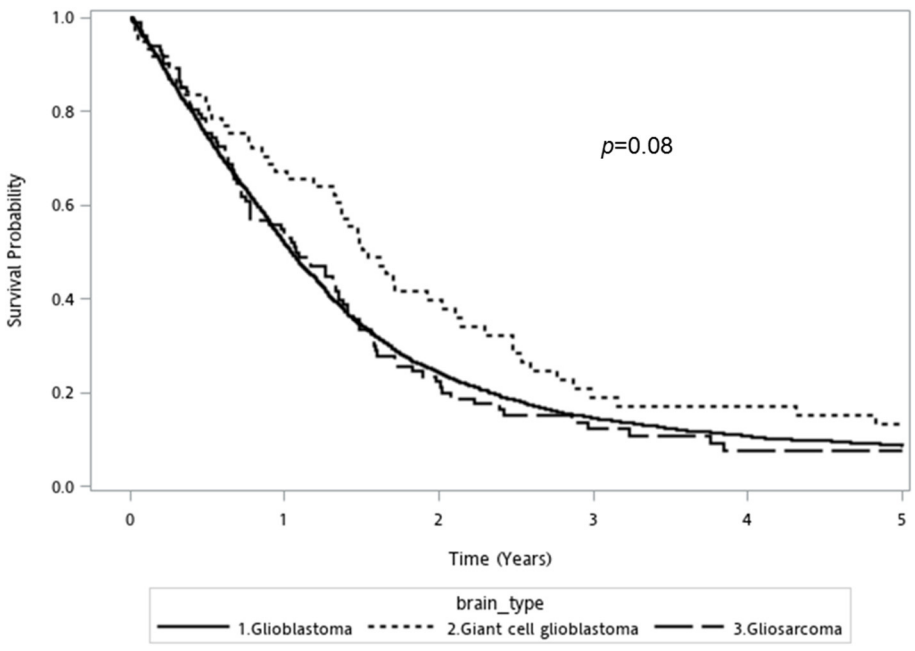

FIGURE 1 | Kaplan-Meier overall survival curve for conventional glioblastoma, giant cell glioblastoma, and gliosarcoma (log rank *p*-value = 0.08).

TABLE 2 | Univariate and multivariate Cox regression analyses of potential factors associated the survival of overall glioblastoms cohort.

Variables	Univariate		Multivariate[a]	
	HR (95% CI)	*p*-Value	HR (95% CI)	*p*-Value
Variants				
Conventional GBM	(reference)		(reference)	
Giant cell GBM	0.73 (0.55–0.97)	0.03	0.91 (0.69–1.20)	0.51
Gliosarcoma	1.03 (0.83–1.27)	0.82	1.06 (0.86–1.31)	0.59
Age at diagnosis (year)				
≤40	(reference)		(reference)	
40–70	1.34 (1.20–1.49)	< 0.01	1.42 (1.27–1.59)	< 0.01
≥70	2.64 (2.35–2.98)	< 0.01	2.56 (2.27–2.88)	< 0.01
Sex				
Female	(reference)		(reference)	
Male	1.16 (1.09–1.24)	< 0.01	1.12 (1.05–1.20)	< 0.01
Resection[b]				
No	(reference)		(reference)	
Yes	0.64 (0.59–0.70)	< 0.01	0.82 (0.75–0.89)	< 0.01
Radiation				
No	(reference)		(reference)	
Yes	0.51 (0.48–0.55)	< 0.01	0.65 (0.59–0.70)	< 0.01
Chemotherapy				
No	(reference)		(reference)	
Yes	0.57 (0.53–0.61)	< 0.01	0.72 (0.67–0.78)	<0.01

GBM, glioblastoma; HR, hazard ratio; CI, confidence interval.
[a]*Adjusted for age, sex, and treatment modality.*
[b]*Subtotal or gross-total resection, other than biopsy only.*

DISCUSSION

Glioblastoma comprise a group of morphologically highly heterogeneous neoplasms, as the original designation "multiforme" implies. The cellular composition, even within a GBM tumor *per se*, can vary widely, and mixed histologic features are typical. "Glioblastoma" is synonymous with WHO grade IV astrocytoma in the previous WHO classification or GBM multiforme (6–8). The 2016 WHO classification of central nervous tumors first introduced molecular parameters to define GBM tumor entities, preserved two (GC-GBM and GSM) variants under the umbrella of isocitrate dehydronase (IDH)-wild type GBM. The variants GSM and GC-GBM possess distinct histologic identities, whereas it is seemingly a coherent category of GBM variants, at least based on microscopic tumor morphology alone without regard to biological markers. The GSM variant retains morphologic features of the conventional GBM, while the tumor has differentiated into both biphasic glial and sarcomatous components, and the tumor behavior possesses a higher potential of metastasizing to different lobes of the brain or even to extra-cranial sites clinically. The prognosis of GSM appears to be equal or even worse than that of conventional GBM (9–13). The GC-GBM variant has conventional GBM differentiation, and is further characterized to share a predominance of bizarre multinucleated giant cells and lymphocytic infiltration. GC-GBM also manifests distinct clinical pictures, traditionally thought to occur more often in younger patients and has better outcome compared to conventional GBM (13–16).

We aimed to recruit a large GBM cohort to define the epidemiology and survival factors using the population-based databases in Taiwan. Our results suggest that GSM and GC-GBM variants represent approximately 2.6% and 1.6% of all GBM patients in Taiwan, respectively. Surveillance, Epidemiology, and End Results (SEER) in the US showed that GSM and GC-GBM only accounted for 2.2% and 1% of overall GBM (11, 14), and the ratio of GBM variants National Cancer Database and SEER in the US reported 2.2%–2.9% for GSM and 0.8%–1% for GC-GBM (11, 13–17). The GSM variant, like conventional GBM, shows a propensity to affect the elderly, with a median age at diagnosis around 60 years old in Taiwan and the US. Similarly, both GBM and GSM variants demonstrate comparable male predominance. The occurrence of GC-GBM in Taiwan tended to occur in younger patients with a mean age at 49.5 years, in contrast to 51–56 years in the US (11, 13–17). Nonetheless, with regard to the Asian or Chinese population, reported data on GBM variants were limited. From a hospital-based series, 51 GSM patients were identified with slightly male predominance (59%) and younger age (median age 45 years) in 518 GBM patients at a Chinese hospital (18). The report showed a higher incidence of GSM (9.8%) and a younger age compared to our analysis. However, the hospital-based study might not have sufficient power to precisely characterize Asian GBM variants. Our study is population-based, which enhances generalizability relative to *ad-hoc* hospital-based case series.

Glioblastoma GSM is the most deadly primary brain tumor, with a 5-year survival rate of only about 5%–10%, there are no clinical or pathologic stage classifications of GBMs that are generally accepted (5, 6, 19). Conventional GBM and its histologic variants had a similar worse outcome in our study, and the 5-year mortality rates (87.9% for conventional GBM, 86.3% for GSM, and 82.0% for GC-GBM) are in line with the reported literature (9–19). Our database analyses found GC-GBM patients had a higher median survival of 18.5 months, compared to conventional GBM (12.5 months) and GSM (12.8 months). Our population study had slightly lower median OS than that reported by Stupp et al. (12.6 vs. 14.6 months) (20). Differences in eligibility for the clinical trial in the study by Stupp et al. and the inclusion criteria in our population-based study might explain the discrepancy. In univariate analysis, GC-GBM was found to be associated with a 27% lower risk of mortality in comparison with conventional GBM, but the difference was not significant in multivariable analysis. The prognosis of GC-GBM variant and conventional GBM was found to be equally poor in a review of cases series and hospital-based cancer database (6, 7). However, other studies found a slightly better prognosis for the GC-GBM variant in comparison with conventional GBM (11, 15). The US cancer registry study reported median survival of 11–15.5 months in GC-GBM patients, which is better than conventional GBM in the period of 1988–2004, 1998–2011, and 2004–2014 reported from US SEER or National Cancer Database, respectively (13–15). However, an analysis of the US SEER database of years 1985–2014 showed that GC-GBM and

TABLE 3 | Univariate and multivariate stratified Cox regression analyses of survival of conventional glioblastoms and histologic variants.

Variables	Conventional glioblastoma		Giant cell glioblastoma		Gliosarcoma	
	Univariate HR (95%CI)	Multivariate HR (95%CI)	Univariate HR (95%CI)	Multivariate HR (95%CI)	Univariate HR (95%CI)	Multivariate HR (95%CI)
Age at diagnosis (year)						
≤40	(reference)	(reference)	(reference)	(reference)	(reference)	(reference)
40–70	1.37 (1.22–1.53)*	1.46 (1.30–1.63)*	0.65 (0.34–1.25)	0.69 (0.35–1.38)	0.92 (0.39–2.15)	0.91 (0.38–2.20)
≥70	2.68 (2.37–3.02)*	2.58 (2.29–2.92)*	1.53 (0.68–3.46)	1.29 (0.40–3.34)	2.33 (0.98–5.57)	2.32 (0.95–5.67)
Sex						
Female	(reference)	(reference)	(reference)	(reference)	(reference)	(reference)
Male	1.17 (1.10–1.26)*	1.13 (1.06–1.21)*	1.05 (0.60–1.83)	1.20 (0.65–2.21)	0.75 (0.49–1.15)	0.87 (0.54–1.40)
Resection[a]						
No	(reference)	(reference)	(reference)	(reference)	(reference)	(reference)
Yes	0.64 (0.59–0.70)*	0.81 (0.74–0.89)*	1.12 (0.35–3.59)	2.49 (0.63–9.93)	0.47 (0.20–1.07)	0.74 (0.31–1.81)
Radiotherapy						
No	(reference)	(reference)	(reference)	(reference)	(reference)	(reference)
Yes	0.51 (0.48–0.55)*	0.65 (0.60–0.71)*	0.50 (0.26–0.94)*	0.51 (021–1.21)	0.36 (0.22–0.57)*	0.46 (0.28–0.78)*
Chemotherapy						
No	(reference)	(reference)	(reference)	(reference)	(reference)	(reference)
Yes	0.58 (0.54–0.62)*	0.73 (0.67–0.79)*	0.28 (0.21–0.70)*	0.51 (0.24–1.07)	0.51 (0.33–0.78)*	(0.40–1.08)

HR, hazard ratio; CI, confidence interval.

**p-value < 0.05.*

[a]*Subtotal or gross-total resection, other than biopsy only.*

conventional GBM shared similar poor prognosis (16). This indicates that a longer study period with a large sample size might reflect the true outcome between the GC-GBM and GBM cohort.

Some previous studies reported that GSM had a similar survival to conventional GBM, or even worse (9, 10, 12, 13). Our survival analysis showed that GSM and conventional GBM had similar poor overall survival (12.8 vs. 12.5 months). The US cancer registry database showed that, the median survival for GSM was 9–10.7 months (11–13, 17). A review article identified 219 cases of GSM from 34 reports before 2010 and found survival ranging from 4 to 11.5 months. This review provided distinct clinical and pathogenetic features of GSM, including increased metastatic dissemination and worse prognosis than conventional GBM (10). Our analysis is also in line with our previous study that showed no difference in survival between conventional GBM and GSM, and two GSM cases progressed to intra- or extra-cranial metastasis (21, 22). A Chinese study reported a similar median overall survival between GSM (13.0 months) and conventional GBM (14.0 months) (18). Despite the dismal outcome of GSM, adjuvant radiotherapy was found to be an independent predictor in the study.

To the best of our knowledge, this is the first population-based study in Asian patients. Therefore, this is a useful study looking into these rare histologic variants of GBM especially for patients of Asian nationality or heritage. We conducted a literature review to identify epidemiologic studies on the clinical features and prognosis of GBM variants in the databases of Medline and PubMed. **Table 4** listed various epidemiologic reports in different national population-based studies, including the US SEER and National Cancer database, and three national registries from Australia, France, and England. However, the three studies only reported case numbers of the variants of GBM without detailed demographics and outcomes (23–25). The results reported the incidence with 1.3%–2.7% GSM and 0.7%–1.8% GC-GBM in other population-based studies. Our study does provide authoritative demographic and survival information on GBM variants in an Asian population, considering that a majority of studies are from American and European populations.

Currently, all GBM patients underwent tri-modal therapy, including tumor excision, following chemo-radiotherapy as the standard therapy. We found GBM patients survived longer following standard therapy including operation, radiotherapy, and chemotherapy. These findings parallel the literature, which all confirmed more favorable survival through tri-modality therapy (6, 20, 26). However, regarding GSM patients, we only found the radiotherapy was associated with favorable survival. For GC-GBM patients, we were unable to find favorable prognostic predictors, even following operation, radiotherapy, or chemotherapy. Due to the rarity, even TCR case number might not be sufficiently powered to precisely characterize GSM and GC-GBM. To sum up, the clinical implications of the prognosis of GC-GBM or GSM might share similar or different risk factors compared with conventional GBM. So, the best management of the two rare entities (GSM and GC-GBM) should be further investigated in future clinical trials with hints taken from the epidemiologic study.

The 2016 WHO classification of central nervous tumors introduced molecular parameters in addition to histology to define GBM tumor entities (7). Although there is a trend to incorporate molecular markers into the classification of GBM,

TABLE 4 | Literature review on the epidemiologic data on histologic variants of glioblastoma from population-based cancer registries.

Registry [year, reference]	Period	All GBM patients	Histologic variants						
			Conventional GBM		GC-GBM		GSM		Survival outcomes
			N (%)	Median age (year)	*N* (%)	Median age (year)	*N* (%)	Median age (year)	Median survival (month)
US, SEER, [2009, (11)]	1988–2004	16,388	16,035 (97.8)	62	–	–	353 (2.2)	63	NS 9 (GBM) 8 (GSM)
US, SEER, [2009, (14)]	1988–2004	16,430	16,259 (99.0)	62	171 (1.0)	51	–	–	GC-GBM > GBM 8 (GBM) 11 (GC-GBM)
Australia, [2011, (23)]	2000–2008	2,275	2,197 (96.5)	–	17 (0.7)	–	62 (2.7)	–	–
US, NCDB, [2014, (13)]	1998–2011	69,935	67,509 (96.5)	61	592 (0.8)	56	1,834 (2.6)	61	GC-GBM > (GBM, GSM) 9.8 (GBM) 13.4 (GC-GBM) 8.8 (GSM)
US, NCDB, [2018, (17)]	2004–2013	37,760	36,658 (97.1)	61.7[a]	–	–	1,102 (2.9)	61.1[a]	NS 11.9 (GBM) 10.7 (GSM)
England, [2018, (24)]	1995–2015	37,786	37,046 (98.0)	–	263 (0.7)	–	477 (1.3)	–	–
US, SEER, [2019, (16)]	1985–2014	25,117	24,909 (99.2)	–	208 (0.8)	–	–	–	NS No survival data
US, SEER, [2019, (15)]	2004–2014	79,543	78,860 (99.1)	62	683 (0.9)	57			GC-GBM > GBM 11.7 (GBM) 15.5 (GC-GBM)
France, FBTDB, [2019, (25)]	2008–2015	2,053	1,988 (96.8)	–	36 (1.8)	–	29 (1.4)	–	–
Taiwan, current study	2000–2016	3,895	3,732 (95.8)	58.7[a]	61 (1.6)	49.5[a]	102 (2.6)	61.3[a]	NS 12.5 (GBM) 18.5 (GC-GBM) 12.8 (GSM)

FBTDB, French brain tumor database; GBM, glioblastoma; GC-GBM, giant cell glioblastoma; GSM, gliosarcoma; NCDB, National Cancer Database; NS, difference not statistically significant; SEER, surveillance epidemiology and end results.
[a]*Mean age.*

none of the markers has been introduced to routine clinical practice before 2016. That is why data on such markers from population-based studies are very limited. Taking SEER for example, we found there were no molecular data between 2001 and 2011 (5), which cover most of our study period. Likewise, IDH1 mutation status was not available in the National Cancer Database between 2004 and 2014 (5). We enrolled GBM patients between the period of 2000 and 2016, and the IDH marker was not mandatory for routine pathologic reports during that period and not registered in the TCR database in Taiwan. Due to lack of data, we were unable to evaluate the prognostic significance of these molecular markers in our study. Further, the more recently defined subtype of epithelioid GBM, there were no registered case data in the study.

It is well-known a younger age is significantly associated with good survival in conventional GBM patients in the literature (6, 20, 26–28). A younger age experienced favorable survival in our GBM cohort. In contrast, aging was not a prognostic factor in GSM or GC-GBM. This may indicate GBM variants possibly differ in clinical manifestation, or it may reflect the relevant chance of hidden bias from a small case number; so caution is advised in interpreting these results.

In the US analysis of GBM variants, the sex factor revealed conflicting results, with some studies showing the female sex experienced a favorable survival in GSM and GC-GBM, yet others reported no difference (11–17). Nonetheless, the sex disparity was not identified in GSM or GC-GBM variants in the study. However, the female sex was associated with improved survival of GBM in the literature (29–31).

The TCR database, similar to other national databases, lacks accuracy in documenting pre-existing comorbidities, and detailed cancer management, which could all impact the outcome analysis. Genetic factors also contribute closely to the prognosis of conventional GBM and its variants. Due to the lack of data, we were unable to evaluate the prognostic significance of these molecular markers in our study. Furthermore, even with large number of cases (3,895 in total), the case number in some subgroup were relatively small and thus might

not able to provide sufficient statistical power. For example, chemotherapy was associated with better survival for both GC-GBM and GSM, and the HRs (0.51 and 0.65) were even smaller than that for GBM (0.73), but did not reach statistical significance.

CONCLUSION

Utilizing a large national cohort and literature review, this paper adds more information on the epidemiology of GBM in both Asian and Western populations. We confirmed the similar incidence of GSM and GC-GBM in Asian and Western population. Our study showed GBM and its variants shared similar worse outcomes. Resection, post-operative radiotherapy, and chemotherapy did improve survival in conventional GBM, but had different effects on histologic variants.

DATA AVAILABILITY STATEMENT

The datasets presented in this study can be found in online repositories. The name of the repository and accession number can be found below: Open Science Framework (OSF), https://osf.io/, HFN3D (project name: histologic variants of glioblastoma in Taiwan).

ETHICS STATEMENT

The studies involving human participants were reviewed and approved by the Chi Mei Medical Center Institutional Review Board (IRB No. 10710-L05). Written informed consent for participation was not required for this study in accordance with the national legislation and the institutional requirements.

AUTHOR CONTRIBUTIONS

S-YH contributed to conception and design of the study. C-HH organized the database. C-HH and H-RG performed the statistical analysis. L-TS and S-YH wrote the first draft of the manuscript. H-RG, C-CH, and Y-CH wrote sections of the manuscript. All authors contributed to manuscript revision, read, and approved the submitted version.

FUNDING

This study was supported by a grant from Chi Mei Medical Center (No. CLFH10724).

ACKNOWLEDGMENTS

We are grateful to Health Data Science Center, National Cheng Kung University Hospital for providing administrative and technical support.

SUPPLEMENTARY MATERIAL

The Supplementary Material for this article can be found online at: https://www.frontiersin.org/articles/10.3389/fneur.2021.659921/full#supplementary-material

REFERENCES

1. Lin YJ, Chiu HY, Chiou MJ, Huang YC, Wei KC, Kuo CF, et al. Trends in the incidence of primary malignant brain tumors in Taiwan and correlation with comorbidities: a population-based study. *Clin Neurol Neurosurg.* (2017) 159:72–82. doi: 10.1016/j.clineuro.2017.05.021
2. Chien LN, Gittleman H, Ostrom QT, Hung KS, Sloan AE, Hsieh YC, et al. Comparative brain and central nervous system tumor incidence and survival between the United States and Taiwan based on population-based registry. *Front Public Health.* (2016) 4:151. doi: 10.3389/fpubh.2016.00151
3. Ostrom QT, Cote DJ, Ascha M, Kruchko C, Barnholtz-Sloan JS. Adult glioma incidence and survival by race or ethnicity in the United States from 2000 to 2014. *JAMA Oncol.* (2018) 4:1254–62. doi: 10.1001/jamaoncol.2018.1789
4. Ostrom QT, Gittleman H, de Blank PM, Finlay JL, Gurney JG, McKean-Cowdin R, et al. American brain tumor association adolescent and young adult primary brain and central nervous system tumors diagnosed in the United States in 2008–2012. *Neuro Oncol.* 18(Suppl 1). (2016) i1–50. doi: 10.1093/neuonc/nov297
5. Shabihkhani M, Telesca D, Movassaghi M, Naeini YB, Naeini KM, Hojat SA, et al. Incidence, survival, pathology, and genetics of adult Latino Americans with glioblastoma. *J Neurooncol.* (2017) 132:351–8. doi: 10.1007/s11060-017-2377-0
6. Miller CR, Perry A. Glioblastoma. *Arch Pathol Lab Med.* (2007) 131:397–406. doi: 10.1043/1543-2165(2007)131[397:G]2.0.Co;2
7. Louis DN, Perry A, Reifenberger G, von Deimling A, Figarella-Branger D, Cavenee WK, et al. The 2016 World Health Organization classification of tumors of the central nervous system: a summary. *Acta Neuropathol.* (2016) 131:803–20. doi: 10.1007/s00401-016-1545-1
8. Scheithauer BW. Development of the WHO classification of tumors of the central nervous system: a historical perspective. *Brain Pathol.* (2009) 19:551–64. doi: 10.1111/j.1750-3639.2008.00192.x
9. Chen B, Liu B, Wu C, Wang Z. Prognostic factors among single primary gliosarcoma cases: a study using surveillance, epidemiology, and end results data from 1973–2013. *Cancer Med.* (2019) 8:6233–42. doi: 10.1002/cam4.2503
10. Han SJ, Yang I, Tihan T, Prados MD, Parsa AT. Primary gliosarcoma: key clinical and pathologic distinctions from glioblastoma with implications as a unique oncologic entity. *J Neurooncol.* (2010) 96:313–20. doi: 10.1007/s11060-009-9973-6
11. Kozak KR, Moody JS. Giant cell glioblastoma: a glioblastoma subtype with distinct epidemiology and superior prognosis. *Neuro Oncol.* (2009) 11:833–41. doi: 10.1215/15228517-2008-123
12. Smith DR, Wu CC, Saadatmand HJ, Isaacson SR, Cheng SK, Sisti MB, et al. Clinical and molecular characteristics of gliosarcoma and modern prognostic significance relative to conventional glioblastoma. *J Neurooncol.* (2018) 137:303–11. doi: 10.1007/s11060-017-2718-z
13. Ortega A, Nuño M, Walia S, Mukherjee D, Black KL, Patil CG. Treatment and survival of patients harboring histological variants of glioblastoma. *J Clin Neurosci.* (2014) 21:1709–13. doi: 10.1016/j.jocn.2014.05.003
14. Kozak KR, Mahadevan A, Moody JS. Adult gliosarcoma: epidemiology, natural history, and factors associated with outcome. *Neuro Oncol.* (2009) 11:183–91. doi: 10.1215/15228517-2008-076
15. Jin MC, Wu A, Xiang M, Azad TD, Soltys SG, Li G, et al. Prognostic factors and treatment patterns in the management of giant cell glioblastoma. *World Neurosurg.* (2019) 128:e217–24. doi: 10.1016/j.wneu.2019.04.103
16. Bin Abdulrahman AK, Bin Abdulrahman KA, Bukhari YR, Faqihi AM, Ruiz JG. Association between giant cell glioblastoma and glioblastoma multiforme in the United States: a retrospective cohort study. *Brain Behav.* (2019) 9:e01402. doi: 10.1002/brb3.1402

17. Frandsen J, Orton A, Jensen R, Colman H, Cohen AL, Tward J, et al. Patterns of care and outcomes in gliosarcoma: an analysis of the National Cancer Database. *J Neurosurg.* (2018) 128:1133–8. doi: 10.3171/2016.12.Jns162291
18. Zhang G, Huang S, Zhang J, Wu Z, Lin S, Wang Y. Clinical outcome of gliosarcoma compared with glioblastoma multiforme: a clinical study in Chinese patients. *J Neurooncol.* (2016) 127:355–62. doi: 10.1007/s11060-015-2046-0
19. Nizamutdinov D, Stock EM, Dandashi JA, Vasquez EA, Mao Y, Dayawansa S, et al. Prognostication of survival outcomes in patients diagnosed with glioblastoma. *World Neurosurg.* (2018) 109:e67–74. doi: 10.1016/j.wneu.2017.09.104
20. Stupp R, Mason WP, van den Bent MJ, Weller M, Fisher B, Taphoorn MJ, et al. Radiotherapy plus concomitant and adjuvant temozolomide for glioblastoma. *N Engl J Med.* (2005) 352:987–96. doi: 10.1056/NEJMoa043330
21. Shieh LT, Guo HR, Chang YK, Lu NM, Ho SY. Clinical implications of multiple glioblastomas: an analysis of prognostic factors and survival to distinguish from their single counterparts. *J Formos Med Assoc.* (2020) 119:728–34. doi: 10.1016/j.jfma.2019.08.024
22. Liu WL, Lin KL, Chang YK, Lu NM, Chen CH, Chang CH, et al.. The effect of radiotherapy on the outcome of primary gliosarcoma: a clinical study of three cases and a literature review. *Therapeut Radiol Oncol.* (2017) 24:335–48. doi: 10.6316/TRO/201724(4)335
23. Dobes M, Khurana VG, Shadbolt B, Jain S, Smith SF, Smee R, et al. Increasing incidence of glioblastoma multiforme and meningioma, and decreasing incidence of Schwannoma (2000–2008): findings of a multicenter Australian study. *Surg Neurol Int.* (2011) 2:176. doi: 10.4103/2152-7806.90696
24. Philips A, Henshaw DL, Lamburn G, O'Carroll MJ. Brain tumours: rise in glioblastoma multiforme incidence in England 1995–2015 suggests an adverse environmental or lifestyle factor. *J Environ Public Health.* (2018) 2018:7910754. doi: 10.1155/2018/7910754
25. Fabbro-Peray P, Zouaoui S, Darlix A, Fabbro M, Pallud J, Rigau V, et al. Association of patterns of care, prognostic factors, and use of radiotherapy-temozolomide therapy with survival in patients with newly diagnosed glioblastoma: a French national population-based study. *J Neurooncol.* (2019) 142:91–101. doi: 10.1007/s11060-018-03065-z
26. Lacroix M, Abi-Said D, Fourney DR, Gokaslan ZL, Shi W, DeMonte F, et al. A multivariate analysis of 416 patients with glioblastoma multiforme: prognosis, extent of resection, and survival. *J Neurosurg.* (2001) 95:190–8. doi: 10.3171/jns.2001.95.2.0190
27. Shieh LT, Guo HR, Ho CH, Lin LC, Chang CH, Ho SY. Survival of glioblastoma treated with a moderately escalated radiation dose-results of a retrospective analysis. *PLoS ONE.* (2020) 15:e0233188. doi: 10.1371/journal.pone.0233188
28. Lutterbach J, Sauerbrei W, Guttenberger R. Multivariate analysis of prognostic factors in patients with glioblastoma. *Strahlenther Onkol.* (2003) 179:8–15. doi: 10.1007/s00066-003-1004-5
29. Tian M, Ma W, Chen Y, Yu Y, Zhu D, Shi J, et al. Impact of gender on the survival of patients with glioblastoma. *Biosci Rep.* (2018) 38:BSR20180752. doi: 10.1042/bsr20180752
30. Barone TA, Gorski JW, Greenberg SJ, Plunkett RJ. Estrogen increases survival in an orthotopic model of glioblastoma. *J Neurooncol.* (2009) 95:37–48. doi: 10.1007/s11060-009-9904-6
31. Ostrom QT, Rubin JB, Lathia JD, Berens ME, Barnholtz-Sloan JS. Females have the survival advantage in glioblastoma. *Neuro Oncol.* (2018) 20:576–7. doi: 10.1093/neuonc/noy002

Conflict of Interest: The authors declare that the research was conducted in the absence of any commercial or financial relationships that could be construed as a potential conflict of interest.

Publisher's Note: All claims expressed in this article are solely those of the authors and do not necessarily represent those of their affiliated organizations, or those of the publisher, the editors and the reviewers. Any product that may be evaluated in this article, or claim that may be made by its manufacturer, is not guaranteed or endorsed by the publisher.

frontiers | Frontiers in Oncology

ORIGINAL RESEARCH
published: 14 April 2022
doi: 10.3389/fonc.2022.621460

The Profiles of Tet-Mediated DNA Hydroxymethylation in Human Gliomas

Aneta Brągiel-Pieczonka[1†], Gabriela Lipka[1†], Angelika Stapińska-Syniec[2], Michał Czyżewski[2], Katarzyna Żybura-Broda[1], Michał Sobstyl[2], Marcin Rylski[1,3] and Marta Grabiec[1]*

[1] Department of Clinical Cytology, Centre of Postgraduate Medical Education, Warsaw, Poland, [2] Department of Neurosurgery, Institute of Psychiatry and Neurology, Warsaw, Poland, [3] Department of Radiology, Institute of Psychiatry and Neurology, Warsaw, Poland

OPEN ACCESS

Edited by:
Kamalakannan Palanichamy, The Ohio State University, United States

Reviewed by:
Joerg Robert Leheste, New York Institute of Technology, United States
Rasime Kalkan, Near East University, Cyprus

***Correspondence:**
Marta Grabiec
marta.grabiec@cmkp.edu.pl

[†]These authors have contributed equally to this work

Specialty section:
This article was submitted to Neuro-Oncology and Neurosurgical Oncology, a section of the journal Frontiers in Oncology

Received: 26 October 2020
Accepted: 17 March 2022
Published: 14 April 2022

Citation:
Brągiel-Pieczonka A, Lipka G, Stapińska-Syniec A, Czyżewski M, Żybura-Broda K, Sobstyl M, Rylski M and Grabiec M (2022) The Profiles of Tet-Mediated DNA Hydroxymethylation in Human Gliomas. Front. Oncol. 12:621460. doi: 10.3389/fonc.2022.621460

Gliomas are the most common primary malignant intracranial brain tumors. Their proliferative and invasive behavior is controlled by various epigenetic mechanisms. 5-hydroxymethylcytosine (5-hmC) is one of the epigenetic DNA modifications that employs ten-eleven translocation (TET) enzymes to its oxidation. Previous studies demonstrated altered expression of 5-hmC across gliomagenesis. However, its contribution to the initiation and progression of human gliomas still remains unknown. To characterize the expression profiles of 5-hmC and TET in human glioma samples we used the EpiJET 5-hmC and 5-mC Analysis Kit, quantitative real-time PCR, and Western blot analysis. A continuous decline of 5-hmC levels was observed in solid tissue across glioma grades. However, in glioblastoma (GBM), we documented uncommon heterogeneity in 5-hmC expression. Further analysis showed that the levels of TET proteins, but not their transcripts, may influence the 5-hmC abundance in GBM. Early tumor-related biomarkers may also be provided by the study of aberrant DNA hydroxymethylation in the blood of glioma patients. Therefore, we explored the patterns of TET transcripts in plasma samples and we found that their profiles were variously regulated, with significant value for *TET2*. The results of our study confirmed that DNA hydroxymethylation is an important mechanism involved in the pathogenesis of gliomas, with particular reference to glioblastoma. Heterogeneity of 5-hmC and TET proteins expression across GBM may provide novel insight into define subtype-specific patterns of hydroxymethylome, and thus help to interpret the heterogeneous outcomes of patients with the same disease.

Keywords: epigenetics, 5-hydroxymethylcytosine, ten-eleven translocation enzymes, brain tumors, glioblastoma

INTRODUCTION

The vast majority (80%) of malignant brain tumors is represented by gliomas (1). They have been classified by the World Health Organization into four grades, with Grade IV glioblastoma (GBM) as the most aggressive form. From 2016 the WHO grading is based on histological and molecular characteristics that are observed amongst various stages of gliomas (2). Many studies focused on

genomic or transcriptomic profiles of human gliomas demonstrated that although histologically similar, they constitute distinct subtypes (3–5) that are associated with different survival outcomes (6, 7). Therefore, systematic molecular analysis of human gliomas is essential for their comprehensive understanding. Aberrations in genes and molecular pathways, include *IDH1/IDH2* and *H3.1/H3.3* mutation or loss of *TP53* tumor suppressor gene, can be used together with histopathological findings for gliomas classification (8, 9).

However, dysregulation of epigenomes seems to be the primary molecular mechanism involved in the pathogenesis of human gliomas. Epigenetic alterations, such as modifications of DNA (10, 11) and histones (12, 13), nucleosome remodeling (14, 15) and RNA-mediated silencing (16–18) are pointed out as a source of gliomas phenotypic heterogeneity. DNA methylation is the best-studied epigenetic change in this field (19–21), but some reports revealed the existence of other modifications in DNA methylome.

The ten-eleven translocation (TET) enzymes can alter DNA methylation status by converting 5-methylcytosine (5-mC) to 5-hydroxymethylcytosine (5-hmC), and later to 5-formylcytosine (5-fC) and 5-carboxylcytosine (5-caC) (22). 5-hmC may act as a transient intermediate in the process of 5-mC demethylation, as well as, may epigenetically regulate gene expression. Several reports found the relationship between 5-hmC level and glioma grades (10, 23–26). However, 5-hmC modification and its direct effect on gliomas biology need to be investigated.

Here, we picture the TET-dependent hydroxymethylation patterns in human gliomas. Using solid tumor tissues samples we demonstrate heterogeneity in 5-hmC expression across glioblastoma which can provide novel insight into define subtype-specific patterns of 5-hmC, and thus help to interpret the heterogeneous outcomes of patients with the same disease.

MATERIALS AND METHODS

Clinical Samples

34 pairs of matched glioma tissues and blood samples were collected during standard neurosurgical tumor removals at the Department of Neurosurgery, Institute of Psychiatry and Neurology (Warsaw, Poland). Additionally, five independent random controls of blood samples were obtained from healthy volunteers. All solid tissues were submerged in the stayRNA solution (A&A Biotechnology) and stored at –80°C. Blood was collected into EDTA-treated tubes and centrifuged at 3500 rpm (MPW, Centrifuge MPW-350R, Rotor 1236B) for 10 min at 4°C. Then supernatant (plasma) was immediately transferred into the clean Eppendorf tubes and stored at –80°C.

5-hmC Quantification

The absolute level of 5-hmC in genomic DNA, previously extracted from 34 glioma tissues, was estimated with the EpiJET 5-hmC and 5-mC Analysis Kit (ThermoFisher Scientific). Briefly, 100 ng of DNA was glucosylated by T4 phage β-glucosyltransferase (T4 BGT), followed by subsequent digestion with Epi MspI and Epi HpaII enzymes. Then the percentage of cytosine modifications within CCGG sites was determined by quantitative real-time PCR (qRT-PCR) with a primer pair flanking recognition sequence. Primer sequences were as follows:

primer1_forward 5′-CTGTCATGGTGACAAAGGCATC-3′,
primer2_reverse 5′-CAGGATTTCTCTATTATGAAGACCT TG-3′.

The experiment was run in triplicate and the amount of 5-hmC was calculated as a percentage based on controls included in the kit.

Quantitative Real-Time PCR

Following Chomczynski`s protocol (27), total RNA of glioma tissues was extracted by TRIzol Reagent (Life Technologies), whereas Total RNA Mini Concentrator Kit (A&A Biotechnology) was used for the extraction of RNA from plasma samples. The concentration and purity of RNA samples were assessed by measuring the 260/280 ratio of absorbance values with the Synergy H4 spectrophotometer (BioTek). cDNA was synthesized from 500 ng of RNA using random hexamers and TaqMan Reverse Transcription Reagents (ThermoFisher Scientific) according to the manufacturer`s instructions. Transcript levels of *TET* family genes were determined by the quantitative real-time PCR using 5x HOT FirePolEvaGreen qPCR Mix (Solis Biodyne) and primer sets for *TET1*, *TET2*, *TET3*, and the housekeeping gene *GAPDH*. The primer sequences are listed in **Supplementary Table S1**. All samples were run in triplicate, and data were normalized to the expression of *GAPDH* (28), according to the ΔCt method. While the ΔΔCt method was applied for relative quantification in blood samples.

Western Blot

Thirty-four human glioma tissues were homogenized with TissueLyser LT homogenizer (Qiagen) in lysis buffer containing 2% SDS, pH 6.8 and protease inhibitors (Sigma). According to the protocol of Ericsson et al. (29), homogenates were incubated at 70°C and shaking at 1400 rpm (BioSan, Thermo-Shaker TS-100) for 10 min and then centrifuged at 12000 rpm (Eppendorf, Centrifuge 5415R, Rotor F45-24-11) for 5 min. The concentration of protein extracts was determined with the Bradford protein assay (Sigma). 15 μg of each protein sample was separated with 7% SDS-polyacrylamide gels and transferred onto nitrocellulose membranes using the Bio-Rad MINI Protean system. Immunoblotting with primary antibodies against TET1, TET2, TET3 (1:3000, ThermoFisher Scientific) and GAPDH (1:5000, Millipore) was performed overnight at 4°C, whereas secondary antibodies (a-mouse and a-rabbit, Vector) diluted 1:10000 were incubated with the membranes for one hour at room temperature. Blots were visualized with the WesternBright Quantum detection system (Advansta) on the UVITEC Cambridge scanner. Densitometry analysis was conducted using GelAnalyzer 2010 software.

Statistical Analysis

GraphPad Prism 7.02 software was used to analyze the data. Statistical significance of differences between groups was determined by One-way ANOVA or nonparametric Kruskal-

Wallis tests followed by *post hoc* Tukey or Dunn analysis, as well as with Mann-Whitney U test (*p < 0.05, **p < 0.01, ***p < 0.001). The results are presented as the mean ± standard deviation of the mean (SD).

RESULTS

Global Changes in 5-hmC Abundance in Gliomas

So far, decreased 5-hmC levels have been presented in a variety of tumors (30–32), suggesting that the loss of 5-hmC may be considered as an epigenetic hallmark of the disease. To evaluate the global changes in 5-hmC abundance in human brain tumors, we selected DNA of 34 glioma samples represented by different WHO grades and analyzed them with EpiJET 5-hmC and 5-mC Analysis Kit and quantitative real-time PCR. Clinical and epigenetic characteristics of glioma samples are shown in **Table 1**.

As can be seen in **Figure 1** and **Table 1**, gliomagenesis has generated the changes of DNA hydroxymethylation. The 5-hmC expression correlated negatively with WHO grading, ranged from 8.2% in Grade II gliomas to 3.0% in Grade IV-low$_{5\text{-hmC}}$ GBM. Significant differences were observed between Grades II and III ($p < 0.01$), as well as Grades II and IV-low$_{5\text{-hmC}}$ ($p < 0.01$). While we observed a decreasing trend in 5-hmC expression with a higher tumor stage, we documented a strong elevation in 5-hmC level in around 30% of Grades IV GBM (Grade IV-high$_{5\text{-hmC}}$). In this study group, the 5-hmC level was 20% and was significantly higher than in Grade IV-low$_{5\text{-hmC}}$ samples (3%, $p < 0.001$). To our knowledge, this is one of the few reports describing high variability in 5-hmC abundance at the tumor mass (10, 24). To clarify observed diversity, the GBMs samples were categorized according to their *IDH1*, and developmental status. The results had not revealed molecular differences between both categories in this scope. A great majority of samples (95%) were primary glioblastomas, while all of them demonstrated the absence of mutation in *IDH1* gene.

Recognized differences might be a consequence of alterations in the expression of TET enzymes that catalyze the conversion of 5-mC to 5-hmC.

TET Expression in Gliomas

To define the impact of TET enzymes on changes in DNA hydroxymethylation, we analyzed their expression at the gene and protein levels in solid tumor tissues. Quantitative real-time PCR was performed to examine the mRNA expression of *TET* family genes (*TET1*, *TET2*, and *TET3*) in 34 samples, including 6 Grade II gliomas, 7 Grade III gliomas and 21 Grade IV GBM. We found that the relative mRNA levels of all three *TET* genes were strongly reduced during glioma grades (**Figures 2A, C, E**). Their downregulation was significantly higher in Grade IV GBM in comparison with Grade II gliomas (*TET1* and *TET3* $p < 0.001$, *TET2* $p < 0.01$) and Grade III gliomas (*TET1* $p < 0.001$, *TET2* and *TET3* $p < 0.01$). As the decline in *TET* mRNA was associated with glioma grades and 5-hmC expression, we determined the levels of *TET* transcripts in two groups with high variability in total 5-hmC abundance across GBM (Grade IV-low$_{5\text{-hmC}}$ and Grade IV-high$_{5\text{-hmC}}$, **Figure 1**). There were no significant differences in *TET1 ($p = 0.1322$)*, *TET2 ($p = 0.2434$)* and *TET3 ($p = 0.8208$)* mRNA levels between glioblastoma Grade IV-low$_{5\text{-}}$

TABLE 1 | Characteristics of glioma patients.

Total cases = 34				
WHO grade	**II**	**III**	**IV-low $_{5\text{-hmC}}$**	**IV-high $_{5\text{-hmC}}$**
Number of patients	6	7	15	6
Age at diagnosis (years)				
Mean	39.3	41.4	65.9	63.2
Range	24 - 54	26 - 59	53 - 77	52 - 77
Gender				
Male/Female	3/3	4/3	9/6	3/3
Hemisphere				
Left/Right	1/5	4/3	8/7	1/5
Location				
Frontal	2	2	5	–
Temporal	3	5	4	4
Pariental	1	–	2	–
Occipital	–	–	4	2
Tumor status				
Primary/Recurrent	5/1	6/1	15/0	5/1
IDH1 status				
IDH1 wild-type	6	6	15	6
IDH1 mutant	0	1 (R132G)	0	0
5-hmC (%)	8.2	3.5	3.0	20.0

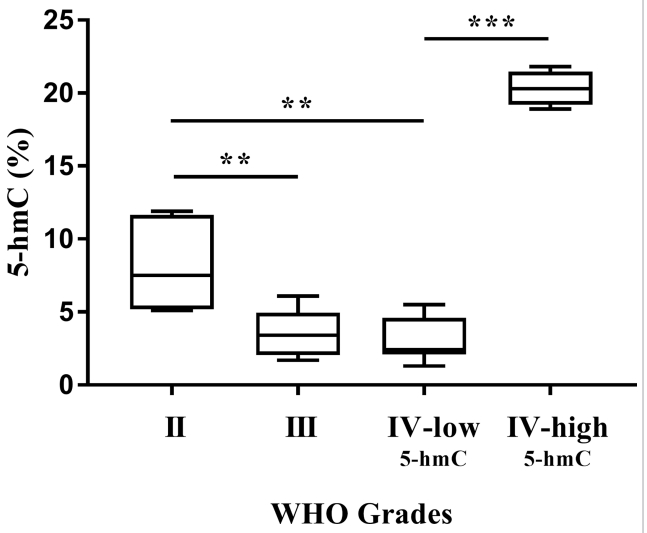

FIGURE 1 | Global 5-hmC abundance (%) in gliomas. Increasing WHO grades of glioma are associated with a continuous decline in 5-hmC levels, except for glioblastoma (IV-low$_{5\text{-hmC}}$ and IV-high$_{5\text{-hmC}}$). Differences among group means were evaluated by one-way ANOVA test (**$p < 0.01$, ***$p < 0.001$).

$_{hmC}$ and Grade IV-high$_{5\text{-hmC}}$ (**Figures 2B, D, F**). Next, we evaluated the levels of TET proteins in the same samples by Western blot. Expression levels of each TET proteins are shown in **Supplementary Table S2**. Immunoblotting revealed the absence of TET1 isoform at 235 kDa, which is mainly detected in embryonic stem cells. But, two additional bands at 162 kDa and 150 kDa were found in the majority of instances. TET2 and TET3 isoforms were discovered at 224 and 194 kDa, respectively (**Figure 3A**). As in the case of *TET* transcripts expression (**Figures 2A, C, E**), levels of TET proteins were negatively associated with advanced stages of gliomas. From Grade II gliomas to Grade IV GBM, we noticed 2-, 4- and 6-fold reduction in TET1$_{162 \text{ and } 150 \text{ kDa}}$, TET2$_{224 \text{ kDa}}$ and TET3$_{194 \text{ kDa}}$ levels, respectively. Interestingly, in Grade IV samples, we observed high variability in TET isoforms expression pattern, which could affect 5-hmC abundance. Quantification of normalized values showed significant differences in TET1$_{162 \text{ and } 150 \text{ kDa}}$ ($p < 0.01$, $p < 0.05$), TET2$_{224 \text{ kDa}}$ ($p < 0.001$) and TET3$_{194 \text{ kDa}}$ ($p < 0.05$) protein levels between GBM Grade IV-low$_{5\text{-hmC}}$ and Grade IV-high$_{5\text{-hmC}}$ (**Figures 3B–E**). These findings suggested the potential role of TET proteins patterns in setting the 5-hmC level in Grade IV glioblastoma.

TET Transcripts Profiling in Plasma Samples

The prospect of distinguishing the aberrant DNA hydroxymethylation in the blood of glioma patients may indicate a powerful tool for early cancer detection or monitoring its progress. To explore the potential diagnostic features of *TET* transcripts profiling, we performed the quantitative real-time PCR on 34 plasma samples obtained from patients with Grade II or III or IV gliomas, and 5 healthy controls. Expression of *TET* genes was observed in the majority of examined samples, followed by specific numbers for *TET1* (control: 80% vs. Grade: II-83%, III-57%, IV-70%), *TET2* (control: 80% vs. Grade: II-83%, III-71%, IV-91%) and *TET3* (control: 80% vs. Grade: II-50%, III-86%, IV-91%) transcript. Our results confirmed that the employed method was sensitive to low-input mRNA presented in plasma samples. The further analysis evaluated the relative mRNA levels of *TET* genes in plasma samples obtaining from patients with different WHO grades gliomas and compared them to healthy controls (**Figures 4A–C**). The results displayed various profiles for each transcript. While *TET1* characterized slightly lower expression than control, *TET3* was similar to control values. The expression of both transcripts was unaffected by WHO grading (**Figures 4A, C**). Whereas, the level of *TET2* was significantly increased in plasma samples derived from patients with Grade II gliomas compared to controls ($p < 0.01$, **Figure 4B**). Validation of our preliminary results in a larger population of patients is needed to evaluate their use as potential biomarkers for early-stage gliomas diagnostics.

DISCUSSION

Currently, the molecular landscape of brain tumors is described by epigenetic mechanisms include DNA methylation and hydroxymethylation (10, 11), histone modifications (12, 13), nucleosome remodeling (14, 15) and RNA-mediated silencing (16–18), that may clarify their etiologic evolution. Recently rediscovered, oxidized form of 5-methylcytosine (5-hmC) may act as a transient intermediate in the process of 5-mC demethylation or may epigenetically mark the cellular state itself with different biological roles.

In the present study, we characterize the epigenetic profile of DNA hydroxymethylation in human gliomas. Decreased level of 5-hmC was observed in glioma patients compared to healthy controls (33–35), but also it was related to glioma grades (10, 23–26). Our results confirm that the loss of 5-hmC is a hallmark of high-grade gliomas. However, we documented a significant increase of global 5-hmC abundance in almost a third of Grades IV GBM. This is one of the few findings that demonstrated heterogeneity in 5-hmC expression across the bulk of the glioblastoma (10, 24). According to recent research, the intra-tumoral diversity of 5-hmC levels among single GBM cells, that represent the proliferative, stem-like and tumorigenic states, could clarify unexpected results (36). But, dysregulation of TET enzymes function may be a possible biological explanation for the observed variability as well. The influence of TETs, including their genetic alterations and subcellular localization, on 5-hmC status in glioma cells, was described by several studies (23–25, 37, 38). Recently, epigenetic repression of histone marks (H4K16ac, H3K4me3, H3K9ac, H3K36me3, H3K4me1, H3K27ac) in *TET3* gene has been postulated as a driver of glioblastoma development *via* genome-wide alteration of 5-hmC (39). Generally, it is believed that the decline in *TET* genes expression causes a widespread reduction of 5-hmC and poorer

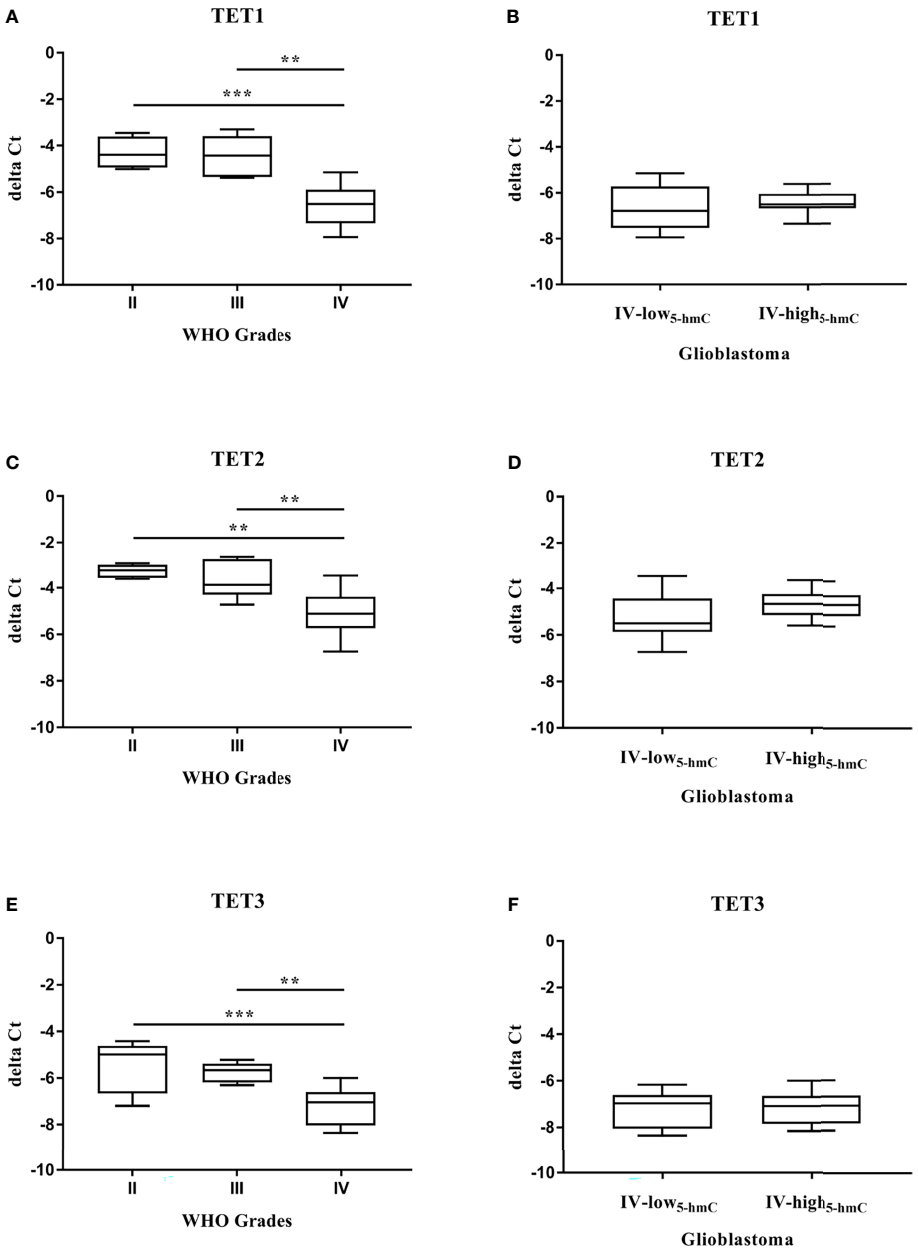

FIGURE 2 | Quantitation of *TET* transcripts in gliomas. qRT–PCR analysis of *TET* mRNA **(A–F)**. The expression of *TET1* **(A)**, *TET2* **(C)**, *TET3* **(E)** mRNA significantly decreased at a higher WHO grade of glioma. Differences among group means were evaluated by one-way ANOVA test (**$p < 0.01$, ***$p < 0.001$). High variability in 5-hmC abundance across glioblastoma (Grade IV-low$_{5\text{-hmC}}$ and Grade IV-high$_{5\text{-hmC}}$) was not linked with levels of *TET1* **(B)**, *TET2* **(D)**, *TET3* **(F)** transcripts.

prognosis in glioma patients. We found that *TET1*, *TET2*, *TET3* mRNA, and 5-hmC levels were decreased during glioma grades. However, similarly to Jin and Glowacka results (40, 41), there was no correlation between expression of *TET* transcripts and variability in 5-hmC abundance across the bulk of the glioblastoma. To define the complete impact of TETs on changes in DNA hydroxymethylation, we evaluated their protein levels in the same samples. Proteins produced by the TET2 and TET3 isoforms were expressed as expected bands at 224 kDa and 194 kDa. Instead of the 235 kDa canonical TET1 protein, we found two short isoforms (162 kDa and ~150 kDa). According to previous reports, they are exclusively activated from an alternate promoter in somatic cancer cells (42, 43). The levels of TET proteins, just as *TET* transcripts, were negatively associated with high-grade gliomas. However, Grade IV GBM samples were more variable in this field. Significant heterogeneity in the expression of TET2 protein in glioblastoma was also noted by Briand (44). We furthermore pointed out the relation between variable levels of TET proteins and

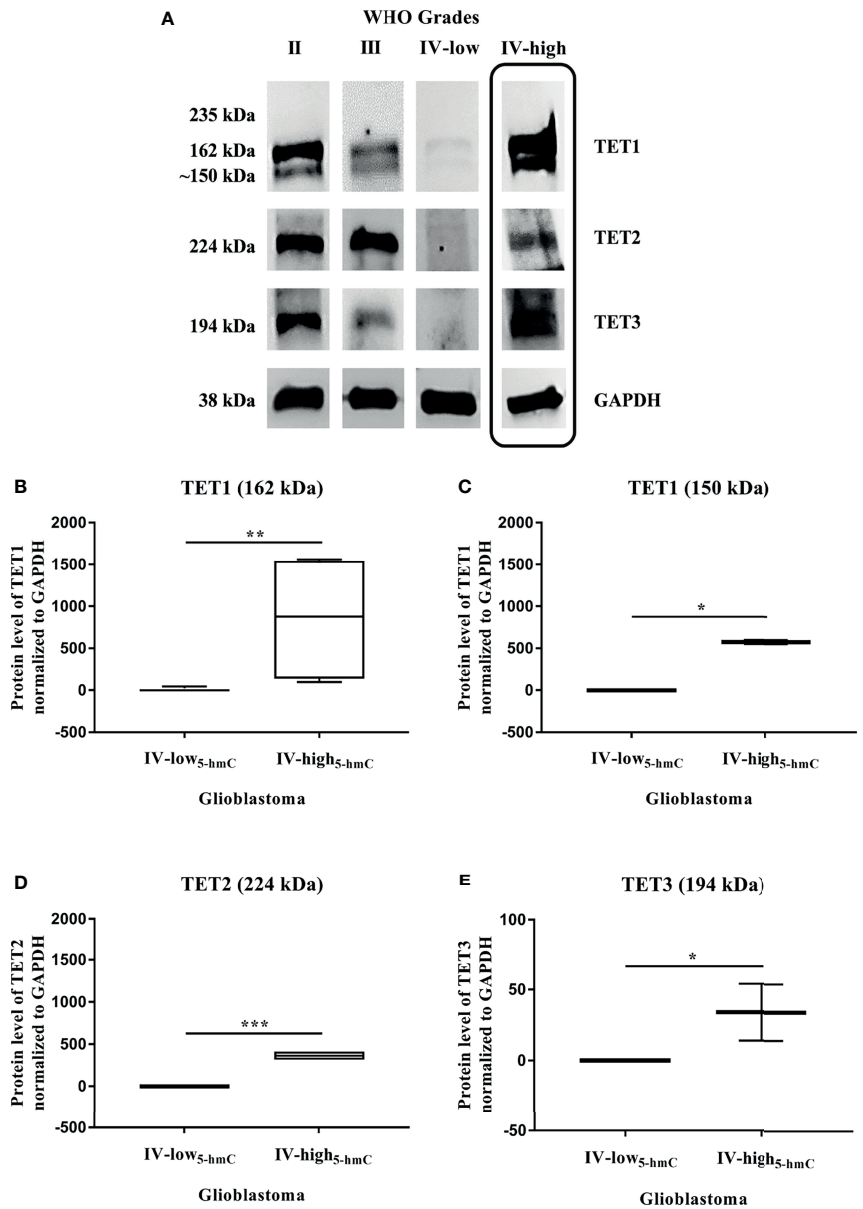

FIGURE 3 | TET proteins expression in gliomas. Western blot analysis of TET proteins **(A–E)**. Exemplary immunoblots of TET1, TET2, and TET3 proteins pictured loss of their expression across glioma stages, except some Grade IV samples (last column). Expression levels of these proteins were normalized with GAPDH **(A)**. High variability in protein levels of TET1 **(B, C)**, TET2 **(D)** and TET3 **(E)** correlated with 5-hmC abundance across glioblastoma (Grade IV-low$_{5\text{-hmC}}$ and Grade IV-high$_{5\text{-hmC}}$). Differences between two groups were evaluated by Mann-Whitney U test (*$p < 0.05$, **$p < 0.01$, ***$p < 0.001$).

5-hmC abundance across glioblastoma. Our findings suggest that the regulation of TET transcription and translation can be made in a different way. For example, this observed imbalance may be a result of different actions of transcription factors, RNA binding proteins, miRNAs targeting mRNA or post-translational modifications (like phosphorylation, acetylation, glycosylation, etc.). Based on the patient-derived glioma stem cells (GSCs) model, the transcription factor (SOX2)-oncomiR (miR-10b-5p)-TET2 axis was identified, which plays an important role in promoting GBM oncogenesis (45). However, it is one of many potential mechanisms involved in glioblastoma growth.

In summary, we demonstrated that expression patterns of TET proteins and the 5-hmC abundance are changed in Grade IV GBM, but the molecular mechanism of this process still needs to be clarified.

Recently, many studies on gliomas indicated the presence of circulating cell-free coding and non-coding nucleic acids in blood or other biofluid samples (46–48). Therefore, liquid

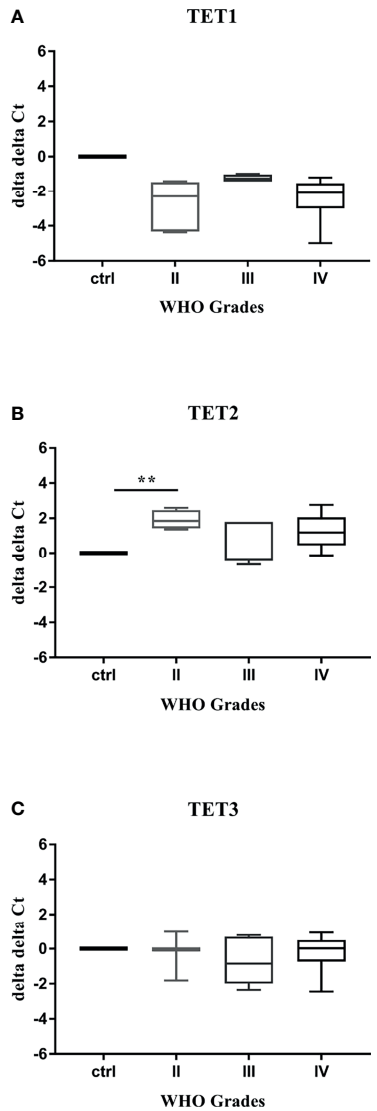

FIGURE 4 | *TET* transcripts profiling in plasma samples. qRT–PCR analysis of *TET* mRNA **(A–C)**. Levels of *TET1* **(A)**, *TET2* **(B)**, and TET3 **(C)** transcripts were variously regulated in plasma samples obtained from patients with gliomas. Statistical analysis performed using non-parametric Kruskal-Wallis test (**$p < 0.01$).

biopsy has become a new diagnostic tool that may establish and track the stage of cancer with particular biomarkers. Cai's group, for example, has developed a noninvasive 5-hmC detection method in circulating cell-free DNA of glioma patients, which was able to distinguish the difference between GBM and lower-grade gliomas regardless of *IDH1* mutation status (49). Here, we explore the potential diagnostic features of *TET* transcripts in plasma samples obtained from patients with gliomas. All three *TET* transcripts were detected in plasma, but their profiles differed from those in solid tissue. We showed that the plasma relative mRNA level for *TET1* was decreased in every stage of glioma, while the *TET3* level remained unchanged. The most promising results were provided by *TET2* gene that was significantly increased in Grade II glioma. Validation of our preliminary results in a larger population of patients is needed to evaluate their use as potential biomarkers for glioma diagnostics.

To conclude, we found that global abundance of 5-hmC was negatively correlated with glioma WHO grades and variable across the bulk of the glioblastoma. It was followed by various TET proteins patterns in solid tumor tissues. In contrast, profiles of *TET* transcripts in plasma samples displayed its heterogeneity. However, significant overexpression of *TET2* in Grade II gliomas might offer a new tool for effective diagnosis of lower-grade glioma patients. Our findings provide novel information about the potential role of TET epigenetic regulation in human gliomas, with particular reference to glioblastoma.

DATA AVAILABILITY STATEMENT

All data generated during this study are included in the article. Further inquiries can be directed to the corresponding author.

ETHICS STATEMENT

The study was conformed to the standards set by the Declaration of Helsinki and approved by the ethics committee of the Centre of Postgraduate Medical Education (code: 34/PB/2017). Written informed consent was obtained from participants prior to specimen collection.

AUTHOR CONTRIBUTIONS

MG designed all experiments, interpreted the results, and wrote the manuscript. AB-P, GL performed the experiments, analyzed the data. KŻ-B performed part of molecular analysis. AS-S, MC contributed to sample collection and registered clinical information. MS and MR managed sample collection; critically commented on the manuscript. All authors read and approved the final version.

FUNDING

This study was supported by a statutory grant 501-1-027-03-19 from the Centre of Postgraduate Medical Education in Warsaw.

ACKNOWLEDGMENTS

The authors thank Mrs. Monika Kubiak for help with the management of clinical information.

SUPPLEMENTARY MATERIAL

The Supplementary Material for this article can be found online at: https://www.frontiersin.org/articles/10.3389/fonc.2022.621460/full#supplementary-material

REFERENCES

1. Ostrom QT, Cioffi G, Gittleman H, Patil N, Waite K, Kruchko C, et al. CBTRUS Statistical Report: Primary Brain and Other Central Nervous System Tumors Diagnosed in the United States in 2012-2016. *Neuro Oncol* (2019) 21 (Suppl 5):v1–v100. doi: 10.1093/neuonc/noz150
2. Louis DN, Perry A, Reifenberger G, von Deimling A, Figarella-Branger D, Cavenee WK, et al. The 2016 World Health Organization Classification of Tumors of the Central Nervous System: A Summary. *Acta Neuropathol* (2016) 131:803–20. doi: 10.1007/s00401-016-1545-1
3. Sottoriva A, Spiteri I, Piccirillo SGM, Touloumis A, Collins VP, Marioni JC, et al. Intratumor Heterogeneity in Human Glioblastoma Reflects Cancer Evolutionary Dynamics. *Proc Natl Acad Sci USA* (2013) 110:4009–14. doi: 10.1073/pnas.1219747110
4. Nomura M, Mukasa A, Nagae G, Yamamoto S, Tatsuno K, Ueda H, et al. Distinct Molecular Profile of Diffuse Cerebellar Gliomas. *Acta Neuropathol* (2017) 134:941–56. doi: 10.1007/s00401-017-1771-1
5. Perrech M, Dreher L, Rohn G, Stavrinou P, Krischek B, Toliat M, et al. Qualitative and Quantitative Analysis of IDH1 Mutation in Progressive Gliomas by Allele-Specific qPCR and Western Blot Analysis. *Technol Cancer Res Treat* (2019) 18:1533033819828396. doi: 10.1177/1533033819828396
6. Marko NF, Toms SA, Barnett GH, Weil R. Genomic Expression Patterns Distinguish Long-Term From Short-Term Glioblastoma Survivors: A Preliminary Feasibility Study. *Genomics* (2008) 91:395–406. doi: 10.1016/j.ygeno.2008.01.002
7. Bernal Rubio YL, Gonzalez-Reymundez A, Wu KHH, Griguer CE, Steibel JP, de Los Campos G, et al. Whole-Genome Multi-Omic Study of Survival in Patients With Glioblastoma Multiforme. *G3 (Bethesda)* (2018) 8:3627–36. doi: 10.1534/g3.118.200391
8. Verhaak RGW, Hoadley KA, Purdom E, Wang V, Qi Y, Wilkerson MD, et al. Integrated Genomic Analysis Identifies Clinically Relevant Subtypes of Glioblastoma Characterized by Abnormalities in PDGFRA, IDH1, EGFR, and NF1. *Cancer Cell* (2010) 17:98–110. doi: 10.1016/j.ccr.2009.12.020
9. Aldape K, Zadeh G, Mansouri S, Reifenberger G, von Deimling A. Glioblastoma: Pathology, Molecular Mechanisms and Markers. *Acta Neuropathol* (2015) 129:829–48. doi: 10.1007/s00401-015-1432-1
10. Orr BA, Haffner MC, Nelson WG, Yegnasubramanian S, Eberhart CG. Decreased 5-Hydroxymethylcytosine is Associated With Neural Progenitor Phenotype in Normal Brain and Shorter Survival in Malignant Glioma. *PloS One* (2012) 7:e41036. doi: 10.1371/journal.pone.0041036
11. Ma J, Hou X, Li M, Ren H, Fang S, Wang X, et al. Genome-Wide Methylation Profiling Reveals New Biomarkers for Prognosis Prediction of Glioblastoma. *J Cancer Res Ther* (2015) 11(Suppl 2):C212–5. doi: 10.4103/0973-1482.168188
12. Vettermann FJ, Felsberg J, Reifenberger G, Hasselblatt M, Forbrig R, Berding G, et al. Characterization of Diffuse Gliomas With Histone H3-G34 Mutation by MRI and Dynamic 18F-FET PET. *Clin Nucl Med* (2018) 43:895–8. doi: 10.1097/RLU.0000000000002300
13. Castel D, Kergrohen T, Tauziede-Espariat A, Mackay A, Ghermaoui S, Lechapt E, et al. Histone H3 Wild-Type DIPG/DMG Overexpressing EZHIP Extend the Spectrum Diffuse Midline Gliomas With PRC2 Inhibition Beyond H3-K27M Mutation. *Acta Neuropathol* (2020) 139:1109–13. doi: 10.1007/s00401-020-02142-w
14. Diehl KL, Ge EJ, Weinberg DN, Jani KS, Allis CD, Muir TW. PRC2 Engages a Bivalent H3K27M-H3K27me3 Dinucleosome Inhibitor. *Proc Natl Acad Sci USA* (2019) 116:22152–7. doi: 10.1073/pnas.1911775116
15. Lu VM, Power EA, Zhang L, Daniels DJ. Unlocking the Translational Potential of Circulating Nucleosomes for Liquid Biopsy in Diffuse Intrinsic Pontine Glioma. *biomark Med* (2019) 13:597–600. doi: 10.2217/bmm-2019-0139
16. Cui H, Mu Y, Yu L, Xi YG, Matthiesen R, Su X, et al. Methylation of the miR-126 Gene Associated With Glioma Progression. *Fam Cancer* (2016) 15:317–24. doi: 10.1007/s10689-015-9846-4
17. Xue L, Wang Y, Yue S, Zhang J. The Expression of miRNA-221 and miRNA-222 in Gliomas Patients and Their Prognosis. *Neurol Sci* (2017) 38:67–73. doi: 10.1007/s10072-016-2710-y
18. Liu ZQ, Ren JJ, Zhao JL, Zang J, Long QF, Du JJ, et al. MicroRNA-144 Represses Gliomas Progression and Elevates Susceptibility to Temozolomide by Targeting CAV2 and FGF7. *Sci Rep* (2020) 10:4155. doi: 10.1038/s41598-020-60218-9
19. Hegi ME, Diserens AC, Gorlia T, Hamou MF, de Tribolet N, Weller M, et al. MGMT Gene Silencing and Benefit From Temozolomide in Glioblastoma. *N Engl J Med* (2005) 352:997–1003. doi: 10.1056/NEJMoa043331
20. Capper D, Jones DTW, Sill M, Hovestadt V, Schrimpf D, Sturm D, et al. DNA Methylation-Based Classification of Central Nervous System Tumours. *Nature* (2018) 555:469–74. doi: 10.1038/nature26000
21. Zhang M, Lv X, Jiang Y, Li G, Qiao Q. Identification of Aberrantly Methylated Differentially Expressed Genes in Glioblastoma Multiforme and Their Association With Patient Survival. *Exp Ther Med* (2019) 18:2140–52. doi: 10.3892/etm.2019.7807
22. Ito S, D`Alessio AC, Taranova OV, Hong K, Sowers LC, Zhang Y. Role of Tet Proteins in 5mc to 5hmc Conversion, ES-Cell Self-Renewal and Inner Cell Mass Specification. *Nature* (2010) 466:1129–33. doi: 10.1038/nature09303
23. Muller T, Gessi M, Waha A, Isselstein LJ, Luxen D, Freihoff D, et al. Nuclear Exclusion of TET1 Is Associated With Loss of 5-Hydroxymethylcytosine in IDH1 Wild-Type Gliomas. *Am J Pathol* (2012) 181:675–83. doi: 10.1016/j.ajpath.2012.04.017
24. Takai H, Masuda K, Sato T, Sakaguchi Y, Suzuki T, Suzuki T, et al. 5-Hydroxymethylcytosine Plays a Critical Role in Glioblastomagenesis by Recruiting the CHTOP-Methylosome Complex. *Cell Rep* (2014) 9:48–60. doi: 10.1016/j.celrep.2014.08.071
25. Kraus TFJ, Kolck G, Greiner A, Schierl K, Guibourt V, Kretzschmar HA. Loss of 5-Hydroxymethylcytosine and Intratumoral Heterogeneity as an Epigenomic Hallmark of Glioblastoma. *Tumour Biol* (2015) 36:8439–46. doi: 10.1007/s13277-015-3606-9
26. Zhang F, Liu Y, Zhang Z, Li J, Wan Y, Zhang L, et al. 5-Hydroxymethylcytosine Loss Is Associated With Poor Prognosis for Patients With WHO Grade II Diffuse Astrocytomas. *Sci Rep* (2016) 6:20882. doi: 10.1038/srep20882
27. Chomczynski P, Sacchi N. Single-Step Method of RNA Isolation by Acid Guanidinium Thiocyanate-Phenol-Chloroform Extraction. *Anal Biochem* (1987) 162:156–9. doi: 10.1006/abio.1987.9999
28. Grube S, Gottig T, Freitag D, Ewald C, Kalff R, Walter J. Selection of Suitable Reference Genes for Expression Analysis in Human Glioma Using RT-qPCR. *J Neurooncol* (2015) 123:35–42. doi: 10.1007/s11060-015-1772-7
29. Ericsson C, Peredo I, Nister M. Optimized Protein Extraction From Cryopreserved Brain Tissue Samples. *Acta Oncol* (2007) 46:10–20. doi: 10.1080/02841860600847061
30. Kudo Y, Tateishi K, Yamamoto K, Yamamoto S, Asaoka Y, Ijichi H, et al. Loss of 5-Hydroxymethylcytosine is Accompanied With Malignant Cellular Transformation. *Cancer Sci* (2012) 103:670–6. doi: 10.1111/j.1349-7006.2012.02213.x
31. Yang H, Liu Y, Bai F, Zhang JY, Ma SH, Liu J, et al. Tumor Development is Associated With Decrease of TET Gene Expression and 5-Methylcytosine Hydroxylation. *Oncogene* (2013) 32:663–9. doi: 10.1038/onc.2012.67
32. Chen Z, Shi X, Guo L, Li Y, Luo M, He J. Decreased 5-Hydroxymethylcytosine Levels Correlate With Cancer Progression and Poor Survival: A Systematic Review and Meta-Analysis. *Oncotarget* (2017) 8:1944–52. doi: 10.18632/oncotarget.13719
33. Johnson KC, Houseman EA, King JE, von Herrmann KM, Fadul CE, Christensen BC. 5-Hydroxymethylcytosine Localizes to Enhancer Elements and is Associated With Survival in Glioblastoma Patients. *Nat Commun* (2016) 7:13177. doi: 10.1038/ncomms13177
34. Fernandez AF, Bayon GF, Sierra MI, Urdinguio RG, Torano EG, Garcia MG, et al. Loss of 5hmc Identifies a New Type of Aberrant DNA Hypermethylation in Glioma. *Hum Mol Genet* (2018) 27:3046–59. doi: 10.1093/hmg/ddy214
35. Fu R, Ding Y, Luo J, Huang KM, Tang XJ, Li DS, et al. Ten-Eleven Translocation 1 Regulates Methylation of Autophagy-Related Genes in Human Glioma. *Neuroreport* (2018) 29:731–8. doi: 10.1097/WNR.0000000000001024
36. El-Habr EA, Dubois LG, Burel-Vandenbos F, Bogeas A, Lipecka J, Turchi L, et al. A Driver for GABA Metabolism in Controlling Stem and Proliferative Cell State Through GHB Production in Glioma. *Acta Neuropathol* (2017) 133:645–60. doi: 10.1007/s00401-016-1659-5
37. Putiri EL, Tiedemann RL, Thompson JJ, Liu C, Ho T, Choi JH, et al. Distinct and Overlapping Control of 5-Methylcytosine and 5-Hydroxymethylcytosine by the TET Proteins in Human Cancer Cells. *Genome Biol* (2014) 15:R81. doi: 10.1186/gb-2014-15-6-r81
38. Garcia MG, Carella A, Urdinguio RG, Bayon GF, Lopez V, Tejedor JR, et al. Epigenetic Dysregulation of TET2 in Human Glioblastoma. *Oncotarget* (2018) 9:25922–34. doi: 10.18632/oncotarget.25406

39. Carella A, Tejedor JR, Garcia MG, Urdinguio RG, Bayon GF, Sierra M, et al. Epigenetic Downregulation of TET3 Reduces Genome-Wide 5hmc Levels and Promotes Glioblastoma Tumorigenesis. *Int J Cancer* (2020) 146:373–87. doi: 10.1002/ijc.32520
40. Jin SG, Jiang Y, Qiu R, Rauch TA, Wang Y, Schackert G, et al. 5-Hydroxymethylcytosine Is Strongly Depleted in Human Cancers But its Levels Do Not Correlate With IDH1 Mutations. *Cancer Res* (2011) 71:7360–5. doi: 10.1158/0008-5472.CAN-11-2023
41. Glowacka WK, Jain H, Okura M, Maimaitiming A, Mamatjan Y, Nejad R, et al. 5-Hydroxymethylcytosine Preferentially Targets Genes Upregulated in Isocitrate Dehydrogenase 1 Mutant High-Grade Glioma. *Acta Neuropathol* (2018) 135:617–34. doi: 10.1007/s00401-018-1821-3
42. Zhang W, Xia W, Wang Q, Towers AJ, Chen J, Gao R, et al. Isoform Switch of TET1 Regulates DNA Demethylation and Mouse Development. *Mol Cell* (2016) 64:1062–73. doi: 10.1016/j.molcel.2016.10.030
43. Good CR, Madzo J, Patel B, Maegawa S, Engel N, Jelinek J, et al. A Novel Isoform of TET1 That Lacks a CXXC Domain Is Overexpressed in Cancer. *Nucleic Acids Res* (2017) 45:8269–81. doi: 10.1093/nar/gkx435
44. Briand J, Nadaradjane A, Vallette FM, Cartron P-F. The TET2 Expression Level Correlates With a Short Relapse Time in Glioblastoma Multiforme. *J Clin Epigenet* (2018) 4:12. doi: 10.21767/2472-1158.100097
45. Lopez-Bertoni H, Johnson A, Rui Y, Lal B, Sall S, Malloy M, et al. Sox2 Induces Glioblastoma Cell Stemness and Tumor Propagation by Repressing TET2 and Deregulating 5hmc and 5mc DNA Modifications. *Signal Transduct Target Ther* (2022) 7:37. doi: 10.1038/s41392-021-00857-0
46. Schwaederle M, Husain H, Fanta PT, Piccioni DE, Kesari S, Schwab RB, et al. Detection Rate of Actionable Mutations in Diverse Cancers Using a Biopsy-Free (Blood) Circulating Tumor Cell DNA Assay. *Oncotarget* (2016) 7:9707–17. doi: 10.18632/oncotarget.7110
47. Mouliere F, Mair R, Chandrananda D, Marass F, Smith CG, Su J, et al. Detection of Cell-Free DNA Fragmentation and Copy Number Alterations in Cerebrospinal Fluid From Glioma Patients. *EMBO Mol Med* (2018) 10:e9323. doi: 10.15252/emmm.201809323
48. Piccioni DE, Achrol AS, Kiedrowski LA, Banks KC, Boucher N, Barkhoudarian G, et al. Analysis of Cell-Free Circulating Tumor DNA in 419 Patients With Glioblastoma and Other Primary Brain Tumors. *CNS Oncol* (2019) 8:CNS34. doi: 10.2217/cns-2018-0015
49. Cai J, Zeng C, Hua W, Qi Z, Song Y, Lu X, et al. An Integrative Analysis of Genome-Wide 5-Hydroxymethylcytosines in Circulating Cell-Free DNA Detects Noninvasive Diagnostic Markers for Gliomas. *Neurooncol Adv* (2021) 3:vdab049. doi: 10.1093/noajnl/vdab049

Conflict of Interest: The authors declare that the research was conducted in the absence of any commercial or financial relationships that could be construed as a potential conflict of interest.

Publisher's Note: All claims expressed in this article are solely those of the authors and do not necessarily represent those of their affiliated organizations, or those of the publisher, the editors and the reviewers. Any product that may be evaluated in this article, or claim that may be made by its manufacturer, is not guaranteed or endorsed by the publisher.

frontiers | Frontiers in Oncology

TYPE Original Research
PUBLISHED 25 August 2022
DOI 10.3389/fonc.2022.696037

OPEN ACCESS

EDITED BY
Christopher Hong,
Yale Medicine, United States

REVIEWED BY
Jian L. Campian,
Mayo Clinic, United States
Jacek Furtak,
10th Military Research Hospital and Polyclinic, Poland

*CORRESPONDENCE
Feng Qiu
lukeqiubmu@163.com
Jinhong Mei
mjhdoctor@126.com
Chunliang Wang
wang330006@126.com

†These authors have contributed equally to this work and share first authorship

SPECIALTY SECTION
This article was submitted to Neuro-Oncology and Neurosurgical Oncology, a section of the journal Frontiers in Oncology

RECEIVED 16 April 2021
ACCEPTED 12 July 2022
PUBLISHED 25 August 2022

CITATION
Zhang Z, Gu W, Hu M, Zhang G, Yu F, Xu J, Deng J, Xu L, Mei J, Wang C and Qiu F (2022) Based on clinical Ki-67 expression and serum infiltrating lymphocytes related nomogram for predicting the diagnosis of glioma-grading.
Front. Oncol. 12:696037.
doi: 10.3389/fonc.2022.696037

Based on clinical Ki-67 expression and serum infiltrating lymphocytes related nomogram for predicting the diagnosis of glioma-grading

Zhi Zhang[1†], Weiguo Gu[2,3†], Mingbin Hu[2†], Guohua Zhang[3], Feng Yu[2,4], Jinbiao Xu[4], Jianxiong Deng[4], Linlin Xu[5,6], Jinhong Mei[5,6*], Chunliang Wang[1*] and Feng Qiu[3,4*]

[1]Department of Neurosurgery, The First Affiliated Hospital of Nanchang University, Nanchang, China, [2]Department of Oncology, The First Affiliated Hospital of Nanchang University, Nanchang, China, [3]Nanchang Key Laboratory of Tumor Gene Diagnosis and Innovative Treatment Research, Nanchang, China, [4]Department of Oncology, Gaoxin Branch of the First Affiliated Hospital of Nanchang University, Nanchang, China, [5]Department of Pathology, The First Affiliated Hospital of Nanchang University, Nanchang, China, [6]Molecular Pathology Center, The First Affiliated Hospital of Nanchang University, Nanchang, China

Background: Compelling evidence indicates that elevated peripheral serum lymphocytes are associated with a favorable prognosis in various cancers. However, the association between serum lymphocytes and glioma is contradictory. In this study, a nomogram was established to predict the diagnosis of glioma-grading through Ki-67 expression and serum lymphocytes.

Methods: We performed a retrospective analysis of 239 patients diagnosed with LGG and 178 patients with HGG. Immunohistochemistry was used to determine the Ki-67 expression. Following multivariate logistic regression analysis, a nomogram was established and used to identify the most related factors associated with HGG. The consistency index (C-index), decision curve analysis (DCA), and a calibration curve were used to validate the model.

Results: The number of LGG patients with more IDH1/2 mutations and 1p19q co-deletion was greater than that of HGG patients. The multivariate logistic analysis identified Ki-67 expression, serum lymphocyte count, and serum albumin (ALU) as independent risk factors associated with HGG, and these factors were included in a nomogram in the training cohort. In the validation cohort, the nomogram demonstrated good calibration and high consistency (C-index = 0.794). The Spearman correlation analysis revealed a significant association between HGG and serum lymphocyte count ($r = -0.238$, $P < 0.001$), ALU ($r = -0.232$, $P < 0.001$), and Ki-67 expression ($r = 0.457$, $P < 0.001$). Furthermore, the Ki-67 expression was negatively correlated with the serum lymphocyte count ($r = -0.244$, $P < 0.05$). LGG patients had lower Ki-67

expression and higher serum lymphocytes compared with HGG patients, and a combination of these two variables was significantly higher in HGG patients.

Conclusion: The constructed nomogram is capable of predicting the diagnosis of glioma-grade. A decrease in the level of serum lymphocyte count and increased Ki-67 expression in HGG patients indicate that their immunological function is diminished and the tumor is more aggressive.

KEYWORDS

glioma, ki67, lymphocytes, isocitrate dehydrogenase 1, nomogram

Introduction

Gliomas continue to be one of the most prevalent and malignant primary cancer-related morbidities in the central nervous system (CNS) (1). According to the World Health Organization (WHO, 2016), low-grade glioma (LGG) is classified as grade I–II, while high-grade glioma (HGG) is classified as grade III-IV (2). Although glioblastomas (GBMs, grade IV) are treated with maximally safe surgical resection and combined radio-chemotherapy, the median overall survival (OS) is 15 months and the 5-year survival rate is less than 5% due to the complexity of tumors, widespread invasiveness, and heterogeneity (3, 4). Furthermore, several studies have demonstrated that approximately 20%–25% of secondary glioblastomas are derived from previously lower grade (WHO grades II or III) gliomas (5, 6). Therefore, numerous studies indicate that the basic clinical–pathological features of serum laboratory indices or immunohistochemical (IHC) staining are significant variables in identifying secondary glioblastomas (7–10).

Histological, molecular features, and anatomical sites play an important role in the classification and diagnosis of glioma by the fifth edition of the WHO Classification of Tumors of the CNS (WHO CNS5) (11). The isocitrate dehydrogenase (IDH) gene encodes an enzyme that is involved in the control of cellular metabolism, epigenetic regulation, redox states, and DNA repair (12). The IDH mutation is critical for diagnosis, treatment efficacy evaluation, survival prediction, and reduced invasiveness of biomarkers associated with glioma, and is widely deemed the most significant genetic alteration (13, 14). It is associated with better outcomes in IDH1-mutant patients than in IDH1 wild-type patients (15, 16). Therefore, according to the new classification, all IDH-mutant diffuse astrocytic tumors are considered a single type (astrocytoma, IDH-mutant) and are graded as 2, 3, or 4. The restriction of the diagnosis of glioblastoma to IDH wild-type tumors means that IDH-mutant gliomas are not GBMs anymore (11, 17). This is perhaps one of the most important changes to the older version of the 2016 WHO classification. Theresia et al. found an association between the Ki-67 labeling index and histopathological grading of glioma. LGG patients had a significantly lower Ki-67 labeling index than HGG patients, and a cut-off of 10% was used to differentiate LGG from HGG (18, 19). The relationship between Ki-67 expression and IDH1 mutation status demonstrated by Zeng et al. (20) showed that Ki-67 expression along with IDH1/2 can significantly differentiate prognosis in glioma, with low Ki-67 expression associated with increased IDH1/2 mutation and IDH1/2 mutant patients with low and moderate Ki-67 expression having the best prognosis. However, it is not known whether Ki-67 expression along with IDH1 can differentiate glioma-grading.

Tumor immune infiltration of the microenvironment with inflammatory factors is critical for the occurrence, development, and prognosis of glioma. Tumor locations, in particular, release immune infiltrates and inflammatory factors into the peripheral blood, triggering an inflammatory immune response that might provide prognostic information. Accumulating evidence suggests that elevated peripheral blood lymphocytes are associated with a favorable prognosis, particularly in lung, breast, and colorectal cancers (21–23). Additionally, macrophages originating from bone marrow mononuclear cells generate an inflammatory immune response, including the release of pro-inflammatory factors such as TNF-α, chronic factors IL-6 and IL-1, which migrate to the glioma site across the blood–brain barrier (24, 25). Numerous studies indicate that T-lymphocyte subsets may affect the prognosis of breast, melanoma, pancreatic, and colorectal cancers (21–23, 26). Kmiecik et al. (27) found a correlation between tumor-infiltrating lymphocytes and prolonged survival in GBS patients. However, Zhao et al. (28) found that local tumor-infiltrating lymphocytes were a poor prognostic marker in GBS. Therefore, the correlation between peripheral serum lymphocyte or lymphocyte infiltration at the tumor site and glioma grade or prognosis is contradictory, and only a few studies have been published.

Finally, the relationship between the immunohistochemical index of IDH1, Ki-67 expression, and the peripheral serum

lymphocyte count in glioma grading is unknown. Therefore, we conducted a retrospective study to determine the prognostic usefulness of preoperative peripheral serum lymphocyte count, postoperative immunohistochemical index of IDH1 mutation status, and Ki-67 expression for glioma grading. Because nomograms are widely used to predict the risk of cancer, we established a nomogram that uses Ki-67 expression and serum lymphocyte count to predict the differences between LGG and HGG. This nomogram will aid clinical doctors in predicting the glioma-grading and identifying potential risk factors for HGG patients and allow for early treatment intervention.

Materials and methods

Patients and data collection

Between January 2012 and December 2020, we conducted a retrospective review of glioma patients. This study was approved by the Ethics Committee of the First Affiliated Hospital of Nanchang University. The WHO classifies glioma grades I–II as LGG and grades III–IV as HGG. Data of patients included their age, sex, immunohistochemistry index, serum clinical laboratory indicators, and glioma grade. The inclusion criteria were as follows: 1) all patients were admitted for surgery and histologically-confirmed glioma postoperatively; and 2) patients with complete information and Ki-67 testing. The exclusion criteria were as follows: 1) preoperative chemoradiotherapy or incomplete information; 2) along with other malignant tumors; and 3) patients with previous blood system diseases and infection or antibiotic use.

Establishment and validation of the nomogram

The R package "rms" was used to randomly divide the patients into two groups in a ratio of 2:1 training cohort (n = 292) and validation cohort (n = 125) (Figure 1A). A nomogram was established in the training cohort using multivariate logistic regression analysis, which revealed the most important predictive risk factors associated with HGG. The consistency index (C-index) ranged between 0.5 (no discrimination) and 1 (perfect discrimination), and a high C-index indicated a good prediction model. The calibration curve was used to determine the prediction compliance, while the decision curve analysis (DCA) was used to assess the clinical utility and threshold probability of the model.

Statistical analysis

The continuous variables were represented as mean ± standard deviation, and if the variables followed a normal distribution, the comparison between the two groups was carried out using the Student's t-test. To perform univariate analysis, continuous variables were converted to categorical variables. Univariate and multivariate logistic regression

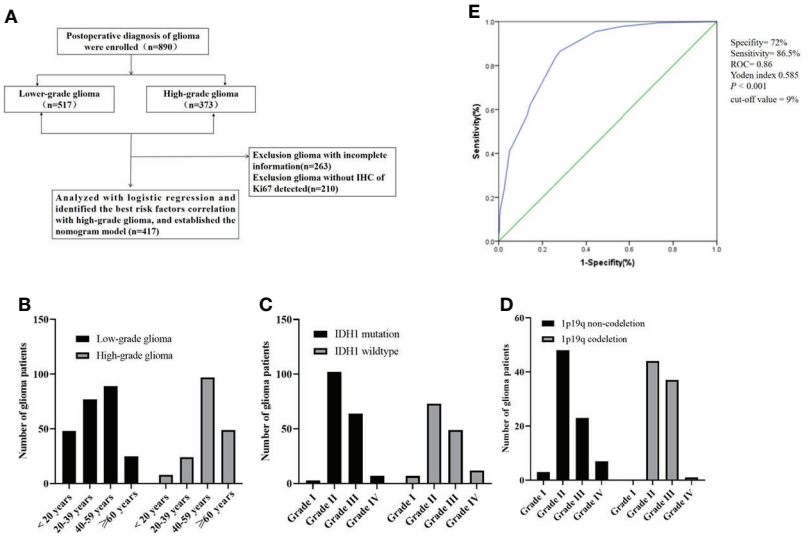

FIGURE 1
(A) Consort diagram, enrollment, and outcome; **(B)** the age distribution of patients with glioma; **(C)** IDH1 mutation status of patients with glioma; **(D)** the number of glioma patients with 1p19q codeletion status; **(E)** the Ki-67 curve of cut-off value (according to the LGG and HGG). ROC, Receiver operating characteristic; IDH1, Isocitrate dehydrogenase 1.

analyses were used to determine the independent risk factors as well as the odds ratio (OR) and 95% confidence interval (CI). The Spearman correlation coefficient was used to determine the correlation between the independent risk factors and HGG. IBM SPSS 22.0 software (SPSS Inc., Chicago, IL, USA) and GraphPad Prism version 8.0 software (Inc., La Jolla, CA, USA) were used to analyze the data. R statistical software version 4.0.0 (http://www.R-project.org/) was used to construct the nomogram model, calibration curve, and DCA. The optimal cut-off values for Ki-67 expression were determined by plotting the receiver operating characteristic (ROC) curves for glioma grading. The normal serum lactate dehydrogenase (LDH) levels were determined using appropriate assay kits (29, 30). P <0.05 was considered statistically significant.

Results

Correlation between glioma and clinicopathological characteristics

A total of 417 (239 with LGG and 178 with HGG) patients were postoperatively diagnosed with glioma and did not receive any treatment preoperatively. The clinicopathological features of glioma are summarized in Table 1. Serum white blood cells (WBCs), lymphocytes, neutrophils, neutrophil-to-lymphocytes ratio (NLR), platelets (PLTs), platelet-to-lymphocytes ratio (PLR), albumin (ALU), and LDH were used as hematological markers. There were 13 cases of grade I glioma, 226 cases of grade II glioma, 157 cases of grade III glioma, and 21 cases of grade IV glioma. The median age of the patients was 45 years (a range of 3–79). The relationship between age distribution and glioma grading revealed that the morbidity in LGG patients was mostly in the 20–59 year age range, while in HGG patients it was primarily in the more than 40 year age range (Figure 1B). A total of 141 IDH1 mutant patients were identified, 176 patients were identified as IDH1 wild-type, and 100 patients were identified as unknown. A total of 82 patients had co-deletion of chromosome 1 and the long arm of chromosome 19 (1p19q), 81 patients had non-codeletion, and 254 were unknown. There were more IDH1 mutation patients in grades II and III than in grades I and IV, with grade II having the highest number of patients with IDH1 mutations (Figure 1C). The number of grade II and III patients with 1p19q codeletion was more than those in grades I and IV, and there were no grade I patients with 1p19q codeletion (Figure 1D). Figure 1E shows the cut-off point for the Ki-67 ROC curve calculated using glioma grading (by LGG and HGG). Because the cut-off value of 9% had the highest sensitivity and specificity (sensitivity was 86.5%, specificity was 72%, Yoden index 0.585, ROC = 0.86, P <0.001), we divided the Ki-67 into low and high groups using a cut-off value of 10%.

Univariate and multivariate logistic analyses in the training cohort

All glioma patients were randomly assigned to the training cohort (n = 292) or the validation cohort (n = 125) using the R package "rms." There were 167 patients with LGG and 125 with HGG in the training cohort. Univariate logistic analysis revealed a significant correlation between age, Ki-67 expression, NLR, serum lymphocyte count, serum ALU, and glioma-grading (P <0.05) (Table 2). All significant factors in the univariate analysis were included in the multivariate logistic regression analysis. The result showed that Ki-67 >10%, serum lymphocytes count ≤1.7 ($\times 10^9$/L), and serum ALU ≤42.7 g/L were all independent risk factors associated with HGG (P <0.05) (Table 3).

Correlation analysis between the independent risk factors and HGG in all cohorts

The Spearman correlation analyses were used to determine the correlation between the independent risk factors and HGG in all cohorts. The serum lymphocyte count (r = −0.238, P <0.001), ALU (r = −0.232, P <0.001), and Ki-67 expression (r = 0.457, P <0.001) were all shown to be significantly associated with glioma-grading (Table 4). Ki-67 expression increased gradually from grades I to IV and was significantly higher in HGG patients than in LGG patients (P <0.05), regardless of glioma type, IDH1 mutation, or wild type (Figures 2A–D). We performed subgroup analysis to determine the correlation between IDH1, 1p19q codeletion, and Ki-67 expression. The result indicated that Ki-67 expression was not associated with IDH1 mutation or 1p19q codeletion Figures 2C–H). Additionally, serum ALU levels significantly decreased from grades I to IV, and the LGG group had better nutritional status than those in the HGG group (Figures 2K–L).

The serum inflammatory index plays an important role in the differentiation and proliferation of tumor cells. Therefore, we examined the relationship between serum lymphocyte count and glioma grade. The serum lymphocyte count significantly decreased from grades I to IV (Figure 3A). The serum lymphocyte count in LGG patients was significantly higher than in HGG patients, regardless of glioma type, IDH1 mutation, or wild-type status (P<0.05) (Figures 3B–D). Additionally, we performed a subgroup analysis of serum lymphocytes according to their IDH mutation status or 1p19q co-deletion status. Regardless of LGG or HGG status, the serum lymphocyte count in 1p19q codeletion groups, as well as in IDH1 mutation or wild-type groups, was not correlated with them (P >0.05) (Figures 3E–J). The serum lymphocytes in high Ki-67 expression groups were significantly lower than serum lymphocytes in low Ki-67 expression groups in all glioma patients (Figure 3K); the two groups exhibited a negative

10.3389/fonc.2022.696037

TABLE 1 Demographic and clinical–pathological characteristics of the training cohort and validation cohort.

Characteristic	Groups	All cohort (n = 417, %)	Training cohort (n = 292, %)	Validation cohort (n = 125, %)
Gender	Male	230 (55.2)	160 (54.8)	70 (56.0)
	Female	187 (44.8)	132 (45.2)	55 (44.0)
Age (years)	<60	343 (82.3)	235 (80.5)	108 (86.4)
	≥60	74 (17.7)	57 (19.5)	17 (13.6)
Tumor diameter	≤2 cm	68 (16.3)	46 (15.8)	22 (17.6)
	>2 cm	349 (83.7)	246 (84.2)	103 (82.4)
Glioma grades	WHO I	13 (3.1)	6 (2.1)	7 (5.6)
	WHO II	226 (54.2)	161 (55.1)	65 (52)
	WHO III	157 (37.7)	112 (38.4)	45 (36)
	WHO IV	21 (5)	13 (4.4)	8 (6.4)
IDH1 mutation	Wilds	141 (33.8)	96 (32.9)	45 (36)
	Mutations	176 (42.2)	118 (40.4)	58 (46.4)
	Unknown	100 (24.0)	78 (26.7)	22 (17.6)
1p/19q codeletion	Negative	81 (19.4)	58 (19.9)	23 (18.4)
	Positive	82 (19.7)	56 (19.2)	26 (20.8)
	Unknown	254 (60.9)	178 (60.9)	76 (60.8)
Ki-67[a]	≤10%	273 (65.5)	202 (69.2)	71 (56.8)
	>10%	144 (34.5)	90 (30.8)	54 (43.2)
ATRX	Negative	24 (5.8)	15 (5.1)	9 (7.2)
	Positive	87 (20.9)	63 (21.6)	24 (19.2)
	Unknown	306 (73.3)	214 (73.3)	92 (73.6)
CD56	Negative	5 (1.2)	5 (1.7)	0 (0)
	Positive	272 (65.2)	190 (65.1)	82 (65.6)
	Unknown	140 (33.6)	97 (33.2)	43 (34.4)
P53	Negative	96 (23)	68 (23.3)	28 (22.4)
	Positive	141 (33.8)	93 (31.8)	48 (38.4)
	Unknown	180 (43.2)	131 (44.9)	49 (39.2)
EMA	Negative	247 (59.2)	175 (59.9)	72 (57.6)
	Positive	60 (14.4)	38 (13)	22 (17.6)
	Unknown	110 (26.4)	79 (27.1)	31 (24.8)
GFAP	Negative	15 (3.6)	11 (3.8)	4 (3.2)
	Positive	279 (66.9)	195 (66.8)	84 (67.2)
	Unknown	123 (29.5)	86 (29.4)	37 (29.6)
WBC (10^9/L)[b]	≤7.07	255 (61.2)	178 (61.0)	77 (61.6)
	>7.07	162 (38.8)	114 (39.0)	48 (38.4)
RBC (10^{12}/L)[b]	≤4.54	212 (50.8)	153 (52.4)	59 (47.2)
	>4.54	205 (49.2)	139 (47.6)	66 (52.8)
HB (g/L)[b]	≤134	202 (48.4)	142 (48.6)	60 (48.0)
	>134	215 (51.6)	150 (51.4)	65 (52.0)
PLT (10^9/L)[b]	≤223	216 (51.8)	155 (53.1)	61 (48.8)
	>223	201 (48.2)	137 (46.9)	64 (51.2)
Lymphocyte (10^9/L)[b]	≤1.7	216 (51.8)	149 (51.0)	67 (53.6)
	>1.7	201 (48.2)	143 (49.0)	58 (46.4)
Neutrophils (10^9/L)[b]	≤4.78	270 (64.7)	193 (66.1)	77 (61.6)
	>4.78	147 (35.3)	99 (33.9)	48 (38.4)
NLR[b]	≤3.6	323 (77.5)	230 (78.8)	93 (74.4)
	>3.6	94 (22.5)	62 (21.2)	32 (25.6)
PLR[b]	≤152.7	259 (62.1)	190 (65.1)	69 (55.2)

(Continued)

TABLE 1 Continued

Characteristic	Groups	All cohort (n = 417, %)	Training cohort (n = 292, %)	Validation cohort (n = 125, %)
	>152.7	158 (37.9)	102 (34.9)	56 (44.8)
ALU(g/L)	≤42.7	214 (51.3)	150 (51.4)	64 (51.2)
	>42.7	203 (48.7)	142 (48.6)	61 (48.8)
LDH (U/L) [c]	≤250	318 (76.3)	220 (75.3)	98 (78.4)
	>250	99 (23.7)	72 (24.7)	27 (21.6)

IDH1, isocitrate dehydrogenase-1; 1p/19q co-deletion, chromosome 1 and the long arm of chromosome 19; ATRX, alpha-thalassemia/mental retardation syndrome X-linked; Ki-67, nuclear proliferation antigen 67; GFAP, glial fibrillary acidic protein; EMA, epithelial membrane antigen; PLR, platelet-to-lymphocyte ratio; NLR, neutrophil-to-lymphocyte ratio; ALU, albumin; LDH, lactate dehydrogenase; WHO, World Health Organization. [a]The cut-off points was used by ROC curve (according to LGG and HGG); [b]The cut-off points was used mean value; [c]The cut-off points was used relevant assay kits, and all those factors divided into high and low groups for statistical analysis.

correlation (Figure 3L). We then analyzed the diagnostic value of Ki-67 expression and serum lymphocyte count in glioma. The HGG patients were mostly classified as having a high Ki-67 expression and a low lymphocyte count. The Ki-67 index, along with serum lymphocytes, may be used to distinguish LGG from HGG. This approach may be critical in the diagnosis of glioma patients (Figure 3M).

Construction and validation of the nomogram

The multivariate logistic analysis identified Ki-67 expression, serum lymphocyte count, and serum albumin (ALU) as independent risk factors associated with HGG in the training cohort, and these variables were included in a nomogram. The weight of each variable was assigned a value between 0 and 100, and the HGG possibility was calculated as a sum of the corresponding scores shown on the coordinates (Figure 4).

The bootstrap c-index of the nomogram was 0.794 (0.71–0.90), indicating that the nomogram model established had a high degree of accuracy in distinguishing LGG from HGG patients. Additionally, the calibration curve indicated that the regression fitting curve was very close to the standard curve and that there was no statistically significant difference between the two curves (P = 0.616), indicating that the model had a high degree of calibration and was very close to the actual outcome (Figure 5). Additionally, the DCA demonstrated that the clinical value of the model presented more net benefits at 30%–73% and 78%–82% threshold probabilities, indicating that the postoperative LGG patients with high-risk factors who received treatment had a greater net benefit than either the treat all patients or treat none patients (Figure 6).

Discussion

Numerous studies have demonstrated that approximately 20%–25% of LGG can develop into HGG and eventually lead to death, and the 5-year survival rate of HGG is less than 5% (4, 32). Due to the limitations of imaging technology, we were unable to detect micrometastasis sites in local tumor lesions even when sophisticated magnetic resonance imaging (MRI) was used to examine the postoperative LGG patients, resulting in the patients missing out on their best opportunity for therapy. IHC and serum Systemic Inflammatory Reaction (SIR) have been shown in several studies to play an essential role in glioma grading and prognosis (7–10). Therefore, MRI combined with immunohistochemistry and blood inflammatory biomarkers will be a highly effective method for predicting HGG in future studies.

In this study, we collected the postoperative IHC and preoperative serum inflammatory-related indicators and establish a correlation with HGG. We found that the Ki-67 expression gradually increased, but the peripheral blood lymphocyte count decreased with the grading of gliomas. Spearman correlation analysis showed that Ki-67 expression had a negative linear correlation with serum lymphocytes, thus, high Ki-67 expression was associated with a lower serum lymphocyte count. Furthermore, the nomogram model was established using Ki-67 and serum lymphocytes, and it was found to be highly accurate in predicting the HGG. This is the first study to incorporate Ki-67 expression, serum lymphocytes, and clinicopathological factors in predicting the glioma-grading, which may help clinical doctors in identifying potential risk factors for HGG patients.

The SIR tumor immune infiltration microenvironment releases immune cytokines and inflammatory factors into the peripheral blood, activating the inflammatory immune response, which is critical for regulating proliferation, invasion, distant metastasis, and prognosis in lung cancer, breast cancer, colon cancer, and glioma (21–25). This study discovered a correlation between the preoperative neutrophil-lymphocyte ratio (NLR) and glioma grade, and that an elevated NLR was an independent predictor of poor outcome in glioblastoma patients (33). Marinari et al. (34) found that peripheral immune signatures associated with increased inflammation, immune infiltration, and activation were associated with poor survival in HGG patients, and that lymphocyte infiltration at the tumor site was also associated with poor survival, implying that immune responses may play a pro-tumorigenic role in glioma. Kmiecik et al. (27) described the mechanisms of immunological escape in

10.3389/fonc.2022.696037

TABLE 2 Univariate logistic proportional hazards regression analysis in the training cohort.

Characteristic		Glioma		OR (95% CI)	*P-value*
		Low grades	High grades		
Gender	Male	89	71	Ref	
	Female	78	54	0.868 (0.544–1.384)	0.551
Age (years)	<60	148	87	Ref	
	≥60	19	38	3.402 (1.847–6.268)	<0.001
Tumor diameter	≤2 cm	29	17	Ref	
	>2 cm	138	108	1.335 (0.697–2.556)	0.383
IDH1 mutation	Negative	58	38	Ref	
	Positive	68	50	1.122 (0.649–1.942)	0.68
1p/19q codeletion	Negative	37	21	Ref	
	Positive	30	26	1.527 (0.721–3.233)	0.269
Ki-67	≤10%	146	56	Ref	
	>10%	21	69	8.566 (4.808–15.262)	<0.001
ATR-X	Negative	9	6	Ref	0.841
	Positive	36	27	1.125 (0.357–3.543)	
CD56	Negative	4	1	Ref	
	Positive	104	86	3.308 (0.363–30.147)	0.289
P53	Negative	44	24	Ref	
	Positive	47	46	1.794 (0.944–3.411)	0.074
EMA	Negative	100	75	Ref	
	Positive	21	17	1.079 (0.533–2.187)	0.832
GFAP	Negative	5	6	Ref	
	Positive	116	79	0.568 (0.167–1.924)	0.363
WBC (10^9/L)[a]	≤7.07	102	76	Ref	
	>7.07	65	49	1.012 (0.629–1.627)	0.962
RBC (10^{12}/L)[a]	≤4.54	80	73	Ref	
	>4.54	87	52	0.655 (0.41–1.046)	0.072
HB (g/L)[a]	≤134	76	66	Ref	
	>134	91	59	0.747 (0.469–1.188)	0.218
PLT (10^9/L)[a]	≤223	81	74	Ref	
	>223	86	51	0.649 (0.406–1.037)	0.071
Lymphocyte (10^9/L)[a]	≤1.7	68	81	Ref	
	>1.7	99	44	0.373 (0.231–0.603)	<0.001
Neutrophils (10^9/L)[a]	≤4.78	115	78		
	>4.78	52	47	1.333 (0.818–2.171)	0.249
NLR[a]	≤3.6	142	88	Ref	
	>3.6	25	37	2.388 (1.347–4.235)	0.003
PLR[a]	≤152.7	115	75	Ref	
	>152.7	52	50	1.474 (0.908–2.395)	0.117
ALU (g/L)	≤42.7	69	81	Ref	
	>42.7	98	44	0.382 (0.237–0.618)	<0.001
LDH (U/L) [b]	≤250	126	94	Ref	
	>250	41	31	1.013 (0.592–1.735)	0.961

IDH1, isocitrate dehydrogenase-1; 1p/19q co-deletion, chromosome 1 and the long arm of chromosome 19; ATRX, alpha-thalassemia/mental retardation syndrome X-linked; Ki67, nuclear proliferation antigen 67; GFAP, glial fibrillary acidic protein; EMA, epithelial membrane antigen; PLR, platelet-to-lymphocyte ratio; NLR, neutrophil-to-lymphocyte ratio; ALU, albumin; LDH, lactate dehydrogenase.

TABLE 3 Multivariate logistic proportional hazards regression analysis in the training cohort.

Characteristic	Groups	OR (95% CI)	*P*-value
Ki-67	≤10%	Ref	
	>10%	8.758 (4.754–16.136)	<0.001
Lymphocyte (10^9/L)	≤1.7	Ref	0.003
	>1.7	0.436 (0.252–0.755)	
ALU (g/L)	≤42.7	Ref	0.001
	>42.7	0.378 (0.217–0.659)	

Ki67, nuclear proliferation antigen 67; ALU, albumin.

GBM, demonstrating that increased CD3(+) tumor-infiltrating T-lymphocyte cells were associated with prolonged survival in GBM patients and were also correlated with integrated immunosuppressive mechanisms in the tumor microenvironment and at the systemic level. Therefore, the association between tumor location and peripheral blood infiltrating lymphocytes in glioma is controversial. In this study, we found that the peripheral blood infiltrating lymphocyte count in LGG was higher than in HGG, and that grade I had the highest serum lymphocyte count. Additionally, a low serum lymphocyte count is an independent risk factor for HGG. Numerous studies have also demonstrated that IDH mutations play an important role in diagnosing, evaluating medication effectiveness, predicting survival, and reducing the invasiveness of biomarkers associated with glioma, and are widely deemed the most significant genetic alteration (13–16). Then, we further performed a correlation analysis between serum lymphocyte count and IDH1 mutation or 1p19q codeletion. In HGG or LGG patients, serum lymphocyte count showed no correlation with IDH1 mutation or 1p19q codeletion.

Additionally, we examined the IHC expression of Ki-67 and serum lymphocytes in glioma. The Ki-67 expression was gradually elevated with glioma grade, and the GBM had the highest Ki-67 expression, however, there was no association between the IDH1 mutation or 1p19q codeletion status and Ki-67 expression. Spearman correlation analysis revealed a negative linear association between Ki-67 expression and serum lymphocytes, with a higher Ki-67 expression corresponding to a lower serum lymphocyte count. Then, we examined the diagnostic utility of Ki-67 expression in glioma by combining with the serum lymphocyte count. We discovered that LGG patients have lower Ki-67 expression and a higher blood lymphocyte count than HGG patients and that a combination of these two factors may significantly distinguish LGG from HGG, perhaps playing a role in diagnosing HGG patients. Taken together, a decrease in serum lymphocytes and increased expression of Ki-67 in HGG patients indicates that the tumor immune capacity of patients is diminished and tumors are more aggressive, which may contribute to the overall survival of LGG patients being longer than HGG patients. Furthermore, there was no association between Ki-67 expression and IDH1 mutation or 1p19q codeletion. As several studies have demonstrated that overexpression of Ki-67 increases tumor proliferation, invasion, and metastasis, it is also a critical reference index for the diagnosis and prognosis of breast cancer, lung cancer, and prostate cancer (35–39). Theresia et al. (18) demonstrated an association between the Ki-67 labeling index and the histopathological grade of glioma, with LGG having a significantly lower grade than HGG. Ki-67 expression may be utilized to quantify lymphocyte proliferation (40). Li et al. (41) demonstrated a negative correlation between pre-and postoperative expression and alterations of peripheral blood lymphocytes and their CD25 and Ki-67 expression in renal cell carcinoma cells using flow cytometry and immunohistochemistry. However, no investigation has been reported to determine the correlation between Ki-67 expression and serum lymphocytes.

Nomograms are widely used for predicting the risk of cancer, and using basic hematological and clinicopathological data to identify risk factors for survival prediction is also a useful and valuable tool in tumors (42, 43). Wu et al. (44) established and validated a novel nomogram for the preoperative diagnosis of GBM using feasible baseline characteristics and preoperative tests. The nomogram demonstrated excellent calibration and a significant clinical advantage in predicting GBM. Another study suggested that a nomogram based on inflammatory biomarkers can accurately predict overall survival rates in patients with glioma, with a high NLR rate associated with a poor prognosis (45). However, no relevant studies have been reported using the Ki-67 expression and serum lymphocytes of the nomogram to

TABLE 4 Spearman correlation analysis independent risk factors with HGG in all cohorts.

Spearman		Ki-67	Lymphocyte	ALU
Glioma	r	0.457	−0.238	−0.232
	P	<0.001	<0.001	<0.001

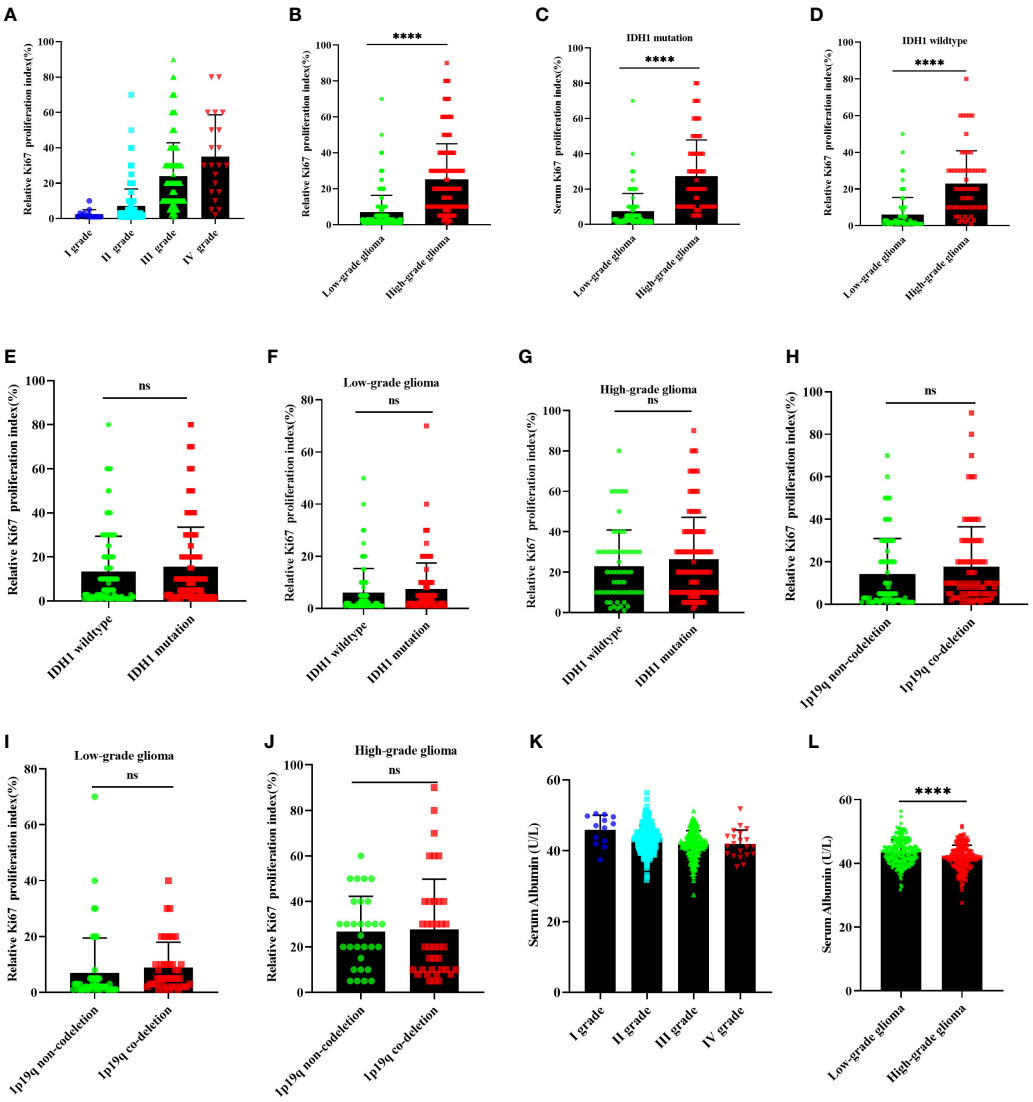

FIGURE 2
The relationship between Ki-67 expression and glioma, IDH1 mutation status, 1p19q co-deletion status. **(A, B)** the Ki-67 expression in glioma; **(E–G)** Ki-67 expression correlation with IDH1 mutation status in all glioma, LGG, and HGG; **(H–J)** Ki-67 expression correlation with 1p19q co-deletion status in all glioma, LGG, and HGG; **(C, D)**, Ki-67 expression correlation with glioma in IDH1 mutation group and IDH1 wild type group; **(K, L)** serum ALU correlation with glioma. LGG, lower-grade glioma; HGG, high-grade glioma; ALU, albumin. $^{ns}P > 0.05$, $^{****}P < 0.0001$, mean ± standard deviation, t-test.

predict the risk of glioma grade. In this study, univariate and multivariate logistic regression analysis revealed that Ki-67 expression and serum lymphocytes were independent risk factors for HGG, and the established nomogram may be used to accurately predict HGG. This is the first study to assess the predictive value of Ki-67 expression and serum lymphocytes in patients with glioma.

There are some limitations to our study. Firstly, this study only examined the correlation between peripheral blood lymphocyte count and glioma grade, but not the survival of patients following surgery or adjuvant chemoradiotherapy. Secondly, we only examined the relationship between serum lymphocytes and IDH1 mutation or 1p19q codeletion status. However, the overall survival was unclear based on both mutation status and analysis of serum lymphocytes. Thirdly, we analyzed and verified the correlation between peripheral lymphocytes and HGG retrospectively, but the expression of O6-methylguanine-DNA methyltransferase (MGMT), CD3, CD4, or CD8, etc. in peripheral blood T-lymphocytes and which inflammatory factors were released and passed through the blood–brain barrier to influence tumors were unknown. Additionally, we classified glioma-grade and pathological classification according to WHO 2016 guidelines; nevertheless, the most recent pathological classification of glioma has undergone significant changes. Finally, because this was a single-center,

10.3389/fonc.2022.696037

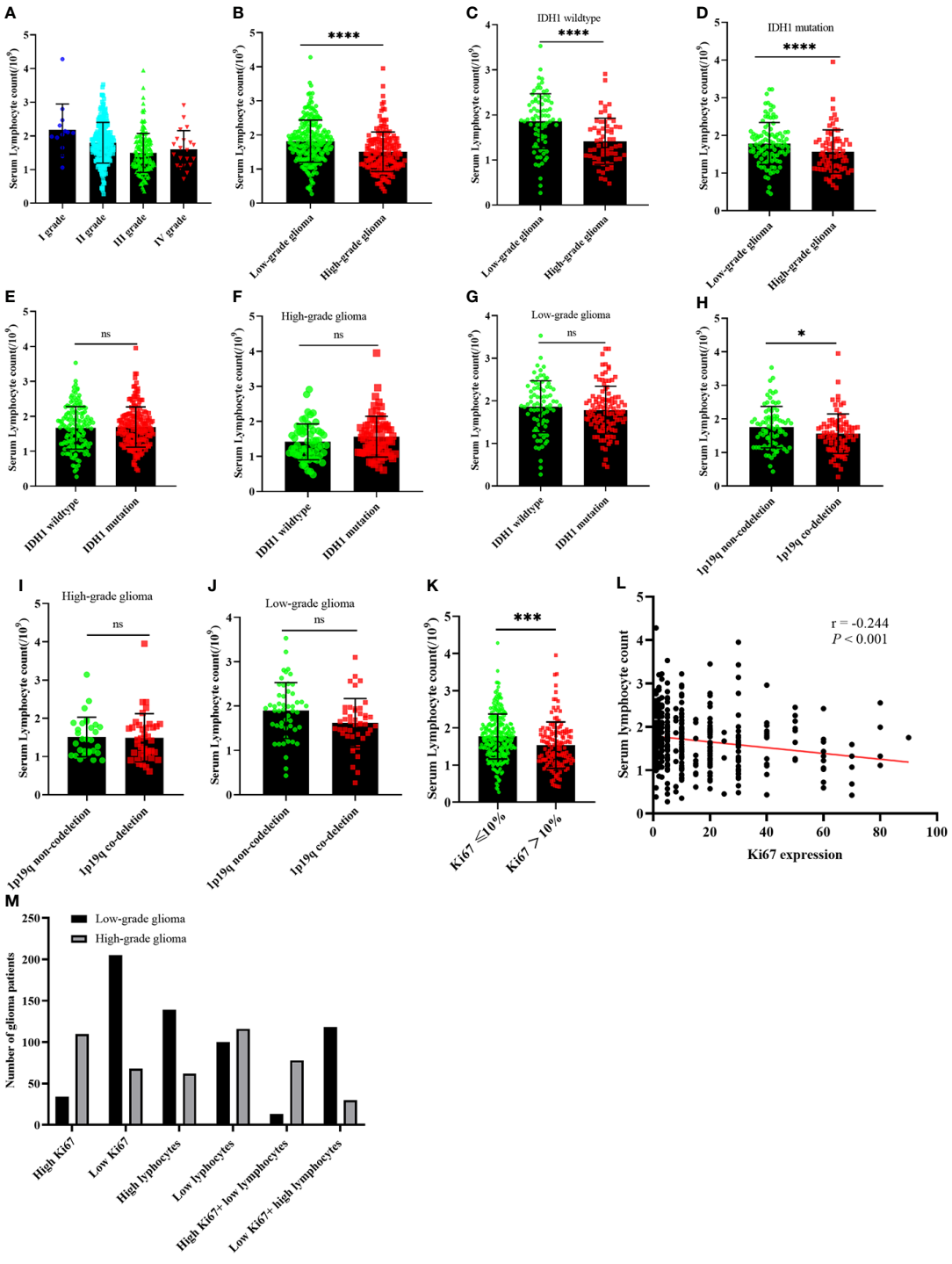

FIGURE 3
The relationship between serum lymphocyte count and glioma, IDH1 mutation status, 1p19q co-deletion status, and serum ALU correlation with glioma. **(A, B)** serum lymphocyte count in glioma; **(C, D)** serum lymphocyte count correlation with glioma in IDH1 mutation group and IDH1 wild-type group; **(E–G)** serum lymphocyte count correlation with IDH1 mutation status in all glioma, HGG, and LGG; **(H–J)** serum lymphocyte count correlation with 1p19q co-deletion status in all glioma, HGG, and LGG; **(K)** serum lymphocyte count correlation with Ki-67 expression in all glioma; **(L)** linear correlation between serum lymphocyte count and Ki-67 expression; **(M)** the number of patients with Ki-67 expression and serum lymphocytes count. LGG, lower-grade glioma; HGG, High-grade glioma; ALU, albumin. $^{ns}P > 0.05$, $*P < 0.05$, $***P < 0.001$, $****P < 0.0001$, mean ± standard deviation, t-test.

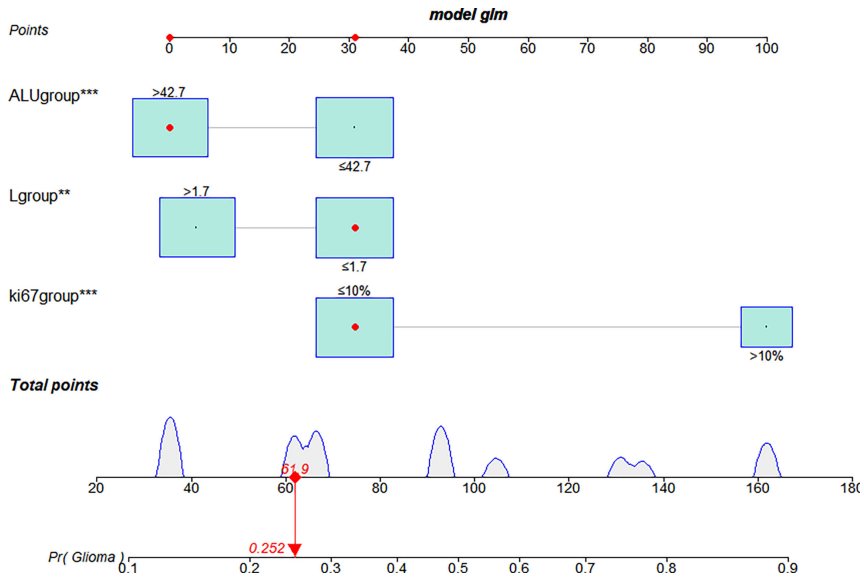

FIGURE 4
The nomogram used to predict the glioma grading in the training cohort. Three independent risk factors were incorporated into the nomogram model, and the data for those variables are shown on the interactive nomogram. Each predictive variable had a value ranging from 0 to 100, and the overall score was calculated by summing those variables. The red dot on the scale represents the corresponding score of the variable. LGG, lower-grade glioma; HGG, High-grade glioma; ALU, albumin. $^{**}P$ <0.01, $^{***}P$ <0.001.

retrospective study with a limited sample size and a small number of grade I or IV glioma patients, the results may have been subject to selection bias. Therefore, a larger sample size, multi-centered clinical study of serum lymphocytes with glioma grade should be considered in the future.

In conclusion, the established nomogram may be used to predict HGG, and the HGG patients with greater serum lymphocyte counts and lower Ki-67 expression. The reduction in serum lymphocytes and increased expression of Ki-67 in HGG patients indicate that their immunological function is

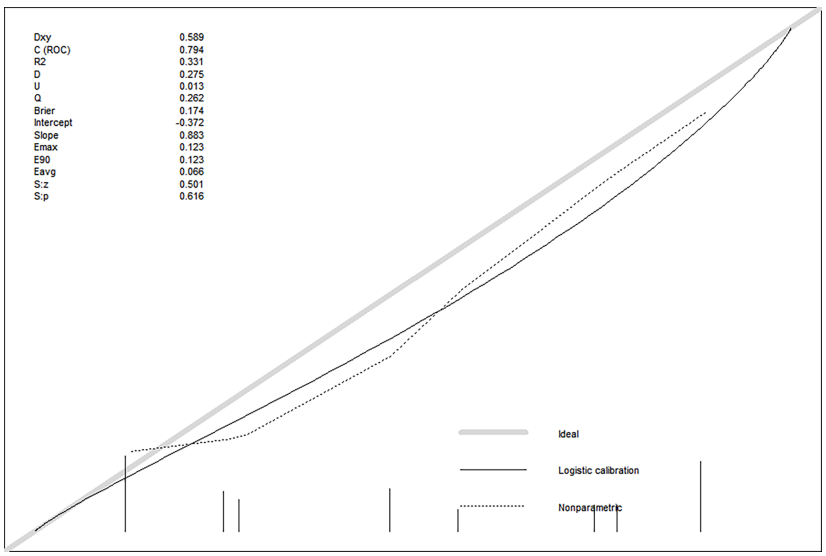

FIGURE 5
The discrimination and calibration curves of prediction model.

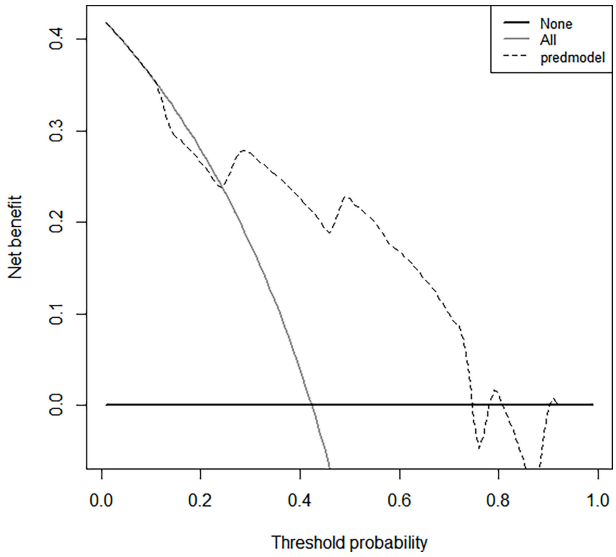

FIGURE 6
The clinical values of this nomogram model for decision curve analyses (DCA). The Y-axis represents the net benefit. The dotted line represents the clinicopathologic nomogram. The gray line represents the hypothesis that all patients are involved in HGG. The black solid line represents the hypothesis that no patients are involved in HGG. The X-axis represents the HGG possibility (31).

compromised and their tumors are more aggressive. Moreover, IHC of Ki-67 expression along with serum lymphocytes may accurately detect HGG. Therefore, we will further conduct long-term follow-up of patients and predict the risk of whose LGG will transform into HGG in the future. This may be useful in assisting clinical doctors in predicting secondary glioma in patients at high risk of postoperative LGG and allowing for early treatment intervention.

Data availability statement

The raw data supporting the conclusions of this article will be made available by the authors, without undue reservation.

Ethics statement

The studies involving human participants were reviewed and approved by the First Affiliated Hospital of Nanchang University, Nanchang, China. The ethics committee waived the requirement of written informed consent for participation. All the patients' data are keep confidential.

Author contributions

WG and ZZ were involved in collected the data and patient follow-up. WG and MH were responsible for the conception and design of the study, assisted with the statistical analysis and wrote the manuscript. CW, FQ, and JM contributed in the correction of the manuscript. LX, FY, JX, JD, and GZ helped correcting and revising the manuscript. All authors approved the manuscript prior to submission.

Funding

This work was supported by the National Natural Science Foundation of China (81960495 to FQ, 81760448 to CW) and the Nanchang Key Laboratory of Tumor Gene Diagnosis and Innovative Treatment Research (2021-NCZDSY-009). The funding sources had no role in the data collection, analysis or interpretation.

Acknowledgments

We appreciate the effort of the physicians for enrolling patients and thank all the patients involved for allowing us to analyze their clinical data.

Conflict of interest

The authors declare that the research was conducted in the absence of any commercial or financial relationships that could be construed as a potential conflict of interest.

Publisher's note

References

1. Molinaro AM, Taylor JW, Wiencke JK, Wrensch MR. Genetic and molecular epidemiology of adult diffuse glioma. *Nat Rev Neurol* (2019) 15(7):405–17. doi: 10.1038/s41582-019-0220-2

2. Louis DN, Perry A, Reifenberger G, von Deimling A, Figarella-Branger D, Cavenee WK, et al. The 2016 world health organization classification of tumors of the central nervous system: a summary. *Acta Neuropathol* (2016) 131(6):803–20. doi: 10.1007/s00401-016-1545-1

3. van Meir EG, Hadjipanayis CG, Norden AD, Shu HK, Wen PY, Olson JJ. Exciting new advances in neuro-oncology: the avenue to a cure for malignant glioma. *CA Cancer J Clin* (2010) 60(3):166–93. doi: 10.3322/caac.20069

4. Stupp R, Hegi ME, Mason WP, van den Bent MJ, Taphoorn MJ, Janzer RC, et al. Effects of radiotherapy with concomitant and adjuvant temozolomide versus radiotherapy alone on survival in glioblastoma in a randomised phase III study: 5-year analysis of the EORTC-NCIC trial. *Lancet Oncol* (2009) 10(5):459–66. doi: 10.1016/S1470-2045(09)70025-7

5. Ohgaki H, Kleihues P. Genetic pathways to primary and secondary glioblastoma. *Am J Pathol* (2007) 170(5):1445–53. doi: 10.2353/ajpath.2007.070011

6. Gross MW, Kraus A, Nashwan K, Mennel HD, Engenhart-Cabillic R, Schlegel J. Expression of p53 and p21 in primary glioblastomas. *Strahlenther Onkol* (2005) 181(3):164–71. doi: 10.1007/s00066-005-1304-z

7. Kleihues P, Ohgaki H. Primary and secondary glioblastomas: from concept to clinical diagnosis. *Neuro Oncol* (1999) 1(1):44–51. doi: 10.1093/neuonc/1.1.44

8. Nakamura M, Shimada K, Nakase H, Konishi N. [Clinicopathological diagnosis of gliomas by genotype analysis]. *Brain Nerve* (2009) 61(7):773–80.

9. Hilmani S, Abidi O, Benrahma H, Karkouri M, Sahraoui S, El Azhari A, et al. Clinicopathological features and molecular analysis of primary glioblastomas in Moroccan patients. *J Mol Neurosci* (2013) 49(3):567–73. doi: 10.1007/s12031-012-9868-4

10. Nakamura M, Shimada K, Ishida E, Nakase H, Konishi N. Genetic analysis to complement histopathological diagnosis of brain tumors. *Histol Histopathol* (2007) 22(3):327–35.

11. Louis DN, Perry A, Wesseling P, Brat DJ, Cree IA, Figarella-Branger D, et al. The 2021 WHO classification of tumors of the central nervous system: a summary. *Neuro Oncol* (2021) 23(8):1231–51. doi: 10.1093/neuonc/noab106

12. July J, Patricia D, Gunawan PY, Setiajaya H, Ginting TE, Putra TP, et al. Clinicopathological associations and prognostic values of IDH1 gene mutation, MGMT gene promoter methylation, and PD-L1 expressions in high-grade glioma treated with standard treatment. *Pan Afr Med J* (2020) 36:309. doi: 10.11604/pamj.2020.36.309.24831

13. Sun C, Xiao L, Zhao Y, Shi J, Yuan Y, Gu Y. Wild-type IDH1 and mutant IDH1 opposingly regulate podoplanin expression in glioma. *Transl Oncol* (2020) 13(4):100758. doi: 10.1016/j.tranon.2020.100758

14. Karpel-Massler G, Nguyen TTT, Shang E, Siegelin MD. Novel IDH1-targeted glioma therapies. *CNS Drugs* (2019) 33(12):1155–66. doi: 10.1007/s40263-019-00684-6

15. Kim W, Liau LM. IDH mutations in human glioma. *Neurosurg Clin N Am* (2012) 23(3):471–80. doi: 10.1016/j.nec.2012.04.009

16. Yan H, Parsons DW, Jin G, McLendon R, Rasheed BA, Yuan W, et al. IDH1 and IDH2 mutations in gliomas. *N Engl J Med* (2009) 360(8):765–73. doi: 10.1056/NEJMoa0808710

17. Wen PY, Packer RJ. The 2021 WHO classification of tumors of the central nervous system: clinical implications. *Neuro Oncol* (2021) 23(8):1215–7. doi: 10.1093/neuonc/noab120

18. Theresia E, Malueka RG, Pranacipta S, Kameswari B, Dananjoyo K, Asmedi A, et al. Association between ki-67 labeling index and histopathological grading of glioma in Indonesian population. *Asian Pac J Cancer Prev* (2020) 21(4):1063–8. doi: 10.31557/APJCP.2020.21.4.1063

19. Skjulsvik AJ, Mørk JN, Torp MO, Torp SH. Ki-67/MIB-1 immunostaining in a cohort of human gliomas. *Int J Clin Exp Pathol* (2014) 7(12):8905–10.

20. Zeng A, Hu Q, Liu Y, Wang Z, Cui X, Li R, et al. IDH1/2 mutation status combined with ki-67 labeling index defines distinct prognostic groups in glioma. *Oncotarget* (2015) 6(30):30232–8. doi: 10.18632/oncotarget.4920

21. Kim CG, Hong MH, Kim KH, Seo IH, Ahn BC, Pyo KH, et al. Dynamic changes in circulating PD-1+CD8+ T lymphocytes for predicting treatment response to PD-1 blockade in patients with non-small-cell lung cancer. *Eur J Cancer* (2021) 143:113–26. doi: 10.1016/j.ejca.2020.10.028

22. Li X, Tan Q, Li H, Yang X. Predictive value of tumor-infiltrating lymphocytes for response to neoadjuvant chemotherapy and breast cancer prognosis. *J Surg Oncol* (2021) 123(1):89–95. doi: 10.1002/jso.26252

23. Loupakis F, Depetris I, Biason P, Intini R, Prete AA, Leone F, et al. Prediction of benefit from checkpoint inhibitors in mismatch repair deficient metastatic colorectal cancer: Role of tumor infiltrating lymphocytes. *Oncologist* (2020) 25(6):481–7. doi: 10.1634/theoncologist.2019-0611

24. Fridman WH, Zitvogel L, Sautes-Fridman C, Kroemer G. The immune contexture in cancer prognosis and treatment. *Nat Rev Clin Oncol* (2017) 14(12):717–34. doi: 10.1038/nrclinonc.2017.101

25. Ginhoux F, Lim S, Hoeffel G, Low D, Huber T. Origin and differentiation of microglia. *Front Cell Neurosci* (2013) 7:45. doi: 10.3389/fncel.2013.00045

26. Zhang L, Conejo-Garcia JR, Katsaros D, Gimotty PA, Massobrio M, Regnani G, et al. Intratumoral T cells, recurrence, and survival in epithelial ovarian cancer. *N Engl J Med* (2003) 348(3):203–13. doi: 10.1056/NEJMoa020177

27. Kmiecik J, Poli A, Brons NH, Waha A, Eide GE, Enger PØ, et al. Elevated CD3+ and CD8+ tumor-infiltrating immune cells correlate with prolonged survival in glioblastoma patients despite integrated immunosuppressive mechanisms in the tumor microenvironment and at the systemic level. *J Neuroimmunol* (2013) 264(12):71–83. doi: 10.1016/j.jneuroim.2013.08.013

28. Zhai L, Ladomersky E, Lauing KL, Wu M, Genet M, Gritsina G, et al. Infiltrating T cells increase IDO1 expression in glioblastoma and contribute to decreased patient survival. *Clin Cancer Res* (2017) 23(2):6650–60. doi: 10.1158/1078-0432.CCR-17-0120

29. Yang Q, Zhang P, Wu R, Lu K, Zhou H. Identifying the best marker combination in CEA, CA125, CY211, NSE, and SCC for lung cancer screening by combining ROC curve and logistic regression analyses: Is it feasible? *Dis Markers* (2018) 2018:1–12. doi: 10.1155/2018/2082840

30. Karimi S, Vyas MV, Gonen L, Tabasinejad R, Ostrom QT, Barnholtz-Sloan J, et al. Prognostic significance of preoperative neutrophilia on recurrence-free survival in meningioma. *Neuro Oncol* (2017) 19(11):1503–10. doi: 10.1093/neuonc/nox089

31. Gu W, Hu M, Wang W, Shi C, Mei J. Development and validation of a novel nomogram for predicting tumor-Distant-Metastasis in patients with early T1-2 stage lung adenocarcinoma. *Ther Clin Risk Manage* (2020) 16:1213–25. doi: 10.2147/TCRM.S272748

32. Patil V, Mahalingam K. A four-protein expression prognostic signature predicts clinical outcome of lower-grade glioma. *Gene* (2018) 679:57–64. doi: 10.1016/j.gene.2018.08.001

33. Weng W, Chen X, Gong S, Guo L, Zhang X. Preoperative neutrophil-lymphocyte ratio correlated with glioma grading and glioblastoma survival. *Neurol Res* (2018) 40(11):917–22. doi: 10.1080/01616412.2018.1497271

34. Marinari E, Allard M, Gustave R, Widmer V, Philippin G, Merkler D, et al. Inflammation and lymphocyte infiltration are associated with shorter survival in patients with high-grade glioma. *Oncoimmunology* (2020) 9(1):1779990. doi: 10.1080/2162402X.2020.1779990

35. Pascale M, Aversa C, Barbazza R, Marongiu B, Siracusano S, Stoffel F, et al. The proliferation marker ki-67, but not neuroendocrine expression, is an independent factor in the prediction of prognosis of primary prostate cancer patients. *Radiol Oncol* (2016) 50(3):313–20. doi: 10.1515/raon-2016-0033

36. Guarneri V, Dieci MV, Bisagni G, Frassoldati A, Bianchi GV, De Salvo GL, et al. De-escalated therapy for HR+/HER2+ breast cancer patients with ki-67 response after 2-week letrozole: results of the PerELISA neoadjuvant study. *Ann Oncol* (2019) 30(6):921–6. doi: 10.1093/annonc/mdz055

37. Warth A, Cortis J, Soltermann A, Meister M, Budczies J, Stenzinger A, et al. Tumour cell proliferation (Ki-67) in non-small cell lung cancer: a critical reappraisal of its prognostic role. *Br J Cancer* (2014) 111(6):1222–9. doi: 10.1038/bjc.2014.402

38. Peng H, Tan X, Wang Y, Dai L, Liang G, Guo J, et al. Clinical significance of ki-67 and circulating tumor cells with an epithelial-mesenchymal transition phenotype in non-small cell lung cancer. *Am J Transl Res* (2020) 12(6):2916–28.

39. Mitchell KG, Parra ER, Nelson DB, Zhang J, Wistuba II, Fujimoto J, et al. Tumor cellular proliferation is associated with enhanced immune checkpoint expression in stage I non-small cell lung cancer. *J Thorac Cardiovasc Surg* (2019) 158:911–9. doi: 10.1016/j.jtcvs.2019.04.084

40. Laštovička J, Rataj M, Bartůňková J. Assessment of lymphocyte proliferation for diagnostic purpose: Comparison of CFSE staining, ki-67 expression and 3H-thymidine incorporation. *Hum Immunol* (2016) 77(12):1215–22. doi: 10.1016/j.humimm.2016.08.012

41. Li Y, Chen YR, Ju J, Shi B. Alterations in the peripheral blood lymphocyte CD25 and ki-67 indices in renal cell carcinoma and their significance: a preliminary study. *Urol Int* (2008) 81(4):447–51. doi: 10.1159/000167845

42. Wang L, Liang S, Li C, Sun X, Pang L, Meng X, et al. A novel nomogram and risk classification system predicting radiation pneumonitis in patients with esophageal cancer receiving radiation therapy. *Int J Radiat Oncol Biol Phys* (2019) 105(5):1074–85. doi: 10.1016/j.ijrobp.2019.08.024

43. Zhu M, Cao B, Li X, Li P, Wen Z, Ji J, et al. Risk factors and a predictive nomogram for lymph node metastasis of superficial esophagogastric junction cancer. *J Gastroenterol Hepatol* (2020) 35(9):1524–31. doi: 10.1111/jgh.15004

44. Wu W, Deng Z, Alafate W, Wang Y, Xiang J, Zhu L, et al. Preoperative prediction nomogram based on integrated profiling for glioblastoma multiforme in glioma patients. *Front Oncol* (2020) 10:1750. doi: 10.3389/fonc.2020.01750

45. Yang T, Mao P, Chen X, Niu X, Xu G, Bai X, et al. Inflammatory biomarkers in prognostic analysis for patients with glioma and the establishment of a nomogram. *Oncol Lett* (2019) 17(2):2516–22. doi: 10.3892/ol.2018.9870

Advantages of publishing in Frontiers

OPEN ACCESS
Articles are free to read for greatest visibility and readership

FAST PUBLICATION
Around 90 days from submission to decision

HIGH QUALITY PEER-REVIEW
Rigorous, collaborative, and constructive peer-review

TRANSPARENT PEER-REVIEW
Editors and reviewers acknowledged by name on published articles

Frontiers
Avenue du Tribunal-Fédéral 34
1005 Lausanne | Switzerland

Visit us: www.frontiersin.org
Contact us: frontiersin.org/about/contact

REPRODUCIBILITY OF RESEARCH
Support open data and methods to enhance research reproducibility

DIGITAL PUBLISHING
Articles designed for optimal readership across devices

FOLLOW US
@frontiersin

IMPACT METRICS
Advanced article metrics track visibility across digital media

EXTENSIVE PROMOTION
Marketing and promotion of impactful research

LOOP RESEARCH NETWORK
Our network increases your article's readership